ISSN 2307-8960 (online)

World Journal of *Clinical Cases*

World J Clin Cases 2023 September 6; 11(25): 5840-6030

Published by Baishideng Publishing Group Inc

World Journal of Clinical Cases

Contents

Thrice Monthly Volume 11 Number 25 September 6, 2023

World Journal of Clinical Cases

Thrice Monthly Volume 11 Number 25 September 6, 2023

Contents

World Journal of Clinical Cases

Thrice Monthly Volume 11 Number 25 September 6, 2023

Contents

NAME OF JOURNAL
World Journal of Clinical Cases

ISSN
ISSN 2307-8960 (online)

LAUNCH DATE
April 16, 2013

FREQUENCY
Thrice Monthly

EDITORS-IN-CHIEF
Bao-Gan Peng, Jerzy Tadeusz Chudek, George Kontogeorgos, Maurizio Serati, Ja Hyeon Ku

EDITORIAL BOARD MEMBERS
https://www.wjgnet.com/2307-8960/editorialboard.htm

PUBLICATION DATE
September 6, 2023

COPYRIGHT
© 2023 Baishideng Publishing Group Inc

INSTRUCTIONS TO AUTHORS
https://www.wjgnet.com/bpg/gerinfo/204

GUIDELINES FOR ETHICS DOCUMENTS
https://www.wjgnet.com/bpg/GerInfo/287

GUIDELINES FOR NON-NATIVE SPEAKERS OF ENGLISH
https://www.wjgnet.com/bpg/gerinfo/240

PUBLICATION ETHICS
https://www.wjgnet.com/bpg/GerInfo/288

PUBLICATION MISCONDUCT
https://www.wjgnet.com/bpg/gerinfo/208

ARTICLE PROCESSING CHARGE
https://www.wjgnet.com/bpg/gerinfo/242

STEPS FOR SUBMITTING MANUSCRIPTS
https://www.wjgnet.com/bpg/GerInfo/239

ONLINE SUBMISSION
https://www.f6publishing.com

E-mail: bpgoffice@wjgnet.com https://www.wjgnet.com

World Journal of Clinical Cases

Submit a Manuscript: https://www.f6publishing.com

World J Clin Cases 2023 September 6; 11(25): 5840-5856

DOI: 10.12998/wjcc.v11.i25.5840

ISSN 2307-8960 (online)

REVIEW

Mechanism and recent updates on insulin-related disorders

Shashank Kumar, Sabyasachi Senapati, Neetu Bhattacharya, Amit Bhattacharya, Shashank Kumar Maurya, Hadiya Husain, Jasvinder Singh Bhatti, Abhay Kumar Pandey

Specialty type: Medicine, research and experimental

Provenance and peer review: Invited article; Externally peer reviewed.

Peer-review model: Single blind

Peer-review report's scientific quality classification

Grade A (Excellent): 0
Grade B (Very good): 0
Grade C (Good): C, C, C
Grade D (Fair): D
Grade E (Poor): E

P-Reviewer: Amin A, United Arab Emirates; Emran TB, Bangladesh; Pappachan JM, United Kingdom

Received: June 3, 2023
Peer-review started: June 3, 2023
First decision: June 14, 2023
Revised: July 6, 2023
Accepted: August 7, 2023
Article in press: August 7, 2023
Published online: September 6, 2023

Shashank Kumar, Department of Biochemistry, Central University of Punjab, Bathinda 151401, Punjab, India

Sabyasachi Senapati, Jasvinder Singh Bhatti, Department of Human Genetics and Molecular Medicine, Central University of Punjab, Bathinda 151401, Punjab, India

Neetu Bhattacharya, Department of Zoology, Dyal Singh College, University of Delhi, New Delhi 110003, India

Amit Bhattacharya, Department of Zoology, Ramjas College, University of Delhi, New Delhi 110007, India

Shashank Kumar Maurya, Department of Zoology, University of Delhi, New Delhi 110007, India

Hadiya Husain, Department of Zoology, University of Lucknow, Lucknow 226007, India

Abhay Kumar Pandey, Department of Biochemistry, University of Allahabad, Allahabad (Prayagraj) 211002, India

Corresponding author: Abhay Kumar Pandey, PhD, Professor, Department of Biochemistry, University of Allahabad, University Road, Allahabad (Prayagraj) 211002, India. akpandey23@rediffmail.com

Abstract

Insulin, a small protein with 51 amino acids synthesized by pancreatic β-cells, is crucial to sustain glucose homeostasis at biochemical and molecular levels. Numerous metabolic dysfunctions are related to insulin-mediated altered glucose homeostasis. One of the significant pathophysiological conditions linked to the insulin associated disorder is diabetes mellitus (DM) (type 1, type 2, and gestational). Insulin resistance (IR) is one of the major underlying causes of metabolic disorders despite its association with several physiological conditions. Metabolic syndrome (MS) is another pathophysiological condition that is associated with IR, hypertension, and obesity. Further, several other patho-physiological disorders/diseases are associated with the insulin malfunctioning, which include polycystic ovary syndrome, neuronal disorders, and cancer. Insulinomas are an uncommon type of pancreatic β-cell-derived neuroendocrine tumor that makes up 2% of all pancreatic neoplasms. Literature revealed that different biochemical events, molecular signaling pathways, microRNAs, and microbiota act as connecting links between insulin disorder and associated

pathophysiology such as DM, insuloma, neurological disorder, MS, and cancer. In this review, we focus on the insulin-related disorders and the underlying mechanisms associated with the pathophysiology.

Key Words: Insulin disorder; Diabetes; Metabolic syndrome; Neurological disorder; Obesity; Cancer

Core Tip: Insulin mediated glucose homeostasis is an important event in human physiology as it fuels the life. Malfunctioning of insulin and its secretion has been linked to initiation and progression of altered pathophysiological conditions at biochemical and molecular levels. This review will help the scientific community to understand the biochemical and molecular axis of insulin-related disorders and associated pathophysiological complications and thus devise their treatment strategy.

Citation: Kumar S, Senapati S, Bhattacharya N, Bhattacharya A, Maurya SK, Husain H, Bhatti JS, Pandey AK. Mechanism and recent updates on insulin-related disorders. *World J Clin Cases* 2023; 11(25): 5840-5856
URL: https://www.wjgnet.com/2307-8960/full/v11/i25/5840.htm
DOI: https://dx.doi.org/10.12998/wjcc.v11.i25.5840

INTRODUCTION

Insulin is a relatively tiny protein with 51 amino acids. Preproinsulin, an immature form, is converted into proinsulin, which in turn produces active insulin protein after proteolysis. Insulin is arranged in tightly grouped "granules" made of insoluble crystalline hexameric insulin in β-cells. Although a number of variables influence insulin biosynthesis in pancreatic beta-cells, glucose metabolism is the primary physiological event that triggers insulin gene transcription and protein translation[1]. Protein translation is generally accelerated by β-cells in response to nutrients, which is at least in part regulated by dephosphorylation of eukaryotic initiation factor 2a *via* protein phosphatase 1[2]. In particular, β-cells react by releasing corresponding amounts of insulin in reaction to changes in plasma glucose concentration[3]. In β-cells, the glucose transporter 2 (GLUT2) is expressed constitutively, allowing glucose entrance through GLUT2-mediated facilitated diffusion. Glucokinase (GCK), a variant of hexokinase, is the rate-limiting enzyme that phosphorylates glucose after it enters β-cells[4]. Through a series of biochemical reactions, phosphorylated glucose produces ATP, which eventually causes the release of insulin *via* ATP-sensitive potassium channels[5]. In general, insulin secretion is a process that includes the plasma membrane fusion of insulin granules and the exocytosis of granule substance.

Several diseases are connected with abnormal insulin secretion and usage inside the body. Insulin resistance (IR) is defined as the decreased ability of cells or tissues to respond to physiological levels of insulin. IR causes metabolic abnormalities as insulin plays a major role in maintaining glucose homeostasis through its actions on carbohydrate, protein, and lipid metabolism. Growing experimental and clinical evidence suggests that IR may be the underlying fundamental metabolic defect which gives chance to the establishment of different diseases such as diabetes mellitus (DM), insulinoma, metabolic syndrome (MS), polycystic ovary syndrome (PCOS), neuronal disorder, and cancer. In the present review article, we have briefly discussed about insulin-signaling pathways and emphasized their association with glycemic imbalance having implications in disease pathogenesis. Here we review the recent evidence in the field and present it in the context of common insulin-related disorders. For the current review, the literature published in English and indexed in the PubMed, Scopus, and other databases was used. The relevant studies were found by using the keywords "insulin; insulin-related disorders; diabetes; insulin and neurological disorders; insulin and cancer; and insulin disorder and miRNA" in database searches.

DM

Type 1 diabetes

Increased blood glucose level (hyperglycemia) is a hallmark of type 1 DM (T1DM), a chronic autoimmune illness caused by an insulin deficiency that results from the death of pancreatic islet β-cells[6]. One of the most prevalent endocrine and metabolic disorders affecting children is T1DM. The loss of β-cells is a result of T1DM-related autoimmunity in the overwhelming majority of patients; these individuals have autoimmune T1DM. Idiopathic T1DM, also known as type 1b DM, is a rarer form of the disease in which no immune responses or autoantibodies are found and the reason of cell death is unknown[7]. T1DM is due to cellular-mediated autoimmune destruction of pancreatic β-cells. Several autoimmune markers such as islet cell autoantibodies, and autoantibodies to insulin, glutamic acid decarboxylase 65 (GAD65), tyrosine phosphatases (IA-2 and IA-2β), and zinc transporter 8 (ZnT8) specific to T1DM have been identified[7]. Uncertainty surrounds the cause of a first-appearing cell-targeting autoantibody, but it is being investigated in a number of trials involving children who have been monitored since birth[8]. According to some theories, the pathogenesis of T1DM can be

viewed as a continuum with distinct phases that start with the discovery of autoantibodies and move on to cell death, dysglycemia, and hyperglycemia-related symptoms[9]. The cause of β-cell-targeted autoimmunity, which is still unknown, is thought to involve a confluence of genetic and environmental factors that either initiate or facilitate the autoimmune reaction against β-cells[8]. Although not proven, it is widely accepted that ongoing exposure to β-cell autoantigens causes the autoantibodies to be produced[10]. A juvenile possessing HLA-DR4-DQ8 haplotype typically develops insulin autoantibodies at a peak rate between the ages of one and two years. These two serotypes, *i.e.*, HLA-DR4 and HLA-DQ8, are coded by HLA-DRB1 and HLA-DQB1 genes, respectively. Autoantibodies that target the protein tyrosine phosphatase-like entities IA2 and IA2β or ZnT8 can form after autoantibodies to insulin or GAD65[8].

Type 2 diabetes

Genetic and environmental factors play a part in the multifactorial illness known as T2DM. T2DM is defined by dysregulation of the metabolism of carbohydrates, lipids, and proteins and is brought on by either impaired insulin secretion, IR, or both. T2DM is by far the most prevalent of the three main types of diabetes, accounting for 90% of all cases. Its primary consequence is progressive impairment of pancreatic cell insulin secretion, which typically occurs against a backdrop of pre-existing IR in skeletal muscle, the liver, and adipose tissue. Pre-diabetes, a high-risk condition that increases the chance of developing T2DM and is characterized by impaired fasting glucose, impaired glucose tolerance, or elevated hemoglobin A1C (HbA1c), precedes overt hyperglycemia[11]. HbA1c levels in people with prediabetes range from 5.7% to 6.4%; they are clinically very diverse and reflect a pathophysiologically heterogeneous group. Prediabetes to T2DM conversion rates vary from 3% to 11% annually[12]. β-cell dysfunction, IR, and persistent inflammation are the hallmarks of the pathophysiological changes, which all work together to gradually impair blood glucose regulation and promote the emergence of micro/macro-vascular complications. The first abnormality that can be seen in people who are prone to develop T2DM is IR[11]. Overt T2DM, however, does not happen unless the cells are unable to produce enough insulin to counteract the IR[13]. Cell failure is caused by a variety of variables, such as toxicity caused by lipids and glucose, inflammation, and cell stress brought on by IR, among others. Inter-individual differences have an impact on how β-cells modify insulin release in response to changing demands on a minute-by-minute basis in order to maintain normal blood glucose levels[14]. The rate of β-cell proliferation in islets with and without diabetes does not appear to vary. Dysregulated autophagy and apoptosis are probable reasons for the loss of β-cells in T2DM[15].

Gestational diabetes

Although Carrington first used the word "gestational diabetes" in 1957, it was not until John O'Sullivan's publications in 1961 and 1964 that it became more widely known[16]. Therefore, gestational DM (GDM) includes a wide range of hyperglycaemia. It ranges from mild impaired glucose tolerance/fasting glucose found in early pregnancy to glucose levels indicative of overt diabetes found in late pregnancy. GDM is characterized by greater IR and β-cell defects, which are metabolic abnormalities. These defects, however, are almost completely asymptomatic and are typically only discovered as a result of frequent testing of blood glucose levels during pregnancy. The metabolic changes that occur during pregnancy put β-cells under extra strain. A patient having a history of GDM has a greater chance to develop T2DM in the years after giving birth, and this increased risk is caused by both baseline abnormalities that were present before the index GDM pregnancy but were not previously diagnosed and further, progressive β-cell dysfunction that developed after that pregnancy. These factors include increased IR and gestational weight gain. Approximately 5% of women with GDM have monogenic variants of DM, which most frequently involve mutations in GCK in white populations, while only a tiny percentage (2%-13%) of women with GDM have antibodies against specific β-cell antigens [17,18]. If the fetus does not have the heterozygous GCK mutation, the mother's slightly elevated fasting glucose levels can increase the risk of excessive fetal growth. GCK phosphorylates glucose to create glucose-6-phosphate in the pancreas and liver. Fascinatingly, fetal growth is normal if the GCK mutation is present in both the mother and the fetus, whereas if the GCK mutation is present only in the fetus, there is a higher chance of fetal growth restriction due to altered glucose sensing by the fetal pancreas[19]. Due to the pancreatic β-cells' capacity to boost their insulin response, these women initially adaptively sustain normoglycaemia in the early stages of pregnancy. The increase in IR, however, makes the insulin response insufficient by the end of pregnancy[20]. The binding of insulin to the cell surface insulin receptor in peripheral tissues such as skeletal muscle causes glucose uptake by cells in non-pregnant women with adequate glucose tolerance. As was already stated, sensitivity decreases with growing gestation during pregnancy, and this decreases even more in women who develop GDM, both before and during pregnancy[14].

According to reports, epigenetic modifications involve several molecular pathways, including traditional epigenetic changes affecting DNA methylation and histone modifications and small RNA-mediated processes, especially those involving microRNAs (miRNAs). It is understood that epigenetic modifications are important mediators of gene regulation concerning diabetes[21]. Impairment in histone modifications (such as H3 Lysine 9demethylation and SIRT1/2/6-dependent deacetylation) have been known to associate with T2DM[22,23]. Recent studies showed the role of miRNAs in the pathogenesis of diabetes. Pancreatic β-cells of individuals with diabetes have a cluster of miRNAs (such as miR-375, miR-1203, miR-412, miR-216a, and miR-101-3p), and their impaired epigenetic regulation is involved in glucose tolerance, insulin secretion, and β cell functioning[24-26]. In addition, to understand the newer mechanism of diabetes, scientists are also trying to explore novel therapeutic strategies for diabetes. Besides currently available anti-diabetic therapy (biguanides, sulfonylureas, thiazolidinediones, dipeptidyl peptidase-4 inhibitors, glucagon-like peptide 1 analogs, and sodium-glucose co-transporter-2 inhibitors), nowadays some newer anti-diabetic treatment strategies (oral hypoglycemics incorporated nanocarriers, insulin pump, pancreatic islet cell transplantation, artificial pancreas, tissue engineering, gene therapy, and stem cell therapy) are in emerging stage[27].

INSULINOMA

Insulinomas are rare neuroendocrine tumors originating from pancreatic beta-cells[28,29]. Due to this, the pancreas makes extra insulin, more than that body can use to keep the blood sugar level balanced. This condition causes blood sugar levels to drop significantly. Insulinomas occur in 1 in 100000 of the population and represent 1% to 2% of all pancreatic neoplasms[30]. Ninety percent or more of all insulinomas are benign in nature, whereas larger tumors are more likely to be malignant[31]. Insulinomas can arise at any age and have an equal gender distribution. Gastroenteropancreatic neuroendocrine tumors (GEPNETs), also known as ascarcinoids and islet cell tumors, based on tumor diameter and stage are commonly graded and classified according to the World Health Organization (WHO) classification of endocrine tumors[32-34]. They are divided into four groups: (1) Well-differentiated endocrine tumor (benign, restricted to the pancreas, < 2 cm in diameter, ≤ 2 mitoses per 10 high power fields (HPFs), ≤ 2% Ki-67 positive cells, no angioinvasion or perineural invasion); (2) Well-differentiated endocrine tumor with uncertain behavior (WDETUB) (restricted to the pancreas with one or more of the following features: 2 cm in diameter, > 2 mitoses per 10 HPFs, > 2% Ki-67 positive cells, angioinvasion, and perineural invasion); (3) Well-differentiated endocrine carcinoma (low grade malignant; gross local invasion and/or metastases); and (4) Poorly differentiated endocrine carcinoma (high grade malignant; > 10 mitoses per 10 HPFs)[25]. The WHO 2000/2004 classification was not extensively recognized because of stage-related classification and the category of 'uncertain behavior' such as WDETUB[34]. The European Neuroendocrine Tumor Society proposed a grading classification and site-specific staging system in 2010[34]. GEPNETs were separated into three groups based on mitoses and the Ki-67 index: NET grade 1 (G1), NET grade 2 (G2), and neuroendocrine carcinoma grade 3 (G3).

In the 1860s, Langerhans[35] made the first careful and detailed description of the microscopic structure of the pancreas. In 1893, the French histologist GE Languesse named the spots described by him 'ilots de Langerhans'. These cells were later established to have insulin secreting property. Several years later, in 1922, Banting and Best isolated insulin (or 'isletin', as they called it) from a solution extract of a dog's pancreas. In 1923, Harris proposed a clinical likelihood of hyperinsulinism and compared it with the diabetes-induced hypoinsulinism[36]. Albert Nicholls described the first adenoma arising from the islets of Langerhans in 1902. He also gave the first report of a pancreatic neuroendocrine tumor (PNET). In 1927, the first insulinoma was defined in Mayo Clinic and was dissected out in 1929 (Toronto). At the St. Jouis hospital in 1931, the first enucleation of insulinoma was done. In 1935, Allen Whipple and Virginia Kneeland Frantz published a classic paper describing the historical diagnostic criteria for insulinoma in *Annals of Surgery*. The Whipple's triad, the diagnostic hallmark of insulinomas, includes: Symptoms of hypoglycemia triggered by fasting, circulating glucose level less than 50 mg/dL at the time when symptoms exist, and respite of symptoms with administration of glucose[37].

Hypoglycemic episodes caused by inappropriate insulin secretion are divided into two main categories, adrenergic symptoms (caused through activation of the sympathetic nervous system/catecholamine release) and neuroglycopenic symptoms (caused through decreased central nervous system glucose supply and may result in serious and debilitating neurological symptoms)[38,39]. Adrenergic symptoms include sweating, tremor, palpitations, tachycardia, agitation, nervosity, and increased appetite. Neuroglycopenic symptoms include impairment of consciousness, mental concentration, visual disturbances, blurred vision, ataxia, disorientation, memory deficits, stupor, seizures, and coma. Most patients testified with insulinomas present neuroglycopenic symptoms and less than 10% of insulinomas are reported to be malignant[40]. It has been found that the majority of malignant insulinomas progress slowly. Due to the rarity of insulinoma, it is often misdiagnosed as epilepsy[40] or juvenile myoclonic epilepsy[41]. Timely diagnosis of occult or non-detectable insulinomas is a diagnostic challenge for radiologists and critical to medical treatments, as well as how to manage cases of malignant insulinoma for surgeons. Most insulinomas are intrapancreatic, benign, and solitary. Various biochemical diagnosis and imaging techniques provide advanced knowledge of the site of the mass and vital information for preoperative localization and intraoperative detection of an insulinoma. The biochemical diagnosis 72-h fasting test is considered as the gold standard for confirmation of insulinoma diagnosis[42]. This test consists of consecutive measurement of plasma glucose, insulin, C-peptide, and proinsulin in adults with signs of neuroglycopenia or known low blood glucose levels. The combination of computerized tomography, magnetic resonance imaging, and endoscopic ultrasound has been reported to be highly sensitive in the localization of insulinomas and metastatic disease. In addition, intraoperative palpation combined with intraoperative ultrasound has been also found very effective with a high detection rate (up to 93%)[39,43,44]. Treatment for insulinomas is largely surgical procedure (such as open surgery and laparoscopic excision) (Figure 1). However, the patient is operated only if the diagnosis is established. Blind pancreatectomy is not an appropriate and preferred therapeutic choice in the treatment of undetected insulinomas.

Insulinomas can occur sporadically or in conjunction with multiple endocrine neoplasia type 1 (MEN-1) syndrome (previously known as Wermer's syndrome). MEN-1 syndrome, an autosomal dominant disorder, was linked with mutations in the *MEN1* gene[45]. The *MEN-1* locus was mapped to chromosome 11 by family studies, and it revealed fitted linkage with the human muscle phosphorylase gene. Several lines of evidence have suggested a role of MEN-1 as a recessive tumor suppressor gene and the two-hit hypothesis for tumor suppressor genes (first proposed by Knudson for tumorigenesis of retinoblastomas) applies to MEN-1 syndrome[46,47]. The inactivation of the *MEN-1* tumor suppressor gene, encoding a 610 amino acid nuclear protein-Menin, in patients leads to a collection of changes in endocrine tissues, including parathyroid neoplasia, pituitary adenomas, PNETs, and carcinoids. Menin is involved in the regulation of multiple important signaling pathways with a variety of nuclear and cytosolic proteins, such as JunD, nuclear transcription factor-kappa B (NF-κB), Smad3, FANCD2, RPA2, and ASK[46]. Thus, Menin regulates critical steps in cell proliferation, apoptosis, and maintenance of genome integrity.

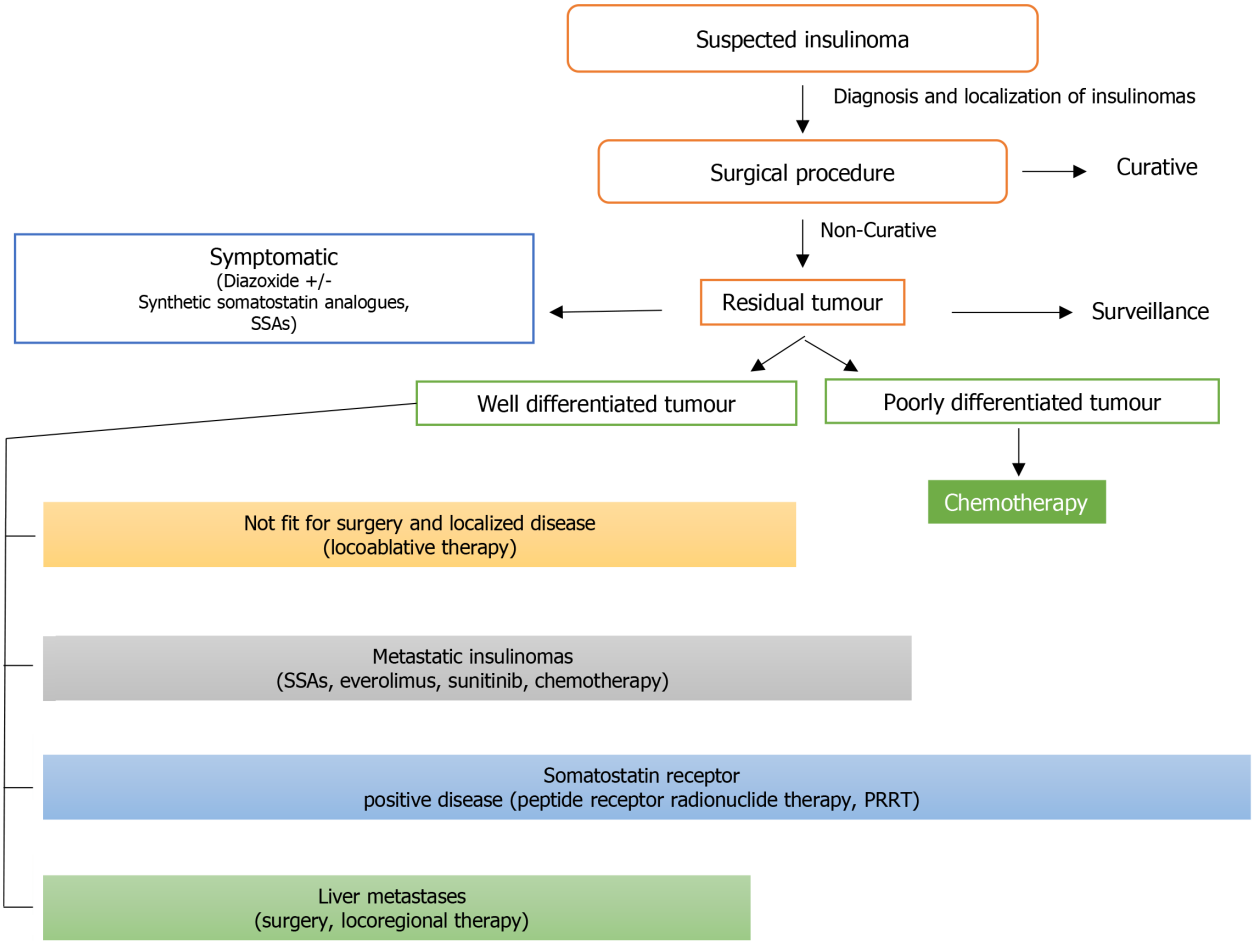

DOI: 10.12998/wjcc.v11.i25.5840

Figure 1 Different treatment options based on suspected aggressiveness of insulinomas[33]. SSAs: Supramolecular self-associating amphiphiles; PRRT: Peptide receptor radionuclide therapy.

The phosphatidylinositol-3-kinase (PI3K)/Akt and mammalian target of rapamycin (mTOR) signaling pathways are intracellular signaling pathways that play a critical role in the regulation of cell cycle, cell growth, and survival, as well as in pathological conditions (such as pancreatic endocrine tumors). The Akt/mTOR pathway is also involved in the regulation of glucose homeostasis and dysregulated mTOR signaling is networked in peripheral IR through numerous distinct mechanisms[48,49]. mTOR inhibitors have an antiproliferative outcome by blocking signaling in the PI3K/Akt/mTOR pathway. Clinical studies suggest that the mTOR inhibitor Everolimus (EVR) normalized plasma glucose levels in metastatic insulinoma within 14 d[50]. EVR, a rapamycin analog, affects tumor progression, rapidly controls hypoglycemia, and causes hyperglycemia by several mechanisms synergistically. Sunitinib, an oral multitargeted receptor tyrosine kinase inhibitor, displayed antiangiogenic and antitumor activity against advanced PNETs[51]. The diagnostic approaches, understanding of biomarker histology, and therapeutic management of PNETs have improved during the last two decades. However, the etiology of these tumors is poorly understood. The correct diagnostic criteria, improved classification, and specific therapeutic approaches are important to protect patients from misdiagnosis and pitfalls. Emerging therapeutic options and a better understanding of PNETs certainly offer the potential to diagnose suspected cases, improve preoperative localization of insulinomas and patient outcomes, and provide symptom control to improve quality of life. However, improved therapy combinations and safety of treatment remain areas for future research.

MS

MS is an accumulation of several disorders due to assemblage of cardiometabolic risk factors, such as obesity, IR, hypertension, and dyslipidemia, which together increase the risk of developing atherosclerotic cardiovascular disease (CVD), neurological problems, and DM[52]. MS adversely affects several body systems. Metabolic disorder becomes a syndrome if an individual has few of the following criteria: (1) Waist size greater than 40 inches in men and 35 inches in women (obesity); (2) Higher fasting glucose of l00 mg/dL or greater (hyperglycemia); (3) Blood triglycerides values equal to or greater than 150 mg/dL (dyslipidemia); (4) High-density lipoprotein (HDL) cholesterol level lower than 40 mg/dL in men or less than 50 mg/dL in women (low HDL/good cholesterol); and (5) Elevated blood pressure values of systolic

(130 mmHg or higher) and/or diastolic (85 mmHg or higher) (hypertension)[52]. The WHO first established its definition in 1998 and was the first to document the cluster of crucial components of IR, obesity, dyslipidemia, and hypertension, which are known to be interrelated[53]. The WHO criteria (1998) were set as IR or diabetes, plus two of the five criteria above. In 1999, the European Group for the Study of Insulin Resistance, proposed a modification to the WHO definition, hyperinsulinemia, plus two of the four criteria[54].

In 2001, the National Cholesterol Education Program (NCEP) Adult Treatment Panel III (ATP III) defined that MS is present if three or more of the above five criteria are present[55]. The NCEP ATP III description is one of the most widely accepted criteria for MS[56]. In 2005, the International Diabetes Foundation issued new criteria for MS which said obesity, plus two of the four criteria[57]. A study showed the association of sleep-related characteristics (such as sleep duration, insomnia, and day-time napping) with a higher prevalence of MS in the general population[58]. A cross-sectional study of MS and sleep duration exhibited that women have a higher risk of MS and higher MS severity scores due to short and long sleep duration[58]. While in men, higher risk of MS and higher MS severity scores were associated with short sleep duration[59].

Understanding of the four central features (IR, visceral adiposity, atherogenic dyslipidemia, and endothelial dysfunction) helps us to broadly define MS and their interrelationships. Insulin produced by beta-cells of the pancreas in response to hyperglycemia kindles glucose uses differently in various tissues (such as glucose uptake by translocation of the GLUT4 to the cell surfaces in skeletal muscle and adipose tissue). The primary effect of these different mechanisms is to increase glucose uptake, decrease circulating glucose levels, and enhance its conversion into the key storage molecules, such as glycogen or fats. IR (also referred as IR syndrome) is a main underlying mechanism responsible for MS. IR is also described as a convincing interpreter of T2DM[60,61]. In IR, adipose, muscle, and liver cells do not respond correctly to insulin, thus circulating glucose levels remain high, leading to physiological and pathological changes. Hyperinsulinemia is a surrogate pointer for IR in the body. Physiological insulin signaling is triggered by binding of insulin to the insulin receptor (a ligand-activated tyrosine kinase) and it transpires *via* activation of two parallel pathways: The PI3K or PI3K-Akt pathway and mitogen-activated protein kinase (MAPK) pathway. The protein kinase B (PKB or Akt) is involved in the regulation of multiple cellular physiological processes like cell metabolism, growth, proliferation, and survival. PKB or Akt initiation is measured by a multi-step process that involves PI3K. The PI3K-Akt pathway is responsible for many of the downstream metabolic effects of insulin. In IR, the PI3K-Akt pathway is dysregulated, whereas the MAPK pathway is not[56]. This leads to a change in the balance between these two critical intracellular signaling pathways.

Abdominal obesity, also referred as visceral or central obesity, categorized by increased adipose tissue surrounding the intra-abdominal organs, has been linked with several medical conditions such as MS, CVD, and some malignancies[62]. In 1991, Björntorp[63] described the role of abdominal obesity in the development of IR and MS. Visceral obesity based on epidemiological, clinical, experimental, cellular, and molecular evidence has also been denoted as an expression of a 'Civilization Syndrome'[64]. Abdominal or visceral obesity leads to variation of the normal physiological equilibrium of adipokines, endothelial dysfunction, IR, and a pro-atherogenic state[65]. Adiponectin, an anti-atherosclerotic adipokine, is a 244-amino acid protein secreted largely by the adipocytes and a recognized homeostatic factor for regulating glucose levels, lipid metabolism, and insulin sensitivity in the body[66]. Adiponectin signaling in mammals is mediated *via* two adiponectin receptors, which occur as two isoforms: AdipoR1 and AdipoR2. Its level decreases in obesity-related diseases such as T2DM, CVD, and MS[67,68]. The adipokines, free fatty acids (released from visceral fat), and bioactive lipid intermediates together disturb the PI3K-Akt pathway and increase oxidative stress. Adiponectin elicits a few downstream signaling events in adiponectin signal transduction (Figure 2). The adaptor protein APPL1 is the first recognized protein that networks directly with adiponectin receptors (AdipoR1 and AdipoR2) and acts as a signaling pathway mediator in cross-talk with adiponectin and insulin[67,69]. Adiponectin-dependent insulin sensitization in insulin responsive tissues is mediated by activation of IR substrate (IRS)1/2. Adiponectin exerts its effect primarily by activating AMP-activated protein kinase (AMPK), p38 mitogen-activated protein kinase, and peroxisome proliferator-activated receptor-α promoting fatty acid oxidation, vasodilation, glucose uptake, and energy expenditure, thereby decreasing the levels of glucose and lipids[65,67] (Figure 2). Furthermore, activated AMPK by adiponectin prevents IkappaB kinase/NFκB/PTEN triggered apoptosis.

Biomarkers of inflammation and endothelial dysfunction, a type of non-obstructive coronary artery disease, have been associated with MS and diabetes[70,71]. Vascular endothelium (VE) regulates vascular homeostasis through a delicate balance between the secretion of vasodilators and vasoconstrictors (Figure 3). Recently, Ganguly *et al*[72] discussed the role of inflammation in obesity and its mitigation by natural products. Endothelial dysfunction in obesity-induced inflammation due to excessive deposition of fat leads to uneven secretion and release of inflammatory mediators or proinflammatory cytokines, like interleukin (IL)-6, IL-1β, tumor necrotic factor-α (TNF-α), leptin, and activation of monocyte chemo-attractant protein-1 (MCP-1)[72]. These biomolecules subsequently reduce the formation of adiponectin, leading to commencement of a proinflammatory state in the obese body[71,72]. Under normal physiology, there is a balanced release of various vasodilator agents but an imbalance in their production, mainly nitric oxide (NO), endothelial-derived hyperpolarizing factors, prostacyclin, and vasoconstricting agents, including prostaglandin, endothelin-1, and angiotensin-II, results in advancement to endothelial dysfunction[73]. The mechanisms of endothelial cell dysfunction associated with inflammation is mainly due to alterations in the balance between proinflammatory and procoagulant state, and anti-inflammatory and anticoagulant properties of the endothelium influencing the VE shift towards the prothrombotic and proatherogenic states[72,74]. These prothrombotic and proatherogenic states alter cell processes, leading to vascular inflammation, platelet activation, leukocyte adherence, mitogenesis, vasoconstriction, pro-oxidation, impaired coagulation, atherosclerosis, and thrombosis with consequent CVDs.

MS is a distinctive constellation of abnormalities through the interaction of genetic, hormonal, and lifestyle factors. However, a distinct understanding of the molecular mechanisms in the pathogenesis of endothelial dysfunction and other abnormalities may allow the development of new diagnostic tools and early therapeutic measures to improve health in

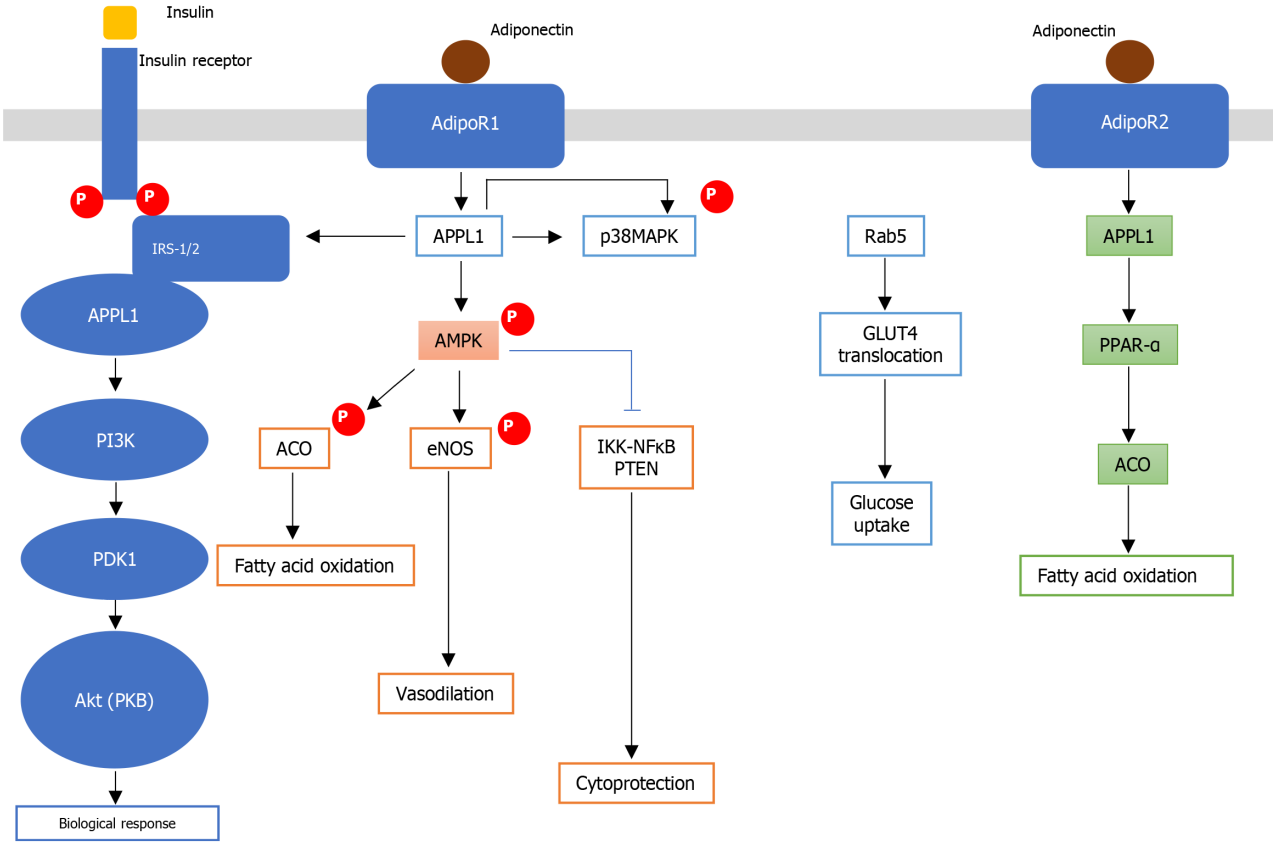

DOI: 10.12998/wjcc.v11.i25.5840

Figure 2 Schematic representation showing downstream signaling events in cross-talk between adiponectin signal transduction and insulin signaling pathway[67]. IRS: Insulin receptor substrate; APPL1: Adaptor protein containing a pleckstrin homology domain, phosphotyrosine binding domain, and leucine zipper motif; PPAR: Peroxisome proliferator-activated receptor; ACO: Asthma-COPD overlap; GLUT: Glucose transporter; PI3K: Phosphatidylinositol-3-kinase; PDK: Phosphoinositide-dependent kinases; PKB: Protein kinase B; eNOS: Endothelial nitric oxide synthase; IKK: IkappaB kinase; NF-κB: Nuclear transcription factor-kappa B; PTEN: Phosphatase and tensin homolog deleted on chromosome 10.

the next generations. A pleotropic polygenic architecture underlying MS tends to cluster together, resulting in an augmented risk for CVD, T2DM, and various cancers. Research will continue to uncover this fascinating complex trait and its subsequent cardiometabolic risk factors.

PCOS

PCOS is one of the most common metabolic diseases among women of the reproductive age group. Very frequently PCOS is classified as an endocrine disorder due to the direct involvement of the hypothalamic-ovarian axis, where IR is considered as the primary pathological basis. The typical presentation of PCOS includes hyperandrogenism and evidence of ovarian dysfunction such as chronic oligo-anovulation and/or micro-polycystic morphology of the ovary[75]. Although the familial aggregation of PCOS is very frequently reported, the heritability of the disease is not well explained [76]. Moreover, the literature indicates controversies regarding possible role of IR in PCOS. Recently, Armanini *et al*[76] summarized IR related controversies in PCOS therapy and diagnosis. Clinically, PCOS is heterogeneous where several non-genetic modifiable factors such as intrauterine environment, gut microbiota, nutritional status, endocrine regulation, and environmental exposure to heavy metals and toxins, have been reported to play critical roles in determining the PCOS pathogenesis[77].

Although the particular molecular trigger of PCOS is unclear, clinical and molecular studies have well-established the link between IR and PCOS without a clear cause-effect relationship[75]. PCOS subjects were frequently reported to have a higher magnitude of IR when compared to healthy controls where the magnitude is mild among lean compared to obese individuals[78]. Recent evidence from clinical, pathological, *ex vivo*, and *in vivo* studies indicated the implication of aberrations in insulin signaling-associated pathways in PCOS. IR in terms of impaired downstream metabolic insulin signaling through increased serine phosphorylation and reduced tyrosine phosphorylation of IR and its substrate IRS-1 among PCOS subjects was reported[79]. Unlike metabolic signaling, activated mitogenic signaling (such as androgen production) which is regulated through IR was also found significantly affected by IR-induced hyperinsulinemia[80]. However, other findings have also suggested that there can be insulin-independent increased androgen production in the ovary due to reduced levels of activated mitogen-activated protein kinase 1/2 and extracellular signal-regulated kinase

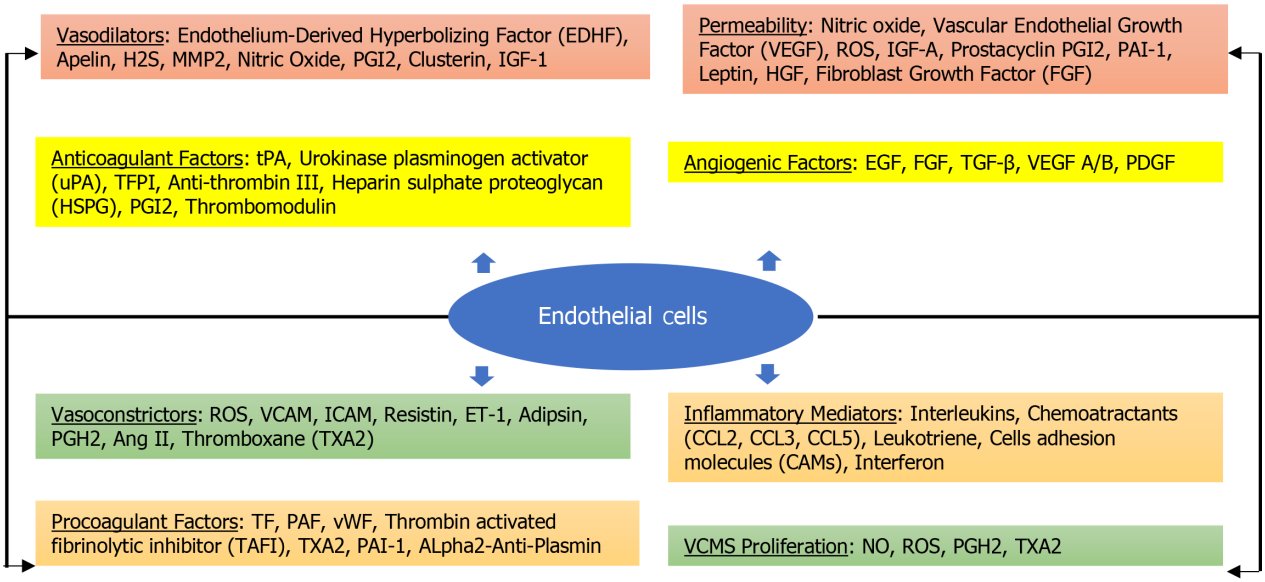

DOI: 10.12998/wjcc.v11.i25.5840

Figure 3 Important molecular functions of endothelial cells and the link between obesity-induced inflammation and endothelial dysfunction[74]. MMP2: Matrix metalloproteinase 2; PGI2: Prostacyclin; IGF-1: Insulin-like growth factor-1;ROS: Reactive oxygen species; FGF: Fibroblast growth factor; tPA: Tissue plasminogen activator; TFPI: Tissue factor pathway inhibitor; EGF: Epidermal growth factor; TGF-β: Transforming growth factor-β; PDGF: Platelet-derived growth factor; VCAM: Vascular cell adhesion molecule; ICAM: Intercellular adhesion molecule; ET-1: Endothelin-1; PAF: Platelet activating factor; vWF: von Willebrand factor; TXA2: Thromboxane A2; NO: Nitric oxide.

1/2 (ERK1/2) with impaired mitogenic pathways[81].

Studies on insulin-resistant PCOS have also confirmed that PCOS-IR is independent of the proximal insulin signaling cascade[82]. Recent studies highlight defects in insulin receptor downstream signaling comprising activation of phosphorylated IRS-1 through protein kinase C or GLUT-4 translocation *via* PI3K/Akt that cause IR in PCOS[83]. Serum levels of several IR induced obesity associated proinflammatory molecules such as TNF, C-reactive protein, MCP-1, and IL-18 were found to be elevated in women with PCOS[84]. Recent research to uncover the effects of IR-induced hyperandrogenemia (HA) associated with PCOS was tested in endometrial organoids. It was reported that excess androgen promotes endometrial cell proliferation which is seen in endometrial disorders associated with PCOS[85].

miRNAs in PCOS

Identification of novel miRNAs in PCOS has highlighted the extent of cross-talk with IR. Cross-sectional expression studies in the last decade have identified several miRNAs that are associated with PCOS-IR and non-insulin resistant PCOS. An elevated serum level of miR-222 was reported in PCOS, which is positively correlated with serum insulin and associated with T2DM[25,86]. Additionally, miR-146a and miR-30 were identified and implicated in PCOS *via* insulin-related signaling pathways[87]. Significantly reduced serum level of miR-24 was identified in both PCOS and T2DM, which was also found to downregulate insulin production. Downregulation of miR-29a was found associated with PCOS, which targets IRS-1, StAR-related lipid transfer protein 3, and androgen receptor that are key regulators of insulin signaling and ovarian steroidogenesis, respectively[88,89]. Significantly higher expression of miR-32, miR-34c, miR-135a, miR18b, and miR-9 in ovarian follicular fluid was identified among PCOS patients compared to healthy controls. Target genes of these miRNAs, namely, Synaptotagmin 1 and *IRS-2,* are directly implicated in carbohydrate metabolism and insulin response[90]. Overexpression of miR-145 inhibits IRS-1 expression, which ultimately inhibits MAKP/ERK signaling pathways in ovarian granulose cells. Elevated insulin level suppresses miR-145, upregulates IRS-1, and promotes cell proliferation. miR-145 is considered a novel and promising molecular target for improving granulose cell dysfunction in PCOS-IR patients[91]. Figure 4 depicts the involvement of clinically relevant miRNAs regulating insulin signaling pathways implicated in PCOS.

Microbiota in PCOS

The role of gut microbiota in regulating metabolism and endocrine function is well illustrated. The early hypothesis stated the possible cause-effect axis between dysbiosis of gut microflora and PCOS, considering that high-fat diet induced leaky gut allows systemic circulation of lipopolysaccharide which induces IR/hyperinsulinemia and promotes the synthesis of testosterone that dysregulates follicular development implicated in PCOS[92]. A triad of HA, IR, and inflammation connects PCOS with the gut microbiota. The vicious cycle of IR-induced HA leads to decreased production of sex hormone-binding globulin and promotes ovarian follicular maturation and ovulation disorder. Prenatal exposure to excess androgen was found to influence gut microbial dysbiosis that affects the production of short-chain fatty acids such as acetate, butyrate, and propionate. An *in vivo* study on rats with prenatal androgen identified a higher relative abundance of *Nocardiaceae* and *Clostridiaceae* that are associated with steroid hormone synthesis, and a lower abundance

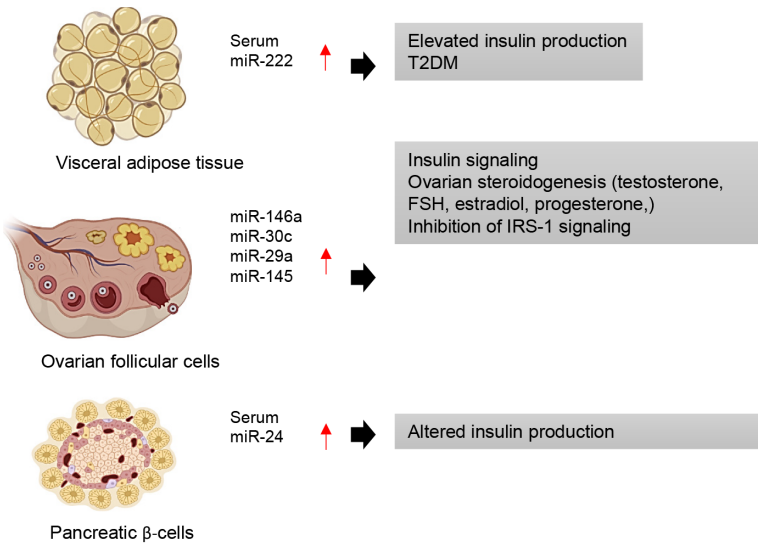

DOI: 10.12998/wjcc.v11.i25.5840

Figure 4 Schematic diagram summarizing the involvement of clinically relevant microRNAs expressed in major tissues in regulating insulin signaling pathways implicated in polycystic ovary syndrome. T2DM: Type 2 diabetes mellitus; FSH: Follicle-stimulating hormone; IRS: Insulin receptor substrate.

of *Akkermansia*, *Bacteroides*, *Lactobacillus*, and *Clostridium* that are known to lower the systemic inflammation[93]. A recent study by Zeng *et al*[94] reported that the abundance of *Prevotellaceae* significantly decreases in PCOS-IR patients, which is negatively correlated with IR, sex hormones, and inflammation. Gut microbial dysbiosis was reported most dramatically among PCOS-IR groups. A better understanding of gut microfloral association with IR and PCOS paved the path for developing novel treatment and disease management approaches for PCOS[95].

INSULIN AND NEURONAL DISORDERS

The majority of insulin in the brain is transported through blood circulation after its synthesis in the pancreas[96]. However, studies also suggest synthesis of insulin from neurons[97]. Further, neurons and glial cells also express insulin receptors, which facilitate the insulin signaling in the brain essential for various crucial functions including metabolic activity and cognition[98,99]. In humans with type 1 and type 2 diabetes, reduction in size of the hippocampus and altered functional connectivity between different brain regions have been reported, followed by a higher risk of behavioural changes and accelerated cognitive decline with the aging process[100,101]. Neuron-specific insulin receptor knockout (NIRKO) mice were observed to show the absolute loss of insulin linked PI3K activation and neuronal apoptosis inhibition. NIRKO mice also showed reduced phosphorylation of Akt and glycogen synthase kinase 3 beta (GSK3β) and increased tau protein phosphorylation[102]. Insulin is shown to cause an increase in activity of dopamine neurons, regulate transmission of N-methyl-D-aspartate receptors in hippocampal neurons, and contribute to the development of long-term hippocampal potentiation[103]. Insulin also regulates α-amino-3-hydroxy-5-methyl-4-isoxazolepropionic acid (AMPA) receptor activity and plays an essential role in insulin-induced long-term depression, indicating importance of insulin in memory flexibility and consolidation[98]. Insulin receptors are also known to regulate GABA receptor activity, structural plasticity of the brain, and postsynaptic density protein 95 expression, which is essential for the postsynaptic junction formation, indicating the impact of insulin on synaptic plasticity and behavior[104-106].

Direct infusion of insulin to the cerebral ventricles is reported to cause increased production of brain derived neurotrophic factor and hippocampal neurogenesis in rodent models[107]. In another study, improvement in mood assessments and self-confidence and word-recall memory scores in healthy human subjects treated with intranasally delivered insulin was reported[108]. IR was observed in various instances of neurodegenerative diseases[109] and neurotrauma[110,111]. In Alzheimer disease (AD) patients, glucose uptake markedly decreases, and cerebral IR and glucose metabolism were also reported to be impaired[112]. The PI3K/AKT pathway, a major branch of insulin pathway that is also known to be a major contributor to IR, was downregulated in AD[65,113]. Further, abnormal serine phosphorylation of IRS1, a homeostatic regulator of PI3K signaling, gets localized with neurofibrillary tangles and hinders the actions of insulin[114]. Downregulation of the PI3K/AKT pathway leads to alteration in expression of GSK-3β and protein phosphatase 2A, two downstream targets, and causes increase in tau phosphorylation and neurofibrillary tangle formation[115]. Deficiency of insulin in the brain also induces hyperphosphorylation of c-Jun N-terminal kinases, neurofilament, and tau followed by cellular ultra-structural damage, which further induces cognitive and learning disabilities.

Insulin causes enhanced excitability of cholinergic interneurons, which activate nicotinic acetylcholine receptors leading to dopamine release in the brain followed by its uptake *via* the PI3K pathway[116]. In Parkinson's disease (PD)

also, the PI3K/Akt pathway gets altered with GSK-3β overexpression, leading to increased neurofibrillary tangle formation contributing to PD dementia[117]. T2DM mouse models are reported to show more expression of α-synuclein and are more susceptible to toxin-induced dopaminergic loss[118]. Further, genetic PD due to mutation in α-synuclein can also influence insulin sensitivity and inhibit AKT activation[119,120]. Thus, insulin mediated signaling plays an important role in maintaining brain homeostasis.

CANCER AND INSULIN

The association of insulin and cancer is specifically significant to researchers working in areas of coalescent cancer approach. It furnishes a prospective biological foundation for several approaches to cancer therapeutics which consist of exercise, diet, *etc.* This shall also be helpful in discovering the function of stress in cancer instigation and advancement. Moreover, there is rising evidentiary support for obesity and cancer relationship which may ultimately help restore the various contradictions in the context of cancer that usually occur. There have been reports on circulating plasma insulin/insulin-like growth factor (IGF)-1 levels to exhibit specific prognosis of cancer variants in humans[121]. The correlation between cancer instigation and plasma insulin/IGF-1 levels is probably because of a straight reaction of these compounds on tumor cells. The insulin receptor is frequently expressed in cancers, along with other transcription factors in the insulin pathway[122].

Disparate human trials are under way for the investigation of the influence of the decrease in insulin levels in humans suffering from cancer. These are basically established on various other preclinical reports exhibiting a substantial impression of insulin in instigating cell proliferation *in vitro* and *in vivo*[123]. At present, approximately 12 trials on the effect of metformin with regard to decrease in cancer growth are ongoing[124]. Metformin is basically an inhibitor of hepatic gluconeogenesis instead of being related to insulin[125].

There are several pathways *via* which IR may influence the malignant condition. Cancer is a sequential phenomenon showing acquired genetic variations steering the step-by-step conversion, from typical usual cells to precancerous to malignant[126]. Insulin may augment the anabolic condition which is mandatory for growth of cells, in turn enabling continued presence of substrates which include amino acids and glucose.

Breast cancer

Insulin is an influential hormone that instigates various mechanisms associated with breast cancer biology. A greater number of reports have concentrated on scrutinizing the prospective connections between body mass index (BMI) and breast cancers. In recent times, there are documentations regarding the assessment of the possible relation between variables of metabolic health like insulin and HbA1c. An association between T2DM and cancers including breast cancer has been reported by the American Diabetes Association and the American Cancer Society[127]. In humans with breast cancer, diabetes is linked with a high fatality hazard ratio of 1.41 (95% confidence interval: 1.28-1.55)[128]. These reports in post-menopausal women furnish support that metabolic disturbances, rather than BMI, may be a better indicator of breast cancer risk. However, more investigations are the need of the hour as there is a dearth of information regarding the possible link between metabolic discrepancies, insulin, and breast cancer risk in post-menopausal women. In spite of diabetes/IR and breast cancer being two separate diseases, insulin signaling plays major role in both ailments. Insulin promotes cancer associated activities which consist of tissue inflammation, angiogenesis, and motility[129]. Very few reports are available regarding the influence of adjuvant chemotherapy or aromatase inhibitors on glucose and insulin physiology in women suffering from breast cancer[130].

Lung cancer

Lung cancer, one of the most common cancers, is highly invasive, metastatically active, and resistant to drugs[131,132]. Non-small cell lung cancer (NSCLC) is the most frequently occurring lung cancer type constituting about 85% of all lung cancer cases[133]. The IGF-1 signaling pathway has been insinuated in lung cancer cases that helps in defiance towards therapeutic interventions[134]. IGF-1 ligand and IGF-1 receptor (IGF-1R) expression is enhanced in NSCLC, and increased IGF-1R level is related with decreased survival in skin squamous cell carcinoma patients[135]. NSCLC individuals have high levels of both IGF-1R and epidermal growth factor receptor (EGFR) with decreased relapse-free survival and overall survival[136,137]. Occurrence of separate expression levels for IRS-1 and IRS-2 in adenocarcinoma and squamous cell carcinoma hints towards involvement of IRS-1 and IRS-2 in NSCLC biology[138]. IGF binding proteins (IGFBPs) are proteins that regulate the IGF pathway by sequestering the IGFs and ultimately modulating the mitogenic effect of IGF receptors[139]. The traditional IGFBP family has six members (IGFBP1-6), which attach IGFs with increased affinity[140], although the notion of IGFBPs has lately been reconceptualised and finally more proteins have been added that enhance half-life of IGFs. Now at least ten members of the IGFBP superfamily have been recognized, which also include the proteins that bind IGFs with low affinity[141]. Currently, typically IGFBPs have enticed enhanced awareness because of their function in NSCLC. Prior reports have exhibited abnormal expression of IGFBPs in NSCLC[142]. The threat of tumor proliferation and metastasis in NSCLC is greatly enhanced by the rise in the levels of IGF1 and IGF2, elevation in IGF-1R, and impairment of transcription factors concerned with PI3K/Akt and MAPK cascades[143]. The molecular association of hyperinsulinemia/hyperglycaemia and cancer is depicted in Figure 5.

Prostate cancer

Metabolic disorders such as obesity[144,145] and hyperinsulinemia[146] are related with prostate cancer risk. Lifestyle parameters like excess energy consumption[147] and physical inactivity[148,149] are usually linked with prostate cancer

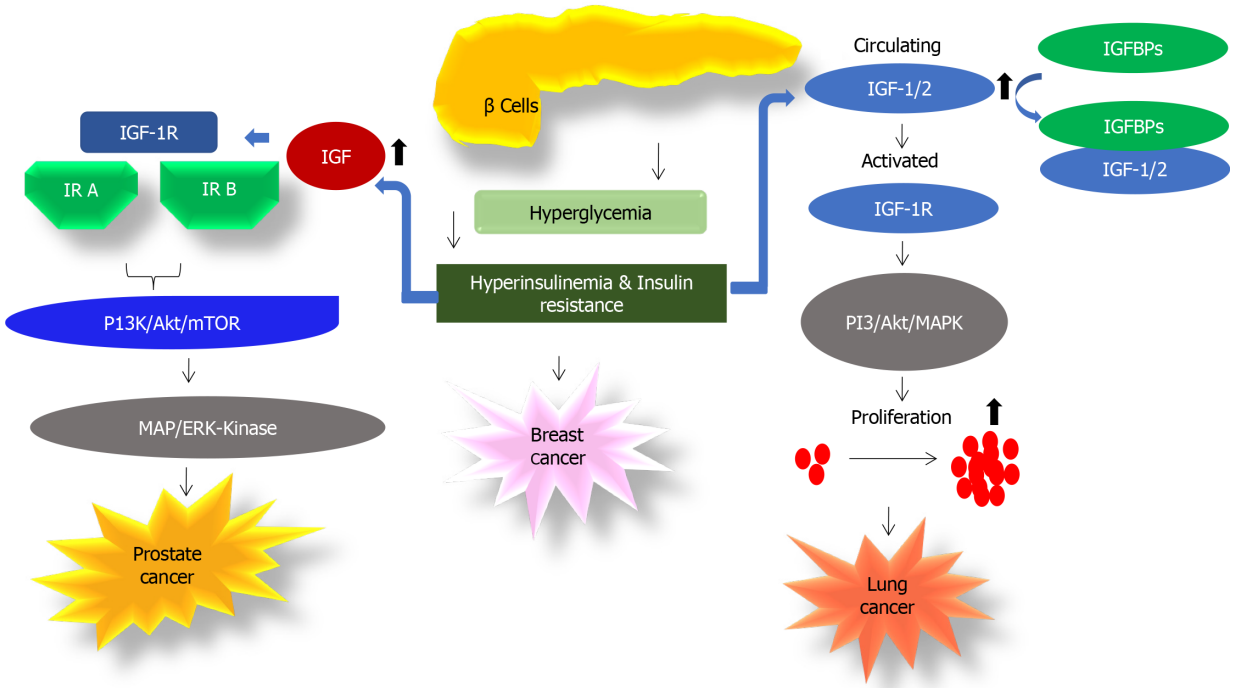

DOI: 10.12998/wjcc.v11.i25.5840

Figure 5 Molecular association of hyperinsulinemia/hyperglycaemia and cancer. Increased insulin-like growth factor (IGF) due to hyperinsulinemia increases IGF-1R activation which in turn activates downstream signaling and causes prostate cancer[135]. Hyperinsulinemia, hyperglycemia, and insulin resistance may lead to breast cancer[129]. Increased insulin in diabetic patients increases IGF-1/IGF-2 circulating levels which interact with IGF-1R present on lung cells. Thus, the activation of the receptor and thereby activated downstream signaling increase carcinogenesis in lung cells. Most of the IGF binding proteins are known to bind circulating IGF-1/IGF-2 and thereby interrupt their interaction with IGF-1R[133,137]. IGF: Insulin-like growth factor; IGFBPs: Insulin-like growth factor binding proteins; PI3K: Phosphatidylinositol-3-kinase; mTOR: Mammalian target of rapamycin; MAP: Mitogen-activated protein; ERK: Extracellular signal-regulated kinase; MAPK: Mitogen-activated protein kinase; IR: Insulin receptor.

that finds linkage with metabolic dysfunction leading to IR, pro-inflammation, and hormonal fluctuations[150]. Insulin acts *via* a tyrosine kinase receptor (insulin receptor), which is present in two isoforms, insulin receptor-A and insulin receptor-B. Instigation of the insulin receptor further triggers P13K/Akt/mTOR mechanism and MAP/ERK-kinase cascade, leading to cell proliferation and metastasis[151]. Hence, enhanced levels of insulin linked with IR, banded together with augmented level of insulin receptors in prostate cancers, suggest that insulin is an important supporter of prostate cancer progression. IGF-1 attaches to both the IGF-1R and insulin receptor to further propagate mitogenic signaling processes that enhance cell proliferation and reduce apoptosis[134]. Both IGF-1R and insulin receptor are elevated in prostate cancer tissues[152] and combating forces attacking the IGF-1R/insulin receptor mechanism are under process[153,154]. A rising number of reports hint towards the fact that the IGF/insulin mechanism may be significant to the transmembrane protease serine 2: ETS transcription factor gene fusion, which is known to be the most frequently occurring somatic process in primary prostate cancer[155,156].

CONCLUSION

Insulin, a small protein with 51 amino acids produced by pancreatic β-cells, plays an important role in metabolism. It is essential for maintaining glucose homeostasis at biochemical and molecular levels under varied physiological conditions. Insulin mediated altered glucose homeostasis has been associated with several pathophysiological ailments such as diabetes, insulinomas, PCOS, neuronal disorders, and cancer. T1DM, T2DM, and GDM are the important patho-physiological conditions primarily associated with the insulin disorder. Insulinomas are a rare neuroendocrine tumor originating from pancreatic beta-cells and represent 2% of all pancreatic neoplasms. Obesity, IR, hypertension, and dyslipidemia are just a few of the cardiometabolic risk factors that can lead to MS and raise chance of atherosclerotic CVD. IR is a main underlying mechanism for MS. One of the most prevalent metabolic disorders in women of childbearing age is PCOS. It is classified as an endocrine disorder due to the direct involvement of the hypothalamic-ovarian axis with IR as the primary pathological factor. IR in PCOS has been linked to impaired downstream metabolic insulin signaling. Recent evidence from clinical, pathological, *ex vivo*, and *in vivo* studies has implicated aberrations in insulin signaling-associated pathways in PCOS. IR is observed in various instances of neurodegenerative diseases and neurotrauma, causing abnormal serine phosphorylation of IRS1 and neurofibrillary tangles and hindering the actions of insulin. Insulin also regulates AMPA receptor activity and plays an essential role in insulin-induced long-term depression. Circulating plasma insulin/IGF-1 levels are associated with specific prognosis of cancer variants in humans. Further, human trials are under way to investigate the relationship between insulin and cancer for devising strategies to

alleviate human suffering from cancer.

ACKNOWLEDGEMENTS

Shashank Kumar acknowledges DST-FIST, India and Central University of Punjab, India, for providing Departmental Grant to Department of Biochemistry, Central University of Punjab, Bathinda, India. Sabyasachi Senapati acknowledges DST-FIST support to Department of Human Genetics and Molecular Medicine, Central University of Punjab. Neetu Bhattacharya acknowledges support from Dyal Singh College, University of Delhi. Amit Bhattacharya acknowledges support from Ramjas College, University of Delhi. Shashank Kumar Maurya acknowledges financial support from the Institute of Eminence, University of Delhi, Delhi. Hadiya Husain acknowledges DST-FIST, DST-PURSE and UGC-SAP India for providing Departmental Grant to Department of Zoology, University of Lucknow, Lucknow, India. Abhay Kumar Pandey acknowledges DST-FIST and UGC-SAP facilities of the Department of Biochemistry, University of Allahabad, Prayagraj, India.

FOOTNOTES

Author contributions: Kumar S, Senapati S, Bhattacharya N, Bhattacharya A, Maurya SK, Husain H, and Bhatti JS performed the literature search; Kumar S, Senapati S, Bhattacharya N, Bhattacharya A, Maurya SK, and Husain H wrote the first draft of the manuscript and validated the references; Pandey AK and Kumar S conceptualized the idea and critically reviewed and revised the manuscript; and all authors have read and approved the final manuscript.

Conflict-of-interest statement: All the authors report no relevant conflicts of interest for this article.

Country/Territory of origin: India

ORCID number: Shashank Kumar 0000-0002-9622-0512; Sabyasachi Senapati 0000-0002-9448-7432; Jasvinder Singh Bhatti 0000-0001-5480-2584; Abhay Kumar Pandey 0000-0002-4774-3085.

S-Editor: Wang JJ
L-Editor: Wang TQ
P-Editor: Zhao S

REFERENCES

1 **Poitout V**, Hagman D, Stein R, Artner I, Robertson RP, Harmon JS. Regulation of the insulin gene by glucose and fatty acids. *J Nutr* 2006; **136**: 873-876 [PMID: 16549443 DOI: 10.1093/jn/136.4.873]
2 **Vander Mierde D**, Scheuner D, Quintens R, Patel R, Song B, Tsukamoto K, Beullens M, Kaufman RJ, Bollen M, Schuit FC. Glucose activates a protein phosphatase-1-mediated signaling pathway to enhance overall translation in pancreatic beta-cells. *Endocrinology* 2007; **148**: 609-617 [PMID: 17082262 DOI: 10.1210/en.2006-1012]
3 **Ganguly R**, Singh SV, Jaiswal K, Kumar R, Pandey AK. Modulatory effect of caffeic acid in alleviating diabetes and associated complications. *World J Diabetes* 2023; **14**: 62-75 [PMID: 36926656 DOI: 10.4239/wjd.v14.i2.62]
4 **Suckale J**, Solimena M. Pancreas islets in metabolic signaling--focus on the beta-cell. *Front Biosci* 2008; **13**: 7156-7171 [PMID: 18508724 DOI: 10.2741/3218]
5 **Chang TW**, Goldberg AL. The metabolic fates of amino acids and the formation of glutamine in skeletal muscle. *J Biol Chem* 1978; **253**: 3685-3693 [PMID: 649596]
6 **Kumar R**, Gupta A, Singh AK, Bishayee A, Pandey AK. The Antioxidant and Antihyperglycemic Activities of Bottlebrush Plant (Callistemon lanceolatus) Stem Extracts. *Medicines (Basel)* 2020; **7** [PMID: 32143382 DOI: 10.3390/medicines7030011]
7 **American Diabetes Association**. (2) Classification and diagnosis of diabetes. *Diabetes Care* 2015; **38** Suppl: S8-S16 [PMID: 25537714 DOI: 10.2337/dc15-S005]
8 **Katsarou A**, Gudbjörnsdottir S, Rawshani A, Dabelea D, Bonifacio E, Anderson BJ, Jacobsen LM, Schatz DA, Lernmark Å. Type 1 diabetes mellitus. *Nat Rev Dis Primers* 2017; **3**: 17016 [PMID: 28358037 DOI: 10.1038/nrdp.2017.16]
9 **Insel RA**, Dunne JL, Atkinson MA, Chiang JL, Dabelea D, Gottlieb PA, Greenbaum CJ, Herold KC, Krischer JP, Lernmark Å, Ratner RE, Rewers MJ, Schatz DA, Skyler JS, Sosenko JM, Ziegler AG. Staging presymptomatic type 1 diabetes: a scientific statement of JDRF, the Endocrine Society, and the American Diabetes Association. *Diabetes Care* 2015; **38**: 1964-1974 [PMID: 26404926 DOI: 10.2337/dc15-1419]
10 **Krischer JP**, Lynch KF, Schatz DA, Ilonen J, Lernmark Å, Hagopian WA, Rewers MJ, She JX, Simell OG, Toppari J, Ziegler AG, Akolkar B, Bonifacio E; TEDDY Study Group. The 6 year incidence of diabetes-associated autoantibodies in genetically at-risk children: the TEDDY study. *Diabetologia* 2015; **58**: 980-987 [PMID: 25660258 DOI: 10.1007/s00125-015-3514-y]
11 **Gupta A**, Kumar R, Pandey AK. Antioxidant and antidiabetic activities of Terminalia bellirica fruit in alloxan induced diabetic rats. *South Afr*

J Bot 2020; **130**: 308-315 [DOI: 10.1016/j.sajb.2019.12.010]
12 **Gerstein HC**, Santaguida P, Raina P, Morrison KM, Balion C, Hunt D, Yazdi H, Booker L. Annual incidence and relative risk of diabetes in people with various categories of dysglycemia: a systematic overview and meta-analysis of prospective studies. *Diabetes Res Clin Pract* 2007; **78**: 305-312 [PMID: 17601626 DOI: 10.1016/j.diabres.2007.05.004]
13 **Ferrannini E**, Mari A. β-Cell function in type 2 diabetes. *Metabolism* 2014; **63**: 1217-1227 [PMID: 25070616 DOI: 10.1016/j.metabol.2014.05.012]
14 **DeFronzo RA**, Ferrannini E, Groop L, Henry RR, Herman WH, Holst JJ, Hu FB, Kahn CR, Raz I, Shulman GI, Simonson DC, Testa MA, Weiss R. Type 2 diabetes mellitus. *Nat Rev Dis Primers* 2015; **1**: 15019 [PMID: 27189025 DOI: 10.1038/nrdp.2015.19]
15 **Marchetti P**, Masini M. Autophagy and the pancreatic beta-cell in human type 2 diabetes. *Autophagy* 2009; **5**: 1055-1056 [PMID: 19657235 DOI: 10.4161/auto.5.7.9511]
16 **McIntyre HD**, Catalano P, Zhang C, Desoye G, Mathiesen ER, Damm P. Gestational diabetes mellitus. *Nat Rev Dis Primers* 2019; **5**: 47 [PMID: 31296866 DOI: 10.1038/s41572-019-0098-8]
17 **Catalano PM**, Tyzbir ED, Sims EA. Incidence and significance of islet cell antibodies in women with previous gestational diabetes. *Diabetes Care* 1990; **13**: 478-482 [PMID: 2190774 DOI: 10.2337/diacare.13.5.478]
18 **Ellard S**, Bellanné-Chantelot C, Hattersley AT; European Molecular Genetics Quality Network (EMQN) MODY group. Best practice guidelines for the molecular genetic diagnosis of maturity-onset diabetes of the young. *Diabetologia* 2008; **51**: 546-553 [PMID: 18297260 DOI: 10.1007/s00125-008-0942-y]
19 **Hattersley AT**, Beards F, Ballantyne E, Appleton M, Harvey R, Ellard S. Mutations in the glucokinase gene of the fetus result in reduced birth weight. *Nat Genet* 1998; **19**: 268-270 [PMID: 9662401 DOI: 10.1038/953]
20 **Buchanan TA**. Pancreatic B-cell defects in gestational diabetes: implications for the pathogenesis and prevention of type 2 diabetes. *J Clin Endocrinol Metab* 2001; **86**: 989-993 [PMID: 11238474 DOI: 10.1210/jcem.86.3.7339]
21 **Ramzan F**, Vickers MH, Mithen RF. Epigenetics, microRNA and Metabolic Syndrome: A Comprehensive Review. *Int J Mol Sci* 2021; **22** [PMID: 34068765 DOI: 10.3390/ijms22095047]
22 **Inagaki T**, Tachibana M, Magoori K, Kudo H, Tanaka T, Okamura M, Naito M, Kodama T, Shinkai Y, Sakai J. Obesity and metabolic syndrome in histone demethylase JHDM2a-deficient mice. *Genes Cells* 2009; **14**: 991-1001 [PMID: 19624751 DOI: 10.1111/j.1365-2443.2009.01326.x]
23 **Singh AK**, Bishayee A, Pandey AK. Targeting Histone Deacetylases with Natural and Synthetic Agents: An Emerging Anticancer Strategy. *Nutrients* 2018; **10** [PMID: 29882797 DOI: 10.3390/nu10060731]
24 **Wang X**, Chang X, Li J, Yin L, Sun K. DNA methylation of microRNA-375 in impaired glucose tolerance. *Exp Ther Med* 2014; **8**: 775-780 [PMID: 25120598 DOI: 10.3892/etm.2014.1816]
25 **Kumar S**, Pandey AK. Oxidative Stress-Related MicroRNAs as Diagnostic Markers: A Newer Insight in Diagnostics. In: Maurya P, Chandra P. Oxidative Stress: Diagnostic Methods and Applications in Medical Science. *Singapore: Springer* 2017; 113-125
26 **Juaid N**, Amin A, Abdalla A, Reese K, Alamri Z, Moulay M, Abdu S, Miled N. Anti-Hepatocellular Carcinoma Biomolecules: Molecular Targets Insights. *Int J Mol Sci* 2021; **22** [PMID: 34639131 DOI: 10.3390/ijms221910774]
27 **Mishra V**, Nayak P, Sharma M, Albutti A, Alwashmi ASS, Aljasir MA, Alsowayeh N, Tambuwala MM. Emerging Treatment Strategies for Diabetes Mellitus and Associated Complications: An Update. *Pharmaceutics* 2021; **13** [PMID: 34683861 DOI: 10.3390/pharmaceutics13101568]
28 **Moldow RE**, Connelly RR. Epidemiology of pancreatic cancer in Connecticut. *Gastroenterology* 1968; **55**: 677-686 [PMID: 4302500]
29 **Service FJ**, McMahon MM, O'Brien PC, Ballard DJ. Functioning insulinoma--incidence, recurrence, and long-term survival of patients: a 60-year study. *Mayo Clin Proc* 1991; **66**: 711-719 [PMID: 1677058 DOI: 10.1016/S0025-6196(12)62083-7]
30 **Oberg K**, Eriksson B. Endocrine tumours of the pancreas. *Best Pract Res Clin Gastroenterol* 2005; **19**: 753-781 [PMID: 16253899 DOI: 10.1016/j.bpg.2005.06.002]
31 **Mittendorf EA**, Liu YC, McHenry CR. Giant insulinoma: case report and review of the literature. *J Clin Endocrinol Metab* 2005; **90**: 575-580 [PMID: 15522939 DOI: 10.1210/jc.2004-0825]
32 **Chang SM**, Yan ST, Wei CK, Lin CW, Tseng CE. Solitary concomitant endocrine tumor and ductal adenocarcinoma of pancreas. *World J Gastroenterol* 2010; **16**: 2692-2697 [PMID: 20518094 DOI: 10.3748/wjg.v16.i21.2692]
33 **Brown E**, Watkin D, Evans J, Yip V, Cuthbertson DJ. Multidisciplinary management of refractory insulinomas. *Clin Endocrinol (Oxf)* 2018; **88**: 615-624 [PMID: 29205458 DOI: 10.1111/cen.13528]
34 **Pasaoglu E**, Dursun N, Ozyalvacli G, Hacihasanoglu E, Behzatoglu K, Calay O. Comparison of World Health Organization 2000/2004 and World Health Organization 2010 classifications for gastrointestinal and pancreatic neuroendocrine tumors. *Ann Diagn Pathol* 2015; **19**: 81-87 [PMID: 25702616 DOI: 10.1016/j.anndiagpath.2015.01.001]
35 **Langerhans P**. Ueber die Nerven der menschlichen Haut. *Archiv f pathol Anat* 1868; **44**: 325-337 [DOI: 10.1007/BF01959006]
36 **Mathur A**, Gorden P, Libutti SK. Insulinoma. *Surg Clin North Am* 2009; **89**: 1105-1121 [PMID: 19836487 DOI: 10.1016/j.suc.2009.06.009]
37 **Whipple AO**, Frantz VK. Adenoma of islet cells with hyperinsulinism: A review. *Ann Surg* 1935; **101**: 1299-1335 [PMID: 17856569 DOI: 10.1097/00000658-193506000-00001]
38 **Nikfarjam M**, Warshaw AL, Axelrod L, Deshpande V, Thayer SP, Ferrone CR, Fernández-del Castillo C. Improved contemporary surgical management of insulinomas: a 25-year experience at the Massachusetts General Hospital. *Ann Surg* 2008; **247**: 165-172 [PMID: 18156937 DOI: 10.1097/SLA.0b013e31815792ed]
39 **Giannis D**, Moris D, Karachaliou GS, Tsilimigras DI, Karaolanis G, Papalampros A, Felekouras E. Insulinomas: from diagnosis to treatment. A review of the literature. *J BUON* 2020; **25**: 1302-1314 [PMID: 32862570]
40 **Louda F**, Chadli A, Elaziz S, Elghomari H, Farouqi A. Malignant insulinoma misdiagnosed and treated as epilepsy. *Ann Endocrinol (Paris)* 2013; **74**: 53-55 [PMID: 23351560 DOI: 10.1016/j.ando.2012.11.002]
41 **Jaladyan V**, Darbinyan V. Insulinoma misdiagnosed as juvenile myoclonic epilepsy. *Eur J Pediatr* 2007; **166**: 485-487 [PMID: 17123109 DOI: 10.1007/s00431-006-0365-z]
42 **Service FJ**, Natt N. The prolonged fast. *J Clin Endocrinol Metab* 2000; **85**: 3973-3974 [PMID: 11095416 DOI: 10.1210/jcem.85.11.6934]
43 **Abboud B**, Boujaoude J. Occult sporadic insulinoma: localization and surgical strategy. *World J Gastroenterol* 2008; **14**: 657-665 [PMID: 18205253 DOI: 10.3748/wjg.14.657]
44 **de Herder WW**, Hofland J. Insulinoma. 2023 Apr 4. In: Endotext [Internet]. South Dartmouth (MA): MDText.com, Inc.; 2000– [PMID:

25905215]
45 **Larsson C**, Skogseid B, Oberg K, Nakamura Y, Nordenskjöld M. Multiple endocrine neoplasia type 1 gene maps to chromosome 11 and is lost in insulinoma. *Nature* 1988; **332**: 85-87 [PMID: 2894610 DOI: 10.1038/332085a0]
46 **Shin JJ**, Gorden P, Libutti SK. Insulinoma: pathophysiology, localization and management. *Future Oncol* 2010; **6**: 229-237 [PMID: 20146582 DOI: 10.2217/fon.09.165]
47 **Ludwig L**, Schleithoff L, Kessler H, Wagner PK, Boehm BO, Karges W. Loss of wild-type MEN1 gene expression in multiple endocrine neoplasia type 1-associated parathyroid adenoma. *Endocr J* 1999; **46**: 539-544 [PMID: 10580746 DOI: 10.1507/endocrj.46.539]
48 **Missiaglia E**, Dalai I, Barbi S, Beghelli S, Falconi M, della Peruta M, Piemonti L, Capurso G, Di Florio A, delle Fave G, Pederzoli P, Croce CM, Scarpa A. Pancreatic endocrine tumors: expression profiling evidences a role for AKT-mTOR pathway. *J Clin Oncol* 2010; **28**: 245-255 [PMID: 19917848 DOI: 10.1200/JCO.2008.21.5988]
49 **Singh AK**, Singh SV, Kumar R, Kumar S, Senapati S, Pandey AK. Current therapeutic modalities and chemopreventive role of natural products in liver cancer: Progress and promise. *World J Hepatol* 2023; **15**: 1-18 [PMID: 36744169 DOI: 10.4254/wjh.v15.i1.1]
50 **Fiebrich HB**, Siemerink EJ, Brouwers AH, Links TP, Remkes WS, Hospers GA, de Vries EG. Everolimus induces rapid plasma glucose normalization in insulinoma patients by effects on tumor as well as normal tissues. *Oncologist* 2011; **16**: 783-787 [PMID: 21482586 DOI: 10.1634/theoncologist.2010-0222]
51 **Raymond E**, Dahan L, Raoul JL, Bang YJ, Borbath I, Lombard-Bohas C, Valle J, Metrakos P, Smith D, Vinik A, Chen JS, Hörsch D, Hammel P, Wiedenmann B, Van Cutsem E, Patyna S, Lu DR, Blanckmeister C, Chao R, Ruszniewski P. Sunitinib malate for the treatment of pancreatic neuroendocrine tumors. *N Engl J Med* 2011; **364**: 501-513 [PMID: 21306237 DOI: 10.1056/NEJMoa1003825]
52 **Swarup S**, Goyal A, Grigorova Y, Zeltser R. Metabolic Syndrome. 2022 Oct 24. In: StatPearls [Internet]. Treasure Island (FL): StatPearls Publishing; 2023 Jan- [PMID: 29083742]
53 **Alberti KG**, Zimmet PZ. Definition, diagnosis and classification of diabetes mellitus and its complications. Part 1: diagnosis and classification of diabetes mellitus provisional report of a WHO consultation. *Diabet Med* 1998; **15**: 539-553 [PMID: 9686693 DOI: 10.1002/(SICI)1096-9136(199807)15:7<539::AID-DIA668>3.0.CO;2-S]
54 **Balkau B**, Charles MA. Comment on the provisional report from the WHO consultation. European Group for the Study of Insulin Resistance (EGIR). *Diabet Med* 1999; **16**: 442-443 [PMID: 10342346 DOI: 10.1046/j.1464-5491.1999.00059.x]
55 **National Cholesterol Education Program (NCEP) Expert Panel on Detection**, Evaluation; and Treatment of High Blood Cholesterol in Adults (Adult Treatment Panel III). Third Report of the National Cholesterol Education Program (NCEP) Expert Panel on Detection, Evaluation, and Treatment of High Blood Cholesterol in Adults (Adult Treatment Panel III) final report. *Circulation* 2002; **106**: 3143-3421 [PMID: 12485966 DOI: 10.1161/circ.106.25.3143]
56 **Huang PL**. A comprehensive definition for metabolic syndrome. *Dis Model Mech* 2009; **2**: 231-237 [PMID: 19407331 DOI: 10.1242/dmm.001180]
57 **Zimmet P**, Magliano D, Matsuzawa Y, Alberti G, Shaw J. The metabolic syndrome: a global public health problem and a new definition. *J Atheroscler Thromb* 2005; **12**: 295-300 [PMID: 16394610 DOI: 10.5551/jat.12.295]
58 **van der Pal KC**, Koopman ADM, Lakerveld J, van der Heijden AA, Elders PJ, Beulens JW, Rutters F. The association between multiple sleep-related characteristics and the metabolic syndrome in the general population: the New Hoorn study. *Sleep Med* 2018; **52**: 51-57 [PMID: 30278295 DOI: 10.1016/j.sleep.2018.07.022]
59 **Smiley A**, King D, Bidulescu A. The Association between Sleep Duration and Metabolic Syndrome: The NHANES 2013/2014. *Nutrients* 2019; **11** [PMID: 31717770 DOI: 10.3390/nu11112582]
60 **Singh AK**, Singla RK, Pandey AK. Chlorogenic Acid: A Dietary Phenolic Acid with Promising Pharmacotherapeutic Potential. *Curr Med Chem* 2023; **30**: 3905-3926 [PMID: 35975861 DOI: 10.2174/0929867329666220816154634]
61 **Hamza AA**, Fikry EM, Abdallah W, Amin A. Mechanistic insights into the augmented effect of bone marrow mesenchymal stem cells and thiazolidinediones in streptozotocin-nicotinamide induced diabetic rats. *Sci Rep* 2018; **8**: 9827 [PMID: 29959408 DOI: 10.1038/s41598-018-28029-1]
62 **Shuster A**, Patlas M, Pinthus JH, Mourtzakis M. The clinical importance of visceral adiposity: a critical review of methods for visceral adipose tissue analysis. *Br J Radiol* 2012; **85**: 1-10 [PMID: 21937614 DOI: 10.1259/bjr/38447238]
63 **Björntorp P**. Metabolic implications of body fat distribution. *Diabetes Care* 1991; **14**: 1132-1143 [PMID: 1773700 DOI: 10.2337/diacare.14.12.1132]
64 **Björntorp P**. Visceral obesity: a "civilization syndrome". *Obes Res* 1993; **1**: 206-222 [PMID: 16350574 DOI: 10.1002/j.1550-8528.1993.tb00614.x]
65 **Joshi T**, Singh AK, Haratipour P, Sah AN, Pandey AK, Naseri R, Juyal V, Farzaei MH. Targeting AMPK signaling pathway by natural products for treatment of diabetes mellitus and its complications. *J Cell Physiol* 2019; **234**: 17212-17231 [PMID: 30916407 DOI: 10.1002/jcp.28528]
66 **Golbidi S**, Mesdaghinia A, Laher I. Exercise in the metabolic syndrome. *Oxid Med Cell Longev* 2012; **2012**: 349710 [PMID: 22829955 DOI: 10.1155/2012/349710]
67 **Achari AE**, Jain SK. Adiponectin, a Therapeutic Target for Obesity, Diabetes, and Endothelial Dysfunction. *Int J Mol Sci* 2017; **18** [PMID: 28635626 DOI: 10.3390/ijms18061321]
68 **Paley CA**, Johnson MI. Abdominal obesity and metabolic syndrome: exercise as medicine? *BMC Sports Sci Med Rehabil* 2018; **10**: 7 [PMID: 29755739 DOI: 10.1186/s13102-018-0097-1]
69 **Deepa SS**, Dong LQ. APPL1: role in adiponectin signaling and beyond. *Am J Physiol Endocrinol Metab* 2009; **296**: E22-E36 [PMID: 18854421 DOI: 10.1152/ajpendo.90731.2008]
70 **Pischon T**, Hu FB, Rexrode KM, Girman CJ, Manson JE, Rimm EB. Inflammation, the metabolic syndrome, and risk of coronary heart disease in women and men. *Atherosclerosis* 2008; **197**: 392-399 [PMID: 17681508 DOI: 10.1016/j.atherosclerosis.2007.06.022]
71 **Farzaei MH**, Singh AK, Kumar R, Croley CR, Pandey AK, Coy-Barrera E, Kumar Patra J, Das G, Kerry RG, Annunziata G, Tenore GC, Khan H, Micucci M, Budriesi R, Momtaz S, Nabavi SM, Bishayee A. Targeting Inflammation by Flavonoids: Novel Therapeutic Strategy for Metabolic Disorders. *Int J Mol Sci* 2019; **20** [PMID: 31597283 DOI: 10.3390/ijms20194957]
72 **Ganguly R**, Gupta A, Pandey AK. Role of baicalin as a potential therapeutic agent in hepatobiliary and gastrointestinal disorders: A review. *World J Gastroenterol* 2022; **28**: 3047-3062 [PMID: 36051349 DOI: 10.3748/wjg.v28.i26.3047]
73 **Dhananjayan R**, Koundinya KS, Malati T, Kutala VK. Endothelial Dysfunction in Type 2 Diabetes Mellitus. *Indian J Clin Biochem* 2016; **31**: 372-379 [PMID: 27605734 DOI: 10.1007/s12291-015-0516-y]

74 **Kwaifa IK**, Bahari H, Yong YK, Noor SM. Endothelial Dysfunction in Obesity-Induced Inflammation: Molecular Mechanisms and Clinical Implications. *Biomolecules* 2020; **10** [PMID: 32069832 DOI: 10.3390/biom10020291]

75 **Moghetti P**, Tosi F. Insulin resistance and PCOS: chicken or egg? *J Endocrinol Invest* 2021; **44**: 233-244 [PMID: 32648001 DOI: 10.1007/s40618-020-01351-0]

76 **Armanini D**, Boscaro M, Bordin L, Sabbadin C. Controversies in the Pathogenesis, Diagnosis and Treatment of PCOS: Focus on Insulin Resistance, Inflammation, and Hyperandrogenism. *Int J Mol Sci* 2022; **23** [PMID: 35456928 DOI: 10.3390/ijms23084110]

77 **Khan MJ**, Ullah A, Basit S. Genetic Basis of Polycystic Ovary Syndrome (PCOS): Current Perspectives. *Appl Clin Genet* 2019; **12**: 249-260 [PMID: 31920361 DOI: 10.2147/TACG.S200341]

78 **Dahan MH**, Reaven G. Relationship among obesity, insulin resistance, and hyperinsulinemia in the polycystic ovary syndrome. *Endocrine* 2019; **64**: 685-689 [PMID: 30900204 DOI: 10.1007/s12020-019-01899-9]

79 **Dunaif A**, Xia J, Book CB, Schenker E, Tang Z. Excessive insulin receptor serine phosphorylation in cultured fibroblasts and in skeletal muscle. A potential mechanism for insulin resistance in the polycystic ovary syndrome. *J Clin Invest* 1995; **96**: 801-810 [PMID: 7635975 DOI: 10.1172/JCI118126]

80 **Diamanti-Kandarakis E**, Dunaif A. Insulin resistance and the polycystic ovary syndrome revisited: an update on mechanisms and implications. *Endocr Rev* 2012; **33**: 981-1030 [PMID: 23065822 DOI: 10.1210/er.2011-1034]

81 **Nelson-Degrave VL**, Wickenheisser JK, Hendricks KL, Asano T, Fujishiro M, Legro RS, Kimball SR, Strauss JF 3rd, McAllister JM. Alterations in mitogen-activated protein kinase kinase and extracellular regulated kinase signaling in theca cells contribute to excessive androgen production in polycystic ovary syndrome. *Mol Endocrinol* 2005; **19**: 379-390 [PMID: 15514033 DOI: 10.1210/me.2004-0178]

82 **Hansen SL**, Svendsen PF, Jeppesen JF, Hoeg LD, Andersen NR, Kristensen JM, Nilas L, Lundsgaard AM, Wojtaszewski JFP, Madsbad S, Kiens B. Molecular Mechanisms in Skeletal Muscle Underlying Insulin Resistance in Women Who Are Lean With Polycystic Ovary Syndrome. *J Clin Endocrinol Metab* 2019; **104**: 1841-1854 [PMID: 30544235 DOI: 10.1210/jc.2018-01771]

83 **Li T**, Mo H, Chen W, Li L, Xiao Y, Zhang J, Li X, Lu Y. Role of the PI3K-Akt Signaling Pathway in the Pathogenesis of Polycystic Ovary Syndrome. *Reprod Sci* 2017; **24**: 646-655 [PMID: 27613818 DOI: 10.1177/1933719116667606]

84 **Zhang YF**, Yang YS, Hong J, Gu WQ, Shen CF, Xu M, Du PF, Li XY, Ning G. Elevated serum levels of interleukin-18 are associated with insulin resistance in women with polycystic ovary syndrome. *Endocrine* 2006; **29**: 419-423 [PMID: 16943580 DOI: 10.1385/ENDO:29:3:419]

85 **Wiwatpanit T**, Murphy AR, Lu Z, Urbanek M, Burdette JE, Woodruff TK, Kim JJ. Scaffold-Free Endometrial Organoids Respond to Excess Androgens Associated With Polycystic Ovarian Syndrome. *J Clin Endocrinol Metab* 2020; **105**: 769-780 [PMID: 31614364 DOI: 10.1210/clinem/dgz100]

86 **Ortega FJ**, Mercader JM, Moreno-Navarrete JM, Rovira O, Guerra E, Esteve E, Xifra G, Martínez C, Ricart W, Rieusset J, Rome S, Karczewska-Kupczewska M, Straczkowski M, Fernández-Real JM. Profiling of circulating microRNAs reveals common microRNAs linked to type 2 diabetes that change with insulin sensitization. *Diabetes Care* 2014; **37**: 1375-1383 [PMID: 24478399 DOI: 10.2337/dc13-1847]

87 **Long W**, Zhao C, Ji C, Ding H, Cui Y, Guo X, Shen R, Liu J. Characterization of serum microRNAs profile of PCOS and identification of novel non-invasive biomarkers. *Cell Physiol Biochem* 2014; **33**: 1304-1315 [PMID: 24802714 DOI: 10.1159/000358698]

88 **Nanda D**, Chandrasekaran SP, Ramachandran V, Kalaivanan K, Carani Venkatraman A. Evaluation of Serum miRNA-24, miRNA-29a and miRNA-502-3p Expression in PCOS Subjects: Correlation with Biochemical Parameters Related to PCOS and Insulin Resistance. *Indian J Clin Biochem* 2020; **35**: 169-178 [PMID: 32226248 DOI: 10.1007/s12291-018-0808-0]

89 **Melkman-Zehavi T**, Oren R, Kredo-Russo S, Shapira T, Mandelbaum AD, Rivkin N, Nir T, Lennox KA, Behlke MA, Dor Y, Hornstein E. miRNAs control insulin content in pancreatic β-cells *via* downregulation of transcriptional repressors. *EMBO J* 2011; **30**: 835-845 [PMID: 21285947 DOI: 10.1038/emboj.2010.361]

90 **Roth LW**, McCallie B, Alvero R, Schoolcraft WB, Minjarez D, Katz-Jaffe MG. Altered microRNA and gene expression in the follicular fluid of women with polycystic ovary syndrome. *J Assist Reprod Genet* 2014; **31**: 355-362 [PMID: 24390626 DOI: 10.1007/s10815-013-0161-4]

91 **Cai G**, Ma X, Chen B, Huang Y, Liu S, Yang H, Zou W. MicroRNA-145 Negatively Regulates Cell Proliferation Through Targeting IRS1 in Isolated Ovarian Granulosa Cells From Patients With Polycystic Ovary Syndrome. *Reprod Sci* 2017; **24**: 902-910 [PMID: 27799458 DOI: 10.1177/1933719116673197]

92 **Tremellen K**, Pearce K. Dysbiosis of Gut Microbiota (DOGMA)--a novel theory for the development of Polycystic Ovarian Syndrome. *Med Hypotheses* 2012; **79**: 104-112 [PMID: 22543078 DOI: 10.1016/j.mehy.2012.04.016]

93 **Sherman SB**, Sarsour N, Salehi M, Schroering A, Mell B, Joe B, Hill JW. Prenatal androgen exposure causes hypertension and gut microbiota dysbiosis. *Gut Microbes* 2018; **9**: 400-421 [PMID: 29469650 DOI: 10.1080/19490976.2018.1441664]

94 **Zeng B**, Lai Z, Sun L, Zhang Z, Yang J, Li Z, Lin J. Structural and functional profiles of the gut microbial community in polycystic ovary syndrome with insulin resistance (IR-PCOS): a pilot study. *Res Microbiol* 2019; **170**: 43-52 [PMID: 30292647 DOI: 10.1016/j.resmic.2018.09.002]

95 **Giampaolino P**, Foreste V, Di Filippo C, Gallo A, Mercorio A, Serafino P, Improda FP, Verrazzo P, Zara G, Buonfantino C, Borgo M, Riemma G, Angelis C, Zizolfi B, Bifulco G, Della Corte L. Microbiome and PCOS: State-of-Art and Future Aspects. *Int J Mol Sci* 2021; **22** [PMID: 33669557 DOI: 10.3390/ijms22042048]

96 **Banks WA**, Owen JB, Erickson MA. Insulin in the brain: there and back again. *Pharmacol Ther* 2012; **136**: 82-93 [PMID: 22820012 DOI: 10.1016/j.pharmthera.2012.07.006]

97 **Kuwabara T**, Kagalwala MN, Onuma Y, Ito Y, Warashina M, Terashima K, Sanosaka T, Nakashima K, Gage FH, Asashima M. Insulin biosynthesis in neuronal progenitors derived from adult hippocampus and the olfactory bulb. *EMBO Mol Med* 2011; **3**: 742-754 [PMID: 21984534 DOI: 10.1002/emmm.201100177]

98 **Kleinridders A**, Ferris HA, Cai W, Kahn CR. Insulin action in brain regulates systemic metabolism and brain function. *Diabetes* 2014; **63**: 2232-2243 [PMID: 24931034 DOI: 10.2337/db14-0568]

99 **Pomytkin I**, Costa-Nunes JP, Kasatkin V, Veniaminova E, Demchenko A, Lyundup A, Lesch KP, Ponomarev ED, Strekalova T. Insulin receptor in the brain: Mechanisms of activation and the role in the CNS pathology and treatment. *CNS Neurosci Ther* 2018; **24**: 763-774 [PMID: 29691988 DOI: 10.1111/cns.12866]

100 **Zilliox LA**, Chadrasekaran K, Kwan JY, Russell JW. Diabetes and Cognitive Impairment. *Curr Diab Rep* 2016; **16**: 87 [PMID: 27491830 DOI: 10.1007/s11892-016-0775-x]

101 **Antal B**, McMahon LP, Sultan SF, Lithen A, Wexler DJ, Dickerson B, Ratai EM, Mujica-Parodi LR. Type 2 diabetes mellitus accelerates brain aging and cognitive decline: Complementary findings from UK Biobank and meta-analyses. *Elife* 2022; **11** [PMID: 35608247 DOI: 10.7554/eLife.73138]

102 **Schubert M**, Gautam D, Surjo D, Ueki K, Baudler S, Schubert D, Kondo T, Alber J, Galldiks N, Küstermann E, Arndt S, Jacobs AH, Krone W, Kahn CR, Brüning JC. Role for neuronal insulin resistance in neurodegenerative diseases. *Proc Natl Acad Sci U S A* 2004; **101**: 3100-3105 [PMID: 14981233 DOI: 10.1073/pnas.0308724101]

103 **Zhao F**, Siu JJ, Huang W, Askwith C, Cao L. Insulin Modulates Excitatory Synaptic Transmission and Synaptic Plasticity in the Mouse Hippocampus. *Neuroscience* 2019; **411**: 237-254 [PMID: 31146008 DOI: 10.1016/j.neuroscience.2019.05.033]

104 **Wan Q**, Xiong ZG, Man HY, Ackerley CA, Braunton J, Lu WY, Becker LE, MacDonald JF, Wang YT. Recruitment of functional GABA(A) receptors to postsynaptic domains by insulin. *Nature* 1997; **388**: 686-690 [PMID: 9262404 DOI: 10.1038/41792]

105 **Lee CC**, Huang CC, Wu MY, Hsu KS. Insulin stimulates postsynaptic density-95 protein translation *via* the phosphoinositide 3-kinase-Akt-mammalian target of rapamycin signaling pathway. *J Biol Chem* 2005; **280**: 18543-18550 [PMID: 15755733 DOI: 10.1074/jbc.M414112200]

106 **Chiu SL**, Chen CM, Cline HT. Insulin receptor signaling regulates synapse number, dendritic plasticity, and circuit function in vivo. *Neuron* 2008; **58**: 708-719 [PMID: 18549783 DOI: 10.1016/j.neuron.2008.04.014]

107 **Haas CB**, Kalinine E, Zimmer ER, Hansel G, Brochier AW, Oses JP, Portela LV, Muller AP. Brain Insulin Administration Triggers Distinct Cognitive and Neurotrophic Responses in Young and Aged Rats. *Mol Neurobiol* 2016; **53**: 5807-5817 [PMID: 26497034 DOI: 10.1007/s12035-015-9494-6]

108 **Shaughness M**, Acs D, Brabazon F, Hockenbury N, Byrnes KR. Role of Insulin in Neurotrauma and Neurodegeneration: A Review. *Front Neurosci* 2020; **14**: 547175 [PMID: 33100956 DOI: 10.3389/fnins.2020.547175]

109 **Diehl T**, Mullins R, Kapogiannis D. Insulin resistance in Alzheimer's disease. *Transl Res* 2017; **183**: 26-40 [PMID: 28034760 DOI: 10.1016/j.trsl.2016.12.005]

110 **Franklin W**, Krishnan B, Taglialatela G. Chronic synaptic insulin resistance after traumatic brain injury abolishes insulin protection from amyloid beta and tau oligomer-induced synaptic dysfunction. *Sci Rep* 2019; **9**: 8228 [PMID: 31160730 DOI: 10.1038/s41598-019-44635-z]

111 **Kim BH**, Kelschenbach J, Borjabad A, Hadas E, He H, Potash MJ, Nedelcovych MT, Rais R, Haughey NJ, McArthur JC, Slusher BS, Volsky DJ. Intranasal insulin therapy reverses hippocampal dendritic injury and cognitive impairment in a model of HIV-associated neurocognitive disorders in EcoHIV-infected mice. *AIDS* 2019; **33**: 973-984 [PMID: 30946151 DOI: 10.1097/QAD.0000000000002150]

112 **Willette AA**, Bendlin BB, Starks EJ, Birdsill AC, Johnson SC, Christian BT, Okonkwo OC, La Rue A, Hermann BP, Koscik RL, Jonaitis EM, Sager MA, Asthana S. Association of Insulin Resistance With Cerebral Glucose Uptake in Late Middle-Aged Adults at Risk for Alzheimer Disease. *JAMA Neurol* 2015; **72**: 1013-1020 [PMID: 26214150 DOI: 10.1001/jamaneurol.2015.0613]

113 **Gabbouj S**, Ryhänen S, Marttinen M, Wittrahm R, Takalo M, Kemppainen S, Martiskainen H, Tanila H, Haapasalo A, Hiltunen M, Natunen T. Altered Insulin Signaling in Alzheimer's Disease Brain - Special Emphasis on PI3K-Akt Pathway. *Front Neurosci* 2019; **13**: 629 [PMID: 31275108 DOI: 10.3389/fnins.2019.00629]

114 **Yarchoan M**, Toledo JB, Lee EB, Arvanitakis Z, Kazi H, Han LY, Louneva N, Lee VM, Kim SF, Trojanowski JQ, Arnold SE. Abnormal serine phosphorylation of insulin receptor substrate 1 is associated with tau pathology in Alzheimer's disease and tauopathies. *Acta Neuropathol* 2014; **128**: 679-689 [PMID: 25107476 DOI: 10.1007/s00401-014-1328-5]

115 **Wang Y**, Yang R, Gu J, Yin X, Jin N, Xie S, Wang Y, Chang H, Qian W, Shi J, Iqbal K, Gong CX, Cheng C, Liu F. Cross talk between PI3K-AKT-GSK-3β and PP2A pathways determines tau hyperphosphorylation. *Neurobiol Aging* 2015; **36**: 188-200 [PMID: 25219467 DOI: 10.1016/j.neurobiolaging.2014.07.035]

116 **Stouffer MA**, Woods CA, Patel JC, Lee CR, Witkovsky P, Bao L, Machold RP, Jones KT, de Vaca SC, Reith ME, Carr KD, Rice ME. Insulin enhances striatal dopamine release by activating cholinergic interneurons and thereby signals reward. *Nat Commun* 2015; **6**: 8543 [PMID: 26503322 DOI: 10.1038/ncomms9543]

117 **Lei P**, Ayton S, Bush AI, Adlard PA. GSK-3 in Neurodegenerative Diseases. *Int J Alzheimers Dis* 2011; **2011**: 189246 [PMID: 21629738 DOI: 10.4061/2011/189246]

118 **Hong CT**, Chen KY, Wang W, Chiu JY, Wu D, Chao TY, Hu CJ, Chau KD, Bamodu OA. Insulin Resistance Promotes Parkinson's Disease through Aberrant Expression of α-Synuclein, Mitochondrial Dysfunction, and Deregulation of the Polo-Like Kinase 2 Signaling. *Cells* 2020; **9** [PMID: 32192190 DOI: 10.3390/cells9030740]

119 **Chung JY**, Lee SJ, Lee SH, Jung YS, Ha NC, Seol W, Park BJ. Direct interaction of α-synuclein and AKT regulates IGF-1 signaling: implication of Parkinson disease. *Neurosignals* 2011; **19**: 86-96 [PMID: 21474915 DOI: 10.1159/000325028]

120 **Rothman SM**, Griffioen KJ, Fishbein KW, Spencer RG, Makrogiannis S, Cong WN, Martin B, Mattson MP. Metabolic abnormalities and hypoleptinemia in α-synuclein A53T mutant mice. *Neurobiol Aging* 2014; **35**: 1153-1161 [PMID: 24239384 DOI: 10.1016/j.neurobiolaging.2013.10.088]

121 **Hursting SD**, Berger NA. Energy balance, host-related factors, and cancer progression. *J Clin Oncol* 2010; **28**: 4058-4065 [PMID: 20697088 DOI: 10.1200/JCO.2010.27.9935]

122 **Rabin-Court A**, Rodrigues MR, Zhang XM, Perry RJ. Obesity-associated, but not obesity-independent, tumors respond to insulin by increasing mitochondrial glucose oxidation. *PLoS One* 2019; **14**: e0218126 [PMID: 31188872 DOI: 10.1371/journal.pone.0218126]

123 **Perry RJ**, Shulman GI. Mechanistic Links between Obesity, Insulin, and Cancer. *Trends Cancer* 2020; **6**: 75-78 [PMID: 32061306 DOI: 10.1016/j.trecan.2019.12.003]

124 **Saraei P**, Asadi I, Kakar MA, Moradi-Kor N. The beneficial effects of metformin on cancer prevention and therapy: a comprehensive review of recent advances. *Cancer Manag Res* 2019; **11**: 3295-3313 [PMID: 31114366 DOI: 10.2147/CMAR.S200059]

125 **Singh AK**, Rana HK, Singh V, Chand Yadav T, Varadwaj P, Pandey AK. Evaluation of antidiabetic activity of dietary phenolic compound chlorogenic acid in streptozotocin induced diabetic rats: Molecular docking, molecular dynamics, in silico toxicity, in vitro and in vivo studies. *Comput Biol Med* 2021; **134**: 104462 [PMID: 34148008 DOI: 10.1016/j.compbiomed.2021.104462]

126 **Hahn WC**, Weinberg RA. Rules for making human tumor cells. *N Engl J Med* 2002; **347**: 1593-1603 [PMID: 12432047 DOI: 10.1056/NEJMra021902]

127 **Giovannucci E**, Harlan DM, Archer MC, Bergenstal RM, Gapstur SM, Habel LA, Pollak M, Regensteiner JG, Yee D. Diabetes and cancer: a consensus report. *Diabetes Care* 2010; **33**: 1674-1685 [PMID: 20587728 DOI: 10.2337/dc10-0666]

128 **Barone BB**, Yeh HC, Snyder CF, Peairs KS, Stein KB, Derr RL, Wolff AC, Brancati FL. Long-term all-cause mortality in cancer patients with preexisting diabetes mellitus: a systematic review and meta-analysis. *JAMA* 2008; **300**: 2754-2764 [PMID: 19088353 DOI: 10.1001/jama.2008.824]

129 **Yee LD**, Mortimer JE, Natarajan R, Dietze EC, Seewaldt VL. Metabolic Health, Insulin, and Breast Cancer: Why Oncologists Should Care About Insulin. *Front Endocrinol (Lausanne)* 2020; **11**: 58 [PMID: 32153503 DOI: 10.3389/fendo.2020.00058]

130 **Buch K**, Gunmalm V, Andersson M, Schwarz P, Brøns C. Effect of chemotherapy and aromatase inhibitors in the adjuvant treatment of breast

cancer on glucose and insulin metabolism-A systematic review. *Cancer Med* 2019; **8**: 238-245 [PMID: 30561133 DOI: 10.1002/cam4.1911]

131 **Jemal A**, Bray F, Center MM, Ferlay J, Ward E, Forman D. Global cancer statistics. *CA Cancer J Clin* 2011; **61**: 69-90 [PMID: 21296855 DOI: 10.3322/caac.20107]

132 **Torre LA**, Bray F, Siegel RL, Ferlay J, Lortet-Tieulent J, Jemal A. Global cancer statistics, 2012. *CA Cancer J Clin* 2015; **65**: 87-108 [PMID: 25651787 DOI: 10.3322/caac.21262]

133 **Chen Z**, Fillmore CM, Hammerman PS, Kim CF, Wong KK. Non-small-cell lung cancers: a heterogeneous set of diseases. *Nat Rev Cancer* 2014; **14**: 535-546 [PMID: 25056707 DOI: 10.1038/nrc3775]

134 **Pollak M**. Insulin and insulin-like growth factor signalling in neoplasia. *Nat Rev Cancer* 2008; **8**: 915-928 [PMID: 19029956 DOI: 10.1038/nrc2536]

135 **Zhao J**, Shi X, Wang T, Ying C, He S, Chen Y. The Prognostic and Clinicopathological Significance of IGF-1R in NSCLC: a Meta-Analysis. *Cell Physiol Biochem* 2017; **43**: 697-704 [PMID: 28946136 DOI: 10.1159/000480655]

136 **Ludovini V**, Flacco A, Bianconi F, Ragusa M, Vannucci J, Bellezza G, Chiari R, Minotti V, Pistola L, Tofanetti FR, Siggillino A, Baldelli E, Sidoni A, Daddi N, Puma F, Varella-Garcia M, Crinò L. Concomitant high gene copy number and protein overexpression of IGF1R and EGFR negatively affect disease-free survival of surgically resected non-small-cell-lung cancer patients. *Cancer Chemother Pharmacol* 2013; **71**: 671-680 [PMID: 23314677 DOI: 10.1007/s00280-012-2056-y]

137 **Gately K**, Forde L, Cuffe S, Cummins R, Kay EW, Feuerhake F, O'Byrne KJ. High coexpression of both EGFR and IGF1R correlates with poor patient prognosis in resected non-small-cell lung cancer. *Clin Lung Cancer* 2014; **15**: 58-66 [PMID: 24210543 DOI: 10.1016/j.cllc.2013.08.005]

138 **Piper AJ**, Clark JL, Mercado-Matos J, Matthew-Onabanjo AN, Hsieh CC, Akalin A, Shaw LM. Insulin Receptor Substrate-1 (IRS-1) and IRS-2 expression levels are associated with prognosis in non-small cell lung cancer (NSCLC). *PLoS One* 2019; **14**: e0220567 [PMID: 31393907 DOI: 10.1371/journal.pone.0220567]

139 **LeRoith D**. Insulin-like growth factor receptors and binding proteins. *Baillieres Clin Endocrinol Metab* 1996; **10**: 49-73 [PMID: 8734451 DOI: 10.1016/S0950-351X(96)80298-9]

140 **Clemmons DR**. Insulin-like growth factor binding proteins and their role in controlling IGF actions. *Cytokine Growth Factor Rev* 1997; **8**: 45-62 [PMID: 9174662 DOI: 10.1016/S1359-6101(96)00053-6]

141 **Hu Q**, Zhou Y, Ying K, Ruan W. IGFBP, a novel target of lung cancer? *Clin Chim Acta* 2017; **466**: 172-177 [PMID: 28104361 DOI: 10.1016/j.cca.2017.01.017]

142 **Wang J**, Hu ZG, Li D, Xu JX, Zeng ZG. Gene expression and prognosis of insulinlike growth factor-binding protein family members in non-small cell lung cancer. *Oncol Rep* 2019; **42**: 1981-1995 [PMID: 31545451 DOI: 10.3892/or.2019.7314]

143 **Xu X**, Qiu Y, Chen S, Wang S, Yang R, Liu B, Li Y, Deng J, Su Y, Lin Z, Gu J, Li S, Huang L, Zhou Y. Different Roles of the Insulin-like Growth Factor (IGF) Axis in Non-small Cell Lung Cancer. *Curr Pharm Des* 2022; **28**: 2052-2064 [PMID: 36062855 DOI: 10.2174/1381612828666220608122934]

144 **Keum N**, Greenwood DC, Lee DH, Kim R, Aune D, Ju W, Hu FB, Giovannucci EL. Adult weight gain and adiposity-related cancers: a dose-response meta-analysis of prospective observational studies. *J Natl Cancer Inst* 2015; **107** [PMID: 25757865 DOI: 10.1093/jnci/djv088]

145 **Zhang X**, Zhou G, Sun B, Zhao G, Liu D, Sun J, Liu C, Guo H. Impact of obesity upon prostate cancer-associated mortality: A meta-analysis of 17 cohort studies. *Oncol Lett* 2015; **9**: 1307-1312 [PMID: 25663903 DOI: 10.3892/ol.2014.2841]

146 **Pandeya DR**, Mittal A, Sathian B, Bhatta B. Role of hyperinsulinemia in increased risk of prostate cancer: a case control study from Kathmandu Valley. *Asian Pac J Cancer Prev* 2014; **15**: 1031-1033 [PMID: 24568446 DOI: 10.7314/APJCP.2014.15.2.1031]

147 **Ma RW**, Chapman K. A systematic review of the effect of diet in prostate cancer prevention and treatment. *J Hum Nutr Diet* 2009; **22**: 187-99; quiz 200 [PMID: 19344379 DOI: 10.1111/j.1365-277X.2009.00946.x]

148 **Kruk J**, Czerniak U. Physical activity and its relation to cancer risk: updating the evidence. *Asian Pac J Cancer Prev* 2013; **14**: 3993-4003 [PMID: 23991944 DOI: 10.7314/APJCP.2013.14.7.3993]

149 **Young-McCaughan S**. Potential for prostate cancer prevention through physical activity. *World J Urol* 2012; **30**: 167-179 [PMID: 22198724 DOI: 10.1007/s00345-011-0812-y]

150 **De Nunzio C**, Aronson W, Freedland SJ, Giovannucci E, Parsons JK. The correlation between metabolic syndrome and prostatic diseases. *Eur Urol* 2012; **61**: 560-570 [PMID: 22119157 DOI: 10.1016/j.eururo.2011.11.013]

151 **Arcidiacono B**, Iiritano S, Nocera A, Possidente K, Nevolo MT, Ventura V, Foti D, Chiefari E, Brunetti A. Insulin resistance and cancer risk: an overview of the pathogenetic mechanisms. *Exp Diabetes Res* 2012; **2012**: 789174 [PMID: 22701472 DOI: 10.1155/2012/789174]

152 **Cox ME**, Gleave ME, Zakikhani M, Bell RH, Piura E, Vickers E, Cunningham M, Larsson O, Fazli L, Pollak M. Insulin receptor expression by human prostate cancers. *Prostate* 2009; **69**: 33-40 [PMID: 18785179 DOI: 10.1002/pros.20852]

153 **Fahrenholtz CD**, Beltran PJ, Burnstein KL. Targeting IGF-IR with ganitumab inhibits tumorigenesis and increases durability of response to androgen-deprivation therapy in VCaP prostate cancer xenografts. *Mol Cancer Ther* 2013; **12**: 394-404 [PMID: 23348048 DOI: 10.1158/1535-7163.MCT-12-0648]

154 **Ibuki N**, Ghaffari M, Reuveni H, Pandey M, Fazli L, Azuma H, Gleave ME, Levitzki A, Cox ME. The tyrphostin NT157 suppresses insulin receptor substrates and augments therapeutic response of prostate cancer. *Mol Cancer Ther* 2014; **13**: 2827-2839 [PMID: 25267499 DOI: 10.1158/1535-7163.MCT-13-0842]

155 **Tomlins SA**, Bjartell A, Chinnaiyan AM, Jenster G, Nam RK, Rubin MA, Schalken JA. ETS gene fusions in prostate cancer: from discovery to daily clinical practice. *Eur Urol* 2009; **56**: 275-286 [PMID: 19409690 DOI: 10.1016/j.eururo.2009.04.036]

156 **Cancer Genome Atlas Research Network**. The Molecular Taxonomy of Primary Prostate Cancer. *Cell* 2015; **163**: 1011-1025 [PMID: 26544944 DOI: 10.1016/j.cell.2015.10.025]

World Journal of Clinical Cases

Submit a Manuscript: https://www.f6publishing.com

World J Clin Cases 2023 September 6; 11(25): 5857-5862

DOI: 10.12998/wjcc.v11.i25.5857

ISSN 2307-8960 (online)

MINIREVIEWS

Progress in the study and treatment of peri-device leak after left atrial appendage closure

Ying-Bo Qi, Hui-Min Chu

Specialty type: Cardiac and cardiovascular systems

Provenance and peer review: Unsolicited article; Externally peer reviewed.

Peer-review model: Single blind

Peer-review report's scientific quality classification

Grade A (Excellent): 0
Grade B (Very good): B
Grade C (Good): C
Grade D (Fair): 0
Grade E (Poor): 0

P-Reviewer: Mishra AK, United States; Patel L, United States

Received: February 18, 2023
Peer-review started: February 18, 2023
First decision: May 8, 2023
Revised: May 28, 2023
Accepted: August 9, 2023
Article in press: August 9, 2023
Published online: September 6, 2023

Ying-Bo Qi, Department of Cardiology, Health Science Center, Ningbo University, Ningbo 315000, Zhejiang Province, China

Hui-Min Chu, Department of Cardiology, Arrhythmia Center, Ningbo First Hospital, Ningbo 3153000, Zhejiang Province, China

Corresponding author: Hui-Min Chu, MD, Professor, Department of Cardiology, Arrhythmia Center, Ningbo First Hospital, No. 59 Liuting Street, Ningbo 3153000, Zhejiang Province, China. epnbheart@163.com

Abstract

For patients with atrial fibrillation with an increased risk of stroke and contraindications to long-term anticoagulation, percutaneous left atrial appendage closure (LAAC) has become an important alternative to long-term oral anticoagulation. Incomplete closure of the LAAC during the procedure leads to faster blood flow in the interstitial space around the device, resulting in peri-device leak (PDL), which is not uncommon. Studies are still inconclusive in determining the incidence, long-term safety, and management of PDL. Therefore, this article reviewed the progress made in the research and treatment of PDL after LAAC.

Key Words: Atrial fibrillation; Left atrial appendage closure; Peri-device leak; Thromboembolism; Cardiac computed tomography angiography; Treatment

Core Tip: For patients with atrial fibrillation with an increased risk of stroke and contraindications to long-term anticoagulation, percutaneous left atrial appendage closure has become an important alternative to long-term oral anticoagulation. Incomplete closure of the left atrial appendage closure during the procedure leads to faster blood flow in the interstitial space around the device, resulting in peri-device leak. The incidence, long-term safety, and management of peri-device leak are still inconclusive.

Citation: Qi YB, Chu HM. Progress in the study and treatment of peri-device leak after left atrial appendage closure. *World J Clin Cases* 2023; 11(25): 5857-5862
URL: https://www.wjgnet.com/2307-8960/full/v11/i25/5857.htm
DOI: https://dx.doi.org/10.12998/wjcc.v11.i25.5857

INTRODUCTION

As one of the most common type of arrhythmias, atrial fibrillation (AF) can lead to the development of atrial thrombi. After a thrombus detaches from the vessel wall, it travels with the blood to the brain and the whole body. In nonvalvular AF, 90% of thrombi are formed in the left atrial appendage (LAA)[1]. Therefore, LAA closure (LAAC) has become an effective alternative to long-term oral anticoagulation for the prevention of stroke in AF patients with increased stroke risk or contraindications to long-term anticoagulation therapy[2]. LAAC uses a catheter delivery system to transport and fix the prefabricated and preinstalled LAA occlusion device to plug or seal off the LAA to block the blood flow between the LAA and the left atrium. Variability in the anatomical morphology, size, and orientation of LAAs between patients can result in the failure of the occluder in sealing the LAA, causing high-velocity blood flow to pass through the gap around the occluder and can possibly cause peri-device leak (PDL). The clinical significance of PDL is now still a controversial issue, while the main concern is its relationship to thromboembolic events.

CAUSES, ASSESSMENT METHODS, AND GRADING CRITERIA OF PDL

Causes of PDL

Plugs and cups are the two widely used occluders in clinical practice, and they can lead to PDL for slightly different reasons. PDL occurs with plug occluders when they cannot fully cover the LAA. PDL occurs with cup occluders mostly due to the gap under the blocking disc that does not fully cover the wall of the LAA[3].

Methods of PDL assessment

Methods to assess PDL include digital subtraction angiography (DSA), intracardiac echocardiography, transesophageal echocardiography (TEE), and cardiac computed tomography angiography (CCTA). A single-center observational study in Denmark studied 415 patients who underwent LAAC with the Amplatzer occluder between 2010 and 2018[4]. In total, 346 patients who received CCTA and TEE at 8 wk postoperatively were included in the research. The results of the study showed that PDL was observed in 110 patients (32%) by TEE, of which 29 (8%) had PDL > 3 mm. PDL was present in 210 patients (61%) by CCTA, of which 63 patients (18%) had PDL > 3 mm. This study suggested that CCTA is more sensitive than TEE in detecting PDL, which was similar to the findings from other studies[5,6].

In contrast, a study from Zhang *et al*[7] included a total of 208 patients with nonvalvular AF who underwent LAAC. Among them, 101 patients received standard surgery (intraoperative TEE confirmation required, retrospective cohort) and 107 patients with fluoroscopy alone (prospective cohort). The study analyzed individual occluder position, anchorage, compression, and PDL to assess clinical outcomes in both cohorts and found that both DSA angiography and TEE assessment intraoperatively showed better performance in assessing the occluder position and anchorage. However, no significant improvement in assessing PDL was observed (P = 0.304). Other data on intracardiac echocardiography and DSA are lacking, and further studies are needed.

Grading criteria

There are no well-recognized criteria for the assessment of PDL. For plugging occluders (*e.g.*, Watchman[8]), a PDL ≤ 5 mm is generally considered a mild PDL, and PDL > 5 mm is considered severe PDL. PDL in some studies of cap occluders (*e.g.*, LAmbre, ACP/Amulet[9]) strictly defined PDL< 1 mm as mild, PDL between 1-3 mm as moderate, and PDL > 3 mm as severe. Most experts agree that PDL of 5 mm is recommended as a grading criterion for either plug or cap occluders (Figure 1).

INCIDENCE OF PDL

Most LAAC-related studies have statistically analyzed the incidence of PDL (Table 1). The PROTECT AF study was the first randomized controlled study of LAAC in which 468 patients successfully underwent LAAC (Watchman) with their PDL assessed by TEE[8]. If TEE found no thrombus on the surface of the occluder and the LAA was effectively occluded (complete occlusion or PDL < 5 mm), then the TEE criteria were met. Then, warfarin could be discontinued in favor of aspirin and clopidogrel for continued antithrombotic therapy. However, only 349 patients in this study met the TEE criteria at the 45-d follow-up, with the initial results of the study showing that the incidence of occluder surface thrombosis and PDL at 45 d (14%) might be higher than expected. In the subsequent PROTECT AF 2study, it was shown that during the follow-up after LAAC, 30 patients (7.5%), 14 patients (3.6%), and 10 patients (2.7%) continued warfarin after PDL (> 5 mm) was detected by TEE at 45 d, 6 mo, and 1 year after the procedure, respectively[10]. In contrast, the

Table 1 Studies reporting the peri-device leak after left atrial appendage closure

Ref.	Study population	Type of study	Type of LAA closure	Incidence of PDL	Findings
Holmes *et al* [8]	485	Randomized controlled study	Watchman	14%: ≥ 5 mm	No difference between patients with any PDL in terms of primary effectiveness
Dukkipati *et al*[12]	1205	Randomized controlled study	Watchman	0.7%: > 5 mm; 27.7%: 1-5 mm; and 71.6%: no PDL	PDL ≤ 5 mm was associated with an increased risk of stroke, systemic embolism, cardiovascular, unexplained death, or all-cause mortality
Korsholm *et al*[13]	153	Retrospective study	Amplatzer Amulet, Amplatzer Cardiac Plug	61%	PDL did not increase the incidence of events related to thromboembolism.
Wang *et al* [14]	152	Retrospective study	LAmbre	15.7%: > 3 mm	PDL was not associated with an increased risk for thromboembolic events
Alkhouli *et al*[15]	51333	Retrospective studies	Watchman, ACP	73.4%: no PDL; 25.8%: moderate; and 0.7%: severe	Patients with PDL at 1 yr had a 2-fold increase in ischemic stroke/SE at 5 yr compared with patients without PDL
Miller *et al* [17]	43	Retrospective study	Watchman FLX	More than 40%	3 TIAs (6.98%) and 3 strokes (6.98%) were documented each within the 6-mo to 1-yr period

TIA: Transient ischemic attack; PDL: Peri-device leak; SE: Systemic embolization; LAA: Left atrial appendage.

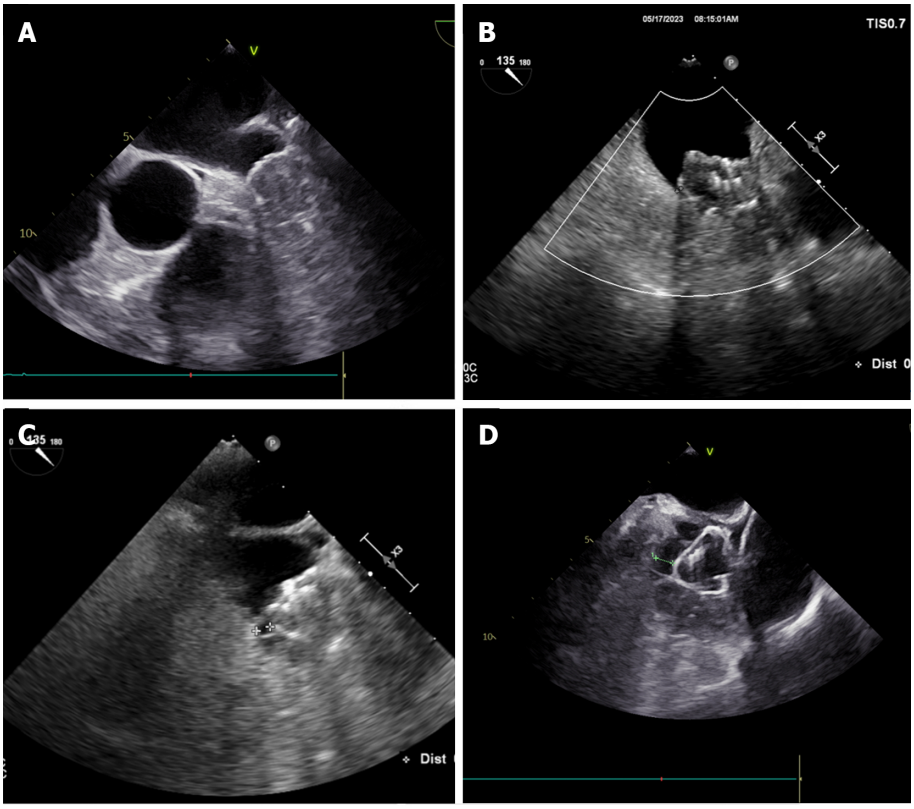

DOI: 10.12998/wjcc.v11.i25.5857 **Copyright** ©The Author(s) 2023.

Figure 1 Different grades of peri-device leak using transesophageal echocardiographic imaging. A: No peri-device leak (PDL); B: 0-3 mm PDL; C: 3-5 mm PDL; D: > 5 mm PDL.

early PROTECT-AF study showed that the incidence of any degree of PDL was 40.9%, 33.8%, and 32.1% at 45 d, 6 mo, and 12 mo postoperatively, respectively[11]. Of these, mild (1 mm), moderate (1-3 mm), and severe (≥ 3 mm) PDL accounted for 7.7% of patients, 59.9% of patients, and 32.4% of patients, respectively.

A total of 1205 patients who were implanted with Watchman occluders from three studies, PROTECT-AF, PREVAIL, and CAP2, were included in another 5-year follow-up study[12]. By TEE at 45 d, 634 patients (60.2%) had no PDL, 404 patients (38.3%) had PDL < 5 mm, and 16 patients (1.5%) had PDL > 5 mm (TEE information was missing for the remaining 151 patients). Of the 404 patients with PDL < 5 mm, 255 patients (63.1%) had PDL ≤ 3 mm, and 149 patients (36.9%) had 3 mm < PDL ≤ 5 mm. At the 1-year TEE follow-up, a total of 983 patients reported PDL, of which 704 patients

(71.6%) had no PDL, 272 patients (27.7%) had PDL ≤ 5 mm, and 7 patients (0.7%) had PDL > 5 mm.

A study from Denmark on the Amplatzer occluder included 153 patients who received LAAC and underwent 2-mo and 12-mo cardiac computed tomography at a single center between 2010 and 2017[13]. The Amplatzer Cardiac Plug Occluder was implanted in 43 patients (28%). The 2-mo and 12-mo follow-ups showed PDL in 103 patients (67%) and 93 patients (61%), respectively (P = 0.08). The mean PDL size at 2 mo and 12 mo was 2.9 ± 1.7 and 2.4 ± 1.4 mm, respectively (P = 0.07).

In a study from Wuhan University People's Hospital, 152 AF patients were implanted with LAmbre occluders[14]. At the 3-mo follow-up, 123 patients underwent TEE, of whom 21 patients (17%) had PDL, 19 patients (15.4%) had mild PDL (1-3 mm), and 2 patients (1.6%) had moderate PDL (> 3 and ≤ 5 mm). Of the 121 patients who underwent TEE at the 12-mo follow-up, 19 patients (15.7%) had PDL (> 3 mm).

Another retrospective study through the NCDR-LAAO registry included all patients who underwent LAAO between January 1, 2016 and December 31, 2019[15]. Patients were classified according to PDL size on a 45-d echocardiogram: PDL= 0 mm, no PDL; PDL > 0-5 mm, moderate PDL; and PDL > 5 mm, severe PDL. A total of 51333 patients were included, of whom 37696 patients (73.4%) had no PDL, 13258 patients (25.8%) had moderate PDL, and 379 patients (0.7%) had severe PDL.

In the Amulet IDE study published in 2021, a head-to-head comparison of the safety and efficacy of the plug occluder (Watchman) *vs* the cap occluder (Amulet) was performed[16]. The study was randomized to the Amulet or Watchman groups, with 934 patients in the Amulet group and 944 patients in the Watchman group. It was discovered that the occluder blocking rate was better in the Amulet group than in the Watchman group at 45 d postoperatively (the proportion of those with PDL ≥ 3 mm was significantly lower in the Amulet group than in the Watchman group, 11% and 26%, respectively; P < 0.001) and lasted until 1 year postoperatively (9% and 22% in the Amulet group compared with the Watchman group for PDL ≥ 3 mm, respectively; P < 0.001). As seen in this study, the incidence of PDL was lower with the cap occluder than with the plug occluder.

However, the conclusion was different in another recent single-center retrospective study[17]. Miller *et al*[17] included 43 patients who underwent Watchman FLX implantation from July 2020 to September 2021, and the final results showed that more than 40% of patients (17/43) implanted with Watchman FLX had PDL. Only 53% of patients (23/43) had complete closure of the LAA. In this study, the incidence of PDL was not low for the Watchman FLX implantation group and still requires a long follow-up.

It can be easily seen from the above studies that the incidence of PDL ranges from 9% to 40%, and the incidence of PDL with different grades also differs. The incidence of PDL may be lower with a cap occluder than with a plug occluder.

PROGNOSTIC IMPACT OF PDL

The prognostic impact of PDL is currently the focus of attention in related studies. Data from the early PROTECT AF study suggested that patients without PDL were not statistically different than patients with any PDL in terms of primary effectiveness (P = 0.572) or ischemic stroke or systemic embolism (P = 0.669)[11]. In addition, further analysis found no statistically significant relationship between PDL severity and the primary endpoint [hazard ratio (HR): 0.84; P = 0.256].

Similarly, the aforementioned study on the Amplatzer occluder noted that with continued follow-up after completion of cardiac computed tomography at 12 mo and a median follow-up at 2.1 years, 52 patients (34%) had a composite endpoint of ischemic stroke, systemic embolism, transient ischemic attack, or all-cause death between the 12-mo visit and the last known follow-up[13]. The study divided PDL into four different grades: no PDL; grade 1; grade 2; and grade 3. The risk of the composite endpoint was 63% higher in the PDL group than in the no-PDL group, yet no statistical significance was found [HR: 1.63, 95% confidence interval: 0.90-2.93; P = 0.11]. The study further noted that PDL did not increase the incidence of events related to thromboembolism.

Although the two studies showed that PDL after Watchman and Amplatzer implantation did not increase the incidence of thromboembolic events, small sample sizes, small number of thromboembolic events, and short follow-up periods of both studies may undermine the statistical efficacy.

The retrospective NCDR-LAAO registry study also showed a trend toward increased ischemic stroke or systemic embolism in patients with any PDL at 45 d (5-year incidence 9.2% *vs* 6.6%), but this was not statistically significant (P = 0.14)[15]. However, patients with PDL at 1 year had a 2-fold increase in ischemic stroke/systemic embolism at 5 years compared with patients with no PDL (9.9% *vs* 5.1%; P = 0.008). This study is the first to show a correlation between PDL (although only detected at 1 year) and subsequent adverse ischemic events.

A similar view was shared in the 5-year follow-up study[12]. Compared with the no-PDL group, a 45-d TEE showing PDL ≤ 5 mm was not associated with an increased risk of ischemic stroke or systemic embolism (9.2% *vs* 6.6%; P = 0.141), cardiovascular or unexplained death (8.8% *vs* 10.3%; P = 0.547), or all-cause death (18.5% *vs* 21.5%; P = 0.350). However, 1-year TEE showing PDL ≤ 5 mm was associated with an increased risk of subsequent ischemic stroke or systemic embolism (9.9% *vs* 5.1%) with an unadjusted HR of 1.92 (95% confidence interval: 1.14-3.25; P = 0.0149), but 1-year TEE showed that PDL ≤ 5 mm was not associated with an increase in cardiovascular or unexplained death (10.1% *vs* 8.6%; P = 0.382) or all-cause mortality (16.2% *vs* 18.3%; P = 0.515).

A prospective observational registry study enrolled 1047 patients and classified PDL as < 1 mm, 1-3 mm, and > 3 mm [18]. After a mean follow-up period of 13 mo, the incidence of PDL at all levels was found to be 4.3%, 5.4% and 1.9%, respectively. There were nine strokes (0.9%) and nine transient ischemic attack (0.9%) during follow-up, which was not related to different grades of PDL.

Although the conclusions on the prognostic impact of PDL are mixed, the current findings favor that PDL can increase the risk of ischemic stroke or systemic embolism, especially in severe (≥ 5 mm) PDL.

CURRENT TREATMENT FOR PDL

PDL of more than 5 mm detected after LAAC will be considered a failure of occlusion, and TEE or CCTA are important follow-up tools to assess the PDL. Current treatment options for PDL include anticoagulation, spring-ring embolization, and radiofrequency ablation.

A study from the United States treated PDL by releasing a spring coil into the LAA[18]. The study included 30 patients with PDL after LAAC, of whom 10 patients (33.3%) had severe PDL (≥ 5 mm) and 20 patients (66.7%) had moderate PDL (3-4 mm). The immediate procedural success rate was 100%, and immediate angiographic and TEE results showed complete occlusion in 25 patients (83.3%), very mild PDL (1-2 mm) in 3 patients (10.0%), and partial occlusion with moderate PDL (3-4 mm) in 2 patients (6.7%). All patients underwent follow-up TEE after a median of 52 d (43–90 d). The majority of patients [n = 23 (76.7%)] showed complete occlusion, except for 2 patients (6.6%) with minor PDL (1-2 mm) and 5 patients (16.7%) with moderate PDL (3-4 mm), where spring coil placement resulted in a mean reduction in leak size of 86.3% (P < 0.001). This study provided a new means of treating PDL.

Another study shed light on the effectiveness of radiofrequency ablation for PDL management[19]. This study included 43 patients (PDL ≥ 4 mm) who underwent radiofrequency ablation of atrial tissue at the site of the PDL, and TEE was performed 48 ± 12 d after the procedure. The study found that 23 patients (53.5%) had complete occlusion of the LAA, 15 patients (34.9%) had mild or very mild (1-2 mm) PDL, and 5 patients (11.6%) had moderate (3-4 mm) PDL. The long-term success rate was 88.4% (n = 38). This study suggested that radiofrequency ablation may be effective in the treatment of PDL.

However, anticoagulation is still used clinically as the primary solution to treat large PDL. Although the small-sample study mentioned above has provided a new insight into the treatment of PDL, a large-scale clinical study is still needed to validate the results.

CONCLUSION

Since PDL after LAAC is not uncommon, it should be taken seriously by clinicians through achieving complete occlusion in LAA as much as possible. Both TEE and CCTA are powerful tools to assess PDLs after LAAC, with CCTA being more sensitive. With longer follow-up and larger sample sizes, it has been found that PDL may increase the risk of thromboembolic events, even though the overall incidence is low. Management of PDL includes anticoagulation, spring-ring embolization, and radiofrequency ablation, but further studies are needed to validate their safety and efficacy.

ACKNOWLEDGEMENTS

We appreciate all the medical staff for their efforts.

FOOTNOTES

Author contributions: Qi YB reviewed the literature and contributed to the manuscript drafting; Chu HM reviewed the manuscript; All authors issued approval of the final version.

Supported by Zhejiang Provincial Foundation for Medical and Health Sciences, No. 2021KY980.

Conflict-of-interest statement: All authors declare having no potential conflicts of interests for this article.

Country/Territory of origin: China

ORCID number: Ying-Bo Qi 0000-0002-4929-0817; Hui-Min Chu 0000-0002-2791-6831.

S-Editor: Liu JH
L-Editor: Filipodia
P-Editor: Zhang XD

REFERENCES

1 **Blackshear JL**, Odell JA. Appendage obliteration to reduce stroke in cardiac surgical patients with atrial fibrillation. *Ann Thorac Surg* 1996; **61**: 755-759 [PMID: 8572814 DOI: 10.1016/0003-4975(95)00887-X]

2 **January CT**, Wann LS, Calkins H, Chen LY, Cigarroa JE, Cleveland JC Jr, Ellinor PT, Ezekowitz MD, Field ME, Furie KL, Heidenreich PA, Murray KT, Shea JB, Tracy CM, Yancy CW. 2019 AHA/ACC/HRS Focused Update of the 2014 AHA/ACC/HRS Guideline for the Management of Patients With Atrial Fibrillation: A Report of the American College of Cardiology/American Heart Association Task Force on Clinical Practice Guidelines and the Heart Rhythm Society in Collaboration With the Society of Thoracic Surgeons. *Circulation* 2019; **140**: e125-e151 [PMID: 30686041 DOI: 10.1161/CIR.0000000000000665]

3 **Jang SJ**, Wong SC, Mosadegh B. Leaks after Left Atrial Appendage Closure: Ignored or Neglected? *Cardiology* 2021; **146**: 384-391 [PMID: 33735867 DOI: 10.1159/000513901]

4 **Korsholm K**, Jensen JM, Nørgaard BL, Samaras A, Saw J, Berti S, Tzikas A, Nielsen-Kudsk JE. Peridevice Leak Following Amplatzer Left Atrial Appendage Occlusion: Cardiac Computed Tomography Classification and Clinical Outcomes. *JACC Cardiovasc Interv* 2021; **14**: 83-93 [PMID: 33413869 DOI: 10.1016/j.jcin.2020.10.034]

5 **Goitein O**, Fink N, Hay I, Di Segni E, Guetta V, Goitein D, Brodov Y, Konen E, Glikson M. Cardiac CT Angiography (CCTA) predicts left atrial appendage occluder device size and procedure outcome. *Int J Cardiovasc Imaging* 2017; **33**: 739-747 [PMID: 28070743 DOI: 10.1007/s10554-016-1050-6]

6 **Saw J**, Fahmy P, Spencer R, Prakash R, McLaughlin P, Nicolaou S, Tsang M. Comparing Measurements of CT Angiography, TEE, and Fluoroscopy of the Left Atrial Appendage for Percutaneous Closure. *J Cardiovasc Electrophysiol* 2016; **27**: 414-422 [PMID: 26728988 DOI: 10.1111/jce.12909]

7 **Zhang X**, Jin Q, Kong D, Jiang Y, Chen S, Chen D, Hou CR, Zhang L, Pan C, Zhou D, Ge J. Comparison of fluoroscopy and transesophageal echocardiogram for intra-procedure device surveillance assessment during implantation of Watchman. *Int J Cardiol* 2021; **324**: 72-77 [PMID: 32882298 DOI: 10.1016/j.ijcard.2020.08.070]

8 **Holmes DR**, Reddy VY, Turi ZG, Doshi SK, Sievert H, Buchbinder M, Mullin CM, Sick P; PROTECT AF Investigators. Percutaneous closure of the left atrial appendage *vs* warfarin therapy for prevention of stroke in patients with atrial fibrillation: a randomised non-inferiority trial. *Lancet* 2009; **374**: 534-542 [PMID: 19683639 DOI: 10.1016/S0140-6736(09)61343-X]

9 **Urena M**, Rodés-Cabau J, Freixa X, Saw J, Webb JG, Freeman M, Horlick E, Osten M, Chan A, Marquis JF, Champagne J, Ibrahim R. Percutaneous left atrial appendage closure with the AMPLATZER cardiac plug device in patients with nonvalvular atrial fibrillation and contraindications to anticoagulation therapy. *J Am Coll Cardiol* 2013; **62**: 96-102 [PMID: 23665098 DOI: 10.1016/j.jacc.2013.02.089]

10 **Reddy VY**, Doshi SK, Sievert H, Buchbinder M, Neuzil P, Huber K, Halperin JL, Holmes D; PROTECT AF Investigators. Percutaneous left atrial appendage closure for stroke prophylaxis in patients with atrial fibrillation: 2.3-Year Follow-up of the PROTECT AF (Watchman Left Atrial Appendage System for Embolic Protection in Patients with Atrial Fibrillation) Trial. *Circulation* 2013; **127**: 720-729 [PMID: 23325525 DOI: 10.1161/CIRCULATIONAHA.112.114389]

11 **Viles-Gonzalez JF**, Kar S, Douglas P, Dukkipati S, Feldman T, Horton R, Holmes D, Reddy VY. The clinical impact of incomplete left atrial appendage closure with the Watchman Device in patients with atrial fibrillation: a PROTECT AF (Percutaneous Closure of the Left Atrial Appendage Versus Warfarin Therapy for Prevention of Stroke in Patients With Atrial Fibrillation) substudy. *J Am Coll Cardiol* 2012; **59**: 923-929 [PMID: 22381428 DOI: 10.1016/j.jacc.2011.11.028]

12 **Dukkipati SR**, Holmes DR Jr, Doshi SK, Kar S, Singh SM, Gibson D, Price MJ, Natale A, Mansour M, Sievert H, Houle VM, Allocco DJ, Reddy VY. Impact of Peridevice Leak on 5-Year Outcomes After Left Atrial Appendage Closure. *J Am Coll Cardiol* 2022; **80**: 469-483 [PMID: 35902169 DOI: 10.1016/j.jacc.2022.04.062]

13 **Korsholm K**, Jensen JM, Nørgaard BL, Nielsen-Kudsk JE. Temporal changes and clinical significance of peridevice leak following left atrial appendage occlusion with Amplatzer devices. *Catheter Cardiovasc Interv* 2022; **99**: 2071-2079 [PMID: 35582829 DOI: 10.1002/ccd.30178]

14 **Wang G**, Kong B, Qin T, Liu Y, Huang C, Huang H. Incidence, risk factors, and clinical impact of peridevice leak following left atrial appendage closure with the LAmbre device-Data from a prospective multicenter clinical study. *J Cardiovasc Electrophysiol* 2021; **32**: 354-359 [PMID: 33251673 DOI: 10.1111/jce.14824]

15 **Alkhouli M**, Du C, Killu A, Simard T, Noseworthy PA, Friedman PA, Curtis JP, Freeman JV, Holmes DR. Clinical Impact of Residual Leaks Following Left Atrial Appendage Occlusion: Insights From the NCDR LAAO Registry. *JACC Clin Electrophysiol* 2022; **8**: 766-778 [PMID: 35387751 DOI: 10.1016/j.jacep.2022.03.001]

16 **Lakkireddy D**, Thaler D, Ellis CR, Swarup V, Sondergaard L, Carroll J, Gold MR, Hermiller J, Diener HC, Schmidt B, MacDonald L, Mansour M, Maini B, O'Brien L, Windecker S. Amplatzer Amulet Left Atrial Appendage Occluder Versus Watchman Device for Stroke Prophylaxis (Amulet IDE): A Randomized, Controlled Trial. *Circulation* 2021; **144**: 1543-1552 [PMID: 34459659 DOI: 10.1161/CIRCULATIONAHA.121.057063]

17 **Miller T**, Hana D, Patibandla S, Guzman DB, Avalon JC, Zeb I, Kadiyala M, Mills J, Balla S, Kim C, Lisle M, Kawsara M, Raybuck B, Daggubati R, Sengupta PP, Hamirani YS. Cardiac Computed Tomography Angiography for Device-Related Thrombus Assessment After WATCHMAN FLX™ Occluder Device Implantation: A Single-Center Retrospective Observational Study. *Cardiovasc Revasc Med* 2022; **41**: 35-46 [PMID: 35140053 DOI: 10.1016/j.carrev.2022.01.028]

18 **Tzikas A**, Shakir S, Gafoor S, Omran H, Berti S, Santoro G, Kefer J, Landmesser U, Nielsen-Kudsk JE, Cruz-Gonzalez I, Sievert H, Tichelbäcker T, Kanagaratnam P, Nietlispach F, Aminian A, Kasch F, Freixa X, Danna P, Rezzaghi M, Vermeersch P, Stock F, Stolcova M, Costa M, Ibrahim R, Schillinger W, Meier B, Park JW. Left atrial appendage occlusion for stroke prevention in atrial fibrillation: multicentre experience with the AMPLATZER Cardiac Plug. *EuroIntervention* 2016; **11**: 1170-1179 [PMID: 25604089 DOI: 10.4244/EIJY15M01_06]

19 **Della Rocca DG**, Horton RP, Di Biase L, Bassiouny M, Al-Ahmad A, Mohanty S, Gasperetti A, Natale VN, Trivedi C, Gianni C, Burkhardt JD, Gallinghouse GJ, Hranitzky P, Sanchez JE, Natale A. First Experience of Transcatheter Leak Occlusion With Detachable Coils Following Left Atrial Appendage Closure. *JACC Cardiovasc Interv* 2020; **13**: 306-319 [PMID: 31954677 DOI: 10.1016/j.jcin.2019.10.022]

World Journal of Clinical Cases

Submit a Manuscript: https://www.f6publishing.com

World J Clin Cases 2023 September 6; 11(25): 5863-5869

DOI: 10.12998/wjcc.v11.i25.5863

ISSN 2307-8960 (online)

ORIGINAL ARTICLE

Case Control Study

Application of lesser trochanteric reduction fixator in the treatment of unstable intertrochanteric fractures

Yao-Min Hui, Guang Zeng, Pei-Yi Liu, Bin Chai

Specialty type: Medicine, research and experimental

Provenance and peer review: Unsolicited article; Externally peer reviewed.

Peer-review model: Single blind

Peer-review report's scientific quality classification

Grade A (Excellent): 0
Grade B (Very good): 0
Grade C (Good): C
Grade D (Fair): 0
Grade E (Poor): 0

P-Reviewer: Ghimire R, Nepal

Received: March 30, 2023
Peer-review started: March 30, 2023
First decision: July 3, 2023
Revised: July 5, 2023
Accepted: August 3, 2023
Article in press: August 3, 2023
Published online: September 6, 2023

Yao-Min Hui, Guang Zeng, Pei-Yi Liu, Bin Chai, Department of Orthopedics, Tong Ren Hospital, School of Medicine Shanghai Jiao Tong University, Shanghai 200336, China

Corresponding author: Pei-Yi Liu, MD, PhD, Academic Research, Attending Doctor, Department of Orthopedics, Tong Ren Hospital, School of Medicine Shanghai Jiao Tong University, No. 1111 Xianxia Road, Shanghai 200336, China. liupeiyi_sjtu@163.com

Abstract

BACKGROUND

Closed reduction and internal fixation with intramedullary nails has been widely accepted for treating intertrochanteric fractures.

AIM

To focus on how to avoid displacement of the lesser trochanter in unstable intertrochanteric fractures.

METHODS

We developed a lesser trochanteric reduction fixator for treating intertrochanteric fractures through fixing the lesser trochanter by combining the loop plate through the fixator after reduction by the reducer. Five patients with intertrochanteric fractures treated with the newly developed lesser trochanteric reduction fixator and loop plate combined with intramedullary nails, and 20 patients with intertrochanteric fractures treated with simple intramedullary nails were selected from December 2020 to March 2021.

RESULTS

The postoperative Harris hip score was significantly higher in patients treated with the lesser trochanteric reduction fixator than in patients treated without the lesser trochanteric reduction fixator, which indicated that this lesser trochanteric reduction fixator had a positive impact on rehabilitation of the hip joint after surgery and could significantly improve the quality of life of patients.

CONCLUSION

We fully realize the significance of trochanteric reduction and fixation, namely, reconstruction of structures under pressure, in the treatment of intertrochanteric fractures. As long as the general condition of patients is favorable and they are willing to undergo surgery, fixation of the main fracture end should be performed and the lesser trochanter should be reduced and fixed at the same time.

Key Words: Lesser trochanteric; Intertrochanteric fractures; Reduction fixator; Loop plate; Unstable fractures

Core Tip: After reliable reduction and fixation, a newly developed lesser trochanteric reduction fixator can be introduced into the loop plate through the customized holes, and the loop plate can pass through the muscle space of the lesser trochanter, which can achieve the reduction and fixation of the lesser trochanter. This fixator can improve the quality of reducing the lesser trochanter, and the loop plate can achieve elastic fixation. There is no risk of nail breakage caused by nail fixation.

Citation: Hui YM, Zeng G, Liu PY, Chai B. Application of lesser trochanteric reduction fixator in the treatment of unstable intertrochanteric fractures. *World J Clin Cases* 2023; 11(25): 5863-5869
URL: https://www.wjgnet.com/2307-8960/full/v11/i25/5863.htm
DOI: https://dx.doi.org/10.12998/wjcc.v11.i25.5863

INTRODUCTION

As the population ages, an increase in the incidence of low-energy injuries, such as intertrochanteric fractures induced by trauma-related osteoporosis, has been reported. Based on the Evans classification system, an intertrochanteric fracture can be categorized into the following five types[1]: (1) Type I: Syn-intertrochanteric fractures; non-displaced, stable fractures that account for 11.1% of all intertrochanteric fractures; (2) Type II: Lesser trochanteric fractures, showing mild displacement and stable reduction; stable fractures that account for 17.4% of all intertrochanteric fractures; (3) Type III: Lesser trochanteric comminuted fractures, with the absence of stable reduction; unstable fractures that account for 45.1% of all intertrochanteric fractures; (4) Type IV: Type III combined with greater trochanteric fractures; unstable fractures that account for 20.1% of all intertrochanteric fractures; and (5) Type V: Reverse intertrochanteric fractures, showing a tendency for displacement due to traction of the adductor; unstable fractures which account for 6.3% of all intertrochanteric fractures. Closed reduction and internal fixation using intramedullary nails has been widely accepted for treating intertrochanteric fractures with established efficacy in clinical practice. However, there may be a lack of medial support structure in patients with types II and III intertrochanteric fractures combined with lesser trochanteric fractures. Meanwhile, the iliopsoas muscle and psoas major muscle attach to the lesser trochanter. In the short term, an unfixed lesser trochanter will affect the hip flexion function, and in the long term, it can cause coxa vara. A tendency for coxa vara has been reported after intramedullary fixation of the femur. There are clinical case reports of postoperative nail breakage caused by lateral stress concentration and fracture nonunion or delayed union caused by a bone defect in the medial wall. Currently, it is thought that these cases are related to the local defect caused by displacement of lesser trochanteric fracture fragments. Therefore, in this study, we aimed to focus on exploring an approach that can avoid lesser trochanter displacement in unstable intertrochanteric fractures, reduce the lesser trochanter during surgery, support the medial wall of the proximal femur, and avoid the development of complications.

MATERIALS AND METHODS

Newly developed lesser trochanteric reduction fixator

After consulting the relevant literature and conducting explorations in clinical practice, we developed a lesser trochanteric reduction fixator for treating intertrochanteric fractures through fixing the lesser trochanter by combining the loop plate through the fixator after reduction by the reducer (Figure 1A and B).

We have applied for a patent for the lesser trochanteric reduction fixator for intertrochanteric fractures to the China National Intellectual Property Administration (No. 202122899022.4).

General patient data

Five patients with intertrochanteric fractures treated with the newly developed lesser trochanteric reduction fixator and loop plate combined with intramedullary nails, and 20 patients with intertrochanteric fractures treated with simple intramedullary nails were selected from December 2020 to March 2021 for a 6-mo follow-up comparison.

Treatment methods

Preoperative preparation: Before surgery, all patients underwent complete routine auxiliary examinations. Data collection, measurement, and classification of X-ray and computed tomography imaging of the hip joint were performed. Besides, the diagnosis and treatment of patients complicated with internal medicine diseases were also conducted whenever necessary.

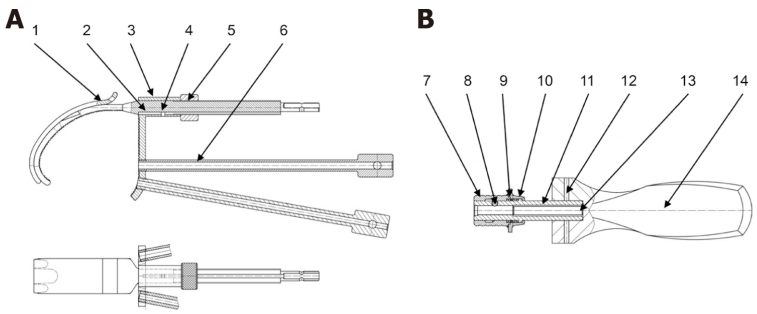

DOI: 10.12998/wjcc.v11.i25.5863

Figure 1 Computer aided design of the newly developed lesser trochanteric reduction fixator. A: Structural schematic diagram of the novel lesser trochanteric reduction fixator for the treatment of intertrochanteric fractures; B: Structural schematic diagram of the handle and connecting rod. 1: Retractor; 2: Grasping rod; 3: Movable pusher; 4: Locating rivet; 5: Movable nut; 6: Drill sleeve; 7: Movable sleeve; 8: Steel ball; 9: Spring; 10: Locking sleeve; 11: Connecting rod; 12: Rivet; 13: Inner core; 14: Handle.

Surgical methods: Surgery was performed under general anesthesia. The patient was placed in a supine position. After being anesthetized, the patient was placed on an orthopedic traction bed. Manual traction reduction was performed, followed by fluoroscopy under a C-arm machine. After at least two qualified doctors confirmed that reduction was achieved, routine disinfection and draping were performed. An opening of about 4-5 cm was made on the proximal femur, and the lesser trochanteric reduction fixator was placed to reduce the lesser trochanter and maintain the fixed state (Figure 2). Proximal femoral nail-anti-rotation Asia II or integrated cephalomedullary nail placement was completed by routine opening at fixed points of the femur. The lesser trochanteric reduction fixator was introduced into the loop plate through a guiding hole. Subsequently, the button end of the loop plate was placed at the apex of the lesser trochanter and was tightened. Then, the newly developed lesser trochanteric reduction fixator was gradually loosened to observe whether there was any displacement of the lesser trochanter. After the position was stable, the loop plate was fixed to complete the surgery.

Postoperative treatment: After surgery, antibiotics were administered as per the requirements, and anticoagulants were administered as appropriate based on venous thromboembolism scores. Physiatrists guided the patients to conduct passive movement 6-8 h after surgery, and to actively move the knee joint and conduct quadriceps femoris function exercise 24 h after surgery. From four weeks after surgery, patients walked with a partial weight-bearing walking aid with the permission of the attending physician, who judged the timing to walk with full weight-bearing according to the postoperative image data.

Statistical analysis

IBM SPSS 26 was used for data analyses. An independent samples *t*-test was used for comparison of means between groups. A P value of < 0.05 was considered statistically significant.

RESULTS

Patient grouping

The patients were divided into either an experimental group or a control group. The experimental group comprised five patients (two males and three females; age range, 51-70 years, with an average age of 60.2 years) who experienced intertrochanteric fractures and were treated using the lesser trochanteric reduction fixator, loop plates, and intramedullary nails. These five cases included three cases with the left side affected and two cases with the right side affected.

The control group comprised 20 patients (4 males and 16 females; age range, 51-95 years, with an average age of 83.9 years) who experienced intertrochanteric fractures and were treated using simple intramedullary nails. These 20 cases included 13 cases with the left side affected and 7 cases with the right side affected.

Patient characteristics

Bone mineral density, age, fracture type, preoperative duration, operative duration, intraoperative blood loss, hospital stay, Harris hip score[2], and proximal incision length were compared between patients who were treated with and without the lesser trochanteric reduction fixator.

No significant difference was noted in age, fracture type, bone mineral density, preoperative duration, operative duration, or hospital stay between the two groups ($P > 0.05$). The postoperative Harris hip score in patients who were treated with the lesser trochanteric reduction fixator was significantly higher than that in patients who were treated without the lesser trochanteric reduction fixator ($P < 0.05$), which suggested that the lesser trochanteric reduction fixator had a positive impact on rehabilitation of the hip joint after surgery and could significantly enhance the quality of life of patients. In addition, the proximal incision in patients who were treated with the lesser trochanteric reduction fixator was larger than that in patients who were treated without the lesser trochanteric reduction fixator ($P < 0.05$). However, no

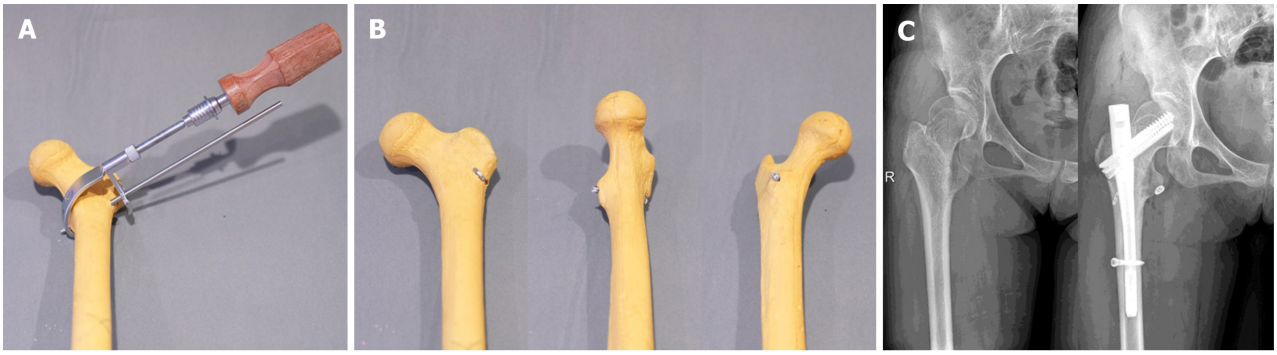

DOI: 10.12998/wjcc.v11.i25.5863

Figure 2 Example diagram of the novel lesser trochanteric reduction fixator for treatment of intertrochanteric fractures. A: Simulation of fixed position of a fixator; B: Simulation of a loop plate through the guiding hole; C: Imaging data of surgical internal fixation.

significant difference was noted in the intraoperative blood loss between the two groups ($P > 0.05$) (Table 1).

DISCUSSION

From the perspective of mechanics, the biomechanical structure of the proximal femur is similar to that of a truss, and the calcar femorale receives support from the bony trabeculae in the posterior medial cortex of the upper femur, which is mainly the trochanter. The calcar femorale, the upper part of the femur, and three bundles of bony trabeculae form a reasonable weight-bearing system. From the biomechanical perspective, this system is the most important part to resist buckling and varus stress.

A defect in the lesser trochanter significantly compromises the biomechanical properties of the upper part of the femur. Biomechanical experiments have shown that defects in the lesser trochanter and extensive defects in the femur could induce obvious stress concentration in the upper part of the femur, increase the load strain and load displacement of the femoral head, reduce the stiffness of the femur, and impair the torsional strength and stiffness, which could decrease the mechanical performance of the femur significantly to resist external load and torsion. Severe torsional instability and failure of anti-deformation ability may cause hip instability. Defects in the lesser trochanter and extensive defects in the femur could induce femoral stress concentration. The strength could increase by 31% and 37%, respectively; femoral stiffness could decrease by 29% and 51%, respectively; and torsional strength of the femur could decrease by 33% and 54%, respectively. After fixing the lesser trochanter, stress concentration could decrease by 25% and 28%, respectively; stiffness could increase by 20% and 31%, respectively; and torsional strength could increase by 23% and 29%, respectively. Thus, significant restoration of the mechanical properties could be achieved.

Chen *et al*[3] conducted a mechanical analysis and test of type III fractures. The results showed that the average maximum load on the upper part of the femur was increased by 57% after anatomical reduction and fixation of a larger posterior medial bone block; however, the increase in the average maximum load on the upper part of the femur was 17% after anatomical reduction and fixation of a smaller posterior medial bone block. Therefore, reduction and fixation of the lesser trochanter is the key to mechanical stability of fractures. Domingo *et al*[4] simulated the femoral head under vertical compression by performing relevant experimental analysis. Besides, they measured the change in the force on the medial side of the lesser trochanter. Results showed that tensile stress on the medial side of the femoral head was obviously increased, and it reached 60% after the lesser trochanter was obviously displaced or defective. Therefore, they stated that displacement of the lesser trochanter could have a significant impact on surgical efficacy. Liu *et al*[5] suggested that the lesser trochanter is located under the calcar femorale, which is the medial cortex extending downwards from the femoral neck to the lesser trochanter. Its main function comprised ensuring that the local composition could bear a higher pressure and could transmit the force evenly to the medial femur. If the fracture affected the lesser trochanter or calcar femorale, displacement of local fracture blocks could occur, which may cause disruption of the normal physiological structure of the medial side, thus inducing coxa vara after surgery. Park *et al*[6] believed that if there was a defect in the lesser trochanter, the contralateral tension could significantly increase. In case of type II intertrochanteric fractures with lesser trochanteric defects, the contralateral tension could increase by 60%, and in case of type IV intertrochanteric fractures with lesser trochanteric defects, the contralateral tension could increase by 370%. Therefore, there may be an increase in the risk of fracture displacement, internal fixation loosening, rupture, femoral head cutting, and coxa vara as a result of only using internal fixation materials to maintain the weight load.

Reduction of the lesser trochanter is one of the most important key factors affecting fracture healing. Currently, many scholars believe that performing reduction of the lesser trochanter and restoring its anatomical function and shape are an optimal option.

Reduction of the lesser trochanter and reconstruction of calcar femorale are important for the treatment of intertrochanteric fractures. If reduction of the lesser trochanter is achieved by extensive soft tissue stripping, there will be disruption of the local blood supply to a certain extent, which would increase the fracture healing time. Although damage to the local blood supply will be reduced if the intertrochanteric fracture is fixed with a steel wire, the steel wire will

Table 1 Comparison of characteristics of patients treated with and without the lesser trochanteric reduction fixator

	Simple intramedullary nails	Lesser trochanteric reduction fixators	*P* value
Sex			
Male	4	3	
Female	16	2	
Age (yr)	83.95 ± 9.539	60.2 ± 7.463	0.066
Fracture location			
Left	13	3	
Right	7	2	
Bone mineral density	-1.635 ± 1.214	-1.6 ± 1.474	0.956
Preoperative duration (d)	3.6 ± 2.414	2.6 ± 0.894	0.378
Operation method			
interTAN	6	5	
PFNA	14	0	
Operative duration (min)	43.95 ± 17.251	69.4 ± 37.031	0.202
Intraoperative blood loss (mL)	81.5 ± 81.517	160 ± 54.772	0.055
Hospital stay (d)	12.85 ± 7.050	11.2 ± 3.768	0.622
Harris hip score	86.865 ± 5.653	91.94 ± 2.639	0.011
Proximal incision length (cm)	4.925 ± 0.293	6 ± 0.3536	0.000

interTAN: Integrated cephalomedullary nail; PFNA: Proximal femoral nail-anti-rotation Asia.

affect the growth of the callus and the stability will not be favorable[7-8]. If the intertrochanteric fracture is fixed with the newly developed lesser trochanteric reduction fixator combined with loop plates, damage to the blood supply will be avoided and reliable fixation will also be achieved, which will not hamper the growth of the callus and can provide certain biological tension for elastic fixation.

There are some advantages of the newly developed lesser trochanteric reduction fixator: (1) After reliable reduction and fixation, the fixator can be introduced into the loop plate through customized holes, and the loop plate can pass through the muscle space of the lesser trochanter, which can achieve reduction and fixation of the lesser trochanter; (2) This fixator can improve the quality of reduction of the lesser trochanter, and the loop plate can achieve elastic fixation; and (3) The risk of nail breakage caused by nail fixation is minimized.

CONCLUSION

We fully realize the significance of trochanteric reduction and fixation, namely, reconstruction of structures under pressure, in the treatment of intertrochanteric fractures. As long as the general condition of patients is favorable and they are willing to undergo surgery, fixation should be carried out at the main fracture end and the lesser trochanter should be reduced and fixed at the same time. Some foreign scholars have proposed another method for performing nail fixation through a medial incision. However, as a medial incision causes greater trauma, we advocate that the lateral intramedullary nail incision should be appropriately lengthened and the soft tissue should be properly stripped from the anterior and posterior aspects of the greater trochanter, followed by placement of the newly developed lesser trochanteric reduction fixator.

ARTICLE HIGHLIGHTS

Research background

We invented a new device for better treatment of femoral intertrochanteric fractures. During the treatment of intertrochanteric fractures, we fully realize the significance of trochanteric reduction and fixation, namely, reconstruction of structures under pressure.

Research motivation

As long as the general condition of patients is suitable and they are willing to undergo surgery, fixation should be carried out at the main fracture end and the lesser trochanter should be reduced and fixed at the same time. Some foreign scholars have proposed another method for performing nail fixation through a medial incision. However, as a medial incision causes larger trauma, we advocate that the lateral intramedullary nail incision shall be appropriately lengthened and the soft tissue shall be properly stripped from the anterior and posterior aspects of the greater trochanter, followed by placement of the newly developed lesser trochanteric reduction fixator.

Research objectives

We aimed to focus on how to avoid displacement of the lesser trochanter in unstable intertrochanteric fractures.

Research methods

IBM SPSS 26 was used for data analyses. An independent samples *t*-test was used for comparison of means between groups. A P value of < 0.05 was considered statistically significant.

Research results

The postoperative Harris hip score in patients who were treated with the lesser trochanteric reduction fixator was significantly higher than that in patients who were treated without the lesser trochanteric reduction fixator ($P < 0.05$), which indicated that the lesser trochanteric reduction fixator had a positive impact on rehabilitation of the hip joint after surgery and could significantly improve the quality of life of patients. In addition, the proximal incision in patients who were treated with the lesser trochanteric reduction fixator was larger than that in patients who were treated without the lesser trochanteric reduction fixator ($P < 0.05$).

Research conclusions

We fully realize the significance of trochanteric reduction and fixation, namely, reconstruction of structures under pressure, in the treatment of intertrochanteric fractures. As long as the general condition of patients is favorable and they are willing to undergo surgery, fixation should be carried out at the main fracture end and the lesser trochanter should be reduced and fixed at the same time. Some foreign scholars have proposed another method for performing nail fixation through a medial incision. However, as a medial incision causes greater trauma, we advocate that the lateral intramedullary nail incision should be appropriately lengthened and the soft tissue should be properly stripped from the anterior and posterior aspects of the greater trochanter, followed by placement of the newly developed lesser trochanteric reduction fixator.

Research perspectives

This newly developed lesser trochanteric reduction fixator has some advantages: (1) After reliable reduction and fixation, this fixator can be introduced into the loop plate through the customized holes, and the loop plate can pass through the muscle space of the lesser trochanter, which can achieve reduction and fixation of the lesser trochanter; and (2) This fixator can improve the quality of reduction of the lesser trochanter, and the loop plate can achieve elastic fixation. There is no risk of nail breakage caused by nail fixation.

ACKNOWLEDGEMENTS

We thank Medjaden Inc. for scientific editing of this manuscript.

FOOTNOTES

Author contributions: Liu PY designed the study, wrote the main manuscript text, and prepared the figures; Hui YM prepared the utility model patents tool for surgery; Zeng G prepared the surgery; Chai B collected the data and performed the statistical analysis; all authors have read and approved the final manuscript.

Institutional review board statement: The Institutional Review Board of the TongRen Hospital, School of Medicine Shanghai Jiao Tong University approved this study, and it was conducted in accordance with the Declaration of Helsinki. All participants provided written informed consent before their data were stored in our hospital database and used for study purposes.

Informed consent statement: All participants provided written informed consent before their data were stored in our hospital database and used for study purposes.

Conflict-of-interest statement: The authors declare no competing interests for this article.

Data sharing statement: The generated and analysed datasets are available from the corresponding author upon reasonable request.

STROBE statement: The authors have read the STROBE Statement—checklist of items, and the manuscript was prepared and revised

according to the STROBE Statement—checklist of items.

Country/Territory of origin: China

ORCID number: Yao-Min Hui 0000-0002-1815-875X; Pei-Yi Liu 0000-0003-1072-3889.

S-Editor: Lin C
L-Editor: Wang TQ
P-Editor: Zhang YL

REFERENCES

1 **Evans EM**. The treatment of trochanteric fractures of the femur. *J Bone Joint Surg Br* 1949; **31B**: 190-203 [PMID: 18150534]
2 **Harris WH**. Traumatic arthritis of the hip after dislocation and acetabular fractures: treatment by mold arthroplasty. An end-result study using a new method of result evaluation. *J Bone Joint Surg Am* 1969; **51**: 737-755 [PMID: 5783851]
3 **Chen WH**, Guo WX, Gao SH, Wei QS, Li ZQ, He W. Arthroplasty *vs* proximal femoral nails for unstable intertrochanteric femoral fractures in elderly patients: A systematic review and meta-analysis. *World J Clin Cases* 2021; **9**: 9878-9888 [PMID: 34877326 DOI: 10.12998/wjcc.v9.i32.9878]
4 **Domingo LJ**, Cecilia D, Herrera A, Resines C. Trochanteric fractures treated with a proximal femoral nail. *Int Orthop* 2001; **25**: 298-301 [PMID: 11794263 DOI: 10.1007/s002640100275]
5 **Liu X**, Liu Y, Pan S, Cao H, Yu D. Does integrity of the lesser trochanter influence the surgical outcome of intertrochanteric fracture in elderly patients? *BMC Musculoskelet Disord* 2015; **16**: 47 [PMID: 25879412 DOI: 10.1186/s12891-015-0492-7]
6 **Park SY**, Yang KH, Yoo JH, Yoon HK, Park HW. The treatment of reverse obliquity intertrochanteric fractures with the intramedullary hip nail. *J Trauma* 2008; **65**: 852-857 [PMID: 18849802 DOI: 10.1097/TA.0b013e31802b9559]
7 **Kim GM**, Nam KW, Seo KB, Lim C, Kim J, Park YG. Wiring technique for lesser trochanter fixation in proximal IM nailing of unstable intertrochanteric fractures: A modified candy-package wiring technique. *Injury* 2017; **48**: 406-413 [PMID: 27887702 DOI: 10.1016/j.injury.2016.11.016]
8 **Cho SH**, Lee SH, Cho HL, Ku JH, Choi JH, Lee AJ. Additional fixations for sliding hip screws in treating unstable pertrochanteric femoral fractures (AO Type 31-A2): short-term clinical results. *Clin Orthop Surg* 2011; **3**: 107-113 [PMID: 21629470 DOI: 10.4055/cios.2011.3.2.107]

World Journal of Clinical Cases

Submit a Manuscript: https://www.f6publishing.com

World J Clin Cases 2023 September 6; 11(25): 5870-5877

DOI: 10.12998/wjcc.v11.i25.5870

ISSN 2307-8960 (online)

ORIGINAL ARTICLE

Case Control Study

Risk factors for post-traumatic stress disorder among young and middle-aged cancer patients in the intensive care unit: A case-control study

Lei Chen, Guo-Zhou Wang, Yuan-Yuan Chi, Jing Zhao

Specialty type: Nursing

Provenance and peer review: Unsolicited article; Externally peer reviewed.

Peer-review model: Single blind

Peer-review report's scientific quality classification

Grade A (Excellent): 0
Grade B (Very good): B
Grade C (Good): C
Grade D (Fair): 0
Grade E (Poor): 0

P-Reviewer: Kadogami D, Japan; Ruane PT, United Kingdom

Received: May 21, 2023
Peer-review started: May 21, 2023
First decision: June 1, 2023
Revised: June 13, 2023
Accepted: August 9, 2023
Article in press: August 9, 2023
Published online: September 6, 2023

Lei Chen, Intensive Care Unit, Tianjin Medical University Cancer Institute and Hospital, National Clinical Research Center for Cancer, Tianjin's Clinical Research Center for Cancer, Tianjin 300060, China

Guo-Zhou Wang, Yuan-Yuan Chi, Department of Intensive Care Unit, Tianjin Medical University Cancer Institute and Hospital, National Clinical Research Center for Cancer, Tianjin's Clinical Research Center for Cancer, Tianjin 300060, China

Jing Zhao, Nursing Department, Tianjin Medical University Cancer Institute and Hospital, National Clinical Research Center for Cancer, Tianjin's Clinical Research Center for Cancer, Tianjin 300060, China

Corresponding author: Jing Zhao, MD, RN, Deputy Director, Department of Nursing, Tianjin Medical University Cancer Institute and Hospital, National Clinical Research Center for Cancer, Tianjin's Clinical Research Center for Cancer, West Huan-Hu Road, Ti Yuan Bei, Hexi District, Tianjin 300060, China. chl-415@163.com

Abstract

BACKGROUND

Young and middle-aged cancer patients in intensive care unit (ICU) often suffer from stress and pressure, causing huge physical and mental damage. Currently, there is few research on post-traumatic stress disorder (PTSD) among young and middle-aged cancer patients in ICU in China, and the psychological status of patients who have experienced both cancer development and ICU stay is still unclear.

AIM

To explore the risk factors for PTSD in young and middle-aged patients with cancer in ICU.

METHODS

Using convenient sampling method, we enrolled 150 young and middle-aged patients with cancer who were admitted to the ICU of our center during the period from July to December 2020. The general data of the patients and PTSD-related indicators were collected. The Impact of Event Scale-Revised (IES-R) was used for assessing PTSD one month after the discharge from the ICU. Binary

Logistic regression analysis was performed to assess the independent risk factors for PTSD in these patients.

RESULTS

Among these 150 patients, 32 (21.33%) were found to be with PTSD. Binary Logistic regression analysis revealed that factors significantly associated with PTSD among young and middle-aged patients with cancer in ICU included monthly income (OR = 0.24, *P* = 0.02), planned transfers (OR = 0.208, *P* = 0.019), and Acute Physiology and Chronic Health Evaluation (APACHE II) score (OR = 1.171, *P* = 0.003).

CONCLUSION

The low monthly income, unplanned transfers, and increased APACHE II score are the risk factors for PTSD in young and middle-aged patients with cancer in ICU.

Key Words: Post-traumatic stress disorder; Cancer; Intensive care unit; Risk factors

Core Tip: In this study, we investigated and analyzed the incidence of post-traumatic stress disorder (PTSD) and related risk factors in young and middle-aged cancer patients in intensive care unit. We found that young and middle-aged cancer patients are prone to suffer from more serious psychological pain and often bear greater psychological burdens, which cause additional damage to patients' physical and mental health. Therefore, understanding the occurrence and influencing factors for PTSD is crucial for these patients.

Citation: Chen L, Wang GZ, Chi YY, Zhao J. Risk factors for post-traumatic stress disorder among young and middle-aged cancer patients in the intensive care unit: A case-control study. *World J Clin Cases* 2023; 11(25): 5870-5877
URL: https://www.wjgnet.com/2307-8960/full/v11/i25/5870.htm
DOI: https://dx.doi.org/10.12998/wjcc.v11.i25.5870

INTRODUCTION

Malignant tumors have become major causes of harm to the health the Chinese residents. In 2015, there were approximately 3.93 million new cancer cases across China, with a significant increase in the incidence rate among individuals aged > 40 years, and with a highest number of cases in those aged 60-64[1]. The diagnosis of a malignant tumor and the accompanying physical and psychological symptoms bring both physical and mental pain to the patients, which may ultimately result in post-traumatic stress disorder (PTSD)[2-4]. PTSD is a long-lasting psychiatric disorder that occurs or is delayed after an individual experiences or witnesses an unusually catastrophic or threatening event[5]. Several studies [6-8] have shown that tumors have been identified as a source of traumatic stress, and the prevalence of cancer-related PTSD is estimated to range from 7.3% to 15.3%[9]. As young and middle-aged people play crucial roles in families and society, once diagnosed with cancer, they often have to face stress from a variety of aspects including illness, family, work place, and financial burden[10,11]. Research indicates that young and middle-aged cancer patients suffer more serious emotional pain and often bear greater psychological burden, which leads to increased medical costs[12] and, even worse, risk of suicide[13]. Evidence has shown that cancer patients in intensive care unit (ICU) have more serious mental problems such as anxiety, fear, and loneliness, and the prevalence of PTSD among survivors within the first 6 mo after discharge was 25%[14-16]. Unfortunately, few literatures in China have described PTSD in young and middle-aged patients who have experienced both malignancy development and ICU admission. Here we investigated the occurrence of PTSD and its relevant risk factors in young and middle-aged cancer patients in the ICU, in an attempt to provide new evidence for the development of effective prevention and treatment strategies.

MATERIALS AND METHODS

Study design and setting

A case-control study was conducted from July 2020 to December 2020, at the Department of Intensive Care Unit of Tianjin Medical University Cancer Institute and Hospital.

Subjects

Using convenient sampling method, we enrolled young and middle-aged patients with cancer who were admitted to the ICU of our center. The inclusion criteria were: (1) Aged 18-65 years; (2) with a diagnosis of cancer confirmed by clinical, imaging, and pathological examinations; (3) with the ability to communicate; and (4) signed informed consent documents and participated in the study voluntarily. The exclusion criteria were: (1) Patients with severe mental illness or cognitive

impairment; (2) those with drop-out, withdrawal, or loss to the follow-up; and (3) recent sufferings from other major life events or traumatic events.

Determination of sample size

Kendall's statistic[17] was applied for sample size estimation in this observational study. The sample size was set to be 5-10 times greater than the number of variables. Since patients might fail to respond to the survey or get lost during follow-up, an additional 20% of the sample size was added. Thus, the final sample size of this study was determined to be 167 cases.

Research tools

General information questionnaire: This self-designed questionnaire covers data including patients' age, gender, marital status, education level, disease diagnosed, disease treatments, and psychosocial factors.

Impact of Event Scale-Revised: The Impact of Event Scale—Revised (IES-R) was developed by Weiss and Marmar in 1997 based on the DSM-IV (Diagnostic and Statistical Manual of Mental Disorders, 4th edition) criteria and the Horowitz's Impact of Event Scale (IES)[18]. It is mostly used to assess the symptoms and severity of PTSD in survivors after critical care[13]. Bienvenu *et al*[19]. Validated the performance of IES-R and concluded that IES-R was a useful tool in detecting PTSD symptoms in patients discharged from the ICU. The Chinese version of the IES-R was revised by Guo *et al*[20], and has a Cronbach's α coefficient of 0.89. This 22-item scale is divided into three dimensions including intrusion, avoidance, and hyperarousal. For each item, participants respond on a 5-point Likert scale ranging from point 0 "Never" to point 4 "Always", and a higher score indicates more severe PTSD symptoms. It has a cut-off score of 33: A total score of ≥ 33 denotes positive PTSD symptoms, whereas a total score of < 33 indicates negative PTSD symptoms[21].

Data collection

According to the literature review[9], a diagnosis of PTSD can be made if the relevant symptoms last more than one month. In the present study, patients who met the inclusion criteria were surveyed by the investigators *via* telephone one month after ICU discharge. The surveys typically lasted 10–15 min. All the investigators had passed China's national counselor level-3 examination and had certain clinical experience and good communication skills. Researchers collected general information about patients from the Hospital Information System and established good patient-consultant relationships during the patient's stay in the ICU. The surveys were conducted after informing the patients of the purpose and values of this survey and obtaining their content. Double data entry was applied to ensure the quality of the responses.

Statistical analysis

All the statistical analyses were performed using the SPSS 19.0 software package (IBM Corporation, Somers, NY, United States). All tests were two-sided, and a P value of < 0.05 was considered statistically significant. The measurement data are expressed as mean ± standard deviation (mean ± SD) or medians/quartiles. The independent t test for two samples was used for the comparisons of normally distributed measurement data, and the rank sum test was used for non-normally distributed ones. Count data are described by frequency and rate, and intergroup comparisons were performed by chi-square test or Fisher's exact test. Risk factors for PTSD in young and middle-aged cancer patients in the ICU were firstly screened using univariate analysis, and then the significant variables were included in a binary Logistic regression model for further analysis. The forest plots were created using GraphPad Prism 8.0 software (GraphPad Software Inc., San Diego, CA, United States).

RESULTS

Subjects enrolled

A total of 169 patients were included in this study, among whom 150 patients entered the final analysis. Nineteen patients were ruled out due to the following reasons: loss to telephone follow-up (n = 6); died after discharge (n = 6); lost after transfer to other hospitals (n = 4); and withdrew voluntarily during the study period (n = 3).

Univariate analysis of PTSD and its risk factors in young and middle-aged cancer patients in the ICU 1 mo after discharge from ICU

PTSD occurred in 32 of the 150 included patients, yielding an incidence rate of 21.33%, which was consistent with the results reported in a previous study[22]. Nine influencing factors were statistically significant: gender, monthly income, use of analgesics, physical restraint, APACHEII score, family burden, unplanned transfers, tracheal intubation, and duration of ICU admission (Table 1).

Multivariate Logistic regression analysis of risk factors for PTSD in young and middle-aged cancer patients in the ICU

With the occurrence of PTSD as the dependent variable, the factors that were statistically significant in the univariate analysis were assigned as independent variables. An unconditional binary multivariate Logistic regression analysis was performed, as shown in Table 2.

Table 1 Univariate analysis of independent variables between post-traumatic stress disorder (PTSD)-positive and PTSD-negative patients

Patient information		PTSD-positive group	PTSD-negative group	χ^2/Z	*P* value
Gender	Males	11	64	3.972[a]	0.046
	Females	21	54		
Age (yr)		58 (53.25, 61)	59 (54, 62)	-1.306[b]	0.192
Marital status	Unmarried	1	31		0.213[c]
	Married	0	118		
Place of residence	Rural	11	39	0.153[a]	0.927
	Suburban	4	18		
	Urban	17	61		
Education level	Elementary school and below	4	21	0.554[a]	0.799
	Middle or high school	17	61		
	College and above	11	36		
Monthly income	≤ 3000 *yuan*	0	9	7.537[a]	0.024
	3000-6000 *yuan*	14	71		
	> 6000 *yuan*	18	38		
History of trauma	Yes	6	29	0.478[a]	0.639
	None	26	89		
Hypertension	Yes	10	44	0.398[a]	0.544
	None	22	74		
Diabetes	Yes	7	20	0.414[a]	0.604
	None	25	98		
Smoking	Yes	16	41	2.486[a]	0.15
	None	16	77		
Alcohol consumption	Yes	12	25	3.605[a]	0.067
	None	20	93		
Fertility	With children	29	116		0.065[c]
	Without children	3	2		
Use of sedatives	Yes	29	98		0.41[c]
	None	3	20		
Use of analgesics	Yes	28	67	10.23[a]	0.002
	None	4	51		
Physical restraint	Yes	23	42	13.495[a]	< 0.001
	None	9	76		
Sputum suctioning	Yes	18	45	3.391[a]	0.073
	None	14	73		
Use of glucocorticoids	Yes	3	29	3.466[a]	0.087
	None	29	89		
APACHE II score		16.5 (13.25, 21)	9 (6.75, 14)	-5.38[b]	< 0.001
Family burden	Yes	25	67	4.836[a]	0.04
	None	7	51		

Family breadwinner	Yes	6	13		0.243[c]
	No	26	105		
Planned transfers	Yes	6	72	18.018[a]	< 0.001
	No	26	46		
Tracheal intubation	Yes	24	64	4.475[a]	0.043
	No	8	54		
Length of ICU stay		147 (115.375, 205.25)	67 (42.875, 114.25)	-5.366[b]	< 0.001

[a]Chi-square test.
[b]Z value.
[c]Fisher's exact test. APACHE II: Acute Physiology and Chronic Health Evaluation; ICU: Intensive care unit; PTSD: Post-traumatic stress disorder.

Table 2 Value assignment for factors potentially related to post-traumatic stress disorder

Factors	Variables	Assignment methods
Occurrence of PTSD	Y	PTSD-negative = 0, PTSD-positive = 1
Gender	X_1	Male = 0, Female = 1
Monthly income,	X_2	≤ 3000 = 0, 3000 – 6000 = 1, > 6000 = 2
Use of analgesics	X_3	No = 0, Yes = 1
Physical restraint	X_4	No =0, Yes= 1
APACHE II score	X_5	Actual measurement value
Family burden	X_6	No = 0, Yes = 1
Planned transfers	X_7	No = 0, Yes = 1
Tracheal intubation	X_8	No = 0, Yes = 1
Length of ICU stay	X_9	Actual measurement value

APACHE II: Acute Physiology and Chronic Health Evaluation; ICU: Intensive care unit; PTSD: Post-traumatic stress disorder.

Binary Logistic regression analysis showed that monthly income, APACHEII score, and planned transfers were risk factors for PTSD in young and middle-aged cancer patients in the ICU. Hosmer-Lemeshow test for the PTSD risks in the ICU patients showed a *P* value of 0.265, suggesting that the binary Logistic regression model established in the present study fit well with the real-world data and could reliably reflect the relationship among the variables (Figure 1).

DISCUSSION

In the present study, patients with an unplanned transfer to the ICU were those who experienced unexpected acute deterioration of their condition during the treatment process. As shown by Logistic regression analysis, the incidence of PTSD in the planned transfer subgroup was 0.208 times that of the incidence in the unplanned transfer subgroup, suggesting that PTSD is more likely to occur after unplanned transfers. It may be explained that the planned ICU patients have been informed about their admissions in advance and therefore have milder stress response. Evidence shows that patients who were unfamiliar with their surroundings and had more fear memories, also had higher PTSD scores[23]. In the present study, patients in the unplanned transfer subgroup felt lonely and panic when they suddenly came to an unfamiliar environment and were not accompanied by their families; meanwhile, the individual psychological response to ICU admission due to disease deterioration can also aggravate their PTSD symptoms. Therefore, adequate psychological care should be offered to unplanned ICU patients to alleviate their anxiety.

Young and middle-aged adults are in the prime of their lives, and they are often the primary breadwinners of their families. In our present study, regression analysis showed that low monthly income was a risk factor for the occurrence of PTSD in young and middle-aged cancer patients in the ICU, as already suggested by Liu *et al*[24]. Treatment expenditure is a major concern among cancer patients. Young and middle-aged cancer patients with low monthly family income typically play the most important roles in their families, and the cost of ICU admission is often much higher than that of a general ward. Thus, the dual economic and psychological pressure can be even more torturous. Patients may feel guilty

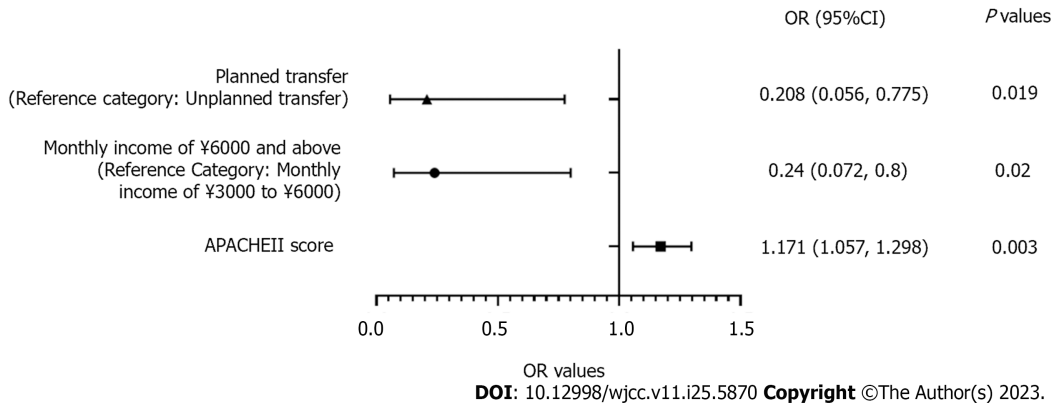

DOI: 10.12998/wjcc.v11.i25.5870

Figure 1 A forest plot based on the Logistic regression analysis of factors associated with the occurrence of post-traumatic stress disorder. APACHE II: Acute Physiology and Chronic Health Evaluation.

and self-blaming to their family members, and some even lose confidence in the future and request to give up the treatment; suicidal behaviors may occur[25,26]. These negative emotions make it difficult for patients to adjust their psychological stress levels, and patients become more susceptible to emotional disorders that can lead to PTSD. Therefore, it is important to carefully observe the body language and facial expressions of these patients and learn their innermost thoughts in a timely manner. Efforts should be made to encourage the patients and stop their worries, helping them to regain confidence in their future life and thus reduce the occurrence of PTSD after discharge.

The APACHEII score is calculated within 24 h after ICU admission and is used to for assess disease severity and predict treatment outcomes[27]. In the present study, cancer patients in the ICU with higher APACHEII scores were more likely to have PTSD-positive symptoms, which was consistent with the findings of Ye *et al*[28]. In fact, patients with advanced cancer are at higher risk of disease deterioration or even life-threatening events at any time during a specific treatment process, which will aggravate their anxiety, depression, and other disturbing emotions. Research has shown that negative emotions such as anxiety and depression were positively correlated with the occurrence of PTSD[29]. Therefore, early interventions targeting the psychological problems of critically ill patients should be offered to reduce the risk of long-term PTSD[30].

There are some limitations in this study. First, as a single-center study, its findings may not represent the clinical characteristics of the cancer patients in ICUs at hospitals of different levels in different regions. Second, long-term follow-up was not carried out due to the limited study period, and some risk factors were not analyzed. Third, limited by the budget, we followed up our patients only *via* telephone, and no customized clinical interviews on PTSD diagnosis by clinical professionals were arranged. In future, we will further screen PTSD patients by this method in multi-center large-sample studies.

CONCLUSION

PTSD in young and middle-aged cancer patients in the ICU can lead to varying degrees of psychological distress and mental disorders, which can seriously reduce patients' quality of life after hospital discharge. Without timely diagnosis and management, these problems can further affect the long-term prognosis of the patients. It was found in our study that low monthly income, unplanned transfers, and increased APACHE II score were the risk factors for PTSD in young and middle-aged cancer patients in the ICU. Early identification and effective preventive interventions may help to reduce the occurrence of PTSD and improve the quality of life in this population.

ARTICLE HIGHLIGHTS

Research background

Young and middle-aged cancer patients in intensive care unit (ICU) often suffer from stress and pressure from many aspects, causing huge physical and mental damage. Currently, there is few research on post-traumatic stress disorder (PTSD) among young and middle-aged cancer patients in ICU in China, and the psychological status of patients who have experienced both cancer development and ICU stay is still unclear.

Research motivation

Few literatures in China have described PTSD in young and middle-aged patients who have experienced both malignancy development and ICU admission. Here we investigated the occurrence of PTSD and its relevant risk factors in young and middle-aged cancer patients in the ICU, in an attempt to provide new evidence for the development of effective prevention and treatment strategies.

Research objectives
To explore the risk factors for PTSD in young and middle-aged patients with cancer in ICU.

Research methods
Using convenient sampling method, we enrolled 150 young and middle-aged patients with cancer who were admitted to the ICU of our center during the period from July to December 2020. The general data of the patients and PTSD-related indicators were collected. The Impact of Event Scale-Revised (IES-R) was used for assessing PTSD one month after the discharge from the ICU. Binary Logistic regression analysis was performed to assess the independent risk factors for PTSD in these patients.

Research results
Among these 150 patients, 32 (21.33%) were found to have PTSD. Binary Logistic regression analysis revealed that factors significantly associated with PTSD among young and middle-aged patients with cancer in ICU included monthly income (OR = 0.24, P = 0.02), planned transfers (OR = 0.208, P = 0.019), and Acute Physiology and Chronic Health Evaluation (APACHE II) score (OR = 1.171, P = 0.003).

Research conclusions
PTSD in young and middle-aged cancer patients in the ICU can lead to varying degrees of psychological distress and mental disorders, which can seriously reduce patients' quality of life after hospital discharge. Without timely diagnosis and management, these problems can further affect the long-term prognosis of the patients. It was found in our study that low monthly income, unplanned transfers, and increased APACHE II score were the risk factors for PTSD in young and middle-aged cancer patients in the ICU.

Research perspectives
Young and middle-aged cancer patients suffer from more serious psychological pain and often bear greater psychological burdens, which cause additional damage to patients' physical and mental health. Therefore, understanding the occurrence and influencing factors of PTSD is crucial for these patients.

FOOTNOTES

Author contributions: Chen L designed the study; Chen L and Wang GZ analyzed the data and wrote the manuscript; Chi YY and Wang GZ performed the research; Zhao J supervised the study. All authors have read and approved the final manuscript.

Institutional review board statement: The study was reviewed and approved by the Medical Ethics Committee of Tianjin Medical University Cancer Institute and Hospital (Approval No. bc2023050).

Informed consent statement: All study participants, or their legal guardian, provided informed written consent prior to study enrollment.

Conflict-of-interest statement: No conflict of interest has been declared by the authors.

Data sharing statement: No additional data are available.

STROBE statement: The authors have read the STROBE Statement—checklist of items, and the manuscript was prepared and revised according to the STROBE Statement—checklist of items.

Country/Territory of origin: China

ORCID number: Lei Chen 0009-0005-8054-2639; Guo-Zhou Wang 0000-0001-9820-8202; Jing Zhao 0009-0009-5127-1568.

S-Editor: Liu JH
L-Editor: A
P-Editor: Cai YX

REFERENCES

1 **Chen W**, Sun K, Zheng R, Zeng H, Zhang S, Xia C, Yang Z, Li H, Zou X, He J. Cancer incidence and mortality in China, 2014. *Chin J Cancer Res* 2018; **30**: 1-12 [PMID: 29545714 DOI: 10.21147/j.issn.1000-9604.2018.01.01]

2 **Li X**. [The symptomatic characteristics and socio-psychological factors of cancer patients posttraumatic stress disorder]. Shihezi University, 2013

3 Diagnostic and statistical manual of mental disorders. 5th ed. Washington, DC: American Psychiatric Association Press, 2013 [DOI: 10.1007/s11019-013-9529-6]

4 **Wang Y**, Hou K, Jin Y, Bao B, Tang S, Qi J, Yang Y, Che X, Liu Y, Hu X, Zheng C. Lung adenocarcinoma-specific three-integrin signature contributes to poor outcomes by metastasis and immune escape pathways. *J Transl Int Med* 2021; **9**: 249-263 [PMID: 35136724 DOI: 10.2478/jtim-2021-0046]

5 **Wang Y**, Feng W. Cancer-related psychosocial challenges. *Gen Psychiatr* 2022; **35**: e100871 [PMID: 36311374 DOI: 10.1136/gpsych-2022-100871]

6 **Amone-P'Olak K**, Omech B, Kakinda AI, Kibedi H. Echoes of the past: prevalence and correlates of PTSD among formerly abducted youths in northern Uganda: findings from the WAYS study. *Gen Psychiatr* 2022; **35**: e100840 [PMID: 36447754 DOI: 10.1136/gpsych-2022-100840]

7 **Cordova MJ**, Riba MB, Spiegel D. Post-traumatic stress disorder and cancer. *Lancet Psychiatry* 2017; **4**: 330-338 [PMID: 28109647 DOI: 10.1016/S2215-0366(17)30014-7]

8 **Andrykowski MA**, Steffens RF, Bush HM, Tucker TC. Lung Cancer Diagnosis and Treatment as a Traumatic Stressor in DSM-IV and DSM-5: Prevalence and Relationship to Mental Health Outcomes. *J Trauma Stress* 2015; **28**: 206-213 [PMID: 25990718 DOI: 10.1002/jts.22005]

9 **Mulligan EA**, Wachen JS, Naik AD, Gosian J, Moye J. Cancer as a Criterion A Traumatic Stressor for Veterans: Prevalence and Correlates. *Psychol Trauma* 2014; **6**: S73-S81 [PMID: 25741406 DOI: 10.1037/a0033721]

10 **Abbey G**, Thompson SB, Hickish T, Heathcote D. A meta-analysis of prevalence rates and moderating factors for cancer-related post-traumatic stress disorder. *Psychooncology* 2015; **24**: 371-381 [PMID: 25146298 DOI: 10.1002/pon.3654]

11 **Lu M**, Luo Z, Zhang X, Nian W. The prevalence study analysis of psychological distress in young and middle-aged patients with advanced cancer. *Tianjin Journal of Nursing* 2019; **027**: 253-256 [DOI: 10.21203/rs.3.rs-1878362/v2]

12 **Fang CK**, Chang MC, Chen PJ, Lin CC, Chen GS, Lin J, Hsieh RK, Chang YF, Chen HW, Wu CL, Lin KC, Chiu YJ, Li YC. A correlational study of suicidal ideation with psychological distress, depression, and demoralization in patients with cancer. *Support Care Cancer* 2014; **22**: 3165-3174 [PMID: 24935648 DOI: 10.1007/s00520-014-2290-4]

13 **Zhang M**. [Study on the economic burden and cost-effectiveness analysis of screening in six common cancers]. Lanzhou University, 2014

14 **Wang S**. [Suicidal ideation screening and the study of psychological experience in hospitalized cancer patients]. Huazhong University of Science and Technolog, 2017

15 **Wang N**, Wang Z, Meng J. Analysis of psychological status of cancer patients in emergency ICU and the effect of humanized nursing intervention. *Chin J Cancer Prev Treat* 2018; **25**: 271-272 [DOI: 10.47939/mh.v2i10.185]

16 **Parker AM**, Sricharoenchai T, Raparla S, Schneck KW, Bienvenu OJ, Needham DM. Posttraumatic stress disorder in critical illness survivors: a metaanalysis. *Crit Care Med* 2015; **43**: 1121-1129 [PMID: 25654178 DOI: 10.1097/CCM.0000000000000882]

17 Research Methods in Nursing. Chapter 2. Beijing: People's Medical Publishing House; 2012

18 **Weiss DS**. The impact of event scale: revised. In: Wilson JP, Tang CSK, editors, Cross-Cultural Assessment of Psychological Trauma and PTSD. Boston, MA: Springer US. 2007; 219–38 [DOI: 10.1007/978-0-387-70990-1_10]

19 **Bienvenu OJ**, Williams JB, Yang A, Hopkins RO, Needham DM. Posttraumatic stress disorder in survivors of acute lung injury: evaluating the Impact of Event Scale-Revised. *Chest* 2013; **144**: 24-31 [PMID: 23699588 DOI: 10.1378/chest.12-0908]

20 **Guo S**, Xin Z, Geng L. Reliability and validity of Chinese version of the Impact of Event Scale-Revised. *Chinese Journal of Clinical Psychology* 2007; **15**: 15-17 [DOI: 10.3969/j.issn.1005-3611.2007.01.006]

21 **Creamer M**, Bell R, Failla S. Psychometric properties of the Impact of Event Scale - Revised. *Behav Res Ther* 2003; **41**: 1489-1496 [PMID: 14705607 DOI: 10.1016/j.brat.2003.07.010]

22 **Morrissey M**, Collier E. Literature review of post-traumatic stress disorder in the critical care population. *J Clin Nurs* 2016; **25**: 1501-1514 [PMID: 27108662 DOI: 10.1111/jocn.13138]

23 **Rattray J**, Crocker C, Jones M, Connaghan J. Patients' perceptions of and emotional outcome after intensive care: results from a multicentre study. *Nurs Crit Care* 2010; **15**: 86-93 [PMID: 20236435 DOI: 10.1111/j.1478-5153.2010.00387.x]

24 **Liu L**, Liu J, Ma L. Analysis of cancer related posttraumatic stress disorder and its related effect factors. Journal of Nurses Training 2017; 32: 1063-1066 [DOI: 10.26226/morressier.5885d712d462b8028d892242]

25 **Ahn E**, Shin DW, Cho SI, Park S, Won YJ, Yun YH. Suicide rates and risk factors among Korean cancer patients, 1993-2005. *Cancer Epidemiol Biomarkers Prev* 2010; **19**: 2097-2105 [PMID: 20696665 DOI: 10.1158/1055-9965.EPI-10-0261]

26 **Petralia A**, Bisso E, Concas I, Maglitto A, Bucolo N, Alaimo S, Di Cataldo A, Signorelli MS, Pulvirenti A, Aguglia E. Psychopathological outcomes and defence mechanisms in clinically healed adults with a paediatric cancer history: an exploratory study. *Gen Psychiatr* 2021; **34**: e100307 [PMID: 34308150 DOI: 10.1136/gpsych-2020-100307]

27 **Hou Y**, Deng Y, Hu L, He L, Yao F, Wang Y, Deng J, Xu J, Xu F, Chen C. Assessment of 17 clinically available renal biomarkers to predict acute kidney injury in critically ill patients. *J Transl Int Med* 2021; **9**: 273-284 [PMID: 35136726 DOI: 10.2478/jtim-2021-0047]

28 **Ye Q**, Ma H. A study of post-traumatic stress disorder in ICU patients. *Journal of Nurses Training* 2012; **27**: 2096-2097 [DOI: 10.1186/cc11095]

29 **Wang J**, Bao M, Wang J. Progress of post-traumatic stress disorder in critical illness survivors. *Chin J Pract Nursing* 2017; **033**: 1510-1513 [DOI: 10.1093/med/9780199653461.003.0021]

30 **Fei S**, Feng X, Luo J, Guo L, Pan Q. Obesity and Coronavirus Disease 2019. *J Transl Int Med* 2022; **10**: 207-218 [PMID: 36776236 DOI: 10.2478/jtim-2022-0020]

World Journal of Clinical Cases

Submit a Manuscript: https://www.f6publishing.com

World J Clin Cases 2023 September 6; 11(25): 5878-5886

DOI: 10.12998/wjcc.v11.i25.5878

ISSN 2307-8960 (online)

ORIGINAL ARTICLE

Retrospective Cohort Study

Effect of different ventilation methods combined with pulmonary surfactant on neonatal acute respiratory distress syndrome

Qing Qing, Ping Zha, Li-Ying Dai, Yang Wang

Specialty type: Pediatrics

Provenance and peer review: Unsolicited article; Externally peer reviewed.

Peer-review model: Single blind

Peer-review report's scientific quality classification

Grade A (Excellent): 0
Grade B (Very good): B
Grade C (Good): C
Grade D (Fair): 0
Grade E (Poor): 0

P-Reviewer: Lee S, Japan; Washio T, Japan

Received: July 12, 2023
Peer-review started: July 12, 2023
First decision: August 2, 2023
Revised: August 7, 2023
Accepted: August 11, 2023
Article in press: August 11, 2023
Published online: September 6, 2023

Qing Qing, Yang Wang, Department of Pediatrics, The First Affiliated Hospital of Anhui Medical University, Hefei 230001, Anhui Province, China

Ping Zha, Li-Ying Dai, Department of Neonatology, Anhui Provincial Children's Hospital, Hefei 230001, Anhui Province, China

Corresponding author: Yang Wang, Doctor, Professor, Department of Pediatrics, The First Affiliated Hospital of Anhui Medical University, No. 218 Jixi Road, Shushan District, Hefei 230001, Anhui Province, China. yangwang202302@163.com

Abstract

BACKGROUND

Acute respiratory distress syndrome precipitates is widespread pulmonary injury in impacted individuals, the neonatal respiratory distress syndrome (NRDS), primarily observed in preterm infants, represents a prevalent critical condition in neonatal clinical settings.

AIM

To investigate the clinical efficacy of various ventilation strategies combined with pulmonary surfactant (PS) therapy in the treatment of NRDS.

METHODS

A total of 20 neonates diagnosed with respiratory distress syndrome, admitted between May 2021 and June 2022, were randomly assigned to either a research group or a control group. Neonates in the research group received treatment involving high-frequency oscillatory ventilation (HFOV) in conjunction with PS. In contrast, neonates in the control group were administered either controlled mechanical ventilation or synchronous intermittent mandatory ventilation, combined with PS. Arterial blood samples from the neonates in both groups were collected before treatment, as well as 6 h, 12 h, 24 h, and 48 h post-treatment. These samples underwent blood gas analysis, with measurements taken for pH value, partial pressures of oxygen (O_2) and carbon dioxide. Concurrently, data was collected on the duration of ventilator use, length of hospitalization time, O_2 treatment time, treatment outcomes, and complications of the ventilator.

RESULTS

From 6-48 h post-treatment, both groups demonstrated significant improvements in arterial blood pH and oxygen partial pressure, along with a significant decrease

in carbon dioxide partial pressure compared to pre-treatment values ($P < 0.05$). Although these changes progressed over time, there were no significant differences between the two groups ($P > 0.05$). However, the research group had significantly lower X-ray scores, shorter hospitalization time, and less time on O_2 therapy compared to the control group ($P < 0.05$). Mortality rates were similar between the two groups ($P > 0.05$), but the research group had a significantly lower incidence of complications ($P < 0.05$).

CONCLUSION

The integration of HFOV combine with PS has proven to effectively expedite the treatment duration, decrease the occurrence of complications, and secure the therapeutic efficacy in managing NRDS.

Key Words: Neonatal respiratory distress syndrome; Pulmonary surfactant; Mechanical ventilation; Respiratory distress syndrome; Acute respiratory distress syndrome

Core Tip: We observed 20 children with respiratory distress syndrome who received different ventilation strategies combined with pulmonary surfactant (PS) therapy, we divided into two groups: The observation group received high-frequency oscillatory ventilation (HFOV) combined with PS, and the control group received controlled mechanical ventilation or synchronous intermittent mandatory ventilation combined with PS. The observed indicators included blood gas analysis pH value partial pressures of oxygen and carbon dioxide. Our research results showed that the integration of HFOV combine with PS has proven to effectively expedite the treatment duration, decrease the occurrence of complications, and secure the therapeutic efficacy in managing neonatal respiratory distress syndrome.

Citation: Qing Q, Zha P, Dai LY, Wang Y. Effect of different ventilation methods combined with pulmonary surfactant on neonatal acute respiratory distress syndrome. *World J Clin Cases* 2023; 11(25): 5878-5886
URL: https://www.wjgnet.com/2307-8960/full/v11/i25/5878.htm
DOI: https://dx.doi.org/10.12998/wjcc.v11.i25.5878

INTRODUCTION

Acute respiratory distress syndrome (ARDS) precipitates a widespread pulmonary injury in impacted individuals, which attributable to the damage inflicted on alveolar epithelial cells and capillaries during an excessive efflux of inflammatory mediators and cells[1-3], is starkly reflected in the loss of pulmonary surfactant (PS). Alarmingly, when ARDS strikes neonates, it carries a considerable risk of causing neonatal mortality and high disability rates[4]. Key risk factors encompass selective cesarean section hypoxia, asphyxia, and meconium aspiration. Neonatal respiratory distress syndrome (NRDS), primarily observed in preterm infants, represents a prevalent critical condition in neonatal clinical settings. Mechanical ventilation and PS administration emerge as the prevailing treatment strategies for NRDS.

Commonly implemented modes of mechanical ventilation in neonates include[5,6]: Controlled Mechanical Ventilation (CMV), Synchronous Intermittent Mandatory Ventilation (SIMV), and Non-invasive High-Frequency Positive Pressure Ventilation (NHFPPV). While CMV and SIMV offer assured therapeutic outcomes, they are intricate, invasive, and associated with numerous adverse reactions. In contrast, NHFPPV, a non-physiological positive pressure ventilation approach, is less complex and non-invasive but carries the risk of amplifying lung injury[7]. High-Frequency Oscillatory Ventilation (HFOV) has been demonstrated to exert a lung-protective effect by leveraging a tidal volume equal to or smaller than the anatomical dead space for rapid gas exchange[8,9]. Furthermore, exogenous PS replacement therapy has been promoted and proven efficacious in mitigating NRDS. Presently, respiratory ailments such as NRDS, congenital diaphragmatic hernia, and meconium aspiration syndrome can be effectively managed with HFOV combined with PS (HFOV+PS) inhalation therapy in neonates and infants[10,11]. However, additional investigations are required to elucidate the impacts of the HFOV and PS combination on ARDS[12,13].

The aim of this study is to compare the effectiveness and safety of HFOV+PS with CMV and PS (CMV+PS) in treating ARDS, thereby offering a foundational guide for the clinical implementation of HFOV in ARDS therapy.

MATERIALS AND METHODS

Population and study criteria

In this study, the research group comprised 35 patients, and the control group also had 35 patients. In the research group, there were 20 males and 15 females. The gestational ages ranged from 34 to 41 wk, with an average of 37.09 ± 1.12 wk. And the birth weights varied between 2000 g and 4317 g, with an average of 3456.09 ± 866.70 g. In the control group, there were 19 males and 16 females. Here, the gestational ages spanned from 35 to 40 wk, with an average of 37.67 ± 1.87 wk

and the birth weights ranged from 2145 g to 4021 g, with an average of 3170.33 ± 767.18 g. Here, the guardians of the children participated voluntarily in this study.

This study represents a single-center, prospective, randomized controlled trial conducted at a provincial hospital in China spanning from May 2020 to June 2022. The investigation received approval from our institutional Ethics Committee and adhered to the principles outlined in the Helsinki Declaration (revised in 2013). Furthermore, written informed consent was obtained from the parents of all participating subjects. The study population comprised 70 neonates diagnosed with RDS, who were admitted to our hospital during the study period.

The inclusion criteria included: (1) Diagnosis conforming to the Montreux diagnostic criteria of 2017; and (2) clinical indications for mechanical ventilation treatment.

Exclusion criteria included congenital malformations of the respiratory tract, congenital heart disease, and intrauterine infectious pneumonia.

Sample size estimation

Utilizing the two independent sample r test sample size estimation module of PASS 15.0 software, with set parameters of $\alpha = 0.05$ and $\beta = 0.10$, and assuming equal sample sizes, we referred to the expression levels of vascular endothelial growth factor, soluble receptor for advanced glycation endproducts, surfactant protein-D, and Ang-2 in research group and control group. Based on these calculations, the required sample size for this study was determined to be 30 subjects, $n = 15$ for each group. However, due to missed visits or incomplete data during the study, the final sample included 11 subjects in the research group and 9 in the control group.

Respiratory management

PS (Calf Pulmonary Surfactant for Injection, CR Shuanghe Keli Su, China) was administered *via* intratracheal injection. All infants received a single dosage of 100 mg/kg within 6 h of ARDS diagnosis. Prior to administration, airway secretions were suctioned, and measures were taken to stabilize circulation and correct acid-base imbalances. Following PS injection, rapid ventilation under pressure was applied for 1 minute, after which the infants were connected to a ventilator to maintain either HFOV/CMV or SIMV ventilation.

In the research group, 35 patients received routine endotracheal intubation (Babylog, VN500; Drager, Germany) coupled with HFOV and PS (100 mg/kg). The PS was re-administered, up to 4 times, if hypoxemia persisted beyond 12 h. Initial ventilator settings were as follows.

Here, frequency set between 812 Hz and inhalation-exhalation ratio at 1:1. Mean airway pressure (MAP) initiated at 10-15 cm H_2O, gradually increased by 1 cm H_2O every 2 to 3 minutes until oxygenation ceased to improve. Thereafter, MAP was incrementally reduced by 1-2 cm H_2O every 2 to 3 minutes until Transcutaneous Oxygen Saturation ($TcSaO_2$) decreased, subsequently increasing MAP by 1-2 cm H_2O from this point. The initial setting for amplitude was 30-40 cm H_2O. The right diaphragm was maintained at the ninth rib level following an hour of mechanical ventilation, using chest radiographs to ascertain optimal lung function. Parameters were adjusted in accordance with the dynamic monitoring results of blood gas analysis. PS was injected into the endotracheal tube after at least 10 minutes of continuous ventilation. Throughout the treatment, variations in heart rate, respiration, blood pressure, and oxygen saturation (SaO_2) were meticulously observed. If apnea, a drop in SaO_2, or heart rate was observed, the PS injection was halted and oxygen was promptly administered until the infant's condition stabilized. Following PS administration, mechanical ventilation was continued with ventilator settings adjusted in line with SaO_2 findings, blood gas analyses, and chest radiography. The infant was extubated when the following conditions were met: hemodynamic stability, MAP of 8 cm H_2O, Fraction of Inspired Oxygen (FiO_2) of 40%, and weaning from sedation. Before extubation, the infant was put on conventional ventilation. Post weaning, nasal continuous positive airway pressure (NCPAP) was administered.

In the control group, 35 patients received standard endotracheal intubation coupled with CMV using a Stephanie ventilator (Fritz Stephan GmbH, Gackenbach, Germany), and PS (100 mg/kg). If hypoxemia lasted beyond 12 h, PS was re-administered, up to 4 times. Initial parameters were set as follows.

FiO_2: 30%-50%. Peak inspiratory pressure: 18-25cm H_2O. Positive end-expiratory pressure: 4-6 cm H_2O, I/E: 1:1.5. Respiratory Rate (RR): 30-40 breaths/min. The ventilator parameters were adjusted in line with SaO_2 results, arterial blood gas (ABG) analysis, and chest radiographs. Post weaning, NCPAP was administered.

Peripheral venous blood was drawn from the children in both groups at the following intervals: before treatment, 6 h post-treatment, 12 h post-treatment, 24 h post-treatment, and 48 h post-treatment. Blood gas analysis was performed, and pH, blood oxygen partial pressure (PaO_2), and $PaCO_2$ were recorded. The duration of key treatment components, including ventilation, hospitalization time and O_2 treatment time were noted. Moreover, treatment outcomes and complications were tracked and documented.

Statistical analysis

The data were analyzed using the 25.0 version of SPSS software for Windows (IBM SPSS Inc., Chicago, IL, United States). The measurement data are expressed as mean ± standard deviation, and the analysis of variance and *t*-test are used. The counting data was expressed in percentage (%), and perform χ^2 test the difference was statistically significant with $P < 0.05$.

RESULTS

Baseline information

As is shown in Table 1, there was no statistically significant differences were observed in the baseline data between the two groups ($P > 0.05$), indicating that they were comparable.

Comparison of pH, blood PaO_2, and $PaCO_2$ at different time points between the two groups

In this study, there was no significant difference was observed between the two groups before treatment ($P > 0.05$). As is shown in Figure 1, following treatment, both the arterial blood pH and blood PaO_2 significantly increased compared to their pre-treatment levels, while the $PaCO_2$ significantly decreased. The oxygen deficiency index (OI) was lower post-treatment, and the oxygenation index (PaO_2/FiO_2) was notably higher than the pre-treatment values ($P < 0.05$). As treatment duration increased, the arterial blood pH, PaO_2, and PaO_2/FiO_2 in both groups showed significant increases, while $PaCO_2$ and OI demonstrated significant decreases. However, no significant differences were noted between the two groups in terms of arterial blood pH, blood PaO_2, and $PaCO_2$ at different post-treatment time points ($P > 0.05$).

Comparison of ventilator use, treatment time and O_2 treatment time between the two groups

The duration of ventilator use, hospitalization and O_2 therapy in the research group were significantly shorter than those in the control group ($P < 0.05$), as shown in Table 2.

Comparison of curative effect between two groups of children

The cure rate of children in the research group was significantly higher than that in the control group ($P < 0.05$). Moreover, there was no significant difference in mortality between the two groups ($P > 0.05$) (Table 3).

Comparison of chest X-ray scores and Apgar scores between two groups of patients

Before treatment, there was no statistically significant difference in chest X-ray score and Apgar score between the two groups of patients ($P > 0.05$). After treatment, the research group had higher chest X-ray score and Apgar score than the control group ($P < 0.05$) (Table 4).

Comparison of complications between two groups of children

As is shown in Table 5, the total incidence of complications such as air leakage in the control group was 37.1%, and that in the research group was 11.4%. The incidence of complications in the research group was significantly lower than that in the control group ($P < 0.05$).

DISCUSSION

Due to immature lung development and surfactant deficiency, ARDS is characterized by alveolar collapse, decreased lung compliance, and diminished ventilation-perfusion ratio. The primary manifestations include refractory hypoxemia and significant enhancement of alveolar permeability. Hypoxia and acidosis can induce injury to alveolar epithelial cells and pulmonary vascular endothelial cells. Moreover, ARDS-related fluid leakage and heightened vascular permeability not only exacerbate acidosis and hypoxia but also diminish the production and secretion of PS, establishing a self-perpetuating cycle. Increased pulmonary microvascular permeability can lead to alveolar and interstitial edema, injury to alveolar type II cells, and decreased generation or release and activity of endogenous PS. This, in turn, decreases lung compliance, escalates alveolar surface tension, compromises lung function, and reduces SaO_2 levels[14,15]. Acute hemodynamic alterations induced by hypoxia and acidosis could exacerbate the state of decreased cardiac output, potentially culminating in multiple organ failure.

PS can enhance the clinical prognosis of neonates with RDS, promoting the regeneration of pulmonary epithelial cells and the release of endogenous surfactant. Beyond preserving functional residual capacity, stabilizing alveolar pressure, and minimizing fluid leakage from capillaries to alveoli, PS replacement therapy can also reduce alveolar surface tension, preventing alveolar collapse at the end of the expiratory phase. Moreover, it can decrease ventilator parameters while concurrently improving lung compliance and ventilation function[16,17]. Early administration of PS in neonates with ARDS has demonstrated a reduction in the necessity for mechanical ventilation and an enhancement in oxygenation[18, 19]. Clinical observations suggest that mechanical ventilation should be employed in conjunction with PS therapy, as this therapy alone exhibits limited efficacy in addressing NRDS. Mechanical ventilation, which has been shown to significantly improve the oxygenation capacity in children with respiratory dysfunction, is currently the most favored treatment approach for neonates with acute and severe respiratory difficulties.

Study has linked the repetitive opening and closing of collapsed alveoli, mainly induced by high airway pressure, large lung capacity, and recurrent alveolar collapse, to the release of inflammatory mediators and subsequent multi-organ dysfunction[20]. Consequently, the focus of mechanical ventilation lies in lung-protective strategies. The two primary goals are to prevent the recurrent closure of end-expiratory alveoli and to limit excessive alveolar expansion to mitigate lung injury and enhance disease recovery. HFOV is characterized by low-cycle pressure changes, biphasic pressure changes, tidal volume at or below the level of the anatomical dead space, and supra-physiological respiratory frequency oscillations. This facilitates an effective gas exchange ventilation mode at the alveolar level, rapidly achieving even alveolar expansion, enhanced gas exchange, and increased lung compliance. HFOV supports the processes of inhalation

Table 1 Baseline information, *n* (%)

Item	Research group	Control group	*P* value
Gestational age (d)	37.09 ± 1.12	37.67 ± 1.87	0.658
Gender			
Male	20 (57.1)	19 (54.3)	0.810
Female	15 (42.9)	16 (45.7)	
Birth weight (g)	3456.09 ± 866.70	3170.33 ± 767.18	0.453

Table 2 Comparison of treatment of two groups of patients (mean ± SD, *n* = 70)

Group	Ventilator use time (h)	Treatment time (d)	O_2 treatment time (h)
Control group	83.28 ± 10.35	22.37 ± 6.63	131.47 ± 19.32
Research group	38.59 ± 8.91[a]	16.20 ± 4.05[a]	92.45 ± 10.13[a]

[a]Compared with the control group, $P < 0.05$.

Table 3 Comparison of curative effects between two groups of patients [*n* (%), *n* = 70]

Group	Cure rate	Improvement rate	Case fatality rate
Control group	3 (8.6)	27 (77.1)	5 (14.3)
Research group	14 (40.0)	19 (54.3)	2 (5.7)
χ^2	9.401	4.058	1.429
P value	0.002	0.044	0.232

Table 4 Comparison of chest X-ray scores and Apgar scores between two groups of patients

Group	X-ray scores		Apgar scores	
	Before	After	Before	After
Control group	2.98 ± 0.42	3.45 ± 0.27	4.12 ± 0.92	6.17 ± 1.02
Research group	3.04 ± 0.39	3.98 ± 0.35[a]	3.96 ± 0.83	7.85 ± 0.98[a]

[a]Compared with the control group, $P < 0.05$.

Table 5 Comparison of complications between the two groups [*n* (%), *n* = 70]

Group	Emphysema	Ventilator-associated pneumonia	Intraventricular hemorrhage	Patent ductus arteriosus	Total complications
Control group	4	2	3	3	13 (37.1)
Research group	2	1	1		4 (11.4)
χ^2					6.293
P value					0.012

and exhalation during ventilation, improving oxygenation and carbon dioxide removal while minimizing barotrauma. Its hypoventilation approach can protect the lungs during mechanical ventilation, thus improving survival rates[21,22]. The research conducted by Poddutoor *et al*[23] studied 675 neonates who were administered CMV. They found that of those, 97 neonates had to be switched to HFOV due to failure of CMV treatment. Impressively, there was a significant improvement in lung oxygenation and ABG parameters within 2 h of switching to HFOV. Our study aligns with these

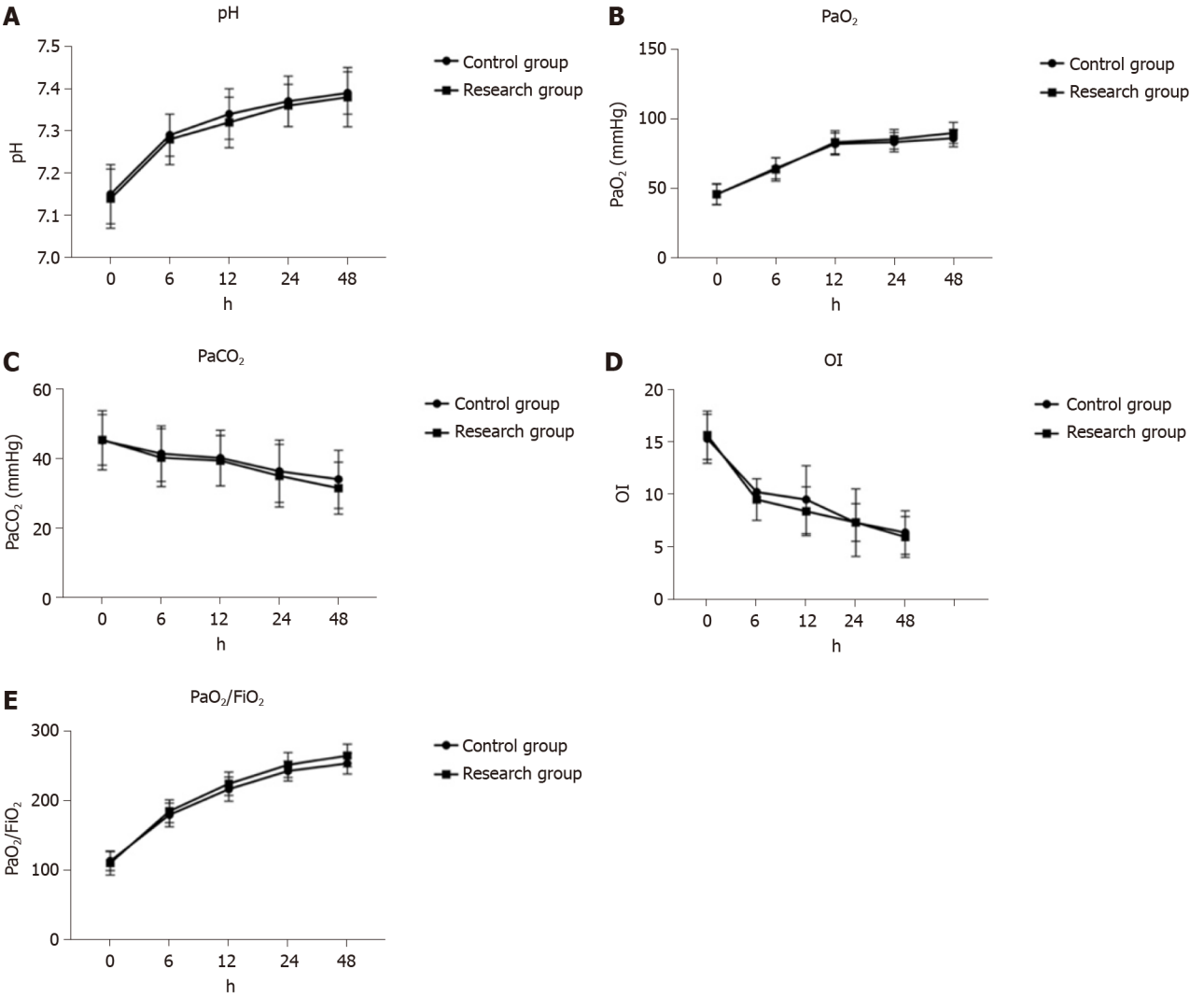

DOI: 10.12998/wjcc.v11.i25.5878

Figure 1 Comparison of pH, PaO_2, $PaCO_2$, oxygen deficiency index and PaO_2/FiO_2 at different time points between the control group and research group. A: Comparison of two groups of PH; B: Comparison of two groups of PaO_2; C: Comparison of two groups of $PaCO_2$; D: Comparison of two groups of oxygen deficiency index; E: Comparison of two groups of PaO_2/FiO_2.

findings. We observed that the ABG parameters in the HFOV+PS group improved significantly after treatment. The CMV+PS group also showed improvements in their ABG parameters, however, the effect was not as pronounced as in the HFOV+PS group.

Moreover, infants treated with the HFOV+PS method experienced significantly reduced hospitalization and boarding durations compared to those in the CMV+PS group. The duration of hospital-stay and the need for mechanical ventilation were markedly less for the HFOV+PS group, demonstrating its effectiveness over the CMV+PS approach. This can be attributed to the fact that, in comparison to CMV, the rapid airflow created by HFOV can swiftly disperse PS across the alveolar surface, reducing surface tension. This effect further expands the alveoli, ensuring their stability, enhancing alveolar ventilation and respiration function, and alleviating symptoms of hypoxia and acidosis. Furthermore, when combined with mechanical ventilation, PS can notably augment the PaO_2/FiO_2 ratio, decrease OI, and significantly improve oxygenation capabilities in children with ARDS[21,24]. This study also discovered that the duration of mechanical ventilation and the need for oxygen therapy was notably reduced in the HFOV+PS group as compared to the CMV+PS group. This might be attributed to the ability of HFOV, which can clear obstructions in the small airways and alveoli. The distinct mode of gas exchange and rapid ventilation frequency foster a uniform distribution of PS along the alveolar wall. Additionally, surfactants exert immunomodulatory, physicochemical, and antibacterial effects which contribute to the stabilization of alveoli, reduction in alveolar capillary edema, and ultimately an enhancement in lung function[24]. The combination of PS with HFOV significantly optimizes respiration and diminishes the time needed for ventilation.

Based on the findings of the study, post-treatment arterial blood pH value, blood PaO_2, and blood $PaCO_2$ of both groups were significantly higher than their pre-treatment levels. Meanwhile, the oxygenation index (PaO_2/FiO_2) was markedly lower post-treatment compared to its pre-treatment value. As the duration of treatment extended, the arterial blood pH value, PaO_2, and PaO_2/FiO_2 of both groups significantly rose, while $PaCO_2$ and OI saw a substantial decrease.

To enhance oxygenation and pulmonary ventilation function in children with NRDS, this study suggests no significant difference between HFOV, CMV, or SIMV when used in conjunction with PS. Children in the research group spent notably less time on ventilators, had significantly shorter hospitalization durations, and required oxygen treatments for a significantly shorter period than those in the control group. Furthermore, the recovery rate among children in the research group was significantly higher than in the control group, whereas the mortality rate remained fairly consistent across both groups. However, the incidence of complications was lower in the research group compared to the control group, suggesting a positive impact of HFOV.

Limits of the study

Our study has some limitations. Firstly, the sample size used in our research was small, with only 20 cases in total, 11 in the observation group and 9 in the control group, which could affect the persuasiveness of our research results. Additionally, we lacked long-term follow-up on patients after discharge, which means we were unable to provide evidence for the long-term therapeutic effects of HFOV combined with PS.

CONCLUSION

In conclusion, our findings suggest that for infants with ARDS, the utilization of HFOV in conjunction with PS demonstrates a significant advantage over the use of CMV with PS. Specifically, the HFOV+PS approach notably reduces both the duration of hospitalization and the necessity for prolonged mechanical ventilation. Importantly, these benefits are achieved without any attendant increase in the incidence of complications. This evidence provides a compelling case for the preferential use of HFOV+PS in the management of infant ARDS, to optimize patient outcomes and enhance the efficiency of care.

ARTICLE HIGHLIGHTS

Research background

Acute respiratory distress syndrome (ARDS) precipitates is widespread pulmonary injury in impacted individuals, the neonatal respiratory distress syndrome (NRDS), primarily observed in preterm infants, represents a prevalent critical condition in neonatal clinical settings.

Research motivation

Presently, respiratory ailments such as NRDS, congenital diaphragmatic hernia, and meconium aspiration syndrome can be effectively managed with high-frequency oscillatory ventilation (HFOV) combined with pulmonary surfactant (PS) (HFOV+PS) inhalation therapy in neonates and infants. However, additional investigations are required to elucidate the impacts of the HFOV and PS combination on ARDS.

Research objectives

The aim of this study is to investigate the clinical efficacy of various ventilation strategies combined with PS therapy in the treatment of NRDS.

Research methods

A total of 20 neonates diagnosed with RDS, admitted between May 2021 and June 2022, were randomly assigned to either a research group or a control group. Neonates in the research group received treatment involving HFOV in conjunction with PS. In contrast, neonates in the control group were administered either controlled mechanical ventilation (CMV) or synchronous intermittent mandatory ventilation, combined with PS.

Research results

From 6-48 h post-treatment, both groups demonstrated significant improvements in arterial blood pH and oxygen partial pressure, along with a significant decrease in carbon dioxide partial pressure compared to pre-treatment values ($P < 0.05$). Although these changes progressed over time, there were no significant differences between the two groups ($P > 0.05$). However, the research group had significantly lower X-ray scores, shorter hospitalization time, and less time on O_2 therapy compared to the control group ($P < 0.05$). Mortality rates were similar between the two groups ($P > 0.05$), but the research group had a significantly lower incidence of complications ($P < 0.05$).

Research conclusions

Our findings suggest that for infants with ARDS, the utilization of HFOV in conjunction with PS demonstrates a significant advantage over the use of CMV with PS. Specifically, the HFOV+PS approach notably reduces both the duration of hospitalization and the necessity for prolonged mechanical ventilation. Importantly, these benefits are achieved without any attendant increase in the incidence of complications. This evidence provides a compelling case for the preferential use of HFOV+PS in the management of infant ARDS, to optimize patient outcomes and enhance the efficiency of care.

Research perspectives

Our future research will be based on alleviating the economic pressure of patients and finding the cheapest treatment to treat Infant respiratory distress syndrome.

ACKNOWLEDGEMENTS

We would like to express our gratitude to all medical research institutes and patients who participated in this study, as well as to all reviewers for their review of this article.

FOOTNOTES

Author contributions: Qing Q and Wang Y contributed to conception and design, provision of study materials or patients; Wang Y contributed to administrative support; All authors contributed to collection and assembly of data; Qing Q contributed to data analysis and interpretation, manuscript writing; All authors contributed to final approval of manuscript.

Institutional review board statement: The ethical audit certificate of this study was provided by the Ethics Committee of the First Affiliated Hospital of Anhui Medical University. (NO. AHYKD-LLWYH-036).

Informed consent statement: All study participants or their legal guardian provided informed written consent about personal and medical data collection prior to study enrolment.

Conflict-of-interest statement: All the Authors have no conflict of interest related to the manuscript.

Data sharing statement: The datasets generated during and/or analyzed during the current study are available from the corresponding author on reasonable request.

STROBE statement: The authors have read the STROBE Statement – checklist of items, and the manuscript was prepared and revised according to the STROBE Statement – checklist of items.

Country/Territory of origin: China

ORCID number: Li-Ying Dai 0000-0003-3914-9155; Yang Wang 0000-0003-0846-4750.

S-Editor: Liu JH
L-Editor: A
P-Editor: Liu JH

REFERENCES

1 **Froese AB**, McCulloch PR, Sugiura M, Vaclavik S, Possmayer F, Moller F. Optimizing alveolar expansion prolongs the effectiveness of exogenous surfactant therapy in the adult rabbit. *Am Rev Respir Dis* 1993; **148**: 569-577 [PMID: 8368625 DOI: 10.1164/ajrccm/148.3.569]
2 **Dreyfuss D**, Saumon G. Ventilator-induced lung injury: lessons from experimental studies. *Am J Respir Crit Care Med* 1998; **157**: 294-323 [PMID: 9445314 DOI: 10.1164/ajrccm.157.1.9604014]
3 **Amatullah H**, Maron-Gutierrez T, Shan Y, Gupta S, Tsoporis JN, Varkouhi AK, Teixeira Monteiro AP, He X, Yin J, Marshall JC, Rocco PRM, Zhang H, Kuebler WM, Dos Santos CC. Protective function of DJ-1/PARK7 in lipopolysaccharide and ventilator-induced acute lung injury. *Redox Biol* 2021; **38**: 101796 [PMID: 33246293 DOI: 10.1016/j.redox.2020.101796]
4 **Stephens RS**, Shah AS, Whitman GJ. Lung injury and acute respiratory distress syndrome after cardiac surgery. *Ann Thorac Surg* 2013; **95**: 1122-1129 [PMID: 23352419 DOI: 10.1016/j.athoracsur.2012.10.024]
5 **Rong LQ**, Di Franco A, Gaudino M. Acute respiratory distress syndrome after cardiac surgery. *J Thorac Dis* 2016; **8**: E1177-E1186 [PMID: 27867583 DOI: 10.21037/jtd.2016.10.74]
6 **Fink MP**. Role of reactive oxygen and nitrogen species in acute respiratory distress syndrome. *Curr Opin Crit Care* 2002; **8**: 6-11 [PMID: 12205400 DOI: 10.1097/00075198-200202000-00002]
7 **Acute Respiratory Distress Syndrome Network**, Brower RG, Matthay MA, Morris A, Schoenfeld D, Thompson BT, Wheeler A. Ventilation with lower tidal volumes as compared with traditional tidal volumes for acute lung injury and the acute respiratory distress syndrome. *N Engl J Med* 2000; **342**: 1301-1308 [PMID: 10793162 DOI: 10.1056/NEJM200005043421801]
8 **Yildizdas D**, Yapicioglu H, Bayram I, Yilmaz L, Sertdemir Y. High-frequency oscillatory ventilation for acute respiratory distress syndrome. *Indian J Pediatr* 2009; **76**: 921-927 [PMID: 19475349 DOI: 10.1007/s12098-009-0151-9]

9 **Bojan M**, Gioanni S, Mauriat P, Pouard P. High-frequency oscillatory ventilation and short-term outcome in neonates and infants undergoing cardiac surgery: a propensity score analysis. *Crit Care* 2011; **15**: R259 [PMID: 22035562 DOI: 10.1186/cc10521]

10 **Rettwitz-Volk W**, Veldman A, Roth B, Vierzig A, Kachel W, Varnholt V, Schlösser R, von Loewenich V. A prospective, randomized, multicenter trial of high-frequency oscillatory ventilation compared with conventional ventilation in preterm infants with respiratory distress syndrome receiving surfactant. *J Pediatr* 1998; **132**: 249-254 [PMID: 9506636 DOI: 10.1016/s0022-3476(98)70440-8]

11 **Lin X-Z**, Lai JD, Lv M, Zhu Y, Wang L, Chen C. [Clinical efficacy of high-frequency oscillatory ventilation combined with pulmonary surfactant in treatment of neonatal pulmonary hemorrhage]. *Zhongguo Dang Dai Er Ke Za Zhi* 2015; **17:** 345–349. Available from: https://pubmed.ncbi.nlm.nih.gov/25919553/

12 **Khemani RG**, Smith LS, Zimmerman JJ, Erickson S; Pediatric Acute Lung Injury Consensus Conference Group. Pediatric acute respiratory distress syndrome: definition, incidence, and epidemiology: proceedings from the Pediatric Acute Lung Injury Consensus Conference. *Pediatr Crit Care Med* 2015; **16**: S23-S40 [PMID: 26035358 DOI: 10.1097/PCC.0000000000000432]

13 **Willson DF**, Thomas NJ, Markovitz BP, Bauman LA, DiCarlo JV, Pon S, Jacobs BR, Jefferson LS, Conaway MR, Egan EA; Pediatric Acute Lung Injury and Sepsis Investigators. Effect of exogenous surfactant (calfactant) in pediatric acute lung injury: a randomized controlled trial. *JAMA* 2005; **293**: 470-476 [PMID: 15671432 DOI: 10.1001/jama.293.4.470]

14 **Deterding RR**. Infants and Young Children with Children's Interstitial Lung Disease. *Pediatr Allergy Immunol Pulmonol* 2010; **23**: 25-31 [PMID: 22332029 DOI: 10.1089/ped.2010.0011]

15 **Matthay MA**, Zemans RL. The acute respiratory distress syndrome: pathogenesis and treatment. *Annu Rev Pathol* 2011; **6**: 147-163 [PMID: 20936936 DOI: 10.1146/annurev-pathol-011110-130158]

16 **Walsh BK**, Daigle B, DiBlasi RM, Restrepo RD; American Association for Respiratory Care. AARC Clinical Practice Guideline. Surfactant replacement therapy: 2013. *Respir Care* 2013; **58**: 367-375 [PMID: 23359726 DOI: 10.4187/respcare.02189]

17 **De Luca D**. Respiratory distress syndrome in preterm neonates in the era of precision medicine: A modern critical care-based approach. *Pediatr Neonatol* 2021; **62** Suppl 1: S3-S9 [PMID: 33358440 DOI: 10.1016/j.pedneo.2020.11.005]

18 **Amigoni A**, Pettenazzo A, Stritoni V, Circelli M. Surfactants in Acute Respiratory Distress Syndrome in Infants and Children: Past, Present and Future. *Clin Drug Investig* 2017; **37**: 729-736 [PMID: 28510235 DOI: 10.1007/s40261-017-0532-1]

19 **Volsko TA**, Parker SW, Deakins K, Walsh BK, Fedor KL, Valika T, Ginier E, Strickland SL. AARC Clinical Practice Guideline: Management of Pediatric Patients With Tracheostomy in the Acute Care Setting. *Respir Care* 2021; **66**: 144-155 [PMID: 33380501 DOI: 10.4187/respcare.08137]

20 **Möller JC**, Schaible T, Roll C, Schiffmann JH, Bindl L, Schrod L, Reiss I, Kohl M, Demirakca S, Hentschel R, Paul T, Vierzig A, Groneck P, von Seefeld H, Schumacher H, Gortner L; Surfactant ARDS Study Group. Treatment with bovine surfactant in severe acute respiratory distress syndrome in children: a randomized multicenter study. *Intensive Care Med* 2003; **29**: 437-446 [PMID: 12589529 DOI: 10.1007/s00134-003-1650-1]

21 **Rodríguez-Moya VS**, Gallo-Borrero CM, Santos-Áreas D, Prince-Martínez IA, Díaz-Casañas E, López-Herce Cid J. Exogenous surfactant and alveolar recruitment in the treatment of the acute respiratory distress syndrome. *Clin Respir J* 2017; **11**: 1032-1039 [PMID: 26881996 DOI: 10.1111/crj.12462]

22 **Yapicioğlu H**, Yildizdaş D, Bayram I, Sertdemir Y, Yilmaz HL. The use of surfactant in children with acute respiratory distress syndrome: efficacy in terms of oxygenation, ventilation and mortality. *Pulm Pharmacol Ther* 2003; **16**: 327-333 [PMID: 14580923 DOI: 10.1016/S1094-5539(03)00088-9]

23 **Poddutoor PK**, Chirla DK, Sachane K, Shaik FA, Venkatlakshmi A. Rescue high frequency oscillation in neonates with acute respiratory failure. *Indian Pediatr* 2011; **48**: 467-470 [PMID: 21555797 DOI: 10.1007/s13312-011-0073-2]

24 **Sun H**, Cheng R, Kang W, Xiong H, Zhou C, Zhang Y, Wang X, Zhu C. High-frequency oscillatory ventilation versus synchronized intermittent mandatory ventilation plus pressure support in preterm infants with severe respiratory distress syndrome. *Respir Care* 2014; **59**: 159-169 [PMID: 23764865 DOI: 10.4187/respcare.02382]

World Journal of Clinical Cases

Submit a Manuscript: https://www.f6publishing.com

World J Clin Cases 2023 September 6; 11(25): 5887-5896

DOI: 10.12998/wjcc.v11.i25.5887

ISSN 2307-8960 (online)

ORIGINAL ARTICLE

Retrospective Study

Hepatic MR imaging using IDEAL-IQ sequence: Will Gd-EOB-DTPA interfere with reproductivity of fat fraction quantification?

Yuan Tian, Peng-Fei Liu, Jia-Yu Li, Ya-Nan Li, Peng Sun

Specialty type: Radiology, nuclear medicine and medical imaging

Provenance and peer review: Unsolicited article; Externally peer reviewed.

Peer-review model: Single blind

Peer-review report's scientific quality classification

Grade A (Excellent): 0
Grade B (Very good): 0
Grade C (Good): C, C
Grade D (Fair): 0
Grade E (Poor): 0

P-Reviewer: Bangalore S, United States; Pope JE, Canada

Received: April 11, 2023
Peer-review started: April 11, 2023
First decision: April 26, 2023
Revised: May 31, 2023
Accepted: July 14, 2023
Article in press: July 14, 2023
Published online: September 6, 2023

Yuan Tian, Peng-Fei Liu, Jia-Yu Li, Ya-Nan Li, Peng Sun, Department of Magnetic Resonance Imaging, The First Affiliated Hospital of Harbin Medical University, Harbin 150001, Heilongjiang Province, China

Corresponding author: Peng Sun, MM, Attending Doctor, Department of Magnetic Resonance, The First Affiliated Hospital of Harbin Medical University, No. 23 Youzheng Street, Nangang District, Harbin 150001, Heilongjiang Province, China. 19526333113@163.com

Abstract

BACKGROUND

Iterative decomposition of water and fat with echo asymmetry and least squares estimation quantification sequence (IDEAL-IQ) is based on chemical shift-based water and fat separation technique to get proton density fat fraction. Multiple studies have shown that using IDEAL-IQ to test the stability and repeatability of liver fat is acceptable and has high accuracy.

AIM

To explore whether Gadoxetate Disodium (Gd-EOB-DTPA) interferes with the measurement of the hepatic fat content quantified with the IDEAL-IQ and to evaluate the robustness of this technique.

METHODS

IDEAL-IQ was used to quantify the liver fat content at 3.0T in 65 patients injected with Gd-EOB-DTPA contrast. After injection, IDEAL-IQ was estimated four times, and the fat fraction (FF) and R2* were measured at the following time points: Pre-contrast, between the portal phase (70 s) and the late phase (180 s), the delayed phase (5 min) and the hepatobiliary phase (20 min). One-way repeated-measures analysis was conducted to evaluate the difference in the FFs between the four time points. Bland-Altman plots were adopted to assess the FF changes before and after injection of the contrast agent. $P < 0.05$ was considered statistically significant.

RESULTS

The assessment of the FF at the four time points in the liver, spleen and spine showed no significant differences, and the measurements of hepatic FF yielded good consistency between T1 and T2 [95% confidence interval: -0.6768%, 0.6658%], T1 and T3 (-0.3900%, 0.3178%), and T1 and T4 (-0.3750%, 0.2825%). R2* of the liver, spleen and spine increased significantly after injection ($P < 0.0001$).

CONCLUSION
Using the IDEAL-IQ sequence to measure the FF, we can obtain results that will not be affected by Gd-EOB-DTPA. The high reproducibility of the IDEAL-IQ sequence makes it available in the scanning interval to save time during multiphase examinations.

Key Words: Gadoxetate Disodium; Iterative decomposition of water and fat with echo asymmetry and least squares estimation quantification sequence; Fat fraction; Enhanced-Magnetic resonance imaging; R2*

Core Tip: The measurement of fat fraction was stable when using Iterative decomposition of water and fat with echo asymmetry and least squares estimation quantification sequence (IDEAL-IQ) before and after injection of hepatocyte-specific contrast agent. Such strong reproducibility makes IDEAL-IQ available in the interval for saving time during examination and optimizes the scanning protocol.

Citation: Tian Y, Liu PF, Li JY, Li YN, Sun P. Hepatic MR imaging using IDEAL-IQ sequence: Will Gd-EOB-DTPA interfere with reproductivity of fat fraction quantification? *World J Clin Cases* 2023; 11(25): 5887-5896
URL: https://www.wjgnet.com/2307-8960/full/v11/i25/5887.htm
DOI: https://dx.doi.org/10.12998/wjcc.v11.i25.5887

INTRODUCTION

The defining characteristic of hepatic steatosis (HS) lies in the intracellular accumulation of fat deposits within hepatocytes. Formerly regarded as a comparatively benign entity, it (HS) has the potential to advance towards the development of steatohepatitis, advanced fibrosis, and ultimately cirrhosis[1,2]. Fortunately, if intervention is performed in a timely manner, isolated steatosis is reversible, and a reduction in liver fat may diminish many of its associated risks. The fat fraction, which represents the quantitative ratio of fat mass to liver mass, serves as a pivotal parameter in the diagnosis and ongoing assessment of nonalcoholic fatty liver disease (NAFLD), the prevalence of which is approximately 25%[3]. Rapid radiological detection and diagnosis are essential in the management of patients with NAFLD[2,4,5].

Quantitative diagnosis and efficacy evaluation of HS have been studied clinically. Liver biopsy is not frequently used for HS diagnosis because of its invasive nature, and sampling errors can be caused by heterogeneous fat distribution[6]. Ultrasound detection is economical and convenient but is highly dependent on the procedure and lacks quantitative and objective criteria[7]. Computed tomography (CT) values cannot be used as a noninvasive technique in the evaluation of fat content, but the deposits of iron, copper, glycogen and amiodarone can increase the liver density and severely interfere with the accuracy of CT in the quantification of liver steatosis[8,9].

Currently, magnetic resonance spectroscopy (MRS) is commonly used as a standard fat quantification method[10-12]. However, the accuracy of this technique depends on the homogeneity of the magnetic field, and single spectral data cannot reflect the whole liver condition[11,12]. Recently, multipoint water-fat separation methods based on chemical shifts have been applied to quantitative analyses of liver fat[12-16]. Among these methods, the iterative decomposition of water and fat with echo asymmetry and least-squares estimation (IDEAL-IQ) not only generates an accurate evaluation of the FF (0%-100%) but also allows the quantitative analysis of the fat composition. This method utilizes a multiecho acquisition technique to facilitate T2* fitting, enabling the subsequent application of T2* correction. By eliminating the inherent T2* effect, this correction accounts for various factors that can impact the accuracy of FF measurements in chemical shift-based approaches. These factors include field inhomogeneity, T1 relaxation, noise bias, and eddy currents [16]. It facilitates the quantitative measurement of the whole liver and promising clinical application for testing the efficacy of drugs for hepatic disorders. The new quantitative scanning regimen not only facilitates accurate prognosis by monitoring dynamic changes in patients but also provides an objective basis for evaluating the treatment effect.

The primary objective of this study was to assess the potential interference of the liver-specific contrast medium Gd-EOB-DTPA on the measurement of hepatic fat content using the IDEAL-IQ sequence. Additionally, the study aimed to evaluate the reliability and resilience of this technique. By exploring these aspects, the researchers sought to identify and address the challenges associated with the widespread application of Gd-EOB-DTPA in clinical settings.

MATERIALS AND METHODS

Patients

In this institutional review board-approved study, patients with liver disease who visited the First Affiliated Hospital of Harbin Medical University between October 2015 and June 2016 were enrolled. All patients were diagnosed with hepatopathy using early imaging and subsequently screened with Gd-EOB-DTPA magnetic resonance imaging. The

Table 1 Baseline patient characteristics and treatment history

Demographics	Parameter	No. of patients (%)
Age	< 60 yr	51 (65)
	> 60 yr	28 (35)
Sex	Male	48 (60)
	Female	17 (40)
Cause	HBV	20 (30)
	HCV	9 (14)
	HBV and HCV	2 (3)
	Alcohol	25 (38)
	Cryptogenic	9 (14)
Cirrhosis	Present	35 (54)
	Absent	30 (46)
Methods of diagnosis	Biopsy	15 (23)
	MR imaging	50 (77)
Tumor characteristics	Unifocal	43 (66)
	Multifocal	22 (34)
Diameter of lesion	< 3 cm	42 (65)
	> 3 cm	23 (35)
No treatment		45 (69)
Treated	Surgical treatment	9 (14)
	Internal medicine	11 (17)

Numbers in parentheses are percentages, and percentages were rounded. HBV: Hepatitis B virus; HCV: Hepatitis C virus.

IDEAL-IQ sequence was used before and after injection to detect liver fat levels. In total, 79 patients were enrolled in this study. We excluded 14 cases for the following criteria: (1) Poor image quality caused by factors such as incompatible breath-holding; (2) Focal liver lesions exceeding 50% of the liver volume; and (3) Patients who underwent an abdominal operation. Finally, 65 patients were enrolled (48 males and 17 females with an average age of 54 years old and a range of 36 to 67 years old). Baseline patient characteristics and treatment history are shown in Table 1, and all the patients signed informed consent forms before the study.

Magnetic resonance imaging

A GE Signa HDxt magnetic resonance imaging (MRI) scanner (Milwaukee, United States) was used with 8-channel TORSOPA phased array coils. The patients fasted for 6 h before the test. Fat detection with the IDEAL-IQ sequence was performed four times before and after Gd-EOB-DTPA enhancement. The acquisition parameters were consistent at the four time points, indicating changes in the FF value and R2*. The scanning parameters were as follows: Breath-hold scanning, IDEAL-IQ (a three-dimensional volumetric imaging sequence): repetition time (TR)/first echo time (TE): 3.7 ms/1.7 ms, thickness 5 mm, receiver bandwidth 125 kHz, view: 44 cm× 40 cm, matrix: 256 × 256, flip angle 3°, NEX1. Six echoes in total were obtained for the T2* correction in two consecutive TRs with a 3-echo acquisition maintained for each. Two-dimensional parallel acceleration was used to maintain the scan time, approximately 21 s, within a single breath hold. The breath-hold double arterial phase LAVA enhanced scanning (BH Ax Dual LAVA+C) parameters were as follows: Turn over time 5.0 ms; flip angle 11°; bandwidth 125 kHz; matrix 256×152; view 44 × 40 cm; and the front and back range was 25% larger than the body surface with a thickness of 4-6 mm. The array spatial sensitivity encoding technique (ASSET) was used with a phase accelerating factor of 2.25 Ph. The injection speed of the contrast agent was 2.0-3.0 mL/s. The dosage was 0.025 mmol/kg, which is approved by the FDA, followed by injection of 20 mL saline at the same speed. After the contrast agent was injected, Dynamic-enhanced scanning using LAVA-Flex was employed to capture images during different phases, namely the arterial phase, portal phase, and equilibrium phase. Additionally, IDEAL-IQ was performed four times throughout the study, including a pre-contrast scan, scans between the portal phase (70 s) and late phase (180 s), a delayed phase scan (5 min), and a hepatobiliary phase scan (20 min). These scans were individually labeled as t1, t2, t3, and t4 in the subsequent statistical analyses and tables.

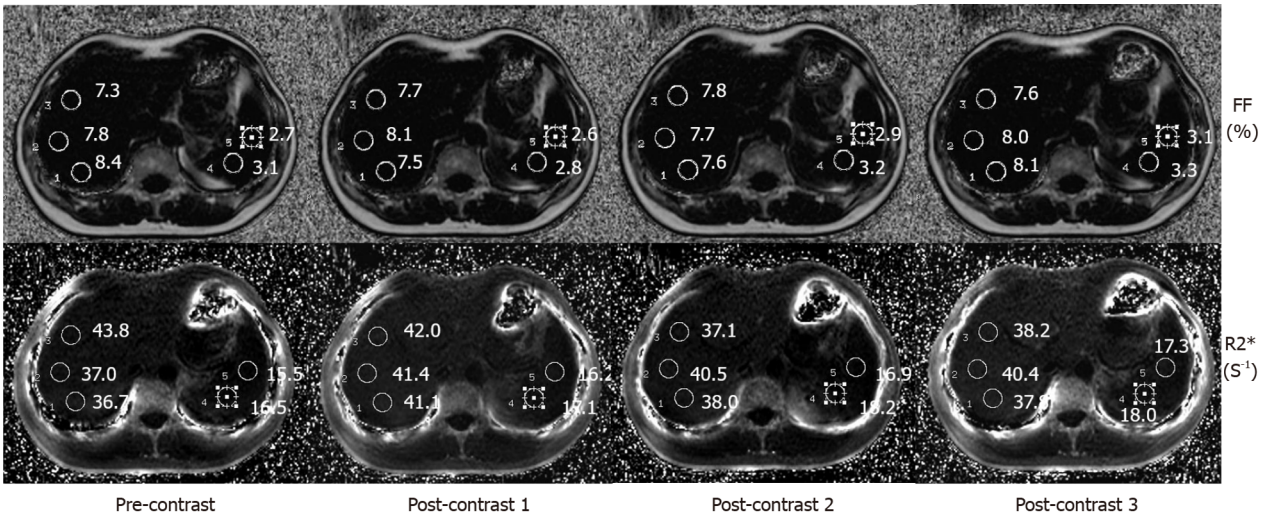

DOI: 10.12998/wjcc.v11.i25.5887 **Copyright** ©The Author(s) 2023.

Figure 1 Fat fraction (%, upper row) and R2* (Hz, bottom row) mappings of the right liver lobe and spleen of a 57-year-old male patient with primary hepatocellular carcinoma. The mean FF and R2∗ values of the right liver lobe and spleen are shown on the images. FF: Fat fraction.

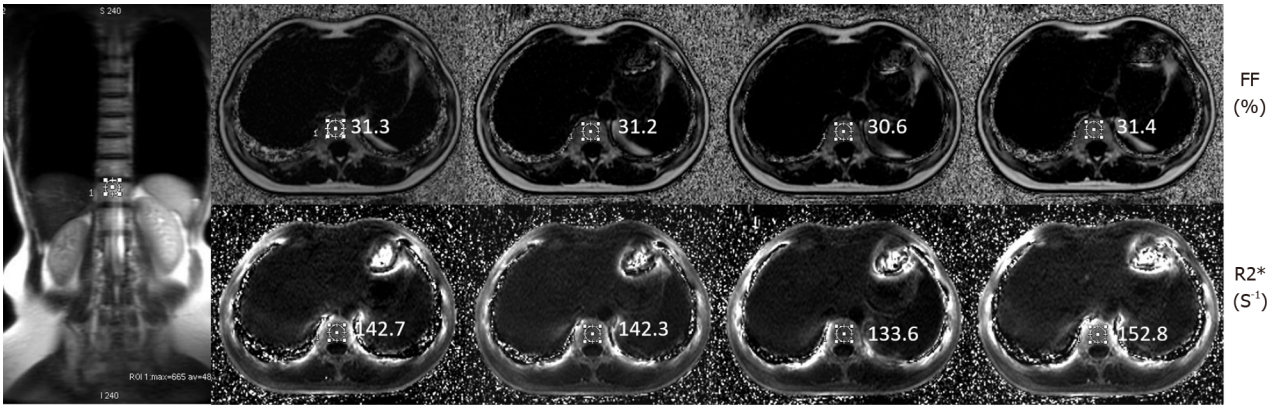

DOI: 10.12998/wjcc.v11.i25.5887 **Copyright** ©The Author(s) 2023.

Figure 2 Fat fraction (%, upper row) and R2* (Hz, bottom row) mappings of the spine of a 47-year-old patient with hepatic hemangioma. The obtained anatomical images were referred to the region of interest in the vertebral body bone marrow to avoid inclusion of the intervertebral disk. FF: Fat fraction.

Data analysis

Two radiologists (with 5-7 years of experience in MR imaging of the abdomen) reviewed the image data of the patients in terms of the known pathological and comprehensive diagnosis. FF and R2∗ maps were autogenerated on the host scanner after each acquisition of the IDEAL-IQ sequence. All the images were independently evaluated by function tool 9.4 on an AW4.5 workstation (Advantage Workstation 4.5; GE Healthcare). Three regions of interest (ROIs) with a diameter of 16 mm in the right liver lobe were used to calculate the mean values (Figure 1). To ensure accurate measurements, regions of interest were carefully selected by excluding intrahepatic bile ducts, blood vessels, and focal liver lesions. The fat fraction detected in the images reflected the amount of fat present in the liver mass, which typically does not exceed 5% in healthy individuals. Similarly, employing the same approach, two ROIs with a diameter of 16 mm were delineated within the spleen for further analysis (Figure 1), one ROI was drawn in the spinal vertebral layer (Figure 2), and the FF and R2∗ values were recorded. The obtained anatomical images of the spine were considered the region of interest in the vertebral body bone marrow to avoid inclusion of the intervertebral disk. Finally, the FF and R2∗ values in the liver, spleen and spine determined by the two physicians were averaged to calculate the final result.

Statistics

The FF and R2∗ values at the four time points were evaluated, and the data were expressed as the means ± SDss and analyzed by ANOVA for repeated measurements. Furthermore, in each region, the values before and after injecting the contrast agent at each time point were compared, and Bland-Altman plots were applied to analyze the differences. $P < 0.05$ was considered statistically significant. SAS 9.13 software (SAS Institute Inc, China) was used to perform the statistical analysis.

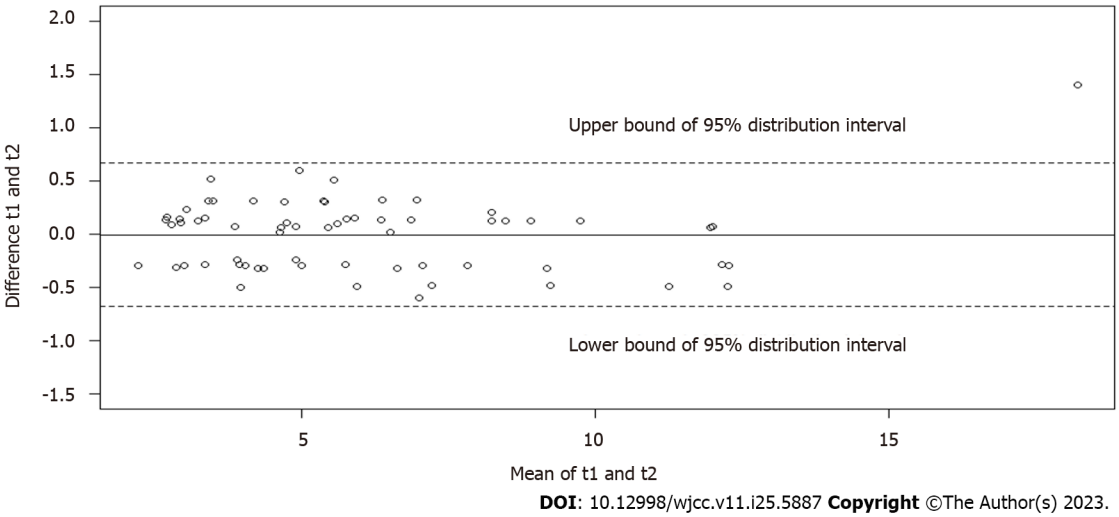

DOI: 10.12998/wjcc.v11.i25.5887 **Copyright** ©The Author(s) 2023.

Figure 3 Agreement of fat fraction measurements between T1 (pre-contrast) and T2 (between portal phase and equilibrium phase). Bland-Altman plots indicating 95% of confidence interval in the hepatic fat fraction measurements (-0.6768, 0.6658).

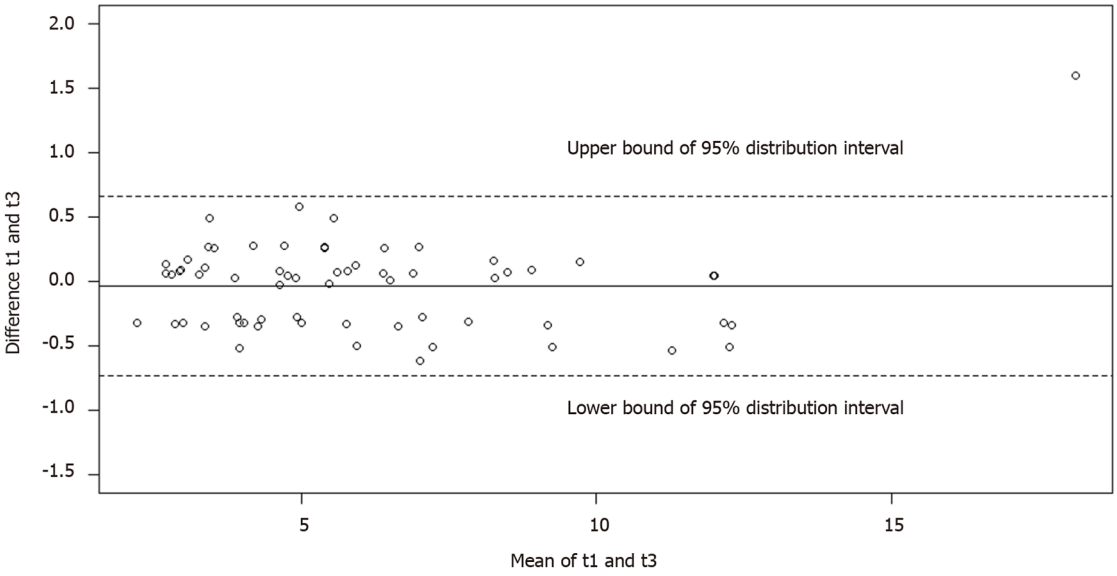

DOI: 10.12998/wjcc.v11.i25.5887 **Copyright** ©The Author(s) 2023.

Figure 4 Agreement of fat fraction measurements between T1 (pre-contrast) and T3 (delayed phase). Bland-Altman plots indicating 95% of confidence interval in the haptic fat fraction measurements (-0.3900, 0.3178).

RESULTS

For the 65 patients, the final FF and R2* values (mean ± SD, n = 65) of the liver, spleen and spine are shown in Table 2. The FF values of the liver, spleen and spine were compared before (time point of T1) and after injection of the contrast agent (T2, T3, and T4). The results showed no significant differences between them (T1-T2, $P = 0.85$; T1-T3, $P = 0.24$; T1-T4, $P = 0.13$), and the FF values were acceptable (Table 3). The R2* value increased from T1 to T2 from 43.14 to 46.21 s-1, respectively ($P < 0.0001$) in the liver and from 42.97 to 46.08 s-1 ($P < 0.0001$) in the spleen. Thereafter, the values reached 46.60 s-1 and 47.10 s-1 at t3 and t4 in the liver ($P < 0.0001$) and 46.38 s-1 and 46.76 s-1 in the spleen ($P < 0.0001$). R2* values in the spine were 121.75 s-1 at t1 and 124.90 s-1, 125.75 s-1 and 126.45 -1 at t2, t3, and t4, respectively ($P < 0.0001$). In summary, the R2* of the liver, spleen and spine increased significantly after injection ($P < 0.0001$), showing a T2* effect of Gd-EOB-DTPA (Table 4).

The Bland-Altman plots (Figures 3-5) demonstrated good agreement of hepatic FF measurements between T1 and T2 (95% confidence interval: -0.6768%, 0.6658%), T1 and T3 (-0.3900%, 0.3178%), and T1 and T4 (-0.3750%, 0.2825%). These findings suggested considerable stability and repeatability of the IDEAL-IQ FF measurements under the impact of Gd-EOB-DTPA.

Table 2 Fat fraction and R2* (mean ± SD, *n* = 65) of the liver, spleen and spine at four time instants

Index	T1	T2	T3	T4
Liver FF	6.0567 ± 3.1295	6.0622 ± 3.1026	6.0928 ± 3.0863	6.103 ± 3.1272
Spleen FF	2.0183 ± 0.7687	2.0363 ± 0.7531	2.0478 ± 0.7633	2.0652 ± 0.7494
Spine FF	25.6275 ± 6.6189	25.6422 ± 6.5966	25.6495 ± 6.5979	25.6648 ± 6.5941
Liver R2*	43.1359 ± 9.95	48.211 ± 10.0155	49.5981 ± 10.0038	52.0894 ± 10.0021
Spleen R2*	42.9711 ± 13.9805	46.0781 ± 13.7729	46.3787 ± 13.7615	46.7647 ± 13.796
Spine R2*	121.7495 ± 20.602	124.902 ± 20.3045	125.7506 ± 20.263	126.4444 ± 20.3439

T1: Pre-contrast; T2: Between portal phase (70 s) and equilibrium phase (180 s); T3: Delayed phase (5 min); T4: Hepatobiliary phase (20 min).

Table 3 The comparison of fat fraction (*n* = 65) before and after hepatocyte-specific contrast media injection

Variation	DF	SS	MS	F	*P* value
T1-T2 (liver)	1	0.001	0.001	0.0319	0.8584
T1-T3 (liver)	1	0.0417	0.0417	1.3901	0.2399
T1-T4 (liver)	1	0.0685	0.0685	2.2825	0.1325
T1-T2 (spleen)	1	0.0103	0.0103	0.4911	0.4843
T1-T3 (spleen)	1	0.0328	0.0328	1.5601	0.2132
T1-T4 (spleen)	1	0.0703	0.0703	3.3418	0.0691
T1-T2 (spleen)	1	0.0069	0.0069	0.1703	0.6803
T1-T3 (spleen)	1	0.0157	0.0157	0.3859	0.5352
T1-T4 (spleen)	1	0.045	0.045	1.1053	0.2944

DF: Degree of freedom; SS: Variance; MS: Mean square; F: Statistics.

Table 4 The comparison of R2* (*n* = 65) before and after injection of Gadoxetate disodium

Variation	DF	SS	MS	F	*P* value
T1-T2 (liver)	1	297.9598	297.9598	476.8081	< 0.0001
T1-T3 (liver)	1	377.59	377.59	604.2357	< 0.0001
T1-T4 (liver)	1	492.3481	492.3481	787.8766	< 0.0001
T1-T2 (spleen)	1	299.2445	299.2445	1035.896	< 0.0001
T1-T3 (spleen)	1	359.9598	359.9598	1246.074	< 0.0001
T1-T4 (spleen)	1	446.1213	446.1213	1544.34	< 0.0001
T1-T2 (spleen)	1	313.126	313.126	317.1906	< 0.0001
T1-T3 (spleen)	1	504.28	504.28	510.826	< 0.0001
T1-T4 (spleen)	1	694.3318	694.3318	703.3447	< 0.0001

DF: Degree of freedom; SS: Variance; MS: Mean square; F: Statistics.

DISCUSSION

Unlike the R2* values, the FF values of the liver, spleen and spine obtained by the IDEAL-IQ sequence showed no significant differences at the four time points before and after the injection of Gd-EOB-DTPA. Our findings demonstrated that this technique for fat quantification can overcome the strong susceptibility effect induced by contrast media, including hepatocyte-specific contrast agents.

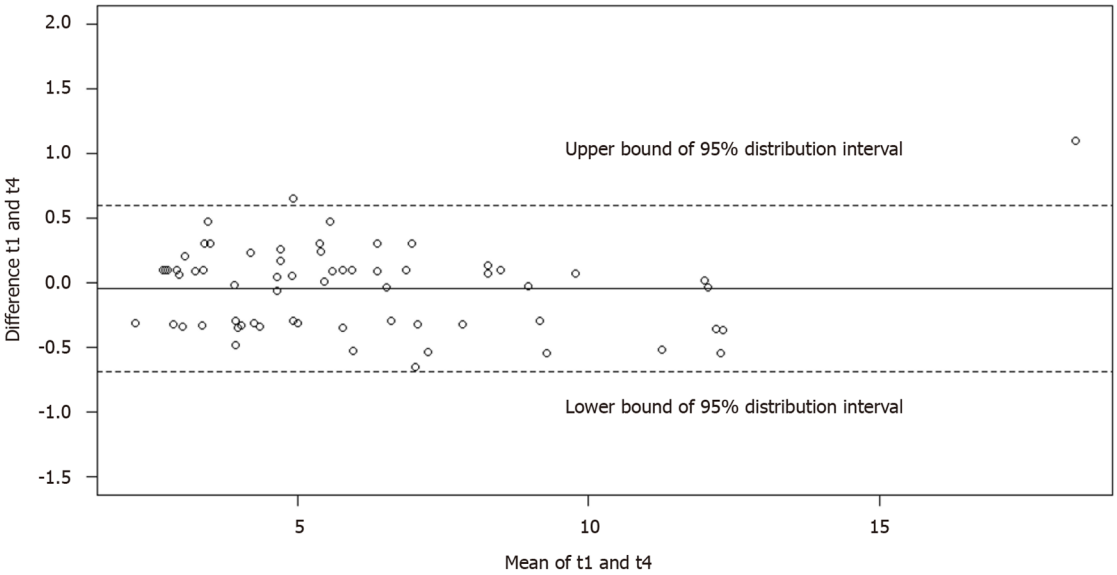

DOI: 10.12998/wjcc.v11.i25.5887

Figure 5 Agreement of fat fraction measurements between T1 (pre-contrast) and T4 (hepatobiliary phase). Bland-Altman plots indicating 95% of confidence interval in the hepatic fat fraction measurements (-0.3750, 0.2825).

IDEAL-IQ is based on a chemical shift-based water and fat separation technique to obtain the proton density fat fraction (PDFF)[14,17,18]. The accuracy of water-fat separation is affected by many factors, including T2* attenuation and the multiple fat peak model. According to the chemical characteristics of triglycerides, the nine-peak fat model was formed. To remove the influence of T2*, a multiecho technique is used to predict the attenuation rate of R2*, and it is used in the calculation of the water and fat maps[16,19]. As a noninvasive liver fat analysis method, several result maps can be reconstructed in one scan, including the FF, R2*, water and fat phases. Moreover, to decrease the signal deviation between water and fat due to the T1 effect, a small flip angle pulse was used to ensure proton density (PD)[19,20]. The stability and repeatability of testing for liver fat using IDEAL-IQ was acceptable and achieved a high accuracy[12,20].

Approximately 50% of the hepatic cells absorbed Gd-EOB-DTPA, which is derived from a lipophilic EOB compound containing gadolinium. This absorption occurred through the organic anion transporting polypeptide (OATP) mechanism [21]. Although the contrast agent partially entered the hepatic cells *via* the intercellular space, it did not affect the water or fat composition but altered the magnetic field environment and T2* effect. However, such attenuation was eliminated by IDEAL-IQ. IDEAL-IQ imaging estimated a complex field map *via* six echo signals using the iterative least-squares method. A complex field map was used to differentiate water and fat and to obtain the dynamic 0 to 100% fat fraction. Amplitude reconstruction was used to quantify the fat fraction, and the phase error was removed. Finally, combined with the results of the two reconstructions, T2* was estimated[20,22]. Thus, elimination of the T2* effect by IDEAL-IQ was relatively stable. A few studies also evaluated the confounding effects of fat detection after injecting a contrast agent, especially SPIO, and found that IDEAL-IQ has stable performance[23]. As a liver-specific contrast agent, SPIO is absorbed by Kupffer cells into hepatic cells. The mechanism was similar to that of Gd-EOB-DTPA, and the difference was mainly in the amounts deposited in hepatic cells. Under T1 deviation, noise difference, T2* decay, a complicated fat resonance spectrum and vortex, the accuracy of the chemical shift in fat quantification was influenced differently[12,20]. However, IDEAL-IQ compensated for and neutralized the effects of interfering factors. Another study illustrated that the FF had no significant difference after injection with Gd-DTPA instead of with Gd-EOB-DTPA in our case[24]. Thus, the presence of contrast agent inside or outside cells does not alter the FF value theoretically.

As a reciprocal of T2*, R2* is related to the water and fat components[17,22]. Due to the application of small 3D flip angle acquisition with gradient echo flyback, the R2* value and FF value can be calculated simultaneously. Therefore, R2* is used to describe the decay of T2* caused by Gd-EOB-DTPA. In our study, the injection of a contrast agent slightly increased R2* due to transverse relaxation of Gd-EOB-DTPA. In the case of contrast agents with similar paramagnetic ions, the R2* influencing factors mainly included micro viscosity, hydrogen proton nuclear dispersion caused by susceptible echo, and the combining capacity with cells[23]. The combining capacity of Gd was lower than that of Gd-EOB-DTPA. However, the influence was limited, which requires further exploration. Being a widely employed liver-specific contrast agent, Gd-EOB-DTPA was similar to Gd in influencing T2* and the T1 relaxation time. At similar dosages, Gd-EOB-DTPA showed a higher relaxation time than Gd, and the paramagnetic effect greatly decreased the T1 relaxation time[25-27]. Nevertheless, IDEAL-IQ effectively addressed the confounding factors that could potentially disrupt accurate fat quantification. It rectified issues such as T2* decay, the distribution of multifat spectrum peaks, and generated separate water and fat images. Additionally, IDEAL-IQ provided valuable information through the fat fraction and R2* maps, further enhancing the reliability of fat quantification[27,28].

However, our study still has a few limitations. First, despite the accuracy and reliability of IDEAL-IQ, Gd-EOB-DTPA intake by hepatic cells was up to 50%, and the role of hepatic function still requires clinical investigation. Second, unstable

breath holding resulted in a slight shift in the local scan layer and further deviation in the inconsistent ROI before and after contrast agent administration. However, we used the image calibration software of the AW4.5 workstation and drew ROIs in the same layer as much as possible. Third, in the four periods of IDEAL-IQ after contrast agent injection, the initial time was influenced by several factors. A deviation in the FF value and other parameters was caused by a failure to achieve the target time. Control of the scan time is important for further study.

CONCLUSION

The measurement of fat fraction was stable when using IDEAL-IQ to detect the FF values in patients scanned by EOB-MRI before and after injecting a hepatocyte-specific contrast agent. The R2* values in the liver, spleen and spine increased after injection of Gd-EOB-DTPA but had no significant effect on fat quantification. Such strong reproducibility makes IDEAL-IQ available in the interval for saving time during examination and optimizing the scanning protocol.

ARTICLE HIGHLIGHTS

Research background

Iterative decomposition of water and fat with echo asymmetry and least squares estimation quantification sequence (IDEAL-IQ) is based on chemical shift-based water and fat separation technique to get proton density fat fraction. Multiple studies have shown that using IDEAL-IQ to test the stability and repeatability of liver fat is acceptable and has high accuracy.

Research motivation

At present, there are few studies on comparing the fat content of different Gadoxetate Disodium (Gd-EOB-DTPA) enhanced organs at different periods. This research can further solve the problem of whether Gd-EOB-DTPA affects fat fraction measurement, and test repeatability of ideal-IQ at Different Periods, which can optimize clinical examination items.

Research objectives

The challenges associated with the widespread applications of liver-specific contrast medium Gd-EOB-DTPA, the purpose of this study is to evaluate whether the Gd-EOB-DTPA would interfere with the measurement of hepatic fat content that was quantified with IDEAL IQ sequence, and the robustness of this technique was also evaluated.

Research methods

In this study, IDEAL-IQ was employed to quantify liver fat content in a cohort of 65 patients who received injections of Gd-EOB-DTPA contrast material during imaging at 3.0T. Following the injection, IDEAL-IQ was performed four times, and measurements of the fat fraction (FF) and R2* were obtained at specific time points: pre-contrast, between the portal phase (70 s) and late phase (180 s), delayed phase (5 min), and hepatobiliary phase (20 min). These measurements allowed for the assessment of liver fat content at different stages of contrast material uptake and clearance.

Research results

The evaluation of the FF at four different time points in the liver, spleen, and spine revealed no significant differences. Furthermore, the measurements of hepatic FF demonstrated good consistency between T1 and T2, T1 and T3, as well as T1 and T4. On the other hand, the R2* values of the liver, spleen, and spine exhibited a significant increase following the injection of the contrast material.

Research conclusions

Using IDEAL-IQ sequence in the measurement of FF, we can get results that won't be affected by Gd-EOB-DTPA. The high reproducibility of IDEAL IQ makes it available in the interval of scanning for saving time during multi-phase examination.

Research perspectives

Multi-center prospective studies with larger sample sizes are required to investigate whether the dosage of GD-EOB-DTPA affects IDEAL-IQ FF.

ACKNOWLEDGEMENTS

We would like to thank all the study participants and the staff of our hospital. Thanks the National Natural Science Foundation of China.

FOOTNOTES

Author contributions: Tian Y and Sun P contributed equally to this work; Tian Y, Liu PF, and Sun P designed the research study; Tian Y, Li JY performed the research; Li YN and Li JY scanned patients and collected data; Tian Y, Sun P and Li JY analyzed the data and wrote the manuscript; all authors have read and approve the final manuscript.

Supported by National Natural Science Foundation of China, No. 82272053.

Institutional review board statement: The study was reviewed and approved by The First Affiliated Hospital of Harbin Medical University Institutional Review Board [(Approval No. 2020JS09)].

Conflict-of-interest statement: All authors disclosed no relevant relationships.

Data sharing statement: No additional data are available.

Country/Territory of origin: China

ORCID number: Yuan Tian 0000-0003-1867-0793; Peng-Fei Liu 0000-0003-2503-8761; Peng Sun 0009-0000-9036-8922.

S-Editor: Ma YJ
L-Editor: A
P-Editor: Wu RR

REFERENCES

1 **Clark JM**, Cryer DRH, Morton M, Shubrook JH. Nonalcoholic fatty liver disease from a primary care perspective. *Diabetes Obes Metab* 2023; **25**: 1421-1433 [PMID: 36789676 DOI: 10.1111/dom.15016]
2 **Sheka AC**, Adeyi O, Thompson J, Hameed B, Crawford PA, Ikramuddin S. Nonalcoholic Steatohepatitis: A Review. *JAMA* 2020; **323**: 1175-1183 [PMID: 32207804 DOI: 10.1001/jama.2020.2298]
3 **Younossi ZM**, Koenig AB, Abdelatif D, Fazel Y, Henry L, Wymer M. Global epidemiology of nonalcoholic fatty liver disease-Meta-analytic assessment of prevalence, incidence, and outcomes. *Hepatology* 2016; **64**: 73-84 [PMID: 26707365 DOI: 10.1002/hep.28431]
4 **Permutt Z**, Le TA, Peterson MR, Seki E, Brenner DA, Sirlin C, Loomba R. Correlation between liver histology and novel magnetic resonance imaging in adult patients with non-alcoholic fatty liver disease-MRI accurately quantifies hepatic steatosis in NAFLD. *Aliment Pharmacol Ther* 2012; **36**: 22-29 [PMID: 22554256 DOI: 10.1111/j.1365-2036.2012.05121.x]
5 **Saadeh S**, Younossi ZM, Remer EM, Gramlich T, Ong JP, Hurley M, Mullen KD, Cooper JN, Sheridan MJ. The utility of radiological imaging in nonalcoholic fatty liver disease. *Gastroenterology* 2002; **123**: 745-750 [PMID: 12198701 DOI: 10.1053/gast.2002.35354]
6 **Khalifa A**, Rockey DC. The utility of liver biopsy in 2020. *Curr Opin Gastroenterol* 2020; **36**: 184-191 [PMID: 32097176 DOI: 10.1097/MOG.0000000000000621]
7 **Graif M**, Yanuka M, Baraz M, Blank A, Moshkovitz M, Kessler A, Gilat T, Weiss J, Walach E, Amazeen P, Irving CS. Quantitative estimation of attenuation in ultrasound video images: correlation with histology in diffuse liver disease. *Invest Radiol* 2000; **35**: 319-324 [PMID: 10803673 DOI: 10.1097/00004424-200005000-00006]
8 **Starekova J**, Hernando D, Pickhardt PJ, Reeder SB. Quantification of Liver Fat Content with CT and MRI: State of the Art. *Radiology* 2021; **301**: 250-262 [PMID: 34546125 DOI: 10.1148/radiol.2021204288]
9 **Guo Z**, Blake GM, Li K, Liang W, Zhang W, Zhang Y, Xu L, Wang L, Brown JK, Cheng X, Pickhardt PJ. Liver Fat Content Measurement with Quantitative CT Validated against MRI Proton Density Fat Fraction: A Prospective Study of 400 Healthy Volunteers. *Radiology* 2020; **294**: 89-97 [PMID: 31687918 DOI: 10.1148/radiol.2019190467]
10 **Wang YS**, Ye J, Cao YH, Zhang R, Han XF, Zou LL, Kuang L, Zhang J, Lian H, Xia JX, Zhang Q, Dai W. Association of [(1)H]-MRS quantified liver fat content with glucose metabolism status. *Diabetol Metab Syndr* 2020; **12**: 51 [PMID: 32528557 DOI: 10.1186/s13098-020-00558-8]
11 **Idilman IS**, Keskin O, Celik A, Savas B, Elhan AH, Idilman R, Karcaaltincaba M. A comparison of liver fat content as determined by magnetic resonance imaging-proton density fat fraction and MRS versus liver histology in non-alcoholic fatty liver disease. *Acta Radiol* 2016; **57**: 271-278 [PMID: 25855666 DOI: 10.1177/0284185115580488]
12 **Heba ER**, Desai A, Zand KA, Hamilton G, Wolfson T, Schlein AN, Gamst A, Loomba R, Sirlin CB, Middleton MS. Accuracy and the effect of possible subject-based confounders of magnitude-based MRI for estimating hepatic proton density fat fraction in adults, using MR spectroscopy as reference. *J Magn Reson Imaging* 2016; **43**: 398-406 [PMID: 26201284 DOI: 10.1002/jmri.25006]
13 **Ren W**, Feng Y, Li J, Zhang C, Feng L, Cui L, Ran J. Relationship of liver fat content with systemic metabolism and chronic complications in patients with type 2 diabetes mellitus. *Lipids Health Dis* 2023; **22**: 11 [PMID: 36694216 DOI: 10.1186/s12944-023-01775-6]
14 **Eskreis-Winkler S**, Corrias G, Monti S, Zheng J, Capanu M, Krebs S, Fung M, Reeder S, Mannelli L. IDEAL-IQ in an oncologic population: meeting the challenge of concomitant liver fat and liver iron. *Cancer Imaging* 2018; **18**: 51 [PMID: 30541635 DOI: 10.1186/s40644-018-0167-3]
15 **Hui SCN**, So HK, Chan DFY, Wong SKH, Yeung DKW, Ng EKW, Chu WCW. Validation of water-fat MRI and proton MRS in assessment of hepatic fat and the heterogeneous distribution of hepatic fat and iron in subjects with non-alcoholic fatty liver disease. *Eur J Radiol* 2018;

107: 7-13 [PMID: 30292275 DOI: 10.1016/j.ejrad.2018.08.008]

16 **Wu B**, Han W, Li Z, Zhao Y, Ge M, Guo X, Wu X. Reproducibility of Intra- and Inter-scanner Measurements of Liver Fat Using Complex Confounder-corrected Chemical Shift Encoded MRI at 3.0 Tesla. *Sci Rep* 2016; **6**: 19339 [PMID: 26763303 DOI: 10.1038/srep19339]

17 **Reeder SB**, Pineda AR, Wen Z, Shimakawa A, Yu H, Brittain JH, Gold GE, Beaulieu CH, Pelc NJ. Iterative decomposition of water and fat with echo asymmetry and least-squares estimation (IDEAL): application with fast spin-echo imaging. *Magn Reson Med* 2005; **54**: 636-644 [PMID: 16092103 DOI: 10.1002/mrm.20624]

18 **Corrias G**, Krebs S, Eskreis-Winkler S, Ryan D, Zheng J, Capanu M, Saba L, Monti S, Fung M, Reeder S, Mannelli L. MRI liver fat quantification in an oncologic population: the added value of complex chemical shift-encoded MRI. *Clin Imaging* 2018; **52**: 193-199 [PMID: 30103108 DOI: 10.1016/j.clinimag.2018.08.002]

19 **Hernando D**, Sharma SD, Aliyari Ghasabeh M, Alvis BD, Arora SS, Hamilton G, Pan L, Shaffer JM, Sofue K, Szeverenyi NM, Welch EB, Yuan Q, Bashir MR, Kamel IR, Rice MJ, Sirlin CB, Yokoo T, Reeder SB. Multisite, multivendor validation of the accuracy and reproducibility of proton-density fat-fraction quantification at 1.5T and 3T using a fat-water phantom. *Magn Reson Med* 2017; **77**: 1516-1524 [PMID: 27080068 DOI: 10.1002/mrm.26228]

20 **Liu CY**, McKenzie CA, Yu H, Brittain JH, Reeder SB. Fat quantification with IDEAL gradient echo imaging: correction of bias from T(1) and noise. *Magn Reson Med* 2007; **58**: 354-364 [PMID: 17654578 DOI: 10.1002/mrm.21301]

21 **Caraiani CN**, Dan M, Fenesan DI, Badea R. Description of focal liver lesions with Gd-EOB-DTPA enhanced MRI. *Clujul Med* 2015; **88**: 438-448 [PMID: 26733231 DOI: 10.15386/cjmed-414]

22 **Yu H**, McKenzie CA, Shimakawa A, Vu AT, Brau AC, Beatty PJ, Pineda AR, Brittain JH, Reeder SB. Multiecho reconstruction for simultaneous water-fat decomposition and T2* estimation. *J Magn Reson Imaging* 2007; **26**: 1153-1161 [PMID: 17896369 DOI: 10.1002/jmri.21090]

23 **Liau J**, Shiehmorteza M, Girard OM, Sirlin CB, Bydder M. Evaluation of MRI fat fraction in the liver and spine pre and post SPIO infusion. *Magn Reson Imaging* 2013; **31**: 1012-1016 [PMID: 23602721 DOI: 10.1016/j.mri.2013.01.016]

24 **Ge M**, Zhang J, Wu B, Liu Z, Song H, Meng X, Wu X. Effect of gadolinium on hepatic fat quantification using multi-echo reconstruction technique with T2* correction and estimation. *Eur Radiol* 2016; **26**: 1913-1920 [PMID: 26376885 DOI: 10.1007/s00330-015-3981-z]

25 **Shuter B**, Tofts PS, Wang SC, Pope JM. The relaxivity of Gd-EOB-DTPA and Gd-DTPA in liver and kidney of the Wistar rat. *Magn Reson Imaging* 1996; **14**: 243-253 [PMID: 8725190 DOI: 10.1016/0730-725x(95)02097-d]

26 **Bydder M**, Yokoo T, Hamilton G, Middleton MS, Chavez AD, Schwimmer JB, Lavine JE, Sirlin CB. Relaxation effects in the quantification of fat using gradient echo imaging. *Magn Reson Imaging* 2008; **26**: 347-359 [PMID: 18093781 DOI: 10.1016/j.mri.2007.08.012]

27 **Sofue K**, Zhong X, Nickel MD, Dale BM, Bashir MR. Stability of liver proton density fat fraction and changes in R 2* measurements induced by administering gadoxetic acid at 3T MRI. *Abdom Radiol (NY)* 2016; **41**: 1555-1564 [PMID: 27052456 DOI: 10.1007/s00261-016-0728-5]

28 **Meisamy S**, Hines CD, Hamilton G, Sirlin CB, McKenzie CA, Yu H, Brittain JH, Reeder SB. Quantification of hepatic steatosis with T1-independent, T2-corrected MR imaging with spectral modeling of fat: blinded comparison with MR spectroscopy. *Radiology* 2011; **258**: 767-775 [PMID: 21248233 DOI: 10.1148/radiol.10100708]

World Journal of Clinical Cases

Submit a Manuscript: https://www.f6publishing.com

World J Clin Cases 2023 September 6; 11(25): 5897-5902

DOI: 10.12998/wjcc.v11.i25.5897

ISSN 2307-8960 (online)

ORIGINAL ARTICLE

Retrospective Study

Conservative management of multi-trauma induced peritonitis: Experience, outcomes, and indications

Qi Chen, Tao Zhu, Jia-Kang Liu, Jun Ding, Lina Chen

Specialty type: Surgery

Provenance and peer review: Unsolicited article; Externally peer reviewed.

Peer-review model: Single blind

Peer-review report's scientific quality classification

Grade A (Excellent): 0
Grade B (Very good): B
Grade C (Good): 0
Grade D (Fair): D
Grade E (Poor): 0

P-Reviewer: Ghimire R, Nepal; Lieto E, Italy

Received: May 17, 2023
Peer-review started: May 17, 2023
First decision: June 15, 2023
Revised: June 27, 2023
Accepted: August 7, 2023
Article in press: August 7, 2023
Published online: September 6, 2023

Qi Chen, Tao Zhu, Jia-Kang Liu, Jun Ding, Department of Surgery, Shuguang Hospital Affiliated to Shanghai University of Traditional Chinese Medicine, Shanghai 201203, China

Lina Chen, Department of Laboratory Medicine and Pathobiology, University of Toronto, Toronto M5S 1A8, Ontario, Canada

Corresponding author: Lina Chen, FRCPC, MD, MMed, MSc, Assistant Professor, Attending Doctor, Consultant Physician-Scientist, Department of Laboratory Medicine and Pathobiology, University of Toronto, No. 1 King's College Circle, Toronto M5S 1A8, Ontario, Canada. lina.chen@utoronto.ca

Abstract

BACKGROUND

The concept of mandatory laparotomy in treating traumatic peritonitis has been increasingly questioned recently.

AIM

To summarize and share the experience of conservative treatment of patients with multi-trauma induced peritonitis.

METHODS

A retrospective review was performed on patients with multiple injury induced traumatic peritonitis.

RESULTS

A total of 184 patients with multiple injury induced traumatic peritonitis were reviewed. 46 of them underwent conservative treatment. None of the 46 patients with conservative treatment switched to surgical treatment, and all of them were cured and discharged after successful conservative treatment. No significant abnormal findings were observed at regular follow-up after discharge.

CONCLUSION

Conservative management is safe, effective, feasible, and beneficial in hemodynamically stable patients with traumatic peritonitis if there is no definite evidence of severe abdominal visceral organ injury.

Key Words: Trauma; Peritonitis; Damage control; Conservative treatment

Core Tip: A retrospective review was performed on 184 patients with multiple injury induced peritonitis. It reveals that conservative management is safe, effective, feasible, and beneficial in hemodynamically stable patients with traumatic peritonitis if there is no definite evidence of severe abdominal visceral organ injury.

Citation: Chen Q, Zhu T, Liu JK, Ding J, Chen L. Conservative management of multi-trauma induced peritonitis: Experience, outcomes, and indications. *World J Clin Cases* 2023; 11(25): 5897-5902
URL: https://www.wjgnet.com/2307-8960/full/v11/i25/5897.htm
DOI: https://dx.doi.org/10.12998/wjcc.v11.i25.5897

INTRODUCTION

Peritonitis refers to the inflammation of the peritoneum. Symptoms and signs may include abdominal pain and tenderness, abdominal guarding and rigidity, rebound tenderness, and fever. A diagnosis of peritonitis is based primarily on the clinical manifestations described above. Rigidity is the most specific exam finding for diagnosing peritonitis. Peritonitis can be caused by infection, chemical, and injuries. Traumatic peritonitis is caused by injury and in most cases requires surgical treatment[1]. Given the great risk of missing occult injuries, mandatory laparotomy has been a well-known guideline in treating traumatic peritonitis. However, recently, this concept has been increasingly questioned[2,3], especially in patients with low risk of a true rupture or bleeding of intraabdominal viscera. In fact, such patients are complicated by severe injury. Their conditions may deteriorate if an inappropriate exploratory laparotomy is performed, causing serious physiological dysfunction, even death[4]. The recent study retrospectively reviewed 43 cases of blunt trauma to abdominal solid organs and found 20 (47%) cases attempted conservative management with successful rate of 90% (18 out of 20 cases)[5]. We aim to review the outcomes of conservative management of traumatic peritonitis and explore the indications for managing it conservatively.

MATERIALS AND METHODS

Patients presented with traumatic peritonitis caused by multiple injuries to the Shuguang Hospital, China from April 2016 to June 2022 were reviewed. Confidentiality of all patients´ information was maintained and permission from the hospital ethical committee for the use of medical data and publishing of the study results was obtained.

Demographic data, clinical parameters, laboratory values, diagnostic examinations, management strategies and outcomes were analyzed. Hemodynamic instability was defined as systolic blood pressure < 90 mmHg, or > 90 mmHg but requiring bolus infusions/transfusions and/or vasopressor drugs. Positive abdominal findings included abdominal pain, rigidity of abdominal wall muscles and positive rebound sign on examination. The injury severity score (ISS) was calculated using the organ injury scaling committee of the American association for the surgery of trauma[6].The amount of peritoneum fluid was calculated by abdominal ultrasound and defined as: Small when the fluid was limited in pelvis or only between bowels with the maximal fluid depth (AP diameter) of 2-4 cm; medium when the maximal fluid depth (AP diameter) was 4-8 cm; large when the fluid was diffusely present in pelvis and abdomen with the maximal fluid depth (AP diameter) more than 8 cm.

RESULTS

A total of 184 patients with multiple traumas induced traumatic peritonitis were admitted from April 2016 to June 2022, including 116 males and 68 females with a mean age of 35.3 ± 10.5 years old. The causes of trauma included 85 cases of traffic injuries, 63 cases of falls from height, 20 cases of injuries from hitting by heavy objects, 16 cases of fights and assaults. The average ISS score was 26.5 points ± 14.9 points, including 42 cases of combined brain trauma, 67 cases of thoracic trauma, and 64 cases of spinopelvic or extremity fracture.

All the patients completed the relevant laboratory examination after admission in emergency room, including physical exam, routine urinalysis for hematuria, serology for cardiac enzymes, blood lactate, liver and kidney function, electrolytes, coagulation test, arterial blood gas analysis. All had emergency electrocardiogram, focused assessment with sonography in trauma (FAST), head, chest, abdomen and pelvis rapid spiral computed tomography (CT) examination, and extremity X-rays.

We identified that 46 patients were treated conservatively, accounting for 25% of the total cases. All of them were managed successfully by conservative treatment alone. None of them switched to surgical treatment. The patient demographics and outcomes are summarized in Table 1. The causes of peritonitis are listed in Table 2.

Table 1 Patient demographics and outcomes

Characteristics	OM (*n* = 138)	CM (*n* = 46)	*P* value
Age (yr), mean ± SD	42.38 ± 15.75	40.30 ± 12.63	$P = 0.418$
Median (range)	38 (16-83)	39.5 (22-67)	$P = 0.602$
M/F	100/38	16/30	$P < 0.001$
ISS score ± SD	28.38 ± 8.99	25.39 ± 8.84	$P = 0.037$
Hemodynamic instability	102	9	$P < 0.001$
Spleen injury	38	26	$P < 0.001$
Liver injury	18	8	$P = 0.305$
Pancreas injury	4	5	$P = 0.045$
Multiple abdominal solid organ injury	5	4	$P = 0.067$
Bowel injury	106	3	$P < 0.001$
ICU admission	138	31	$P < 0.001$
Mortality	6	0	$P = 0.339$

OM: Operative management; CM: Conservative management; SD: Standard deviation; M/F: Males/females; ISS: Injury severity score; ICU: Intensive care unit.

Table 2 Causes of peritonitis

Causes		OM (*n* = 138)	CM (*n* = 46)
Major abdominal visceral damage	Major solid organ injury	60	0
	Hollow organ perforation	106	0
Bleeding	Minor injury to solid organs	0	43
	Injury to vessels	16	3
Extra-abdominal injuries	Multiple rib fractures	48	19
	Anterior abdominal wall contusion	112	10
	Low back fractures or soft tissue injuries	12	14
	Pelvic fracture, pelvic hematoma, retroperitoneum hematoma	46	6

OM: Operative management; CM: Conservative management.

A case-by-case review of the 46 conservatively managed case revealed the following characteristics: For 15 cases with a small amount of peritoneal effusion, ISS grade III or less, no definite visceral damage found, and no hemodynamic instability, conservative treatment with close observation in emergency room was performed.

Thirsty-one cases with moderate peritoneal effusion, visceral damage or hemodynamic instability were admitted into intensive care unit with close monitoring, open central venous access, active anti-shock treatment, and transfusion as needed. These cases were under close observation of abdominal symptoms and signs and image studies were repeated if clinically indicated.

The conservative management included fasting, gastrointestinal decompression, acid suppression, broad-spectrum antibiotics against infection, and TPN nutritional support. Clinical and laboratory monitoring included frequent assessment of clinical symptoms and signs, urine output, hemoglobin, hematocrit, and arterial blood gas analysis (every six hour in first 24 h, at least daily for 3 d, and the interval of reexamination was increased after the condition was stable). In addition to the FAST exam performed in emergency room, abdominal ultrasound or CT scan was repeated on the second day after admission to confirm the peritoneal effusion and assess the progress of the injury, followed with another ultrasound or CT 3-7 d post-admission. Patients were immobilized in a flat position and were guaranteed not to be at risk for possible bleeding if moved. Emotional support was provided to relieve patient anxiety and sedatives were use when necessary.

There was no conversion to surgical treatment in these 46 conservatively managed patients. All were discharged after successful conservative treatment. The average hospital stay was 14 d. Patients were followed up after discharge. All laboratory parameters were normal after 3 mo and repeated ultrasound and CT confirmed no obvious abnormal findings

in the abdominal cavity.

DISCUSSION

The peritoneum is a very thin layer of serosa composed of mesothelial cells and divided into two parts, the parietal peritoneum and the visceral peritoneum. The parietal peritoneum is mainly innervated by intercostal nerves and lumbar nerves so it is sensitive to pain. When the peritoneum of the anterior abdominal wall is stimulated, it can cause reflex abdominal muscle tension, called rigidity. It is pathognomonic for the diagnosis of peritonitis. Most peritonitis are treated with surgical operation, especially secondary peritonitis, which is often caused by injury or perforation of abdominal visceral organs[7].

In patient with multi-trauma, many second hits such as surgery and resuscitation are inappropriately applied, which may trap these patients in a vicious cycle of lethal triad consisting of hypothermia, coagulopathy and metabolic acidosis [8-10]. Therefore, damage control plays an increasing role in patient care for severe multiple trauma. The rational and cautious application of damage control surgery is extremely important in patients with severe trauma, especially abdominal injury. The current concept of damage control is applicable to all surgical specialties, and the core idea is to consider surgery as part of the overall resuscitation process[11]. The consequences of excessive surgical intervention for severely traumatized patients are dreadful[12]. Therefore, for multi-trauma patients with peritonitis, explorative laparotomy must be minimized to alleviate the unnecessary damage caused by the second hit. The cause of peritonitis must be clarified as soon as possible to decide on further treatment modalities.

The etiology of peritonitis in patients with multiple trauma is broadly classified into the following three conditions: major abdominal visceral damage including major solid organ injury and hollow organ perforation, bleeding due to minor injury to solid organs or vessels, and effect from extra-abdominal injuries[13]. Patients with major abdominal visceral damage need to undergo surgical treatment. Most of them can be done by routine laparotomy. However, damage control laparotomy should be performed if the patient condition requires. Peritonitis caused by bleeding due to minor visceral damage such as liver and spleen damage in grade three or less organ damage, conservative treatment can be performed to avoid the second hit caused by surgery[14,15]. Peritonitis caused by extra-abdominal injuries, including pelvic fracture, pelvic hematoma, retroperitoneum hematoma, frequent reassessment and repeated image studies should be performed[16,17].

In addition, symptoms from some extra-abdominal injuries can mimic peritonitis[18]. Multiple rib fractures especially of the lower quarter ribs can commonly cause abdominal pain and abdominal muscle tension. Low back fractures or soft tissue injuries can stimulate the lumbar nerves, resulting in extensive anterior abdominal wall tension and tenderness. Anterior abdominal wall contusion especially intramuscular hemorrhage can present as localized abdominal pain and tenderness. These symptoms and signs can be misleading. Surgeons need to be caution to not rush to surgical exploration and always have these in the differential diagnoses when assessing multi-trauma patients. In the absence of definitive evidence of intra-abdominal visceral injury, patients need to be closely observed for changes in clinical symptoms and signs, ancillary tests, and image. To our knowledge, these "pseudoperitonitis" has not been well studies and reported.

In this study, we retrospectively reviewed a total of 184 cases of multi trauma induced peritonitis with 46 cases treated conservatively. Under the guidance of damage control concept, these patients avoided unnecessary damage from exploratory surgery, eliminated the risk of surgical complications, and achieved good therapeutic outcomes.

CONCLUSION

Therefore, we conclude that for multi trauma patients with peritonitis, if there is no definite evidences for severe intra-abdominal visceral organ damage and patients are hemodynamically stable, conservative treatment is safe and beneficial. We recommended that conservative treatment of traumatic peritonitis should be attempted in centers with experienced surgeons, capability for precise diagnosing (ultrasound, CT, and magnetic resonance imaging), ample medical staff and equipment for uninterrupted close monitoring, and instant accessibility to operation.

ARTICLE HIGHLIGHTS

Research background

With damage control plays an increasing role in patient care for severe multiple trauma, the concept of mandatory laparotomy in treating traumatic peritonitis has been increasingly questioned recently.

Research motivation

By reveiwing the treatment modalities and outcomes of patients with multiple injury induced traumatic peritonitis, we propose the indications and share the experience of conservative managment of multi-trauma induced peritonitis.

Research objectives

To review the outcomes of conservative management of traumatic peritonitis and explore the indications for managing it

conservatively.

Research methods

A retrospective review was performed on a total of 184 patients with multiple injury induced traumatic peritonitis.

Research results

Out of 184 patients with multiple injury induced traumatic peritonitis, 46 of them underwent conservative treatment. None of the conservatively managed patients switched to surgical treatment and all of them fully recovered.

Research conclusions

In hemodynamically stable patients with traumatic peritonitis, conservative management is safe, effective, feasible, and beneficial if there is no definite evidence of severe abdominal visceral organ injury.

Research perspectives

We aim to seek collaborations from other institutions to conduct a multi-center study to further explore conservative management of multiple injury induced traumatic peritonitis.

FOOTNOTES

Author contributions: Chen Q, Zhu T, and Liu JK contributed equally to this work; Chen L designed the research study; Chen Q, Zhu T, Liu JK, and Ding J performed the research; Chen L, Chen Q, Zhu T, and Liu JK analyzed the data and wrote the manuscript; all authors have read and approved the final manuscript.

Institutional review board statement: The study was reviewed and approved by the Institutional Review Board of Shuguang Hospital Affiliated with Shanghai Univeristy of TCM (Approval No. 2023-1321-88-01).

Informed consent statement: This is a retrospective chart review study. Individual patient consent is waived according to the Research Ethics Board.

Conflict-of-interest statement: The authors have no conflicts of interest to declare.

Data sharing statement: No additional data are available.

Country/Territory of origin: China

ORCID number: Qi Chen 0009-0004-0516-4845; Tao Zhu 0009-0007-1677-1722; Jia-Kang Liu 0009-0006-5006-2148; Jun Ding 0000-0003-3686-1710; Lina Chen 0009-0006-1621-2747.

S-Editor: Chen YL
L-Editor: A
P-Editor: Chen YL

REFERENCES

1 **Feliciano DV**. Abdominal Trauma Revisited. *Am Surg* 2017; **83**: 1193-1202 [PMID: 29183519]
2 **Leenellett E**, Rieves A. Occult Abdominal Trauma. *Emerg Med Clin North Am* 2021; **39**: 795-806 [PMID: 34600638 DOI: 10.1016/j.emc.2021.07.009]
3 **Thomas MN**, Whaba R, Datta RR, Bunck AC, Stippel DL, Bruns CJ. [Management and treatment of liver injuries after blunt abdominal trauma]. *Chirurgie (Heidelb)* 2023 [PMID: 37142798 DOI: 10.1007/s00104-023-01858-1]
4 **Bonne S**, Sheikh F. Controversies in Surgery: Trauma. *Surg Clin North Am* 2021; **101**: 1111-1121 [PMID: 34774272 DOI: 10.1016/j.suc.2021.06.008]
5 **Karachentsev S**. Blunt trauma to abdominal solid organs: an experience of non-operative management at a rural hospital in Zambia. *Pan Afr Med J* 2021; **38**: 89 [PMID: 33889255 DOI: 10.11604/pamj.2021.38.89.20061]
6 **Linn S**. The injury severity score--importance and uses. *Ann Epidemiol* 1995; **5**: 440-446 [PMID: 8680606 DOI: 10.1016/1047-2797(95)00059-3]
7 **Ross JT**, Matthay MA, Harris HW. Secondary peritonitis: principles of diagnosis and intervention. *BMJ* 2018; **361**: k1407 [PMID: 29914871 DOI: 10.1136/bmj.k1407]
8 **van Veelen MJ**, Brodmann Maeder M. Hypothermia in Trauma. *Int J Environ Res Public Health* 2021; **18** [PMID: 34444466 DOI: 10.3390/ijerph18168719]

9 **Moore EE**, Moore HB, Kornblith LZ, Neal MD, Hoffman M, Mutch NJ, Schöchl H, Hunt BJ, Sauaia A. Trauma-induced coagulopathy. *Nat Rev Dis Primers* 2021; **7**: 30 [PMID: 33927200 DOI: 10.1038/s41572-021-00264-3]

10 **Benz D**, Balogh ZJ. Damage control surgery: current state and future directions. *Curr Opin Crit Care* 2017; **23**: 491-497 [PMID: 29035926 DOI: 10.1097/MCC.0000000000000465]

11 **Pape HC**, Moore EE, McKinley T, Sauaia A. Pathophysiology in patients with polytrauma. *Injury* 2022; **53**: 2400-2412 [PMID: 35577600 DOI: 10.1016/j.injury.2022.04.009]

12 **Roberts DJ**, Bobrovitz N, Zygun DA, Ball CG, Kirkpatrick AW, Faris PD, Brohi K, D'Amours S, Fabian TC, Inaba K, Leppäniemi AK, Moore EE, Navsaria PH, Nicol AJ, Parry N, Stelfox HT. Indications for Use of Damage Control Surgery in Civilian Trauma Patients: A Content Analysis and Expert Appropriateness Rating Study. *Ann Surg* 2016; **263**: 1018-1027 [PMID: 26445471 DOI: 10.1097/SLA.0000000000001347]

13 **Kanlerd A**, Auksornchart K, Boonyasatid P. Non-operative management for abdominal solidorgan injuries: A literature review. *Chin J Traumatol* 2022; **25**: 249-256 [PMID: 34654595 DOI: 10.1016/j.cjtee.2021.09.006]

14 **Duron V**, Stylianos S. Strategies in liver Trauma. *Semin Pediatr Surg* 2020; **29**: 150949 [PMID: 32861453 DOI: 10.1016/j.sempedsurg.2020.150949]

15 **Malloum Boukar K**, Moore L, Tardif PA, Soltana K, Yanchar N, Kortbeek J, Champion H, Clement J. Value of repeat CT for nonoperative management of patients with blunt liver and spleen injury: a systematic review. *Eur J Trauma Emerg Surg* 2021; **47**: 1753-1761 [PMID: 33484276 DOI: 10.1007/s00068-020-01584-x]

16 **Schnüriger B**, Lam L, Inaba K, Kobayashi L, Barbarino R, Demetriades D. Negative laparotomy in trauma: are we getting better? *Am Surg* 2012; **78**: 1219-1223 [PMID: 23089438]

17 **Nicolau AE**, Craciun M, Vasile R, Kitkani A, Beuran M. The Role of Laparoscopy in Abdominal Trauma: A 10-Year Review. *Chirurgia (Bucur)* 2019; **114**: 359-368 [PMID: 31264574 DOI: 10.21614/chirurgia.114.3.359]

18 **Osterwalder I**, Özkan M, Malinovska A, Nickel CH, Bingisser R. Correction: Osterwalder *et al*. Acute Abdominal Pain: Missed Diagnoses, Extra-Abdominal Conditions, and Outcomes. *J Clin Med* 2023; **12** [PMID: 36836243 DOI: 10.3390/jcm12041403]

World Journal of Clinical Cases

Submit a Manuscript: https://www.f6publishing.com

World J Clin Cases 2023 September 6; 11(25): 5903-5909

DOI: 10.12998/wjcc.v11.i25.5903

ISSN 2307-8960 (online)

ORIGINAL ARTICLE

Retrospective Study

Analysis of prognostic factors in patients with emergency sepsis

Xian-Li Ning, Min Shao

Specialty type: Critical care medicine

Provenance and peer review: Unsolicited article; Externally peer reviewed.

Peer-review model: Single blind

Peer-review report's scientific quality classification

Grade A (Excellent): 0
Grade B (Very good): B
Grade C (Good): C
Grade D (Fair): 0
Grade E (Poor): 0

P-Reviewer: Maraka S, United States; Volk HA, Germany

Received: July 4, 2023
Peer-review started: July 4, 2023
First decision: July 19, 2023
Revised: July 21, 2023
Accepted: August 7, 2023
Article in press: August 7, 2023
Published online: September 6, 2023

Xian-Li Ning, Department of Emergency, Anqing Municipal Hospital, Anqing 246000, Anhui Province, China

Min Shao, Department of Critical Care Medicine, The First Affiliated Hospital of Anhui Medical University, Hefei 230031, Anhui Province, China

Corresponding author: Min Shao, PhD, Chief Physician, Department of Critical Care Medicine, The First Affiliated Hospital of Anhui Medical University, No. 218 Jixi Road, Shushan District, Hefei 230031, Anhui Province, China. minicu2021@163.com

Abstract

BACKGROUND

Emergency sepsis is a common and serious infectious disease, and its prognosis is influenced by a number of factors.

AIM

To analyse the factors influencing the prognosis of patients with emergency sepsis in order to provide a basis for individualised patient treatment and care. By retrospectively analysing the clinical data collected, we conducted a comprehensive analysis of factors such as age, gender, underlying disease, etiology and site of infection, inflammatory indicators, multi-organ failure, cardiovascular function, therapeutic measures, immune status and severity of infection.

METHODS

Data collection: Clinical data were collected from patients diagnosed with acute sepsis, including basic information, laboratory findings, medical history and treatment options. Variable selection: Variables associated with prognosis were selected, including age, gender, underlying disease, etiology and site of infection, inflammatory indicators, multi-organ failure, cardiovascular function, treatment measures, immune status and severity of infection. Data analysis: The data collected are analysed using appropriate statistical methods such as multiple regression analysis and survival analysis. The impact of each factor on prognosis was assessed according to prognostic indicators, such as survival, length of stay and complication rates.

RESULTS

Descriptive statistics: Descriptive statistics were performed on the data collected from the patients, including their basic characteristics and clinical presentation.

CONCLUSION

Type 2 diabetes mellitus were independent factors affecting the prognosis of patients with sepsis.

Key Words: Platelet count; Length of ICU stay; Mechanical ventilation; Abdominal infection; Combined coronary artery disease

Core Tip: Age, gender, underlying disease, etiology and site of infection, inflammatory indicators, multi-organ failure, cardiovascular function, therapeutic measures, immune status, and severity of infection are important factors influencing the prognosis of emergency sepsis patients.

Citation: Ning XL, Shao M. Analysis of prognostic factors in patients with emergency sepsis. *World J Clin Cases* 2023; 11(25): 5903-5909
URL: https://www.wjgnet.com/2307-8960/full/v11/i25/5903.htm
DOI: https://dx.doi.org/10.12998/wjcc.v11.i25.5903

INTRODUCTION

Sepsis is a life-threatening condition caused by a dysregulated host response to infection resulting in organ dysfunction and is a common high mortality syndrome[1-5]. With the treatment of underlying infections, optimisation of organ perfusion is the mainstay of sepsis treatment, including the use of intravenous fluids and antihypertensive agents. The heart is one of the key organs involved in sepsis, and myocardial injury and cardiac insufficiency including diastolic and/or systolic dysfunction often occurs in patients with sepsis and is a significant cause of death in septic patients[6,7]. Diastolic dysfunction in sepsis is associated with fluid resuscitation in septic patients, and elevated left ventricular filling pressures are strongly associated with mortality[8,9]. With the development of haemodynamic monitoring and cardiac ultrasound technology, the American Society of Echocardiography revised the definition of diastolic dysfunction in 2009, but operational measurement is often difficult due to the complexity of its measurement and the frequent occurrence of arrhythmias such as tachycardia or atrial fibrillation in critically ill patients. The ratio of peak early mitral diastolic flow velocity to early mitral annular diastolic motion velocity (E/e') is commonly used to reflect elevated left heart filling pressures and is easily measured in critically ill patients. Based on a simplified classification of diastolic function in sepsis [10], the aim of this study was to investigate the factors that influence the prognosis of patients with sepsis according to their clinical characteristics and to provide a theoretical basis for the prognosis of patients with sepsis. It is reported as follows.

Age: Age is an important prognostic factor, with older patients usually having a poorer prognosis. Gender: Gender may have an impact on prognosis, as women usually have a better prognosis than men. Underlying disease: Patients with some chronic diseases (*e.g.* diabetes, heart disease, kidney disease, *etc.*) usually have a poorer prognosis[11-17]. Etiology and site of infection: Different sites and causes of infection may have different prognostic implications. Certain sites of infection (*e.g.* bloodstream infection) may have a poorer prognosis. Inflammatory indicators: Abnormal levels of inflammatory indicators (*e.g.* C-reactive protein, white blood cell count, calcitoninogen, *etc.*) are associated with prognosis. Higher inflammatory markers are usually associated with a poorer prognosis. Multi-organ failure: Multi-organ failure is one of the complications of severe sepsis and has a significant impact on prognosis[18-26]. Cardiovascular function: Instability of cardiovascular function is associated with prognosis. Hypotension and arrhythmias may predict a poorer prognosis. Therapeutic measures: Early and appropriate therapeutic measures, such as antibiotic therapy and haemodynamic support, are essential for prognosis. Immune status: Patients with impaired immune function (*e.g.* immunosuppressant users, HIV-infected patients, *etc.*) usually have a poorer prognosis. Severity of infection: The severity of the infection and the level of sepsis scoring systems (*e.g.* SOFA score, APACHE II score) are associated with prognosis. These are only some of the possible factors, and the specific influences will also depend on the study design, patient sample and data availability. When conducting specific analyses, statistical methods such as multiple regression analysis and survival analysis can be used to determine which factors have the most significant impact on prognosis.

MATERIALS AND METHODS

General information

Retrospective analysis of the clinical data of 102 patients with sepsis in the emergency care unit [collectively referred to as intensive care unit (ICU)] of our hospital from May 2018 to April 2023. (1) Inclusion criteria: Meeting the latest diagnostic criteria of sepsis 3.0 promulgated by the American Society of Critical Care Medicine and the European Society of Critical Care Medicine in 2016, with a SOFA score ≥ 2 (a baseline SOFA score of 0 was suspiciously assumed for patients with unknown underlying organ dysfunction); and (2) Exclusion criteria: (I) those who died of disease within 48 h of diagnosis

of sepsis and septic shock; (II) acute coronary syndrome, malignant arrhythmias; (III) unclear ultrasound images; (IV) advanced malignancy; and (V) post-cardiopulmonary resuscitation. Patients were divided into a death group and a survival group according to their clinical outcome in hospital. The study was approved by the hospital ethics committee.

Methodology

Clinical data such as age, gender, body mass index, comorbidities, laboratory tests such as white blood cell count, platelet count, blood creatinine value, blood potassium, glutamate transaminase, classification of the source of infection, duration of ICU stay, acute physiology and chronic health evaluation (APACHE II), sequential organ failure (SOFA) score, and the application of tissue Doppler imaging to determine peak mitral valve diastolic velocity (E) and mitral annular diastolic velocity (SOFA). APACHE II, sequential organ failure (SOFA) score and the use of tissue Doppler imaging to determine peak mitral valve early diastolic flow velocity (E), early mitral annular motion velocity (e') and E/e'.

Observation indicators

The clinical data of the patients were analysed and classified according to their cardiac function as normal cardiac function, abnormal systolic function (LVEF < 50%), diastolic dysfunction, and systolic and diastolic dysfunction. Diastolic dysfunction is graded according to the simplified method: e' < 8 and E/e'. Diastolic dysfunction grade I: e' < 8 and E/e' ≤ 8, diastolic dysfunction grade II: e' < 8 and 8 < E/e' < 13, diastolic dysfunction grade III: e' < 8 and E/e' ≥ 13. Analyse the factors affecting the prognosis of patients with sepsis.

Statistical treatment

SPSS 25.0 software was used for statistical analysis of the data obtained. The measurement data conforming to normal distribution were expressed as (mean ± SD) and compared by *t*-test; the measurement data conforming to non-normal distribution were expressed as M(P25, P75) and the rank sum test was used for comparison between groups. Statistical data were expressed as rates (%), and comparisons were made using the X^2 test. Variables with statistically significant differences in univariate analysis were introduced into a binary logistic regression model for multivariate analysis. Differences were considered statistically significant at $P < 0.05$.

RESULTS

Analysis of the patient's clinical data

The study included 102 patients with sepsis, 60 males and 62 females; age 30-87 years, mean (61.69 ± 8.78) years; 63 patients were mechanically ventilated by tracheal intubation; APACHE II score 16-33, mean (24.38 ± 3.20); SOFA score 7-17, mean (12.27 ± 1.95) points. There were 46 cases in the death group and 56 cases in the survival group.

Univariate analysis of factors

Affecting the prognosis of septic patients comparing E, e', platelet count, creatinine maximum, SOFA score, ICU length of stay, cardiac function classification, abdominal infection, mechanical ventilation, type 2 diabetes and coronary artery disease in both groups were statistically significant ($P < 0.05$), Tables 1-3.

Multi-factor analysis of variables

Affecting the prognosis of patients with sepsis Multi-factor analysis of variables that were significant in the univariate analysis was performed, where E, platelet count, duration of ICU stay, abdominal infection, mechanical ventilation, type 2 diabetes and coronary heart disease were independent influencing factors on the death of patients with sepsis ($P < 0.05$), Table 4.

DISCUSSION

Myocardial injury due to sepsis was previously thought to refer specifically to myocardial systolic dysfunction; however, recent studies have shown that myocardial injury in sepsis can manifest as different types of cardiac dysfunction, such as left ventricular diastolic dysfunction, left ventricular systolic dysfunction, and that the different types of cardiac dysfunction can coexist with each other. Both left ventricular diastolic dysfunction and systolic dysfunction are predictors of mortality in patients with sepsis compared with patients with normal cardiac function[27-31]. The author classified diastolic dysfunction into classes I, II and III based on a simplified classification of diastolic function in sepsis, based on the E/e' ratio. This is more consistent with previous studies reported.

There are limited invasive methods of measuring cardiac diastolic function in patients with sepsis. e/e' correlates well with left ventricular end-diastolic pressure in patients with sepsis[32-35]. In this study, a univariate analysis of cardiac function grading revealed a statistically significant difference ($P < 0.05$) when comparing cardiac function grading between the surviving and deceased groups, but a multifactorial logistic regression analysis failed to show a statistically significant difference, a study that appears to contradict the results of recent studies. The author considers that the reasons for the inconsistent findings may be related to the small sample size of this study, case selection bias, timing of cardiac ultrasound assessment, simplified version of the diastolic function definition, and treatment received.

Table 1 Univariate analysis of factors affecting the breath parameters of patients

Group	Left ventricular end-diastolic internal diameter (mm)	Left ventricular end-systolic internal diameter (mm)	E (m/s)	E/e'	e' (cm/s)
Survival group (n = 56)	49.30 ± 3.57	33.78 ± 3.43	0.84 (0.67, 1.08)	8.67 (7.25, 11.56)	8.87 ± 2.37
Death group (n = 46)	49.03 ± 3.37	34.17 ± 3.44	0.79 (0.63, 1.01)	8.85 (6.92, 11.50)	8.41 ± 2.48
$t/Z/X^2$ values	0.84	1.23	2.48	0.05	2.10
P value	> 0.05	> 0.05	< 0.05	> 0.05	< 0.05

Table 2 Univariate analysis of factors affecting the fundamental factor of patients

Group	Age (yr)	Body mass index (kg/m²)	White blood cell count (×10⁹ /L)	Platelet count (×10⁹ /L)	Admission creatinine (mg/dL)
Survival group (n = 56)	61.96 ± 8.16	24.92 ± 3.15	14.70 ± 3.58	179.43 ± 53.19	0.88 (0.68, 1.13)
Death group (n = 46)	61.31 ± 9.60	24.68 ± 3.36	14.57 ± 3.40	169.55 ± 49.70	0.94 (0.70, 1.20)
$t/Z/X^2$ values	0.78	0.82	0.41	2.09	1.50
P value	> 0.05	> 0.05	> 0.05	< 0.05	> 0.05

Table 3 Univariate analysis of factors affecting the blood system parameters of patients

Group	Creatinine maximum (mg/dL)	Blood potassium (mmol/L)	Glutathione transaminase (U/L)	Lactic acid (mg/dL)	SOFA score (Points)
Survival group (n = 56)	1.43 (0.93, 2.18)	4.75 ± 0.63	34.00 (26.00, 43.00)	51.88 (39.39, 78.79)	12.12 ± 1.87
Death group (n = 46)	1.67 (1.12, 2.67)	4.76 ± 0.58	34.00 (25.00, 44.75)	53.80 (39.39, 71.82)	12.48 ± 2.04
$t/Z/X^2$ values	2.88	0.16	0.61	0.64	2.00
P value	< 0.05	> 0.05	> 0.05	> 0.05	< 0.05

Table 4 Multifactorial analysis affecting the prognosis of patients with sepsis

Factors	B	S.E.	Wald values	*P* value	OR value	95%CI
E	-1.949	0.769	6.416	0.011	0.142	0.032, 0.643
Platelet count	-0.005	0.003	4.440	0.035	0.994	0.989, 0.999
Abdominal infection	0.788	0.288	7.499	0.006	2.200	1.251, 3.868
Mechanical ventilation	3.481	0.305	130.130	0.000	32.491	17.866, 59.089
ICU length of stay	-0.082	0.020	16.925	0.000	0.921	0.886, 0.958
Type 2 diabetes	0.783	0.391	4.001	0.045	2.187	1.016, 4.708
Coronary heart disease	1.727	0.682	6.421	0.011	5.624	1.479, 21.387

ICU: Intensive care unit.

CONCLUSION

The results of this study showed that E, platelet count, days of ICU stay, abdominal infection, mechanical ventilation, type 2 diabetes mellitus and coronary heart disease were independent factors influencing death in patients with sepsis (P < 0.05). Patients in the survivor group had longer ICU stays than those in the death group, and the analysis may be

related to factors such as receiving haemodialysis. Small retrospective studies suggest that early initiation of continuous renal replacement therapy may improve clinical acute kidney injury in septic patients.

ARTICLE HIGHLIGHTS

Research background

Emergency sepsis is a common and serious infectious disease, and its prognosis is influenced by a number of factors.

Research motivation

The aim of this study was to analyse the factors influencing the prognosis of patients with emergency sepsis in order to provide a basis for individualised patient treatment and care. By retrospectively analysing the clinical data collected.

Research objectives

We conducted a comprehensive analysis of factors such as age, gender, underlying disease, etiology and site of infection, inflammatory indicators, multi-organ failure, cardiovascular function, therapeutic measures, immune status and severity of infection.

Research methods

Clinical data were collected from patients diagnosed with acute sepsis, including basic information, laboratory findings, medical history and treatment options. Variable selection: Variables associated with prognosis were selected, including age, gender, underlying disease, etiology and site of infection, inflammatory indicators, multi-organ failure, cardiovascular function, treatment measures, immune status and severity of infection. Data analysis: The data collected are analysed using appropriate statistical methods such as multiple regression analysis and survival analysis. The impact of each factor on prognosis was assessed according to prognostic indicators, such as survival, length of stay and complication rates.

Research results

Descriptive statistics were performed on the data collected from the patients, including their basic characteristics and clinical presentation.

Research conclusions

Type 2 diabetes mellitus were independent factors affecting the prognosis of patients with sepsis.

Research perspectives

The impact of each factor on prognosis was assessed according to prognostic indicators, such as survival, length of stay and complication rates.

FOOTNOTES

Author contributions: These authors contributed equally to this work.

Institutional review board statement: The study was reviewed and approved by the [The First Affiliated Hospital of Anhui Medical University] Institutional Review Board.

Informed consent statement: Informed written consent was obtained from the patient for publication of this study. All participants are confirmed.

Conflict-of-interest statement: All the authors declare that they have no conflict of interest.

Data sharing statement: No additional data are available.

Country/Territory of origin: China

ORCID number: Xian-Li Ning 0009-0001-4533-0471; Min Shao 0000-0001-7307-5570.

S-Editor: Liu JH
L-Editor: A

P-Editor: Liu JH

REFERENCES

1 **Gaieski DF**, Edwards JM, Kallan MJ, Carr BG. Benchmarking the incidence and mortality of severe sepsis in the United States. *Crit Care Med* 2013; **41**: 1167-1174 [PMID: 23442987 DOI: 10.1097/CCM.0b013e31827c09f8]

2 **Brown SM**, Pittman JE, Hirshberg EL, Jones JP, Lanspa MJ, Kuttler KG, Litwin SE, Grissom CK. Diastolic dysfunction and mortality in early severe sepsis and septic shock: a prospective, observational echocardiography study. *Crit Ultrasound J* 2012; **4**: 8 [PMID: 22870900 DOI: 10.1186/2036-7902-4-8]

3 **Sanfilippo F**, Corredor C, Fletcher N, Landesberg G, Benedetto U, Foex P, Cecconi M. Erratum to: Diastolic dysfunction and mortality in septic patients: a systematic review and meta-analysis. *Intensive Care Med* 2015; **41**: 1178-1179 [PMID: 25851394 DOI: 10.1007/s00134-015-3799-9]

4 **Ritzema JL**, Richards AM, Crozier IG, Frampton CF, Melton IC, Doughty RN, Stewart JT, Eigler N, Whiting J, Abraham WT, Troughton RW. Serial Doppler echocardiography and tissue Doppler imaging in the detection of elevated directly measured left atrial pressure in ambulant subjects with chronic heart failure. *JACC Cardiovasc Imaging* 2011; **4**: 927-934 [PMID: 21920328 DOI: 10.1016/j.jcmg.2011.07.004]

5 **Lanspa MJ**, Gutsche AR, Wilson EL, Olsen TD, Hirshberg EL, Knox DB, Brown SM, Grissom CK. Application of a simplified definition of diastolic function in severe sepsis and septic shock. *Crit Care* 2016; **20**: 243 [PMID: 27487776 DOI: 10.1186/s13054-016-1421-3]

6 **Fleischmann C**, Thomas-Rueddel DO, Hartmann M, Hartog CS, Welte T, Heublein S, Dennler U, Reinhart K. Hospital Incidence and Mortality Rates of Sepsis. *Dtsch Arztebl Int* 2016; **113**: 159-166 [PMID: 27010950 DOI: 10.3238/arztebl.2016.0159]

7 **Angus DC**, Linde-Zwirble WT, Lidicker J, Clermont G, Carcillo J, Pinsky MR. Epidemiology of severe sepsis in the United States: analysis of incidence, outcome, and associated costs of care. *Crit Care Med* 2001; **29**: 1303-1310 [PMID: 11445675 DOI: 10.1097/00003246-200107000-00002]

8 **Iba T**, Thachil J. Present and future of anticoagulant therapy using antithrombin and thrombomodulin for sepsis-associated disseminated intravascular coagulation: a perspective from Japan. *Int J Hematol* 2016; **103**: 253-261 [PMID: 26588929 DOI: 10.1007/s12185-015-1904-z]

9 **Iba T**, Yamada A, Hashiguchi N, Nagaoka I. New therapeutic options for patients with sepsis and disseminated intravascular coagulation. *Pol Arch Med Wewn* 2014; **124**: 321-328 [PMID: 24732306 DOI: 10.20452/pamw.2299]

10 **Shankar-Hari M**, Phillips GS, Levy ML, Seymour CW, Liu VX, Deutschman CS, Angus DC, Rubenfeld GD, Singer M; Sepsis Definitions Task Force. Developing a New Definition and Assessing New Clinical Criteria for Septic Shock: For the Third International Consensus Definitions for Sepsis and Septic Shock (Sepsis-3). *JAMA* 2016; **315**: 775-787 [PMID: 26903336 DOI: 10.1001/jama.2016.0289]

11 **Howell MD**, Davis AM. Management of Sepsis and Septic Shock. *JAMA* 2017; **317**: 847-848 [PMID: 28114603 DOI: 10.1001/jama.2017.0131]

12 **Rudd KE**, Johnson SC, Agesa KM, Shackelford KA, Tsoi D, Kievlan DR, Colombara DV, Ikuta KS, Kissoon N, Finfer S, Fleischmann-Struzek C, Machado FR, Reinhart KK, Rowan K, Seymour CW, Watson RS, West TE, Marinho F, Hay SI, Lozano R, Lopez AD, Angus DC, Murray CJL, Naghavi M. Global, regional, and national sepsis incidence and mortality, 1990-2017: analysis for the Global Burden of Disease Study. *Lancet* 2020; **395**: 200-211 [PMID: 31954465 DOI: 10.1016/S0140-6736(19)32989-7]

13 **Zhao L**, Yang J, Zhou C, Wang Y, Liu T. A novel prognostic model for predicting the mortality risk of patients with sepsis-related acute respiratory failure: a cohort study using the MIMIC-IV database. *Curr Med Res Opin* 2022; **38**: 629-636 [PMID: 35125039 DOI: 10.1080/03007995.2022.2038490]

14 **Ren Y**, Zhang L, Xu F, Han D, Zheng S, Zhang F, Li L, Wang Z, Lyu J, Yin H. Risk factor analysis and nomogram for predicting in-hospital mortality in ICU patients with sepsis and lung infection. *BMC Pulm Med* 2022; **22**: 17 [PMID: 34991569 DOI: 10.1186/s12890-021-01809-8]

15 **Sun Q**, Li N, Jia L, Guo W, Jiang H, Liu B, Bao C, Liu M, Huang J, Lei L. Ribosomal Protein SA-Positive Neutrophil Elicits Stronger Phagocytosis and Neutrophil Extracellular Trap Formation and Subdues Pro-Inflammatory Cytokine Secretion Against Streptococcus suis Serotype 2 Infection. *Front Immunol* 2020; **11**: 585399 [PMID: 33603733 DOI: 10.3389/fimmu.2020.585399]

16 **Cheung WK**, Chau LS, Mak II, Wong MY, Wong SL, Tiwari AF. Clinical management for patients admitted to a critical care unit with severe sepsis or septic shock. *Intensive Crit Care Nurs* 2015; **31**: 359-365 [PMID: 26292920 DOI: 10.1016/j.iccn.2015.04.005]

17 **Rhee C**, Zhang Z, Kadri SS, Murphy DJ, Martin GS, Overton E, Seymour CW, Angus DC, Dantes R, Epstein L, Fram D, Schaaf R, Wang R, Klompas M; CDC Prevention Epicenters Program. Sepsis Surveillance Using Adult Sepsis Events Simplified eSOFA Criteria Versus Sepsis-3 Sequential Organ Failure Assessment Criteria. *Crit Care Med* 2019; **47**: 307-314 [PMID: 30768498 DOI: 10.1097/CCM.0000000000003521]

18 **Corl KA**, Prodromou M, Merchant RC, Gareen I, Marks S, Banerjee D, Amass T, Abbasi A, Delcompare C, Palmisciano A, Aliotta J, Jay G, Levy MM. The Restrictive IV Fluid Trial in Severe Sepsis and Septic Shock (RIFTS): A Randomized Pilot Study. *Crit Care Med* 2019; **47**: 951-959 [PMID: 30985449 DOI: 10.1097/CCM.0000000000003779]

19 **Seymour CW**, Rosengart MR. Bedside Ultrasonography for Diagnosis of Septic Shock--Reply. *JAMA* 2016; **315**: 89-90 [PMID: 26746467 DOI: 10.1001/jama.2015.15073]

20 **Kierzkowska M**, Markowska K, Majewska A. Knowledge, Attitude and Practice Regarding Staphylococcus pettenkoferi. *Infect Dis Rep* 2022; **14**: 112-120 [PMID: 35200442 DOI: 10.3390/idr14010015]

21 **Rhee C**, Dantes R, Epstein L, Murphy DJ, Seymour CW, Iwashyna TJ, Kadri SS, Angus DC, Danner RL, Fiore AE, Jernigan JA, Martin GS, Septimus E, Warren DK, Karcz A, Chan C, Menchaca JT, Wang R, Gruber S, Klompas M; CDC Prevention Epicenter Program. Incidence and Trends of Sepsis in US Hospitals Using Clinical vs Claims Data, 2009-2014. *JAMA* 2017; **318**: 1241-1249 [PMID: 28903154 DOI: 10.1001/jama.2017.13836]

22 **Marik PE**, Linde-Zwirble WT, Bittner EA, Sahatjian J, Hansell D. Fluid administration in severe sepsis and septic shock, patterns and outcomes: an analysis of a large national database. *Intensive Care Med* 2017; **43**: 625-632 [PMID: 28130687 DOI: 10.1007/s00134-016-4675-y]

23 **Fine N**, Tasevski N, McCulloch CA, Tenenbaum HC, Glogauer M. The Neutrophil: Constant Defender and First Responder. *Front Immunol* 2020; **11**: 571085 [PMID: 33072112 DOI: 10.3389/fimmu.2020.571085]

24 **Ma F**, Chang X, Wang G, Zhou H, Ma Z, Lin H, Fan H. Streptococcus Suis Serotype 2 Stimulates Neutrophil Extracellular Traps Formation *via* Activation of p38 MAPK and ERK1/2. *Front Immunol* 2018; **9**: 2854 [PMID: 30581435 DOI: 10.3389/fimmu.2018.02854]

25 **Iwashyna TJ**, Cooke CR, Wunsch H, Kahn JM. Population burden of long-term survivorship after severe sepsis in older Americans. *J Am Geriatr Soc* 2012; **60**: 1070-1077 [PMID: 22642542 DOI: 10.1111/j.1532-5415.2012.03989.x]

26 **Wang L**, Chen X, Zhang H, Hong L, Wang J, Shao L, Chen G, Wu J. Comprehensive analysis of transient receptor potential channels-related signature for prognosis, tumor immune microenvironment, and treatment response of colorectal cancer. *Front Immunol* 2022; **13**: 1014834 [PMID: 36389750 DOI: 10.3389/fimmu.2022.1014834]

27 **Stortz JA**, Mira JC, Raymond SL, Loftus TJ, Ozrazgat-Baslanti T, Wang Z, Ghita GL, Leeuwenburgh C, Segal MS, Bihorac A, Brumback BA, Mohr AM, Efron PA, Moldawer LL, Moore FA, Brakenridge SC. Benchmarking clinical outcomes and the immunocatabolic phenotype of chronic critical illness after sepsis in surgical intensive care unit patients. *J Trauma Acute Care Surg* 2018; **84**: 342-349 [PMID: 29251709 DOI: 10.1097/TA.0000000000001758]

28 **Bouma S**. Diagnosing Pediatric Malnutrition. *Nutr Clin Pract* 2017; **32**: 52-67 [DOI: 10.1177/0884533616671861]

29 **Levinson AT**, Casserly BP, Levy MM. Reducing mortality in severe sepsis and septic shock. *Semin Respir Crit Care Med* 2011; **32**: 195-205 [PMID: 21506056 DOI: 10.1055/s-0031-1275532]

30 **Wong W**, Yim YM, Kim A, Cloutier M, Gauthier-Loiselle M, Gagnon-Sanschagrin P, Guerin A. Assessment of costs associated with adverse events in patients with cancer. *PLoS One* 2018; **13**: e0196007 [PMID: 29652926 DOI: 10.1371/journal.pone.0196007]

31 **Kumar G**, Kumar N, Taneja A, Kaleekal T, Tarima S, McGinley E, Jimenez E, Mohan A, Khan RA, Whittle J, Jacobs E, Nanchal R; Milwaukee Initiative in Critical Care Outcomes Research (MICCOR) Group of Investigators. Nationwide trends of severe sepsis in the 21st century (2000-2007). *Chest* 2011; **140**: 1223-1231 [PMID: 21852297 DOI: 10.1378/chest.11-0352]

32 **Seymour CW**, Gesten F, Prescott HC, Friedrich ME, Iwashyna TJ, Phillips GS, Lemeshow S, Osborn T, Terry KM, Levy MM. Time to Treatment and Mortality during Mandated Emergency Care for Sepsis. *N Engl J Med* 2017; **376**: 2235-2244 [PMID: 28528569 DOI: 10.1056/NEJMoa1703058]

33 **Raith EP**, Udy AA, Bailey M, McGloughlin S, MacIsaac C, Bellomo R, Pilcher DV; Australian and New Zealand Intensive Care Society (ANZICS) Centre for Outcomes and Resource Evaluation (CORE). Prognostic Accuracy of the SOFA Score, SIRS Criteria, and qSOFA Score for In-Hospital Mortality Among Adults With Suspected Infection Admitted to the Intensive Care Unit. *JAMA* 2017; **317**: 290-300 [PMID: 28114553 DOI: 10.1001/jama.2016.20328]

34 **Valik JK**, Ward L, Tanushi H, Johansson AF, Färnert A, Mogensen ML, Pickering BW, Herasevich V, Dalianis H, Henriksson A, Nauclér P. Predicting sepsis onset using a machine learned causal probabilistic network algorithm based on electronic health records data. *Sci Rep* 2023; **13**: 11760 [PMID: 37474597 DOI: 10.1038/s41598-023-38858-4]

35 **Green Corkins K**, Teague EE. Pediatric Nutrition Assessment. *Nutr Clin Pract* 2017; **32**: 40-51 [DOI: 10.1177/0884533616679639]

World Journal of Clinical Cases

Submit a Manuscript: https://www.f6publishing.com

World J Clin Cases 2023 September 6; 11(25): 5910-5918

DOI: 10.12998/wjcc.v11.i25.5910

ISSN 2307-8960 (online)

CASE REPORT

Clinicopathological study of malignant peripheral nerve sheath tumors in the head and neck: Case reports and review of literature

Long Li, Xiao-Kun Ma, Yan Gao, Dian-Can Wang, Rong-Fang Dong, Jing Yan, Ran Zhang

Specialty type: Dentistry, oral surgery and medicine

Provenance and peer review: Unsolicited article; Externally peer reviewed.

Peer-review model: Single blind

Peer-review report's scientific quality classification

Grade A (Excellent): 0
Grade B (Very good): B
Grade C (Good): 0
Grade D (Fair): 0
Grade E (Poor): 0

P-Reviewer: D'Orazi V, Italy

Received: March 27, 2023
Peer-review started: March 27, 2023
First decision: July 3, 2023
Revised: July 20, 2023
Accepted: August 8, 2023
Article in press: August 8, 2023
Published online: September 6, 2023

Long Li, Yan Gao, Jing Yan, Ran Zhang, Department of Oral Pathology, Peking University School and Hospital of Stomatology, National Clinical Research Center for Oral Diseases, National Engineering Laboratory for Digital and Material Technology of Stomatology, Beijing Key Laboratory of Digital Stomatology, Beijing 100000, China

Long Li, Yan Gao, Jing Yan, Ran Zhang, Research Unit of Precision Pathologic Diagnosis in Tumors of the Oral and Maxillofacial Regions, Chinese Academy of Medical Sciences, Beijing 100000, China

Long Li, Department of Oral Pathology, Xiangya Stomalogical Hospital & School of Stomatology, Central South University, Changsha 410078, Hunan Province, China

Xiao-Kun Ma, Department of Oral and Maxillofacial Surgery, The Affiliated Stomatological Hospital of Soochow University, Suzhou Stomatological Hospital, Suzhou 215000, Jiangsu Province, China

Dian-Can Wang, Department of Oral and Maxillofacial Surgery, Peking University School and Hospital of Stomatology, Peking University School and Hospital of Stomatology, Beijing 100000, China

Rong-Fang Dong, Department of Pathology, Beijing Jishuitan Hospital, Beijing 100000, China

Corresponding author: Ran Zhang, MD, Assistant Professor, Department of Oral Pathology, Peking University School and Hospital of Stomatology, National Clinical Research Center for Oral Diseases, National Engineering Laboratory for Digital and Material Technology of Stomatology, Beijing Key Laboratory of Digital Stomatology, No. 22 South Zhongguancun Avenue, Haidian District, Beijing 100081, China. rani@bjmu.edu.cn

Abstract

BACKGROUND

Malignant peripheral nerve sheath tumor (MPNST) is a rare and aggressive soft tissue sarcoma that poses a major diagnostic and therapeutic challenge.

CASE SUMMARY

We retrospectively reviewed patients with head and neck MPNSTs treated in our hospital from 2000 to 2021. The clinical features, pathological manifestations, treatments, and prognoses were summarized. We also reviewed the literature, focusing on MPNST in the mandible and maxilla. The study population consisted of five women and five men aged 22–75 years (mean age, 49 years). Of the 10

patients, 7 were initial cases and 3 were recurrent cases. All lesions were sporadic. The most common site was the mandible. The most frequently encountered symptoms were a progressive mass and local swelling. Complete or partial loss of trimethylation at lysine 27 of histone H3 (H3K27me3) was evident on staining in four of nine cases (one case was excluded due to lack of tissue for evaluation of loss of H3K27me3). The 2- and 5-year disease-specific survival rates were 86% and 43%, respectively. The average survival time was 64 mo.

CONCLUSION
MPNST is a highly malignant tumor with a poor prognosis, prone to a high risk of recurrence and distant metastasis. Complete surgical resection is the main treatment.

Key Words: Malignant peripheral nerve sheath tumor; Head and neck; Treatment; Intraosseous; Surgery; Case report

Core Tip: We retrospectively reviewed patients with head and neck malignant peripheral nerve sheath tumors treated in our hospital from 2000 to 2021. The study population consisted of five women and five men aged 22–75 years (mean age, 49 years). The 2- and 5-year disease-specific survival rates were 86% and 43%, respectively. The average survival time was 64 mo. Complete or partial loss of trimethylation at lysine 27 of histone H3 (H3K27me3) was evident on staining in four of nine cases (one case was excluded due to lack of tissue for evaluation of loss of H3K27me3).

Citation: Li L, Ma XK, Gao Y, Wang DC, Dong RF, Yan J, Zhang R. Clinicopathological study of malignant peripheral nerve sheath tumors in the head and neck: Case reports and review of literature. *World J Clin Cases* 2023; 11(25): 5910-5918
URL: https://www.wjgnet.com/2307-8960/full/v11/i25/5910.htm
DOI: https://dx.doi.org/10.12998/wjcc.v11.i25.5910

INTRODUCTION

Malignant peripheral nerve sheath tumor (MPNST) is an uncommon and aggressive tumor that arises from the cells of peripheral nerve sheaths. The most common anatomical sites are the trunk, extremities, and retroperitoneum. The head and neck region accounts for only 2%–9% of cases[1,2]. The clinical presentation of head and neck MPNST includes a rapidly enlarging mass, radicular pain or paresthesia, and neurological defects that depend on the anatomical sites involved[1]. Almost half of all cases are caused by defects in the neurofibromatosis type 1 gene located on chromosome 17; fewer than 10% of cases are radiation-induced (post-radiation sarcomas); the rest are sporadic cases of unknown etiology[3,4]. Histologically, MPNST is a spindle cell sarcoma arising from peripheral nerves, and varies in terms of nerve sheath differentiation; MPNST has been considered as a neurogenic sarcoma, neurofibrosarcoma, malignant schwannoma [1,5]. Most MPNSTs exhibit a tightly packed, stripe-like proliferation of spindle cells, which often complicate the diagnosis for pathologists. It is difficult to differentiate MPNSTs from other spindle cell sarcomas. The level of S-100 expression ranges from 50% to 70%, and is usually focal. In general, more primitive tumors are also more malignant, and are associated with low levels of S-100. Recent studies found that various components of polycomb repressive complex 2 (PRC2) are inactivated in most MPNSTs. Homozygous PRC2 inactivation leads to loss of H3K27me3 (as revealed by immunohistochemical analysis), which may be a new immunohistochemistry marker for MPNST[6-9].

MPNST is a high-grade malignant tumor with a high recurrence rate. The local recurrence rate is almost 50%, and 33% of patients develop bone and lung metastases[1,10]. Similar to most soft tissue sarcomas, wide excision is the main treatment; the utility of adjuvant radiotherapy and chemotherapy remains controversial[1]. In line with the high malignancy, the 5-year overall survival rate is only 20%-51%[3,11,12].

Here, we report on 10 MPNST cases, including 4 in the mandible and one in the maxilla, treated at our institution over a 20-year period. Immunohistochemical evaluation of H3K27me3 was conducted. We also review the literature with a focus on intraosseous MPNST in mandible and maxilla.

CASE PRESENTATION

Chief complaints

Case 1: A 62-year-old woman was referred to our hospital with a chief complaint of pigmented gingival lesions of the left anterior maxilla.

Case 2: A 28-year-old woman had a 6-mo history of a left mandibular gingival mass.

History of present illness

Case 1: The pathological diagnosis was an oral melanotic macule with increased melanocyte activity (Figure 1A). Two years later, clinical examination revealed a mild asymptomatic swelling on the anterior maxilla and two swollen lymph nodes on each side of the neck.

Case 2: The mandibular mass was located in the region of the 1st premolar to 1st molar teeth. The cortex of the buccal side was not continuous and the soft tissues of the cheek and tongue side were thickened.

Personal and family history

Case 1 and Case 2: Personal *and* family history denies the family history of genetic disease.

Laboratory examinations

Case 1 and Cases 2: Laboratory examinations reveal nothing abnormal.

Imaging examinations

Case 1: Computed tomography (CT) revealed a soft tissue mass in the anterior maxilla involving the surgical defect in the incisor region (Figure 1B).

Case 2: CT revealed a poorly-defined lytic lesion in the left mandible.

Clinicopathological characteristics

The clinical characteristics of the 10 patients are presented in Table 1; there were 7 *de novo* cases and 3 recurrences. No patient had a history of NF1 syndrome or radiotherapy before the first consultation. There were five male and five female patients, ranging in age from 22 to 75 years (mean age = 49 years). The mandible was the most common anatomical site. Other locations included the maxilla, gingiva, infratemporal fossa, and palate. The tumor size ranged from 1.5 to 4.5 cm (mean size = 2.9 cm). The most common initial symptoms were a progressive mass and local swelling (10/10 cases), sometimes accompanied by peripheral nerve symptoms including local pain or numbness (4/10 cases).

Morphologically, the tumors were composed predominantly of relatively monomorphic spindle cells arranged in intersecting long fascicles. The lesional cells exhibited hyperchromatic ovoid nuclei, with inconspicuous nucleoli and scant cytoplasm. MPNST is generally considered to be a high-grade sarcoma; in line with this, the mitosis score was relatively high in the current study. Large cells exhibiting obvious pleomorphism, or multinucleated giant cells, were found in three cases. Three other cases had areas of epithelial differentiation (Figure 2A-C). All cases evaluated with S100 staining were positive or focal positive, and melanotic markers such as HMB-45 and Melan-A were negative. H3K27me3 staining was evaluated immunohistochemically in the nine surgical cases; one of these (11.1%) exhibited complete H3K27me3 loss, while three (33.3%) showed partial loss (Figure 2D-F).

Nine of the ten patients were initially treated *via* wide excision; the other patient was prescribed chemotherapy because the tumor was too large to excise. Follow-up information was available for seven patients, who were followed-up for 13–216 mo (mean follow-up = 64 mo). Of these patients, four received both adjuvant radiotherapy and chemotherapy; the remaining patient received radiotherapy only after surgery. Two patients developed local recurrence, and four distant metastasis, within 2 years. Four patients died, while three patients remain under follow-up and are free from disease after 24, 28 and 74 mo, respectively. The 2 and 5-year disease-specific survival (DSS) rates were 86% and 43%, respectively.

FINAL DIAGNOSIS

Case 1 and Cases 2: Biopsies were used to diagnose MPNST.

TREATMENT

Case 1: The patient then underwent partial maxillectomy and radical neck dissection.

Case 2: The patient underwent wide mandibular resection and radical neck dissection, followed by adjuvant radiotherapy and chemotherapy.

OUTCOME AND FOLLOW-UP

Case 1: Two years later, CT performed during regular follow-up revealed multiple pulmonary nodules; further examination confirmed lung and bone metastases.

Cases 2: The patient has remained disease-free for 2 years.

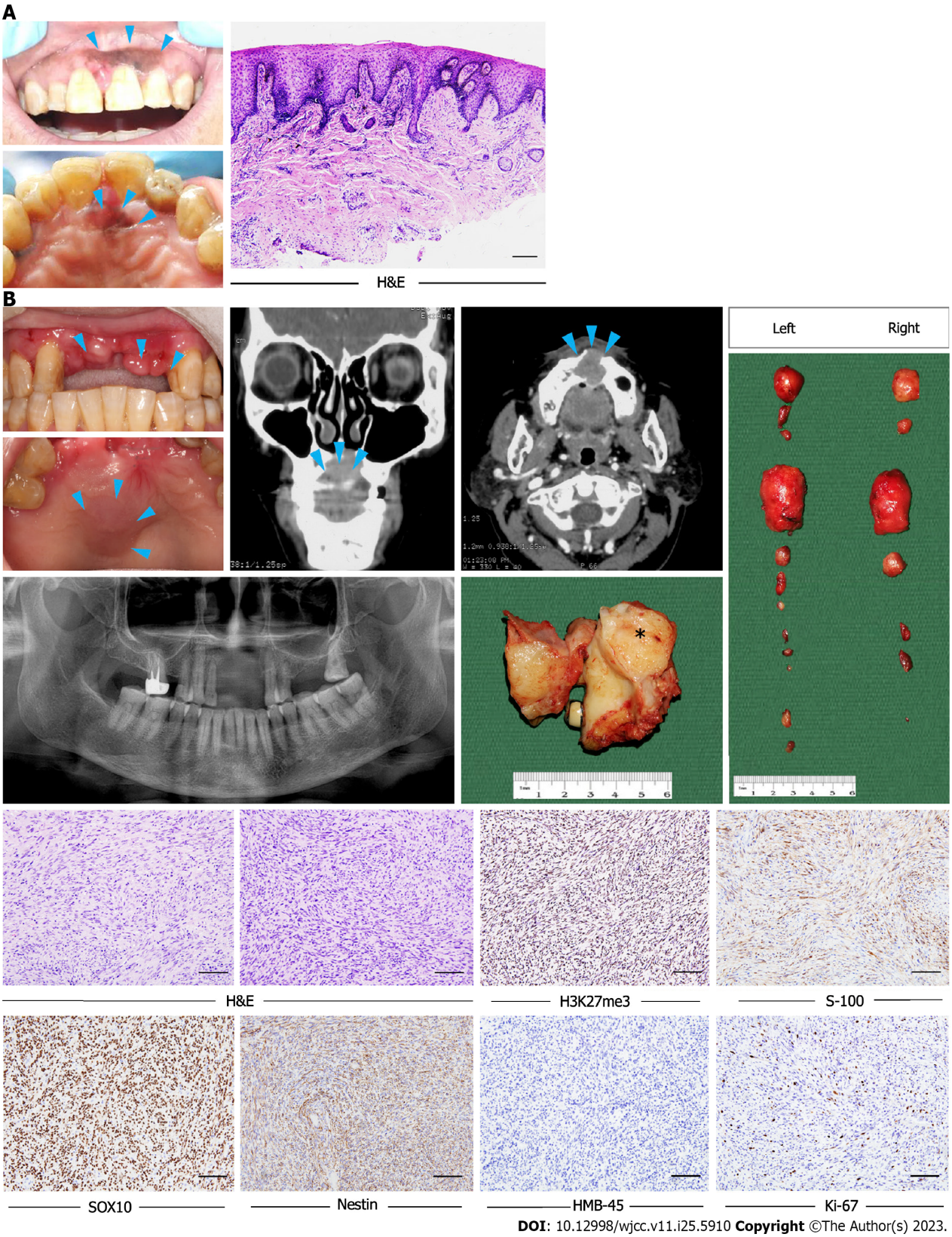

DOI: 10.12998/wjcc.v11.i25.5910

Figure 1 Clinicopathological characteristics of the patient in case 1. A: Clinical and pathological presentations of the patient during the first visit to our hospital. A macular brown to black lesion was on the anterior maxillary gingiva and incisive foramen region (arrows). Histopathological image revealed the lesion was black macule; B: Clinicopathological presentations of the patient during the second visit to our hospital. A multinodular mass was noted on the anterior maxillary gingiva, and a local swelling was on the anterior to median portion of the palate. Coronal head computed tomography scan shows soft tissue masses in the front of the upper jaw with unclear boundary. The masses involved the post-surgical defect in the incisor region and there was lytic destruction of the underlying bone (arrows). Enlarged lymph nodes and the gross specimen of the lesion after the surgery. H&E characteristics of the case confirmed the diagnosis was malignant peripheral nerve sheath tumor. Tumor cells show partial loss of H3K27me3 and positive stain for S-100, SOX10, nestin, and negative stain for HMB-45. The Ki-67

index is about 10%. Scale bar: 250 μm (A), 50 μm (B).

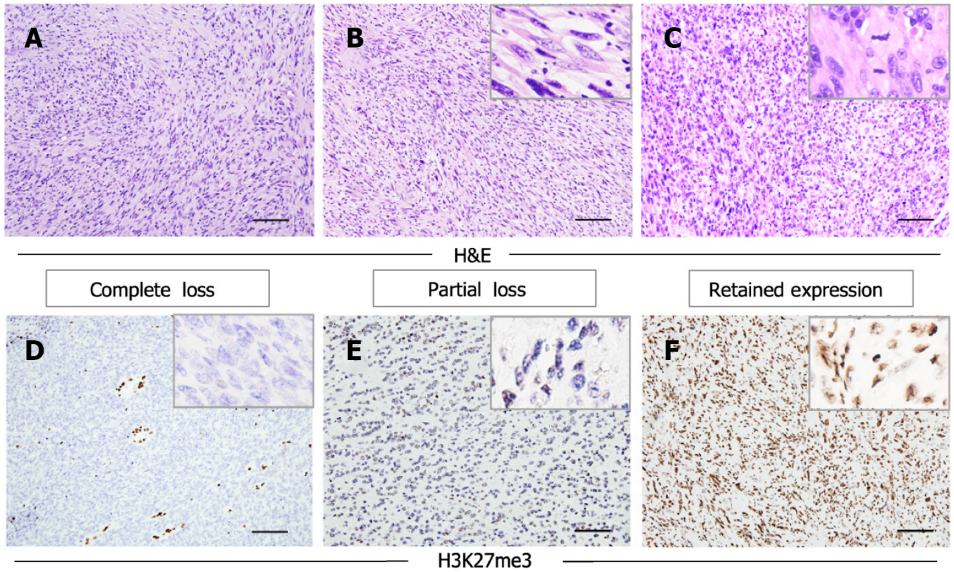

DOI: 10.12998/wjcc.v11.i25.5910

Figure 2 Histological characteristics of malignant peripheral nerve sheath tumor (MPNST) and immunohistochemical analysis of H3K27me3 in MPNST sections. A: The lesion cells display predominantly spindle in an architectural pattern; B: The cells are enlongated and tends to be hyperchromatic with scant cytoplasm; C: There is severe cytologic atypia and nuclear pleomorphism, with focally brisk mitotic activity; D: Complete loss of H3K27me3 expression on sections. Staining of blood vessels and inflammatory cells is the internal positive controls; E: Partial loss of H3K27me3 expression on the section; F: Strong expression of H3K27me3 is retained in some MPNST cases. Scale bars: 50 μm.

DISCUSSION

MPNST is an infiltrating and aggressive tumor of neural origin[13]. Although head and neck MPNSTs are histologically similar to MPNSTs in other regions, there are important clinical differences. Patel *et al*[3] performed a comparative analysis based on the SEER database. The mean age of head and neck MPNST patients was 49.1 years, compared to 46.1 years for patients with MPNSTs in other regions. The former group showed a male predilection (60.2%) while a sex predilection for females (54.2%) in the latter group. Also, the average tumor size of the former group was smaller than in the latter group. The mean age and average tumor size of our patients are consistent with these observations, but we observed no gender differences. This may reflect regional differences among our relatively small sample. MPNSTs develop sporadically, rather than in association with NF-1, in the head and neck region. Ma *et al*[2] reported that 69.8% (30/43) of MPNSTs were sporadic[14]. None of our cases had a history of NF1 syndrome or malignant transformation after radiotherapy, suggesting that they were all sporadic.

Previous studies found that primary intraosseous MPNST was rare[15]. We report four cases in the mandible and one case in the maxilla in this study; our review of the English language literature revealed 48 cases of primary intraosseous MPNST including 27 such cases in the mandible and 21 such cases in the maxilla. In the mandible, Ma *et al*[2] reported five patients, of whom three suffered recurrences. The other 22 cases were single cases; the clinical data of these cases, and our four cases, are shown in Supplementary Table 1[15-26]. Among the 26 patients, there were 19 women and 7 men, ranging in age from 4.5 to 76 years [mean age = 33 years (data were unavailable for three patients)]. One patient had a history of NF1 syndrome, and seventeen did not (data were unavailable for five patients). In the maxilla, Ma *et al*[2] reported 12 patients, of whom seven suffered recurrences. The other 9 cases were single cases; the clinical data of these cases, and our case, are shown in Table 2[19,27-34]. Among the 10 patients, there were 5 women and 5 men, ranging in age from 12 to 65 years (mean age = 44 years). Two patients had a history of NF1 syndrome, and six did not (data were unavailable for two patients). These datas revealed that MPNST in the mandible was more common in women than men, and there were no differences in the maxilla. Most of the patients had no history of NF1 syndrome in both mandible and maxilliary.

Given the lack of unique histological criteria and a specific immunoprofile, diagnosing MPNST can be very challenging. Some tumors have morphological features that overlap with those of MPNST, including fibrosarcomas and leiomyosarcomas; differential diagnosis is therefore essential. Fibrosarcomas have a simple structure, and are rich in collagen and S-100-negative onimmunohistochemistry. Leiomyosarcoma cells exhibit vacuoles around nuclei; the lesions develop in tissues and organs rich in smooth muscle, and stain positively for desmin and smooth muscle actin. When epithelioid cells predominate, MPSNT must be distinguished from malignant melanoma and epithelioid sarcoma. The lesion site of malignant melanoma is more superficial than that of MPSNT; moreover, the cell morphology is more irregular, and the nucleus is larger and more intenselystained. Melanomas stain positively for HMB45 and Melan-A.

Table 2 A review of malignant peripheral nerve sheath tumor cases arising in the maxilla

Ref.	Patients (*n*)	Sex	Age	Treatment	Follow-up (mon)	Recurrence	NF association
Kameyama *et al*[27], 1987	1	F	61	/	/	/	No
Urade *et al*[28], 1990	1	F	47	S+R+C	22	Died of disease	No
Che *et al*[19], 2006	1	F	13	R	/	/	No
Patil *et al*[29], 2007	1	M	45	/	/	/	No
Janardhanan *et al*[30], 2011	1	M	40	S	/	Died of disease	Yes
Ali *et al*[31], 2011	1	M	50	R	8	No	/
Tamgadge *et al*[32], 2014	1	M	65	/	/	/	No
Neetha *et al*[33], 2004	1	F	12	R	/	/	/
Muraki *et al*[34], 1999	1	M	43	R+C	20	Died of disease	Yes
Present study	1	F	62	S+R+C	28	Yes	No

S: Surgery; R: Radiotherapy; C: Chemotherapy; NF: Nuclear factor.

Epithelioid sarcomas are typical granulomas with many collagen fibers, and stain negatively for neuron-specific enolase.

Recent studies have shown that loss of H3K27me3, as revealed by immunohistochemical staining, was described in MPNST.The complete loss rate ranges from 34% to 84%[9,35-42]. Among our patients, 11.1% (n = 1) of the MPNST cases showed complete loss of H3K27me3, while 33.3% (n = 3) showed partial loss. Thus, the H3K27me3 Loss rate was lower than reported previously, perhaps reflecting differences among histological subgroups. Lyskjaer *et al*[43] found that 76% of MPNSTs with classical histological features had lost H3K27me3, compared to only 23% of MPNSTs with heterologous elements or low-grade components. The complete loss rate of the epithelioid MPNST subtype was 0%.

Patel *et al*[3] reported that the 5-year head and neck MPNST DSS rate was 65.1%, based on analysis of the SEER database. Similar studies from single institutions reported 5-year DSS rates of 30% and 20%, and a 2-year DSS rate of 21% [14,44]. In our study, the 2- and 5-year DSS rates were 86% and 43%, respectively. Local recurrence and distant metastasis exerted a major influence on DSS. In our study, 43% (3/7) of patients developed local recurrence; two of these patients died and the other one was lost to follow-up. In total, 57% (4/7) of the patients developed distant metastases and 75% died. Both of the patients without local recurrence or distant metastasis are still alive. Other studies revealed that tumor size, stage, and surgical resection significantly influenced DSS[1,2].

Radical surgical resection is the mainstay of MPNST treatment[44,45]. In our study, 9 of 10 patients underwent wide excision; in the remaining case, the tumor was too large to excise. Adjuvant therapies, such as radiotherapy and chemotherapy, are now prescribed for MPNST patients. Some studies have suggested that radiation should be routine to improve survival and decrease the risk of recurrence[44,46]. Chemotherapy has been prescribed for those with large or recurrent tumors, but any role for chemotherapy as an MPNST treatment remains controversial[2]. In our study, both radiation and chemotherapy were prescribed for four patients, and radiation only for one. As our study included a relatively small number of cases, larger series are needed to validate the results.

CONCLUSION

In summary, MPNST is an uncommon and aggressive soft tissue sarcomas and the head and neck MPNST is extremely rare. Clinical and pathological characteristics of MPNST are not significant. The patients are with poor prognoses and associated with a high risk of recurrence and distant metastasis. Complete surgical resection is the main treatment.

Table 1 Clinicopathological characteristics of malignant peripheral nerve sheath tumor arising in the head and neck

Case	Sex/age	Location	Size (cm)	Treatment	Recurrence (site)	Survival	Follow-up (months)	H3K27Me3
1	F/62	Anterior maxilla	2.5	S+R+C	DR (lung, bone)	Yes	28	Positive
2	F/28	Left mandible	3	S+R+C	NR	Yes	24	Positive
3	M/22	Right submandibular region	2.5	S	/	/	/	Complete loss
4	M/74	Gingival and the left cheek and left temporal	2.5	S	/	/	/	Positive
5	F/48	Mandible	3	S+R+C	LR, DR (lung)	No	70	Positive
6	M/40	Left facial and upper left gingiva	3	S+R	LR, DR (trunk, brain)	No	216	Partial loss
7	F/40	Right mandible	3	S	/	/	/	Partial loss
8	F/44	The left inferior temporal fossa	4.5	R+C	NR	No	13	Partial loss
9	M/58	Right palat	1.5	S	NR	Yes	74	/
10	M/75	Mandibular gingival	3	S	DR (lung, lymph node)	No	24	Positive

S: Surgery; R: Radiotherapy; C: Chemotherapy; LR: Local recurrence; DR: Distant recurrence; NR: No recurrence.

FOOTNOTES

Author contributions: Li L and Ma XK contributed equally to this work; Zhang R, Li L, Ma XK, Wang DC, Gao Y designed the research study; Jing Y, Dong RF performed the research; Li L, Ma XK, Zhang R analyzed the data and wrote the manuscript; All authors have read and approve the final manuscript.

Informed consent statement: All study participants, or their legal guardian, provided informed written consent prior to study enrollment.

Conflict-of-interest statement: All the authors declare that they have no conflicts of interest related to this manuscript.

CARE Checklist (2016) statement: The authors have read the CARE Checklist (2016), and the manuscript was prepared and revised according to the CARE Checklist (2016).

Country/Territory of origin: China

ORCID number: Ran Zhang 0000-0001-5815-2689.

S-Editor: Liu JH
L-Editor: A
P-Editor: Zhang XD

REFERENCES

1 **Arshi A**, Tajudeen BA, St John M. Malignant peripheral nerve sheath tumors of the head and neck: Demographics, clinicopathologic features, management, and treatment outcomes. *Oral Oncol* 2015; **51**: 1088-1094 [PMID: 26442813 DOI: 10.1016/j.oraloncology.2015.08.012]

2 **Ma C**, Ow A, Shan OH, Wu Y, Zhang C, Sun J, Ji T, Pingarron Martin L, Wang L. Malignant peripheral nerve sheath tumours in the head and neck region: retrospective analysis of clinicopathological features and treatment outcomes. *Int J Oral Maxillofac Surg* 2014; **43**: 924-932 [PMID: 24685259 DOI: 10.1016/j.ijom.2014.03.006]

3 **Patel TD**, Shaigany K, Fang CH, Park RC, Baredes S, Eloy JA. Comparative Analysis of Head and Neck and Non-Head and Neck Malignant Peripheral Nerve Sheath Tumors. *Otolaryngol Head Neck Surg* 2016; **154**: 113-120 [PMID: 26408559 DOI: 10.1177/0194599815606700]

4 **do Amaral TL**, Valiati R, de Andrade BA, Rumayor Piña A, Torres SR, Romañach MJ, Agostini M. Malignant peripheral nerve sheath tumor of the lower labial mucosa: case report and literature review. *Oral Surg Oral Med Oral Pathol Oral Radiol* 2016; **122**: e64-e68 [PMID: 26852824 DOI: 10.1016/j.oooo.2015.11.009]

5 **Cunha KS**, Caruso AC, Faria PA, Silva LE, Pires AR, Geller M, Lopes VS, Moura-Neto RS. Malignant peripheral nerve sheath tumors: clinicopathological aspects, expression of p53 and survival. *Clinics (Sao Paulo)* 2012; **67**: 963-968 [PMID: 22948467 DOI: 10.6061/clinics/2012(08)18]

6 **Zhang M**, Wang Y, Jones S, Sausen M, McMahon K, Sharma R, Wang Q, Belzberg AJ, Chaichana K, Gallia GL, Gokaslan ZL, Riggins GJ, Wolinksy JP, Wood LD, Montgomery EA, Hruban RH, Kinzler KW, Papadopoulos N, Vogelstein B, Bettegowda C. Somatic mutations of SUZ12 in malignant peripheral nerve sheath tumors. *Nat Genet* 2014; **46**: 1170-1172 [PMID: 25305755 DOI: 10.1038/ng.3116]

7 **De Raedt T**, Beert E, Pasmant E, Luscan A, Brems H, Ortonne N, Helin K, Hornick JL, Mautner V, Kehrer-Sawatzki H, Clapp W, Bradner J, Vidaud M, Upadhyaya M, Legius E, Cichowski K. PRC2 loss amplifies Ras-driven transcription and confers sensitivity to BRD4-based therapies. *Nature* 2014; **514**: 247-251 [PMID: 25119042 DOI: 10.1038/nature13561]

8 **Lee W**, Teckie S, Wiesner T, Ran L, Prieto Granada CN, Lin M, Zhu S, Cao Z, Liang Y, Sboner A, Tap WD, Fletcher JA, Huberman KH, Qin LX, Viale A, Singer S, Zheng D, Berger MF, Chen Y, Antonescu CR, Chi P. PRC2 is recurrently inactivated through EED or SUZ12 loss in malignant peripheral nerve sheath tumors. *Nat Genet* 2014; **46**: 1227-1232 [PMID: 25240281 DOI: 10.1038/ng.3095]

9 **Prieto-Granada CN**, Wiesner T, Messina JL, Jungbluth AA, Chi P, Antonescu CR. Loss of H3K27me3 Expression Is a Highly Sensitive Marker for Sporadic and Radiation-induced MPNST. *Am J Surg Pathol* 2016; **40**: 479-489 [PMID: 26645727 DOI: 10.1097/PAS.0000000000000564]

10 **Farid M**, Demicco EG, Garcia R, Ahn L, Merola PR, Cioffi A, Maki RG. Malignant peripheral nerve sheath tumors. *Oncologist* 2014; **19**: 193-201 [PMID: 24470531 DOI: 10.1634/theoncologist.2013-0328]

11 **Mullins BT**, Hackman T. Malignant peripheral nerve sheath tumors of the head and neck: a case series and literature review. *Case Rep Otolaryngol* 2014; **2014**: 368920 [PMID: 25548703 DOI: 10.1155/2014/368920]

12 **Wang Y**, Wang RR. Malignant Neurilemmoma of the Head and Neck: a clinicopathologic, Immunohistochemical, and Imaging Study of 8 Cases. 2015; 25: 360-364 [DOI: 10.3969/j.issn.1005-4979.2015.05.011]

13 **Probst M**, Koerdt S, Ritschl LM, Bissinger O, Liesche F, Gempt J, Meyer B, Burian E, Lummel N, Kolk A. Malignant Peripheral Nerve Sheath Tumor in the Course of the Mandibular Nerve. *World Neurosurg* 2018; **117**: e130-e137 [PMID: 29883816 DOI: 10.1016/j.wneu.2018.05.203]

14 **Minovi A**, Basten O, Hunter B, Draf W, Bockmühl U. Malignant peripheral nerve sheath tumors of the head and neck: management of 10 cases and literature review. *Head Neck* 2007; **29**: 439-445 [PMID: 17163467 DOI: 10.1002/hed.20537]

15 **Lee S**, Lee C, Kim JK, Nam W. An unusual presentation of intraosseous malignant peripheral nerve sheath tumour of mandible. *Dentomaxillofac Radiol* 2019; **48**: 20180341 [PMID: 31188646 DOI: 10.1259/dmfr.20180341]

16 **Yaga US**, Shivakumar R, Kumar MA, Sathyaprakash. Malignant peripheral nerve sheath tumor: A rarity. *Indian J Dent* 2015; **6**: 53-56 [PMID: 25767362 DOI: 10.4103/0975-962X.151712]

17 **Majumdar S**, Kotina S, Mahesh N, Uppala D, Kumar SP. Malignant Peripheral Nerve Sheath Tumor -A Rare Malignancy in Mandible. *J Clin Diagn Res* 2016; **10**: ZD12-ZD13 [PMID: 27504425 DOI: 10.7860/JCDR/2016/18263.8010]

18 **Zakhary I**, Elsalanty M, Ishag I, Taher T, Hassan M, Gehani R, Orafi M, El-Mekkawi H. Malignant peripheral nerve sheath tumor of mandible. *J Craniofac Surg* 2011; **22**: 762-766 [PMID: 21415661 DOI: 10.1097/SCS.0b013e318207f447]

19 **Che Z**, Nam W, Park WS, Kim HJ, Cha IH, Kim HS, Yook JI, Kim J, Lee SH. Intraosseous nerve sheath tumors in the jaws. *Yonsei Med J* 2006; **47**: 264-270 [PMID: 16642559 DOI: 10.3349/ymj.2006.47.2.264]

20 **Sham ME**, Ghorpade, Shetty A, Hari S, Vinay. Malignant peripheral nerve cell tumour. *J Maxillofac Oral Surg* 2010; **9**: 68-71 [PMID: 23139572 DOI: 10.1007/s12663-010-0019-6]

21 **Prem S**, Gangothria S, Reddyb KS. Malignant Peripheral Nerve Sheath Tumor of the Mandible: A Case Report and Review of Literature. *Journal of Neurology Research* 2011 [DOI: 10.4021/JNR.V1I5.80]

22 **Salla JT**, Johann AC, Garcia BG, Aguiar MC, Mesquita RA. Retrospective analysis of oral peripheral nerve sheath tumors in Brazilians. *Braz Oral Res* 2009; **23**: 43-48 [PMID: 19488471 DOI: 10.1590/S1806-83242009000100008]

23 **Patel S**, Pathak J, Dekate K, Mohanty N. Malignant peripheral nerve sheath tumour (MPNST) of mandible: solving the perplexity. *BMJ Case Rep* 2015; **2015** [PMID: 25762575 DOI: 10.1136/bcr-2014-207790]

24 **Kumar P**, Surya V, Urs AB, Augustine J, Mohanty S, Gupta S. Sarcomas of the Oral and Maxillofacial Region: Analysis of 26 Cases with Emphasis on Diagnostic Challenges. *Pathol Oncol Res* 2019; **25**: 593-601 [PMID: 30382526 DOI: 10.1007/s12253-018-0510-9]

25 **Naikmasur VG**, Guttal KS, Kaveriappa S, Datta KS. Rapidly progressing soft tissue mass of the anterior mandibular region. Malignant peripheral nerve sheath tumor. *Oral Surg Oral Med Oral Pathol Oral Radiol Endod* 2009; **107**: 607-611 [PMID: 19201222 DOI: 10.1016/j.tripleo.2008.11.025]

26 **Bullock MJ**, Bedard YC, Bell RS, Kandel R. Intraosseous malignant peripheral nerve sheath tumor. Report of a case and review of the literature. *Arch Pathol Lab Med* 1995; **119**: 367-370 [PMID: 7726730 DOI: 10.4172/joo.1000107]

27 **Kameyama Y**, Maeda H, Nakane S, Maeda S, Takai Y, Fukaya M. Malignant schwannoma of the maxilla in a patient without neurofibromatosis. *Histopathology* 1987; **11**: 1205-1208 [PMID: 3121490 DOI: 10.1111/j.1365-2559.1987.tb01860.x]

28 **Urade M**, Fujimoto Y, Ogura T, Matsuya T. Malignant schwannoma and melanoma occurring in the maxilla. *J Osaka Univ Dent Sch* 1990; **30**: 153-156 [PMID: 2130169]

29 **Patil K**, Mahima VG, Ambika L. Malignant peripheral nerve sheath tumour: an elusive diagnosis. *Indian J Dent Res* 2007; **18**: 19-22 [PMID: 17347540 DOI: 10.4103/0970-9290.30917]

30 **Janardhanan M**, Rakesh S, Vinod Kumar R. Intraoral presentation of multiple malignant peripheral nerve sheath tumors associated with neurofibromatosis-1. *J Oral Maxillofac Pathol* 2011; **15**: 46-51 [PMID: 21731277 DOI: 10.4103/0973-029X.80025]

31 **Ali NS**, Junaid M, Aftab K. Malignant peripheral nerve sheath tumour of maxilla. *J Coll Physicians Surg Pak* 2011; **21**: 420-422 [PMID: 21777531]

32 **Tamgadge S**, Modak N, Tamgadge AP, Bhalerao S. Intraosseous malignant peripheral nerve sheath tumor of maxilla: A case report with review of the literature. *Dent Res J (Isfahan)* 2014; **11**: 405-410 [PMID: 25097654]

33 **Neetha MC**, Anupama DH, Shashikanth MC. Malignant peripheral nerve sheath tumor of the maxilla. *Indian J Dent Res* 2004; **15**: 110-3 [PMID: 15915634]

34 **Muraki Y**, Tateishi A, Tominaga K, Fukuda J, Haneji T, Iwata Y. Malignant peripheral nerve sheath tumour in the maxilla associated with von Recklinghausen's disease. *Oral Dis* 1999; **5**: 250-252 [PMID: 10483073 DOI: 10.1111/j.1601-0825.1999.tb00310.x]

35 **Ersen A**, Pekmezci M, Folpe AL, Tihan T. Comparision of New Diagnostic Tools for Malignant Peripheral Nerve Sheath Tumors. *Pathol*

Oncol Res 2017; **23**: 393-398 [PMID: 27734293 DOI: 10.1007/s12253-016-0125-y]

36 **Otsuka H**, Kohashi K, Yoshimoto M, Ishihara S, Toda Y, Yamada Y, Yamamoto H, Nakashima Y, Oda Y. Immunohistochemical evaluation of H3K27 trimethylation in malignant peripheral nerve sheath tumors. *Pathol Res Pract* 2018; **214**: 417-425 [PMID: 29482987 DOI: 10.1016/j.prp.2017.12.015]

37 **Cleven AH**, Sannaa GA, Briaire-de Bruijn I, Ingram DR, van de Rijn M, Rubin BP, de Vries MW, Watson KL, Torres KE, Wang WL, van Duinen SG, Hogendoorn PC, Lazar AJ, Bovée JV. Loss of H3K27 tri-methylation is a diagnostic marker for malignant peripheral nerve sheath tumors and an indicator for an inferior survival. *Mod Pathol* 2016; **29**: 582-590 [PMID: 26990975 DOI: 10.1038/modpathol.2016.45]

38 **Schaefer IM**, Fletcher CD, Hornick JL. Loss of H3K27 trimethylation distinguishes malignant peripheral nerve sheath tumors from histologic mimics. *Mod Pathol* 2016; **29**: 4-13 [PMID: 26585554 DOI: 10.1038/modpathol.2015.134]

39 **Le Guellec S**, Macagno N, Velasco V, Lamant L, Lae M, Filleron T, Malissen N, Cassagnau E, Terrier P, Chevreau C, Ranchere-Vince D, Coindre JM. Loss of H3K27 trimethylation is not suitable for distinguishing malignant peripheral nerve sheath tumor from melanoma: a study of 387 cases including mimicking lesions. *Mod Pathol* 2017; **30**: 1677-1687 [PMID: 28752843 DOI: 10.1038/modpathol.2017.91]

40 **Röhrich M**, Koelsche C, Schrimpf D, Capper D, Sahm F, Kratz A, Reuss J, Hovestadt V, Jones DT, Bewerunge-Hudler M, Becker A, Weis J, Mawrin C, Mittelbronn M, Perry A, Mautner VF, Mechtersheimer G, Hartmann C, Okuducu AF, Arp M, Seiz-Rosenhagen M, Hänggi D, Heim S, Paulus W, Schittenhelm J, Ahmadi R, Herold-Mende C, Unterberg A, Pfister SM, von Deimling A, Reuss DE. Methylation-based classification of benign and malignant peripheral nerve sheath tumors. *Acta Neuropathol* 2016; **131**: 877-887 [PMID: 26857854 DOI: 10.1007/s00401-016-1540-6]

41 **Pekmezci M**, Cuevas-Ocampo AK, Perry A, Horvai AE. Significance of H3K27me3 loss in the diagnosis of malignant peripheral nerve sheath tumors. *Mod Pathol* 2017; **30**: 1710-1719 [PMID: 28776579 DOI: 10.1038/modpathol.2017.97]

42 **Makise N**, Sekimizu M, Kubo T, Wakai S, Hiraoka N, Komiyama M, Fukayama M, Kawai A, Ichikawa H, Yoshida A. Clarifying the Distinction Between Malignant Peripheral Nerve Sheath Tumor and Dedifferentiated Liposarcoma: A Critical Reappraisal of the Diagnostic Utility of MDM2 and H3K27me3 Status. *Am J Surg Pathol* 2018; **42**: 656-664 [PMID: 29309298 DOI: 10.1097/PAS.0000000000001014]

43 **Lyskjaer I**, Lindsay D, Tirabosco R, Steele CD, Lombard P, Strobl AC, Rocha AM, Davies C, Ye H, Bekers E, Ingruber J, Lechner M, Amary F, Pillay N, Flanagan AM. H3K27me3 expression and methylation status in histological variants of malignant peripheral nerve sheath tumours. *J Pathol* 2020; **252**: 151-164 [PMID: 32666581 DOI: 10.1002/path.5507]

44 **Kar M**, Deo SV, Shukla NK, Malik A, DattaGupta S, Mohanti BK, Thulkar S. Malignant peripheral nerve sheath tumors (MPNST)--clinicopathological study and treatment outcome of twenty-four cases. *World J Surg Oncol* 2006; **4**: 55 [PMID: 16923196 DOI: 10.1186/1477-7819-4-55]

45 **Zou C**, Smith KD, Liu J, Lahat G, Myers S, Wang WL, Zhang W, McCutcheon IE, Slopis JM, Lazar AJ, Pollock RE, Lev D. Clinical, pathological, and molecular variables predictive of malignant peripheral nerve sheath tumor outcome. *Ann Surg* 2009; **249**: 1014-1022 [PMID: 19474676 DOI: 10.1097/SLA.0b013e3181a77e9a]

46 **Anghileri M**, Miceli R, Fiore M, Mariani L, Ferrari A, Mussi C, Lozza L, Collini P, Olmi P, Casali PG, Pilotti S, Gronchi A. Malignant peripheral nerve sheath tumors: prognostic factors and survival in a series of patients treated at a single institution. *Cancer* 2006; **107**: 1065-1074 [PMID: 16881077 DOI: 10.1002/cncr.22098]

World Journal of Clinical Cases

Submit a Manuscript: https://www.f6publishing.com

World J Clin Cases 2023 September 6; 11(25): 5919-5925

DOI: 10.12998/wjcc.v11.i25.5919

ISSN 2307-8960 (online)

CASE REPORT

Synchronous multiple lung cancers with hilar lymph node metastasis of small cell carcinoma: A case report

Ryusei Yoshino, Nana Yoshida, Shunsuke Yasuda, Akane Ito, Masaki Nakatsubo, Sayaka Yuzawa, Masahiro Kitada

Specialty type: Medicine, research and experimental

Provenance and peer review: Unsolicited article; Externally peer reviewed.

Peer-review model: Single blind

Peer-review report's scientific quality classification

Grade A (Excellent): 0
Grade B (Very good): B
Grade C (Good): C
Grade D (Fair): 0
Grade E (Poor): E

P-Reviewer: Eccher A, Italy; Lin Q, China; Long X, China

Received: March 25, 2023
Peer-review started: March 25, 2023
First decision: June 21, 2023
Revised: July 5, 2023
Accepted: August 7, 2023
Article in press: August 7, 2023
Published online: September 6, 2023

Ryusei Yoshino, Nana Yoshida, Shunsuke Yasuda, Akane Ito, Masaki Nakatsubo, Masahiro Kitada, Thoracic Surgery and Breast Surgery, Asahikawa Medical University, Asahikawa 078-8510, Japan

Sayaka Yuzawa, Diagnostic Pathology, Asahikawa Medical University Hospital, Hokkaido 078-8510, Japan

Corresponding author: Ryusei Yoshino, MD, Doctor, Thoracic Surgery and Breast Surgery, Asahikawa Medical University, 2-1-1-1 Midorigaoka Higashi, Asahikawa-shi, Hokkaido, Asahikawa 078-8510, Japan. ryusei.0628.ppp@gmail.com

Abstract

BACKGROUND

Synchronous multiple lung cancers are rare and refer to the simultaneous presence of two or more primary lung tumors, which present significant challenges in terms of diagnosis and treatment.

CASE SUMMARY

We report a case of multiple synchronous lung cancers with hilar lymph node metastasis of small cell carcinoma of unknown origin in a 73-year-old man. Transbronchial lung biopsy revealed squamous cell carcinoma. Although enlargement of lymph node 12u was detected, no distant metastases were observed. The patient was preoperatively diagnosed with T1cN0M0 and underwent thoracoscopic right upper lobectomy with nodal dissection (ND2a). Based on histopathological findings, the primary lesion was squamous cell carcinoma. A microinvasive adenocarcinoma was also observed on the cranial side of the primary lesion. Tumors were detected in two resected lymph nodes (#12u and #11s). Both tumors were pathologically diagnosed as small cell carcinomas. The primary lesion of the small cell carcinoma could not be identified even by whole-body imaging; however, chemotherapy was initiated for hilar lymph node metastasis of the small cell carcinoma of unknown origin.

CONCLUSION

Multiple synchronous lung cancers can be accompanied by hilar lymph node metastasis of small cell carcinomas of unknown origin.

Key Words: Small cell carcinoma; Synchronous multiple lung cancers; Squamous cell

carcinoma; Adenocarcinoma; Chemotherapy; Case report

Core Tip: Synchronous multiple lung cancer is relatively rare. We report a case of synchronous multiple lung cancers with lymph node metastasis in the hilar region of a small cell carcinoma of unknown origin. Immunohistochemistry was helpful in aiding the diagnosis. As such cases have a poor prognosis, an accurate diagnosis is necessary to determine treatment options.

Citation: Yoshino R, Yoshida N, Yasuda S, Ito A, Nakatsubo M, Yuzawa S, Kitada M. Synchronous multiple lung cancers with hilar lymph node metastasis of small cell carcinoma: A case report. *World J Clin Cases* 2023; 11(25): 5919-5925
URL: https://www.wjgnet.com/2307-8960/full/v11/i25/5919.htm
DOI: https://dx.doi.org/10.12998/wjcc.v11.i25.5919

INTRODUCTION

Synchronous multiple primary cancerous lesions are rare in patients with primary lung cancer[1]. Such lesions are associated with a poorer prognosis than solitary lung cancer. Moreover, it is necessary to differentiate these lesions from intrapulmonary metastases when these tumors exhibit the same histological type.

Furthermore, hilar and mediastinal lymph node metastases of unknown origin are rare in cases of small cell carcinoma [2]. We report the rare case of a 73-year-old man with a preoperative diagnosis of squamous cell carcinoma of the lung who underwent surgery and was found to have multiple synchronous cancers (squamous cell carcinoma and microinvasive adenocarcinoma) on histopathological examination. Additionally, the histological type of the hilar lymph node metastasis was small cell carcinoma. To the best of our knowledge, a similar case study has not been reported previously. Herein, we describe our case and review the relevant literature.

CASE PRESENTATION

Chief complaints

The patient had no subjective symptoms such as respiratory distress or chest pain. Computed tomography (CT) revealed abnormal shadows in the chest.

History of present illness

The patient had been receiving treatment for diabetes mellitus; during a regular checkup, a mass shadow in the right upper lung was observed on chest radiography. The lesions were closely examined, and the patient was diagnosed with squamous cell carcinoma of the lung using bronchoscopy. Subsequently, the patient was referred to our department for surgical resection.

History of past illness

The patient had a history of diabetes mellitus and hypertension, which were well-controlled. No other cardiac or respiratory disease was observed.

Personal and family history

The patient's family history was unremarkable. The patient had a history of smoking 20 cigarettes per day for 38 years (20–58 years of age).

Physical examination upon admission

Physical findings on admission were as follows: Height, 169 cm; weight, 79.3 kg; body mass index, 27.8 kg/m^2. Respiratory sounds were evident in both lungs. Superficial lymph nodes were not palpable.

Laboratory examinations

The patient's blood count was within the normal range. Blood glucose level was 177 mg/dL, and hemoglobin A1c level was slightly elevated at 6.9%. No abnormal findings were observed for any other biochemical or coagulation marker. Levels of tumor markers (carcinoembryonic antigen, cytokeratin 19 fragment, and pro-gastrin-releasing peptide) were not elevated. Respiratory function tests and electrocardiograms revealed no abnormalities.

Imaging examinations

Chest radiography revealed nodular shadows associated with the surrounding tightening of the right upper lung field (Figure 1). Chest CT images (lung window) showed an irregularly shaped mass measuring 2.5 × 2.0 cm in the upper lobe of the right lung and a slightly increased density on the cranial side (Figure 2A and B). CT (mediastinal window) also revealed enlarged lymph nodes in the right hilar region (Figure 2C). Additionally, abdominal CT showed no findings suggestive of metastasis, and magnetic resonance imaging revealed no evidence of brain metastasis. Fluorodeoxyglucose (FDG) positron emission tomography showed FDG uptake, with a maximum standardized uptake value of approximately 5.0, in the right upper lung field and right hilar region (Figure 3), indicating hilar lymph node metastasis of the primary right upper lobe lung cancer.

FURTHER DIAGNOSTIC WORKUP

The specimen collected from the right upper pulmonary lobe during the transbronchial lung biopsy was histologically diagnosed as squamous cell carcinoma.

Intraoperatively, thoracoscopic right upper lobectomy with nodal dissection (ND2a) was performed *via* a thoracotomy of the fifth intercostal space. The lymph nodes around the truncus artery were enlarged, with strong adhesion. The surgery time was 2 h 4 min, with 10 mL blood loss.

Upon examination of the resected specimen, a tumor measuring 3.0 cm × 2.5 cm × 2.5 cm on cut surfaces was detected in segment 1 of the right upper pulmonary lobe. A lesion with a grayish-white area measuring 1.7 cm × 1.5 cm × 1.0 cm was noted on the cranial side (Figure 4). The lobar bronchial lymph node (#12u) was enlarged to 2.9 cm × 2.8 cm × 2.1 cm.

Using hematoxylin-eosin (HE) staining, histopathological examination of the mass in the right upper pulmonary lobe revealed nested and sheet-like growth of atypical cells with hyperchromatic pleomorphic irregularly-shaped nuclei. The nuclei were centrally located, some cells had intercellular bridges, and focal keratinization was observed. These findings were indicative of squamous cell carcinoma (Figure 5A). Immunohistochemical staining was positive for p40 (Figure 5B) and negative for CD56, synaptophysin, and chromogranin A. Vascular and lymphatic invasion was observed. The pathological diagnosis was pT1cN0M0 (pStage IA3).

The cranial side of the tumor in the right upper pulmonary lobe showed lepidic growth of atypical cuboidal cells with enlarged nuclei and eosinophilic cytoplasm (Figure 5C). Focal invasion measuring ≤ 1 mm was noted, indicating microinvasive adenocarcinoma; neither vascular nor lymphatic invasion was observed. The pathological diagnosis was pT1aN0M0 (pStage IA1). HE staining of a lobar bronchial lymph node (#12u) revealed solid and nested growth of atypical cells with finely granular nuclear chromatin and scant cytoplasm. The tumor cells were less cohesive, with no keratinization or intercellular bridges. Apoptotic cells and mitoses were frequently observed. These findings are indicative of small cell carcinoma (Figure 5D). Immunohistochemical staining was positive for cytokeratin CAM5.2 and negative for p40. A few tumor cells were positive for synaptophysin, chromogranin A, insulinoma-associated protein-1 (INSM1), and CD56. Micrometastases of small cell carcinoma were also observed in the lymph nodes of #11s. The pathological diagnosis was pTXN1M0 (Stage IIB).

FINAL DIAGNOSIS

The final diagnosis was synchronous multiple lung cancers (squamous cell carcinoma and microinvasive adenocarcinoma) with hilar lymph node metastasis of small cell carcinoma of unknown origin.

TREATMENT

The patient had no adverse events postoperatively and was discharged on the eighth postoperative day. One month later, the patient received four courses of chemotherapy consisting of carboplatin [area under the curve (AUC), 5] and etoposide (80 mg/m^2) combination. No prophylactic cranial irradiation was administered.

OUTCOME AND FOLLOW-UP

There was no evidence of recurrence approximately 2 years after surgery. The patient was followed-up every 6 mo.

DISCUSSION

Although synchronous multiple lung cancers have been reported previously, they are relatively rare[1]. Martini and Melamed[3] reported the following diagnostic criteria: (1) Each tumor exists independently; (2) Tumors exhibit different histological types, or if they exhibit identical histological types, intrapulmonary metastasis can be ruled out based on the presence or absence of carcinoma in situ, the extent of histodifferentiation, cellular subtypes, the extent of scar formation

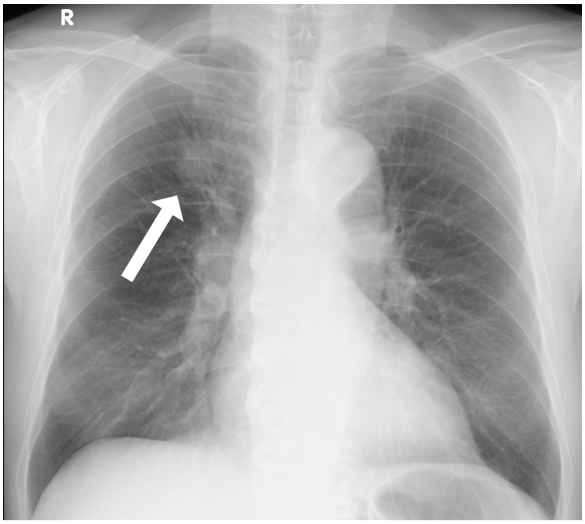

DOI: 10.12998/wjcc.v11.i25.5919 **Copyright** ©The Author(s) 2023.

Figure 1 Chest radiograph (frontal view). Nodular shadows associated with the surrounding tightening are observed in the right upper lung field (arrow).

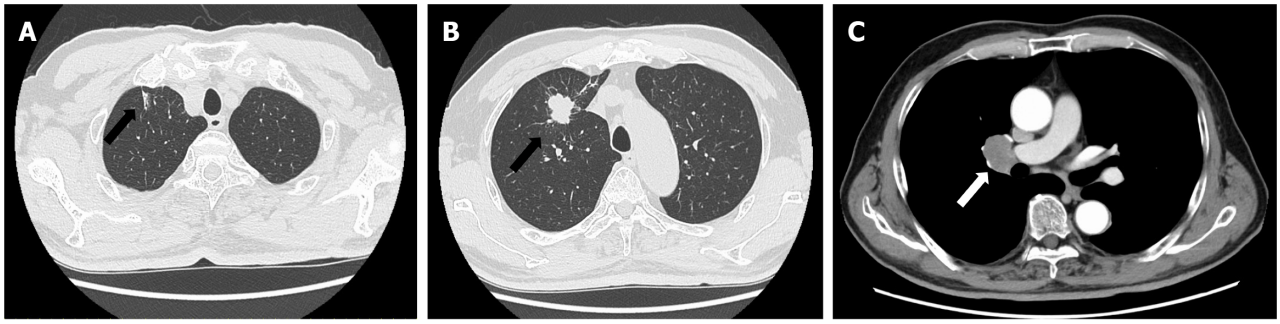

DOI: 10.12998/wjcc.v11.i25.5919 **Copyright** ©The Author(s) 2023.

Figure 2 Chest computed tomography findings. A: Chest computed tomography (CT) using the lung window showing slightly increased density in the periphery (black arrow); B: Primary lesion detected using the lung window. An irregularly shaped mass measuring 25 mm is observed in the right upper pulmonary lobe (black arrow); C: Chest CT using the mediastinal window revealing enlarged lymph nodes in the right hilar region (white arrow).

at the tumor core, and presence or absence of vascular invasion; and (3) Metastasis from other organ cancers can be ruled out. The histological types are often identical. Squamous cell carcinoma is frequently reported in Japan, whereas adenocarcinoma is common in the United States[4]. In the case of simultaneous multiple lung cancers, determining whether these lung cancer foci are separate primary sites is relatively easy when histological examination reveals differences in tumors[5]. However, it is difficult to differentiate between two tumors with similar morphologies[6]. To this end, genetic analysis has recently become a widely used auxiliary diagnostic tool[7,8].

Cancer of unknown origin accounts for approximately 2%–5% of all cancers[9] and can manifest as lymph node metastasis, accounting for approximately 30%–40% of these cases[10]. Cancer detection is even rarer owing to hilar mediastinal lymph node metastasis. In many cases, the primary cancer is assumed to be located in the lungs. Adenocarcinoma is the most common histological type, whereas small cell carcinomas are rare[2]. Cases of synchronous multiple lung cancers with hilar lymph node metastasis of small cell carcinoma of unknown origin are rare, as in the present case. No such cases have been reported in the literature.

Synchronous multiple lung cancers must be differentiated from pulmonary metastases, extrapulmonary metastases, infections, and benign nodules. In the present case, HE staining of the tumor in the right upper pulmonary lobe revealed findings indicative of squamous cell carcinoma. Immunohistochemical staining was positive for p40, consistent with the diagnosis of squamous cell carcinoma[11]. Furthermore, the maximum invasion diameter of the tumor on the cranial side was ≤ 1 mm, and the HE staining results indicated microinvasive adenocarcinoma. HE staining of the lobar bronchial lymph nodes (#12u and #11s) indicated small cell carcinoma. Immunohistochemical staining results were negative for p40; hence, squamous cell carcinoma was excluded. Synaptophysin, chromogranin A, INSM1, and CD56 were focally positive, consistent with small cell carcinoma[12,13]. However, there was no evidence of a primary lesion indicative of small cell carcinoma in the right upper pulmonary lobe. This may be explained as follows: the primary tumor site may be the hilum, a lump of the tumor and lymph node mass may be formed, there may be minute primary lesions in sites that were not collected as specimens, and the primary lesion may be in sites other than the right upper pulmonary lobe. Squamous cell carcinoma is unlikely to transform into small cell carcinoma because squamous cell carcinoma contains no small cell carcinoma components, the lymph nodes contain no squamous cell carcinoma components, and transformation

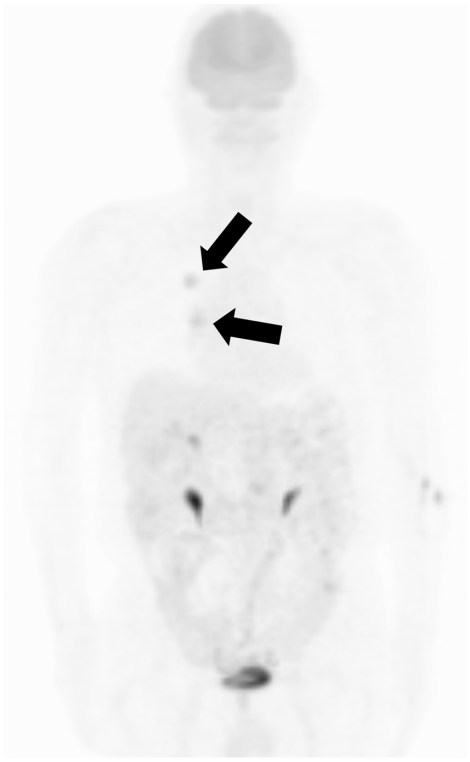

DOI: 10.12998/wjcc.v11.i25.5919 **Copyright** ©The Author(s) 2023.

Figure 3 Fluorodeoxyglucose positron emission tomography findings. Fluorodeoxyglucose uptake with a maximum standardized uptake value of approximately 5.0 is observed in the right upper lung field (up arrow) and right hilar region (down arrow).

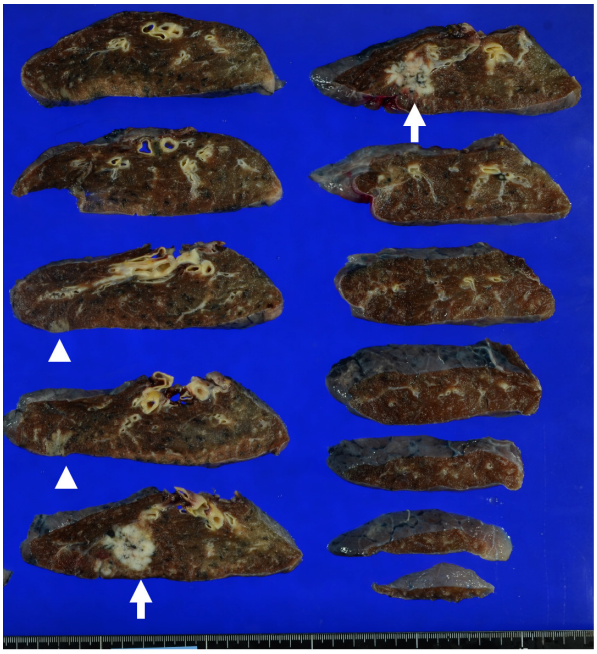

DOI: 10.12998/wjcc.v11.i25.5919 **Copyright** ©The Author(s) 2023.

Figure 4 Resected specimen findings. In addition to the primary lesion, another lesion with a grayish-white area is noted on the cranial side (white arrows).

from squamous cell carcinoma to small cell carcinoma is rare.

Our patient received postoperative chemotherapy with four courses of carboplatin (AUC 5) and etoposide (80 mg/m^2) combination. When the histological types of tumors vary in multiple synchronous lung cancers, each tumor should be evaluated and treated, regardless of the presence of other tumors. When tumors are in stages II or III, postoperative chemotherapy is recommended[14]. However, no standard effective postoperative treatment regimen has been established for stage I tumors, as in the present case. As our patient had hilar lymph node metastasis of small cell carcinoma of unknown origin, postoperative chemotherapy was administered based on the treatment regimen for small

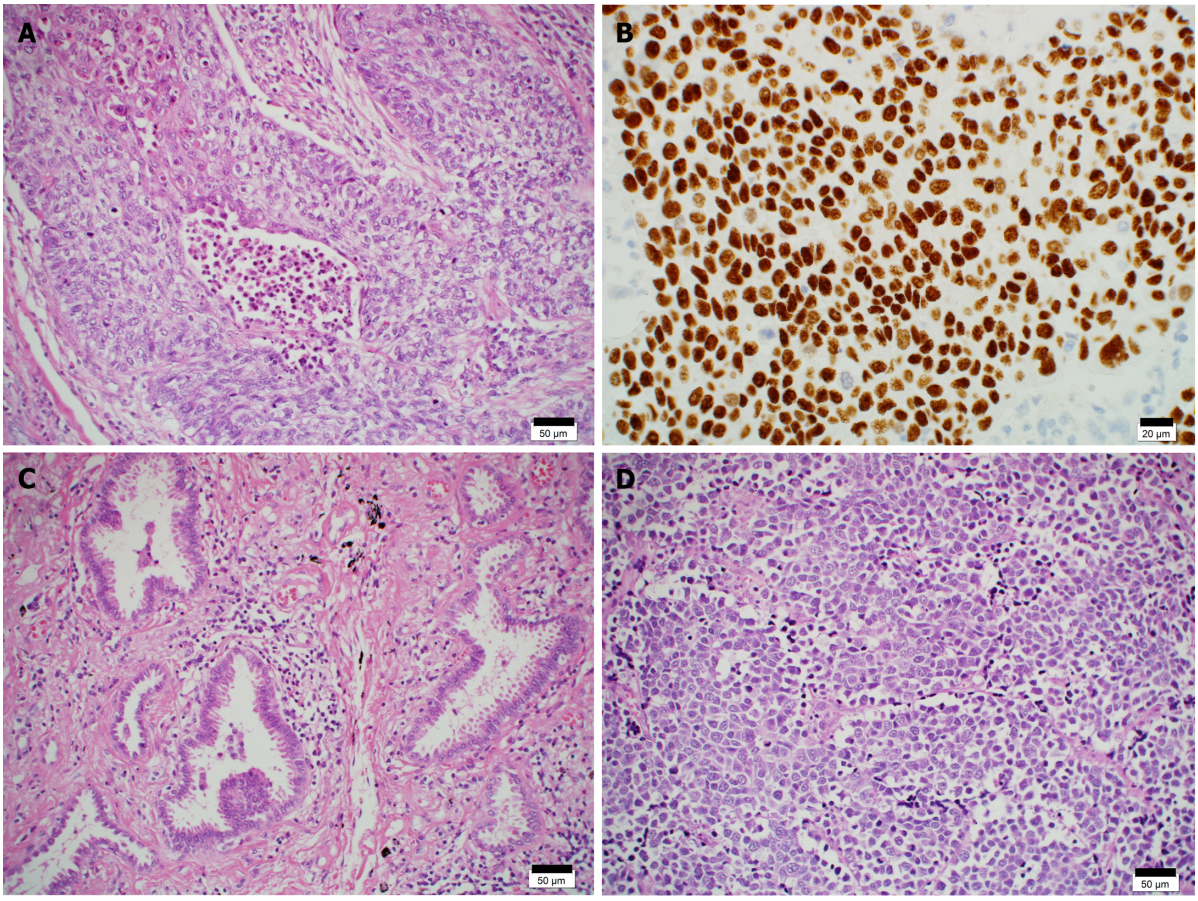

DOI: 10.12998/wjcc.v11.i25.5919

Figure 5 Histopathological findings. A: Primary lesion in the right upper pulmonary lobe. The staining results indicate squamous cell carcinoma [hematoxylin-eosin (HE) staining, Scale bar: 50 μm]; B: Primary lesion in the right upper pulmonary lobe. The immunohistochemical staining results are positive for p40 (Scale bar: 20 μm); C: A lesion located on the cranial side of the primary lesion. The staining results indicate microinvasive adenocarcinoma (HE staining, Scale bar: 50 μm); D: Lobar bronchial lymph node (#12u). The staining results indicate small cell carcinoma (HE staining, Scale bar: 50 μm).

cell lung carcinoma, as stated in the National Comprehensive Cancer Network Clinical Practice Guidelines in Oncology (NCCN Guidelines®). Approximately 2 years postoperatively, there was no evidence of recurrence.

When multiple synchronous lung cancers are accompanied by hilar lymph node metastasis, diagnosis and therapeutic strategies vary according to the histological type of the tumor. Therefore, immunohistochemical staining is a valuable tool for tumor differentiation. As in our case, the coexistence of synchronous multiple lung cancers with different histological types and histologically different carcinomas of unknown origin is rare. Further investigation of such cases is required to clarify this condition.

CONCLUSION

We present a case of multiple synchronous lung cancers with hilar lymph node metastasis of small cell carcinoma of unknown origin. Immunohistochemical staining proved to be a valuable diagnostic tool. In addition, synchronous multiple lung cancers and cancers of unknown origin have poor prognoses; hence, an accurate diagnosis is necessary for selecting postoperative adjuvant therapy.

FOOTNOTES

Author contributions: Yoshino R contributed to the study conceptualization and original draft preparation; Yasuda S, Yoshida N, Yuzawa S, Ito A, and Nakatsubo M contributed to the review and editing of the manuscript; Kitada M validated and visualized the study; and Kitada M supervised the study; all the authors have read and approved the final version of the manuscript.

Informed consent statement: Written informed consent was obtained from the patient.

Conflict-of-interest statement: The authors declare no conflicts of interest.

CARE Checklist (2016) statement: The authors have read the CARE Checklist (2016), and the manuscript was prepared and revised according to the CARE Checklist (2016).

Country/Territory of origin: Japan

ORCID number: Ryusei Yoshino 0000-0002-6904-7267; Shunsuke Yasuda 0000-0003-1773-4070; Akane Ito 0009-0008-2413-7841; Masaki Nakatsubo 0009-0009-4080-4015; Sayaka Yuzawa 0000-0002-2337-4000; Masahiro Kitada 0000-0002-9741-0510.

S-Editor: Lin C
L-Editor: Webster JR
P-Editor: Zhang XD

REFERENCES

1 **Trousse D**, Barlesi F, Loundou A, Tasei AM, Doddoli C, Giudicelli R, Astoul P, Fuentes P, Thomas P. Synchronous multiple primary lung cancer: an increasing clinical occurrence requiring multidisciplinary management. *J Thorac Cardiovasc Surg* 2007; **133**: 1193-1200 [PMID: 17467428 DOI: 10.1016/j.jtcvs.2007.01.012]
2 **Chang SK**, Ano S, Kikuchi N, Masuda M, Osawa H, Kondo Y, Ishii Y. A case of lung and mediastinal and hilar lymph node metastasis in a patient with cancer of unknown primary site. *Clin Exp Metastasis* 2022; **39**: 259-261 [PMID: 34773207 DOI: 10.1007/s10585-021-10134-7]
3 **Martini N**, Melamed MR. Multiple primary lung cancers. *J Thorac Cardiovasc Surg* 1975; **70**: 606-612 [PMID: 170482]
4 **Wakelee HA**, Bernardo P, Johnson DH, Schiller JH. Changes in the natural history of nonsmall cell lung cancer (NSCLC)--comparison of outcomes and characteristics in patients with advanced NSCLC entered in Eastern Cooperative Oncology Group trials before and after 1990. *Cancer* 2006; **106**: 2208-2217 [PMID: 16604529 DOI: 10.1002/cncr.21869]
5 **Wu X**, Huang W, Geng T, Wei Y. Next-Generation Sequencing of Synchronous Multiple Primary Lung Cancers in a Patient with Squamous Cell Carcinoma and Small Cell Lung Cancer. *Onco Targets Ther* 2020; **13**: 11621-11626 [PMID: 33209038 DOI: 10.2147/OTT.S274329]
6 **Jiang L**, Zheng X, Wu S, Zhang J, Ru G, Li Y. A Rare Case Of Synchronous Multiple Primary Lung Cancer: Squamous Cell Cancer And Small Cell Lung Cancer. *Onco Targets Ther* 2019; **12**: 8801-8806 [PMID: 31749623 DOI: 10.2147/OTT.S213259]
7 **Qu R**, Tu D, Ping W, Zhang N, Fu X. Synchronous Multiple Lung Cancers with Lymph Node Metastasis and Different EGFR Mutations: Intrapulmonary Metastasis or Multiple Primary Lung Cancers? *Onco Targets Ther* 2021; **14**: 1093-1099 [PMID: 33623395 DOI: 10.2147/OTT.S294953]
8 **Lim J**, Han YB, Park SY, Ahn S, Kim H, Kwon HJ, Lee CT, Cho S, Chung JH. Gene Expression Profiles of Multiple Synchronous Lesions in Lung Adenocarcinoma. *Cells* 2021; **10** [PMID: 34943992 DOI: 10.3390/cells10123484]
9 **Lee MS**, Sanoff HK. Cancer of unknown primary. *BMJ* 2020; **371**: m4050 [PMID: 33288500 DOI: 10.1136/bmj.m4050]
10 **Greager JA**, Wood D, Das Gupta TK. Metastatic cancer from an undetermined primary site. *J Surg Oncol* 1983; **23**: 73-76 [PMID: 6855244 DOI: 10.1002/jso.2930230204]
11 **Takahashi H**, Asato Y, Ikeda Y, Kijima S, Tamura Y, Hiraki T, Hatanaka K. Tumor-to-tumor metastasis: lung cancer within a thymoma. *Gen Thorac Cardiovasc Surg* 2021; **69**: 147-150 [PMID: 32920748 DOI: 10.1007/s11748-020-01481-5]
12 **Wick MR**. Immunohistology of neuroendocrine and neuroectodermal tumors. *Semin Diagn Pathol* 2000; **17**: 194-203 [PMID: 10968705]
13 **Lantuejoul S**, Moro D, Michalides RJ, Brambilla C, Brambilla E. Neural cell adhesion molecules (NCAM) and NCAM-PSA expression in neuroendocrine lung tumors. *Am J Surg Pathol* 1998; **22**: 1267-1276 [PMID: 9777989 DOI: 10.1097/00000478-199810000-00012]
14 **van Rens MT**, de la Rivière AB, Elbers HR, van Den Bosch JM. Prognostic assessment of 2,361 patients who underwent pulmonary resection for non-small cell lung cancer, stage I, II, and IIIA. *Chest* 2000; **117**: 374-379 [PMID: 10669677 DOI: 10.1378/chest.117.2.374]

World Journal of Clinical Cases

Submit a Manuscript: https://www.f6publishing.com

World J Clin Cases 2023 September 6; 11(25): 5926-5933

DOI: 10.12998/wjcc.v11.i25.5926

ISSN 2307-8960 (online)

CASE REPORT

Ultrasound-guided carotid angioplasty and stenting in a patient with iodinated contrast allergy: A case report

Le Li, Zi-Yan Wang, Bo Liu

Specialty type: Clinical neurology

Provenance and peer review: Unsolicited article; Externally peer reviewed.

Peer-review model: Single blind

Peer-review report's scientific quality classification

Grade A (Excellent): 0
Grade B (Very good): 0
Grade C (Good): C
Grade D (Fair): 0
Grade E (Poor): 0

P-Reviewer: Chow WK, Taiwan

Received: April 28, 2023
Peer-review started: April 28, 2023
First decision: July 18, 2023
Revised: August 3, 2023
Accepted: August 9, 2023
Article in press: August 9, 2023
Published online: September 6, 2023

Le Li, Bo Liu, Department of Neurology, Shenzhen Longhua District Central Hospital, Shenzhen 518110, Guangdong Province, China

Le Li, Zi-Yan Wang, Department of Neurology, The Third Hospital of Mianyang (Sichuan Mental Health Center), Mianyang 621000, Sichuan Province, China

Zi-Yan Wang, Department of Clinical Medicine, North Sichuan Medical College, Nanchong 637000, Sichuan Province, China

Corresponding author: Bo Liu, PhD, Doctor, Department of Neurology, Shenzhen Longhua District Central Hospital, No. 187 Guanlan Avenue, Longhua District, Shenzhen 518110, Guangdong Province, China. liubo200000@126.com

Abstract

BACKGROUND

Ischemic stroke is an entity with high incidence, morbidity, and mortality rates. Carotid artery stenosis is an important and independent risk factor for ischemic stroke. The three current approaches for treating carotid artery stenosis are drug treatment, carotid endarterectomy (CEA), carotid angioplasty and stenting (CAS). The approach is chosen based on the degree of stenosis. CEA or CAS could have been chosen for the current patient, who had severe carotid stenosis and an iodinated contrast allergy. After thoroughly communicating with the patient, the patient chose CAS for treatment. Therefore, we performed ultrasound-guided CAS to avoid the use of iodinated contrast.

CASE SUMMARY

The main symptoms of the patient were numbness and weakness of the left limb. Computed tomography angiography of the head and neck at another hospital indicated multiple sites of stenosis in the arteries of the head and neck. The patient requested CAS for treatment but was allergic to iodinated contrast media. Thus, routine digital subtraction angiography (DSA) with iodinated contrast could not be used for the procedure. The diagnosis of this patient was as follows: (1) Right parietal lobe cerebral infarction; (2) multiple sites of stenosis in the arteries of the head and neck (severe stenosis of the right internal carotid artery, severe stenosis of the right subclavian artery); (3) right subclavian steal syndrome; and (4) hypertension (stage 3, high risk). The interventions included routine treatment for cerebral infarction, oral administration of clopidogrel (75 mg qd) and aspirin (100 mg qd), ultrasound-guided CAS, and postoperative follow-up. Postoperative color Doppler ultrasound and cerebrovascular magnetic resonance

angiography of the carotid artery showed good vascular recovery, and the postoperative follow-up indicated a good prognosis.

CONCLUSION
This case study suggests that ultrasound-guided endovascular treatment is a potential option for patients with contraindications to the iodinated contrast agents used in DSA-guided surgery, although excellent surgical operating skills are needed.

Key Words: Iodinated contrast allergy; Ultrasound-guided; Gadolinium-based contrast agent; Carotid angioplasty and stenting; Subclavian artery angioplasty and stenting; Digital subtraction angiography; Case report

Core Tip: We report a case of patient who had severe stenosis of the right internal carotid artery and severe stenosis of the right subclavian artery. The patient requested carotid angioplasty and stenting (CAS) for treatment but was allergic to iodinated contrast media. Therefore, we performed ultrasound-guided CAS to avoid the use of iodinated contrast. Ultrasound and magnetic resonance examination showed good vascular recovery, and the postoperative follow-up indicated a good prognosis. The case suggests that for patients who are allergic to iodinated contrast media, ultrasound-guided CAS is a feasible alternative.

Citation: Li L, Wang ZY, Liu B. Ultrasound-guided carotid angioplasty and stenting in a patient with iodinated contrast allergy: A case report. *World J Clin Cases* 2023; 11(25): 5926-5933
URL: https://www.wjgnet.com/2307-8960/full/v11/i25/5926.htm
DOI: https://dx.doi.org/10.12998/wjcc.v11.i25.5926

INTRODUCTION

Ischemic stroke is a common life-threatening disease, with high morbidity and mortality rates in China. Carotid artery stenosis is an important and independent risk factor for ischemic stroke. With the advancement of materials science, interventional techniques, and imaging technology, as well as the application of distal protection devices, carotid angioplasty and stenting (CAS) has been applied for the treatment of carotid artery stenosis, especially in high-risk patients, to improve the blood supply of the intracranial artery and prevent the occurrence of stroke. The C-arm fluoroscopy machine is the main equipment used in CAS. Iodinated contrast media is used in digital subtraction angiography (DSA)–guided surgical operations, giving the interventional physician a way to observe local blood vessels in real time in an intuitive way and facilitating successful treatment. However, CAS is not clinically applied in patients with iodinated contrast allergy.

For this reason, with the approval of the Quality Management Committee of our hospital, we performed ultrasound-guided CAS in a patient with a contrast agent allergy and achieved a good outcome. We report this case and review the relevant literature.

CASE PRESENTATION

Chief complaints

A 55-year-old man was admitted to our hospital due to numbness and weakness of the left limb for a month.

History of present illness

The patient was admitted to a local hospital for numbness and weakness in his left limb for a month and was diagnosed with cerebral infarction. After standard treatment, the patient felt that the numbness and weakness in his left limb had improved. He occasionally felt weakness of the limb that would resolve spontaneously. Skin rash and shock developed due to an allergic reaction to iodine when he was undergoing head and neck computed tomography angiography (CTA) at the local hospital. The hospital's management brought him out of the crisis. At that time, valuable head and neck artery images were obtained that showed multiple sites of stenosis in cerebral arteries. To better solve this problem, he was transferred to our hospital.

History of past illness

The patient reported well-controlled hypertension. He denied other systemic diseases such as diabetes, hyperlipidemia, coronary heart disease, hepatitis, and tuberculosis.

Personal and family history

The patient reported no smoking or drinking, and there was no special family history.

Physical examination

Physical examination showed the following: clear mind, fluent language, limb muscle strength level 5, and NIHSS score 0.

Laboratory examinations

There were no significant abnormalities in laboratory examinations.

Imaging examinations

Brain magnetic resonance imaging at our hospital showed multiple small patchy shadows on the right parietal lobe, most of which were deemed cerebral infarctions (new onset). Head and neck CTA performed at the local hospital showed that the V1 segment of the right vertebral artery was occluded, the lumen of the rest of the right vertebral artery was small, and the proximal segment of the right subclavian artery (R-SCA) and the right carotid sinus were severely stenotic (Figure 1G and Figure 2G-J). Carotid artery color Doppler ultrasound showed plaque formation in the bilateral common carotid artery, internal carotid artery (ICA), artery-SCA, brachiocephalic artery, and right vertebral artery; stenosis in the initial segment of the right internal carotid artery (R-ICAC1) (stenosis rate 80%) (Figure 2A) and initial segment of the R-SCA (stenosis rate 80%) (Figure 1A), and R-SCA steal syndrome (partial). There was no obvious blood flow signal in the initial segment of the right vertebral artery, suggesting occlusion.

FINAL DIAGNOSIS

The diagnosis of this patient was as follows: (1) Right parietal lobe cerebral infarction; (2) multiple sites of stenosis in the arteries of the head and neck (severe stenosis of the right internal carotid artery, severe stenosis of the right subclavian artery); (3) right subclavian steal syndrome; and (4) hypertension (stage 3, high risk).

TREATMENT

Routine treatment for cerebral infarction was given to the patient after admission. To treat the multiple stenoses of the head and neck arteries, the patient and his family chose CAS (R-SCA, R-ICAC1) after fully understanding the available options. However, routine endovascular therapy could not be performed due to his iodinated contrast agent allergy. The interventional treatment team discussed the problem and decided to use ultrasound instead of iodinated contrast to locate and visualize local cerebral blood vessels.Then, ultrasound-guided CAS of the R-ICAC1 and the R-SCA was performed.

Oral clopidogrel (75 mg qd) and aspirin (100 mg qd) were administered before surgery. The surgical procedure was as follows: (1) The operative fields for the right radial artery and right femoral artery were disinfected and draped. Under local anesthesia, the Seldinger technique was used to puncture the right radial artery and right femoral artery with a 6-F radial artery access sheath and an 8-F femoral artery access sheath, respectively; (2) Under the guidance of a 5-F pigtail angiographic catheter, a 260-cm-long 0.035" guidewire was inserted from the right radial artery sheath to the right femoral artery sheath. A snare was used to grab the tip of the 260-cm 0.035" guidewire out of the femoral artery sheath to form a stable 0.035" stent placement track with both ends outside the body. A 10 mm × 25 mm Biotronik stent was delivered to the beginning of the R-SCA through the femoral artery sheath over the 0.035" guidewire and deployed in a proper position under ultrasound guidance (Figure 1E and F). Ultrasonography showed that the blood flow of the R-SCA was significantly improved (Figure 1B and D) (the degree of stenosis changed from 80% to 30%) (Figure 1A and C). The stent delivery system and the 260-cm 0.035" guidewire were withdrawn. The radial artery access sheath was removed, and the access site was compressed for hemostasis; (3) An 8-F guide catheter was inserted into the right common carotid artery over a 0.035" guidewire. Ultrasonography and radiography showed that the tip of the guide catheter was positioned accurately (Figure 2E). Ultrasonography showed that the degree of stenosis of R-ICAC1 was approximately 80% (Figure 2A). Under ultrasound and X-ray guidance, the 5-mm eV3 embolic protection device (EPD) was placed at the distal R-ICAC1 segment. A 6-8 mm × 40 mm eV3 self-expanding stent was placed in the stenotic site over the 0.014" guidewire of the EPD and deployed when ultrasonography showed accurate positioning (Figure 2E and F). The degree of residual stenosis was 30% (Figure 2C). The distal blood flow was significantly improved (Figure 2D). The stent delivery system and the EPD were withdrawn. The femoral artery access sheath was removed, and the access site was compressed for hemostasis at the end of the procedure; and (4) The patient's vital signs were stable during the operation, and no particular discomfort was reported. Routine care for carotid artery stent implantation was given after surgery.

OUTCOME AND FOLLOW-UP

The patient was discharged without any symptoms or positive neurological signs and had an NIHSS score of 0. The

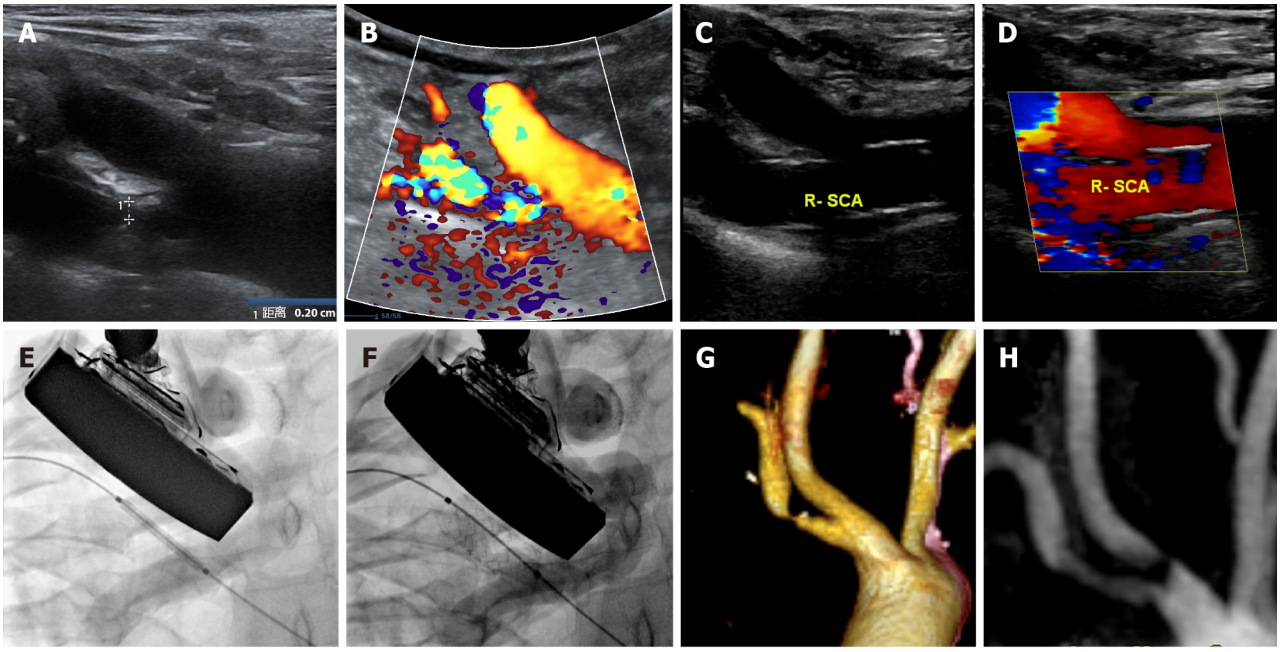

DOI: 10.12998/wjcc.v11.i25.5926

Figure 1 Images before and after subclavian artery stent implantation. A: Ultrasound showing stenosis of the right subclavian artery (R-SCA) before surgery; B: Ultrasound showing blood flow in the region of R-SCA stenosis before surgery; C: Ultrasound showing good stent shape of the R-SCA after surgery; D: Ultrasound showing good blood flow in the region of R-SCA stent after surgery; E: X-ray showing the shape of the stent before stenting; F: X-ray showing the shape of the stent after stenting; G: Computed tomography angiography showing severe stenosis of the R-SCA before surgery; H: Magnetic resonance angiography showing good stent shape after surgery. R-SCA: Right subclavian artery.

follow-up carotid color Doppler ultrasound and cerebrovascular magnetic resonance angiography (MRA) showed normal stent shape and function (Figure 1H and Figure 2K), and the patient's intracranial blood supply was restored (Figure 1D and Figure 2D). Double antiplatelet therapy was continued for 6 mo after stent placement, and then single antiplatelet therapy with clopidogrel was continued lifelong. After 2 years of follow-up, the patient's general condition was good, and no stroke occurred (modified Rankin Scale (mRS) score 0).

DISCUSSION

Advantages and disadvantages of this case study

Advantages: The patient in this study was allergic to iodinated contrast media, which is an absolute contraindication for CAS. In this case, the surgeon avoided the use of iodinated contrast and instead used ultrasound for stent positioning and completion of the operation. Carotid artery color Doppler ultrasound and cerebrovascular MRA showed good vascular recovery after the operation. According to relevant literature in China and abroad, ultrasound-guided interventional therapy can now be applied to treat diseases including coronary artery disease, liver carcinoma, kidney disease, and uterine fibroids. Among cerebrovascular treatments, ultrasound-guided interventional therapy is not common, but it is technically safe and feasible. Reports about carotid artery occlusion and low-dose contrast media for patients with renal insufficiency are available, but arterial stent implantation under ultrasound guidance has not been reported. Therefore, this operation is a technical innovation and can be applied in patients with contraindications to iodinated contrast agents for various reasons.

Shortcomings: The operation was successful because there were no complications or adverse events during the operation, such as arterial wall damage, spasm, plaque detachment, thrombosis, or stent displacement. Moreover, balloon predilation and postdilation were not performed (these can easily cause plaque detachment and embolism). Ultrasound and fluoroscopy alone without contrast cannot be used to completely and accurately detect these unexpected conditions. Therefore, DSA with contrast must be used to observe the local and distal conditions of the artery to make a correct diagnosis and choose the best treatment. If an iodinated contrast agent had been used, another allergic reaction might have occurred, which was a risk the patient could not take. An iodinated contrast agent allergy also increases the difficulty of dealing with various unexpected situations and may eventually cause failure of the operation, threatening the life of the patient. We covered all of these considerations in the preoperative discussion and developed a back-up plan: (1) Effective preoperative preparation was performed to ensure the smooth execution of the operation. To reduce the risk, balloon predilation and postdilation were not performed; and (2) In the case iodinated contrast needed to be used, a large dose of corticosteroids would be intravenously administered in advance to reduce the strength of the allergic reaction, and the patient would be closely monitored to gain time to deal with other unexpected conditions.

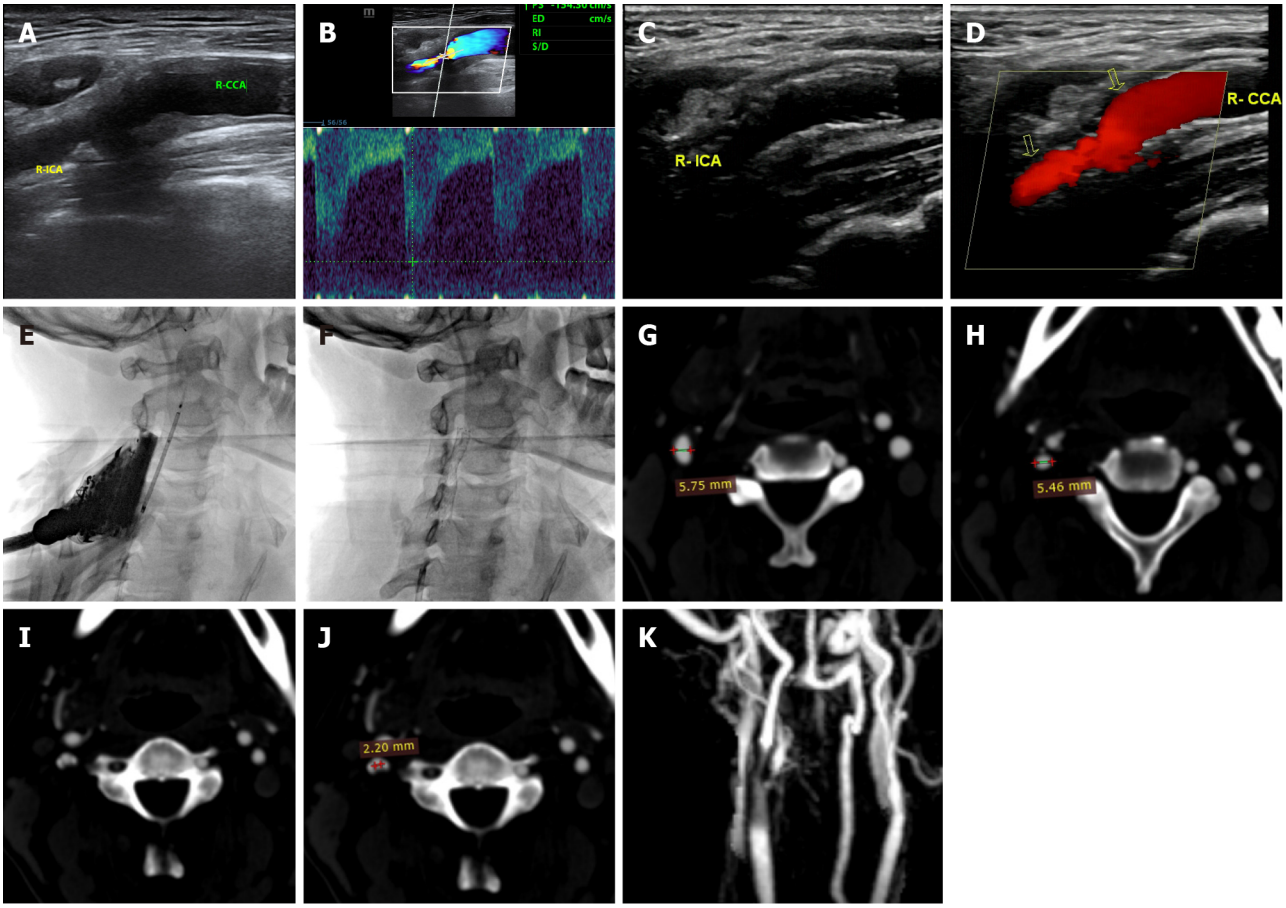

DOI: 10.12998/wjcc.v11.i25.5926

Figure 2 Images before and after carotid artery stent implantation. A: Ultrasound showing stenosis of the right internal carotid artery (R-ICA) before surgery; B: Ultrasound showing blood flow in the region of R-ICA stenosis before surgery; C: Ultrasound showing good stent shape of the R-ICA after surgery; D: Ultrasound showing good blood flow in the region of R-ICA stent after surgery; E: X-ray showing the shape of the stent before stenting; F: X-ray showing the shape of the stent after stenting; G: Preoperative computed tomography angiography (CTA) showing a proximal diameter at the site of R-ICA stenosis of 5.75 mm; H: Preoperative CTA showing a distal diameter at the site of R-ICA stenosis of 5.46 mm; I: CTA showing a cross-section of the site of R-ICA stenosis. The vascular lumen is in the middle, and calcified plaques are present at both ends; J: CTA indicating a lumen diameter at the site of R-ICA stenosis of 2.20 mm; K: Magnetic resonance angiography showing good stent shape after surgery. R-SCA: Right subclavian artery; R-ICA: Right internal carotid artery.

Critical points of technologies: There are two critical points. (1) Identify the narrowed portioned from sonography; and (2) Pass the guidewire through the narrowed portion of the artery. If the guidewire cannot pass through the narrowed portion of the artery, implantation of the stent is impossible. Since both the initial segment of the R-SCA and the initial segment of the R-ICAC1 are thick (8-11 mm), shallow, and not covered by bone, color ultrasound can clearly show these blood vessels and accurately locate the site of stenosis. Ultrasound can detect plaque and blood flow in real-time, and is advantageous in that it is non-invasive, repeatable, and radiation-free. It is often difficult for the guidewire to pass through the stenosis when the stent is placed at the initial segment of the R-SCA through the regular femoral artery approach. This procedure was possibly more difficult because no contrast agent was used in this patient. To overcome this difficulty, we chose the right radial artery approach. Under the guidance of ultrasound and fluoroscopy, the 260-cm-long 0.035" guidewire easily passed through the stenosis of the R-SCA. Then, under the guidance of fluoroscopy, the 260-cm-long 0.035" guidewire was inserted into the right 8F femoral artery sheath, and the head of the guidewire was captured outside the body. This provided a stable track for the 10 mm × 25 mm stent from the femoral artery approach to the stenosis of the R-SCA, and then the stent was precisely and successfully placed under ultrasonic guidance. In this patient, the rate of stenosis in the initial segment of the R-ICAC1 was 80%. Because the degree of stenosis was less than 90%, under the guidance of ultrasound and fluoroscopy, the 0.014 '' micro guidewire easily passed through the stenosis area, and then the stent was successfully placed. If the degree of stenosis is greater than 90% or the lesion is occluded, only ultrasound and fluoroscopy are used, no contrast agent is used for evaluation, passing the guidewire through the stenosis lesion may be relatively difficult, and the surgery may fail.

Treatment selection for symptomatic carotid artery stenosis

Most carotid artery stenosis is caused by atherosclerosis. Lumen stenosis or occlusion, plaque rupture, and embolism can lead to ischemic stroke. There are currently three approaches for treating carotid artery stenosis: medical drug therapy, CEA and CAS. The North American Symptomatic Carotid Endarterectomy Trial and the European Carotid Surgery Trial

have defined a degree of carotid artery stenosis of 0%-49% as no or mild stenosis, 50%-69% as moderate stenosis, 70%-99% as severe stenosis, and 100% as complete occlusion. Patients with moderate stenosis should be closely observed for progression of the lesion, and patients with severe stenosis or occlusion and symptomatic patients should undergo surgery or interventional treatment. That being said, accurate diagnosis of the degree of stenosis is essential[1,2]. In patients with symptomatic carotid artery stenosis and low perioperative risk, when the degree of stenosis exceeds 50%, revascularization should be performed as soon as possible[3].

The patient in the present case had severe carotid artery stenosis, so CEA and CAS were his options. Both methods have advantages and disadvantages. CAS has the advantages of less trauma, fewer surgical complications, high safety, and a high success rate. However, CAS cannot be performed in patients who are allergic to contrast media or have severe heart, liver, or kidney dysfunction; patients in whom interventional devices cannot be placed due to severely tortuous interventional pathways and/or mural thrombosis and vulnerable plaques; patients with chronic complete carotid artery occlusion, in whom contrast media cannot pass; or patients with cerebral hemorrhage within the last 3 mo or large-area cerebral infarction within the last 4 mo. There has been controversy about the pros and cons of the two treatments. According to the results of prospective controlled studies, the consensus of experts is that CAS is a treatment that is not inferior to CEA and can be selectively applied in those with a high surgical risk. CEA has advantages for patients over 75 years of age with severe calcification and thrombosis in the aortic arch and symptomatic carotid stenosis. Current evidence indicates that CEA is absolutely preferred for carotid artery stenosis. In terms of postoperative safety and long-term postoperative efficacy, CEA still has advantages and is still the gold standard for the treatment of carotid artery stenosis. The efficacy of CAS is not superior to that of CEA. However, CEA has become an indispensable treatment for some high-risk patients[4]. CEA was a suitable procedure for treating carotid artery stenosis in this patient but could not be used to manage the stenosis of the R-SCA at the same time. Therefore, CAS was performed at the request of the patient and his family members.

Alternative for patients with iodinated contrast allergy

According to the relevant literature, if iodinated contrast agents cannot be used, such as in patients who are allergic to iodinated contrast agents and those who have a clear history of hyperthyroidism, gadolinium (Gd)-based contrast is feasible as an alternative. The incidence of all side effects of Gd-based contrast media is 1%-2%, while the incidence of all side effects of iodinated contrast media is 3.0%, although the incidence of serious life-threatening side effects of Gd-based contrast media is 10 times that of iodinated contrast media. The probability of severe allergic reaction to gadopentetate meglumine is 0.0002% to 0.001%[5], but it is 3 or 4 times this in patients with a history of iodine allergy, which is still quite low[6]. At present, Gd is mainly used as an MR contrast agent in clinical applications. Gd, as an alternative contrast agent for patients with contraindications to iodinated contrast agents, is mainly used in intravenous pyelography, enhanced computed tomography (CT), CTA, DSA, and interventional therapy. Researchers in China and abroad have reported the successful clinical application of Gd-based contrast agents such as gadopentetate meglumine in pulmonary, aortic, and coronary CTA[7-9]. In 1993, Kinno *et al*[10] first reported the use of a Gd-based contrast agent in arterial angiography and interventional therapy. Since then, the application of Gd-based contrast agents in the cerebral artery, coronary artery, carotid artery, aorta, renal artery, hepatic artery, limb arteries, vena cava, and other blood vessels in most parts of the body has yielded good imaging results[7,11-14]. Moreover, the current application of Gd-based contrast in intracerebrovascular interventional therapy is still associated with some problems, such as high cost and unclear potential for neurotoxic effects, although much evidence has shown that it is safe for the nervous system. Gd-diethylenetriamine pentetic acid (Gd-DTPA) cannot pass through the intact blood–brain barrier. There are currently no guidelines for intra-arterial Gd administration. The maximum safe dose of intra-arterial injection has not yet been determined. The safety of intracardiac and intracoronary injection needs to be further clarified.

Patients who are unable to undergo CAS due to contrast agent-related reasons can undergo CAS under ultrasound guidance. Rostambeigi *et al*[15] reported a case of intravascular revascularization with the aid of duplex ultrasound for chronic internal carotid artery occlusion. Chinese researcher Lu *et al*[16] reported revascularization in two cases of chronic internal carotid artery occlusion by intravascular intervention under ultrasound monitoring. For patients allergic to iodinated contrast media, although ultrasound-guided CAS is an option, it has the disadvantage that ultrasound can only display the vessel approximately 4-5 cm above the bifurcation of the common carotid artery. Thus, excellent surgical operating skills are required[16].

Emphasis

This case study suggests that for patients who are allergic to iodinated contrast agents, ultrasound-guided CAS is a feasible alternative. However, the feasibility is conditional; that is, the lesion must be easy to manage and associated with low risk. For patients with difficult-to-manage lesions, advanced age, or higher surgical risk, who are prone to complications after surgery, CEA is preferred when both CAS and CEA are options.

CONCLUSION

Ultrasound-guided CAS is technically a feasible procedure. However, due to the few patients who have been treated in this way, the limited treatment experience, and the lack of recognized indications, the long-term efficacy needs further observation, and more cases are needed to confirm the outcomes. We believe that with further improvement of this technique, careful selection of patients, and appropriate preoperative evaluation, ultrasound-guided endovascular therapy will benefit more patients with contraindications to iodinated contrast agents and will become a viable option in

the future.

FOOTNOTES

Author contributions: Li L and Wang ZY contributed equally to this work; Li L, Wang ZY and Liu B contributed to manuscript writing and editing, and data collection; Liu B contributed to conceptualization and supervision; all authors have read and approved the final manuscript.

Supported by the Foundation of the Longhua District Health System Project Cooperation 2022 (basic and clinical research in ischemic stroke).

Informed consent statement: Informed written consent was obtained from the patient for publication of this case report and accompanying images.

Conflict-of-interest statement: All the authors have declared that no competing interests exist.

CARE Checklist (2016) statement: The authors have read the CARE Checklist (2016), and the manuscript was prepared and revised according to the CARE Checklist (2016).

Country/Territory of origin: China

ORCID number: Bo Liu 0000-0002-4398-0390.

S-Editor: Liu JH
L-Editor: A
P-Editor: Liu JH

REFERENCES

1 **North American Symptomatic Carotid Endarterectomy Trial Collaborators**, Barnett HJM, Taylor DW, Haynes RB, Sackett DL, Peerless SJ, Ferguson GG, Fox AJ, Rankin RN, Hachinski VC, Wiebers DO, Eliasziw M. Beneficial effect of carotid endarterectomy in symptomatic patients with high-grade carotid stenosis. *N Engl J Med* 1991; **325**: 445-453 [PMID: 1852179 DOI: 10.1056/nejm199108153250701]

2 MRC European Carotid Surgery Trial: interim results for symptomatic patients with severe (70-99%) or with mild (0-29%) carotid stenosis. European Carotid Surgery Trialists' Collaborative Group. *Lancet* 1991; **337**: 1235-1243 [PMID: 1674060]

3 **Espinola-Klein C**. [ESC guidelines 2017 on peripheral arterial diseases: Summary of the most important recommendations and innovations]. *Herz* 2017; **42**: 721-727 [PMID: 29143147 DOI: 10.1007/s00059-017-4638-2]

4 **Bahati KLF**, Guan S, Tang JRK, Ge XH. Meta-analysis of the efficacy and safety of carotid endarterectomy and carotid stenting in the treatment of carotid artery stenosis. *Chinese Journal of Bases and Clinics in General Surgery* 2016; **23**: 676-681 [DOI: 10.7507/1007-9424.20160181]

5 **Spinosa DJ**, Kaufmann JA, Hartwell GD. Gadolinium chelates in angiography and interventional radiology: a useful alternative to iodinated contrast media for angiography. *Radiology* 2002; **223**: 319-25; discussion 326 [PMID: 11997531 DOI: 10.1148/radiol.2232010742]

6 **Wagner HJ**, Kalinowski M, Klose KJ, Alfke H. The use of gadolinium chelates for X-ray digital subtraction angiography. *Invest Radiol* 2001; **36**: 257-265 [PMID: 11323513 DOI: 10.1097/00004424-200105000-00003]

7 **Bridges MD**, St Amant BS, McNeil RB, Cernigliaro JG, Dwyer JP, Fitzpatrick PM. High-dose gadodiamide for catheter angiography and CT in patients with varying degrees of renal insufficiency: Prevalence of subsequent nephrogenic systemic fibrosis and decline in renal function. *AJR Am J Roentgenol* 2009; **192**: 1538-1543 [PMID: 19457816 DOI: 10.2214/AJR.07.3895]

8 **Henes FO**, Groth M, Begemann PG, Adam G, Regier M. Intraindividual comparison of gadolinium- and iodine-enhanced 64-slice multidetector CT pulmonary angiography for the detection of pulmonary embolism in a porcine model. *Emerg Radiol* 2011; **18**: 189-195 [PMID: 21136130 DOI: 10.1007/s10140-010-0926-3]

9 **Carrascosa P**, Merletti PG, Capuñay C, Goldsmit A, Bettinotti M, Carrascosa J. New approach to noninvasive coronary angiography by multidetector computed tomography: initial experience using gadolinium. *J Comput Assist Tomogr* 2007; **31**: 441-443 [PMID: 17538293 DOI: 10.1097/01.rct.0000250113.64714.7d]

10 **Kinno Y**, Odagiri K, Andoh K, Itoh Y, Tarao K. Gadopentetate dimeglumine as an alternative contrast material for use in angiography. *AJR Am J Roentgenol* 1993; **160**: 1293-1294 [PMID: 8388622 DOI: 10.2214/ajr.160.6.8388622]

11 **Yaganti V**, Alani F, Yaganti S, Goldberg S, McCormick D. Use of gadolinium for carotid artery angiography and stenting in patients with renal insufficiency. *J Ren Care* 2009; **35**: 211-218 [PMID: 19909415 DOI: 10.1111/j.1755-6686.2009.00120.x]

12 **Sakamoto S**, Eguchi K, Shibukawa M, Kiura Y, Yamasaki F, Kajiwara Y, Matsushige T, Kurisu K. Cerebral angiography using gadolinium as an alternative contrast medium in a patient with severe allergy to iodinated contrast medium. *Hiroshima J Med Sci* 2010; **59**: 15-16 [PMID: 20518256]

13 **Kane GC**, Stanson AW, Kalnicka D, Rosenthal DW, Lee CU, Textor SC, Garovic VD. Comparison between gadolinium and iodine contrast

for percutaneous intervention in atherosclerotic renal artery stenosis: clinical outcomes. *Nephrol Dial Transplant* 2008; **23**: 1233-1240 [PMID: 18256017 DOI: 10.1093/ndt/gfm725]

14 **Saleh L**, Juneman E, Movahed MR. The use of gadolinium in patients with contrast allergy or renal failure requiring coronary angiography, coronary intervention, or vascular procedure. *Catheter Cardiovasc Interv* 2011; **78**: 747-754 [PMID: 21780275 DOI: 10.1002/ccd.22907]

15 **Rostambeigi N**, Khatri R, Hassan AE, Qureshi AI. Duplex ultrasound assisted endovascular revascularization of chronic internal carotid artery occlusion: technical note. *J Vasc Interv Neurol* 2013; **6**: 42-46 [PMID: 24358416]

16 **Lu XY**, Zhang L, Chen B, Li QY, Qian XQ, Lu PS. Ultrasound assisted endovascular revascularization of chronic internal carotid artery occlusion:two cases report and literature review. *Zhonghua Shenjing Yixue Zazhi* 2017; **16:** 1294-1296.
Available from: https://d.wanfangdata.com.cn/periodical/ChlQZXJpb2RpY2FsQ0hJTmV3UzIwMjMwNDI2EhF6aHNqeXh6ejIwMTcxMjAyMRoIejZxYjJxZ3k%3D

World Journal of Clinical Cases

Submit a Manuscript: https://www.f6publishing.com

World J Clin Cases 2023 September 6; 11(25): 5934-5940

DOI: 10.12998/wjcc.v11.i25.5934

ISSN 2307-8960 (online)

CASE REPORT

Parathyroid carcinoma: Three case reports

Ce Shi, Ning Lu, Yan-Jie Yong, Hai-Di Chu, Ai-Jun Xia

Specialty type: Medicine, research and experimental

Provenance and peer review: Unsolicited article; Externally peer reviewed.

Peer-review model: Single blind

Peer-review report's scientific quality classification

Grade A (Excellent): 0
Grade B (Very good): B
Grade C (Good): C
Grade D (Fair): D
Grade E (Poor): 0

P-Reviewer: Cigrovski Berkovic M, Croatia; Corvino A, Italy; Pappachan JM, United Kingdom

Received: April 12, 2023
Peer-review started: April 12, 2023
First decision: July 3, 2023
Revised: July 14, 2023
Accepted: August 1, 2023
Article in press: August 1, 2023
Published online: September 6, 2023

Ce Shi, Yan-Jie Yong, Ai-Jun Xia, Department of Ultrasound, Yantaishan Hospital, Yantai 264003, Shandong Province, China

Ning Lu, Department of Pathology, Yantaishan Hospital, Yantai 264003, Shandong Province, China

Hai-Di Chu, Department of Thyroid Surgery, Yantaishan Hospital, Yantai 264003, Shandong Province, China

Corresponding author: Ai-Jun Xia, MD, Chief Doctor, Department of Ultrasound, Yantaishan Hospital, No. 10087 Kejidadao Road, Yantai 264003, Shandong Province, China.
xiaaijun1964@sina.com

Abstract

BACKGROUND

Parathyroid carcinoma (PC) is a rare, slow-growing malignant tumor and a rare cause of primary hyperfunctioning of the parathyroid, with a highly variable clinical course, depending on the aggressiveness of the individual tumor and the degree of hypercalcemia.

CASE SUMMARY

The aim of this report is to summarize the diagnosis and treatment of three cases of PC and to review and conclude aspects regarding the three collected cases with reference to other relevant cases to explore the value of ultrasound in the diagnosis of PC. All three patients had hypercalcemia, consisting of a high serum calcium level and a high level of parathyroid hormone that was > 2-fold (even > 30-fold) of the normal upper limit. The ultrasonographic findings of the parathyroid gland showed that the glands were all > 30 mm, and the internal echo was uneven. All patients underwent surgery. PC in three cases was confirmed by routine histopathology and immunohistochemistry.

CONCLUSION

As clinical signs and laboratory results are nonspecific, it is difficult to diagnose PC preoperatively, so imaging examinations are often needed.

Key Words: Parathyroid carcinoma; Parathyroid adenoma; Ultrasound; Parathyroid hormone; Primary parathyroid hyperfunction; Case report

Core tip: Parathyroid carcinoma (PC) is a rare malignant tumor with a highly variable clinical course, depending on the aggressiveness of the individual tumor and the degree of hypercalcemia. As clinical signs and laboratory results are nonspecific, it is difficult to diagnose PC before surgery, so relevant imaging examinations are often needed. The aim of this report is to summarize the diagnosis and treatment of three cases of PC and to review and conclude aspects regarding the three collected cases with reference to other relevant cases to explore the value of ultrasound in the diagnosis of PC.

Citation: Shi C, Lu N, Yong YJ, Chu HD, Xia AJ. Parathyroid carcinoma: Three case reports. *World J Clin Cases* 2023; 11(25): 5934-5940
URL: https://www.wjgnet.com/2307-8960/full/v11/i25/5934.htm
DOI: https://dx.doi.org/10.12998/wjcc.v11.i25.5934

INTRODUCTION

Parathyroid carcinoma (PC) is a rare endocrine carcinoma that accounts for approximately 0.005% of all cancers and has an annual incidence of < 0.001%[1-4]. The main clinical features are hypersecretion of parathyroid hormone (PTH) and high serum calcium. PC has no clear diagnostic criteria, lacks specific manifestations, and is difficult to distinguish from parathyroid adenoma (PA) or hyperplasia. PC should be highly suspected if the serum calcium level exceeds 3.5 mmol/L, PTH exceeds 2-5 times the upper limit of normal, or the tumor touches the neck or is accompanied by vocal cord paralysis, or bone, kidney or other related manifestations[5]. In this study, ultrasound images of three patients with pathologically confirmed PC are summarized, and related literature was reviewed to explore the value of ultrasound in the diagnosis of PC.

CASE PRESENTATION

Chief complaints

Case 1: A 59-year-old man had a neck mass detected 10 d previously.

Case 2: A 28-year-old woman presented with weakness in the left lower limb.

Case 3: A 65-year-old woman presented with a neck mass that was noticed 6 mo previously and that had recently gradually increased in size.

History of present illness

Case 1: No tenderness was observed.

History of past illness

Case 1: Blood sugar control was satisfactory, and the patient had a history of diabetes for > 3 years.

Case 2: The patient had a 3-year history of kidney stones and presented with lumbago with pain.

Case 3: None.

Laboratory examinations

Case 1: Serum calcium level was 2.78 mmol/L (normal range 2.11-2.52 mmol/L), and PTH was 207.6 pg/mL (normal range 12.3-88.3 pg/mL).

Case 2: Serum calcium was 3.47 mmol/L, and PTH was 2723 pg/mL.

Case 3: Serum calcium was 3.19 mmol/L, and PTH was 1388 pg/mL.

Imaging examinations

Case 1: Doppler ultrasound revealed a 3.9 cm × 3.5 cm × 2 cm regularly shaped complex nodule (with mixed echogenicity); that is, with solid and fluid components at the lower pole of the thyroid on the right side. The boundary between the nodule and the thyroid parenchyma was unclear (Figure 1A). Color doppler flow imaging (CDFI) indicated multiple blood flow signals in the internal solid part and around the nodule (Figure 1B). Computed tomography (CT) displayed circular shadow density at the lower pole of the right thyroid gland with a clear boundary. Mild-to-moderate enhancement was observed around the lesion, but no obvious enhancement was detected inside the lesion.

Case 2: Doppler ultrasound revealed a 5.4 cm × 4.4 cm × 2.8 cm regularly shaped solid nodule with small internal cystic foci in the lower right lobe of the thyroid gland. The nodule had a clear boundary (Figure 2A). CDFI revealed multiple blood flow signals in the solid part of the nodule (Figure 2B).

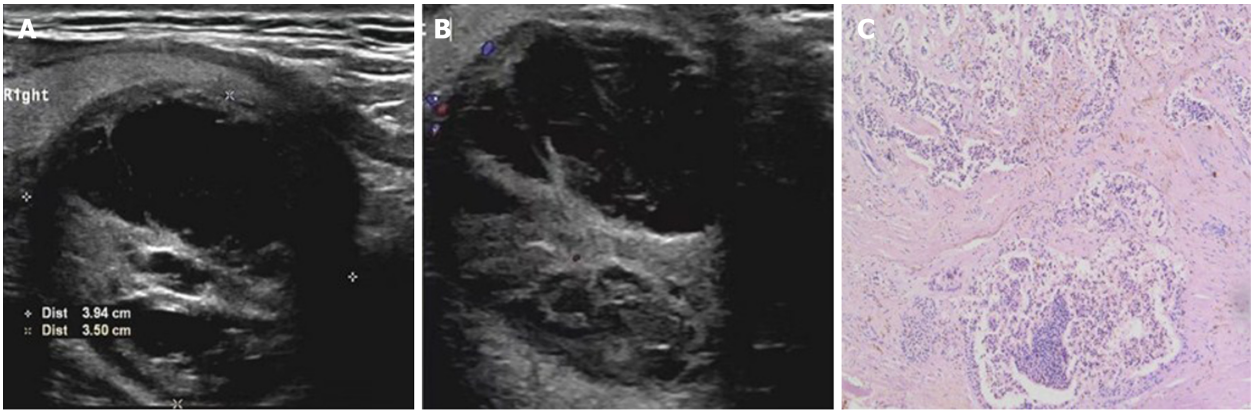

DOI: 10.12998/wjcc.v11.i25.5934 **Copyright** ©The Author(s) 2023.

Figure 1 Parathyroid carcinoma of the lower pole of the thyroid on the right side in a 59-year-old man. A: Doppler ultrasound revealed a complex nodule (with mixed echogenicity), *i.e.*, with solid and fluid components; B: Color doppler flow imaging indicated punctate blood flow signals were detected in the solid part of the nodule and its periphery; C: The neoplastic chief cells of the parathyroid glands were arranged in solid sheets, nests and acini, indicating diffuse infiltrative growth.

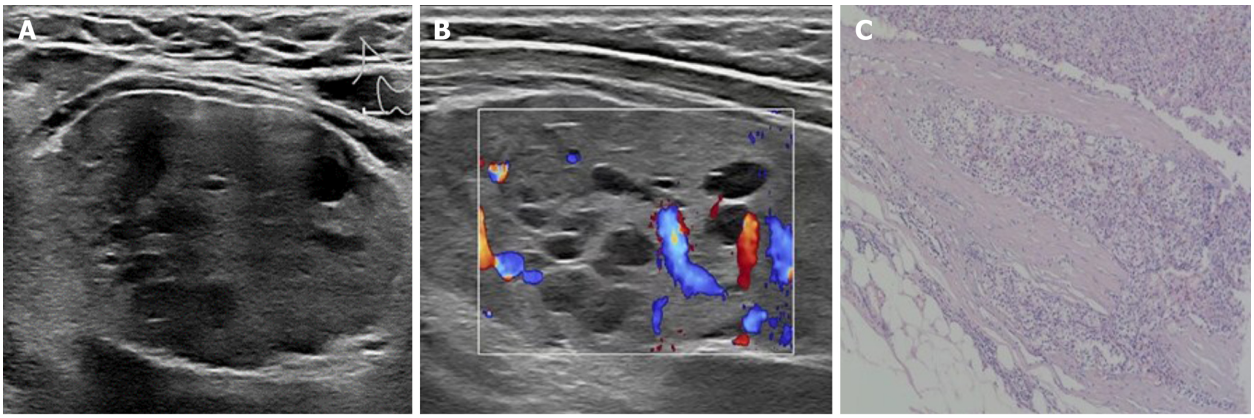

DOI: 10.12998/wjcc.v11.i25.5934 **Copyright** ©The Author(s) 2023.

Figure 2 Parathyroid adenocarcinoma of the lower right lobe of the thyroid gland in a 28-year-old woman. A: Doppler ultrasound revealed a solid nodule with small internal cystic foci; B: Color doppler flow imaging indicated multiple streaks of blood flow signals were observed in the solid part of the nodule; C: Parathyroid chief cells with neoplastic hyperplasia; some of the tumor cells were atypical, and the tumor capsule was of different thicknesses with focal capsule invasion.

Case 3: Doppler ultrasound revealed a 3.2 cm × 2.6 cm × 2.4 cm, irregularly shaped, solid nodule with an inhomogeneous echo-structure at the lower right lobe of the thyroid gland. The boundary was unclear, and the internal echo was uneven (Figure 3A). CDFI indicated multiple blood flow signals within the nodule (Figure 3B). Several lymph nodes were detected on the right side of the neck; the larger lymph node was 1.3 cm × 0.5 cm, with poorly defined boundaries and no tenderness. A CT scan revealed an oval low-density lesion with a clear boundary in the middle and lower lobes of the right thyroid gland.

Intraoperative findings and immunohistochemistry

Case 1: A 3.5 cm × 3.0 cm × 2 cm mass was observed under the right thyroid gland, which was closely associated with the surrounding tissues. The mass surface was smooth, and the envelope was complete with a variable thickness. The section was a solid cyst. The cystic part was multilocular, the inner wall of the sac was smooth, and the solid part was grayish-red, soft and brittle. The parathyroid neoplastic master cells were arranged in a solid flaky-like, nest-like, acinar pattern with diffuse infiltrating growth that invaded a nerve and locally infiltrated but did not penetrate the capsule. A small amount of thyroid tissue was seen in the tumor margin focus (Figure 1C). Immunohistochemistry revealed PTH (+), calcitonin (-), carcinoembryonic antigen (-), chromogranin A (CgA) (+), synaptophysin (Syn) (-), thyroid transcription factor-1 (TTF-1) (-), thyroglobulin (Tg) (-) and Ki67 (1%).

Case 2: An enlarged parathyroid gland (6 cm × 4 cm × 3 cm) was observed below the right thyroid gland during the operation. The general surface of the nodule was smooth, the capsule was intact, and the section surface was dark red, multinodular and soft. The main cells of the parathyroid gland were neoplastic and hyperplastic, and coarse fiber segmentation was seen in the tumor. Some tumor cells were atypical, with mitotic images of approximately 2/50 per

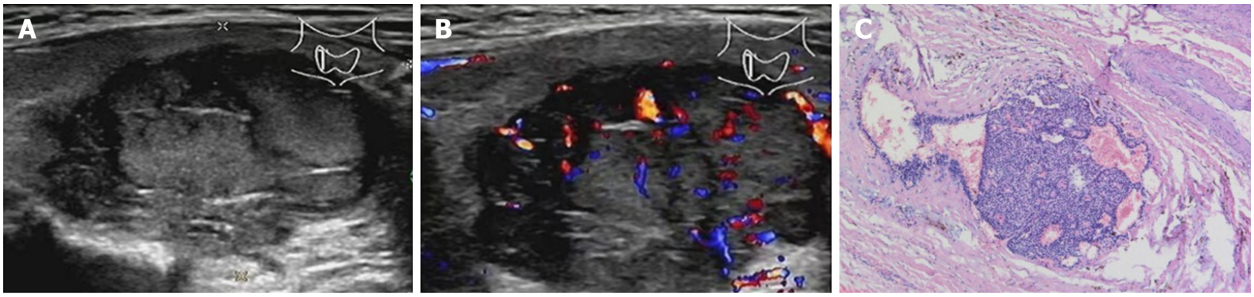

DOI: 10.12998/wjcc.v11.i25.5934 **Copyright** ©The Author(s) 2023.

Figure 3 Parathyroid adenocarcinoma of the lower right lobe of the thyroid gland in a 65-year-old woman. A: Doppler ultrasound revealed a solid nodule with an inhomogeneous echostructure; B: Color doppler flow imaging indicated multiple spots and strips of blood flow signals were observed in the nodules; C: Parathyroid tumor with an unclear local capsule. A vascular tumor thrombus can be seen.

high-power field (HPF). The tumor envelope was of different thicknesses, and the tumor had invaded the envelope. The blood vessels had invaded the thyroid, and a tumor plug was seen in the blood vessels (Figure 2C). Immunohistochemistry revealed PTH (+) and Ki67 (4%).

Case 3: A 3.4 cm × 2.4 cm × 2.2 cm mass was found at the lower pole of the right thyroid gland, which had adhered to the surrounding esophageal and recurrent laryngeal nerves. The general surface was smooth, the envelope was relatively complete, and the section surface was grayish-brown, soft and slightly brittle. The local envelope of the tumor was not obvious, there were visible mitoses (< 2/10 HPF), and the tumor had invaded the thyroid tissue (Figure 3C). Immunohistochemistry revealed PTH (+), calcitonin (-), cytokeratin pan (+), cytokeratin19 (+), CgA (+), neural cell adhesion molecule (NCAM; CD56) (-), Syn (weak +), TTF-1 (-), Tg (-) and Ki67 (5%).

FINAL DIAGNOSIS

Case 1: The patient was pathologically diagnosed with highly differentiated PC (low grade).

Case 2: The pathological diagnosis was parathyroid adenocarcinoma.

Case 3: The lesion was pathologically diagnosed as parathyroid adenocarcinoma.

TREATMENT

Case 1: The right inferior pole of the parathyroid and the right thyroid were resected.

Case 2: The right parathyroid lesion was resected.

Case 3: The right parathyroid gland was explored, the right parathyroid lesion, the right thyroid and the isthmus were resected, and a regional lymphadenectomy was performed.

OUTCOME AND FOLLOW-UP

Case 1: The 5-year follow-up did not show residual–recurrent disease.

Case 2: The 1-year follow-up did not show residual–recurrent disease.

Case 3: The 1-year follow-up did not show residual–recurrent disease.

DISCUSSION

PC is a rare, slow-growing malignant tumor and a rare cause of primary hyperfunctioning of the parathyroid (PHPT), with an incidence of 0.5%-7.0%[6,7]. Approximately 95% of PC tumors are functional and clinically manifested by various symptoms and signs caused by excessive secretion of PTH and hypercalcemia, including moderate to severe hypercalcemia (a parathyroid crisis may occur in some patients), kidney stones, renal calcinosis, osteoporosis, osteitis cystic fibrosis, brown tumors, fractures, constipation, abdominal pain, peptic ulcers and pancreatitis[8,9]. The PTH and serum calcium were increased in these three patients, and PTH was 2.35, 30.84 and 15.72 times the upper limit of normal,

respectively. Case 2 presented with osteoporosis and recurrent kidney stones. Cases 1 and 3 presented at the clinic for painless anterior neck masses. It has been reported that 30%-76% of patients with PC have a palpable mass in the neck [10], which is uncommon in patients with PA. PC is considered a slow-growing malignant tumor with a highly variable clinical course, depending on the aggressiveness of the individual tumor and the degree of hypercalcemia. As clinical signs and laboratory results are nonspecific, it is difficult to diagnose PC before surgery, so relevant imaging examinations are often needed.

A variety of techniques can be used to image the parathyroid gland, including ultrasound, methoxy isobutyl isonitrile (MIBI) imaging, CT and magnetic resonance imaging (MRI). Ultrasound is the first choice to accurately assess the size of a tumor without radiation and at a low cost and has significant value for detecting parathyroid disease. Studies have shown that ultrasound has a sensitivity of 67%-96% and a positive predictive value of 82%-98% in patients undergoing PHPT surgery[11-14]. The ultrasonographic findings of normal parathyroid glands are oval hypoechoic or hyperechoic nodules with a maximum diameter of 4-7 mm, clear boundaries and a uniform echo. PC is usually larger, lobulated, hypoechoic, heterogeneous and ill-defined compared with PA. A high positive predictive value is obtained when the parathyroid lesion is > 30 mm, calcified, and has an unclear boundary with the surrounding tissue[15,16]. In this group of three patients, the tumors were > 30 mm, and the internal echo was uneven. In cases 1 and 2, the tumors were cystic and solid, and in cases 1 and 3, the tumors had unclear boundaries with the surrounding tissue, which was consistent with malignant signs. However, ultrasound has some limitations. Parathyroid diseases can be difficult to distinguish from thyroid nodules and lymph nodes, so the clinical manifestations and a laboratory examination should be combined for identification. In addition, when the parathyroid lesion is cystic, it should be distinguished from other cystic neck lesions. For cystic neck lesions, close attention should be paid to the age of presentation, lesion location, and association with surrounding structures[17,18]. If located on the midline, the differential diagnosis narrows to thyroglossal duct cysts, ranulas or dermoid cysts. Off-midline lesions can be, instead, branchial cleft cysts or lymphangiomas[17]. Due to interference by the sternum and clavicle, ultrasound examination of hypolocated parathyroid tumors or ectopic parathyroid tumors in the retropharyngeal space or mediastinum is limited, so other imaging examinations are needed. Tc-99 m-MIBI is widely used to localize parathyroid tumors, but there is no significant specificity between benign and malignant parathyroid diseases. CT and MRI have limited diagnostic value in patients with parathyroid disease but can be used to assess cervical lymph node status, detect ectopic parathyroid tumors and assess preoperative risk[19].

There are some difficulties when preoperatively and intraoperatively diagnosing PC. Fine-needle aspiration can be used to distinguish thyroid from parathyroid tissues, but it has limited value in the differential diagnosis of benign and malignant parathyroid tumors and may cause local dissemination and implantation of tumors, so it is not recommended [20,21]. Because the histopathological features of PC may overlap with PA, an intraoperative rapid frozen pathological examination has been demonstrated to lack reliability. Therefore, postoperative pathological examination of the lesion is the gold standard for diagnosing PC. PC is pathologically diagnosed if the tumor is invasive, such as in the capsule, blood vessels or nerves, or has local or distant metastasis[22].

Surgical excision is an effective method to treat PC, and the standard of treatment is total excision of the tumor and surrounding tissues[20]. Selective cervical lymph node dissection is also necessary when the cervical lymph nodes are involved. However, the necessity of prophylactic septal lymphadenectomy remains controversial[23]. In this study, all three patients underwent surgical resection of the diseased parathyroid gland combined with resection of the affected thyroid gland. PC is an indolent, slowly progressive cancer since the tumor has a low malignant potential. Few patients initially present with regional lymph node involvement (< 5%) or with distant metastatic disease (< 2%)[24]. PC can recur 2-5 years after the initial operation, and the local recurrence rate within 5 years is 33%-82%[25]. The prognosis mainly depends on whether the tumor is completely removed during the first operation. Most patients do not die from the tumor disease burden since it is slow growing. Instead, most patients with metastatic disease die from complications of hypercalcemia[26,27]. Consequently, postoperative serum calcium and PTH monitoring are also important to detect whether the tumor was completely removed and whether there is early recurrence and metastasis. This especially applies to serum calcium levels, since most of these patients are highly susceptible to hungry bone syndrome. They require regular monitoring of their calcium and PTH levels every 3 mo for up to 1 year to evaluate for recurrence[28]. If the levels remain stable at this point, the duration between laboratory assessments can gradually be increased.

CONCLUSION

PC is a rare head and neck malignant tumor. Significant increases in serum calcium and PTH should be warning signs of a mass in the neck. The best surgical method should be selected to improve the survival rate of patients.

FOOTNOTES

Author contributions: Shi C and Lu N contributed to manuscript writing and editing, and data collection; Yong YJ contributed to data analysis; Chu HD did the surgical appraisal; Xia AJ contributed to conceptualization and supervision; All authors have read and approved the final manuscript.

Informed consent statement: Informed written consent was obtained from the patient and her parents for the publication of this report and any accompanying images.

Conflict-of-interest statement: All the authors report no relevant conflicts of interest for this article.

CARE Checklist (2016) statement: The authors have read the CARE Checklist (2016), and the manuscript was prepared and revised according to the CARE Checklist (2016).

Country/Territory of origin: China

ORCID number: Ce Shi 0000-0002-0218-0805; Ning Lu 0009-0001-3912-5455; Yan-Jie Yong 0000-0002-5506-4330; Hai-Di Chu 0009-0002-3547-5236; Ai-Jun Xia 0000-0002-9548-1585.

S-Editor: Qu XL
L-Editor: Kerr C
P-Editor: Zhang YL

REFERENCES

1 **Duan K**, Mete Ö. Parathyroid Carcinoma: Diagnosis and Clinical Implications. *Turk Patoloji Derg* 2015; **31** Suppl 1: 80-97 [PMID: 26177319 DOI: 10.5146/tjpath.2015.01316]
2 **Ozolins A**, Narbuts Z, Vanags A, Simtniece Z, Visnevska Z, Akca A, Wirowski D, Gardovskis J, Strumfa I, Goretzki PE. Evaluation of malignant parathyroid tumours in two European cohorts of patients with sporadic primary hyperparathyroidism. *Langenbecks Arch Surg* 2016; **401**: 943-951 [PMID: 26658808 DOI: 10.1007/s00423-015-1361-4]
3 **James BC**, Aschebrook-Kilfoy B, Cipriani N, Kaplan EL, Angelos P, Grogan RH. The Incidence and Survival of Rare Cancers of the Thyroid, Parathyroid, Adrenal, and Pancreas. *Ann Surg Oncol* 2016; **23**: 424-433 [PMID: 26467460 DOI: 10.1245/s10434-015-4901-9]
4 **Lee PK**, Jarosek SL, Virnig BA, Evasovich M, Tuttle TM. Trends in the incidence and treatment of parathyroid cancer in the United States. *Cancer* 2007; **109**: 1736-1741 [PMID: 17372919 DOI: 10.1002/cncr.22599]
5 **Agarwal S**, Kumar T, Sharma MC, Damle NA, Gandhi AK. Parathyroid carcinoma with contralateral subcutaneous and breast recurrences: A rare presentation. *Head Neck* 2016; **38**: E115-E118 [PMID: 26685878 DOI: 10.1002/hed.24317]
6 **Pelizzo MR**, Piotto A, Bergamasco A, Rubello D, Casara D. [Parathyroid carcinoma. Therapeutic strategies derived from 20 years of experience]. *Minerva Endocrinol* 2001; **26**: 23-29 [PMID: 11323564]
7 **Wermers RA**, Khosla S, Atkinson EJ, Achenbach SJ, Oberg AL, Grant CS, Melton LJ 3rd. Incidence of primary hyperparathyroidism in Rochester, Minnesota, 1993-2001: an update on the changing epidemiology of the disease. *J Bone Miner Res* 2006; **21**: 171-177 [PMID: 16355286 DOI: 10.1359/jbmr.050910]
8 **Rodriguez C**, Nadéri S, Hans C, Badoual C. Parathyroid carcinoma: a difficult histological diagnosis. *Eur Ann Otorhinolaryngol Head Neck Dis* 2012; **129**: 157-159 [PMID: 22480967 DOI: 10.1016/j.anorl.2012.01.002]
9 **Kim HK**, Oh YL, Kim SH, Lee DY, Kang HC, Lee JI, Jang HW, Hur KY, Kim JH, Min YK, Chung JH, Kim SW. Parafibromin immunohistochemical staining to differentiate parathyroid carcinoma from parathyroid adenoma. *Head Neck* 2012; **34**: 201-206 [PMID: 21717519 DOI: 10.1002/hed.21716]
10 **Shane E**. Clinical review 122: Parathyroid carcinoma. *J Clin Endocrinol Metab* 2001; **86**: 485-493 [PMID: 11157996 DOI: 10.1210/jcem.86.2.7207]
11 **Haber RS**, Kim CK, Inabnet WB. Ultrasonography for preoperative localization of enlarged parathyroid glands in primary hyperparathyroidism: comparison with (99m)technetium sestamibi scintigraphy. *Clin Endocrinol (Oxf)* 2002; **57**: 241-249 [PMID: 12153604 DOI: 10.1046/j.1365-2265.2002.01583.x]
12 **Whitson BA**, Broadie TA. Preoperative ultrasound and nuclear medicine studies improve the accuracy in localization of adenoma in hyperparathyroidism. *Surg Today* 2008; **38**: 222-226 [PMID: 18306995 DOI: 10.1007/s00595-007-3612-7]
13 **Ulanovski D**, Feinmesser R, Cohen M, Sulkes J, Dudkiewicz M, Shpitzer T. Preoperative evaluation of patients with parathyroid adenoma: role of high-resolution ultrasonography. *Head Neck* 2002; **24**: 1-5 [PMID: 11774396 DOI: 10.1002/hed.10043]
14 **Abboud B**, Sleilaty G, Rabaa L, Daher R, Abou Zeid H, Jabbour H, Hachem K, Smayra T. Ultrasonography: highly accuracy technique for preoperative localization of parathyroid adenoma. *Laryngoscope* 2008; **118**: 1574-1578 [PMID: 18475203 DOI: 10.1097/MLG.0b013e31817aecad]
15 **Sidhu PS**, Talat N, Patel P, Mulholland NJ, Schulte KM. Ultrasound features of malignancy in the preoperative diagnosis of parathyroid cancer: a retrospective analysis of parathyroid tumours larger than 15 mm. *Eur Radiol* 2011; **21**: 1865-1873 [PMID: 21556910 DOI: 10.1007/s00330-011-2141-3]
16 **Cetani F**, Pardi E, Marcocci C. Parathyroid Carcinoma. *Front Horm Res* 2019; **51**: 63-76 [PMID: 30641523 DOI: 10.1159/000491039]
17 **Corvino A**, Pignata S, Campanino MR, Corvino F, Giurazza F, Tafuri D, Pinto F, Catalano O. Thyroglossal duct cysts and site-specific differential diagnoses: imaging findings with emphasis on ultrasound assessment. *J Ultrasound* 2020; **23**: 139-149 [PMID: 32052384 DOI: 10.1007/s40477-020-00433-2]
18 **Wong KT**, Lee YY, King AD, Ahuja AT. Imaging of cystic or cyst-like neck masses. *Clin Radiol* 2008; **63**: 613-622 [PMID: 18455551 DOI: 10.1016/j.crad.2007.12.007]
19 **Mulla M**, Schulte KM. Central cervical lymph node metastases in papillary thyroid cancer: a systematic review of imaging-guided and prophylactic removal of the central compartment. *Clin Endocrinol (Oxf)* 2012; **76**: 131-136 [PMID: 21722150 DOI: 10.1111/j.1365-2265.2011.04162.x]

20 **Owen RP**, Silver CE, Pellitteri PK, Shaha AR, Devaney KO, Werner JA, Rinaldo A, Ferlito A. Parathyroid carcinoma: a review. *Head Neck* 2011; **33**: 429-436 [PMID: 20310041 DOI: 10.1002/hed.21376]

21 **Kassahun WT**, Jonas S. Focus on parathyroid carcinoma. *Int J Surg* 2011; **9**: 13-19 [PMID: 20887820 DOI: 10.1016/j.ijsu.2010.09.003]

22 **Schantz A**, Castleman B. Parathyroid carcinoma. A study of 70 cases. *Cancer* 1973; **31**: 600-605 [PMID: 4693587 DOI: 10.1002/1097-0142(197303)31:3<600::AID-CNCR2820310316>3.0.CO;2-0]

23 **Mohebati A**, Shaha AR. Anatomy of thyroid and parathyroid glands and neurovascular relations. *Clin Anat* 2012; **25**: 19-31 [PMID: 21800365 DOI: 10.1002/ca.21220]

24 **Schulte KM**, Talat N, Miell J, Moniz C, Sinha P, Diaz-Cano S. Lymph node involvement and surgical approach in parathyroid cancer. *World J Surg* 2010; **34**: 2611-2620 [PMID: 20640422 DOI: 10.1007/s00268-010-0722-y]

25 **Kebebew E**. Parathyroid carcinoma. *Curr Treat Options Oncol* 2001; **2**: 347-354 [PMID: 12057115 DOI: 10.1007/s11864-001-0028-2]

26 **Machado NN**, Wilhelm SM. Parathyroid Cancer: A Review. *Cancers (Basel)* 2019; **11** [PMID: 31661917 DOI: 10.3390/cancers11111676]

27 **Salcuni AS**, Cetani F, Guarnieri V, Nicastro V, Romagnoli E, de Martino D, Scillitani A, Cole DEC. Parathyroid carcinoma. *Best Pract Res Clin Endocrinol Metab* 2018; **32**: 877-889 [PMID: 30551989 DOI: 10.1016/j.beem.2018.11.002]

28 **Givi B**, Shah JP. Parathyroid carcinoma. *Clin Oncol (R Coll Radiol)* 2010; **22**: 498-507 [PMID: 20510594 DOI: 10.1016/j.clon.2010.04.007]

World Journal of Clinical Cases

Submit a Manuscript: https://www.f6publishing.com

World J Clin Cases 2023 September 6; 11(25): 5941-5946

DOI: 10.12998/wjcc.v11.i25.5941

ISSN 2307-8960 (online)

CASE REPORT

Median neuropathy after multiple punctures of the forearm for catheterization: A case report

Tomoaki Suzuki, Yuichiro Matsui, Daisuke Momma, Takeshi Endo, Norimasa Iwasaki

Specialty type: Medicine, research and experimental

Provenance and peer review: Unsolicited article; Externally peer reviewed.

Peer-review model: Single blind

Peer-review report's scientific quality classification

Grade A (Excellent): 0
Grade B (Very good): 0
Grade C (Good): C, C
Grade D (Fair): 0
Grade E (Poor): 0

P-Reviewer: Bernardes A, Portugal; Papazafiropoulou A, Greece

Received: May 2, 2023
Peer-review started: May 2, 2023
First decision: July 3, 2023
Revised: July 14, 2023
Accepted: August 9, 2023
Article in press: August 9, 2023
Published online: September 6, 2023

Tomoaki Suzuki, Yuichiro Matsui, Takeshi Endo, Norimasa Iwasaki, Department of Orthopaedic Surgery, Faculty of Medicine and Graduate School of Medicine, Hokkaido University, Sapporo 060-8638, Japan

Yuichiro Matsui, Section for Clinical Education, Faculty of Dental Medicine, Hokkaido University, Sapporo 060-8586, Japan

Daisuke Momma, Center for Sports Medicine, Hokkaido University, Sapporo 060-8638, Japan

Corresponding author: Tomoaki Suzuki, MD, PhD, Doctor, Department of Orthopaedic Surgery, Faculty of Medicine and Graduate School of Medicine, Hokkaido University, No. 15 Kita, No. 7 Nishi, Kita-ku, Sapporo 060-8638, Japan. gmtm32@gmail.com

Abstract

BACKGROUND

Neuropathy may occur at some sites after catheterization for close examination of cardiac disease. Although the radial artery is considered a relatively uncomplicated site for catheterization, the radial artery and median nerve are in relatively close proximity, with the risk of median nerve injury depending on the angle of puncture. The purpose of this study was to report the outcomes of surgery performed for conservative therapy-resistant median neuropathy following forearm catheterization.

CASE SUMMARY

A 50-year-old woman experienced palsy from the right thumb to the radial side of the ring finger after catheterization from the radial artery of the right forearm. Paresthesia developed at the same site and a positive tinel-like sign was seen for the median nerve area at the high level of the puncture site. Nerve conduction study showed reduced compound muscle action potentials and loss of sensory nerve action potentials. Symptoms did not improve despite pharmacotherapy and the patient gradually developed flexion restrictions of the index and middle fingers. Median nerve injury and associated flexor tendon adhesion was diagnosed, and the patient was referred for surgery at 3 mo after injury. When the same area was opened, no injury to the median nerve epithelium was obvious, but the area of the positive tinel-like sign was highly adherent to surrounding tissue and to the flexor digitorum superficialis of the index and middle fingers. The surgery was terminated with adequate adhesion release. Rehabilitation was initiated postoperatively, improving neurological symptoms and range of motion of the fingers. Six months after surgery, the patient returned to daily activities

without discomfort.

CONCLUSION
This case provides the appropriate diagnosis and treatment for a suspected peripheral nerve injury.

Key Words: Catheterization; Median neuropathy; Surgical treatment; Case report

Core Tip: Median neuropathy during forearm puncture is unlikely but possible given the anatomic location. In general, peripheral neuropathy of the upper extremity causes difficulty in performing hand-operated tasks and daily living, leading to a decreased quality of life, so surgery is aggressively considered in cases that are resistant to conservative treatment. Even in examinations where the risk of complications is considered low, accurate diagnosis based on clinical symptoms is important to provide appropriate treatment.

Citation: Suzuki T, Matsui Y, Momma D, Endo T, Iwasaki N. Median neuropathy after multiple punctures of the forearm for catheterization: A case report. *World J Clin Cases* 2023; 11(25): 5941-5946
URL: https://www.wjgnet.com/2307-8960/full/v11/i25/5941.htm
DOI: https://dx.doi.org/10.12998/wjcc.v11.i25.5941

INTRODUCTION

The radial artery is the most common site for arterial catheters, and radial artery catheters are considered relatively safe. The incidence of serious complications of radial artery catheterization is less than 0.2%[1]. One potential complication is nerve injury[2], most often in the form of median neuropathy at the forearm level. Median nerve injury related to radial artery catheterization has been reported to be caused by prolonged dorsiflexion of the wrist joint[3] and increased intra-carpal pressure due to hematoma formation[4,5], but the possibility of direct injury cannot be ruled out. We report a case of median nerve injury diagnosed and operated on after radial artery catheterization.

CASE PRESENTATION

Chief complaints

A 50-year-old woman underwent coronary angiography from the radial artery of the right forearm. When the artery was punctured with a 22-G needle, the patient reported a burning sensation in the right hand, and multiple punctures were made without injecting any drug. Coronary artery bypass grafting was performed the same day under a diagnosis of unstable angina pectoris.

History of present illness

After the patient noticed a burning sensation in the right hand during the initial forearm puncture, anesthesia was induced in emergency surgery. After waking from anesthesia, she perceived paresthesia from the thumb to the radial side of the ring finger and difficulty moving the right hand. Medical treatment with drugs was started but obtained little improvement in symptoms, and the difficulty in bending the index finger gradually worsened.

History of past illness

Unstable angina pectoris.

Personal and family history

Non-contributory.

Physical examination

There was decreased perception of the phalanx and from the thumb to radial side of the ring finger as compared to the other side. Manual muscle testing of the abductor pollicis brevis (APB) had dropped to 4. Range of motion of the wrist joint was preserved, but flexion of the metacarpophalangeal and proximal interphalangeal joints of the index and middle fingers was limited (Figure 1), and a complete O could not be made. A positive tinel-like sign was seen for the two proximal lateral digits from the wrist crease and negative at the carpal tunnel. In peripheral nerve conduction studies (NCS), motor and sensory latencies at the wrists did not differ between left and right. Compound muscle action potential (CMAP) of the APB was reduced and no waveform was recorded for sensory nerve action potential (SNAP) of the right

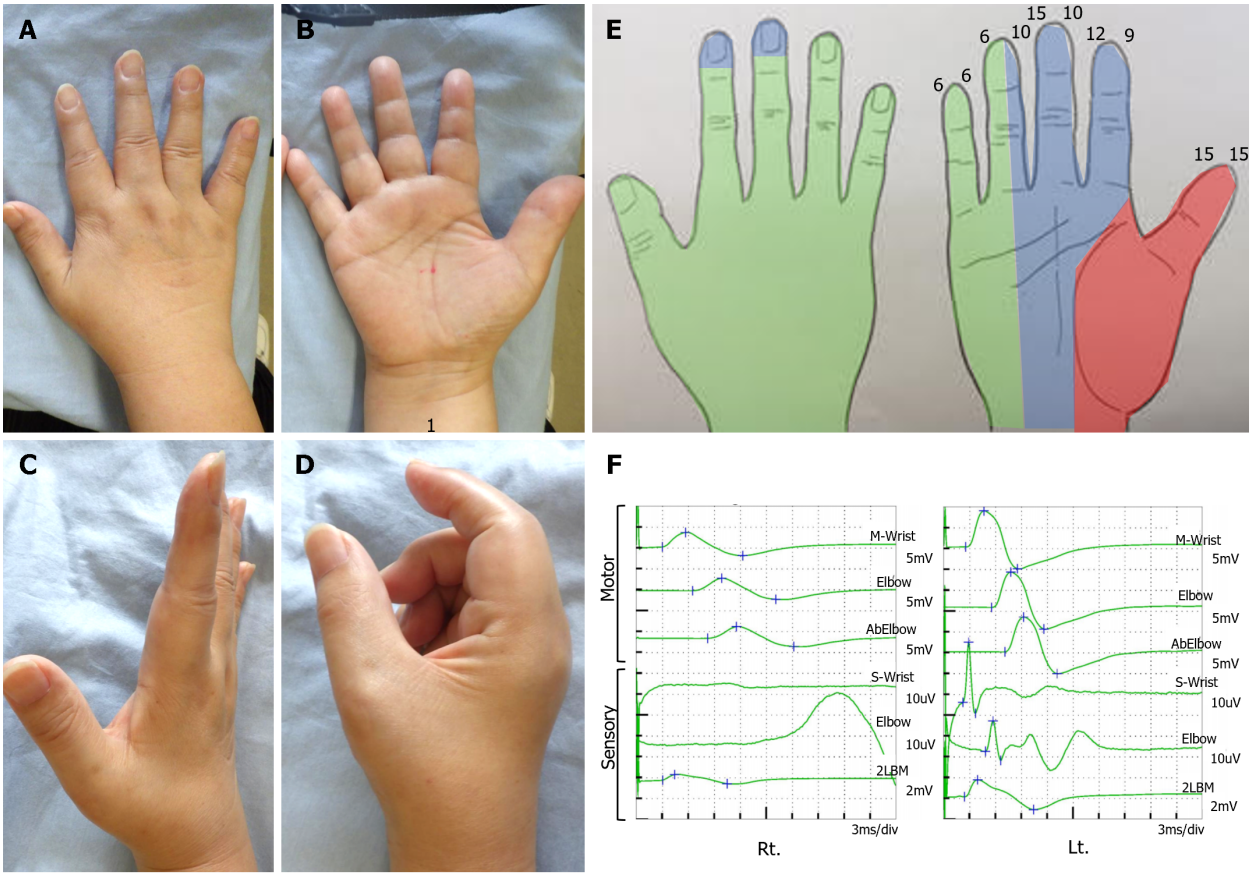

DOI: 10.12998/wjcc.v11.i25.5941

Figure 1 Preoperative physical examination. A and B: Inspection of the right hand. The Tinel like sign was positive at the 2 proximal lateral digits from the wrist crease (1); C: Finger extension. Allowable without restriction; D: Finger flexion. Restriction of the index and middle fingers prevents full grip; E: Right hand perception. Numbers represent two-point discrimination test, colors represent semmes weinstein test results. There is a decreased perception in the median nerve area; F: Nerve conduction studies results of the median nerve. Compound muscle action potential was reduced and sensory nerve action potential showed no waveform appearance.

second finger (Figure 1). Ultrasonography and magnetic resonance imaging did not show any median nerve swelling or hematoma formation.

Laboratory examinations

No special abnormal findings.

Imaging examinations

No special abnormal findings.

FINAL DIAGNOSIS

The patient was finally diagnosed with median nerve injury and flexor digitorum superficialis (FDS) adhesion of the index and middle fingers.

TREATMENT

Three months of conservative treatment with medication failed to improve the condition, so surgery was performed.

A skin incision was made from the proximal median of the palm to the distal median forearm. The median nerve was dissected circumferentially at the proximal level of the second transverse digit of the wrist crease, with erythema of the epineurium and adhesions to fatty tissue and tendons (palmaris longus and FDS for the second and third digits). The carpal tunnel was also released. The wound was closed under microscopy to ensure that there was no obvious injury or defect in the epineural membrane (Figure 2). No external fixation was performed and rehabilitation for hand exercises and prevention of adhesions was started on the third postoperative day.

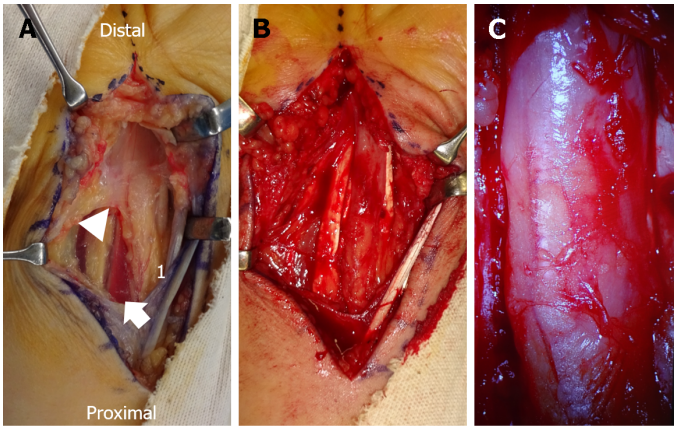

DOI: 10.12998/wjcc.v11.i25.5941 **Copyright** ©The Author(s) 2023.

Figure 2 Intraoperative photographs. A: The median nerve (1) is adherent to a fatty tissue (white arrow head) and flexor digitorum superficialis (FDS) for the second digit (white arrow); B: The median nerve was dissected circumferentially, and FDS muscle belly was resected; C: Microscopic findings. There was mild erythema of the neuroepithelium, but no obvious injury or defect.

OUTCOME AND FOLLOW-UP

Improvement of palsy was observed from the day after surgery. Hand movement improved gradually, with full grip possible 2 wk after surgery. The NCS waveform of SNAP (3.3 μV), which could not be confirmed preoperatively, was confirmed at 3 mo postoperatively (Figure 3). By 6 mo postoperatively, decreased perception was localized only to the phalanges of the index and middle fingers and disability of arm, shoulder and hand score had improved from 62.1 preoperatively to 15.5.

DISCUSSION

A detailed history and thorough clinical examination are the foundations of diagnosing nerve injuries. Electrodiagnostic studies are also commonly performed as an aid to diagnosis. This modality provides important information for identifying the site of compression and neuropathy, determining severity and prognosis, and allowing the identification of relevant phenomena such as denervation, reinnervation, abnormal reinnervation, and motor plate lesions[6,7]. In nerve palsy, stimulation of the nerve proximal to the lesion with distal recording results in loss of CMAP amplitude, partial or complete conduction block, and reduced conduction velocity across the lesion. SNAP is also lost or reduced in amplitude with proximal stimulation, with a 50%-70% reduction in amplitude suggesting conduction block[8]. These changes show complete or partial resolution once remyelination has been completed[9]. The present case showed reduced CMAP amplitude and loss of SNAP, suggesting conduction block due to axonal injury or nerve adhesions. Intraoperative findings were anatomically consistent with the predominance of dysesthesia in this case, since the sensory fibers in the distal forearm run mainly on the radial side of the median nerve[10,11].

Several peripheral neuropathies have been associated with vascular punctures related to venipuncture, with frequencies below 0.0001%[12-15]. Of particular significance is that half of the nerve injuries related to venipuncture improved within 5 wk, and all injuries improved within 18 wk[12]. The lack of spontaneous improvement in this case may have been related to the size of the puncture needle and the surface area of the injured nerve. External denervation has been reported to be effective for peripheral nerve injuries resistant to conservative therapy[16-18], and the same principle was applied in this case. The preoperative findings led to a diagnosis of median nerve injury, and the median nerve did in fact show marked adhesions at the site of the positive tinel-like sign. The coexisting flexion limitations of the index and middle fingers in this patient also completely resolved with adhesion release and postoperative rehabilitation. As of 6 mo postoperatively, neurological symptoms remained mild, but the patient had full use of the hand without any problems in daily life, much to her satisfaction.

CONCLUSION

This case provides insights into the appropriate diagnosis and treatment of suspected peripheral nerve injury. A thorough understanding of the nerve, tendon, and vascular anatomies is important and aggressive performance of surgery may be warranted for neuropathies that prove resistant to conservative therapy.

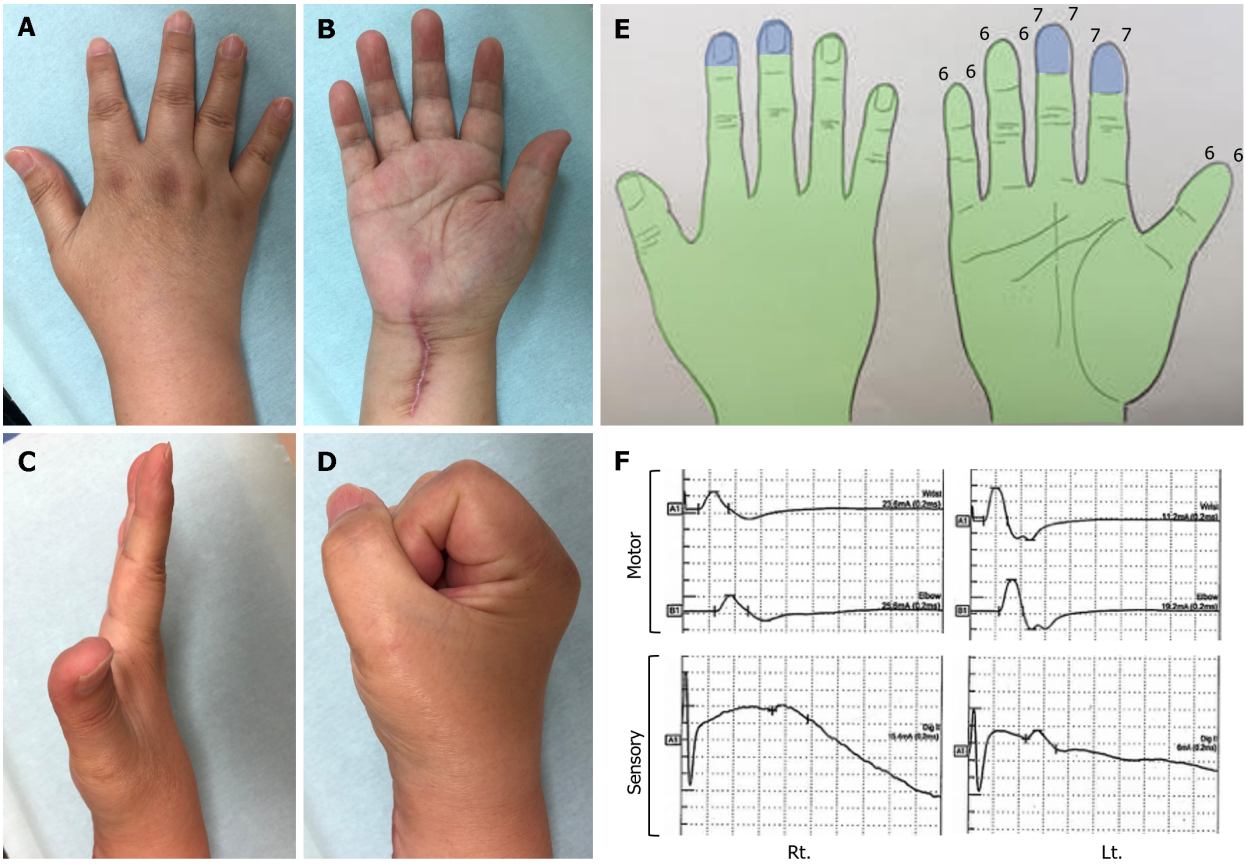

DOI: 10.12998/wjcc.v11.i25.5941

Figure 3 Postoperative physical examination. A and B: Inspection of the right hand. An operation scar is present on the proximal median of the palm to the distal median of the forearm; C: Finger extension. Allowable without restriction; D: Finger flexion. Full grip is available; E: Decreased perception is localized to the phalanges of the index and middle fingers; F: Nerve conduction studies results of the median nerve at 6 mo postoperatively. The waveform of sensory nerve action potential can be confirmed.

FOOTNOTES

Author contributions: Suzuki T was involved in gaining ethical approval, patient recruitment and data analysis; Matsui Y, Momma D and Endo T contributed to editing and conceptualization; Iwasaki N contributed to supervision; All authors have read and approved the final manuscript.

Informed consent statement: Informed written consent was obtained from the patient and her parents for the publication of this report and any accompanying images.

Conflict-of-interest statement: All the authors report no relevant conflicts of interest for this article.

CARE Checklist (2016) statement: The authors have read the CARE Checklist (2016), and the manuscript was prepared and revised according to the CARE Checklist (2016).

Country/Territory of origin: Japan

ORCID number: Tomoaki Suzuki 0000-0001-6552-0515.

S-Editor: Qu XL
L-Editor: A
P-Editor: Chen YX

REFERENCES

1 **Wallach SG**. Cannulation injury of the radial artery: diagnosis and treatment algorithm. *Am J Crit Care* 2004; **13**: 315-319 [PMID: 15293584]
2 **Brzezinski M**, Luisetti T, London MJ. Radial artery cannulation: a comprehensive review of recent anatomic and physiologic investigations. *Anesth Analg* 2009; **109**: 1763-1781 [PMID: 19923502 DOI: 10.1213/ANE.0b013e3181bbd416]
3 **Chowet AL**, Lopez JR, Brock-Utne JG, Jaffe RA. Wrist hyperextension leads to median nerve conduction block: implications for intra-arterial catheter placement. *Anesthesiology* 2004; **100**: 287-291 [PMID: 14739802 DOI: 10.1097/00000542-200402000-00017]
4 **Kokosis G**, Blueschke G, Blanton M, Levinson H, Erdmann D. Acute carpal tunnel syndrome secondary to iatrogenic hemorrhage. A case report. *Hand (N Y)* 2011; **6**: 206-208 [PMID: 22654706 DOI: 10.1007/s11552-010-9298-0]
5 **Lazaro RP**. Complex regional pain syndrome and acute carpal tunnel syndrome following radial artery cannulation: a neurological perspective and review of the literature. *Medicine (Baltimore)* 2015; **94**: e422 [PMID: 25621693 DOI: 10.1097/MD.0000000000000422]
6 **Domkundwar S**, Autkar G, Khadilkar SV, Virarkar M. Ultrasound and EMG-NCV study (electromyography and nerve conduction velocity) correlation in diagnosis of nerve pathologies. *J Ultrasound* 2017; **20**: 111-122 [PMID: 28593000 DOI: 10.1007/s40477-016-0232-3]
7 **Aminoff MJ**. Electrophysiologic testing for the diagnosis of peripheral nerve injuries. *Anesthesiology* 2004; **100**: 1298-1303 [PMID: 15114229 DOI: 10.1097/00000542-200405000-00034]
8 **Kimura J**, Machida M, Ishida T, Yamada T, Rodnitzky RL, Kudo Y, Suzuki S. Relation between size of compound sensory or muscle action potentials, and length of nerve segment. *Neurology* 1986; **36**: 647-652 [PMID: 3703263 DOI: 10.1212/wnl.36.5.647]
9 **Campbell WW**. Evaluation and management of peripheral nerve injury. *Clin Neurophysiol* 2008; **119**: 1951-1965 [PMID: 18482862 DOI: 10.1016/j.clinph.2008.03.018]
10 **Tamura K**. The funicular pattern of Japanese peripheral nerves. *Nihon Geka Hokan* 1969; **38**: 35-58 [PMID: 5813934]
11 **Delgado-Martínez I**, Badia J, Pascual-Font A, Rodríguez-Baeza A, Navarro X. Fascicular Topography of the Human Median Nerve for Neuroprosthetic Surgery. *Front Neurosci* 2016; **10**: 286 [PMID: 27445660 DOI: 10.3389/fnins.2016.00286]
12 **Tsukuda Y**, Funakoshi T, Nasuhara Y, Nagano Y, Shimizu C, Iwasaki N. Venipuncture Nerve Injuries in the Upper Extremity From More Than 1 Million Procedures. *J Patient Saf* 2019; **15**: 299-301 [PMID: 27314202 DOI: 10.1097/PTS.0000000000000264]
13 **Newman BH**, Waxman DA. Blood donation-related neurologic needle injury: evaluation of 2 years' worth of data from a large blood center. *Transfusion* 1996; **36**: 213-215 [PMID: 8604504 DOI: 10.1046/j.1537-2995.1996.36396182137.x]
14 **Newman B**. Venipuncture nerve injuries after whole-blood donation. *Transfusion* 2001; **41**: 571-572 [PMID: 11316914 DOI: 10.1046/j.1537-2995.2001.41040571.x]
15 **Berry PR**, Wallis WE. Venepuncture nerve injuries. *Lancet* 1977; **1**: 1236-1237 [PMID: 68334 DOI: 10.1016/s0140-6736(77)92442-4]
16 **Kuncoro J**, Deapsari F, Suroto H. Clinical and functional outcome after different surgical approaches for brachial plexus injuries: Cohort study. *Ann Med Surg (Lond)* 2022; **78**: 103714 [PMID: 35620046 DOI: 10.1016/j.amsu.2022.103714]
17 **Temiz Ç**, Yaşar S, Kırık A. Surgical treatment of peripheral nerve injuries: Better outcomes with intraoperative NAP recordings. *Ulus Travma Acil Cerrahi Derg* 2021; **27**: 510-515 [PMID: 34476797 DOI: 10.14744/tjtes.2020.95702]
18 **Desai K**, Warade AC, Jha AK, Pattankar S. Injection-related iatrogenic peripheral nerve injuries: Surgical experience of 354 operated cases. *Neurol India* 2019; **67**: S82-S91 [PMID: 30688239 DOI: 10.4103/0028-3886.250703]

World Journal of Clinical Cases

Submit a Manuscript: https://www.f6publishing.com

World J Clin Cases 2023 September 6; 11(25): 5947-5953

DOI: 10.12998/wjcc.v11.i25.5947

ISSN 2307-8960 (online)

CASE REPORT

Novel *COL4A3* synonymous mutation causes Alport syndrome coexistent with immunoglobulin A nephropathy in a woman: A case report

Yu-Ting Chen, Wen-Ze Jiang, Ke-Da Lu

Specialty type: Medicine, research and experimental

Provenance and peer review: Unsolicited article; Externally peer reviewed.

Peer-review model: Single blind

Peer-review report's scientific quality classification
Grade A (Excellent): A
Grade B (Very good): 0
Grade C (Good): C
Grade D (Fair): 0
Grade E (Poor): 0

P-Reviewer: Weinstock BA, United States; Yari D, Iran

Received: June 6, 2023
Peer-review started: June 6, 2023
First decision: July 17, 2023
Revised: July 31, 2023
Accepted: August 8, 2023
Article in press: August 8, 2023
Published online: September 6, 2023

Yu-Ting Chen, Wen-Ze Jiang, The First Clinical Medical College, Zhejiang Chinese Medical University, Hangzhou 310053, Zhejiang Province, China

Ke-Da Lu, Department of Nephrology, The Third Affiliated Hospital of Zhejiang Chinese Medical University, Hangzhou 310005, Zhejiang Province, China

Corresponding author: Ke-Da Lu, MD, Doctor, Professor, Department of Nephrology, The Third Affiliated Hospital of Zhejiang Chinese Medical University, No. 219 Moganshan Road, Xihu District, Hangzhou 310005, Zhejiang Province, China. lukedaq@126.com

Abstract

BACKGROUND

Alport syndrome (AS) is an inherited disease of the glomerular basement membrane caused by mutations in genes encoding α3, α4, or α5 chains of type IV collagen. It manifests with hematuria or proteinuria, which is often accompanied by hearing impairments and ocular abnormalities. Histopathologically, AS shows mesangial proliferation and sometimes incidental immunoglobulin A (IgA) deposition. Hematuria or proteinuria is also a common presentation in patients with IgA nephropathy that makes it difficult to differentially diagnose AS and IgA nephropathy solely based on these clinical and pathological features.

CASE SUMMARY

Herein, we present the case of a 59-year-old female patient who was admitted to our hospital with persistent microscopic hematuria and occasional proteinuria that had lasted for > 2 years. This patient had a familial history of renal disease and was diagnosed with autosomal dominant AS (ADAS) and IgA nephropathy based on the findings of renal biopsy as well as genetic testing performed using whole-exome sequencing, which suggested that the patient carried a novel heterozygous variation (c.888G>A:p.Gln296Gln) in the *COL4A3* gene that enriches the mutation spectrum of ADAS. The proband received an angiotensin receptor blocker therapy after a definitive diagnosis was established. After one year of therapy, a significant reduction in proteinuria was observed. The number of microscopic red blood cells per high-power field decreased to one-quarter of the baseline levels. Renal function also maintained well during the follow-up.

CONCLUSION

Our case highlights the significance of performing kidney biopsy and genetic

testing in the diagnosis of AS and familial IgA nephropathy.

Key Words: Alport syndrome; Immunoglobulin A nephropathy; *COL4A3* gene; Whole-exome sequencing; Renal biopsy; Case report

Core Tip: It is challenging to distinguish between Alport syndrome (AS) and immunoglobulin A (IgA) nephropathy solely based on clinical and pathological findings. This report highlights the diagnostic value of whole-exome sequencing in the precise diagnosis of AS and emphasizes the significance of renal biopsy and genetic detection in the early diagnosis of AS and familial IgA nephropathy.

Citation: Chen YT, Jiang WZ, Lu KD. Novel *COL4A3* synonymous mutation causes Alport syndrome coexistent with immunoglobulin A nephropathy in a woman: A case report. *World J Clin Cases* 2023; 11(25): 5947-5953
URL: https://www.wjgnet.com/2307-8960/full/v11/i25/5947.htm
DOI: https://dx.doi.org/10.12998/wjcc.v11.i25.5947

INTRODUCTION

Both Alport syndrome (AS) and immunoglobulin A (IgA) nephropathy (IgAN) present with persistent hematuria, proteinuria, and progressive renal dysfunction. The prevalence of AS is approximately 1 in 50000 newborns, with males exhibiting a higher propensity for symptomatic manifestations compared with females[1]. AS is a genetically heterogeneous nephropathy that results from the mutations of *COL4A3*, *COL4A4*, and *COL4A5* genes encoding α3, α4, and α5 chains of type IV collagen[2]. AS comprises three hereditary forms: X-linked AS, autosomal recessive AS, and autosomal dominant AS (ADAS). Patients with ADAS typically harbor a heterozygous pathogenic variant in the *COL4A3* or *COL4A4* gene and have a wide spectrum of clinical features, ranging from lack of symptoms to renal failure[3]. The heterogeneity of ADAS phenotypes leads to its underdiagnosis clinically. As next-generation sequencing and whole-exome sequencing (WES) become ever more prevalent, the prevalence of ADAS has been reported increasingly and accounts for approximately 20% of AS[3]. Early diagnosis of AS is important because progression to renal failure can be slowed by renin-angiotensin-aldosterone system blockade[4]. Nephrologists recommend that the renin-angiotensin-aldosterone blockade should be administered to patients with a heterozygous pathogenic *COL4A3* or *COL4A4* mutation from the onset of microalbuminuria, hypertension, or kidney impairment[4-6].

IgAN is the most common primary glomerulonephritis, and patients with IgAN are characterized by the deposition of IgA1 immune complexes in the glomerular mesangium. The global prevalence of IgAN varies widely. IgAN is more common in Asian countries, including China (45%–58% of primary glomerulonephritis), than in European countries (10%–35% of primary glomerulonephritis) and has a higher prevalence among males than females[7]. IgAN usually occurs sporadically, but approximately 15% of cases have an inheritable component[8]. With advances in genetic medicine, pathogenic or likely pathogenic variants in *COL4A3–5* were confirmed in the IgAN family members[9,10]. When hematuria is ascribed to familial IgAN, it is more likely owing to unknown disease-causing *COL4A3–5* variants. In the present study, we performed sequencing on a 59-year-old female patient who was diagnosed with IgAN by renal biopsy. A novel heterozygous mutation (c.888G>A) in the *COL4A3* gene was identified in the patient through WES. The same mutation was also found in the proband's asymptomatic son. Based on the results of genetic testing, histopathological findings, and pedigree analysis, the proband was diagnosed with co-occurring ADAS and IgAN.

CASE PRESENTATION

Chief complaints

A 59-year-old female patient presented with persistent microscopic hematuria and occasional proteinuria for > 2 years.

History of present illness

The patient was admitted to our hospital on November 11, 2020, with persistent microscopic hematuria and occasional proteinuria, in addition to frequent complaints of waist soreness and thirst.

History of past illness

The patient had no prior past medical history.

Personal and family history

The patient had a family history of renal disease. Although her parents had died many years ago with no exact cause, one of her elder brothers was diagnosed with chronic renal failure in December 2021 whose 30-year-old son has been undergoing hemodialysis for many years (Figure 1).

Physical examination

The patient's vital signs were normal, including a body temperature of 37.1 ℃, pulse of 91 beats/minute, respiratory rate of 18 breaths/minute, and blood pressure of 15.7/9.2 kPa. No abnormalities were detected in the eye and ear examinations. Physical examinations showed no abnormalities related to the abdomen, cardiopulmonary system, and lower extremities.

Laboratory examinations

Laboratory tests showed the following results: 24-h urinary protein (223.2 mg), microhematuria (red blood cell count: 302.5/μL), poikilocyte (75%), albumin-to-creatinine ratio (181 mg/g), albumin (36.7 g/L), serum creatinine (0.52 mg/dL), potassium (13.65 mg/dL), total cholesterol (257.16 mg/dL), low-density lipoprotein (150.04 mg/dL), IgA (1.67 g/L), IgG (11.30 g/L), IgM (1.26 g/L), Complement 3 (1.03 g/L), and Complement 4 (0.32 g/L). The biochemical results are summarized in Table 1.

Imaging examinations

No abnormalities were detected in the findings of the electrocardiogram and color Doppler echocardiography. The abdominal ultrasound revealed a left renal cyst and a 1.3 cm right upper ureteral calculus with expansion.

Further diagnostic work-up

A holmium laser lithotripsy through ureteropyeloscopy was performed, and an indwelling double J stent was placed in the patient's right ureter. One month later, the ureteral stent was removed, and a renal biopsy was performed the next day. We used hematoxylin and eosin, periodic acid-Schiff, periodic acid-silver methenamine, and Masson's trichrome staining techniques for histopathological evaluation of tissue specimens. Twenty glomeruli were found in the biopsy specimen. Under light microscopy, the glomeruli showed a mild increase in mesangial cellularity and mesangial matrix. Congo red stain for amyloid gave negative results. Immunofluorescence showed a diffuse deposit of IgA (++) in the glomerular mesangial area. Furthermore, immunostaining for C3 and IgM was weakly positive, while immunostaining for C1q and IgG was negative. The electron microscopy image showed diffuse thinning of the glomerular basement membrane (GBM) and minor electron-dense depositions in a few mesangial areas (Figure 2). Based on the pathologic findings, the patient was diagnosed with IgAN. The MESTC score was M1E0S0T0-C0. We obtained the proband's consent to carry out a genetic analysis to establish the diagnosis. Fresh venous blood was obtained from the patient for genomic DNA extraction. Firstly, the DNA was interrupted and prepared for library construction. Then, the exons of the target gene and the DNA adjacent to the shear region were captured and enriched by Roche KAPA HyperExome microarray. Finally, the mutation was detected by the MGISEQ-2000 sequencing platform. WES showed a unique heterozygous synonymous mutation in *COL4A3*. The mutation of c.888G>A:p.Gln296Gln locates in exon 15 of the *COL4A3* gene (NM_000091.4) on chromosome 2, in which G in the 888th position was changed to A (c.888G>A), resulting in the CAG→CAA codon change without amino change. This mutation has not been reported so far in the literature. SpliceAI, dbscSNV_RF and dbscSNV_ADA indicated that it may have an effect on splicing. To widen the pedigree of patients, we also performed genetic testing of her son without clinical symptoms. Sequencing results demonstrated that the son harbored an identical mutation in the *COL4A3* gene (Figure 3).

FINAL DIAGNOSIS

Based on the histopathological findings, family history, and genetic testing results, the diagnosis was established as ADAS with IgAN.

TREATMENT

The patient was administered with atorvastatin calcium tablets (20 mg qd) and potassium chloride sustained-release tablets (0.5 g bid) when she was admitted. Subsequently, she received losartan potassium tablets (50 mg qd) after a definitive diagnosis.

OUTCOME AND FOLLOW-UP

One year after therapy, significant reduction in proteinuria was observed. Microscopic red blood cells per high-power field decreased to one quarter of the baseline level. Additionally, her renal function was maintained during the follow-up period.

Table 1 Proband's laboratory tests

Biochemical items	Results
Urinary albumin	±
RBCs (/μL)	302.5
24 h urinary protein (mg)	223.2
ACR (mg/g)	181
Poikilocyte	75%
Total serum protein (g/L)	62.8
Albumin (g/L)	36.7
eGFR (mL/min per 1.73m^2)	149.20
Serum creatinine (mg/dL)	0.52
Uric acid (mg/dL)	5.23
Potassium (mg/dL)	13.65
Total cholesterol (mg/dL)	257.16
Low density lipoprotein (mg/dL)	150.04
ANA	Negative
Anti-dsDNA antibody	Negative
IgA (g/L)	1.67
IgG (g/L)	11.30
IgM (g/L)	1.26
C3 (g/L)	1.03
C4 (g/L)	0.32
Anti-SSA antibody	Negative
Anti-SSB antibody	Negative
Hepatitis (A, B, or C) antibody	Negative

RBCs: Red blood cells; ACR: Albumin-creatinine ratio; eGFR: Estimated glomerular filtration rate; ANA: Anti-nuclear antibody; Anti-dsDNA: Anti-double-stranded DNA; C3: Complement 3; C4: Complement 4; Anti-SSA: Anti-Sjögren's syndrome A; Anti-SSB: Anti-Sjögren's syndrome B.

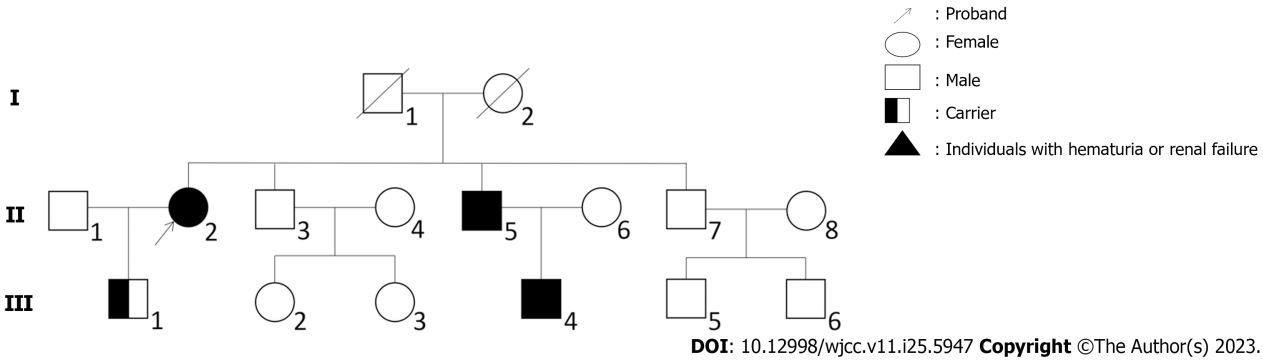

DOI: 10.12998/wjcc.v11.i25.5947

Figure 1 Family pedigrees. The proband and her son were heterozygous for the novel disease-causing variant. One of the proband's brothers was diagnosed with renal failure in December 2021 whose son has been undergoing hemodialysis for many years.

DISCUSSION

Although the patient presented with minor microhematuria and proteinuria, her son had no clinical symptoms. Histologic findings included dominant IgA deposit in the mesangial area of the renal glomerulus and diffuse thinning of the GBM. The clinical manifestations and histologic findings were consistent with both IgAN and AS or thin basement

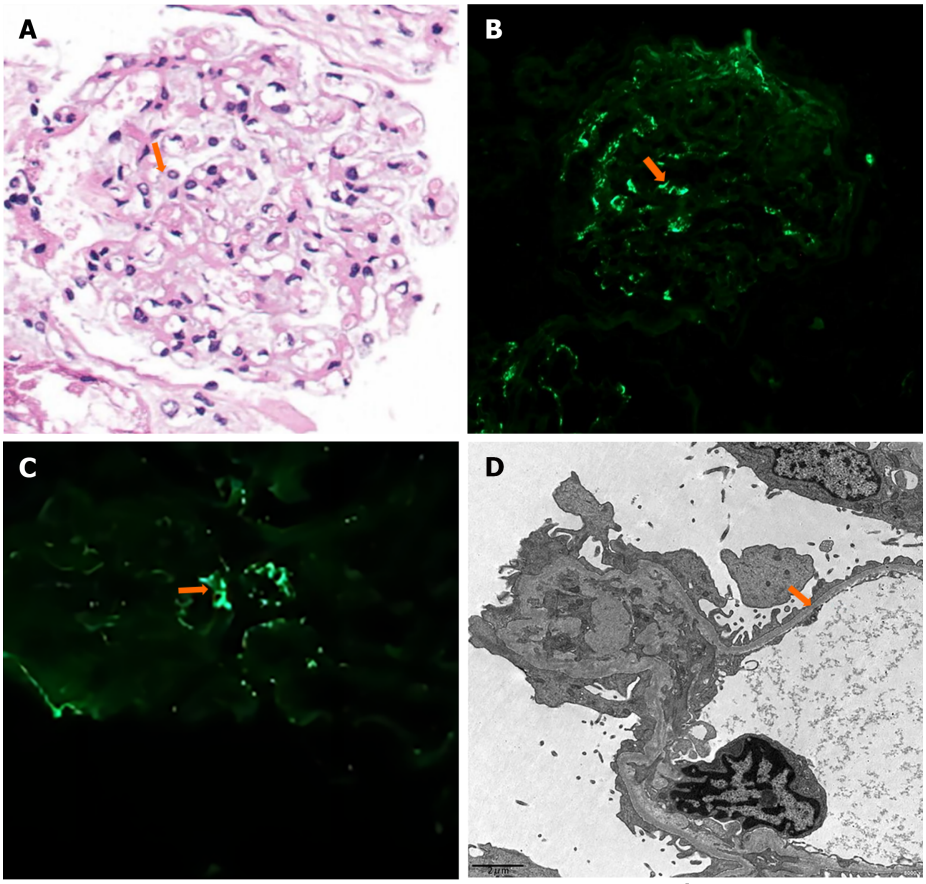

DOI: 10.12998/wjcc.v11.i25.5947 **Copyright** ©The Author(s) 2023.

Figure 2 Findings of the proband's renal biopsy. A: Hematoxylin and eosin stain shows mild mesangial proliferation (as the arrow indicates). Original magnification 400 ×; B: Immunofluorescence shows deposition of immunoglobulin A (as the arrow indicates). Original magnification 400 ×; C: Immunofluorescence shows deposition of C3 (as the arrow indicates). Original magnification 400 ×; D: Electron microscopy shows diffuse thinning of the glomerular basement membrane (as the arrow indicates). Scale bars: 2 μm.

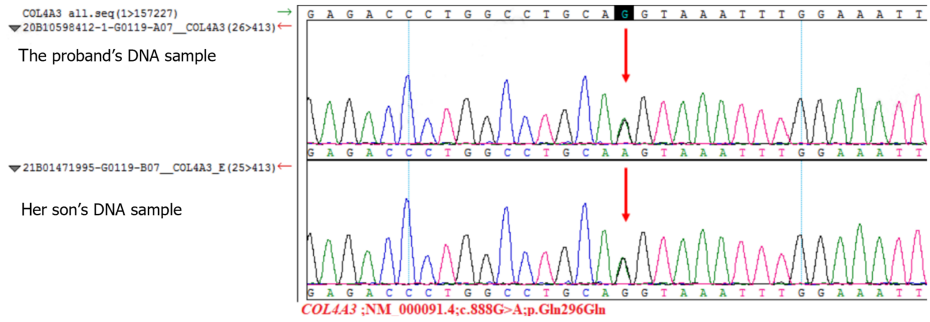

DOI: 10.12998/wjcc.v11.i25.5947 **Copyright** ©The Author(s) 2023.

Figure 3 Findings of *COL4A3* gene mutations. A heterozygous synonymous variant (c.888G>A:p.Gln296Gln) was screened in the *COL4A3* gene from the proband's and her son's DNA sample.

membrane nephropathy (TBMN). The changes in the thickness of GBM as observed with electron microscopy suggested the possibility of TBMN, necessitating genetic testing. We sequenced the proband and her son with WES. WES showed that both the woman and her son had identical heterozygous mutation of c.888G>A:p.Gln296Gln in *COL4A3* gene, which revealed the autosomal dominant pattern of genetic inheritance in the family. A comprehensive search of ESP6500, 1000 Genomes, ExAC, GnomAD and GnomAD-EAS databases showed that this mutation has not been previously reported associated with AS. Considering that her son had no renal symptoms, this hereditary condition showed incomplete penetrance in the family, which is consistent with a multifactorial disease model and confirms that other factors beyond a single causal factor leading to mutations are required to trigger disease onset[11].

The patient had no sensorineural deafness, characteristic retinopathy, or renal function impairment. Histologic findings showed a diffuse thin GBM with an average width of < 250 nm, without duplication, lamellation, or electron-dense deposits. These results suggested the diagnosis of TBMN rather than AS. Both AS and TBMN could result from hetero-

zygous variations in *COL4A3* or *COL4A4* genes[5]. Generally, significant proteinuria, progressive kidney failure, and extrarenal diseases are not associated with TBMN, though some patients can progress to end-stage renal disease in later life. Inconsistent with the presentation of TBMN pedigree, the pedigree includes a brother diagnosed with chronic renal failure and his 30-year-old son has been undergoing hemodialysis for many years. One of the diagnostic criteria of AS is irregular thickening, thinning, and splitting of the GBM, whereas the electron microscopic findings in patients with ADAS commonly show diffuse thinning of the GBM. Therefore, it is difficult to make an accurate distinguishment between ADAS and TBMN. Clifford E. Kashtan[2] suggested establishing an early diagnosis and rendering timely treatment in patients with AS. Some patients with AS are undiagnosed with a label of "benign familial hematuria" or "TBMN" due to their relative lack of clinical signs. Nevertheless, some experts query the diagnosis of ADAS because the electron microscopy findings in many patients with ADAS include diffuse thinning rather than the typical basement membrane splitting, lamellation, and basket weaving[12]. They consider that the diagnosis of ADAS will add to excessive anxiety. However, the diagnostic term "TBMN" is inappropriate because the risk of end-stage renal disease will be underestimated and early treatment will be delayed. In the genomic era, there is growing agreement that patients with a heterozygous pathologic variation in the *COL4A3* and/or *COL4A4* genes should be considered to have ADAS[3].

IgAN may occur in a sporadic or familial form[13]. Intriguingly, clinical manifestations of IgAN can overlap considerably with AS, which results from mutations in the *COL4A3*, *COL4A4*, and *COL4A5* genes[14,15]. Stapleton *et al*[10] conducted WES in 10 Irish families of which at least one member had biopsy-confirmed IgAN. They identified a likely disease-causing mutation in *COL4A5* in one family and a variant of unknown significance in *COL4A3* in another. Xu *et al*[16] confirmed a novel *COL4A5* gene variation (chrX:107814698, c.438 +2->AAACCAATTATA-) in IgAN in a Chinese family and suggested that variable *COL4A5* gene mutations may play different roles in IgAN. Li *et al*[9] discovered putatively disease-causing *COL4A3–5* variations in 9 of the 46 familial IgAN cases (20%), of which 6 showed autosomal dominant inheritance, with 2 carrying heterozygous mutations in *COL4A3* and 4 in *COL4A4*, and the remaining 3 demonstrated X-linked inheritance, with variations in the *COL4A5* gene. These findings demonstrate that *COL4A3–5* variations may be related to IgAN. Herein, our pedigree with biopsy-proven IgAN of the proband should be referred for assessment of familial IgAN. The case proposes a paradigm where AS and familial IgAN might represent two features of a single disease spectrum instead of two different pathologies.

Kamiyoshi *et al*[17] analyzed 25 patients with ADAS and their family members and revealed that the median age at detection of proteinuria was 17 years, the median renal survival time was 70 years, and only one patient developed hearing impairment and another had ocular abnormalities. Extrarenal manifestations in patients with ADAS are relatively rare compared with those in individuals with X-linked AS or autosomal recessive AS. The proband had a milder clinical course without ear and eye abnormalities which may be related to the autosomal dominant form of inheritance that has relatively minor impact on the renal function, and therefore the disturbance in the GBM architecture is milder. Besides, the synonymous variation in the gene loci may have reduced the severity of the disease.

Furlano *et al*[3] conducted a retrospective cohort study of 82 families (252 patients) with ADAS from Spanish hospitals, of which 216 of 252 patients underwent genetic testing. A heterozygous pathogenic mutation in *COL4A3* was confirmed in 107 patients, and a pathogenic mutation in *COL4A4* was confirmed in 133 patients. Digenic inheritance was confirmed in 12 patients. The most common type of pathogenic mutation was the missense variant (62.9%), the second was splicing variant (16.7%), and then in-frame indel > 5 amino acids (12.5%), indel truncating (11.6%), nonsense (6.5%), deletion (indel) < 5 amino acids (0.9%). We identified a heterozygous variation, c.888G>A, in exon 15 of *COL4A3* gene in the proband and her son, which is predicted to lead to a synonymous amino acid change, and p.Gln296Gln. mutation results in illness by affecting the process of splicing primarily[18,19]. This novel mutation potentially caused abnormal exonic splicing and could be responsible for ADAS affecting the family.

CONCLUSION

In conclusion, the patient was diagnosed with ADAS with IgAN based on the findings of kidney biopsy and WES. The diagnosis of ADAS is difficult because of its wide phenotype spectrum. Renal biopsy is necessary to avoid misdiagnosis. Genetic testing is crucial for early diagnosis of patients and relatives at risk. In our case, the proband has a novel heterozygous synonymous mutation in the *COL4A3* gene, which extends the gene mutational spectrum associated with ADAS.

FOOTNOTES

Author contributions: Chen YT contributed to manuscript writing and editing, and data collection; Jiang WZ contributed to data analysis; Lu KD contributed to conceptualization and supervision; all authors have read and approve the final manuscript.

Supported by The Major Project of Zhejiang Administration of Traditional Chinese Medicine, No. 2020ZZ008.

Informed consent statement: Informed written consent was obtained from the patient for publication of this report and any accompanying images.

Conflict-of-interest statement: The authors declare that they have no conflict of interest to disclose.

CARE Checklist (2016) statement: The authors have read the CARE Checklist (2016), and the manuscript was prepared and revised

according to the CARE Checklist (2016).

Country/Territory of origin: China

ORCID number: Yu-Ting Chen 0000-0002-6771-0133; Wen-Ze Jiang 0000-0003-1331-4036; Ke-Da Lu 0000-0002-9934-3630.

S-Editor: Fan JR
L-Editor: A
P-Editor: Cai YX

REFERENCES

1 **Pedrosa AL**, Bitencourt L, Paranhos RM, Leitão CA, Ferreira GC, Simões E Silva AC. Alport Syndrome: A Comprehensive Review on Genetics, Pathophysiology, Histology, Clinical and Therapeutic Perspectives. *Curr Med Chem* 2021; **28**: 5602-5624 [PMID: 33423643 DOI: 10.2174/0929867328666210108113500]
2 **Kashtan CE**. Alport Syndrome: Achieving Early Diagnosis and Treatment. *Am J Kidney Dis* 2021; **77**: 272-279 [PMID: 32712016 DOI: 10.1053/j.ajkd.2020.03.026]
3 **Furlano M**, Martínez V, Pybus M, Arce Y, Crespí J, Venegas MDP, Bullich G, Domingo A, Ayasreh N, Benito S, Lorente L, Ruíz P, Gonzalez VL, Arlandis R, Cabello E, Torres F, Guirado L, Ars E, Torra R. Clinical and Genetic Features of Autosomal Dominant Alport Syndrome: A Cohort Study. *Am J Kidney Dis* 2021; **78**: 560-570.e1 [PMID: 33838161 DOI: 10.1053/j.ajkd.2021.02.326]
4 **Savige J**, Lipska-Zietkiewicz BS, Watson E, Hertz JM, Deltas C, Mari F, Hilbert P, Plevova P, Byers P, Cerkauskaite A, Gregory M, Cerkauskiene R, Ljubanovic DG, Becherucci F, Errichiello C, Massella L, Aiello V, Lennon R, Hopkinson L, Koziell A, Lungu A, Rothe HM, Hoefele J, Zacchia M, Martic TN, Gupta A, van Eerde A, Gear S, Landini S, Palazzo V, Al-Rabadi L, Claes K, Corveleyn A, Van Hoof E, van Geel M, Williams M, Ashton E, Belge H, Ars E, Bierzynska A, Gangemi C, Renieri A, Storey H, Flinter F. Guidelines for Genetic Testing and Management of Alport Syndrome. *Clin J Am Soc Nephrol* 2022; **17**: 143-154 [PMID: 34930753 DOI: 10.2215/CJN.04230321]
5 **Savige J**, Gregory M, Gross O, Kashtan C, Ding J, Flinter F. Expert guidelines for the management of Alport syndrome and thin basement membrane nephropathy. *J Am Soc Nephrol* 2013; **24**: 364-375 [PMID: 23349312 DOI: 10.1681/ASN.2012020148]
6 **Kashtan CE**, Ding J, Garosi G, Heidet L, Massella L, Nakanishi K, Nozu K, Renieri A, Rheault M, Wang F, Gross O. Alport syndrome: a unified classification of genetic disorders of collagen IV α345: a position paper of the Alport Syndrome Classification Working Group. *Kidney Int* 2018; **93**: 1045-1051 [PMID: 29551517 DOI: 10.1016/j.kint.2017.12.018]
7 **Zhang Z**, Zhang Y, Zhang H. IgA Nephropathy: A Chinese Perspective. *Glomerular Dis* 2022; **2**: 30-41 [PMID: 36751266 DOI: 10.1159/000520039]
8 **Bhattacharyya A**, Huang Y, Khan SH, Drachenberg CB, Malone LC. Tale of two nephropathies; co-occurring Alport syndrome and IgA nephropathy, a case report. *BMC Nephrol* 2021; **22**: 358 [PMID: 34717572 DOI: 10.1186/s12882-021-02567-9]
9 **Li Y**, Groopman EE, D'Agati V, Prakash S, Zhang J, Mizerska-Wasiak M, Caliskan Y, Fasel D, Karnib HH, Bono L, Omran SA, Sabban EA, Kiryluk K, Caridi G, Ghiggeri GM, Sanna-Cherchi S, Scolari F, Gharavi AG. Type IV Collagen Mutations in Familial IgA Nephropathy. *Kidney Int Rep* 2020; **5**: 1075-1078 [PMID: 32647767 DOI: 10.1016/j.ekir.2020.04.011]
10 **Stapleton CP**, Kennedy C, Fennelly NK, Murray SL, Connaughton DM, Dorman AM, Doyle B, Cavalleri GL, Conlon PJ. An Exome Sequencing Study of 10 Families with IgA Nephropathy. *Nephron* 2020; **144**: 72-83 [PMID: 31865346 DOI: 10.1159/000503564]
11 **Kiryluk K**, Julian BA, Wyatt RJ, Scolari F, Zhang H, Novak J, Gharavi AG. Genetic studies of IgA nephropathy: past, present, and future. *Pediatr Nephrol* 2010; **25**: 2257-2268 [PMID: 20386929 DOI: 10.1007/s00467-010-1500-7]
12 **Imafuku A**, Nozu K, Sawa N, Nakanishi K, Ubara Y. How to resolve confusion in the clinical setting for the diagnosis of heterozygous COL4A3 or COL4A4 gene variants? Discussion and suggestions from nephrologists. *Clin Exp Nephrol* 2020; **24**: 651-656 [PMID: 32232700 DOI: 10.1007/s10157-020-01880-1]
13 **Fennelly NK**, Kennedy C, Jenkinson AC, Connaughton DM, Stapleton C, Dorman AM, Doyle B, Conlon PJ. Clinical Heterogeneity in Familial IgA Nephropathy. *Nephron* 2018; **139**: 63-69 [PMID: 29402819 DOI: 10.1159/000486018]
14 **Gagliano Taliun SA**, Sulem P, Sveinbjornsson G, Gudbjartsson DF, Stefansson K, Paterson AD, Barua M. GWAS of Hematuria. *Clin J Am Soc Nephrol* 2022; **17**: 672-683 [PMID: 35474271 DOI: 10.2215/CJN.13711021]
15 **Gale DP**. How benign is hematuria? Using genetics to predict prognosis. *Pediatr Nephrol* 2013; **28**: 1183-1193 [PMID: 23325022 DOI: 10.1007/s00467-012-2399-y]
16 **Xu Z**, Chen J, Yu W, Li X, Lin B, Lai D, Xu A, Tang Y. New COL4A5 mutation in IgA nephropathy. *Postgrad Med J* 2022; **98**: 13-17 [PMID: 33087535 DOI: 10.1136/postgradmedj-2020-138625]
17 **Kamiyoshi N**, Nozu K, Fu XJ, Morisada N, Nozu Y, Ye MJ, Imafuku A, Miura K, Yamamura T, Minamikawa S, Shono A, Ninchoji T, Morioka I, Nakanishi K, Yoshikawa N, Kaito H, Iijima K. Genetic, Clinical, and Pathologic Backgrounds of Patients with Autosomal Dominant Alport Syndrome. *Clin J Am Soc Nephrol* 2016; **11**: 1441-1449 [PMID: 27281700 DOI: 10.2215/CJN.01000116]
18 **Pagani F**, Baralle FE. Genomic variants in exons and introns: identifying the splicing spoilers. *Nat Rev Genet* 2004; **5**: 389-396 [PMID: 15168696 DOI: 10.1038/nrg1327]
19 **Chamary JV**, Parmley JL, Hurst LD. Hearing silence: non-neutral evolution at synonymous sites in mammals. *Nat Rev Genet* 2006; **7**: 98-108 [PMID: 16418745 DOI: 10.1038/nrg1770]

World Journal of Clinical Cases

Submit a Manuscript: https://www.f6publishing.com

World J Clin Cases 2023 September 6; 11(25): 5954-5961

DOI: 10.12998/wjcc.v11.i25.5954

ISSN 2307-8960 (online)

CASE REPORT

Non-retroareolar male mucinous breast cancer without gynecomastia development in an elderly man: A case report

Qiang Sun, Xu-Yan Liu, Qi Zhang, Hai Jiang

Specialty type: Medicine, research and experimental

Provenance and peer review: Unsolicited article; Externally peer reviewed.

Peer-review model: Single blind

Peer-review report's scientific quality classification

Grade A (Excellent): 0
Grade B (Very good): B, B
Grade C (Good): 0
Grade D (Fair): 0
Grade E (Poor): 0

P-Reviewer: Kang SY, South Korea; Wu K, United States

Received: May 5, 2023
Peer-review started: May 5, 2023
First decision: June 12, 2023
Revised: June 30, 2023
Accepted: August 9, 2023
Article in press: August 9, 2023
Published online: September 6, 2023

Qiang Sun, Qi Zhang, Hai Jiang, Department of Breast Surgery, General Hospital of Benxi Iron & Steel Industry Group of Liaoning Health Industry Group, Benxi 117000, Liaoning Province, China

Xu-Yan Liu, Department of Pathology, General Hospital of Benxi Iron & Steel Industry Group of Liaoning Health Industry Group, Benxi 117000, Liaoning Province, China

Corresponding author: Qiang Sun, PhD, Chief Doctor, Department of Breast Surgery, General Hospital of Benxi Iron & Steel Industry Group of Liaoning Health Industry Group, No. 29 Renming Road, Benxi 117000, Liaoning Province, China. sq1338@hotmail.com

Abstract

BACKGROUND

Male breast cancer (MBC) is an extremely rare condition and accounts for less than 1% of all breast cancers, and malignant tumors occur in less than 1% of the affected men. Mucinous breast cancer is extremely rare and accounts for 2% of all invasive breast cancers. Generally, MBC is accompanied by a retroareolar mass.

CASE SUMMARY

Herein, we report a case of male mucinous breast carcinoma (MMBC) without gynecomastia development and with mass localization outside the common retroareolar region, wherein the mass was a painless nodule in the right breast of a 64-year-old man. We also discuss the clinical and pathological characteristics of this unusual tumor. The excised breast specimen showed pure mucinous carcinoma. The patient had strong expression of estrogen and progesterone receptors, a low Ki-67 proliferation index of the tumor cells, and negative pathological axillary lymph nodes. The patient underwent modified radical mastectomy and axillary lymph node dissection, followed by tamoxifen hormone therapy.

CONCLUSION

To the best of our knowledge, this is the first case report of MMBC in the non-retroareolar region of the nipple without gynecomastia development. Mucinous tumors are easily missed during diagnosis, and the incidence of axillary lymph node metastases of chest mucinous tumors has increased.

Key Words: Breast cancer; Male; Mucinous adenocarcinoma; Nipple; Case report

Core Tip: We not only report a rare case, but also discuss the clinical and pathological characteristics of this unusual tumor. Though a summary of a limited number of cases and a comparison with female breast cancer, we reveal some interesting features of male mucinous breast cancer. It is helpful to distinguish the rare male disease.

Citation: Sun Q, Liu XY, Zhang Q, Jiang H. Non-retroareolar male mucinous breast cancer without gynecomastia development in an elderly man: A case report. *World J Clin Cases* 2023; 11(25): 5954-5961
URL: https://www.wjgnet.com/2307-8960/full/v11/i25/5954.htm
DOI: https://dx.doi.org/10.12998/wjcc.v11.i25.5954

INTRODUCTION

Male breast cancer (MBC) is particularly uncommon, accounting for approximately 1% of all breast cancer cases[1-3]. Known risk factors for MBC include old age, high estradiol levels, Klinefelter's syndrome, radiation exposure, gynecomastia, family history of breast cancer, and Breast Cancer 1 protein (BRCA1) and BRCA2 mutations[4]. The most common malignancy in MBC patients is invasive ductal carcinoma, and mucinous carcinoma is extremely rare[5,6]. Anatomically, the male breast comprises the external nipple, areola, internal lymph nodes, adipose tissue, and ducts. The glandular portion of the male breast is located mainly posterior to the nipple-areola complex[7]. MBC occurrence most often involves remarkable gynecomastia development and a retroareolar mass[8-10]. We herein report a case of non-retroareolar male mucinous breast carcinoma (MMBC) without gynecomastia development and review similar cases documented in the literature.

CASE PRESENTATION

Chief complaints

A 64-year-old male presented at the hospital with a painless mass in the right chest for 4 mo.

History of present illness

The patient had a mass over the right lateral nipple for 4 mo, which grew from the size of a pea to the size of an egg yolk, without pain.

History of past illness

The patient with no history of smoking or drinking, no history of hepatitis, no history of cardiovascular disease, and no history of long-term drug use.

Personal and family history

There was no significant personal or family history.

Physical examination

The patient was 178 cm in height and 58 kg in weight, with body mass index (BMI): 18.3 kg/m^2. Physical examination indicated an approximately 2.0 cm × 1.5 cm-sized nodule present 2.0 cm above the right lateral nipple.

Laboratory examinations

Serum six-sex hormone test revealed the following findings: (1) Follicle-stimulating hormone: 12.60 IU/L (normal: 1.27-19.26 IU/L); (2) Luteinizing hormone: 7.66 IU/L (normal: 1.24-8.62 IU/L); (3) Estradiol: 0.00 pg/mL (normal: < 25-38.95 pg/mL); (4) Testosterone: 3.37 ng/mL (normal: 1.75-7.81 ng/mL); (5) Prolactin: 16.83 ng/mL (normal: 2.64-13.13 ng/mL); and (6) Progesterone: 0.00 ng/mL (normal: 0.14-2.06 ng/mL).

Imaging examinations

Ultrasound examination revealed the following information: A subcutaneous hypoechoic lesion was located 2.0 cm from the nipple edge on the lateral side of the right nipple and had a size of approximately 1.88 cm × 1.13 cm, with clear borders and no blood flow signal within it. Computerized tomography (CT) reveals posterior nipple glands and postoperative defects from outpatient surgery (Figure 1).

MULTIDISCIPLINARY EXPERT CONSULTATION

According to histopathological examination and immunohistochemistry analysis of the excised tissue, multidisciplinary consultation by the Department of Breast Surgery, Oncology, Ultrasound, and Pathology made the diagnosis - non-

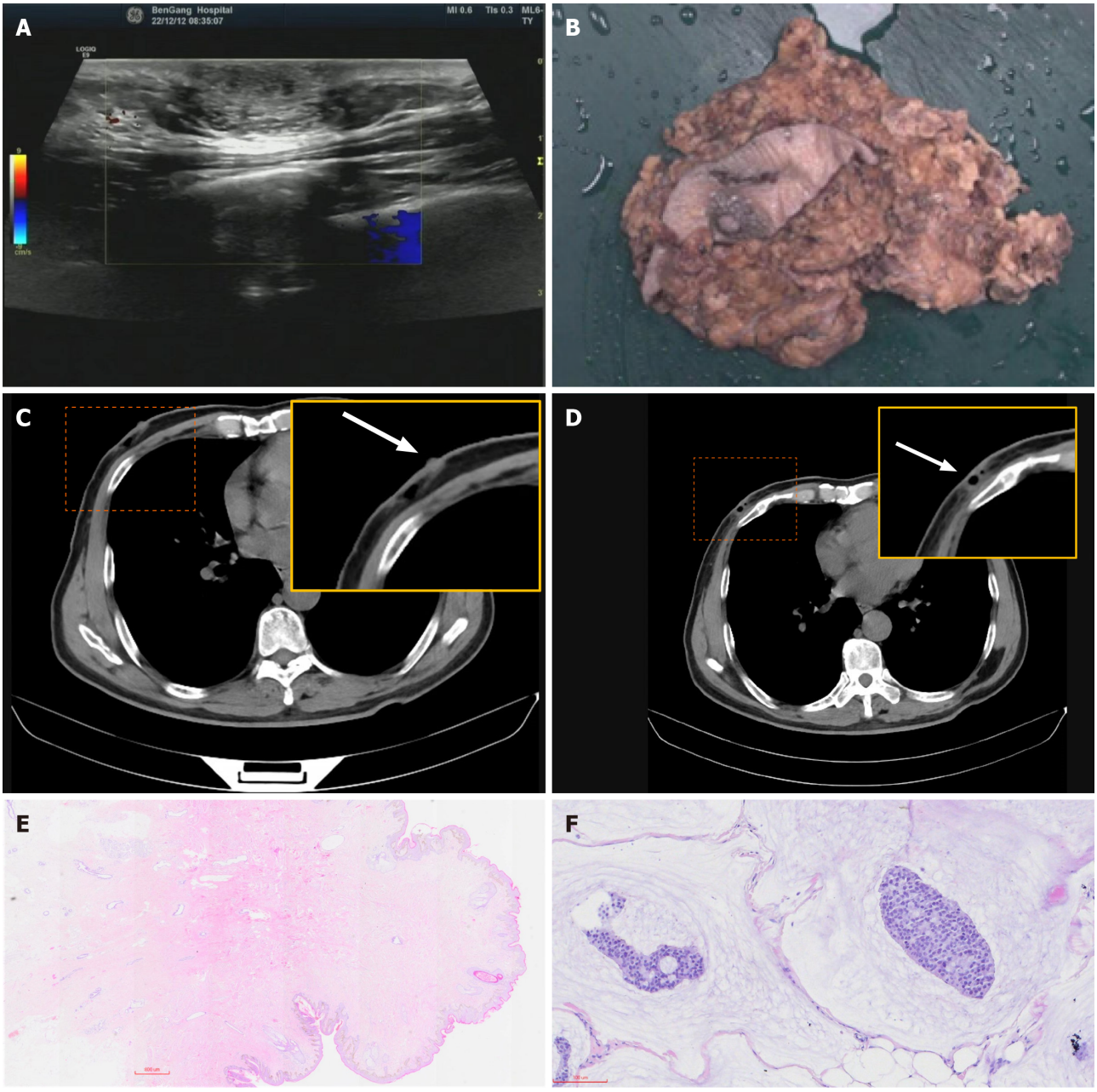

DOI: 10.12998/wjcc.v11.i25.5954

Figure 1 Preoperative and postoperative imaging corresponding surgical specimen and pathology analysis. A: Ultrasound image of the left breast region at the upper outer area of the nipple demonstrating a 1.88-cm oval, parallel isoechoic mass; B: Surgical specimens showing the position of the surgical scar; C: Computerized tomography reveals posterior nipple glands (the arrow points to the position where the back of the nipple is located); D: Postoperative defects from outpatient surgery (the arrow points to the location of the residual cavity after removal of the mass); E: Histopathological examination of the excised breast tissue showing a nodular lesion with relatively clear borders in the breast. Homogeneous clusters of tumor cells containing small nuclei together with slightly larger round nuclei were suspended in abundant mucus material (mucus lake). The tumor invaded the surrounding adipose tissue and muscle tissue and did not invade the skin or subcutaneous tissue. The ductal tissue of the breast was visible in the periphery, and no intraductal cancer changes were seen (hematoxylin-eosin, 200 ×); F: Pathology of the nipple and posterior nipple, and no cancerous tissue invasion was seen in the nipple and subpapillary ducts, and Paget's changes were not seen in the skin (hematoxylin-eosin, 20 ×).

retroareolar MMBC without gynecomastia (Figure 2).

FINAL DIAGNOSIS

The patient was given the diagnosis of male mucinous breast carcinoma.

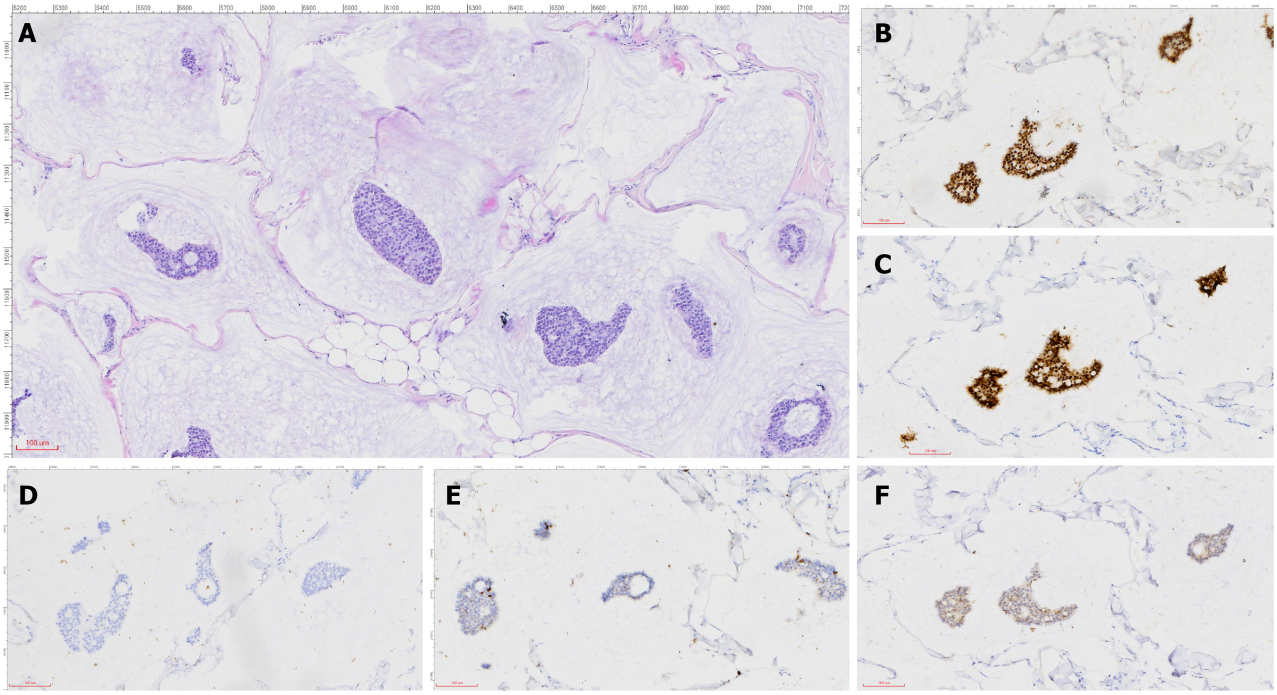

DOI: 10.12998/wjcc.v11.i25.5954

Figure 2 Pathology and immunohistochemistry analysis. A: Image showing clusters of tumor cells suspended in abundant extracellular mucin and separated by ciliated fibrous intervals containing capillaries; B: Estrogen receptor (2+); C: Progesterone receptor (2+); D: AR (−); E: Ki-67 (5%); F: CerbB-2 (−) (scale: 100 μm; 200 ×).

TREATMENT

Examination and ultrasound revealed a mass located anterior to the pectoralis major fascia that can be differentiated from a muscle-derived mass. Subcutaneous fibroadenomas are slow growing and occasionally painful. In gynecomastia, the masses are mostly located behind the nipple and are not very well defined with a soft texture. Lymphomas, which are located in the chest 2.0 cm from the nipple in a non-normal lymphatic anatomical location, are more difficult to distinguish and require pathological analysis for identification. The outpatient surgeon diagnosed a possible benign fibroadenoma, which was surgically removed on December 12, and found the tumor lacked a capsule and the specimen was brittle. According to histopathological examination and immunohistochemistry analysis of the excised tissue, multidisciplinary consultation by the Department of Breast Surgery, Oncology, Ultrasound, and Pathology made the diagnosis - non-retroareolar MMBC without gynecomastia. The patient was hospitalized and underwent modified radical mastectomy (MRM) for breast cancer on December 30, 2022, Intraoperatively, the gynecomastia was seen to be very thin, but the area was equivalent to that of a female. Pathological return: No cancerous tissue invasion of the nipple and pectoralis major fascia, peri-cancerous breast: Granulomatous inflammation, postoperative lymph nodes: 0/20 (extra-pectoralis minor 0/19; post-pectoralis minor 0/1), pT2N0M0.

OUTCOME AND FOLLOW-UP

Postoperative axillary and supracostal arch drains were less than 20 mL for three consecutive days starting on postoperative day 6 and were removed on day 9. The patient had no adverse complaints. The flap hemorrhage in the operative area was normal. Perioperative care was equivalent to that of female breast cancer (FBC) and no significant discomfort for the patient during treatment. Tamoxifen (20 mg/d) was administered as adjuvant therapy (Figure 3). The patient was followed up every three months in the outpatient clinic. The follow-up tumor marker carbohydrate antigen 153 fluctuated in the fifth month, and CT and ultrasound showed no abnormality.

DISCUSSION

MBC occurrence in men accounts for less than 1% of all breast cancer cases, and malignant tumors develop in less than 1% of affected men[11]. Different risk factors concurrently impact MBC development, including clinical disorders related to hormonal imbalance, such as obesity, testicular disease, and radiation exposure; suspected epidemiological risk factors are prostate cancer, prostate cancer treatment, occupational exposure, dietary factors, and alcohol intake[12]. By contrast, carrying a BRCA2 mutation confers a lifetime risk for MBC to the male carrier, which is approximately 80-100 times

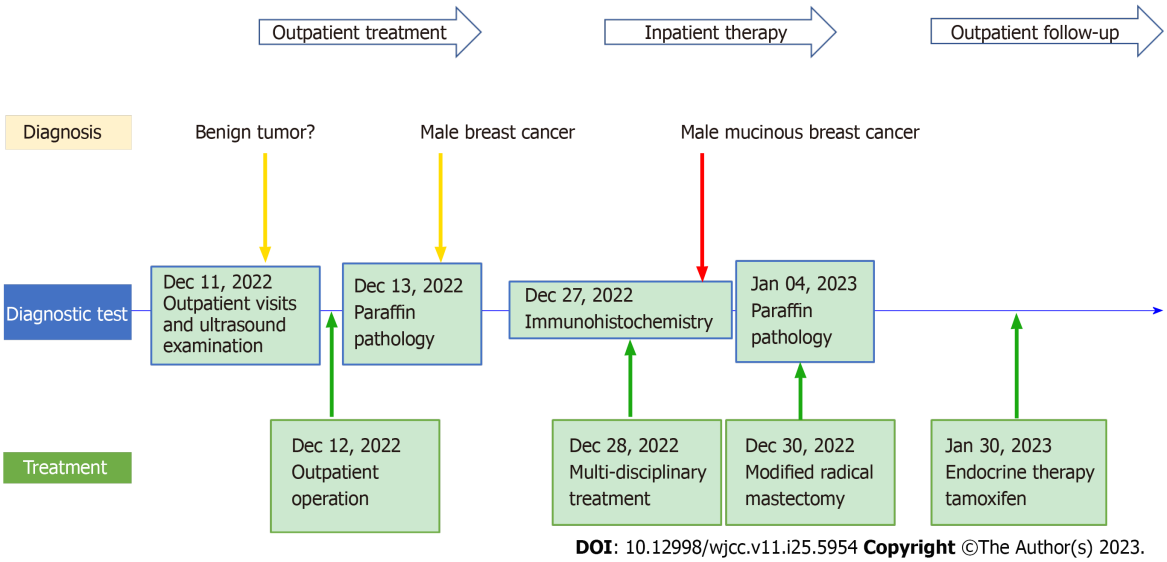

DOI: 10.12998/wjcc.v11.i25.5954

Figure 3 Timeline of disease course.

higher than that in the general population[13]. The rate of mucinous adenocarcinoma of all invasive breast drops from 4% to 2%[2,14]. Mucinous breast cancer rarely occurs in men. A single-center trial retrospectively assessed 16868 breast cancer patients over 10 years, with 72 cases of MBC accounting for 0.42% of the total patient population and six cases of mucinous adenocarcinoma accounting for 8.33% of the total MBC patient population[15].

The presence of extracellular mucin on microscopic observation is the basis for the microscopic diagnosis of mucinous breast cancer, defined as pure mucinous cancer and mixed mucinous cancer (MMC) at a cutoff of 90%. MMC can be further differentiated into partially mixed mucinous adenocarcinoma and mixed mucinous adenocarcinoma at a cutoff of 50%. Immunohistochemistry analysis revealed that the expression of estrogen and progesterone receptors was positive, and that of the androgen receptor was negative.

A 71-year-old MBC patient was treated by a physician in Virginia in the 1970s[16]. Although he had bilateral breast cancer, the pathology was not fully documented. However, searches for PubMed, several cases of male mucinous breast cancer cases have been successfully treated in recent decades. We have summarized and analyzed mucinous adenocarcinoma cases among men (Table 1). As assessed using hematoxylin-eosin staining, all patients had mucinous adenocarcinoma[8-10,17-22]. In one case, the lesion type was mixed invasive ductal carcinoma (IDC) component[17], and in another case, the lesion type was concurrent breast mucinous carcinoma and extramammary lymphoma[8]. The patient's age ranged from 35 to 83 years, with a mean age of 69.3 years. The history of onset ranged from 2-96 mo, with a median time of nearly 12 mo, and swelling of the retroareolar region is the main factor for tumor development. No significant difference was noted in the location of the masses to the left and right (four left and five right). All of them were located posterior to the nipple-areolar region, except for one case wherein the mass was present in the axillary position. The mass diameter was used as a statistical criterion, with a minimum value of 13 mm, a maximum value of 95 mm, and a mean diameter length of 44.5 mm. Four of the eight patients who reported lymph node metastasis had combined lymph node metastasis (50%). HER-2/CerbB-2 was tested in four patients with non-amplified or negative expressions. BRCA testing was negative in two patients with combined diffuse large B-cell tumors and those with an IDC component. All patients had MRM at the correct location. A Japanese patient underwent MRM after two resections of enlarged masses within a period of 3 years until the fifth year, which was when the mass recurred and showed ipsilateral axillary lymph node enlargement[22]. Postoperative adjuvant therapy revealed the following findings: All patients were treated with tamoxifen hormone therapy, and two patients with positive axillary lymph nodes received radiotherapy; chemotherapy combined with hormone therapy was observed in four patients before 2010 but not in four patients after 2010. Patients underwent follow-up for a maximum of 60 mo and a minimum of 8 mo after surgery, and no recurrence or metastasis was reported during the postoperative period of MRM, regardless of whether they had combined axillary lymph node metastases.

Having presented the case, we now move on to discuss the broader implications and findings. In summary, the median age of onset of mucinous adenocarcinoma in men is above 70 years. The history of onset of MMBC patients is longer than a year, and the average mass size is greater than 40 mm; however, MMBC is frequently overlooked. The chief complaint and the primary clinical manifestation of patients are swelling behind the nipple region or skin changes in the nipple region. Patients with axillary metastatic lymph nodes had a predominantly 1-year history and a smaller average mass size than the other patients; hence, it cannot be speculated that the length of history and mass size are the key factors attributed to the occurrence of lymph node metastasis. Generally, the trend in postoperative adjuvant therapy has switched from chemotherapy combined with endocrine therapy before 2010 to predominantly hormone therapy alone after 2010, considering that it was influenced by the treatment of luminal-type FBC, while the treatment strategy changed the same. All patients had better prognoses than men with nonspecific breast cancer. Previous case reports have shown that the retroareolar mass usually occurs with gynecomastia and is in the inner margin of the nipple[22]. Another case of

Table 1 Clinical case characterization

Ref.	Country	Age (yr)	Case history (yr)	Laterality	Past history	Tumor max-diameter	Tumor location	Pathology characteristic	Lymphatic metastasis	ER	PR	HER2/CerbB-2	KI67 %	BRCA	Surgery	Adjuvant therapy	DFS (mo)
Fujikawa *et al* [20], 1998	Japan	35	2	Right	Negative	80	Areola	M	Negative	Positive	Positive	None	None	None	MRM	C + TAM	30
Peschos *et al* [19], 2008	Greece	83	None	Left	None	70	Areola	M	None	Positive	Positive	None	None	None	MRM	C + TAM	None
Hammedi *et al* [10], 2010	Tunisia	75	2 mo	Right	Negative	40	Areola	M	Positive + 2	Negative	Positive	Negative	None	None	MRM	C + R + TAM	36
Dragoumis *et al* [21], 2012	Greece	59	1	Right	Negative	30	Areola	M	Positive	Positive	Positive	Negative	None	None	MRM	C + R + TAM	74
Imakado and Masuda[22], 2012	Japan	72	3	Left	Negative	20	Areola-aside	M	Positive	Positive	Positive	None	None	None	MRM	TAM	60
Gupta *et al*[18], 2015	India	73	8	Right	Negative	95	Areola	M	Negative	Positive	Positive	Middle 2	11	None	MRM	TAM	8
Kim and Lee[8], 2021	Korean	78	1	Left	Negative	35	Areola	M + B-cell	Positive + 2	None	None	None	None	Negative	MRM	C + TAM	11
Takahashi *et al* [17], 2021	Japan	75	None	Right	Sister breast cancer	13	Axilla	M + IDC	Negative	Positive	Positive	Negative	33	Negative	MRM	TAM	24
Ahmed *et al*[9], 2022	United States	74	1	Left	Thyroid cancer	18	Areola	M	Negative	None	None	None	None	None	MRM	TAM	48

ER: Estrogen receptor; PR: Progesterone receptor; BRCA: Breast cancer susceptibility gene; DFS: Disease free survival; TAM: Tamoxifen; MRM: Modified radical mastectomy; M: Mastectomy; C: Chemotherapy; R: Radiotherapy.

mucinous breast cancer combined with Paget's disease also had a nipple-centered clinical presentation[17]. We present the first case of MMBC in the non-retroareolar region of the nipple. The patient had no evident signs of gynecomastia, and the mass was located on the upper outer nipple at an easily misdiagnosed distance. The absence of cancerous tissue in the nipple and posterior glands confirmed this finding. Similar to this finding, Mizutani *et al*[23] reported a rare case of cutaneous mucinous adenocarcinoma in a 78-year-old man. In the fourth year of follow-up review after prostate cancer treatment, an abnormally enlarged axillary lymph node (10 mm) was found, and a whole-body examination revealed the presence of a 30-mm-sized mass in the patient's inner upper right chest. For several years, the patient complained of a mass in the right chest but did not pay close attention to it; eventually, the mass was surgically excised as a benign 1-cm margin plus axillary lymph node dissection, and no breast tissue was found in the pathological specimen, but the enlarged axillary lymph node, which was the patient's chief complaint, demonstrated mucinous adenocarcinoma metastasis [23]. This led to the following conclusions: (1) Mucinous tumors are easily missed; and (2) The incidence of axillary lymph node metastases of chest mucinous tumors is higher than that anticipated. Considering the previously mentioned three

surgical recurrence cases in Japan[22] and the 50% rate of axillary lymph node metastasis in cases of male mucinous adenocarcinoma, as summarized here, MRM, including treatment for axillary lymph nodes, is an essential treatment approach for MMBC patients. Because of the rarity of MBC, most of the affected patients have not been assessed in treatment studies in past studies; therefore, treatment strategies for MBC have been largely extrapolated from evidence for FBC[24,25]. Based on immunohistochemical characteristics, mucinous adenocarcinoma of the male breast is equivalent to the luminal-type treatment strategy for postmenopausal FBC[26].

In our case, the patient's gynecomastia symptoms are not visible because of the patient's low BMI and the absence of fat encapsulation in the gland beneath the skin. The patient was considered to have an atypical clinical presentation of MMBC, and MRM is essential. Because of the strong expression of the hormone receptors (estrogen and progesterone receptors), low tumor cell proliferation index indicated by Ki67, and negative pathological axillary lymph nodes, the patient would have a well-predicted prognosis. A 5-year outpatient follow-up with endocrine treatment is required.

CONCLUSION

We encountered a rare case of MMBC. It was difficult to differentiate from MBC because the patient had no representative clinical indications of gynecomastia, and the mass was located distant from the nipple region. A diagnosis of male mucinous breast cancer should be considered, even when the body surface mass on the male chest is not located in the retroareolar region, and MRM and endocrine treatment is necessary.

FOOTNOTES

Author contributions: Sun Q designed the proposal and drafted the manuscript; Liu XY participated in immunohistochemical stain and analysis; Jiang H and Sun Q carried out the ultrasound analysis; Sun Q participated in data collection; Sun Q, Zhang Q, Liu XY, and Jiang H participated in total data analysis; and all authors read and approved the final manuscript.

Informed consent statement: All study participants, or their legal guardian, provided informed written consent prior to study enrollment.

Conflict-of-interest statement: All the authors report no relevant conflicts of interest for this article.

CARE Checklist (2016) statement: The authors have read the CARE Checklist (2016), and the manuscript was prepared and revised according to the CARE Checklist (2016).

Country/Territory of origin: China

ORCID number: Qiang Sun 0000-0001-5936-8086; Xu-Yan Liu 0000-0002-9892-9752; Qi Zhang 0000-0002-7303-1399; Hai Jiang 0000-0003-4826-8500.

S-Editor: Wang JJ
L-Editor: A
P-Editor: Wang JJ

REFERENCES

1 **Fox S**, Speirs V, Shaaban AM. Male breast cancer: an update. *Virchows Arch* 2022; **480**: 85-93 [PMID: 34458944 DOI: 10.1007/s00428-021-03190-7]
2 **Limaiem F**, Ahmad F. Mucinous Breast Carcinoma. 2023 Feb 12. In: StatPearls [Internet]. Treasure Island (FL): StatPearls Publishing; 2023 Jan- [PMID: 30855918]
3 **McClurg DP**, Urquhart G, McGoldrick T, Chatterji S, Miedzybrodzka Z, Speirs V, Elsberger B. Analysis of the Clinical Advancements for BRCA-Related Malignancies Highlights the Lack of Treatment Evidence for BRCA-Positive Male Breast Cancer. *Cancers (Basel)* 2022; **14** [PMID: 35804947 DOI: 10.3390/cancers14133175]
4 **Gucalp A**, Traina TA, Eisner JR, Parker JS, Selitsky SR, Park BH, Elias AD, Baskin-Bey ES, Cardoso F. Male breast cancer: a disease distinct from female breast cancer. *Breast Cancer Res Treat* 2019; **173**: 37-48 [PMID: 30267249 DOI: 10.1007/s10549-018-4921-9]
5 **Fentiman IS**, Fourquet A, Hortobagyi GN. Male breast cancer. *Lancet* 2006; **367**: 595-604 [PMID: 16488803 DOI: 10.1016/S0140-6736(06)68226-3]
6 **Cardoso F**, Bartlett JMS, Slaets L, van Deurzen CHM, van Leeuwen-Stok E, Porter P, Linderholm B, Hedenfalk I, Schröder C, Martens J, Bayani J, van Asperen C, Murray M, Hudis C, Middleton L, Vermeij J, Punie K, Fraser J, Nowaczyk M, Rubio IT, Aebi S, Kelly C, Ruddy KJ, Winer E, Nilsson C, Lago LD, Korde L, Benstead K, Bogler O, Goulioti T, Peric A, Litière S, Aalders KC, Poncet C, Tryfonidis K, Giordano

SH. Characterization of male breast cancer: results of the EORTC 10085/TBCRC/BIG/NABCG International Male Breast Cancer Program. *Ann Oncol* 2018; **29**: 405-417 [PMID: 29092024 DOI: 10.1093/annonc/mdx651]

7 **Ruddy KJ**, Winer EP. Male breast cancer: risk factors, biology, diagnosis, treatment, and survivorship. *Ann Oncol* 2013; **24**: 1434-1443 [PMID: 23425944 DOI: 10.1093/annonc/mdt025]

8 **Kim SY**, Lee JY. Multiple Primary Malignant Neoplasms: A Case Report of Breast Mucinous Carcinoma and Extramammary Diffuse Large B-Cell Lymphoma in a Male Patient. *Taehan Yongsang Uihakhoe Chi* 2021; **82**: 729-736 [PMID: 36238796 DOI: 10.3348/jksr.2020.0140]

9 **Ahmed U**, Wagner S, Jordan S. Mucinous carcinoma in a male patient: Diagnosis and management of breast cancer in male patients. *Radiol Case Rep* 2022; **17**: 124-128 [PMID: 34815818 DOI: 10.1016/j.radcr.2021.10.015]

10 **Hammedi F**, Trabelsi A, Abdelkrim SB, Abid LB, Jomaa W, Bdioui A, Beizig N, Mokni M. Mucinous carcinoma with axillary lymph node metastasis in a male breast: A case report. *N Am J Med Sci* 2010; **2**: 111-113 [PMID: 22624124]

11 **Siegel RL**, Miller KD, Jemal A. Cancer statistics, 2020. *CA Cancer J Clin* 2020; **70**: 7-30 [PMID: 31912902 DOI: 10.3322/caac.21590]

12 **Khan NAJ**, Tirona M. An updated review of epidemiology, risk factors, and management of male breast cancer. *Med Oncol* 2021; **38**: 39 [PMID: 33721121 DOI: 10.1007/s12032-021-01486-x]

13 **Rizzolo P**, Silvestri V, Tommasi S, Pinto R, Danza K, Falchetti M, Gulino M, Frati P, Ottini L. Male breast cancer: genetics, epigenetics, and ethical aspects. *Ann Oncol* 2013; **24** Suppl 8: viii75-viii82 [PMID: 24131976 DOI: 10.1093/annonc/mdt316]

14 **Anderson WF**, Chu KC, Chang S, Sherman ME. Comparison of age-specific incidence rate patterns for different histopathologic types of breast carcinoma. *Cancer Epidemiol Biomarkers Prev* 2004; **13**: 1128-1135 [PMID: 15247123]

15 **Liu DY**, Xie GR, Chen M. [Analysis on the clinical and prognostic features of 71 male patients with breast cancer]. *Zhonghua Liu Xing Bing Xue Za Zhi* 2013; **34**: 187-190 [PMID: 23751479]

16 **Brodie EM**, King ER. Histologically different, synchronous, bilateral carcinoma of the male breast (a case report). *Cancer* 1974; **34**: 1276-1277 [PMID: 4371379 DOI: 10.1002/1097-0142(197410)34:4<1276::AID-CNCR2820340439>3.0.CO;2-W]

17 **Takahashi E**, Terata K, Nanjo H, Ishiyama K, Hiroshima Y, Yamaguchi A, Yatsuyanagi M, Kudo C, Wakita A, Takashima S, Sato Y, Imai K, Motoyama S, Minamiya Y. A male with primary accessory breast carcinoma in an axilla is strongly suspected of having hereditary breast cancer. *Int Cancer Conf J* 2021; **10**: 107-111 [PMID: 33782642 DOI: 10.1007/s13691-020-00466-8]

18 **Gupta K**, Sharma S, Kudva R, Kumar S. Mixed Mucinous and Infiltrating Carcinoma Occurring in Male Breast- Study of Clinico-Pathological Features: A Rare Case Report. *J Clin Diagn Res* 2015; **9**: ED07-ED08 [PMID: 26266132 DOI: 10.7860/JCDR/2015/12209.6090]

19 **Peschos D**, Tsanou E, Dallas P, Charalabopoulos K, Kanaris C, Batistatou A. Mucinous breast carcinoma presenting as Paget's disease of the nipple in a man: a case report. *Diagn Pathol* 2008; **3**: 42 [PMID: 18950495 DOI: 10.1186/1746-1596-3-42]

20 **Fujikawa T**, Sonobe M, Nishimura S, Matsusue S, Takeda H, Nakamura Y. A case of Mucinous Carcinoma of the Male Breast with Unusual Ultrasonographic Findings Mimicking Phyllodes Tumor. *Breast Cancer* 1998; **5**: 83-86 [PMID: 11091631 DOI: 10.1007/BF02967420]

21 **Dragoumis DM**, Assimaki AS, Tsiftsoglou AP. Pure mucinous carcinoma with axillary lymph node metastasis in a male breast. *Breast Cancer* 2012; **19**: 365-368 [PMID: 19756925 DOI: 10.1007/s12282-009-0163-3]

22 **Imakado S**, Masuda R. A case of carcinoma of the male breast mimicking a mucinous carcinoma of the skin. *Clin Pract* 2012; **2**: e61 [PMID: 24765460 DOI: 10.4081/cp.2012.e61]

23 **Mizutani K**, Taira M, Akiyama M. Primary mucinous carcinoma of the skin on the breast with lymph node metastasis. *J Dermatol* 2014; **41**: 760-761 [PMID: 25040615 DOI: 10.1111/1346-8138.12556]

24 **Yadav S**, Karam D, Bin Riaz I, Xie H, Durani U, Duma N, Giridhar KV, Hieken TJ, Boughey JC, Mutter RW, Hawse JR, Jimenez RE, Couch FJ, Leon-Ferre RA, Ruddy KJ. Male breast cancer in the United States: Treatment patterns and prognostic factors in the 21st century. *Cancer* 2020; **126**: 26-36 [PMID: 31588557 DOI: 10.1002/cncr.32472]

25 **Zheng G**, Leone JP. Male Breast Cancer: An Updated Review of Epidemiology, Clinicopathology, and Treatment. *J Oncol* 2022; **2022**: 1734049 [PMID: 35656339 DOI: 10.1155/2022/1734049]

26 Male Breast Cancer Treatment (PDQ®): Health Professional Version. 2023 Mar 10. In: PDQ Cancer Information Summaries [Internet]. Bethesda (MD): National Cancer Institute (US); 2002– [PMID: 26389234]

World Journal of Clinical Cases

Submit a Manuscript: https://www.f6publishing.com

World J Clin Cases 2023 September 6; 11(25): 5962-5969

DOI: 10.12998/wjcc.v11.i25.5962

ISSN 2307-8960 (online)

CASE REPORT

Autosomal dominant non-syndromic hearing loss caused by a novel mutation in *MYO7A*: A case report and review of the literature

Cai-Feng Xia, Rong Yan, Wen-Wen Su, Yu-He Liu

Specialty type: Medicine, research and experimental

Provenance and peer review: Unsolicited article; Externally peer reviewed.

Peer-review model: Single blind

Peer-review report's scientific quality classification

Grade A (Excellent): 0
Grade B (Very good): 0
Grade C (Good): C
Grade D (Fair): D
Grade E (Poor): 0

P-Reviewer: Mirsalehi M, Iran; Naz S, Pakistan

Received: May 13, 2023
Peer-review started: May 13, 2023
First decision: July 3, 2023
Revised: July 16, 2023
Accepted: August 8, 2023
Article in press: August 8, 2023
Published online: September 6, 2023

Cai-Feng Xia, Rong Yan, Wen-Wen Su, Yu-He Liu, Department of Otolaryngology Head and Neck Surgery, Peking University First Hospital, Beijing 100034, China

Yu-He Liu, Department of Otolaryngology Head and Neck Surgery, Beijing Friendship Hospital, Capital Medical University, Beijing 100050, China

Corresponding author: Yu-He Liu, MD, Chief Doctor, Doctor, Professor, Department of Otolaryngology Head and Neck Surgery, Beijing Friendship Hospital, Capital Medical University, No. 95 Yongan Road, Xicheng District, Beijing 100050, China.
liuyuhefeng@163.com

Abstract

BACKGROUND

Variants in the *MYO7A* gene commonly result in Usher syndrome, and in rare cases lead to autosomal dominant non-syndromic deafness (DFNA11). Currently, only nine variants have been reported to be responsible for DFNA11 and their clinical phenotypes are not identical. Here we present a novel variant causing DFNA11 identified in a three-generation Chinese family.

CASE SUMMARY

The proband was a 53-year-old Han male who presented with post-lingual bilateral symmetrical moderate sensorineural hearing loss. We learned from the patient's medical history collection that multiple family members also had similar hearing loss, generally occurring around the age of 40. Subsequent investigation by high-throughput sequencing identified a novel *MYO7A* variant. To provide evidence supporting that this variant is responsible for the hearing loss in the studied family, we performed Sanger sequencing on 11 family members and found that the variant co-segregated with the deafness phenotype. In addition, the clinical manifestation of the 11 affected family members was found to be late-onset bilateral slowly progressive hearing loss, inherited in this family in an autosomal dominant manner. None of the affected family members had visual impairment or vestibular symptoms; therefore, we believe that this novel *MYO7A* variant is responsible for the rare DFNA11 in this family.

CONCLUSION

We report a novel variant leading to DFNA11 which further enriches the collection of *MYO7A* variants, and our review of the nine previous variants that have been identified to cause DFNA11 provides a reference for clinical genetic counseling.

Key Words: Autosomal dominant hearing loss; *MYO7A* gene; Non-syndromic hearing loss; Variant; Hereditary hearing loss; Case report

Core Tip: Autosomal dominant non-syndromic hearing loss caused by the *MYO7A* variant (DFNA11) is rare and characterized by post-lingual sensorineural hearing loss with no or mild vestibular dysfunction. To date, only nine variants have been identified to be responsible for DFNA11. Here we present a novel variant (c.1531G>A) causing DFNA11 identified in a three-generation Chinese family. Progressive hearing loss is the only clinical manifestation in this family, and the onset age of affected members is later and more concentrated than that of other DFNA11 families. Our findings further enrich the collection of *MYO7A* mutations, and our review of the nine reported DFNA11 families can provide a reference for clinical genetic counseling.

Citation: Xia CF, Yan R, Su WW, Liu YH. Autosomal dominant non-syndromic hearing loss caused by a novel mutation in *MYO7A*: A case report and review of the literature. *World J Clin Cases* 2023; 11(25): 5962-5969
URL: https://www.wjgnet.com/2307-8960/full/v11/i25/5962.htm
DOI: https://dx.doi.org/10.12998/wjcc.v11.i25.5962

INTRODUCTION

Hearing loss is the most common clinical manifestation in otology, with both genetic and environmental etiologies. Genetic factors account for approximately 60% of cases[1,2]. To date, more than 150 genes have been linked to hearing loss (https://hereditaryhearingloss.org), including *GJB2, GJB3, SLC26A4*, and *MYO7A*. *MYO7A* is located at 11q13.5, has 49 exons encoding 2215 amino acids, and is mainly expressed in the inner ear, retina, testis, lungs, and kidneys[3]. Variants in *MYO7A* can cause both syndromic (Usher syndrome)[4-6] and non-syndromic deafness, with the latter including autosomal dominant (DFNA11) and autosomal recessive (DFNB2) inheritance patterns[7-9].

Usher syndrome is the most common consequence of *MYO7A* variants, in which patients experience congenital sensorineural hearing loss, progressive retinitis pigmentosa, and vestibular dysfunction. Furthermore, severe cases can lead to deaf-mutism, total blindness, intellectual disability, and other disorders[10,11]. In contrast, the clinical symptoms of DFNB2 caused by the *MYO7A* gene variant are milder than those of Usher syndrome and are mainly characterized by congenital sensorineural hearing loss and vestibular dysfunction. A study by Astuto *et al*[12] found late-onset mild visual impairment in members of a family with DFNB2. Hence, the authors determined that DFNB2 and Usher syndrome are different stages of the same disease. However, this conclusion remains controversial, and visual impairment is still commonly used as the primary criterion to distinguish syndromic from non-syndromic hearing loss caused by *MYO7A*. Moreover, DFNA11 is the rarest consequence of the *MYO7A* gene variant and mainly manifests as delayed post-lingual sensorineural hearing loss. Most patients with DFNA11 present with mild or no vestibular dysfunction, but all cases exhibit normal vision[13,14]. To date, no specific association between clinical manifestations and variant location has been found, and only nine variants have been identified as causing DFNA11. The rarity of DFNA11 combined with its occult and atypical clinical manifestations makes the diagnosis of DFNA11 more challenging.

Here, we describe a novel variant in the *MYO7A* gene (c.1531G>A) that caused DFNA11 in a three-generation Chinese family. All affected members of this family presented with bilateral progressive sensorineural hearing loss beginning in adulthood. Additionally, we provide a summary of the clinical and genetic features observed in previously reported families with DFNA11.

CASE PRESENTATION

Chief complaints

The proband was a 53-year-old Han male who sought treatment at the outpatient clinic of Peking University First Hospital for progressive hearing loss in both ears, manifested for more than 10 years.

History of present illness

The patient presented with bilateral hearing loss that began around the age of 40 and gradually affected daily listening and communication. There were no vestibular disorders such as vertigo or unsteady walking.

History of past illness

The patient had no history of past illness.

Personal and family history
The patient had no history of noise exposure, otitis media, or ototoxic drug use. However, it was understood that several of the patient's family members had similar symptoms, with slowly progressive bilateral hearing loss, also beginning around the age of 40. Therefore, we contacted 11 additional members of the patient's family (including four members experiencing hearing loss) and obtained their consent to participate in our study (Figure 1). The first member of the third generation (III:1) had a history of noise exposure for about 20 years because of his work. The remaining 11 family members had no history of noise exposure, otitis media, or ototoxic drug use.

Physical examination
No abnormality was found in the ear examination of the 12 family members.

Laboratory examinations
The proband's routine blood, liver function, renal function, and coagulation function tests showed no obvious abnormalities.

Imaging examinations
Five family members with deafness were examined by high-resolution computed tomography of the temporal bone, and no obvious abnormality was found.

Hearing, vestibular function, and eye examinations
We found that all five affected members had bilateral symmetrical moderate to profound sensorineural hearing loss (Figure 2). The audiograms of the affected family members were flat or slightly sloping, and high-frequency hearing loss was particularly severe. And none of them had vestibular dysfunction or visual impairment.

Genetic analysis
After written informed consent was obtained from all participants or their guardians, peripheral blood samples were collected for genetic analysis. High-throughput sequencing was used for the proband, including the exons of 415 genes, and partial deep intron regions of 147 genes reported by the Human Gene Mutation Database (https://www.hgmd.cf.ac.uk/) were also detected. The coverage density of the probe (GenCap deafness gene capture probe V4.0, https://www.mygeno.cn/) was increased in 29 common deafness pathogenic genes, among which *GJB2*, *SLC26A4*, and *POU3F4* were covered in full length. Deafness-related genes in the mitochondrial circular DNA were also detected using GenCap Mitochondrial Loop Gene Capture Probe V1.0 (MyGenostics, Beijing, China). Then five candidate variants were identified in the proband: *MYO7A* (c.1531G>A), *TRIOBP* (c.3689C>T), *WHRN* (c.2090C>T), *USH1C* (1534G>A), and *PDZD7* (c.1529G>A). These variants were annotated using ANNOVAR (v20200607)[15] and compared with the Exome Aggregation Consortium (ExAC, v0.3.1, Broad Institute, United States), 1000 Genomes (http://www.1000genomes.org/), and Genome Aggregation Database (gnomAD, http://www.gnomad-sg.org/) databases. The pathogenicity of the variants was predicted using Rare Exome Variant Ensemble Learner (REVEL, https://sites.google.com/site/revelgenomics/), Mutation Taster (https://www.mutationtaster.org/), and PolyPhen2 (http://genetics.bwh.harvard.edu/pph2/) programs. At the same time, we obtained the spatial structure of the MYO7A protein with AlphaFold2 (https://alphafold.ebi.ac.uk), and then used PyMOL (v2.5.4, Schrodinge, United States) to map and analyze the effect of the mutation on the structure of MYO7A protein. Finally, Sanger sequencing of the remaining 11 family members showed that only *MYO7A* (c.1531G>A) co-segregated with the deafness phenotype. This variant resulted in the conversion of Asp to Asn at position 511 of the MYO7A protein (Figure 3A), an amino acid highly conserved among species (Figure 3B). This variant was not detected in the control group consisting of 200 Chinese Han individuals with normal hearing, or in the ExAC, 1000 Genomes, or gnomAD database. The pathogenicity of this variant was predicted to be "probably damaging" (0.994) by PolyPhen-2, "damaging" (0.853) by REVEL, and "disease-causing" (1.000) by Mutation Taster. As shown in Figure 3C, the Asp at position 511 of wild-type MYO7A protein is located in the motor domain, has three hydrogen bonds with surrounding amino acids, and has electrostatic interaction with Lys at position 515. However, the p.Asp511Asn variant loses one hydrogen bond and the only electrostatic interaction.

FINAL DIAGNOSIS
The phenotype of deafness in this family was typical of late onset and progressive sensorineural hearing loss, which is consistent with that reported in other families with DFNA11. The *MYO7A* (c.1531G>A, p.D511N) variant co-segregated with the deafness phenotype in an autosomal dominant pattern in this family. The variant was not detected in 200 normal hearing controls, or in the ExAC, 1000 Genomes, or gnomAD database. Finally, the variant was predicted to be generally damaging by REVEL, Mutation Taster, and PolyPhen2. The p.511D is highly conserved among species, and PyMOL analysis suggests that the structural stability of the MYO7A protein was destroyed after Asp was replaced by Asn in the variant. Based on the above evidence and following the criteria of the American College of Medical Genetics and Genomics, we diagnosed the affected members of this family with autosomal dominant hearing loss caused by the *MYO7A* (c.1531G>A, p.D511N) variant.

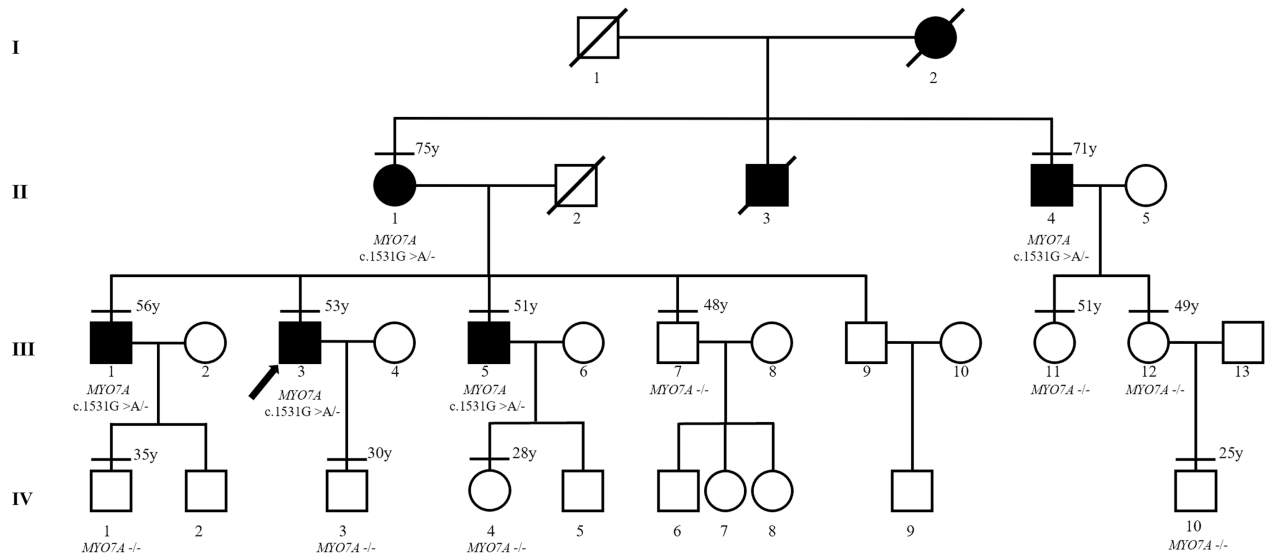

DOI: 10.12998/wjcc.v11.i25.5962 **Copyright** ©The Author(s) 2023.

Figure 1 Pedigree of the DFNA11 family. The arrow indicates the proband. Horizontal lines above the individuals indicate that genetic testing was performed. The age of each subject at the time of genetic testing is listed on the top-right region of each symbol. The genotype of *MYO7A* for each individual is indicated below the symbol, heterozygous mutant: c.1531G>A/- or wild type: -/-.

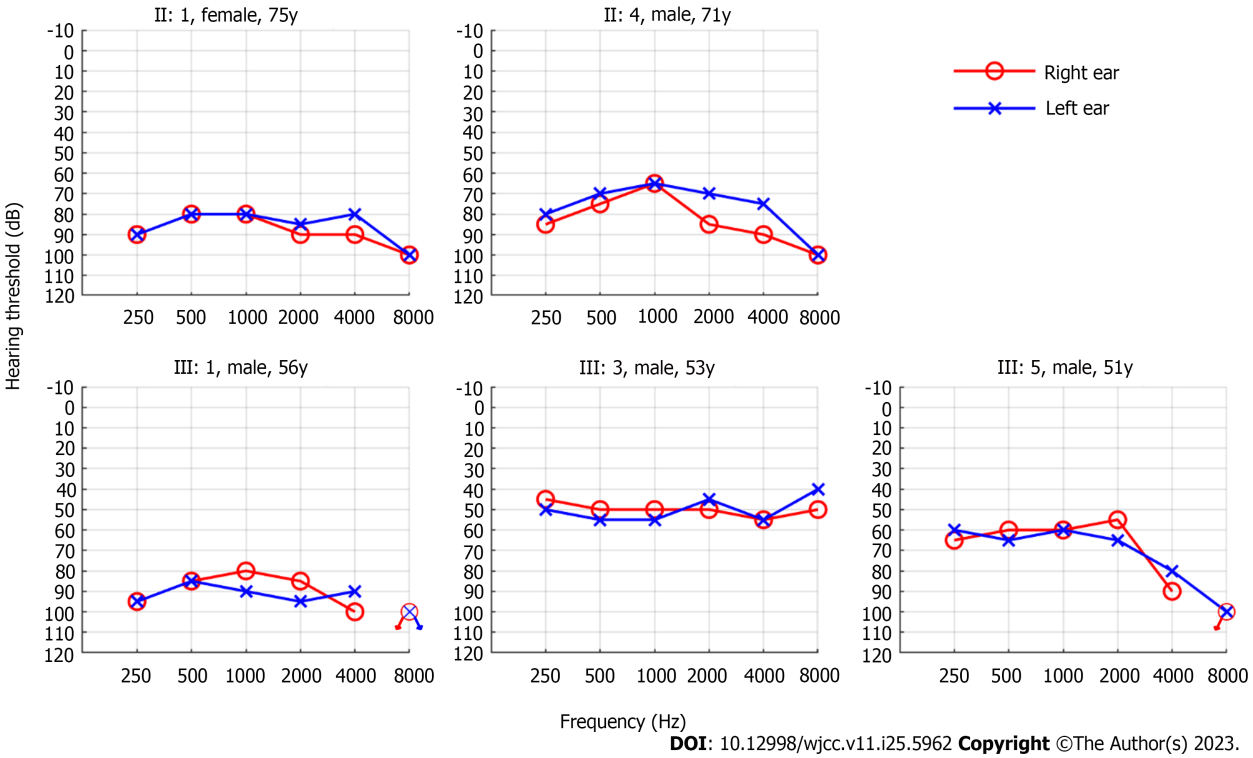

DOI: 10.12998/wjcc.v11.i25.5962 **Copyright** ©The Author(s) 2023.

Figure 2 Pure-tone audiogram of the five affected members in this family. Each person presented bilateral symmetrical moderate-to-profound sensorineural hearing loss, with audiograms that were either flat or slightly downward-sloping at high frequencies. Specifically, III:1 had particularly profound hearing loss owing to occupational noise exposure.

TREATMENT

We advised the five hearing-impaired members to protect their residual hearing by avoiding exposure to noise and ototoxic drugs. In addition, the family members were advised to wear hearing aids to improve hearing and daily communication.

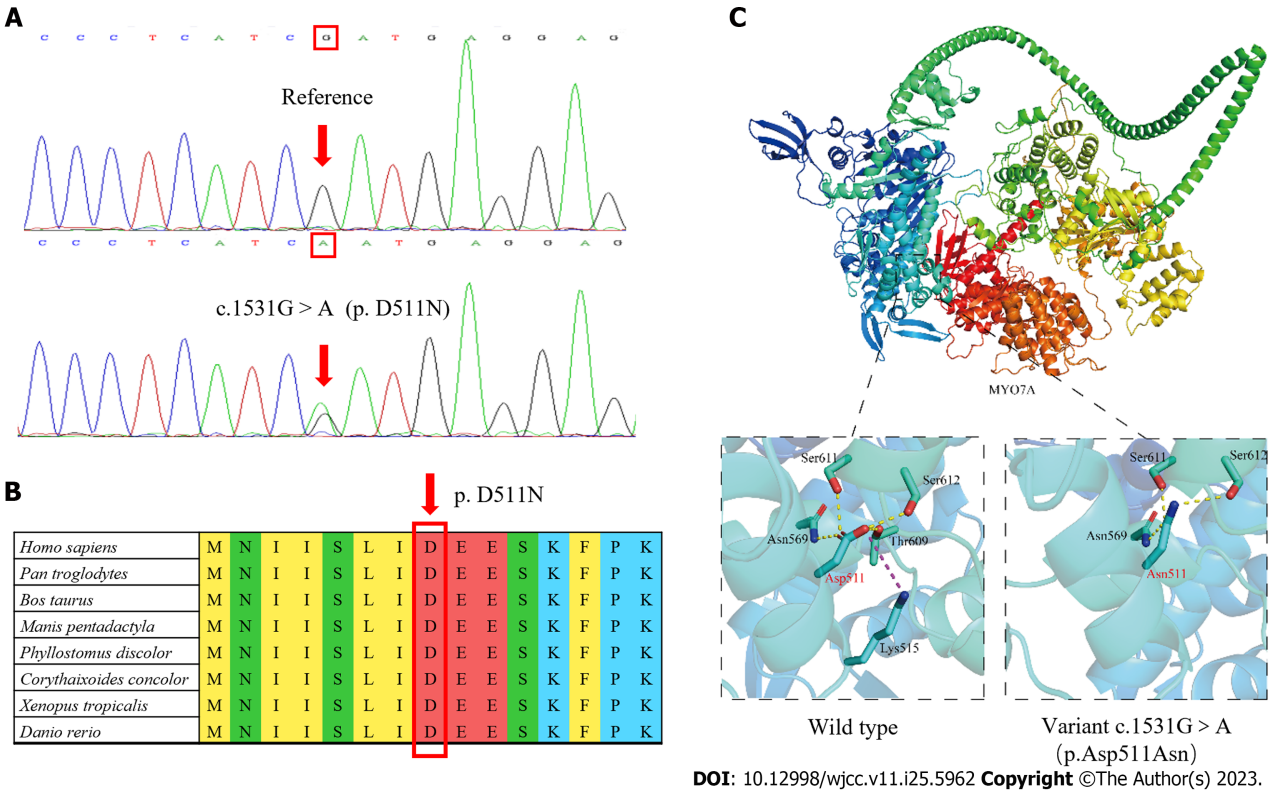

DOI: 10.12998/wjcc.v11.i25.5962

Figure 3 Location of nucleotide changes and functional analysis of the variant. A: DNA sequence chromatograms. Arrows indicate the site of the mutation, which results in the p.D511N variant; B: Evolutionary conservation of Asp at position 511 (indicated by the arrow) on the MYO7A protein; C: The wild-type and variant (p.D511N) of the MYO7A protein. Yellow dashed lines represent hydrogen bonds between amino acids, and the purple dashed line represent electrostatic interaction between amino acids.

OUTCOME AND FOLLOW-UP

Hearing aids greatly improved the hearing and quality of life for the affected family members, as we learned in our telephone follow-ups 3 mo later. Considering that all participants' hearing loss will progress with age, they were encouraged to make regular follow-up visits and facilitate timely adjustment of hearing aid parameters.

Review of the literature

We searched for articles in the PubMed database published up to December 2022 using the keywords "DFNA11", "*MYO7A*", "autosomal dominant inheritance", and "hearing loss". A total of 11 families with DFNA11, including nine *MYO7A* mutation sites, were identified by genetic analysis. The genotype, hearing status, age of onset, and other information of these families are shown in Table 1[8,13,14,16-22].

DISCUSSION

Since the first family with DFNA11 was reported by Liu *et al* in 1997[8], nine variants from 11 families have been identified to be responsible for DFNA11. The clinical phenotypes of deafness in members of these families with DFNA11 varied; however, most presented with post-lingual progressive sensorineural hearing loss[16,20]. In the family of this study, the affected members presented bilateral symmetrical sensorineural hearing loss. The audiograms of the affected family members were flat or slightly sloping, and high-frequency hearing loss was particularly severe, which is consistent with the symptoms previously reported in families with DFNA11[13,14,20]. In the family of this study, the onset age of hearing loss among affected members was relatively late and concentrated, occurring at around 40 years old. This differs from most reported families with DFNA11, where the age span of onset is larger and hearing loss occurred before adulthood in many cases[14,17,22]. The hearing loss of the second-generation members was generally more severe than that of the third-generation members, which also horizontally reflects that hearing loss progresses with age. However, differences were observed between III:1, III:3, and III:5, who were in the same age group. Although the presence of genetic modifications cannot be excluded[23], environmental effects on the phenotype, such as chronic exposure to noise (*i.e.*, III:1), should also be considered. Therefore, the preservation of residual hearing is one of the important therapeutic measures. Moreover, it is essential to select hearing aid devices according to the hearing threshold and actual needs of each patient, to minimize the impact of DFNA11 on their daily life.

Table 1 Summary of the identified DFNA11 variants

Mutation	Exon	Structure	Patient number	Age of onset (yr)	Audiogram	Vestibular symptoms	Family origin	Ref.
c.2656-2664del/A886-K888Del	22	Coiled coil	8/19	12-16	Flat/sloping	Absent	Japan	[8]
c.652G>A/p.D218N	7	Motor domain	11/29	20-47	Flat/sloping	Absent	China	[13]
c.689C>T/p.A230V	7	Motor domain	1 (sporadic case)	4	U-shaped	Absent	Japan	[16]
c.689C>T/p.A230V	7	Motor domain	9/18	Mean 6-7	Flat/sloping	Bilateral areflexia	Italy	[17]
c.1373A>T/p.N458I	13	Motor domain	11/26	4-43	Ascending-flat-sloping	Vertigo and unsteady walking	Netherlands	[18]
c.2003G>A/p.R668H	17	Motor domain	9/15	17-45	Ascending-flat-sloping	-	China	[19]
c.2011G>A/p.G671S	17	Motor domain	9/23	10-39	Ascending-flat-sloping	Absent	China	[13]
c.2011G>A/p.G671S	17	Motor domain	11/29	13-40	Flat/sloping	Absent	China	[20]
c.2164G>C/p.G722R	17	Motor domain	13/43	20-30	Ascending-flat-sloping	Absent	United States	[21]
c.2557C>T/p.R853C	21	IQ 5	5/12	1 mo to puberty	-	Mild dysfunction	Germany	[22]
c.2558G>A/p.A853H	21	IQ 5	12/23	1-33	Flat/sloping	Absent	Japan	[14]
c.1531G>A/p.D511N	13	Motor domain	5/12	35-42	Flat/sloping	Absent	China	This report

In the inner ear, *MYO7A* is expressed in hair cells, utricles, and semicircular canals and is involved in the transmembrane transport of proteins and functional maintenance of hair cells[24,25]. In the eyes, *MYO7A* is mainly expressed in photoreceptors and pigment epithelial cells and its main function is to transport visual proteins together with connecting cilia[26,27]. Therefore, in most cases, variants in *MYO7A* cause dysfunction in the encoded protein, leading to both sensorineural hearing loss and visual impairment. In the eye, the dysfunctional protein may be compensated by other proteins in the retina[18]; nonetheless, its function in the inner ear is unique[25,28]. Therefore, patients with variants in *MYO7A* can present only hearing loss and mild or no vestibular dysfunction with no ocular symptoms[17,18,22], resulting in rare non-syndromic hearing loss. In the family of this study, the phenotype of hearing loss of the study participants is consistent with an autosomal dominant inheritance pattern, and clinical examination revealed no visual impairment or vestibular symptoms in the affected members. This is consistent with the symptoms reported in families with DFNA11. The only symptom of the studied family was slowly progressive hearing loss, which may also have contributed to the delay in seeking medical attention.

The protein encoded by *MYO7A* belongs to the myosin family, which is composed of three regions: the N-terminal head (motor domain), IQ5 neck, and C-terminal tail, the last of which begins with a single α-helix domain[29,30]. The motor domain contains the binding domains of adenosine triphosphate and actin, which are the core functional areas of the molecule[31]. The variant identified in this study leads to the loss of hydrogen bond and electrostatic interaction in the motor domain, which is predicted to cause a decrease in the stability of the local structure and subsequently affect the function of the MYO7A protein.

In a clinical setting, a diagnosis of this type of post-lingual hereditary hearing loss requires ruling out many lesions of the middle and inner ear, as well as nerve damage caused by noise, drugs, autoimmunity, or other factors. The key points of differential diagnosis are to inquire about the characteristics of hearing changes carefully, collect details on the patient's personal and family medical history, and complete various clinical examinations. For rare variants, extensive clinical and genetic data collection from family members is a prerequisite for diagnosis. Based on the results presented above, we made the diagnosis and provided effective treatment recommendations and genetic counseling for all family members. However, owing to the limited experimental conditions, we did not conduct further verification of the pathogenic mechanism of this variant.

CONCLUSION

In this study, we report a new family with DFNA11 caused by a *MYO7A* variant, which provides a new screening site for hereditary deafness. At the same time, the late onset age of hearing loss in the studied family also provides new insights

into the clinical phenotype of DFNA11.

ACKNOWLEDGEMENTS

The authors would like to thank the patients and their families.

FOOTNOTES

Author contributions: Xia CF and Yan R contributed equally to this work. Xia CF and Yan R conducted the clinical investigations of the patients and drafted the manuscript; Su WW participated in the collection of clinical data; Liu YH supervised the study and revised the manuscript; and all authors have contributed to the manuscript and approved the submitted version.

Informed consent statement: Written informed consent was obtained from all participants or their guardians, and they agreed to publish this case report.

Conflict-of-interest statement: All the authors report no relevant conflicts of interest for this article.

CARE Checklist (2016) statement: The authors have read the CARE Checklist (2016), and the manuscript was prepared and revised according to the CARE Checklist (2016).

Country/Territory of origin: China

ORCID number: Cai-Feng Xia 0000-0003-3295-2201; Rong Yan 0009-0000-8118-0442; Wen-Wen Su 0009-0006-7884-4619; Yu-He Liu 0000-0002-7470-1905.

S-Editor: Wang JJ
L-Editor: Wang TQ
P-Editor: Cai YX

REFERENCES

1 **Lin X**, Tang W, Ahmad S, Lu J, Colby CC, Zhu J, Yu Q. Applications of targeted gene capture and next-generation sequencing technologies in studies of human deafness and other genetic disabilities. *Hear Res* 2012; **288**: 67-76 [PMID: 22269275 DOI: 10.1016/j.heares.2012.01.004]
2 **Rehm HL**. Genetics and the genome project. *Ear Hear* 2003; **24**: 270-274 [PMID: 12923418 DOI: 10.1097/01.AUD.0000079806.73761.C8]
3 **Hasson T**, Heintzelman MB, Santos-Sacchi J, Corey DP, Mooseker MS. Expression in cochlea and retina of myosin VIIa, the gene product defective in Usher syndrome type 1B. *Proc Natl Acad Sci U S A* 1995; **92**: 9815-9819 [PMID: 7568224 DOI: 10.1073/pnas.92.21.9815]
4 **Weil D**, Blanchard S, Kaplan J, Guilford P, Gibson F, Walsh J, Mburu P, Varela A, Levilliers J, Weston MD. Defective myosin VIIA gene responsible for Usher syndrome type 1B. *Nature* 1995; **374**: 60-61 [PMID: 7870171 DOI: 10.1038/374060a0]
5 **Weston MD**, Kelley PM, Overbeck LD, Wagenaar M, Orten DJ, Hasson T, Chen ZY, Corey D, Mooseker M, Sumegi J, Cremers C, Moller C, Jacobson SG, Gorin MB, Kimberling WJ. Myosin VIIA mutation screening in 189 Usher syndrome type 1 patients. *Am J Hum Genet* 1996; **59**: 1074-1083 [PMID: 8900236]
6 **Zina ZB**, Masmoudi S, Ayadi H, Chaker F, Ghorbel AM, Drira M, Petit C. From DFNB2 to Usher syndrome: variable expressivity of the same disease. *Am J Med Genet* 2001; **101**: 181-183 [PMID: 11391666 DOI: 10.1002/ajmg.1335]
7 **Liu XZ**, Walsh J, Mburu P, Kendrick-Jones J, Cope MJ, Steel KP, Brown SD. Mutations in the myosin VIIA gene cause non-syndromic recessive deafness. *Nat Genet* 1997; **16**: 188-190 [PMID: 9171832 DOI: 10.1038/ng0697-188]
8 **Liu XZ**, Walsh J, Tamagawa Y, Kitamura K, Nishizawa M, Steel KP, Brown SD. Autosomal dominant non-syndromic deafness caused by a mutation in the myosin VIIA gene. *Nat Genet* 1997; **17**: 268-269 [PMID: 9354784 DOI: 10.1038/ng1197-268]
9 **Tamagawa Y**, Ishikawa K, Ishida T, Kitamura K, Makino S, Tsuru T, Ichimura K. Phenotype of DFNA11: a nonsyndromic hearing loss caused by a myosin VIIA mutation. *Laryngoscope* 2002; **112**: 292-297 [PMID: 11889386 DOI: 10.1097/00005537-200202000-00017]
10 **Fuster-García C**, García-Bohórquez B, Rodríguez-Muñoz A, Aller E, Jaijo T, Millán JM, García-García G. Usher Syndrome: Genetics of a Human Ciliopathy. *Int J Mol Sci* 2021; **22** [PMID: 34201633 DOI: 10.3390/ijms22136723]
11 **Dammeyer J**. Children with Usher syndrome: mental and behavioral disorders. *Behav Brain Funct* 2012; **8**: 16 [PMID: 22449032 DOI: 10.1186/1744-9081-8-16]
12 **Astuto LM**, Kelley PM, Askew JW, Weston MD, Smith RJ, Alswaid AF, Al-Rakaf M, Kimberling WJ. Searching for evidence of DFNB2. *Am J Med Genet* 2002; **109**: 291-297 [PMID: 11992483 DOI: 10.1002/ajmg.10384]
13 **Sun Y**, Chen J, Sun H, Cheng J, Li J, Lu Y, Jin Z, Zhu Y, Ouyang X, Yan D, Dai P, Han D, Yang W, Wang R, Liu X, Yuan H. Novel missense mutations in MYO7A underlying postlingual high- or low-frequency non-syndromic hearing impairment in two large families from China. *J Hum Genet* 2011; **56**: 64-70 [PMID: 21150918 DOI: 10.1038/jhg.2010.147]

14 **Yamamoto N**, Mutai H, Namba K, Goto F, Ogawa K, Matsunaga T. Clinical Profiles of DFNA11 at Diverse Stages of Development and Aging in a Large Family Identified by Linkage Analysis. *Otol Neurotol* 2020; **41**: e663-e673 [PMID: 32097363 DOI: 10.1097/MAO.0000000000002604]

15 **Wang K**, Li M, Hakonarson H. ANNOVAR: functional annotation of genetic variants from high-throughput sequencing data. *Nucleic Acids Res* 2010; **38**: e164 [PMID: 20601685 DOI: 10.1093/nar/gkq603]

16 **Kaneko Y**, Nakano A, Arimoto Y, Nara K, Mutai H, Matsunaga T. The first sporadic case of DFNA11 identified by next-generation sequencing. *Int J Pediatr Otorhinolaryngol* 2017; **100**: 183-186 [PMID: 28802369 DOI: 10.1016/j.ijporl.2017.07.007]

17 **Di Leva F**, D'Adamo P, Cubellis MV, D'Eustacchio A, Errichiello M, Saulino C, Auletta G, Giannini P, Donaudy F, Ciccodicola A, Gasparini P, Franzè A, Marciano E. Identification of a novel mutation in the myosin VIIA motor domain in a family with autosomal dominant hearing loss (DFNA11). *Audiol Neurootol* 2006; **11**: 157-164 [PMID: 16449806 DOI: 10.1159/000091199]

18 **Luijendijk MW**, Van Wijk E, Bischoff AM, Krieger E, Huygen PL, Pennings RJ, Brunner HG, Cremers CW, Cremers FP, Kremer H. Identification and molecular modelling of a mutation in the motor head domain of myosin VIIA in a family with autosomal dominant hearing impairment (DFNA11). *Hum Genet* 2004; **115**: 149-156 [PMID: 15221449 DOI: 10.1007/s00439-004-1137-3]

19 **Sang Q**, Yan X, Wang H, Feng R, Fei X, Ma D, Xing Q, Li Q, Zhao X, Jin L, He L, Li H, Wang L. Identification and functional study of a new missense mutation in the motor head domain of myosin VIIA in a family with autosomal dominant hearing impairment (DFNA11). *PLoS One* 2013; **8**: e55178 [PMID: 23383098 DOI: 10.1371/journal.pone.0055178]

20 **Li L**, Yuan H, Wang H, Guan J, Lan L, Wang D, Zong L, Liu Q, Han B, Huang D, Wang Q. Identification of a MYO7A mutation in a large Chinese DFNA11 family and genotype-phenotype review for DFNA11. *Acta Otolaryngol* 2018; **138**: 463-470 [PMID: 29400105 DOI: 10.1080/00016489.2017.1397743]

21 **Kallman JC**, Phillips JO, Bramhall NF, Kelly JP, Street VA. In search of the DFNA11 myosin VIIA low- and mid-frequency auditory genetic modifier. *Otol Neurotol* 2008; **29**: 860-867 [PMID: 18667942 DOI: 10.1097/MAO.0b013e3181825651]

22 **Bolz H**, Bolz SS, Schade G, Kothe C, Mohrmann G, Hess M, Gal A. Impaired calmodulin binding of myosin-7A causes autosomal dominant hearing loss (DFNA11). *Hum Mutat* 2004; **24**: 274-275 [PMID: 15300860 DOI: 10.1002/humu.9272]

23 **Street VA**, Li J, Robbins CA, Kallman JC. A DNA variant within the MYO7A promoter regulates YY1 transcription factor binding and gene expression serving as a potential dominant DFNA11 auditory genetic modifier. *J Biol Chem* 2011; **286**: 15278-15286 [PMID: 21378158 DOI: 10.1074/jbc.M111.228304]

24 **Kachar B**, Battaglia A, Fex J. Compartmentalized vesicular traffic around the hair cell cuticular plate. *Hear Res* 1997; **107**: 102-112 [PMID: 9165351 DOI: 10.1016/s0378-5955(97)00027-0]

25 **Li S**, Mecca A, Kim J, Caprara GA, Wagner EL, Du TT, Petrov L, Xu W, Cui R, Rebustini IT, Kachar B, Peng AW, Shin JB. Myosin-VIIa is expressed in multiple isoforms and essential for tensioning the hair cell mechanotransduction complex. *Nat Commun* 2020; **11**: 2066 [PMID: 32350269 DOI: 10.1038/s41467-020-15936-z]

26 **Williams DS**. Usher syndrome: animal models, retinal function of Usher proteins, and prospects for gene therapy. *Vision Res* 2008; **48**: 433-441 [PMID: 17936325 DOI: 10.1016/j.visres.2007.08.015]

27 **Liu X**, Udovichenko IP, Brown SD, Steel KP, Williams DS. Myosin VIIa participates in opsin transport through the photoreceptor cilium. *J Neurosci* 1999; **19**: 6267-6274 [PMID: 10414956 DOI: 10.1523/JNEUROSCI.19-15-06267.1999]

28 **Self T**, Mahony M, Fleming J, Walsh J, Brown SD, Steel KP. Shaker-1 mutations reveal roles for myosin VIIA in both development and function of cochlear hair cells. *Development* 1998; **125**: 557-566 [PMID: 9435277 DOI: 10.1242/dev.125.4.557]

29 **Li J**, Chen Y, Deng Y, Unarta IC, Lu Q, Huang X, Zhang M. Ca(2+)-Induced Rigidity Change of the Myosin VIIa IQ Motif-Single α Helix Lever Arm Extension. *Structure* 2017; **25**: 579-591.e4 [PMID: 28262393 DOI: 10.1016/j.str.2017.02.002]

30 **Chen ZY**, Hasson T, Kelley PM, Schwender BJ, Schwartz MF, Ramakrishnan M, Kimberling WJ, Mooseker MS, Corey DP. Molecular cloning and domain structure of human myosin-VIIa, the gene product defective in Usher syndrome 1B. *Genomics* 1996; **36**: 440-448 [PMID: 8884267 DOI: 10.1006/geno.1996.0489]

31 **Joo SY**, Na G, Kim JA, Yoo JE, Kim DH, Kim SJ, Jang SH, Yu S, Kim HY, Choi JY, Gee HY, Jung J. Clinical Heterogeneity Associated with MYO7A Variants Relies on Affected Domains. *Biomedicines* 2022; **10** [PMID: 35453549 DOI: 10.3390/biomedicines10040798]

World Journal of Clinical Cases

Submit a Manuscript: https://www.f6publishing.com

World J Clin Cases 2023 September 6; 11(25): 5970-5976

DOI: 10.12998/wjcc.v11.i25.5970

ISSN 2307-8960 (online)

CASE REPORT

Predicting apical hypertrophic cardiomyopathy using T-wave inversion: Three case reports

Liang Kang, Yi-Hua Li, Rong Li, Qing-Min Chu

Specialty type: Cardiac and cardiovascular systems

Provenance and peer review: Unsolicited article; Externally peer reviewed.

Peer-review model: Single blind

Peer-review report's scientific quality classification

Grade A (Excellent): A
Grade B (Very good): B, B, B
Grade C (Good): 0
Grade D (Fair): 0
Grade E (Poor): 0

P-Reviewer: Buccheri D, Italy; Darbari A, India; Ong H, Malaysia; Vyshka G, Albania

Received: May 22, 2023
Peer-review started: May 22, 2023
First decision: July 6, 2023
Revised: July 11, 2023
Accepted: July 31, 2023
Article in press: July 31, 2023
Published online: September 6, 2023

Liang Kang, Yi-Hua Li, The First Clinical Medical College, Guangzhou University of Chinese Medicine, Guangzhou 510000, Guangdong Province, China

Rong Li, Qing-Min Chu, Department of Cardiovascular Disease, The First Affiliated Hospital of Guangzhou University of Chinese Medicine, Guangzhou 510000, Guangdong Province, China

Corresponding author: Qing-Min Chu, MD, Associate Chief Physician, Associate Professor, Department of Cardiovascular Disease, The First Affiliated Hospital of Guangzhou University of Chinese Medicine, No. 16 Jichang Road, Baiyun District, Guangzhou 510000, Guangdong Province, China. 13929504676@163.com

Abstract

BACKGROUND

Apical hypertrophic cardiomyopathy (AHCM) is a subtype of hypertrophic cardiomyopathy. Due to its location, the thickening of the left ventricular apex can be missed on echocardiography. Giant negative T waves (GNTs) in left-sided chest leads are the hallmark electrocardiogram (ECG) change of AHCM.

CASE SUMMARY

The first patient was a 68-year-old woman complaining of recurrent chest tightness persisting for more than 3 years. The second was a 59-year-old man complaining of spasmodic chest tightness persisting for more than 2 years. The third was a 55-year-old woman complaining of recurrent chest pain persisting for 4 mo. In all three cases, GNTs were observed several years prior to apical cardiac hypertrophy after other causes of T-wave inversion were ruled out.

CONCLUSION

Electrophysiological abnormalities of AHCM appear earlier than structural abnormalities, confirming the early predictive value of ECG for AHCM.

Key Words: Electrocardiogram; Negative T waves; Hypertrophic cardiomyopathy; Apical hypertrophic cardiomyopathy; Echocardiography; Case report

Core Tip: Apical hypertrophic cardiomyopathy (AHCM) is a subtype of hypertrophic cardiomyopathy that is thought to be associated with sudden death. Owing to its atypical clinical symptoms and insidious progression, early diagnosis is difficult. We followed up three patients who eventually progressed to AHCM over a period of several years. Giant negative T waves in the left-sided chest leads of these three patients occurred earlier than thickening of the left ventricular apex as detected *via* echocardiography. Therefore, we suggest that electrophysiological abnormalities in AHCM appear earlier than structural abnormalities and that electrocardiogram may have early predictive value for AHCM.

Citation: Kang L, Li YH, Li R, Chu QM. Predicting apical hypertrophic cardiomyopathy using T-wave inversion: Three case reports. *World J Clin Cases* 2023; 11(25): 5970-5976
URL: https://www.wjgnet.com/2307-8960/full/v11/i25/5970.htm
DOI: https://dx.doi.org/10.12998/wjcc.v11.i25.5970

INTRODUCTION

Apical hypertrophic cardiomyopathy (AHCM) is an uncommon type of hypertrophic cardiomyopathy (HCM) characterized by thickening of the left ventricular apex. The prevalence rate of AHCM is higher in Asia than those in Europe and America[1]. In China, AHCM accounts for 16% of all cases of HCM[2]. It lacks specificity in clinical symptoms with about 50% of patients not having obvious symptoms[3]. The concept of AHCM was first proposed in 1976 by Sakamoto *et al*[4], who summarized its features as giant negative T waves (GNTs) in leads V3-V4 on electrocardiogram (ECG) and a spade-like configuration of the left ventricular cavity at end-diastole on left ventriculography. Because the lesion site of AHCM is the left ventricular apex, its diagnosis may be overlooked on echocardiography. Therefore, patients considered likely to progress to AHCM can initially be screened by ECG. In addition, if patients with AHCM tendencies are identified early, early medical intervention can be initiated to delay disease progression. This could reduce the hospitalization rate and risk of sudden death in patients with AHCM. Before the diagnosis of AHCM, some patients exhibit T-wave changes similar to AHCM on their ECG, but echocardiography at the time shows no left ventricular apical myocardial thickening. Only several years later is AHCM diagnosed by echocardiography. Despite not reaching the diagnostic criteria of AHCM, cardiac hypertrophy in such patients appears in the left ventricular apical myocardium. Here, we report three cases of patients presenting with T-wave changes several years prior to apical cardiac hypertrophy being detected on echocardiography.

CASE PRESENTATION

Chief complaints

Case 1: A 68-year-old woman complained of recurrent chest tightness persisting for more than 3 years.

Case 2: A 59-year-old man complained of spasmodic chest tightness that had persisted for over two years and was aggravated two days prior to his hospital visit.

Case 3: A 55-year-old woman complained of recurrent chest pain persisting for more than 4 mo.

History of present illness

Case 1: For the previous 3 years, the patient had experienced recurrent episodes of chest tightness, each lasting no more than 10 min. Her chest tightness was often induced by exercise and could be relieved by rest. She experienced no marked radiating discomfort in the shoulder or back.

Case 2: The patient had developed spasmodic chest tightness more than 2 years before the current visit. The episodes of chest tightness had no obvious trigger, occurred once or twice a week, lasted 3-5 min each, and resolved spontaneously. In the previous 2 days, the frequency of chest tightness attacks had increased to three to five times per day, prompting the patient's hospital visit.

Case 3: The patient had recurrent episodes of chest pain for nearly 4 mo. Her chest pain was often induced by exercise or emotional excitement, lasted about 5 min per episode, and was relieved after rest. She did not experience marked radiating pain in the shoulder or back when she had chest pain.

History of past illness

Case 1: She had a medical history of rheumatoid arthritis and had been admitted repeatedly for chest tightness or arthralgia from 2016 to 2020.

Case 2: The patient had a medical history of type 2 diabetes and an abnormal lipid profile.

Case 3: The patient had a medical history of systemic lupus erythematosus.

Personal and family history

Case 1: The patient had no related personal or family history.

Case 2: The patient had a history of smoking of more than 30 years and no family history of related diseases.

Case 3: The patient had no relevant personal or family history.

Physical examination

Case 1: Physical examination of the patient's heart, lungs, and abdomen was unremarkable. Her first interphalangeal joint and wrist joint were swollen and painful.

Case 2: Physical examination results were unremarkable.

Case 3: Physical examination of the heart, lungs, and abdomen was unremarkable. The patient had butterfly-shaped erythema on the face, swelling and pain of the knee joints and elbows, and scattered ring erythema on the legs.

Laboratory examinations

Case 1: Laboratory test results were unremarkable.

Case 2: Laboratory test results were unremarkable.

Case 3: Laboratory test results were unremarkable.

Imaging examinations

Case 1: After echocardiography was performed four times over the years, she was finally diagnosed with AHCM in 2020. In 2016, the patient's ECG showed negative or biphasic T waves in leads V4 to V6, which evolved dynamically. ECG changes were seen significantly earlier than hypertrophy in the left ventricular apex and the diagnosis of AHCM (Figure 1). In addition, the patient had undergone coronary angiography in 2016, and the results showed no coronary artery stenosis.

Case 2: The patient underwent echocardiography twice in 2016 and 2020. In 2016, the patient underwent cardiac MR examination, and no obvious abnormalities were found Echocardiography in 2020 showed cardiac hypertrophy in the left ventricular apex. However, the ECG of the patient in 2016 showed GNTs in leads V3-V6 (Figure 2). The patient had undergone coronary angiography in 2016, and the results showed no coronary artery stenosis.

Case 3: The patient underwent echocardiography three times between 2016 and 2020. Echocardiography in 2020 showed cardiac hypertrophy at the left ventricular apex. The ECG of the patient in 2016 showed GNTs in leads V3-V6 (Figure 3). The patient underwent coronary angiography in 2019, and the results showed no coronary artery stenosis.

FINAL DIAGNOSIS

Based on the examination findings, the final diagnosis was AHCM in all three cases.

TREATMENT

The underlying diseases and comorbidities of the three patients were treated with symptomatic treatment.

In case 1, sublingual nitroglycerin was given to relieve the patient's paroxysmal chest tightness and chest pain. Methotrexate and leflunomide were taken continuously and regularly, and oral glucocorticoids were used intermittently for the patient's rheumatoid arthritis. Celecoxib was also administered to relieve joint pain.

In case 2, sublingual nitroglycerin was given to relieve paroxysmal chest tightness, oral metformin and acarbose were given to treat type 2 diabetes mellitus, oral atorvastatin was given to treat dyslipidemia, and aspirin was given to inhibit platelet aggregation.

In case 3, sublingual nitroglycerin was given for relief of paroxysmal chest pain. Cyclophosphamide, taken regularly and continuously, and oral glucocorticoids were used for systemic lupus erythematosus.

OUTCOME AND FOLLOW-UP

The patient in case 1 died from malignant arrhythmia in 2020. The remaining patients are still being monitored.

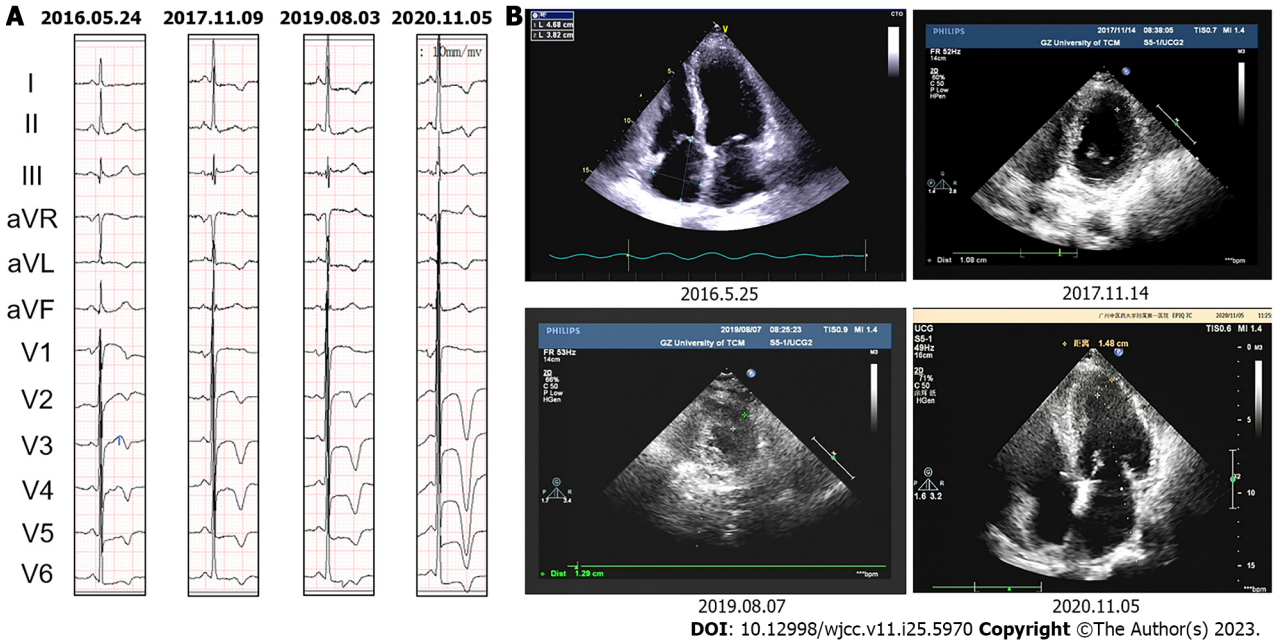

DOI: 10.12998/wjcc.v11.i25.5970 **Copyright** ©The Author(s) 2023.

Figure 1 Evolution of left ventricular apical thickness and T-wave amplitude in chest leads of electrocardiogram in case 1. A: Electrocardiogram showed that T-wave inversion amplitude in chest leads gradually deepened from 2016 to 2020; B: Echocardiography showed that the left ventricular apical thickness gradually increased from 2016 to 2020.

DISCUSSION

The three patients reported herein had extensive T-wave changes in left-sided chest leads (V3-V6) and GNTs on average 2.3 years before the diagnosis of AHCM. These diagnoses were made after excluding myocardial ischemia due to coronary artery disease by coronary angiography. No cerebrovascular accidents had occurred, nor did the patients have Takotsubo syndrome or other possible conditions that might lead to the observed ECG changes. The T-wave changes of these patients did not disappear and showed a trend of continuous evolution even after hypertrophy in the left ventricular apex was found by echocardiography and AHCM was diagnosed. Unexplained T-wave inversion in left-sided chest leads is not uncommon, but the final diagnosis of AHCM by echocardiography after long-term follow-up is rare.

AHCM is considered an autosomal dominant disease with familial clustering. It is more prevalent in men (74.4%)[5]. From the perspective of pathophysiology, left ventricular apical hypertrophy impacts left ventricular diastolic function. This reduces left ventricular filling volume, resulting in lower cardiac output and progressive heart failure. Apical myocardial fibrosis reduces the relaxation and compliance of ventricular muscles, resulting in increased left ventricular filling pressures potentially leading to left atrial enlargement, atrial fibrillation, and an increased risk of stroke. Hypertrophic apical myocardium could lead to myocardial ischemia unrelated to coronary arteries owing to papillary muscle microvascular dysplasia and low blood flow reserve. This could then develop into myocardial infarction or apical ventricular aneurysm, thereby increasing the chances of malignant arrhythmias and sudden death[6,7]. In short, AHCM is a latent threat to patients' lives. Early prediction and early intervention could profoundly delay its progression and prevent complications.

The diagnosis of AHCM is based on echocardiography and myocardial magnetic resonance imaging. Currently, the most accepted diagnostic criteria are a maximum apical thickness ≥ 15 mm, maximum apical thickness/left ventricular posterior wall thickness ≥ 15 mm, and exclusion of other causes of cardiac hypertrophy[6]. Some experts argue that the imaging diagnostic criterion of maximum apical thickness ≥ 15 mm could be lowered to ≥ 13 mm when a patient with a thin myocardium at the apex has typical ECG changes, a family history of HCM, or genetic testing results indicating AHCM[8].

ECG also has value in the diagnosis of AHCM. Sakamoto *et al*[4] emphasized the value of GNTs in the diagnosis of AHCM, which has been affirmed in the European Society of Cardiology HCM Diagnosis and Treatment Guidelines[9]. Studies have shown that approximately 90% of patients with AHCM have T-wave inversion, and the incidence of GNTs is approximately 11%-47%[3].

We found that the ECG showed obvious GNT changes several years before the imaging findings of hypertrophy in the left ventricular apex, which implies the greater sensitivity of ECG for apical hypertrophy compared to imaging. Thus, it follows that for AHCM, cardiac electrophysiological abnormalities are seen earlier than structural abnormalities. In the three patients reported herein, significant T-wave inversion in left-sided chest leads was observed at an average of 2.3 years before the appearance of hypertrophy in the left ventricular apex on echocardiography. The average duration of ECG changes is affected by the frequency of echocardiography and ECG during follow-up. Although the small sample in our report inevitably subjects our results to bias, it suggests the predictive value of ECG on cardiac hypertrophy in the left ventricular apex. It can also prove the importance of long-term follow-up in patients with T-wave inversion in left-sided chest leads.

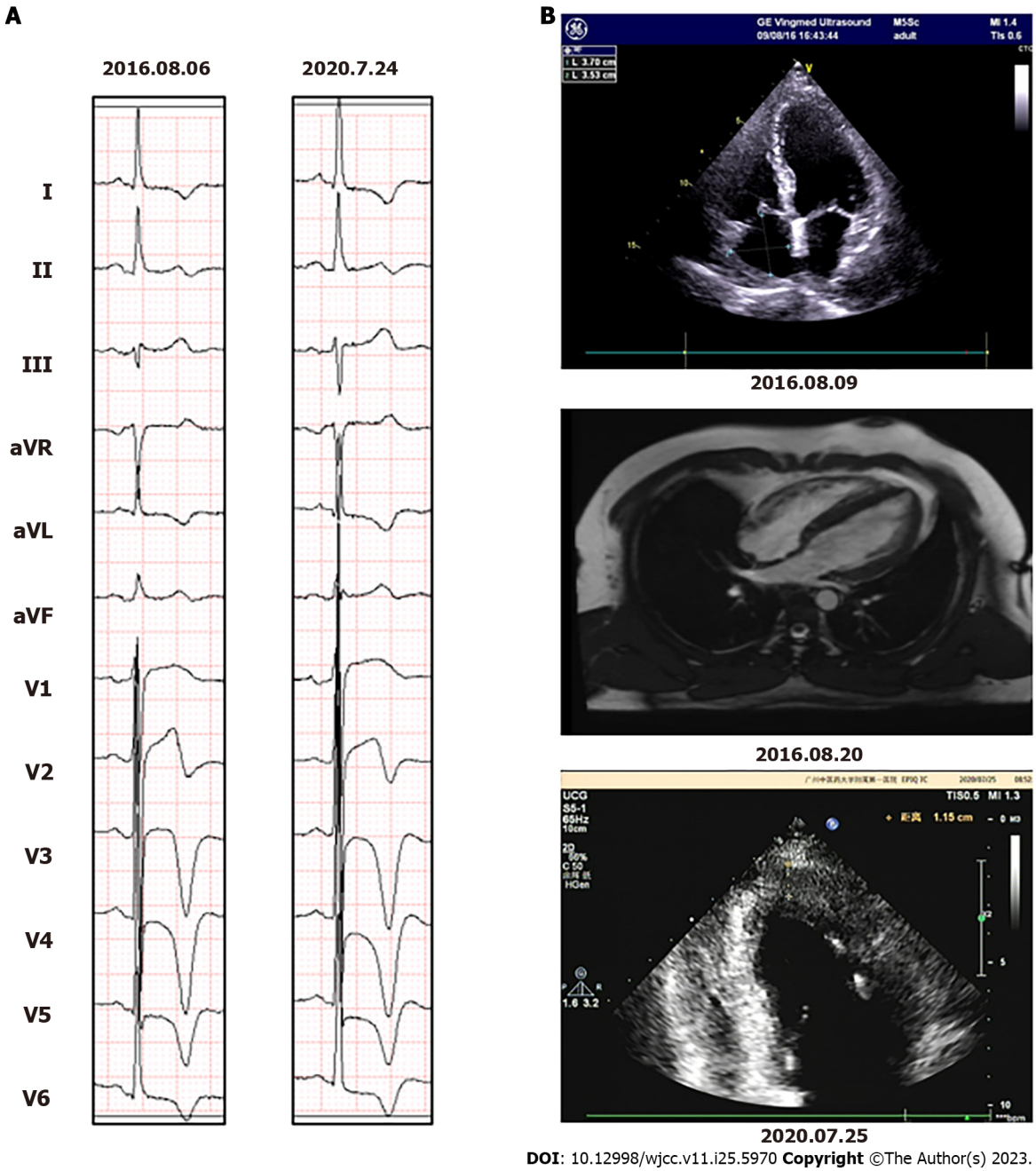

DOI: 10.12998/wjcc.v11.i25.5970

Figure 2 Evolution of left ventricular apical thickness and T-wave amplitude in chest leads of electrocardiogram in case 2. A: Electrocardiogram showed that T-wave inversion amplitude in chest leads gradually deepened from 2016 to 2020; B: Echocardiography and cardiac magnetic resonance showed that the left ventricular apical thickness gradually increased from 2016 to 2020.

In addition, the clinical symptoms of the three patients appeared later than the changes found on echocardiography, and only when cardiac hypertrophy evolved to a certain degree did the symptoms become apparent. Simultaneously, because ECG is more sensitive in the prediction of apical cardiac hypertrophy, its auxiliary diagnostic value for early asymptomatic patients with AHCM should not be ignored.

In the future, more patients with extensive T-wave inversion in left-sided chest leads need to be evaluated in case-control studies with higher levels of evidence in order to enable evidence-based medicine for such patients. At the same time, early genetic testing combined with T-wave changes in ECG should provide a more accurate clinical diagnosis.

CONCLUSION

Extensive T-wave inversion in leads V3-V6 occurred significantly earlier than left ventricular apical cardiac hypertrophy detected by echocardiography. Therefore, after excluding other conditions that may cause extensive T-wave inversion in left-sided chest leads, extensive T-wave inversion in leads V3-V6 may have early predictive value for AHCM. For patients with extensive T-wave inversion in left-sided chest leads, no left ventricular apical cardiac hypertrophy on echocardio-

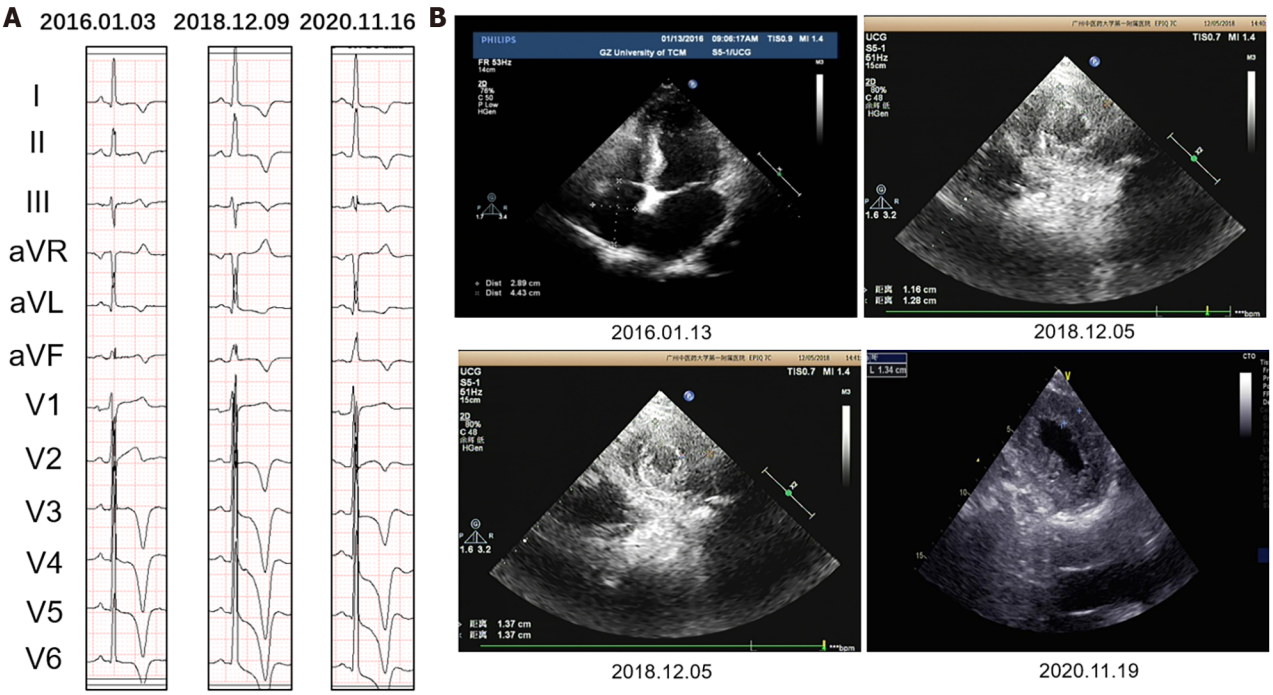

DOI: 10.12998/wjcc.v11.i25.5970

Figure 3 Evolution of left ventricular apical thickness and T-wave amplitude in chest leads of electrocardiogram in case 3. A: Electrocardiogram showed that T-wave inversion amplitude in chest leads gradually deepened from 2016 to 2020; B: Echocardiography showed that the left ventricular apical thickness gradually increased from 2016 to 2020.

graphy, and exclusion of other causes such as ischemia, the possibility of AHCM should be considered. This may improve clinical decision-making.

ACKNOWLEDGEMENTS

The authors wish to thank Dr. Ling Shen and Dr. Xiaolian He for their contribution to the data collection process, and the patients for their cooperation regarding this publication.

FOOTNOTES

Author contributions: Kang L and Li YH reviewed the literature and contributed to manuscript drafting; Li R and Chu QM analyzed and interpreted the electrocardiogram and coronary angiography findings; Chu QM was responsible for the revision of the manuscript for important intellectual content; all authors issued final approval for the version to be submitted.

Informed consent statement: Informed written consent was obtained from the patients for the publication of this report and any accompanying images.

Conflict-of-interest statement: The authors declare that they have no conflict of interest to disclose.

CARE Checklist (2016) statement: The authors have read the CARE Checklist (2016), and the manuscript was prepared and revised according to the CARE Checklist (2016).

Country/Territory of origin: China

ORCID number: Liang Kang 0000-0002-5042-8553; Yi-Hua Li 0000-0002-9056-2386; Rong Li 0000-0001-5771-1178; Qing-Min Chu 0000-0002-1144-5211.

S-Editor: Chen YL

L-Editor: A
P-Editor: Yu HG

REFERENCES

1 **Kitaoka H**, Doi Y, Casey SA, Hitomi N, Furuno T, Maron BJ. Comparison of prevalence of apical hypertrophic cardiomyopathy in Japan and the United States. *Am J Cardiol* 2003; **92**: 1183-1186 [PMID: 14609593 DOI: 10.1016/j.amjcard.2003.07.027]

2 **Tao YK**, Yan LR, Li YS, Xu ZM, Zhang GQ, Zu LM, DU HY, Fan CM. [Clinical features and prognosis of 188 Chinese patients with apical hypertrophic cardiomyopathy]. *Zhonghua Xin Xue Guan Bing Za Zhi* 2011; **39**: 106-109 [PMID: 21426741]

3 **Klarich KW**, Attenhofer Jost CH, Binder J, Connolly HM, Scott CG, Freeman WK, Ackerman MJ, Nishimura RA, Tajik AJ, Ommen SR. Risk of death in long-term follow-up of patients with apical hypertrophic cardiomyopathy. *Am J Cardiol* 2013; **111**: 1784-1791 [PMID: 23540548 DOI: 10.1016/j.amjcard.2013.02.040]

4 **Sakamoto T**, Tei C, Murayama M, Ichiyasu H, Hada Y. Giant T wave inversion as a manifestation of asymmetrical apical hypertrophy (AAH) of the left ventricle. Echocardiographic and ultrasono-cardiotomographic study. *Jpn Heart J* 1976; **17**: 611-629 [PMID: 136532 DOI: 10.1536/ihj.17.611]

5 **Ommen SR**, Semsarian C. Hypertrophic cardiomyopathy: a practical approach to guideline directed management. *Lancet* 2021; **398**: 2102-2108 [PMID: 34600606 DOI: 10.1016/S0140-6736(21)01205-8]

6 **Gruner C**, Care M, Siminovitch K, Moravsky G, Wigle ED, Woo A, Rakowski H. Sarcomere protein gene mutations in patients with apical hypertrophic cardiomyopathy. *Circ Cardiovasc Genet* 2011; **4**: 288-295 [PMID: 21511876 DOI: 10.1161/CIRCGENETICS.110.958835]

7 **Yan L**, Wang Z, Xu Z, Li Y, Tao Y, Fan C. Two hundred eight patients with apical hypertrophic cardiomyopathy in china: clinical feature, prognosis, and comparison of pure and mixed forms. *Clin Cardiol* 2012; **35**: 101-106 [PMID: 22125122 DOI: 10.1002/clc.20995]

8 **Jan MF**, Todaro MC, Oreto L, Tajik AJ. Apical hypertrophic cardiomyopathy: Present status. *Int J Cardiol* 2016; **222**: 745-759 [PMID: 27521551 DOI: 10.1016/j.ijcard.2016.07.154]

9 **Authors/Task Force members**, Elliott PM, Anastasakis A, Borger MA, Borggrefe M, Cecchi F, Charron P, Hagege AA, Lafont A, Limongelli G, Mahrholdt H, McKenna WJ, Mogensen J, Nihoyannopoulos P, Nistri S, Pieper PG, Pieske B, Rapezzi C, Rutten FH, Tillmanns C, Watkins H. 2014 ESC Guidelines on diagnosis and management of hypertrophic cardiomyopathy: the Task Force for the Diagnosis and Management of Hypertrophic Cardiomyopathy of the European Society of Cardiology (ESC). *Eur Heart J* 2014; **35**: 2733-2779 [PMID: 25173338 DOI: 10.1093/eurheartj/ehu284]

World Journal of Clinical Cases

Submit a Manuscript: https://www.f6publishing.com

World J Clin Cases 2023 September 6; 11(25): 5977-5981

DOI: 10.12998/wjcc.v11.i25.5977

ISSN 2307-8960 (online)

CASE REPORT

Bilateral thigh pyomyositis in an otherwise healthy middle-aged woman: A case report

Min Cui, Gang Zhang, Na Zhang, Lei Han, Zai-Qi Ma

Specialty type: Infectious diseases

Provenance and peer review: Unsolicited article; Externally peer reviewed.

Peer-review model: Single blind

Peer-review report's scientific quality classification

Grade A (Excellent): 0
Grade B (Very good): B, B
Grade C (Good): 0
Grade D (Fair): 0
Grade E (Poor): 0

P-Reviewer: Baryshnikova NV, Russia; Ghimire R, Nepal

Received: May 23, 2023
Peer-review started: May 23, 2023
First decision: July 17, 2023
Revised: August 1, 2023
Accepted: August 9, 2023
Article in press: August 9, 2023
Published online: September 6, 2023

Min Cui, Gang Zhang, Na Zhang, Lei Han, Department of Pain Medicine, Central Hospital Affiliated to Shandong First Medical University, Jinan 250013, Shandong Province, China

Zai-Qi Ma, Department of Thoracic Surgery, Qingdao Hiser Hospital Affiliated to Qingdao University, Qingdao 266000, Shandong Province, China

Corresponding author: Zai-Qi Ma, MA, Attending Doctor, Department of Thoracic Surgery, Qingdao Hiser Hospital Affiliated to Qingdao University, No. 4 Renmin Road, Shibei District, Qingdao 266000, Shandong Province, China. 94116845@qq.com

Abstract

BACKGROUND

Pyomyositis generally occurs in otherwise healthy young men. Because this condition is unusual among otherwise healthy women in temperate climates, we present the following case.

CASE SUMMARY

An otherwise healthy 43-year-old woman presented with bilateral pain in her lower extremities and fever. Magnetic resonance imaging (MRI) findings were indicative of myositis with a possible abscess. We initiated empirical antibiotic therapy with ceftriaxone. However, the swelling and pain in her legs persisted even after 7 d of treatment. Contrast MRI revealed multiple pockets of pus in the vastus lateralis and gluteal muscles. We performed needle aspiration of these abscesses with ultrasound guidance and local anesthesia. Upon culturing, the purulent material was positive for *Staphylococcus aureus*. We diagnosed her with *S. aureus*-induced pyomyositis of the vastus lateralis muscle and gluteus region. Based on the antibiotic sensitivity report, ceftriaxone was administered for an additional 7 d. By day 15 post-drainage, the patient was able to start walking. Oral antibiotic therapy was continued for 1 wk following her discharge from hospital, after which her symptoms resolved completely.

CONCLUSION

Pyomyositis may present with muscle pain, swelling, and fever. Ultrasound-guided percutaneous puncture and drainage may enable timely diagnosis and treatment.

Key Words: Pyomyositis; Endoscopic ultrasound-guided fine-needle aspiration; Staphylococcus aureus; Climate; Magnetic resonance imaging; Case report

Core Tip: Pyomyositis generally occurs in otherwise healthy young men. We report a case where pyomyositis occurred in an otherwise healthy 43-year-old woman in a temperate climate. This case is unusual because, in temperate regions, pyomyositis usually occurs in immunocompromised patients, such as those with diabetes mellitus. Owing to its rarity in temperate climates and its presentation being characterized by non-specific signs and symptoms, its diagnosis and treatment can be delayed, which can lead to septic shock and death. We hope that our report will help raise awareness and guide the future treatment of patients with pyomyositis.

Citation: Cui M, Zhang G, Zhang N, Han L, Ma ZQ. Bilateral thigh pyomyositis in an otherwise healthy middle-aged woman: A case report. *World J Clin Cases* 2023; 11(25): 5977-5981
URL: https://www.wjgnet.com/2307-8960/full/v11/i25/5977.htm
DOI: https://dx.doi.org/10.12998/wjcc.v11.i25.5977

INTRODUCTION

Pyomyositis is a bacterial infection of skeletal muscle, usually caused by hematogenous dissemination and often accompanied by abscess formation. Tropical myositis, a suppurative disease, mainly affects children aged 2–5 years and adults aged 20–45 years, whereas pyomyositis in temperate climates mainly affects adult men with coexisting conditions. The reported incidence of pyomyositis in temperate climates has been increasing, owing to the increased use of diagnostic imaging. Pyomyositis generally occurs in otherwise healthy young men, manifesting as muscle swelling, marked tenderness, and indurated muscle swelling that progresses to woody induration of the muscle and overlying tissues[1]. Because this condition is unusual among otherwise healthy women in temperate climates, we present the following case.

CASE PRESENTATION

Chief complaints

A 43-year-old woman, 156 cm in height and 69 kg in weight, who was employed as a cashier in a bakery, was admitted to the department of pain medicine for pain in both of her legs.

History of present illness

The pain had persisted for 3 d, with substantial movement restriction. The patient denied any history of trauma or vaccine injection. She had initially undergone an ultrasound examination of her lower limbs, which had ruled out arteriovenous thrombosis. Despite receiving therapy comprising non-steroidal anti-inflammatory drugs and rest, under the assumption that her pain was caused by muscle strain, the pain and swelling increased and the patient developed a fever and chills.

History of past illness

The patient had no history of diabetes.

Personal and family history

The patient did not report having experienced any injury or trauma, and had no recent history of infection, foreign travel, or immunosuppression.

Physical examination

We admitted the patient to investigate the etiology of her fever and pain. Upon physical examination her temperature was 39.1°C, pulse rate was 90 beats/min, and blood pressure was 100/65 mmHg. Her visual analog scale score was 8 cm. No wounds or breaks in the skin were noted on her lower extremities. She had tenderness in both her thighs and left knee joint, as well as in her bilateral gluteus media and small gluteus muscles. Both of the patient's thighs were swollen and had a sensation of warmth, although no erythema, ecchymosis, or fluctuance were noted in these areas. Respiratory, neurological, and cardiovascular examination results were all normal.

Laboratory examinations

A hematological examination conducted upon the patient's admission to hospital revealed leukocytosis [white blood cell (WBC) = 19.67 × 10^9/L] and neutrophilia (neutrophils = 17.92 × 10^9/L; 91.1%). Her hemoglobin concentration was 83 g/L, C-reactive protein (CRP) concentration was 192 mg/L (normal value: < 7 mg/L), erythrocyte sedimentation rate (ESR) was 96 mm/h (normal value: < 20 mm/h), and her creatine kinase concentration was 306 IU/L (normal value = 24–170

IU/L). Routine urine and stool cultures, liver and kidney function, electrolyte levels, and myocardial enzyme profile were all within the normal range. Tests for autoantibodies associated with rheumatic diseases were negative.

Imaging examinations

Plain radiographs revealed no bony abnormalities of the knee joint. A lower limb venous ultrasonography excluded phlebothrombosis. A computed tomography (CT) scan of the thorax, abdomen, and pelvis revealed no abnormalities. As we suspected that the patient might have pyomyositis, magnetic resonance imaging (MRI) was performed, which revealed widespread infiltrative edema within the vastus lateralis muscle, indicative of myositis with a possible abscess. We observed no signs or symptoms of knee joint effusion, osteomyelitis, or infiltration.

Initial treatment, responses, and further examinations

After obtaining blood cultures, we started the patient on empirical antibiotic therapy with ceftriaxone. She remained febrile during her first 3 d of hospitalization, and after 4 d of antibiotic treatment her temperature decreased to normal levels. Blood cultures taken upon presentation revealed no growth after 3 d. Subsequent laboratory tests revealed improvements in leukocyte (11.31 × 10^9/L) and neutrophil (9.06 × 10^9/L) concentrations.

Because we suspected that the patient might have pyomyositis and as 7 d of antibiotic treatment alone did not significantly relieve the swelling or pain in her legs, a repeat MRI of the thighs and hip joint was performed with enhanced contrast. This revealed multiple pockets of pus in the vastus lateralis and gluteal muscles (Figure 1). We performed needle aspiration of these abscesses with ultrasound guidance and local anesthesia, draining about 40 mL (30 mL from the left leg and 10 mL from the right) of purulent material. The purulent content was sent for culturing. The patient's condition improved after aspiration. Physical examination revealed a reduction in muscle tenderness and localized indurations. A follow-up ultrasound done 3 d after aspiration revealed the accumulation of residual fluid measuring 1.5 cm × 1.2 cm. The patient declined a second round of aspiration. *Staphylococcus aureus* was observed in the aspiration culture.

FINAL DIAGNOSIS

In the end, the patient was diagnosed with *S. aureus*-induced pyomyositis of the vastus lateralis muscle and gluteus region.

TREATMENT

Based on the antibiotic sensitivity report, ceftriaxone was administered for an additional 7 d.

OUTCOME AND FOLLOW-UP

By day 15 post drainage, the patient was able to start walking. Laboratory tests revealed a decrease in her WBCs (within the normal range), ESR (59 mm/h), and CRP concentration (6.2 mg/L). Oral antibiotic therapy was continued for 1 wk after the patient was discharged. The total duration of therapy was 3 wk. Subsequent follow-up visits revealed a gradual relief of her symptoms. By her 4-mo follow-up visit, her ESR and CRP concentration had normalized. The patient experienced complete resolution of her symptoms and had no further complaints.

DISCUSSION

Pyomyositis affects the skeletal muscles, manifesting as high-grade fever with pain in the affected limbs. It is generally considered a tropical infectious disease that affects otherwise healthy children and adults, but it has also been diagnosed with increasing frequency in other parts of the world since the 1970s, with the spread of routine diagnostic imaging tests [2]. The pathogenesis of tropical myositis remains unclear, although it may be related to trauma, parasites, nutritional deficiencies, and viruses.

As this disease is relatively rare in temperate regions and its early presentation is characterized by signs and symptoms that are not very specific, pyomyositis is usually not added to differential diagnoses of muscle pain and swelling until patients fail to respond to treatments of the alternative diagnoses. The case we report here is unusual, as the patient was an otherwise healthy, middle-aged woman with an unremarkable medical history. The muscles involved in pyomyositis are usually deep, so typical inflammatory manifestations may not be visible on the surface. Therefore, pyomyositis should be differentiated from osteomyelitis, malignant tumors, hematoma, septic arthritis, deep vein thrombosis, and thrombotic phlebitis. When pyomyositis is not promptly and properly treated, serious complications such as muscle abscesses, cerebral abscesses, renal failure, septicemia, and death may occur[3,4].

Pyomyositis is characterized by fever, local swelling, and pain. In severe cases, it can lead to shock and death. The large muscle groups of the pelvic girdle and lower extremities are the most common sites of infection. The thigh muscles,

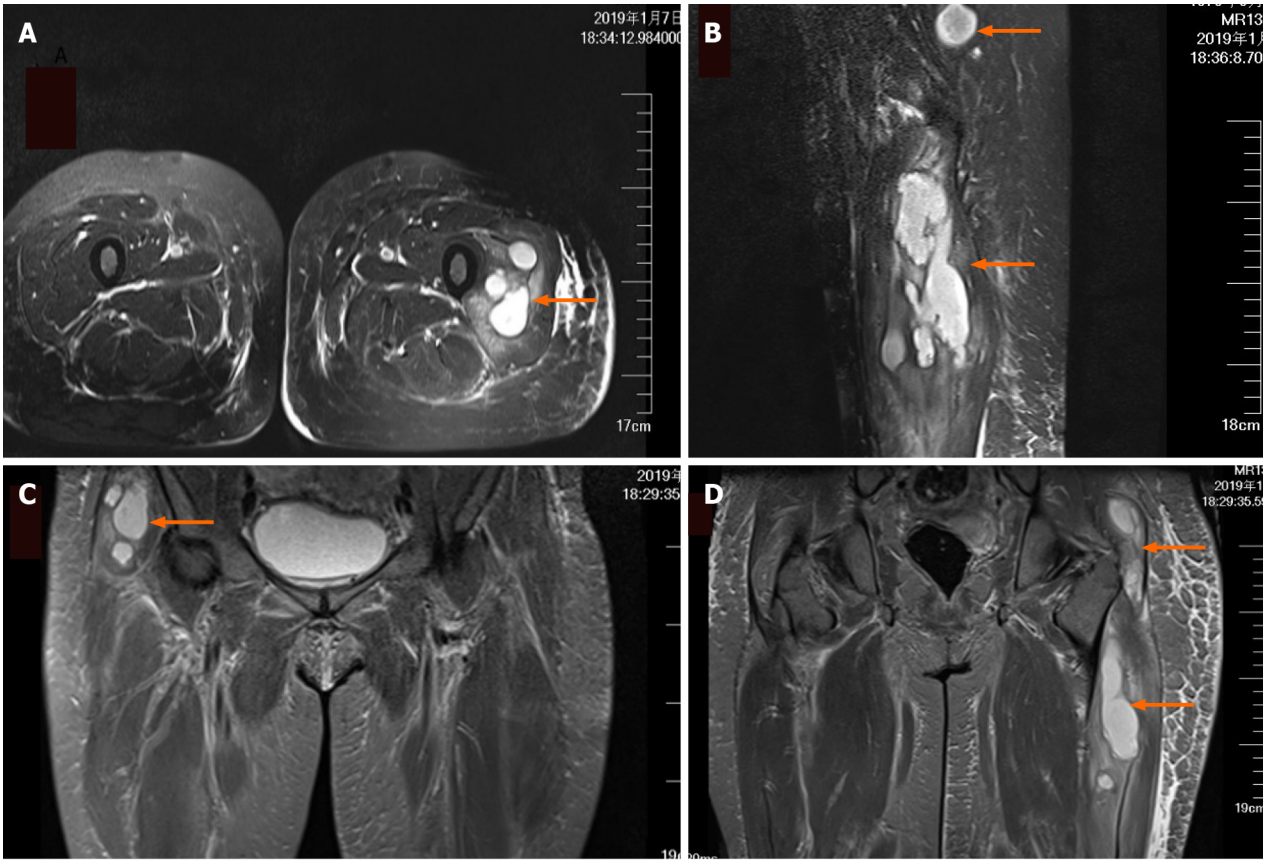

DOI: 10.12998/wjcc.v11.i25.5977

Figure 1 Abscess (arrow) in the gluteal and quadriceps muscles as visualized by T2-weighted magnetic resonance imaging. A: Axillary view; B: Sagittal view; C and D: Coronal view.

particularly the quadriceps (26%), are the most commonly affected muscles, followed by the iliopsoas (14%) and gluteal (10%) muscles[2,5]. The gold standard for the diagnosis of pyomyositis is MRI[6]. In the present case, the patient exhibited swelling and warmth in her thighs, and the final diagnosis was *S. aureus*-induced pyomyositis, based on the results of an MRI and aspirated fluid cultures. In patients with pyomyositis, blood cultures are usually negative, whereas aspirated fluid cultures are usually positive. In > 85% of cases, *S. aureus* is the causative organism[3,7].

The principle treatment for suppurative pyomyositis is surgical incision and drainage combined with intravenous antibiotic administration for 2–3 wk. Such drainage can be performed *via* open surgery, aspiration under ultrasound or CT guidance, or percutaneously. Pyomyositis has been described as having three stages: Invasive, suppurative, and septic, representing a gradual progression from diffuse inflammation to focal abscess formation to a septic state[8]. By the time the disease has progressed for 2–3 wk, suppuration becomes apparent. At that stage, puncture aspiration of the local abscess can be performed. Percutaneous abscess drainage combined with antibiotic therapy is an effective method for the treatment of tropical pyomyositis (also in the suppurative phase). Such drainage can shorten the duration of antibiotic use and hospital stay[9].

The patient in this case was treated with 2 wk of intravenous ceftriaxone, followed by oral antibiotic therapy for 1 wk. As the infection was rather advanced, we performed needle aspiration with ultrasound guidance of the vastus lateralis muscle and gluteus abscess, under local anesthesia. The patient's condition improved following aspiration. No clear guidelines exist for the duration of such antibiotic treatment, but most experts recommend a combination of intravenous and oral antibiotics for 3-8 wk, regardless of whether the abscess is drained[10]. The duration of therapy for our patient was 3 wk. Surprisingly, pyomyositis rarely requires amputation compared to necrotizing fasciitis and myonecrosis. Even when muscle damage is severe, residual deformities and dysfunction are rarely observed. At the 4-month follow-up visit, our patient exhibited complete resolution of her symptoms and had no further complaints.

A preprint of this report was previously published (Min *et al*[11], 2022).

CONCLUSION

The clinical manifestations of pyomyositis, such as muscle pain, swelling, fever, and leukocytosis, can be treated *via* ultrasound-guided percutaneous puncture and drainage. This can aid its diagnosis, facilitating timely treatment and improving the prognosis. We hope that this report will help guide the future treatment of patients with pyomyositis.

FOOTNOTES

Author contributions: Cui M contributed to manuscript writing (original draft preparation); Zhang G contributed to conceptualization; Zhang N contributed to visualization; Han L contributed to investigation; Ma ZQ contributed to manuscript writing (reviewing and editing); all authors have read and approved the final manuscript.

Informed consent statement: Informed written consent was obtained from the patient for publication of this report and any accompanying medical images.

Conflict-of-interest statement: All the authors declare that they have no conflict of interest to disclose.

CARE Checklist (2016) statement: The authors have read the CARE Checklist (2016), and the manuscript was prepared and revised according to the CARE Checklist (2016).

Country/Territory of origin: China

ORCID number: Zai-Qi Ma 0000-0002-2157-931X.

S-Editor: Liu JH
L-Editor: A
P-Editor: Liu JH

REFERENCES

1 **Patel SR**, Olenginski TP, Perruquet JL, Harrington TM. Pyomyositis: clinical features and predisposing conditions. *J Rheumatol* 1997; **24**: 1734-1738 [PMID: 9292796]
2 **Hassan FO**, Shannak A. Primary pyomyositis of the paraspinal muscles: a case report and literature review. *Eur Spine J* 2008; **17** Suppl 2: S239-S242 [PMID: 17932692 DOI: 10.1007/s00586-007-0507-7]
3 **Chauhan S**, Jain S, Varma S, Chauhan SS. Tropical pyomyositis (myositis tropicans): current perspective. *Postgrad Med J* 2004; **80**: 267-270 [PMID: 15138315 DOI: 10.1136/pgmj.2003.009274]
4 **d'Assignies G**, Fangio P, De Jonghe B, Lachérade JC, Outin H. [Septic shock due to tropical pyomyositis]. *Ann Fr Anesth Reanim* 2003; **22**: 913-914 [PMID: 14644377 DOI: 10.1016/j.annfar.2003.09.017]
5 **Gomez-Reino JJ**, Aznar JJ, Pablos JL, Diaz-Gonzalez F, Laffon A. Nontropical pyomyositis in adults. *Semin Arthritis Rheum* 1994; **23**: 396-405 [PMID: 7939725 DOI: 10.1016/0049-0172(94)90090-6]
6 **Stevens DL**, Bisno AL, Chambers HF, Dellinger EP, Goldstein EJ, Gorbach SL, Hirschmann JV, Kaplan SL, Montoya JG, Wade JC; Infectious Diseases Society of America. Practice guidelines for the diagnosis and management of skin and soft tissue infections: 2014 update by the Infectious Diseases Society of America. *Clin Infect Dis* 2014; **59**: e10-e52 [PMID: 24973422 DOI: 10.1093/cid/ciu444]
7 **Lemonick DM**. Non-tropical pyomyositis caused by methicillin-resistant Staphylococcus aureus: an unusual cause of bilateral leg pain. *J Emerg Med* 2012; **42**: e55-e62 [PMID: 19327931 DOI: 10.1016/j.jemermed.2008.12.020]
8 **Spiegel DA**, Meyer JS, Dormans JP, Flynn JM, Drummond DS. Pyomyositis in children and adolescents: report of 12 cases and review of the literature. *J Pediatr Orthop* 1999; **19**: 143-150 [PMID: 10088678 DOI: 10.1097/00004694-199903000-00002]
9 **Palacio EP**, Rizzi NG, Reinas GS, Júnior MM, Júnior AD, Mizobuchi RR, Yanasse RH, da Silva MV, Branco RB, Galbiatti JA. OPEN DRAINAGE VERSUS PERCUTANEOUS DRAINAGE IN THE TREATMENT OF TROPICAL PYOMYOSITIS. PROSPECTIVE AND RANDOMIZED STUDY. *Rev Bras Ortop* 2010; **45**: 260-268 [PMID: 27022550 DOI: 10.1016/S2255-4971(15)30366-9]
10 **Wong CH**, Choi SH, Wong KY. Piriformis pyomyositis: a report of three cases. *J Orthop Surg (Hong Kong)* 2008; **16**: 389-391 [PMID: 19126914 DOI: 10.1177/230949900801600326]
11 **Min C**, Gang Z, Na Z, Lei H, Qi MZ. Bilateral thigh pyomyositis in a healthy middle-aged female: A Case report. SSRN [DOI: 10.2139/ssrn.4133049]

World Journal of Clinical Cases

Submit a Manuscript: https://www.f6publishing.com

World J Clin Cases 2023 September 6; 11(25): 5982-5987

DOI: 10.12998/wjcc.v11.i25.5982

ISSN 2307-8960 (online)

CASE REPORT

Creutzfeldt-Jakob disease presenting as Korsakoff syndrome caused by E196A mutation in *PRNP* gene: A case report

Yong-Kang Zhang, Jia-Rui Liu, Kang-Li Yin, Yuan Zong, Yu-Zhen Wang, Ye-Min Cao

Specialty type: Medicine, research and experimental

Provenance and peer review: Unsolicited article; Externally peer reviewed.

Peer-review model: Single blind

Peer-review report's scientific quality classification

Grade A (Excellent): 0
Grade B (Very good): B
Grade C (Good): C
Grade D (Fair): 0
Grade E (Poor): 0

P-Reviewer: Beran RG, Australia; Toledano A, Spain

Received: May 26, 2023
Peer-review started: May 26, 2023
First decision: July 17, 2023
Revised: July 25, 2023
Accepted: August 9, 2023
Article in press: August 9, 2023
Published online: September 6, 2023

Yong-Kang Zhang, Jia-Rui Liu, Kang-Li Yin, Yuan Zong, Yu-Zhen Wang, Ye-Min Cao, Diagnosis and Treatment Center of Vascular Disease, Shanghai TCM-Integrated Hospital, Shanghai University of Traditional Chinese Medicine, Shanghai 200082, China

Corresponding author: Ye-Min Cao, Doctor, MD, PhD, Academic Research, Chief Doctor, Professor, Diagnosis and Treatment Center of Vascular Disease, Shanghai TCM-Integrated Hospital, Shanghai University of Traditional Chinese Medicine, No. 230 Road Baoding, Hongkou District, Shanghai 200082, China. caoyemin@shutcm.edu.cn

Abstract

BACKGROUND

Prion diseases are a group of degenerative nerve diseases that are caused by infectious prion proteins or gene mutations. In humans, prion diseases result from mutations in the prion protein gene (PRNP). Only a limited number of cases involving a specific PRNP mutation at codon 196 (E196A) have been reported. The coexistence of Korsakoff syndrome in patients with Creutzfeldt-Jakob disease (CJD) caused by E196A mutation has not been documented in the existing literature.

CASE SUMMARY

A 61-year-old Chinese man initially presented with Korsakoff syndrome, followed by rapid-onset dementia, visual hallucinations, akinetic mutism, myoclonus, and hyperthermia. The patient had no significant personal or familial medical history. Magnetic resonance imaging of the brain revealed extensive hyperintense signals in the cortex, while positron emission tomography/computed tomography showed a diffuse reduction in cerebral cortex metabolism. Routine biochemical and microorganism testing of the cerebrospinal fluid (CSF) yielded normal results. Tests for thyroid function, human immunodeficiency virus, syphilis, vitamin B1 and B12 levels, and autoimmune rheumatic disorders were normal. Blood and CSF tests for autoimmune encephalitis and autoantibody-associated paraneoplastic syndrome yielded negative results. A test for 14-3-3 protein in the CSF yielded negative results. Whole-genome sequencing revealed a disease-causing mutation in PRNP. The patient succumbed to the illness 11 months after the initial symptom onset.

CONCLUSION

Korsakoff syndrome, typically associated with alcohol intoxication, also manifests in CJD patients. Individuals with CJD along with PRNP E196A mutation may

present with Korsakoff syndrome.

Key Words: Prion disease; Creutzfeldt-Jakob disease; Korsakoff syndrome; *PRNP* gene; 14-3-3 proteins; Case report

Core Tip: The present case report describes a rare mutation in the prion protein gene at codon 196 causing Creutzfeldt-Jakob disease (CJD) with a clinical presentation of Korsakoff syndrome. This study emphasizes the importance of considering this mutation in CJD patients presenting with Korsakoff syndrome based on clinical, laboratory, and imaging findings.

Citation: Zhang YK, Liu JR, Yin KL, Zong Y, Wang YZ, Cao YM. Creutzfeldt-Jakob disease presenting as Korsakoff syndrome caused by E196A mutation in *PRNP* gene: A case report. *World J Clin Cases* 2023; 11(25): 5982-5987
URL: https://www.wjgnet.com/2307-8960/full/v11/i25/5982.htm
DOI: https://dx.doi.org/10.12998/wjcc.v11.i25.5982

INTRODUCTION

Prion diseases arise from an abnormal transformation of normal cellular prion proteins into abnormal forms. These diseases include Creutzfeldt-Jakob disease (CJD), Kuru disease, Gerstmann-Straussler syndrome and fatal familial insomnia[1]. Sporadic cases account for approximately 85% of the prion diseases, genetic cases account for approximately 10%-15%, and acquired cases account for less than 1%[2]. According to epidemiological studies, the global incidence of CJD ranges from approximately one to two per million per year[3]. The clinical manifestations of CJD involve diffuse or localized dysfunction of the central nervous system, characterized by rapidly progressive dementia, myoclonus, and extrapyramidal, cerebellar, and pyramidal tract signs[4]. Uncommon symptoms include visual abnormalities, cranial nerve palsies, and epileptic seizures[4].

Prion proteins are encoded by the prion protein gene (*PRNP*) located on the 20th human chromosome. Mutations in *PRNP* can lead to the production of pathogenic prion proteins, thereby causing CJD. More than 55 different types of *PRNP* mutations have been associated with CJD, each exhibiting distinct clinical manifestations and neuropathological characteristics[5]. Mutation at codon 196 (E196A) in *PRNP* is a rare mutation that has been reported exclusively in Chinese patients with CJD. No association of Korsakoff syndrome with this mutation has been reported. Korsakoff syndrome is typically characterized by symptoms such as memory impairment, confabulation or falsification, apathy, and disorientation in time and space[6]. While this syndrome is common in individuals with alcoholism, it is rare in CJD patients. The current report presents a case of CJD caused by an E196A mutation that initially presented as Korsakoff syndrome. This case report aimed to provide a detailed description of the clinical manifestations associated with this rare *PRNP* mutation in CJD patients.

CASE PRESENTATION

Chief complaints

A 61-year-old Chinese man with hypertension presented with memory disorders, falsification, time and space disorientation, visual hallucinations, rapidly progressive dementia, akinetic mutism, and myoclonus.

History of present illness

Four months prior, the patient experienced memory disorders, falsification, and time and space disorientation without any identifiable triggers. In the second month after the symptom onset, the patient developed rapidly progressive dementia and visual hallucinations. By the third month, the patient experienced akinetic mutism combined with myoclonus. Hyperthermia occurred in the fourth month after the onset of symptoms.

History of past illness

The patient had a 10-year history of hypertension.

Physical examination

Vital signs were as follows: Body temperature, 36.5 °C; heart rate, 76 beats/min; blood pressure, 119/71 mmHg; and respiratory rate, 20 beats/min. The patient exhibited spontaneous eye opening but was unable to follow commands or exhibit eye tracking. Passive muscle tension, positive pathological reflexes, and myoclonic movements were also observed.

Laboratory examinations

The initial electroencephalogram (EEG) test conducted in the fourth month after symptom onset showed basic rhythmic activity with moderate-potential 8-Hz a waves. Cerebrospinal fluid (CSF) was colorless and transparent without clots or flocculation. Perthes test and oligoclonal bands were negative. CSF analysis revealed normal white blood cell count and immunoglobulin (Ig) G, IgA, IgM, total protein, glucose, and chloride ion levels. Tests for herpes simplex virus, toxoplasmosis, rubella virus, cytomegalovirus, and Epstein-Barr virus in the CSF yielded negative results. Vitamin B1 and B12 levels and thyroid function test results were within normal ranges. Human immunodeficiency virus and syphilis antibody tests were negative. Antibodies associated with autoimmune encephalitis and paraneoplastic syndrome were not detected in the serum and CSF. Rheumatoid and autoimmune disease-related parameters, including erythrocyte sedimentation rate, rheumatoid factor, anti-cyclic citrullinated peptide antibodies, glucose phosphate isomerase, antinuclear antibodies, anti-cardiolipin antibodies, and anti-neutrophil antibodies, were within normal limits.

Imaging examinations

Magnetic resonance imaging (MRI) of the brain revealed hyperintense signals on diffusion-weighted imaging (DWI) sequences in the bilateral occipital, parietal, temporal, and frontal lobes, particularly in the right cortex. These hyperintense signals are referred to as cortical ribbons (Figure 1A). Positron emission tomography/computed tomography showed a diffuse decrease in fluorodeoxyglucose metabolism in the right cerebral cortex (Figure 1B).

Further diagnostic workup

Considering rapid cognitive decline, diffuse brain damage, and hyperthermia, a probable diagnosis of CJD was made. Viral encephalitis, which can be treated, could not be ruled out. Antiviral therapy was attempted by intravenous administration of gamma globulin (300 mg/day) for five days. Physical cooling and benzodiazepines were used to manage the fever and myoclonus.

Despite gamma globulin treatment, the patient's condition did not improve. EEG performed in the fifth month after symptom onset showed bilateral persistent 4-5 Hz q waves, 2-3 Hz d waves, and sharp slow waves. In the sixth month after symptom onset, the EEG showed bilaterally symmetrical low-to-moderate-potential 8-Hz a waves with a large number of moderate-to-high potential 4–6 Hz q waves. Repeated examinations of serum and CSF for autoimmune encephalitis-related antibodies yielded negative results. Other potential diagnoses were ruled out, and CJD remained a potential diagnosis. Although the 14-3-3 protein was not detected in the CSF, the combination of the patient's clinical manifestations and imaging findings further supported the suspicion of CJD. Sequencing of *PRNP* revealed a heterozygous c.A587C base change in the second exon, resulting in a glutamate-to-alanine substitution at E196A that indicated a potential pathogenic mutation (Figure 2).

FINAL DIAGNOSIS

According to diagnostic criteria for CJD[7,8], the final diagnosis in this case was probably CJD caused by an E196A mutation in *PRNP*.

TREATMENT

Physical cooling and antipyretic drugs were administered to manage patient’s hyperthermia. Considering the possibility of viral encephalitis, gamma globulin was initially administered. After the diagnosis of CJD, the patient's family opted for palliative care.

OUTCOME AND FOLLOW-UP

The patient succumbed to illness within 11 mo of onset. The family declined an autopsy.

DISCUSSION

Mutations in *PRNP*, which is located on the 20th human chromosome, can lead to the development of prion diseases. One specific mutation, E196A, has been reported in cases of CJD. Between 2014 and 2019, four cases of CJD with E196A mutation were individually documented[9-11]. In 2021, the Chinese National CJD Surveillance System reported 16 Chinese CJD patients with the E196A mutation, including four previously reported cases[12]. All 16 patients[12] and the patient mentioned in this case study were of Han Chinese ethnicity and had no relevant family history or known exposure to prion diseases. Patients with the E196A mutation exhibit nonspecific symptoms at onset, and disease progression demonstrated typical features of sporadic prion diseases. The disease duration varied between 2 and 28 mo in the reported Chinese cases[12]. No brain tissue biopsy or autopsy was conducted in any of the 17 patients, leading to inconclusive evidence regarding the relationship between the E196A mutation in *PRNP* and occurrence of CJD.

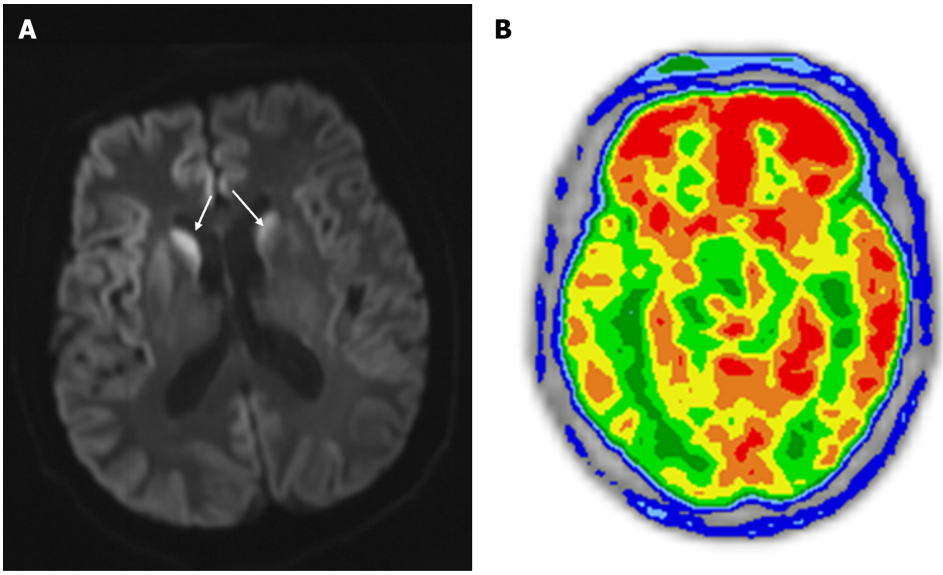

DOI: 10.12998/wjcc.v11.i25.5982 **Copyright** ©The Author(s) 2023.

Figure 1 Diffusion-weighted imaging and positron emission tomography/computed tomography of brain. A: Hyperintense signals observed in bilateral occipital, parietal, temporal, and frontal lobes. Hyperintense signals in bilateral thalamus (white arrow markers); B: Decreased diffuse fluorodeoxyglucose metabolism seen on the right cerebral cortex.

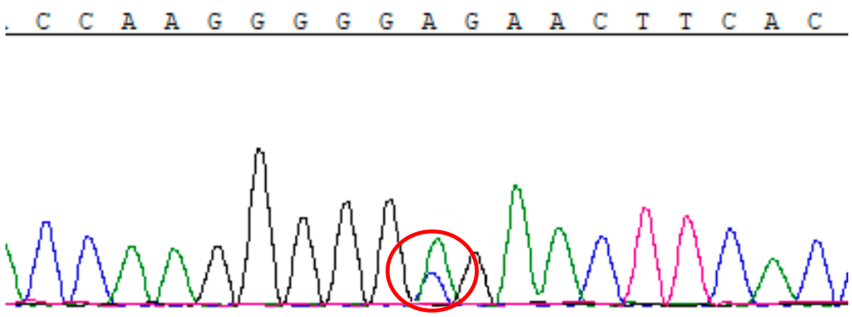

DOI: 10.12998/wjcc.v11.i25.5982 **Copyright** ©The Author(s) 2023.

Figure 2 *PRNP* sequencing outcome. Red circle marks the presence of a c.A587C base heterozygous change in the second exon of *PRNP*.

Based on the clinical manifestations and imaging features, the patient was diagnosed with probable CJD. A recent study have found that the criterion of displaying at least one positive brain region on DWI to diagnose CJD has a sensitivity and specificity higher than 90%[13]. Other possible diagnoses were ruled out during examination. *PRNP* sequencing results firmly established the diagnosis of CJD. CJD patients harboring the E196A mutation present with various clinical manifestations, including mental problems, dementia, cerebellar disorders, visual disturbances, pyramidal dysfunction, and extrapyramidal dysfunction[12,14]. None of the reported patients with the E196A mutation mentioned Korsakoff syndrome. Korsakoff syndrome is a mental disorder caused by vitamin B1 deficiency in the brain, and is characterized by memory impairment, confabulation or falsification, apathy, and time and space disorientation. Although cases of CJD presenting as Korsakoff syndrome have been reported[15], imaging examinations in previous cases, including the present case, did not reveal typical lesions associated with vitamin B1 deficiency. Given the rapidly progressive dementia following Korsakoff syndrome and the normal serum level of vitamin B1, CJD is considered a more likely diagnosis than Wernicke encephalopathy, despite the presence of Korsakoff syndrome in early stages of the disease [16,17]. Current study is the first report of a CJD patient associated with the E196A mutation who displayed Korsakoff syndrome at an early stage. Based on the findings of MRI of the brain, the thalamic region is speculated to be involved in the occurrence of Korsakoff syndrome in this CJD patient. The survival time for CJD patients presenting with Korsakoff syndrome ranges from 2 to 18 mo[18].

The 14-3-3 protein, a classic biomarker of CJD, was not found in the patient's CSF in this case. Similar results were observed in previous cases of CJD with E196A mutation[12]. This may be related to the fact that some patients are in the early stages of the disease or that the 14-3-3 protein has low sensitivity in certain CJD subtypes[19].

Another mutation at the same codon, E196K, was identified in a Caucasian population and confirmed to be associated with CJD[20]. Patients with CJD caused by the E196K mutation were positive for CSF 14-3-3 protein and had a shorter disease course, averaging 6.5 mo. Since the E196A mutation is located adjacent to E196K, it is possible that E196A may have a pathogenic role similar to that of E196K. However, the neuropathological characteristics associated with E196A

mutation have not yet been clarified. The conclusions drawn from the present case report are based on the available information and current understanding of CJD and prion diseases. Further research, including brain tissue analyses and autopsy studies, is required to establish a definitive relationship between the E196A mutation in *PRNP* and CJD, and to elucidate the neuropathological characteristics associated with this mutation.

However, CJD is incurable. Some researchers have recently attempted to inhibit prion duplication to prolong the survival of CJD patients[19,21]. The present study's findings offer new insights for the treatment of CJD.

CONCLUSION

Multiple factors, including clinical manifestations, laboratory test results, and imaging findings, should be considered when diagnosing CJD. The diagnosis of CJD can be challenging owing to its diverse clinical presentations and the need to exclude other possible causes. The rarity of E196A mutation in CJD highlights the complexity of this disease.

ACKNOWLEDGEMENTS

We thank the Department of Vascular Disease nurses who helped draw blood.

FOOTNOTES

Author contributions: Zong Y, Wang YZ and Yin KL conducted data collection and medical history compilation; Zhang YK and Liu JR conducted manuscript writing, manuscript editing, and submission; Cao YM revised and guided the manuscript; All authors read and approved the final manuscript.

Informed consent statement: The patient's immediate family members signed a Chinese informed consent form approved by the Ethics Committee of Shanghai TCM-Integrated Hospital. The consent form covers permission to publish personal information and images. Both the copy of the consent form and the copy of the consent have been uploaded for editor review.

Conflict-of-interest statement: Ye-Min Cao has not received fees for serving as a speaker. Ye-Min Cao has not received research funding from any organization(s). Ye-Min Cao is an employee of Shanghai TCM-Integrated Hospital. Ye-Min Cao doesn't own stocks and/or shares in the hospital. Ye-Min Cao doesn't own a patent.

CARE Checklist (2016) statement: The authors have read the CARE Checklist (2016), and the manuscript was prepared and revised according to the CARE Checklist (2016).

Country/Territory of origin: China

ORCID number: Yong-Kang Zhang 0000-0002-2156-6762; Ye-Min Cao 0000-0001-5961-1058.

S-Editor: Fan JR
L-Editor: A
P-Editor: Cai YX

REFERENCES

1 **Imran M**, Mahmood S. An overview of human prion diseases. *Virol J* 2011; **8**: 559 [PMID: 22196171 DOI: 10.1186/1743-422X-8-559]
2 **Prusiner SB**. The prion diseases. *Brain Pathol* 1998; **8**: 499-513 [PMID: 9669700 DOI: 10.1111/j.1750-3639.1998.tb00171.x]
3 **Uttley L**, Carroll C, Wong R, Hilton DA, Stevenson M. Creutzfeldt-Jakob disease: a systematic review of global incidence, prevalence, infectivity, and incubation. *Lancet Infect Dis* 2020; **20**: e2-e10 [PMID: 31876504 DOI: 10.1016/S1473-3099(19)30615-2]
4 **Shir D**, Lazar EB, Graff-Radford J, Aksamit AJ, Cutsforth-Gregory JK, Jones DT, Botha H, Ramanan VK, Prusinski C, Porter A, Day GS. Analysis of Clinical Features, Diagnostic Tests, and Biomarkers in Patients With Suspected Creutzfeldt-Jakob Disease, 2014-2021. *JAMA Netw Open* 2022; **5**: e2225098 [PMID: 35921110 DOI: 10.1001/jamanetworkopen.2022.25098]
5 **Jeong BH**, Kim YS. Genetic studies in human prion diseases. *J Korean Med Sci* 2014; **29**: 623-632 [PMID: 24851016 DOI: 10.3346/jkms.2014.29.5.623]
6 **Oudman E**, Wijnia JW, Oey MJ, van Dam M, Postma A. Wernicke-Korsakoff syndrome despite no alcohol abuse: A summary of systematic reports. *J Neurol Sci* 2021; **426**: 117482 [PMID: 34000679 DOI: 10.1016/j.jns.2021.117482]

7 **Manix M**, Kalakoti P, Henry M, Thakur J, Menger R, Guthikonda B, Nanda A. Creutzfeldt-Jakob disease: updated diagnostic criteria, treatment algorithm, and the utility of brain biopsy. *Neurosurg Focus* 2015; **39**: E2 [PMID: 26646926 DOI: 10.3171/2015.8.FOCUS15328]

8 **Hermann P**, Appleby B, Brandel JP, Caughey B, Collins S, Geschwind MD, Green A, Haïk S, Kovacs GG, Ladogana A, Llorens F, Mead S, Nishida N, Pal S, Parchi P, Pocchiari M, Satoh K, Zanusso G, Zerr I. Biomarkers and diagnostic guidelines for sporadic Creutzfeldt-Jakob disease. *Lancet Neurol* 2021; **20**: 235-246 [PMID: 33609480 DOI: 10.1016/S1474-4422(20)30477-4]

9 **Zhang H**, Wang M, Wu L, Zhang H, Jin T, Wu J, Sun L. Novel prion protein gene mutation at codon 196 (E196A) in a septuagenarian with Creutzfeldt-Jakob disease. *J Clin Neurosci* 2014; **21**: 175-178 [PMID: 23787189 DOI: 10.1016/j.jocn.2013.03.016]

10 **Shi Q**, Zhou W, Chen C, Zhang BY, Xiao K, Wang Y, Dong XP. Rare E196A mutation in PRNP gene of 3 Chinese patients with Creutzfeldt-Jacob disease. *Prion* 2016; **10**: 331-337 [PMID: 27310471 DOI: 10.1080/19336896.2016.1190897]

11 **Dai Y**, Lang Y, Ding M, Zhang B, Han X, Duan G, Cui L. Rare genetic Creutzfeldt-Jakob disease with E196A mutation: a case report. *Prion* 2019; **13**: 132-136 [PMID: 31238786 DOI: 10.1080/19336896.2019.1631679]

12 **Shi Q**, Xiao K, Chen C, Zhou W, Gao LP, Wu YZ, Wang Y, Hu C, Gao C, Dong XP. Characteristics of Chinese patients with genetic CJD who have E196A or E196K mutation in PRNP: comparative analysis of patients identified in the Chinese National CJD Surveillance System. *BMJ Open* 2021; **11**: e054551 [PMID: 34782343 DOI: 10.1136/bmjopen-2021-054551]

13 **Bizzi A**, Pascuzzo R, Blevins J, Grisoli M, Lodi R, Moscatelli MEM, Castelli G, Cohen ML, Schonberger LB, Foutz A, Safar JG, Appleby BS, Gambetti P. Evaluation of a New Criterion for Detecting Prion Disease With Diffusion Magnetic Resonance Imaging. *JAMA Neurol* 2020; **77**: 1141-1149 [PMID: 32478816 DOI: 10.1001/jamaneurol.2020.1319]

14 **Shi Q**, Chen C, Xiao K, Zhou W, Gao LP, Chen DD, Wu YZ, Wang Y, Hu C, Gao C, Dong XP. Genetic Prion Disease: Insight from the Features and Experience of China National Surveillance for Creutzfeldt-Jakob Disease. *Neurosci Bull* 2021; **37**: 1570-1582 [PMID: 34487324 DOI: 10.1007/s12264-021-00764-y]

15 **Pietrini V**. Creutzfeldt-Jakob disease presenting as Wernicke-Korsakoff syndrome. *J Neurol Sci* 1992; **108**: 149-153 [PMID: 1517746 DOI: 10.1016/0022-510x(92)90045-m]

16 **Chen B**, Zhang S, Xiao Y, Wu Y, Tang W, Yan L, Zhang Z, Qin S, Dai M, You Y. Genetic Creutzfeldt-Jakob disease shows fatal family insomnia phenotype. *Prion* 2021; **15**: 177-182 [PMID: 34486485 DOI: 10.1080/19336896.2021.1968291]

17 **Iwasaki Y**, Hashimoto R, Saito Y, Aiba I, Inukai A, Akagi A, Mimuro M, Miyahara H, Kitamoto T, Yoshida M. An autopsied case of MM1-type sporadic Creutzfeldt-Jakob disease with pathology of Wernicke encephalopathy. *Prion* 2019; **13**: 13-20 [PMID: 30409087 DOI: 10.1080/19336896.2018.1545525]

18 **Goossens K**, van Bruchem-Visser RL. A patient with a 'typical presentation' of Wernicke encephalopathy was found to have sporadic Creutzfeldt-Jakob disease. *Neth J Med* 2017; **75**: 211-214 [PMID: 28653943]

19 **Vallabh SM**, Minikel EV, Schreiber SL, Lander ES. Towards a treatment for genetic prion disease: trials and biomarkers. *Lancet Neurol* 2020; **19**: 361-368 [PMID: 32199098 DOI: 10.1016/S1474-4422(19)30403-X]

20 **Peoc'h K**, Manivet P, Beaudry P, Attane F, Besson G, Hannequin D, Delasnerie-Lauprêtre N, Laplanche JL. Identification of three novel mutations (E196K, V203I, E211Q) in the prion protein gene (PRNP) in inherited prion diseases with Creutzfeldt-Jakob disease phenotype. *Hum Mutat* 2000; **15**: 482 [PMID: 10790216 DOI: 10.1002/(SICI)1098-1004(200005)15:5<482::AID-HUMU16>3.0.CO;2-1]

21 **Minikel EV**, Zhao HT, Le J, O'Moore J, Pitstick R, Graffam S, Carlson GA, Kavanaugh MP, Kriz J, Kim JB, Ma J, Wille H, Aiken J, McKenzie D, Doh-Ura K, Beck M, O'Keefe R, Stathopoulos J, Caron T, Schreiber SL, Carroll JB, Kordasiewicz HB, Cabin DE, Vallabh SM. Prion protein lowering is a disease-modifying therapy across prion disease stages, strains and endpoints. *Nucleic Acids Res* 2020; **48**: 10615-10631 [PMID: 32776089 DOI: 10.1093/nar/gkaa616]

World Journal of Clinical Cases

Submit a Manuscript: https://www.f6publishing.com

World J Clin Cases 2023 September 6; 11(25): 5988-5993

DOI: 10.12998/wjcc.v11.i25.5988

ISSN 2307-8960 (online)

CASE REPORT

Incomplete distal renal tubular acidosis uncovered during pregnancy: A case report

Eun Young Seong, Da Woon Kim, Hyo Jin Kim, Harin Rhee, Sang Heon Song

Specialty type: Urology and nephrology

Provenance and peer review: Unsolicited article; Externally peer reviewed.

Peer-review model: Single blind

Peer-review report's scientific quality classification

Grade A (Excellent): 0
Grade B (Very good): 0
Grade C (Good): C
Grade D (Fair): D, D
Grade E (Poor): 0

P-Reviewer: Fabbian F, Italy; Han J, China

Received: May 24, 2023
Peer-review started: May 24, 2023
First decision: June 15, 2023
Revised: July 12, 2023
Accepted: August 8, 2023
Article in press: August 8, 2023
Published online: September 6, 2023

Eun Young Seong, Hyo Jin Kim, Harin Rhee, Sang Heon Song, Department of Internal Medicine, Biomedical Research Institute, Pusan National University Hospital, Busan 49241, South Korea

Eun Young Seong, Hyo Jin Kim, Harin Rhee, Sang Heon Song, Department of Internal Medicine, School of Medicine, Pusan National University, Yangsan-si 50612, Gyeongsangnam-do, South Korea

Da Woon Kim, Department of Internal Medicine, Pusan National University School of Medicine, Busan 49241, South Korea

Corresponding author: Eun Young Seong, MD, PhD, Professor, Department of Internal Medicine, Biomedical Research Institute, Pusan National University Hospital, 179 Gudeok-ro, Seo-gu, Busan 49241, South Korea. sey-0220@hanmail.net

Abstract

BACKGROUND

Renal tubular acidosis (RTA) is a renal cause of non-anion-gap metabolic acidosis characterized by low urinary ammonia excretion. This condition has a low prevalence, and various congenital and acquired etiologies. To date, only a few cases of idiopathic RTA uncovered during pregnancy have been reported.

CASE SUMMARY

A previously healthy 32-year-old Korean woman at 30 wk of gestation was admitted to Pusan National University Hospital with preterm labor. At admission, the patient presented with hypokalemia, non-anion-gap metabolic acidosis, and nephrocalcinosis. Distal RTA was diagnosed based on laboratory blood and urine findings and imaging examinations. Various tests, including next-generation gene sequencing panels for nephropathy, were performed to determine the etiology of the disease, which indicated that it was idiopathic. The patient received sodium bicarbonate and potassium chloride supplementation. After 3 wk, she delivered a baby who was subsequently diagnosed with corpus callosum agenesis and colpocephaly. During regular follow-ups for 6 mo postpartum, her hypokalemia and metabolic acidosis were gradually resolved, and medications eventually discontinued.

CONCLUSION

Herein we describe a case of idiopathic distal RTA discovered during pregnancy. Hypokalemia and metabolic acidosis resolved spontaneously after delivery.

Key Words: Renal tubular acidosis; Pregnancy; Hypokalemia; Sodium bicarbonate; Case report

Core Tip: Renal tubular acidosis is a rare disease that presents as non-anion-gap metabolic acidosis. To the best of our knowledge, only a few cases of idiopathic distal renal tubular acidosis uncovered during pregnancy have been reported. To date, the exact pathophysiology by which pregnancy activates this condition has not been established.

Citation: Seong EY, Kim DW, Kim HJ, Rhee H, Song SH. Incomplete distal renal tubular acidosis uncovered during pregnancy: A case report. *World J Clin Cases* 2023; 11(25): 5988-5993
URL: https://www.wjgnet.com/2307-8960/full/v11/i25/5988.htm
DOI: https://dx.doi.org/10.12998/wjcc.v11.i25.5988

INTRODUCTION

Renal tubular acidosis (RTA) is a rare disease caused by the failure of net acid excretion in the kidneys. Based on its pathophysiology, RTA is divided into four subtypes, three of which are major and related to the mechanisms of renal acid–base handling. Distal (type 1) RTA results from a reduction in net acid secretion in the distal nephron[1], proximal (type 2) RTA is characterized by a decreased capacity of the proximal tubule to reabsorb filtered bicarbonate, and hyperkalemic (type 4) RTA is characterized by impaired renal excretion of both acid and potassium in the distal nephron [2]. Each can be distinguished based on renal function, serum potassium, serum bicarbonate, urine pH, urine citrate, and the presence of Fanconi syndrome. Mixed (type 3) RTA shows features of both distal and proximal RTA and is most often associated with rare autosomal recessive syndromes[1].

RTA has various causes, including primary (inherited or idiopathic) and secondary (acquired) factors. Only a few cases of idiopathic RTA uncovered during pregnancy have been reported[3,4]. Here, we present the case of a healthy pregnant woman in her third trimester who was diagnosed with idiopathic distal RTA and spontaneously recovered from hypokalemia and metabolic acidosis after delivery.

CASE PRESENTATION

Chief complaints

A 32-year-old unemployed Korean woman presented with lower abdominal pain.

History of present illness

The patient was gravida III at 30 wk of gestation. There was lower abdominal pain due to uterine contractions.

History of past illness

The patient had no significant medical history, including kidney stones. She delivered two preterm babies in 2012 and 2016, both by normal spontaneous vaginal delivery at 35 wk of gestation. The babies were healthy and within the normal range of birth weight. She denied any medication history, including herbal medicines, vaccines, depot injections, and nonprescription medications.

Personal and family history

The patient reported no significant family history of related illnesses.

Physical examination

On admission, she had a height of 168 cm, weight 82.1 kg, blood pressure 120/70 mmHg, regular heart rate of 97 beats per minute, and temperature 36.4 ℃. The patient complained of lower abdominal pain due to periodic uterine contractions with cervical dilatation and was thus thought to be in preterm labor. The fundus height corresponded to 30 wk of gestation. No notable physical examination findings indicated any volume depletion.

Laboratory examinations

On admission, the patient had moderate hypokalemia with potassium level 2.98 mEq/L. She did not show any symptoms indicative of recent potassium loss from the gastrointestinal tract such as diarrhea, and had a healthy appetite.

Further blood tests revealed the following: White blood cells 13520 cells/uL, hemoglobin 10.9 g/dL, platelets 350000 cells/uL, sodium 136 mEq/L, potassium 2.98 mEq/L, chloride 107 mEq/L, bicarbonate 18 mEq/L, blood urea nitrogen 30 mg/dL, creatinine 0.4 mg/dL, glucose 91 mg/dL, albumin 3.3 mg/dL, calcium 8.5 mg/dL, magnesium 1.7 mEq/L, and

serum anion gap of 11 mEq/L. Urine studies revealed a urine pH of 7.0, urine anion gap of 28 mEq/L (urine sodium, 81 mEq/L; urine potassium, 15 mEq/L; and urine chloride, 68 mEq/L), urine osmolar gap of 28 mEq/L, and transtubular potassium gradient of 4.8 (serum osmolality, 282 mOsm/dL/L; urine osmolality, 304 mOsm/dL; urine potassium, 15 mEq/L; and serum potassium 2.98 meq/L). Urine protein and glucose levels were negative and pyuria was absent. Hypercalciuria (440 mg/d) and hypocitraturia (44 mg/d) were also observed.

Imaging examinations

Ultrasonography of the fetus was performed on the day of admission and showed a biparietal diameter of 8.35 cm, abdominal circumference 26.86 cm, femur length 5.22 cm and estimated body weight 1572 g, which was in the 75th percentile at 30 wk of gestation[5]. The amniotic fluid index was 19.37 cm, calculated by adding the anteroposterior diameters of the largest empty fluid pocket in each quadrant (quadrant 1: 4.50 cm, quadrant 2: 5.74 cm, quadrant 3: 3.92 cm, quadrant 4: 5.21 cm) and the value was in the 95th percentile at 30 wk of gestation[6].

Nephrocalcinosis and tiny renal stones were detected on whole abdominal ultrasonography and computed tomography (Figure 1). No radiological findings of medullary sponge kidney were observed.

FINAL DIAGNOSIS

Urine and transtubular potassium gradients indicated increased potassium secretion in the distal portions of the kidney. Because the patient had normal blood pressure, non-anion-gap metabolic acidosis, normal aldosterone to renin ratio (1.32 ng/dL per ng/mL per hour), and nephrocalcinosis, incomplete distal RTA was strongly suspected. However, because the patient refused the provocative acid-loading test, the disease was not confirmed. She had no history or clinical indication of autoimmune disease or renal stones and no history of drug use or toxin exposure. Thyroid-stimulating hormone, human immunodeficiency virus, and hepatitis panel results were normal or nonreactive. Additional studies, including next-generation sequencing (NGS) panels of nephropathy-related genes, were performed to determine the cause of distal RTA. The NGS panels consisted of 39 genes, six of which were related to the proximal and distal RTA. The results indicated that none of these genes were significantly altered. Therefore, we concluded that the distal RTA was idiopathic in this case.

TREATMENT

After the diagnosis of distal RTA, the patient received a daily dose of 1500 mg sodium bicarbonate to correct metabolic acidosis and 1800 mg potassium chloride supplementation. Blood tests returned to normal 12 days after the start of supplementation, with a serum potassium of 4.2 mEq/L and bicarbonate of 21 mEq/L. After 2 wk, as the shortness of the cervix and the interval between uterine contractions did not progress, the patient was discharged with medications.

OUTCOME AND FOLLOW-UP

One week later, the patient was admitted to the hospital for labor and underwent spontaneous vaginal delivery. As agenesis of the corpus callosum was suspected on prenatal ultrasonography, brain magnetic resonance imaging was performed, which confirmed agenesis of the corpus callosum and colpocephaly. Although the baby experienced a brief period of apnea after birth, it spontaneously recovered with supportive care, and no other brain-related complications were detected.

After delivery, the patient visited the hospital monthly for RTA checkups, and her laboratory findings gradually returned to normal. Four months after the diagnosis, all medications were discontinued.

DISCUSSION

Distal RTA (type 1) is a relatively common form of RTA. There are various causes of distal RTA, including primary (idiopathic or familial) and secondary (autoimmune disorders, genetic disorders, drugs or toxins, nephrocalcinosis, and tubulointerstitial diseases). Distal RTA should be suspected in all patients with hypokalemia and non-anion-gap metabolic acidosis. Further urine analysis showing a urine pH above 5.5 and a urine anion gap value greater than zero or lack of an increase in the urine osmolar gap helps confirm the disease[1]. Severe hypokalemia (< 2.5 mEq/L) can result in musculoskeletal weakness and rhabdomyolysis. Nephrocalcinosis can be observed using abdominal ultrasonography or radiography.

Administration of an alkali can correct metabolic acidosis in the distal RTA. In patients with severe potassium deficits, potassium replacement should be the first treatment before acidosis is corrected, because serum potassium levels can be lowered to dangerous levels through bicarbonate replacement. Generally, distal RTA treatment includes bicarbonate and potassium supplementation. In patients with recurrent renal stone disease caused by distal RTA, acidosis may lead to stone dissolution by increasing urinary citrate excretion and slowing further stone formation.

Table 1 Causes and clinical courses of distal renal tubular acidosis diagnosed in pregnant women

Ref.	Cause	Clinical course
Muthukrishnan *et al* [10], 2010	Idiopathic	Recurrent rhabdomyolysis induced by hypokalemia in consecutive pregnancies; successful delivery and potassium replacement was needed on follow-up
Mallett *et al*[14], 2011	Ibuprofen, codeine abuse	RTA resolved after quitting ibuprofen and codeine; successful delivery and renal function did not fully return to baseline on follow-up
Srisuttayasathien[9], 2015	Idiopathic	Rhabdomyolysis induced by hypokalemia; successful delivery and complete resolution of RTA on follow-up
Alkhasoneh *et al*[11], 2019	Not identified (patient refusal of autoimmune disease workup)	Severe metabolic acidosis and hypokalemia; successful delivery and only sodium bicarbonate was needed on follow-up

RTA: Renal tubular acidosis.

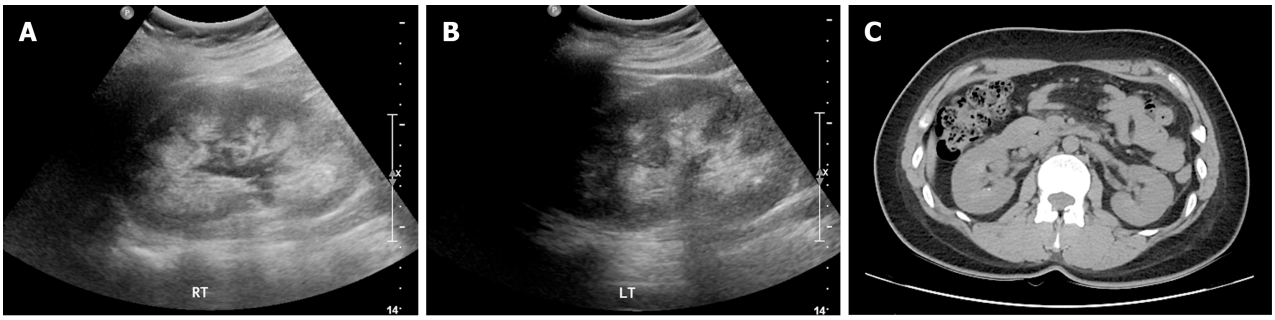

DOI: 10.12998/wjcc.v11.i25.5988

Figure 1 Ultrasonography and computed tomography images of kidney. A: Right kidney; B: Left kidney on ultrasonography; C: Axial computed tomography image. Bilateral medullary nephrocalcinosis.

Table 1 lists case reports of distal RTA diagnosed during pregnancy. Patients who have been diagnosed with distal RTA before pregnancy generally have confirmed causes such as autoimmune diseases or inherited factors[7,8]. However, in most cases of distal RTA presenting for the first time during pregnancy, the etiologies were unknown. Among cases presenting with unidentified causes of distal RTA, only one case has been reported to be completely cured after pregnancy[9]. Another case of rhabdomyolysis induced by severe hypokalemia in consecutive pregnancies involved a distal RTA of an uncertain etiology. After the successful delivery of healthy babies, the patient required continuous potassium replacement during the follow-up[10]. In a recently reported case of a distal RTA, the patient exhibited severe metabolic acidosis and hypokalemia due to distal RTA. After successful delivery, the distal RTA persisted and only sodium bicarbonate was required during the follow-up[11].

Renal physiology changes significantly during a normal pregnancy, and is characterized by marked volume expansion and vasodilation. Renal plasma flow increases by approximately 80% and glomerular filtration rate (GFR) by 50%[12]. An elevated GFR indicates an increase in the filtered solute load, although tubular reabsorption is proportionally increased. This imbalance between the filtered solute load and tubular reabsorption causes an increased loss of some electrolytes, leading to a higher need for potassium and bicarbonate. Typically, chronic mild respiratory alkalosis occurs secondary to hyperventilation, which lowers arterial carbon dioxide tension. Owing to these physiological changes, pregnancy has been reported to worsen RTA[1]. In the current case, idiopathic distal RTA was uncovered during pregnancy and spontaneous resolution of hypokalemia and metabolic acidosis occurred after delivery. Since nephrocalcinosis and renal stones were present on imaging at the time of diagnosis, we suspected that a hidden distal RTA might have existed and was uncovered when it worsened during pregnancy.

Theoretically, prolonged maternal metabolic acidosis due to chronic RTA impairs fetal growth and development and causes fetal distress, commonly resulting in preterm labor[11]. There has been a case of distal RTA secondary to possible Sjögren's syndrome causing multiple pregnancy losses[7,13]. In this case, the patient had a history of preterm delivery of two babies without any congenital brain defects. As she was at 35 wk of gestation, which is near full term, and the babies were healthy, no further evaluations, including laboratory examinations that might suspect RTA, were performed. Since the patient was gravida III diagnosed with RTA, she also had preterm labor, but the gestational age was earlier than that of gravidas I and II. Therefore, further evaluation for the patient was conducted and revealed hypokalemia with metabolic acidosis. The infant also had a congenital brain defect. Although she did not have severe hypokalemia or metabolic acidosis at the time of diagnosis, we cannot rule out the possibility that prolonged maternal metabolic acidosis resulting from an undiagnosed distal RTA was related to consecutive preterm labor and fetal distress.

CONCLUSION

In conclusion, we report a rare case of idiopathic distal RTA uncovered during pregnancy. The patient had an unremarkable medical history and no symptoms or laboratory findings suggestive of other causes of RTA. The patient was treated accordingly, and 3 wk later delivered an infant with corpus callosum agenesis and colpocephaly. After delivery, the hypokalemia and metabolic acidosis resolved spontaneously and completely, and no further treatment was required.

ACKNOWLEDGEMENTS

We thank the patient for her participation and cooperation in this case report.

FOOTNOTES

Author contributions: Kim DW collected clinical data and drafted the manuscript; Kim HJ and Rhee H reviewed the manuscript and provided intellectual input; Song SH and Seong EY reviewed the literature and revised the manuscript; all the authors have read and approved the final version of the manuscript.

Supported by Clinical Research Grant from Pusan National University Hospital in 2022.

Informed consent statement: Written informed consent was obtained from the patient for publication of this report.

Conflict-of-interest statement: The authors declare no conflicts of interest.

CARE Checklist (2016) statement: The authors have read the CARE Checklist (2016), and the manuscript was prepared and revised according to the CARE Checklist (2016).

Country/Territory of origin: South Korea

ORCID number: Eun Young Seong 0000-0002-6006-0051; Da Woon Kim 0000-0002-9471-5976; Sang Heon Song 0000-0002-8218-6974.

S-Editor: Yan JP
L-Editor: A
P-Editor: Cai YX

REFERENCES

1 **Johnson RJ**, Feehally J, Floege J, Tonelli M. Comprehensive Clinical Nephrology. 6th ed. Elsevier, 2018: 150-154, 501-531
2 **Rodríguez Soriano J**. Renal tubular acidosis: the clinical entity. *J Am Soc Nephrol* 2002; **13**: 2160-2170 [PMID: 12138150 DOI: 10.1097/01.asn.0000023430.92674.e5]
3 **Hardardottir H**, Lahiri T, Egan JF. Renal tubular acidosis in pregnancy: case report and literature review. *J Matern Fetal Med* 1997; **6**: 16-20 [PMID: 9029379 DOI: 10.1002/(SICI)1520-6661(199701/02)6:1<16::AID-MFM3>3.0.CO;2-V]
4 **Firmin CJ**, Kruger TF, Davids R. Proximal renal tubular acidosis in pregnancy. A case report and literature review. *Gynecol Obstet Invest* 2007; **63**: 39-44 [PMID: 16902307 DOI: 10.1159/000094942]
5 **Mikolajczyk RT**, Zhang J, Betran AP, Souza JP, Mori R, Gülmezoglu AM, Merialdi M. A global reference for fetal-weight and birthweight percentiles. *Lancet* 2011; **377**: 1855-1861 [PMID: 21621717 DOI: 10.1016/S0140-6736(11)60364-4]
6 **Moore TR**, Cayle JE. The amniotic fluid index in normal human pregnancy. *Am J Obstet Gynecol* 1990; **162**: 1168-1173 [PMID: 2187347 DOI: 10.1016/0002-9378(90)90009-v]
7 **Yuvaraj A**, Ghosh S, Shanmugasundaram L, Abraham G. Sjogren's with distal renal tubular acidosis complicating pregnancy. *J Obstet Gynaecol* 2018; **38**: 429-431 [PMID: 29361865 DOI: 10.1080/01443615.2017.1303466]
8 **Seeger H**, Salfeld P, Eisel R, Wagner CA, Mohebbi N. Complicated pregnancies in inherited distal renal tubular acidosis: importance of acid-base balance. *J Nephrol* 2017; **30**: 455-460 [PMID: 28005240 DOI: 10.1007/s40620-016-0370-x]
9 **Srisuttayasathien M**. Hypokalemia-Induced Rhabdomyolysis as a result of Distal Renal Tubular Acidosis in a Pregnant Woman: A Case Report and Literature Review. *Case Rep Obstet Gynecol* 2015; **2015**: 947617 [PMID: 26788388 DOI: 10.1155/2015/947617]
10 **Muthukrishnan J**, Harikumar K, Jha R, Modi K. Pregnancy predisposes to rhabdomyolysis due to hypokalemia. *Saudi J Kidney Dis Transpl* 2010; **21**: 1127-1128 [PMID: 21060186]
11 **Alkhasoneh M**, Jacobs J, Kaur G. A case of severe metabolic acidosis during pregnancy. *Clin Case Rep* 2019; **7**: 550-552 [PMID: 30899492 DOI: 10.1002/ccr3.2042]

12 **Cheung KL**, Lafayette RA. Renal physiology of pregnancy. *Adv Chronic Kidney Dis* 2013; **20**: 209-214 [PMID: 23928384 DOI: 10.1053/j.ackd.2013.01.012]
13 **Jain SH**, Sainarersh VV, Patel HV, Trivedi HL. Renal tubular acidosis: an uncommon cause of bad obstetric history. *J Obstet Gynaecol India* 2014; **64**: 34-35 [PMID: 25404803 DOI: 10.1007/s13224-013-0440-0]
14 **Mallett A**, Lynch M, John GT, Healy H, Lust K. Ibuprofen-related renal tubular acidosis in pregnancy. *Obstet Med* 2011; **4**: 122-124 [PMID: 27579107 DOI: 10.1258/om.2011.110041]

World Journal of Clinical Cases

Submit a Manuscript: https://www.f6publishing.com

World J Clin Cases 2023 September 6; 11(25): 5994-5999

DOI: 10.12998/wjcc.v11.i25.5994

ISSN 2307-8960 (online)

CASE REPORT

Single omental metastasis of renal cell carcinoma after radical nephrectomy: A case report

Jae-Wook Chung, Jun-Koo Kang, Eun Hye Lee, So Young Chun, Yun-Sok Ha, Jun Nyung Lee, Tae-Hwan Kim, Tae Gyun Kwon, Ghil Suk Yoon

Specialty type: Urology and nephrology

Provenance and peer review: Unsolicited article; Externally peer reviewed.

Peer-review model: Single blind

Peer-review report's scientific quality classification

Grade A (Excellent): 0
Grade B (Very good): 0
Grade C (Good): C
Grade D (Fair): D
Grade E (Poor): 0

P-Reviewer: Sawazaki H, Japan; Taskovska M, Slovenia

Received: May 31, 2023
Peer-review started: May 31, 2023
First decision: July 19, 2023
Revised: July 28, 2023
Accepted: August 8, 2023
Article in press: August 8, 2023
Published online: September 6, 2023

Jae-Wook Chung, Jun-Koo Kang, Yun-Sok Ha, Jun Nyung Lee, Tae-Hwan Kim, Tae Gyun Kwon, Department of Urology, Kyungpook National University Hospital, Daegu 41404, South Korea

Jae-Wook Chung, Yun-Sok Ha, Jun Nyung Lee, Tae-Hwan Kim, Tae Gyun Kwon, Department of Urology, School of Medicine, Kyungpook National University, Daegu 41404, South Korea

Jae-Wook Chung, Eun Hye Lee, So Young Chun, Yun-Sok Ha, Jun Nyung Lee, Tae-Hwan Kim, Tae Gyun Kwon, Biomedical Research Institute, Kyungpook National University, Daegu 41404, South Korea

Jae-Wook Chung, Yun-Sok Ha, Jun Nyung Lee, Tae-Hwan Kim, Tae Gyun Kwon, Joint Institute for Regenerative Medicine, Kyungpook National University, Daegu 41404, South Korea

Ghil Suk Yoon, Department of Pathology, Kyungpook National University Hospital, Daegu 41404, South Korea

Ghil Suk Yoon, Department of Pathology, School of Medicine, Kyungpook National University, Daegu 41404, South Korea

Corresponding author: Ghil Suk Yoon, MD, PhD, Professor, Department of Pathology, Kyungpook National University Hospital, Hakjeong-ro 561, Buk-gu, Daegu 41404, South Korea. gsyoon@knu.ac.kr

Abstract

BACKGROUND

Renal cell carcinoma (RCC) is the third most common malignancy in the genitourinary tract. The lungs, bone, lymph nodes, liver, and brain are common metastatic sites of RCC. However, there is limited literature on single omental metastasis of RCC.

CASE SUMMARY

We present the case of a 44-year-old man with single omental metastasis of RCC after laparoscopic radical nephrectomy. Pathological diagnosis of the resected left kidney revealed pT3a clear cell RCC (Fuhrman grade III). At 6 mo postoperatively, abdominal computed tomography revealed a 12-mm enhancing nodule in the left lower peritoneum. At 7 mo after initial operation, laparoscopic removal of the left omental nodule was performed. The pathological results indicated metastatic clear cell RCC. Currently, the patient is being treated with adjuvant

pembrolizumab.

CONCLUSION
Omental metastasis of RCC owing to laparoscopic radical nephrectomy is rare. Urologists should be aware of the diverse nature of RCC.

Key Words: Metastasis; Omentum; Renal cell carcinoma; Radical nephrectomy; Case report

Core Tip: The authors present the case of a 44-year-old man with single omental metastasis of renal cell carcinoma (RCC) after laparoscopic radical nephrectomy. Omental metastasis of RCC owing to laparoscopic radical nephrectomy is rare. Urologists should be aware of the diverse nature of RCC.

Citation: Chung JW, Kang JK, Lee EH, Chun SY, Ha YS, Lee JN, Kim TH, Kwon TG, Yoon GS. Single omental metastasis of renal cell carcinoma after radical nephrectomy: A case report. *World J Clin Cases* 2023; 11(25): 5994-5999
URL: https://www.wjgnet.com/2307-8960/full/v11/i25/5994.htm
DOI: https://dx.doi.org/10.12998/wjcc.v11.i25.5994

INTRODUCTION

Renal cell carcinoma (RCC) is the third most common malignancy in the genitourinary tract[1]. In South Korea, the incidence of RCC has been rising, with 6952 new cases estimated in both sexes in 2022[2]. The lungs, bone, lymph nodes, liver, and brain are common metastatic sites of RCC[1,3]. However, literature on single omental metastasis of RCC is limited. We herein present the case of a 44-year-old man with single omental metastasis of RCC after laparoscopic radical nephrectomy.

CASE PRESENTATION

Chief complaints

A 44-year-old man with gross hematuria and left flank pain visited our emergency department on July 14, 2022.

History of present illness

The patient's gross hematuria started 1 day before admission. In the morning of the day of visit, the hematuria became more severe and was accompanied with clots. Moreover, he experienced severe pain in the left flank.

History of past illness

The patient was healthy and had a history of appendectomy 10 years earlier.

Personal and family history

The patient denied any history of tobacco or alcohol consumption. He had no medication history. His family history was unremarkable.

Physical examination

At the emergency department, the patient's initial vital signs were stable. His blood pressure level was 129/79 mmHg, pulse rate was 81 beats/min, and respiratory rate was 16 breaths/min. The patient's body weight was 86 kg, and his height was 171.0 cm (body mass index = 29.4 kg/m^2). There was no palpable mass around the left flank area. The patient showed left flank tenderness but no rebound tenderness.

Laboratory examinations

Laboratory serum tests were normal (hemoglobin level: 13.7 g/dL, creatinine level: 1.05 mg/dL, and calcium level: 9.1 mg/dL). Urinalysis revealed the presence of many red blood cells. Electrocardiogram indicated normal sinus rhythm.

Imaging examinations

Initial kidney dynamic computed tomography (CT) (three phases of intravenous contrast enhancement) revealed an 8.8 cm × 6.1 cm heterogeneously enhancing mass in the upper to mid pole of the left kidney abutting the left adrenal gland and pancreas (Figure 1). No metastatic lesions were detected in the enhanced brain and chest CT scans.

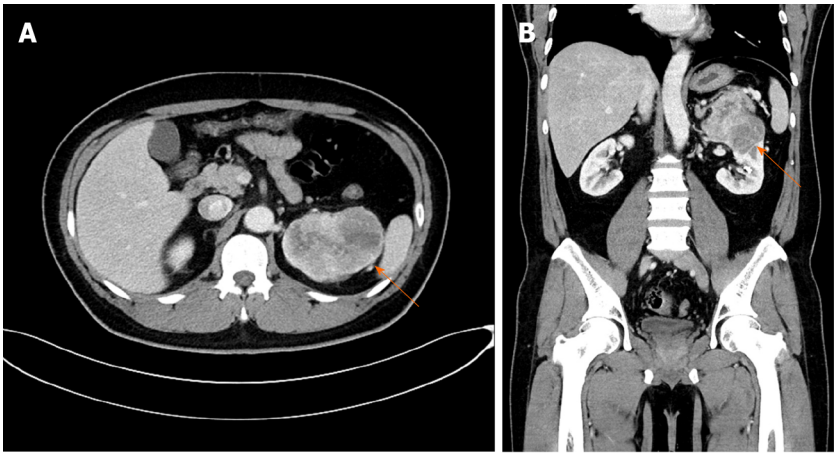

DOI: 10.12998/wjcc.v11.i25.5994

Figure 1 Kidney dynamic computed tomography. A: Axial view; B: Coronal view. Initial kidney dynamic computed tomography showing an 8.8 cm × 6.1 cm heterogeneously enhancing mass in the upper to mid pole of the left kidney abutting onto the left adrenal gland and pancreas (arrows).

Follow-up CT 3 mo after radical nephrectomy showed no metastatic lesions. However, at 6 mo postoperatively, abdominal CT revealed a 12-mm enhancing nodule in the left lower peritoneum (Figure 2). 18F-fluorodeoxyglucose (*FDG*) positron emission tomography/CT (Figure 3) was performed immediately, and the results were the same (mildly hypermetabolic nodule in the left lower peritoneum).

FINAL DIAGNOSIS

Pathological diagnosis of the resected specimen from initial radical nephrectomy revealed pT3a clear cell RCC (Fuhrman grade III). Tumor capsular invasion was absent, but lymphovascular invasion and tumor cell necrosis were present (10%). No tumor was observed in the left adrenal gland.

The pathological results of the second laparoscopic removal of the left omental nodule revealed metastatic clear cell RCC (Figure 4).

TREATMENT

At the time of the patient's visit to emergency department, he experienced severe flank pain and gross hematuria; therefore, we decided to perform emergency surgery rather than elective surgery. Laparoscopic radical nephrectomy and adrenalectomy were performed on the same day. We inserted a 12-mm camera port near the umbilicus. Mild adhesion was observed between the renal mass and pancreas, but pancreatic injury did not occur. No tumor spillage was found during radical nephrectomy. We further opened the 12-mm camera port to remove the specimen from the abdominal cavity using endobag (Lapbag®, SEJONG Medical).

On February 3, 2023, laparoscopic removal of the left omental nodule was performed. The patient underwent the second surgery in the supine position. A 12-mm port was inserted just above the umbilicus, and other 12- and 5-mm ports were inserted in the anterior axillary line at the level of the umbilicus and 2 cm below the xiphoid process. Fortunately, the nodule was visible immediately after entering the abdominal cavity, and the urologist could remove the nodule without any help from a general surgeon.

OUTCOME AND FOLLOW-UP

No metastatic lesion was observed in the most recent CT scan. The most recent brain, chest, and abdomen CT was performed on July 5, 2023. In other words, the interval between the primary surgery and the most recent CT was 12 mo.

Currently, the patient is being treated with adjuvant pembrolizumab. However, adjuvant pembrolizumab is not covered by Korean health insurance. Therefore, immediately after radical nephrectomy, he refused adjuvant pembrolizumab owing to its high cost but agreed to administer it after the second operation.

At our hospital, immunotherapy or targeted therapy for RCC is entirely established by urologists, not medical oncologists. Therefore, JWC decided to initiate treatment with adjuvant pembrolizumab. The duration/scheme of pembrolizumab application is intravenous injection every 3 wk, with at least ten administrations[4].

Thyroid function tests revealed minor abnormalities, but no recent side effects have been reported.

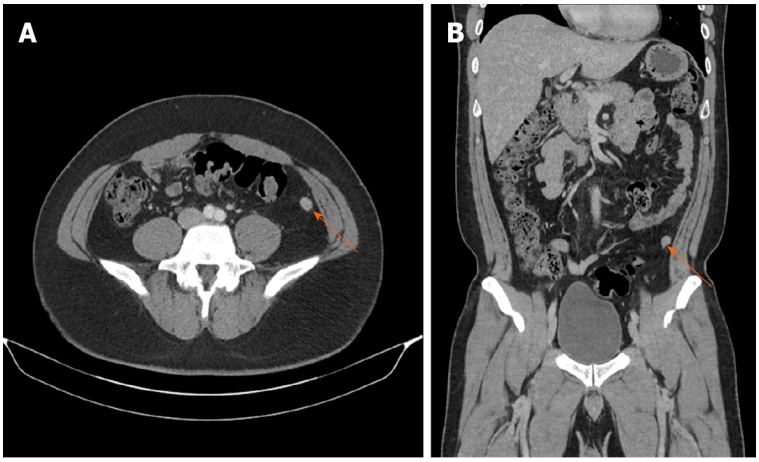

DOI: 10.12998/wjcc.v11.i25.5994 **Copyright** ©The Author(s) 2023.

Figure 2 Abdominal computed tomography. A: Axial view; B: Coronal view. Abdominal computed tomography at 6 mo postoperatively showed a 12 mm enhancing nodule at the left lower peritoneum (arrows).

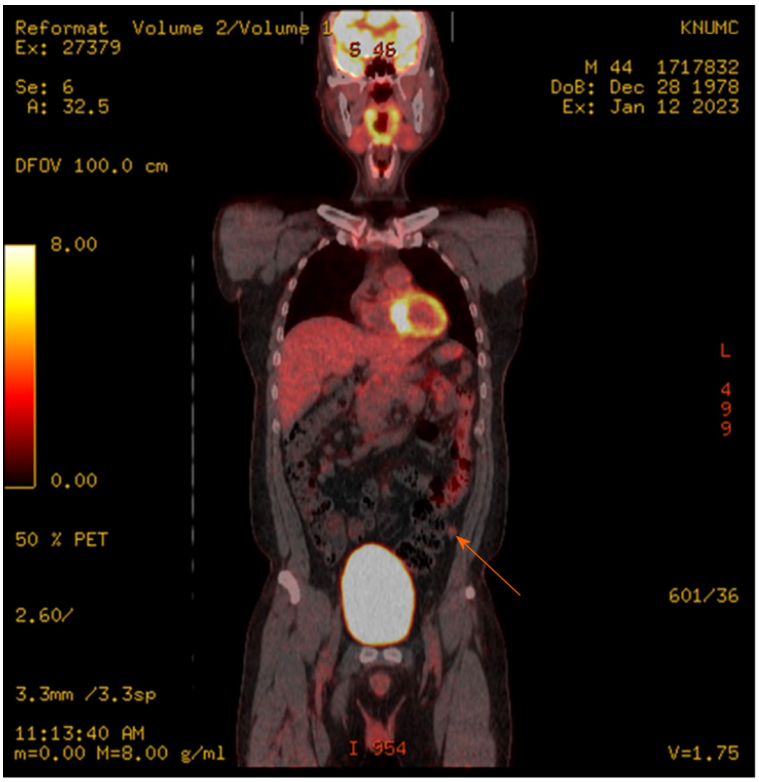

DOI: 10.12998/wjcc.v11.i25.5994 **Copyright** ©The Author(s) 2023.

Figure 3 18F-fluorodeoxyglucose positron emission tomography/computed tomography. F-fluorodeoxyglucose positron emission tomography/computed tomography at 6 mo postoperatively showed a hypermetabolic nodule in the left lower peritoneum (arrow).

DISCUSSION

Kidney cancers are the third most common genitourinary malignancy, accounting for over 431288 new cancer diagnoses and over 179368 deaths worldwide annually[5]. CT and magnetic resonance imaging have increased the diagnosis of early RCC in many patients. The 5-year survival rate for early RCC is approximately 93%; however, the 5-year survival rate of RCC patients with metastases is only 12%[6].

RCC commonly metastasizes to the lung parenchyma (45.2%), bone (29.5%), lymph nodes (20.8%), liver (20.3%), adrenal glands (8.9%), and brain (8.1%)[1]. Metastases into the pancreas are rare and found mostly in asymptomatic patients[7]. Other atypical RCC metastases in the omentum, thyroid, and mediastinum are extremely rare. In particular, port-site metastasis or peritoneal metastasis after a laparoscopic procedure for urological malignancies is a rare event, accounting for approximately 0.09 % and 0.03 % of total cases, respectively[8,9]. RCC is the least common urological

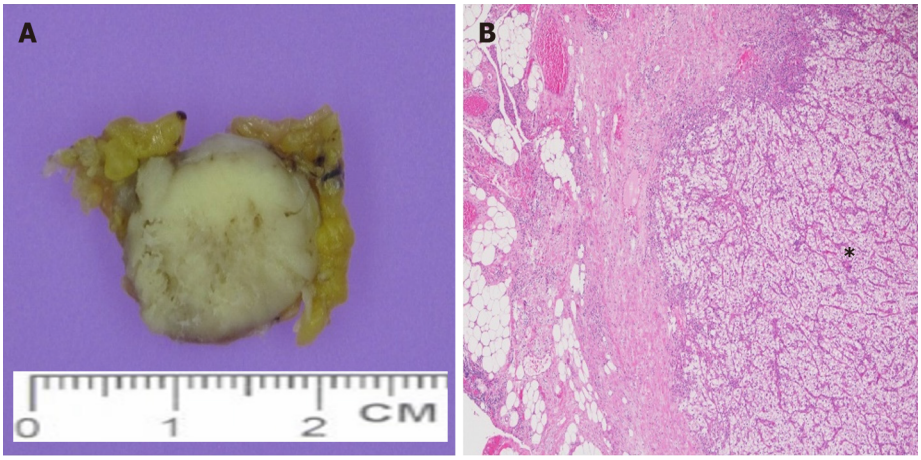

DOI: 10.12998/wjcc.v11.i25.5994 **Copyright** ©The Author(s) 2023.

Figure 4 Histologic outcomes. Gross and microscopic features in this case: A: Gross examination; B: Hematoxylin and eosin (H&E) staining (magnification, × 400). A: Gross finding shows a well-defined pale yellow solid mass in fibroadipose tissue of the abdominal wall; B: Histological finding shows a metastatic clear cell renal cell carcinoma consisting of atypical clear cell nests in fibroadipose tissue (*).

malignancy that leads to port-site metastasis or peritoneal metastasis, with only rare cases being reported in the literature [10].

In 2013, Ploumidis *et al*[9] presented a case report concerning tumor seeding in the omentum found in a 75-year-old female patient after a previous transperitoneal robot-assisted radical nephrectomy for papillary RCC. Two years after the initial surgery, the patient was diagnosed with cervical cancer, leading to radical hysterectomy with lymphadenectomy and omentectomy. Incidentally, a neoplastic omental nodule was discovered during the surgery. Pathological outcome and immunohistochemistry result confirmed the presence of features consistent with papillary RCC. In 2016, Acar *et al*[3] also presented a case report of a 62-year-old male patient who, 13 years after having undergone open extraperitoneal partial nephrectomy for pT1 clear cell RCC, developed an omental metastatic lesion.

Similarly, we present the case of a 44-year-old man with single omental metastasis of RCC after laparoscopic radical nephrectomy. We reviewed the recorded video of the surgery again and did not find intraoperative tumor spillage. We can conjecture that despite the absence of macroscopic surgically induced tumor spillage, there is a possibility that certain tumorigenic yet nonmetastasizing neoplastic cells, which typically do not survive the metastatic cascade under normal circumstances, could have been transferred and aided in establishing a novel neoplastic colony.

CONCLUSION

In summary, omental metastasis of RCC because of laparoscopic radical nephrectomy is rare. Urologists should be aware of the diverse nature of RCC. Various therapeutic approaches should be considered, such as morphological and functional imaging studies together with histopathological assessment of metastatic lesions, and a fundamental treatment for the causative disease should be applied.

FOOTNOTES

Author contributions: Chung JW, Kang JK, Kwon TG, and Yoon GS contributed to manuscript writing and editing and data collection; Lee EH, Chun SY, Ha YS, Lee JN, and Kim TH contributed to data analysis; Kwon TG and Yoon GS contributed to conceptualization and supervision; all authors have read and approved the final manuscript.

Informed consent statement: The present study was approved by the Ethics Committee (IRB Number: KNUCH 2023-03-009) and performed in accordance with the ethical standards laid down in the 1964 Declaration of Helsinki and its later amendments. The need for informed consent was waived by the aforementioned IRB due to the retrospective nature and single case report of the study.

Conflict-of-interest statement: All the authors declare that they have no conflict of interest to disclose.

CARE Checklist (2016) statement: The authors have read the CARE Checklist (2016), and the manuscript was prepared and revised according to the CARE Checklist (2016).

Country/Territory of origin: South Korea

ORCID number: Jae-Wook Chung 0000-0002-1055-2357; Jun-Koo Kang 0000-0002-8857-3406; Eun Hye Lee 0000-0001-5507-2632; So Young Chun 0000-0003-4500-4956; Yun-Sok Ha 0000-0003-3732-9814; Jun Nyung Lee 0000-0002-6342-9846; Tae-Hwan Kim 0000-0003-4924-4826; Tae Gyun Kwon 0000-0002-4390-0952; Ghil Suk Yoon 0000-0002-9941-024X.

S-Editor: Liu JH
L-Editor: Wang TQ
P-Editor: Liu JH

REFERENCES

1 **Bruckschen F**, Gerharz CD, Sagir A. Renal cell carcinoma with unusual metachronous metastasis up to 22 years after nephrectomy: two case reports. *J Med Case Rep* 2021; **15**: 490 [PMID: 34607612 DOI: 10.1186/s13256-021-03098-5]
2 **Jung KW**, Won YJ, Hong S, Kong HJ, Lee ES. Prediction of Cancer Incidence and Mortality in Korea, 2020. *Cancer Res Treat* 2020; **52**: 351-358 [PMID: 32178488 DOI: 10.4143/crt.2020.203]
3 **Acar Ö**, Mut T, Sağlıcan Y, Sag AA, Falay O, Selcukbiricik F, Tabak L, Esen T. Isolated omental metastasis of renal cell carcinoma after extraperitoneal open partial nephrectomy: A case report. *Int J Surg Case Rep* 2016; **21**: 6-11 [PMID: 26874583 DOI: 10.1016/j.ijscr.2016.02.008]
4 **Choueiri TK**, Tomczak P, Park SH, Venugopal B, Ferguson T, Chang YH, Hajek J, Symeonides SN, Lee JL, Sarwar N, Thiery-Vuillemin A, Gross-Goupil M, Mahave M, Haas NB, Sawrycki P, Gurney H, Chevreau C, Melichar B, Kopyltsov E, Alva A, Burke JM, Doshi G, Topart D, Oudard S, Hammers H, Kitamura H, Bedke J, Perini RF, Zhang P, Imai K, Willemann-Rogerio J, Quinn DI, Powles T; KEYNOTE-564 Investigators. Adjuvant Pembrolizumab after Nephrectomy in Renal-Cell Carcinoma. *N Engl J Med* 2021; **385**: 683-694 [PMID: 34407342 DOI: 10.1056/NEJMoa2106391]
5 **Saad AM**, Gad MM, Al-Husseini MJ, Ruhban IA, Sonbol MB, Ho TH. Trends in Renal-Cell Carcinoma Incidence and Mortality in the United States in the Last 2 Decades: A SEER-Based Study. *Clin Genitourin Cancer* 2019; **17**: 46-57.e5 [PMID: 30391138 DOI: 10.1016/j.clgc.2018.10.002]
6 **Kumar S**, Singh V, Singh MK, Sankhwar SN. Management of Metastatic Renal Cell Carcinoma in a Tertiary Care Hospital. *Cureus* 2023; e35623 [DOI: 10.7759/cureus.35623]
7 **Tosoian JJ**, Cameron JL, Allaf ME, Hruban RH, Nahime CB, Pawlik TM, Pierorazio PM, Reddy S, Wolfgang CL. Resection of isolated renal cell carcinoma metastases of the pancreas: outcomes from the Johns Hopkins Hospital. *J Gastrointest Surg* 2014; **18**: 542-548 [PMID: 24163138 DOI: 10.1007/s11605-013-2278-2]
8 **Tanaka K**, Hara I, Takenaka A, Kawabata G, Fujisawa M. Incidence of local and port site recurrence of urologic cancer after laparoscopic surgery. *Urology* 2008; **71**: 728-734 [PMID: 18279936 DOI: 10.1016/j.urology.2007.10.054]
9 **Ploumidis A**, Panoskaltsis T, Gavresea T, Yiannou P, Yiannakou N, Pavlakis K. Tumor seeding incidentally found two years after robotic-Assisted radical nephrectomy for papillary renal cell carcinoma. A case report and review of the literature. *Int J Surg Case Rep* 2013; **4**: 561-564 [PMID: 23632074 DOI: 10.1016/j.ijscr.2013.03.031]
10 **Castillo OA**, Vitagliano G. Port site metastasis and tumor seeding in oncologic laparoscopic urology. *Urology* 2008; **71**: 372-378 [PMID: 18342166 DOI: 10.1016/j.urology.2007.10.064]

World Journal of Clinical Cases

Submit a Manuscript: https://www.f6publishing.com

World J Clin Cases 2023 September 6; 11(25): 6000-6004

DOI: 10.12998/wjcc.v11.i25.6000

ISSN 2307-8960 (online)

CASE REPORT

Myeloid sarcoma as the only manifestation in a rare mixed lineage leukemia-fusion-driven acute myeloid leukemia: A case report

Sheng-Jie Tang, Qi-Guo Zhang

Specialty type: Medicine, research and experimental

Provenance and peer review: Unsolicited article; Externally peer reviewed.

Peer-review model: Single blind

Peer-review report's scientific quality classification

Grade A (Excellent): 0
Grade B (Very good): 0
Grade C (Good): C, C, C
Grade D (Fair): 0
Grade E (Poor): 0

P-Reviewer: Akbulut S, Turkey; Salvadori M, Italy

Received: June 26, 2023
Peer-review started: June 26, 2023
First decision: July 4, 2023
Revised: July 7, 2023
Accepted: August 8, 2023
Article in press: August 8, 2023
Published online: September 6, 2023

Sheng-Jie Tang, The First Clinical Medical College of Xuzhou Medical University, Xuzhou 221004, Jiangsu Province, China

Qi-Guo Zhang, Department of Hematology, Chuzhou Hospital affiliated to Anhui Medical University, Chuzhou 239001, Anhui Province, China

Corresponding author: Qi-Guo Zhang, MD, Chief Physician, Department of Hematology, Chuzhou Hospital affiliated to Anhui Medical University, No. 369 Zuiwen Road, Chuzhou 239001, Anhui Province, China. qgzhang8@sina.com

Abstract

BACKGROUND

The mixed lineage leukemia (MLL)-eleven-nineteen lysine-rich leukemia (ELL) fusion gene is a rare occurrence among the various MLL fusion genes. We present the first case in which myeloid sarcoma (MS) was the only manifestation of adult MLL-ELL-positive acute myeloid leukemia (AML).

CASE SUMMARY

We report a case of a 33-year-old male patient who was admitted in June 2022 with a right occipital area mass measuring approximately 7 cm × 8 cm. Blood work was normal. The patient underwent right occipital giant subscalp mass excision and incisional flap grafting. Immunohistochemistry was positive for myeloperoxidase, CD43 and CD45 and negative for CD3, CD20, CD34, and CD56. The bone marrow aspirate showed hypercellularity with 20% myeloblasts. Flow cytometry showed that myeloblasts accounted for 27.21% of the nucleated cells, which expressed CD33, CD38, and CD117. The karyotype was 46, XY, *t* (11, 19) (q23; p13.1), -12, + mar/46, XY. Next-generation sequencing showed a fusion of MLL exon 7 to exon 2 of ELL. A diagnosis of MLL-ELL-positive AML (M2 subtype) with subcutaneous MS was made.

CONCLUSION

MLL-ELL-positive AML with MS is a rare clinical entity. Additional research is needed to elucidate the molecular mechanisms of the pathogenesis of MS.

Key Words: Myeloid sarcoma; Acute myeloid leukemia; Mixed lineage leukemia-eleven-nineteen lysine-rich leukemia; Transplantation; Case report

Core Tip: This study described myeloid sarcoma as the first and only manifestation in an adult patient with mixed lineage leukemia-eleven-nineteen lysine-rich leukemia-positive acute myeloid leukemia. Based on our findings and information from a few previous reports, we speculate that our patient had (1): Transformation of preleukemia cells in the marrow followed by spread to extramedullary sites; or (2) homing of preleukemia cells to extramedullary sites, followed by spreading back to bone marrow. The current study helps increase the awareness of this particular disease and reduce the clinical underdiagnosis rate.

Citation: Tang SJ, Zhang QG. Myeloid sarcoma as the only manifestation in a rare mixed lineage leukemia-fusion-driven acute myeloid leukemia: A case report. *World J Clin Cases* 2023; 11(25): 6000-6004
URL: https://www.wjgnet.com/2307-8960/full/v11/i25/6000.htm
DOI: https://dx.doi.org/10.12998/wjcc.v11.i25.6000

INTRODUCTION

Myeloid sarcoma (MS) is a rare disease characterized by an extramedullary tumor composed of immature myeloid cells. When differentiating any extramedullary lesion infiltrated by heterogeneous cells, clinicians should consider the possibility of MS[1]. Mixed lineage leukemia (MLL) gene rearrangements define a unique leukemia with distinctive pathophysiology and phenotype. The MLL gene encodes a large histone methyltransferase that directly binds and actively regulates gene transcription. In MLL rearrangement leukemia, menin acts as an oncogenic cofactor leading to leukemogenesis by mediating aberrant gene expression through the HOX gene and cofactor meis homeobox 1[2]. A chromosomal translocation *t* (11; 19) (q23; P13), with breakpoints mainly located within the 19p13.1 subband, generates the MLL-eleven-nineteen lysine-rich leukemia (ELL) fusion gene and is predominantly found in acute myeloid leukemia (AML)[3]. We present a rare case in which MS was the only manifestation of adult MLL-ELL-positive AML.

CASE PRESENTATION

Chief complaints

A 33-year-old male patient was admitted in June 2022 with a right occipital area mass measuring approximately 7 cm × 8 cm.

History of present illness

The patient had scalp swelling for 4 mo prior to this presentation.

History of past illness

The patient had no history of chronic conditions.

Personal and family history

The patients' personal and family histories were not significant.

Physical examination

A hard, immobile mass measuring approximately 7 cm × 8 cm was observed in the right occipital region of the skull. The local scalp color appeared dark brown with no abnormalities in the surrounding area.

Laboratory examinations

Blood work was normal. No malignant cells were seen in the cerebrospinal fluid.

Imaging examinations

No bone erosion or abnormalities were detected in the brain parenchyma by computed tomography scan (Figure 1). The cranial magnetic resonance imaging also showed no significant abnormalities.

Further diagnostic work-up

The patient underwent right occipital giant subscalp mass excision and incisional flap grafting (Figure 2). Resection tissue staining showed a small round-cell tumor, which was suspected to be lymphoma. Immunohistochemistry was positive for myeloperoxidase, CD43 and CD45 and negative for CD3, CD20, CD34, and CD56. The bone marrow (BM) aspirate showed hypercellularity with 20% myeloblasts. Flow cytometry showed that myeloblasts accounted for 27.21% of the nucleated cells, which expressed CD33, CD38, and CD117 (Figure 3). The karyotype was 46, XY, *t* (11, 19) (q23; p13.1), -12, + mar[4]/46, XY[5]. Next-generation sequencing showed a fusion of MLL exon 12 to exon 1 of ELL.

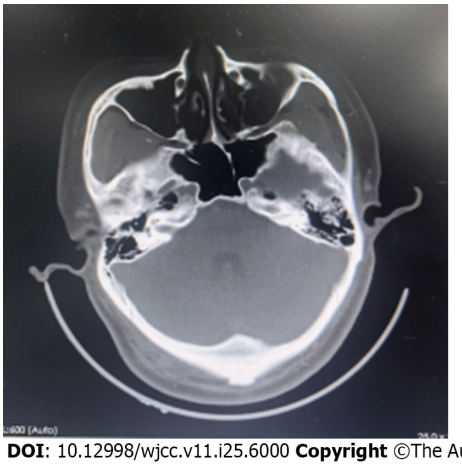

DOI: 10.12998/wjcc.v11.i25.6000 **Copyright** ©The Author(s) 2023.

Figure 1 Head computed tomography. Anomalous density shadow of the right occipital subcutaneous region.

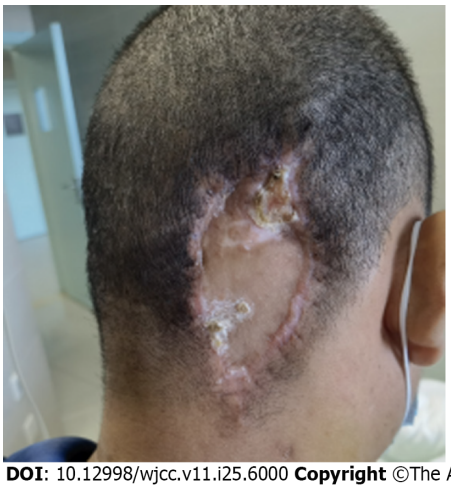

DOI: 10.12998/wjcc.v11.i25.6000 **Copyright** ©The Author(s) 2023.

Figure 2 Skin grafting after myeloid sarcoma resection.

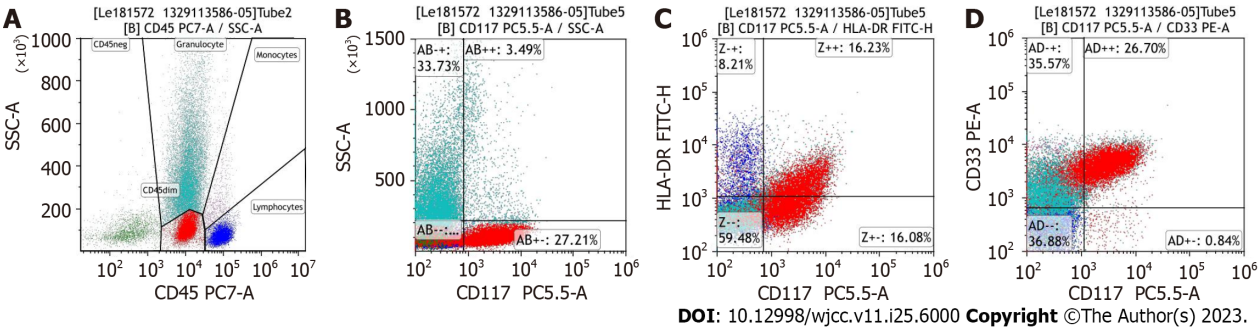

DOI: 10.12998/wjcc.v11.i25.6000 **Copyright** ©The Author(s) 2023.

Figure 3 Flow cytometric analysis of the bone marrow aspirate. A: Expression of CD45 of all cell populations; B: Increase of CD117 positive cells was demonstrated; C: Increase of CD117/HLA-DR positive cells was demonstrated; D: Increase of CD117/CD33 positive cells was demonstrated.

FINAL DIAGNOSIS

A diagnosis of MLL-ELL-positive AML (M2 subtype) with subcutaneous MS was made.

TREATMENT

Complete remission (CR) was achieved after the first course of standard 7 + 3 (idarubicin and cytarabine) induction

chemotherapy. He then received 2 cycles of high-dose cytarabine-based consolidation therapy followed by a myeloablative, allogeneic, matched, unrelated-donor hematopoietic stem cell transplant.

OUTCOME AND FOLLOW-UP

When last seen in May 2023, he was still in CR.

DISCUSSION

To our knowledge, we present the first case in which MS was the only manifestation of adult MLL-ELL-positive AML. The molecular mechanisms underlying extramedullary involvement remain unknown, but 70% of MS cases have concurrent AML. "extramedullary AML tumor" may be a more accurate term for MS[6].

The MLL-ELL fusion gene is a rare occurrence among the various MLL fusion genes. It is associated with the genesis of AML in a mouse model[7]. MLL-ELL fusions are present in 12% of adult AML patients, 7% of pediatric AML patients and 15% of infant AML patients[8]. No concurrent MLL-ELL-positive MS cases have been mentioned in the literature, although two cases of MLL-ELL-positive MS with no evidence of AML have been reported[9,10]. Based on our findings and information from a few previous reports, we speculate that our patient had (1): Transformation of preleukemia cells in the marrow followed by spread to extramedullary sites; or and (2) homing of preleukemia cells to extramedullary sites, followed by spreading back to BM. This hypothesis has been proven in the development of blastic plasmacytoid dendritic cell neoplasm[4].

MLL-ELL-positive AML is associated with high response rates to conventional chemotherapy, but relapse is common, and some patients may benefit from allogeneic hematopoietic stem cell transplantation (allo-HSCT)[11]. Our patient achieved BM minimal residual disease-negative CR, and concurrently, 10% hematogones[5] existed in his BM, which may imply longer overall survival and a lower rate of acute graft-versus-host disease after HSCT.

CONCLUSION

In conclusion, MLL-ELL-positive AML with MS is a rare clinical entity. Additional research is needed to elucidate the molecular mechanisms of the pathogenesis of MS.

FOOTNOTES

Author contributions: Tang SJ performed the study, collected the data, analyzed/interpreted the data, and drafted the article; Zhang QG supervised the study, contributed to the experimental design, and revised the paper.

Supported by Scientific Research Project of Anhui Provincial Health Commission, No. AHWJ2021b005.

Informed consent statement: Informed written consent was obtained from the patient and her parents for the publication of this report and any accompanying images.

Conflict-of-interest statement: All the authors report no relevant conflicts of interest for this article.

CARE Checklist (2016) statement: The authors have read the CARE Checklist (2016), and the manuscript was prepared and revised according to the CARE Checklist (2016).

Country/Territory of origin: China

ORCID number: Sheng-Jie Tang 0009-0000-3563-2567.

S-Editor: Qu XL
L-Editor: A
P-Editor: Zhao S

REFERENCES

1 **Almond LM**, Charalampakis M, Ford SJ, Gourevitch D, Desai A. Myeloid Sarcoma: Presentation, Diagnosis, and Treatment. *Clin Lymphoma Myeloma Leuk* 2017; **17**: 263-267 [PMID: 28342811 DOI: 10.1016/j.clml.2017.02.027]

2 **Krivtsov AV**, Evans K, Gadrey JY, Eschle BK, Hatton C, Uckelmann HJ, Ross KN, Perner F, Olsen SN, Pritchard T, McDermott L, Jones CD, Jing D, Braytee A, Chacon D, Earley E, McKeever BM, Claremon D, Gifford AJ, Lee HJ, Teicher BA, Pimanda JE, Beck D, Perry JA, Smith MA, McGeehan GM, Lock RB, Armstrong SA. A Menin-MLL Inhibitor Induces Specific Chromatin Changes and Eradicates Disease in Models of MLL-Rearranged Leukemia. *Cancer Cell* 2019; **36**: 660-673.e11 [PMID: 31821784 DOI: 10.1016/j.ccell.2019.11.001]

3 **Panagopoulos I**, Gorunova L, Kerndrup G, Spetalen S, Tierens A, Osnes LT, Andersen K, Müller LS, Hellebostad M, Zeller B, Heim S. Rare MLL-ELL fusion transcripts in childhood acute myeloid leukemia-association with young age and myeloid sarcomas? *Exp Hematol Oncol* 2015; **5**: 8 [PMID: 26949571 DOI: 10.1186/s40164-016-0037-2]

4 **Griffin GK**, Booth CAG, Togami K, Chung SS, Ssozi D, Verga JA, Bouyssou JM, Lee YS, Shanmugam V, Hornick JL, LeBoeuf NR, Morgan EA, Bernstein BE, Hovestadt V, van Galen P, Lane AA. Ultraviolet radiation shapes dendritic cell leukaemia transformation in the skin. *Nature* 2023; **618**: 834-841 [PMID: 37286599 DOI: 10.1038/s41586-023-06156-8]

5 **Chantepie SP**, Cornet E, Salaün V, Reman O. Hematogones: an overview. *Leuk Res* 2013; **37**: 1404-1411 [PMID: 23932356 DOI: 10.1016/j.leukres.2013.07.024]

6 **Shallis RM**, Gale RP, Lazarus HM, Roberts KB, Xu ML, Seropian SE, Gore SD, Podoltsev NA. Myeloid sarcoma, chloroma, or extramedullary acute myeloid leukemia tumor: A tale of misnomers, controversy and the unresolved. *Blood Rev* 2021; **47**: 100773 [PMID: 33213985 DOI: 10.1016/j.blre.2020.100773]

7 **Lavau C**, Luo RT, Du C, Thirman MJ. Retrovirus-mediated gene transfer of MLL-ELL transforms primary myeloid progenitors and causes acute myeloid leukemias in mice. *Proc Natl Acad Sci U S A* 2000; **97**: 10984-10989 [PMID: 10995463 DOI: 10.1073/pnas.190167297]

8 **Meyer C**, Burmeister T, Gröger D, Tsaur G, Fechina L, Renneville A, Sutton R, Venn NC, Emerenciano M, Pombo-de-Oliveira MS, Barbieri Blunck C, Almeida Lopes B, Zuna J, Trka J, Ballerini P, Lapillonne H, De Braekeleer M, Cazzaniga G, Corral Abascal L, van der Velden VHJ, Delabesse E, Park TS, Oh SH, Silva MLM, Lund-Aho T, Juvonen V, Moore AS, Heidenreich O, Vormoor J, Zerkalenkova E, Olshanskaya Y, Bueno C, Menendez P, Teigler-Schlegel A, Zur Stadt U, Lentes J, Göhring G, Kustanovich A, Aleinikova O, Schäfer BW, Kubetzko S, Madsen HO, Gruhn B, Duarte X, Gameiro P, Lippert E, Bidet A, Cayuela JM, Clappier E, Alonso CN, Zwaan CM, van den Heuvel-Eibrink MM, Izraeli S, Trakhtenbrot L, Archer P, Hancock J, Möricke A, Alten J, Schrappe M, Stanulla M, Strehl S, Attarbaschi A, Dworzak M, Haas OA, Panzer-Grümayer R, Sedék L, Szczepański T, Caye A, Suarez L, Cavé H, Marschalek R. The MLL recombinome of acute leukemias in 2017. *Leukemia* 2018; **32**: 273-284 [PMID: 28701730 DOI: 10.1038/leu.2017.213]

9 **Ouansafi I**, Arabadjief M, Mathew S, Srivastara S, Orazi A. Myeloid sarcoma with t(11;19)(q23;p13.3) (MLL-ELL) in the uterine cervix. *Br J Haematol* 2011; **153**: 679 [PMID: 21501132 DOI: 10.1111/j.1365-2141.2010.08411.x]

10 **Bao H**, Gao J, Chen YH, Altman JK, Frankfurt O, Wilson AL, Sukhanova M, Chen Q, Lu X. Rare myeloid sarcoma with KMT2A (MLL)-ELL fusion presenting as a vaginal wall mass. *Diagn Pathol* 2019; **14**: 26 [PMID: 30922345 DOI: 10.1186/s13000-019-0804-6]

11 **Muto T**, Takeuchi M, Yamazaki A, Sugita Y, Tsukamoto S, Sakai S, Takeda Y, Mimura N, Ohwada C, Sakaida E, Aotsuka N, Iseki T, Nakaseko C. Efficacy of myeloablative allogeneic hematopoietic stem cell transplantation in adult patients with MLL-ELL-positive acute myeloid leukemia. *Int J Hematol* 2015; **102**: 86-92 [PMID: 25758097 DOI: 10.1007/s12185-015-1779-z]

World Journal of Clinical Cases

Submit a Manuscript: https://www.f6publishing.com

World J Clin Cases 2023 September 6; 11(25): 6005-6011

DOI: 10.12998/wjcc.v11.i25.6005

ISSN 2307-8960 (online)

CASE REPORT

Carotid-cavernous fistula following mechanical thrombectomy of the tortuous internal carotid artery: A case report

Lin-Zhuo Qu, Guang-Hui Dong, En-Bo Zhu, Ming-Quan Lin, Guang-Lin Liu, Hong-Jian Guan

Specialty type: Medicine, research and experimental

Provenance and peer review: Unsolicited article; Externally peer reviewed.

Peer-review model: Single blind

Peer-review report's scientific quality classification

Grade A (Excellent): 0
Grade B (Very good): B
Grade C (Good): C
Grade D (Fair): 0
Grade E (Poor): 0

P-Reviewer: Ng ZQ, Australia; Yarmahmoodi F, Iran

Received: July 4, 2023
Peer-review started: July 4, 2023
First decision: July 18, 2023
Revised: July 26, 2023
Accepted: July 31, 2023
Article in press: July 31, 2023
Published online: September 6, 2023

Lin-Zhuo Qu, Department of Medicine, Yanbian University, Yanji 133000, Jilin Province, China

Guang-Hui Dong, En-Bo Zhu, Ming-Quan Lin, Guang-Lin Liu, Hong-Jian Guan, Department of Neurology, Affiliated Hospital of Yanbian University, Yanji 133000, Jilin Province, China

Corresponding author: Hong-Jian Guan, MD, Chief Doctor, Professor, Department of Neurology, Affiliated Hospital of Yanbian University, No. 1327 Juzi Street, Yanji 133000, Jilin Province, China. hjguan@ybu.edu.cn

Abstract

BACKGROUND

A carotid-cavernous fistula (CCF) is an abnormal connection between the internal carotid artery (ICA) and the cavernous sinus. Although direct CCFs typically result from trauma or as an iatrogenic complication of neuroendovascular procedures, they can occur as surgery-related complications after mechanical thrombectomy (MT). With the widespread use of MT in patients with acute ischemic stroke complicated with large vessel occlusion, it is important to document CCF following MT and how to avoid them. In this study, we present a case of a patient who developed a CCF following MT and describe in detail the characteristics of ICA tortuosity in this case.

CASE SUMMARY

A 60-year-old woman experienced weakness in the left upper and lower limbs as well as difficulty speaking for 4 h. The neurological examination revealed left central facial paralysis and left hemiplegia, with a National Institutes of Health Stroke Scale score of 9. Head magnetic resonance imaging revealed an acute cerebral infarction in the right basal ganglia and radial crown. Magnetic resonance angiography demonstrated an occlusion of the right ICA and middle cerebral artery. Digital subtraction angiography demonstrated distal occlusion of the cervical segment of the right ICA. We performed suction combined with stent thrombectomy. Then, postoperative angiography was performed, which showed a right CCF. One month later, CCF embolization was performed, and the patient's clinical symptoms have significantly improved 5 mo after the operation.

CONCLUSION

Although a CCF is a rare complication after MT, it should be considered. Understanding the tortuosity of the internal carotid-cavernous sinus may help predict the complexity of MT and avoid this complication.

Key Words: Carotid-cavernous fistula; Complication; Mechanical thrombectomy; Internal carotid artery; Tortuosity; Case report

Core Tip: The occurrence of carotid-cavernous fistula (CCF) after mechanical thrombectomy (MT) is rare, with only five cases reported in PubMed. Herein we report a rare case of CCF occurring after MT in a patient with acute ischemic stroke. This paper describes the tortuosity of the cavernous internal carotid artery (ICA). We believe that future analysis of ICA tortuosity will help evaluate the complexity of the surgery and better predict and avoid CCF and other complications.

Citation: Qu LZ, Dong GH, Zhu EB, Lin MQ, Liu GL, Guan HJ. Carotid-cavernous fistula following mechanical thrombectomy of the tortuous internal carotid artery: A case report. *World J Clin Cases* 2023; 11(25): 6005-6011
URL: https://www.wjgnet.com/2307-8960/full/v11/i25/6005.htm
DOI: https://dx.doi.org/10.12998/wjcc.v11.i25.6005

INTRODUCTION

Carotid-cavernous fistula (CCF) is an abnormal connection between arteries and veins of the coronary sinus[1]. The symptoms include headache, nerve palsy and ocular symptoms, which lead to visual impairment, blindness, cerebral infarction and even intracranial haemorrhage[1,2]. Head trauma, ruptured aneurysm and idiopathic CCF represent the main causes of direct CCF[1]. The incidence of iatrogenic CCF in interventional radiology is approximately 0.8%; this includes its occurrence as a complication during neurointerventional procedures, including coil embolization of aneurysms and intracranial percutaneous transluminal angioplasty and rarely after mechanical thrombectomy (MT)[3]. The risk factors for iatrogenic CCF include advanced age, internal carotid artery (ICA) tortuosity, changes in the atherosclerotic vessel wall, cavernous aneurysms as well as vessel wall fragility due to underlying connective tissue weakening (*e.g.*, Ehlers-Danlos syndrome type IV)[4]. To date, there is no literature describing the classification of the carotid artery tortuosity when CCF occurs during MT. In this article, we report a case of CCF, review the clinical manifestations and imaging examination of CCF and describe in detail the twists and turns of the cavernous ICA in this case. The purpose of this case report is to discuss the CCF following MT and how to avoid it considering the classification of carotid tortuosity.

CASE PRESENTATION

Chief complaints

Speech impairment with weakness of the left upper and lower limbs for 4 h.

History of present illness

A 60-year-old female patient presented with poor speech and left upper and lower limbs movement for the last 4 h. The left upper limb could be lifted off the bed surface but with no resistance. The left lower limb could do moderate resistance. Further symptoms included lethargy, slurred speech, a drinking cough and no incontinence. Before coming to our hospital, a head CT was performed in a subordinate hospital with no sign of cerebral hemorrhage. She was then immediately transferred to our hospital.

History of past illness

The patient's medical history included cerebral infarction and coronary heart disease. She had no history of hypertension, diabetes or hyperlipidemia.

Personal and family history

The personal history included smoking twenty cigarettes daily for 40 years. Otherwise no further contributing factors in the remaining personal and family history.

Physical examination

Physical examination on admission: Lethargy, dysarthria, eye deviation to the right, partial facial paralysis left, left upper limb muscle strength level III, left lower limb muscle strength level IV, no pathological reflex. The National Institutes of Health Stroke Scale (NIHSS) score was 9 points (1 point for consciousness, 1 point for gazing, 2 points for dysarthria, 2 points for partial facial paralysis, and 3 points for left limb weakness). The modified Rankin Scale (mRS) score was 4.

Laboratory examinations

The laboratory findings were within the normal range, glucose was 5.85 mmol/L, triglyceride was 1.66 mmol/L, with the exception of the low density lipoprotein cholesterol level measuring 4.3 mmol/L, higher than normal.

Imaging examinations

The result of magnetic resonance angiography and computed tomography angiography indicated the presence of occlusion in both the right ICA and middle cerebral artery (MCA) (Figure 1). MT was required. Digital subtraction angiography (DSA) demonstrated distal occlusion of the right ICA (Figure 2A and B). The A1 segment of the right anterior cerebral artery (ACA) was not developed, and there was no compensatory flow to the right MCA (Figure 2C). After performing the aspiration thrombectomy, the DSA showed occlusion of the terminal bifurcation of the right ICA (Figure 3A). After the first stent removal, the angiography showed poor right MCA reflow and no CCF (Figure 3B). After the second stent retriever thrombectomy, the DSA showed a right CCF (Figure 3C and D). The A1 segment of the right ACA was developed to supply blood to the supply area of the right MCA (Figure 3E). Cavernous ICA tortuosity was observed, with the acute angle of the anterior genu being 37.119°, and that of the posterior genu being 56.618° (Figure 4). Figure 5A and B show the clinical manifestations of the patient before the preoperative internal carotid-cavernous sinus embolization. After five months follow-up, the patient's clinical symptoms were relieved (Figure 5C and D).

FINAL DIAGNOSIS

Carotid thrombosis complicated with intracranial arterial embolism; MT-caused right CCF.

TREATMENT

The patient received aspiration thrombectomy with stent retriever thrombectomy. One month after thrombus removal, the patient underwent CCF embolization.

OUTCOME AND FOLLOW-UP

After 5 mo follow-up, the patient's clinical symptoms showed significant improvement with no new stroke events. At 24 h after MT, the patient's NIHSS score was 6, 1 mo after MT the patient's NIHSS score was 2. After 5 mo follow-up, the patient's NIHSS score was 1 and mRS score was 1. No exacerbation of the symptoms, no complications and no recorded adverse events. The patient expressed satisfaction with the treatment and is now able to resume their normal life. The patient's clinical symptoms were significantly relieved and he was actively rehabilitated.

DISCUSSION

The present report documents a CCF that occurred after MT of the tortuous ICA. To the best of our knowledge, CCF following MT is an uncommon event[4]. A case of CCF caused by vessel injury during the withdrawal of a stent retriever during MT for acute ischemic stroke (AIS) was reported by Matsumoto *et al*[5], where it was suggested that the key mechanism contributing to the pull-out vessel injury was the mechanical stretching of the vessel while withdrawing the stent retriever due to vessel tortuosity. This was probably caused by pull-out vessel injury of the meningohypophyseal trunk branching from the cavernous segment of the ICA. The study of Miyamoto *et al*[3] reported that direct CCF is caused by ICA perforation by a microcatheter body during MT. Our case report suggests that the tortuosity of the ICA could be a potential predisposing factor for iatrogenic CCF[4]. In this case, the initial angiography showed distal occlusion of the right ICA at the beginning, stenosis of the patient's proximal vessels, unclear distal vascular conditions and a large number of load thrombi, resulting in an unclear path and a significant increase in the risk of CCF. Meanwhile, the tortuous ICA would reduce the surgeon's control level of the microcatheter or micro guide wire[6]. Hence, we considered that the CCF might have resulted from not performing a gentle manipulation by the operator. The tortuosity of the ICA leads to an increased risk of inadvertently damaging the apex in case of mistakenly inserting a guide wire[7]. Consequently, it is imperative for the neurointerventionist to proceed with caution and gentleness throughout the procedure.

Proptosis frequently manifests as a symptom of CCF. The CCF-associated symptoms are influenced by the direction of the venous drainage, speed of blood flow through the shunts and a thrombosis-caused obstruction of the venous outflow. Therefore, a range of clinical manifestations may arise, including but not limited to headache, nerve dysfunction and ocular symptoms. Amidst these symptoms, the most dreaded complications are visual impairment, blindness and intracranial haemorrhages[4]. Despite the growing use of MT in the treatment of AIS, limited cases of resulting CCF have been reported. Furthermore, CCFs due to the high curvature of the ICA are even rarer.

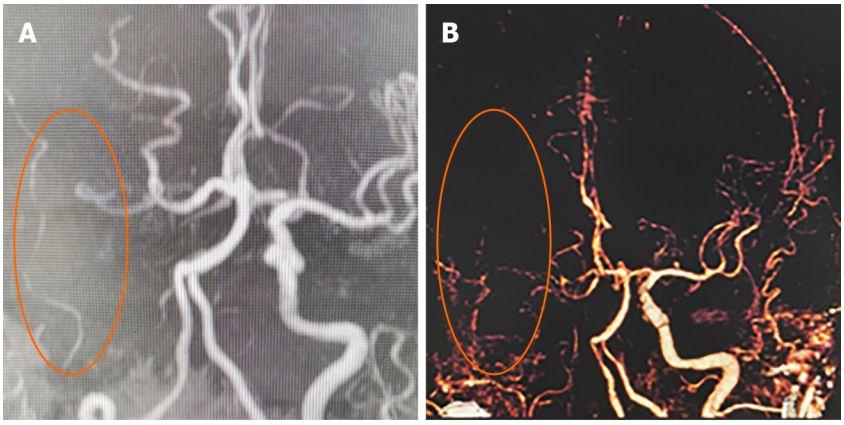

DOI: 10.12998/wjcc.v11.i25.6005 **Copyright** ©The Author(s) 2023.

Figure 1 Image of an intracranial major artery embolism. A and B: Magnetic resonance angiography and computed tomography angiography showing occlusion of the right internal carotid artery and middle cerebral artery (ellipses), respectively.

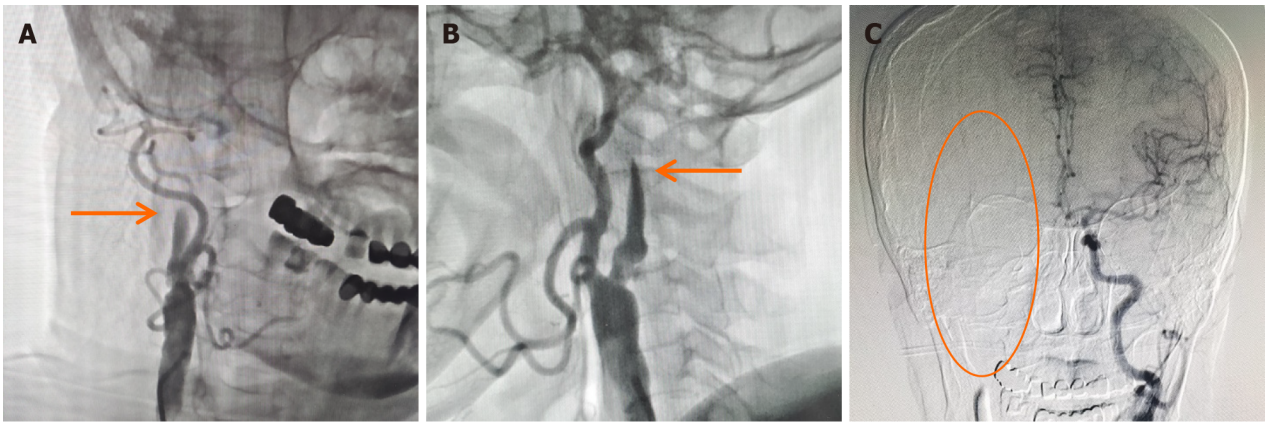

DOI: 10.12998/wjcc.v11.i25.6005 **Copyright** ©The Author(s) 2023.

Figure 2 Angiography before thrombectomy. A and B: Digital subtraction angiography showing an occlusion beyond the origin of the right internal carotid artery (arrows); C: The A1 segment of the right anterior cerebral artery was blocked, and there was no compensatory blood flow to the right middle cerebral artery (ellipse).

Unlike previously reported cases, a focal point in our report is the curvature of the ICA. Given that the ICA is the exclusive pathway to the anterior circulation, its curvature represents an important challenge when performing MT. ICA tortuosity can be categorized into four types based on the geometry of the anterior and posterior curves. Type I ICA tortuosity is characterized by an open configuration or angle, with two subclasses: IA when the angle of the posterior knee is greater than 90°, and IB when the angle is equal to 90°. Type II is characterized by a closed anterior knee configuration with a sharper knee angle compared with Type I. Type III is defined as having the back knee angled backward, and Type IV ICA tortuosity exhibits a highly curved appearance, resembling the shape of a Simmons angiogram catheter. In this type, the posterior knee is curved upwards in comparison with the front knee, making it the most tortuous form of ICA tortuosity. Type I (A or B) represents mild tortuosity, Type II-III represents moderate tortuosity, and Type IV represents severe tortuosity[8,9]. In our case, as shown in Figure 4, this patient has a cavernous ICA tortuosity of type III, which is moderate tortuosity.

According to the study conducted by Ono *et al*[7], 89% of the reported CCFs occurred specifically at the genu (bend) of the cavernous ICA. This can be explained by the increased likelihood of direct perforation by the guidewire or distal access catheter at the curved portion of the ICA. A previous report[10] presented two cases of perforation during catheter navigation, the fistulas were located at the posterior part of the cavernous ICA. It was suggested that this occurrence might be attributed to the acutely angled vasculature in this particular region. Some evidence suggests that vascular tortuosity could depend on connective tissue alterations that weaken the structure of the nasal wall, making it more susceptible to dissection. In this regard, it could be considered a "visual marker" of vassal fragility[11]. Compared with straight arteries, tortuous arteries have a higher likelihood of vasospasm occurring during the passage of balloons, catheters, embolic protection devices and stents. This is due to the increased potential for collisions between these devices and the arterial wall. The presence of tortuosity is challenging during the procedure, typically involving repeated and prolonged mechanical stimulation to the arterial wall. This direct stimulation can induce vasospasm, which might have detrimental effects[12]. The tortuosity of the ICA can impede the advancement of intermediate catheters, microcatheters and retrievers, ultimately diminishing the effectiveness of proximal aspiration and reducing the likelihood of a successful

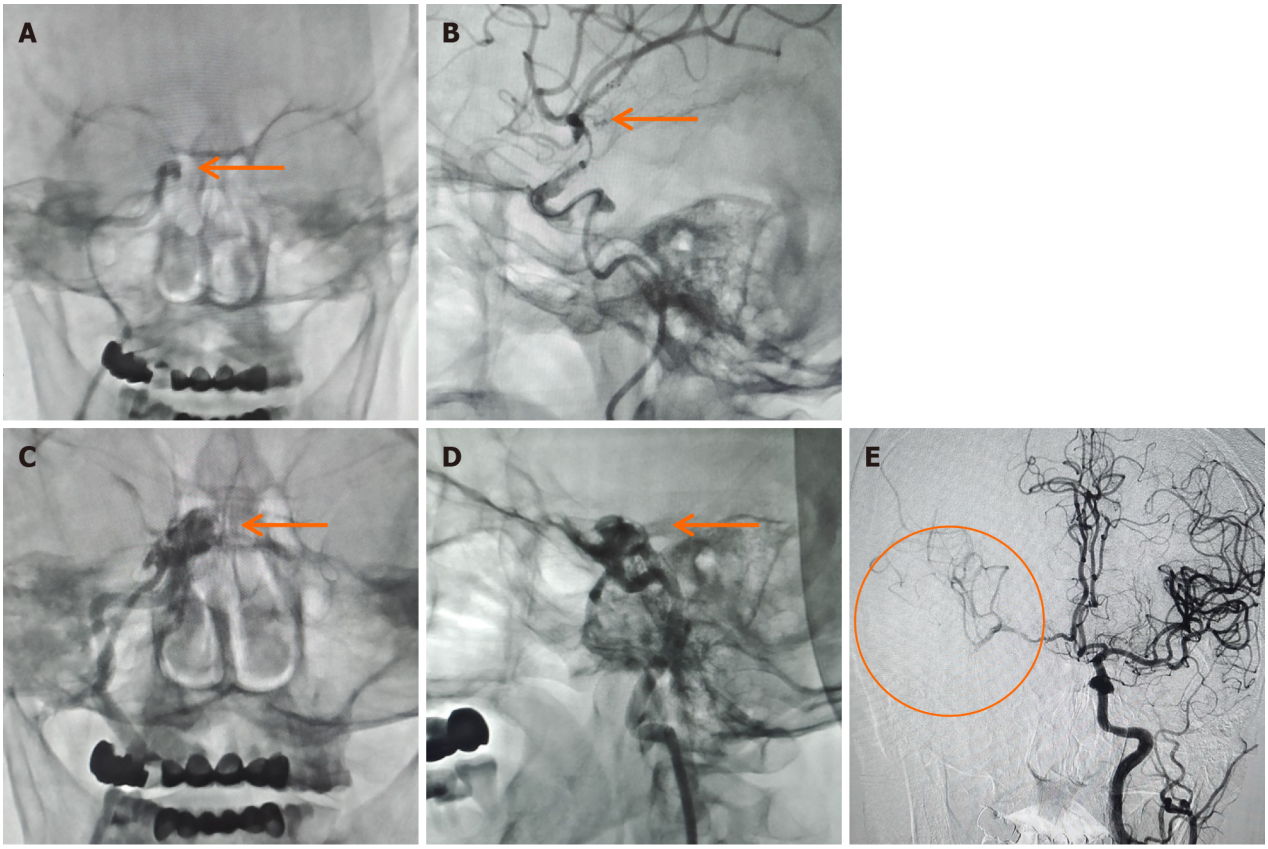

DOI: 10.12998/wjcc.v11.i25.6005 **Copyright** ©The Author(s) 2023.

Figure 3 Thrombectomy and carotid-cavernous fistula formation. A: After the aspiration thrombectomy, the digital subtraction angiography showed occlusion of the terminal bifurcation of the right internal carotid artery (arrow); B: After the first stent removal, angiography showed poor right middle cerebral artery (MCA) reflow and no carotid-cavernous fistula (CCF) (arrow); C and D: After a second stent thrombectomy, reexamination showed CCF (arrows); E: Reflow of the A1 segment of the right anterior cerebral artery to supply blood to the right MCA supply area (circle).

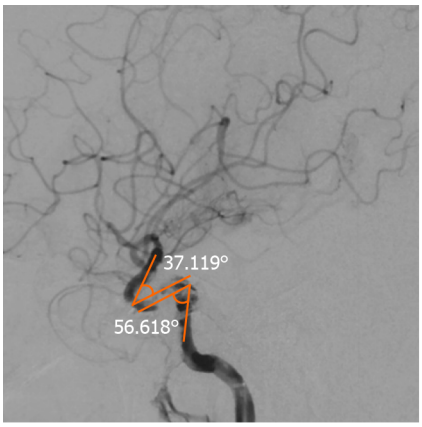

DOI: 10.12998/wjcc.v11.i25.6005 **Copyright** ©The Author(s) 2023.

Figure 4 Cavernous internal carotid artery tortuosity. The acute angle of the anterior genu = 37.119°, the posterior genu angle = 56.618°.

embolectomy[13,14]. Consequently, this can negatively affect vessel recanalization and overall treatment outcome[15].

Complications after MT lead to increased length of stay in intensive care and stroke units, increasing the costs and delaying the commencement of rehabilitation[16]. Iatrogenic CCFs are a subset of traumatic fistulae that may occur during endovascular procedures[17]. With the increasing frequency of MTs performed for AIS, neuro-interventionalists should be aware of this potential rare complication. In future surgery, predicting the curvature of ICA can help to choose a better operation mode. However, in the case of emergency thrombectomy, the curvature of the ICA is mostly unpredictable. Specifically, in patients with ICA occlusion, by understanding the curvature grading of the cavernous sinus segment, the catheter and guidewire could be operated more gently and cautiously when passing through the cavernous sinus segment and stenting for embolization during future cerebral angiography and MT. Hence, the possibility of severe curvature of ICA should be considered. Caution and prudence of the neurointerventionist while

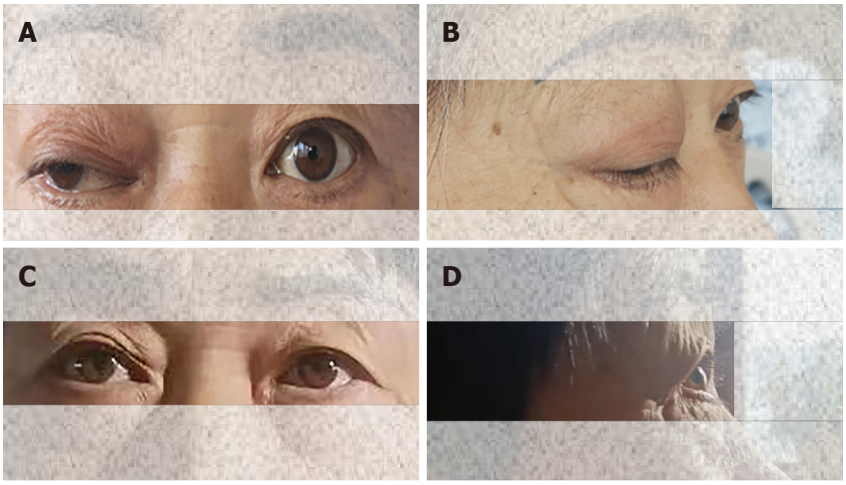

DOI: 10.12998/wjcc.v11.i25.6005

Figure 5 Comparison of the physical characteristics of the patient before and after carotid-cavernous fistula embolization. A and B: Physical examination on admission: Right proptosis, ptosis and limited eye movement; C and D: After five months of follow-up, the symptoms were relieved.

performing the procedure can ensure a discreet approach, thereby minimizing the risk of CCF.

CONCLUSION

Although limited cases of CCF during neurointerventional radiology have been reported, it is anticipated that the number of cases will increase due to the significant rise in MT procedures following AIS. It is important to avoid iatrogenic direct CCF complications, especially that the degree of curvature of the carotid cavernous segment is mostly unknown at the time of MT with ICA occlusion. Therefore, it is advisable for the neurointerventionist to adopt a gentle and cautious approach during the procedure.

ACKNOWLEDGEMENTS

We would like to thank the patient and her family for their informed cooperation and support in our work.

FOOTNOTES

Author contributions: Qu LZ followed up with the patient and wrote the paper; Zhu EB participated in the treatment and management of the patient; Lin MQ and Liu GL collected the data; Dong GH helped to correct the article; Guan HJ conceptualized the idea and finalized the manuscript; All authors have read and approved the final manuscript.

Informed consent statement: Informed written consent was obtained from the patient for publication of this report and any accompanying images.

Conflict-of-interest statement: The authors declare that they have no conflict of interest to disclose.

CARE Checklist (2016) statement: The authors have read CARE Checklist (2016), and the manuscript was prepared and revised according to CARE Checklist (2016).

Country/Territory of origin: China

ORCID number: Lin-Zhuo Qu 0009-0000-2297-8358; Guang-Hui Dong 0000-0002-3641-6628; En-Bo Zhu 0009-0001-1089-0719; Ming-Quan Lin 0009-0002-5317-3151; Guang-Lin Liu 0009-0003-2234-8198; Hong-Jian Guan 0009-0001-8731-3880.

S-Editor: Lin C

L-Editor: A
P-Editor: Yuan YY

REFERENCES

1 **Henderson AD**, Miller NR. Carotid-cavernous fistula: current concepts in aetiology, investigation, and management. *Eye (Lond)* 2018; **32**: 164-172 [PMID: 29099499 DOI: 10.1038/eye.2017.240]
2 **Sheinberg DL**, Brunet MC, Chen SH, Luther E, Starke RM. Iatrogenic Direct Carotid-cavernous Fistula Following Mechanical Thrombectomy: A Case Report and Review of the Literature. *Cureus* 2020; **12**: e7524 [PMID: 32377472 DOI: 10.7759/cureus.7524]
3 **Miyamoto S**, Kato N, Yamazaki T, Yamano A, Akutsu Y, Yasuda S, Matsumaru Y, Ishikawa E. Direct Carotid-Cavernous Fistula Caused by Internal Carotid Artery Perforation by a Microcatheter Body during Mechanical Thrombectomy. *Asian J Neurosurg* 2022; **17**: 638-641 [PMID: 36570747 DOI: 10.1055/s-0042-1757629]
4 **Grüter BE**, Kahles T, Anon J, Berberat J, Andereggen L, Killer HE, Gruber P. Carotid-cavernous sinus fistula following mechanical thrombectomy in acute ischaemic stroke: a rare complication. *Neuroradiology* 2021; **63**: 1149-1152 [PMID: 33755767 DOI: 10.1007/s00234-021-02695-x]
5 **Matsumoto H**, Nishiyama H, Takemoto H, Tetsuo Y, Nakao N. Carotid-cavernous Fistula Caused by Vessel Injury While Withdrawing a Stent Retriever during Mechanical Thrombectomy for Acute Ischemic Stroke: A Case Report. *J Neuroendovascular Ther* 2018; **12**: 235-240 [DOI: 10.5797/jnet.cr.2017-0089]
6 **Ihn YK**, Shin SH, Baik SK, Choi IS. Complications of endovascular treatment for intracranial aneurysms: Management and prevention. *Interv Neuroradiol* 2018; **24**: 237-245 [PMID: 29466903 DOI: 10.1177/1591019918758493]
7 **Ono K**, Oishi H, Tanoue S, Hasegawa H, Yoshida K, Yamamoto M, Arai H. Direct carotid-cavernous fistulas occurring during neurointerventional procedures. *Interv Neuroradiol* 2016; **22**: 91-96 [PMID: 26628454 DOI: 10.1177/1591019915617321]
8 **Koge J**, Tanaka K, Yoshimoto T, Shiozawa M, Kushi Y, Ohta T, Satow T, Kataoka H, Ihara M, Koga M, Isobe N, Toyoda K. Internal Carotid Artery Tortuosity: Impact on Mechanical Thrombectomy. *Stroke* 2022; **53**: 2458-2467 [PMID: 35400203 DOI: 10.1161/STROKEAHA.121.037904]
9 **Lin LM**, Colby GP, Jiang B, Uwandu C, Huang J, Tamargo RJ, Coon AL. Classification of cavernous internal carotid artery tortuosity: a predictor of procedural complexity in Pipeline embolization. *J Neurointerv Surg* 2015; **7**: 628-633 [PMID: 24996435 DOI: 10.1136/neurintsurg-2014-011298]
10 **Kwon HJ**, Jin SC. Spontaneous healing of iatrogenic direct carotid cavernous fistula. *Interv Neuroradiol* 2012; **18**: 187-190 [PMID: 22681734 DOI: 10.1177/159101991201800210]
11 **Venturini G**, Vuolo L, Pracucci G, Picchioni A, Failli Y, Benvenuti F, Sarti C. Association between carotid artery dissection and vascular tortuosity: a case-control study. *Neuroradiology* 2022; **64**: 1127-1134 [PMID: 34766191 DOI: 10.1007/s00234-021-02848-y]
12 **Wang Q**, Liu C, Yan B, Fan X, Zhang M, Li Y, Zhu W, Chen M, Huang X, Zhang Z, Xu G, Liu X. Correlation of extracranial internal carotid artery tortuosity index and intraprocedural complications during carotid artery stenting. *Eur Neurol* 2012; **68**: 65-72 [PMID: 22739099 DOI: 10.1159/000337682]
13 **Kaymaz ZO**, Nikoubashman O, Brockmann MA, Wiesmann M, Brockmann C. Influence of carotid tortuosity on internal carotid artery access time in the treatment of acute ischemic stroke. *Interv Neuroradiol* 2017; **23**: 583-588 [PMID: 28944705 DOI: 10.1177/1591019917729364]
14 **Snelling BM**, Sur S, Shah SS, Chen S, Menaker SA, McCarthy DJ, Yavagal DR, Peterson EC, Starke RM. Unfavorable Vascular Anatomy Is Associated with Increased Revascularization Time and Worse Outcome in Anterior Circulation Thrombectomy. *World Neurosurg* 2018; **120**: e976-e983 [PMID: 30196176 DOI: 10.1016/j.wneu.2018.08.207]
15 **Leker RR**, Kasner SE, El Hasan HA, Sacagiu T, Honig A, Gomori JM, Guan S, Choudhry O, Hurst RW, Kung D, Pukenas B, Sedora-Roman N, Ramchand P, Cohen JE. Impact of carotid tortuosity on outcome after endovascular thrombectomy. *Neurol Sci* 2021; **42**: 2347-2351 [PMID: 33047199 DOI: 10.1007/s10072-020-04813-8]
16 **Balami JS**, White PM, McMeekin PJ, Ford GA, Buchan AM. Complications of endovascular treatment for acute ischemic stroke: Prevention and management. *Int J Stroke* 2018; **13**: 348-361 [PMID: 29171362 DOI: 10.1177/1747493017743051]
17 **Alan N**, Nwachuku E, Jovin TJ, Jankowitz BT, Jadhav AP, Ducruet AF. Management of Iatrogenic Direct Carotid Cavernous Fistula Occurring During Endovascular Treatment of Stroke. *World Neurosurg* 2017; **100**: 710.e15-710.e20 [PMID: 28185973 DOI: 10.1016/j.wneu.2017.01.112]

World Journal of Clinical Cases

Submit a Manuscript: https://www.f6publishing.com

World J Clin Cases 2023 September 6; 11(25): 6012-6018

DOI: 10.12998/wjcc.v11.i25.6012

ISSN 2307-8960 (online)

CASE REPORT

Successful treatment of a case of COVID-19 pneumonia following kidney transplantation using paxlovid and tocilizumab

Qian Chen, Yu-Lin Niu

Specialty type: Medicine, research and experimental

Provenance and peer review: Unsolicited article; Externally peer reviewed.

Peer-review model: Single blind

Peer-review report's scientific quality classification

Grade A (Excellent): 0
Grade B (Very good): 0
Grade C (Good): C, C, C
Grade D (Fair): 0
Grade E (Poor): 0

P-Reviewer: Aydin S, Turkey; Salvadori M, Italy; Sarier M, Turkey

Received: July 6, 2023
Peer-review started: July 6, 2023
First decision: July 18, 2023
Revised: July 26, 2023
Accepted: August 3, 2023
Article in press: August 3, 2023
Published online: September 6, 2023

Qian Chen, Yu-Lin Niu, Department of Organ Transplantation, Affiliated Hospital of Guizhou Medical University, Guiyang 550000, Guizhou Province, China

Corresponding author: Qian Chen, Doctor, Chief Physician, Professor, Researcher, Department of Organ Transplantation, Affiliated Hospital of Guizhou Medical University, No. 28 Gui Medical Street, Beijing Road, Yunyan District, Guiyang 550000, Guizhou Province, China. chenqian1056659393@163.com

Abstract

BACKGROUND

Since its initial detection in 2019, coronavirus disease 2019 (COVID-19) pneumonia has rapidly spread throughout the world in a global pandemic. However, reports of COVID-19 pneumonia among patients following kidney transplantation have been limited and no uniform treatment guidelines for these patients have yet to be established.

CASE SUMMARY

Here, we report the case of a 39-year-old patient recovering from kidney transplantation who contracted perioperative COVID-19 pneumonia that was successfully controlled with oral paxlovid and a single intravenous drip infusion of tocilizumab following the discontinuation of immunosuppressive drugs.

CONCLUSION

Given the rapid spread of severe acute respiratory syndrome coronavirus 2 infections, clinicians should be aware of the potential for more cases of COVID-19 among patients following kidney transplantation and be familiar with appropriate treatment options and likely clinical outcomes.

Key Words: Clinical research; Kidney transplantation; Coronavirus disease 2019 pneumonia; Paxlovid; Tocilizumab; Case report

Core Tip: Here, we report the case of a 39-year-old patient recovering from kidney transplantation who contracted perioperative coronavirus disease 2019 (COVID-19) pneumonia that was successfully controlled with oral paxlovid and a single intravenous drip infusion of tocilizumab following the discontinuation of immunosuppressive drugs. Given the rapid spread of severe acute respiratory syndrome coronavirus 2 infections, clinicians should be aware of the potential for more cases of COVID-19 among patients following kindey transplantation and be familiar with appropriate treatment options and likely clinical outcomes.

Citation: Chen Q, Niu YL. Successful treatment of a case of COVID-19 pneumonia following kidney transplantation using paxlovid and tocilizumab. *World J Clin Cases* 2023; 11(25): 6012-6018
URL: https://www.wjgnet.com/2307-8960/full/v11/i25/6012.htm
DOI: https://dx.doi.org/10.12998/wjcc.v11.i25.6012

INTRODUCTION

The coronavirus disease 2019 (COVID-19) pandemic was first detected as an outbreak of pneumonia in the Wuhan region of China in December 2019[1,2], and it the causative severe acute respiratory syndrome coronavirus 2 (SARS-CoV-2) virus has remained highly transmissible[3-5]. The progression of the pandemic has varied markedly among countries throughout the world, with differences in circulating viral strains and control efforts in different regions. For example, several devastating mutant strains in Italy have rapidly emerged and caused critical illness, particularly among older adults and immunocompromised individuals[6]. Prolonged immunosuppressive treatment is essential among transplant recipients in order to prevent rejection, thus inevitably suppressing the immune status of these individuals as compared to the general population. At present, there is a lack of reported cases of COVID-19 pneumonia in kidney transplant patients, and there are no uniform treatment standards for these individuals[7]. The efficacy of different treatments, the optimal symptomatic management strategies, and the prognostic outcomes in kidney transplant recipients suffering from COVID-19 are also not well understood[8,9]. Here, we describe the case of a 39-year-old male that contracted and was successfully treated for COVID-19 pneumonia after the completion of a kidney transplant procedure. Given the current challenges associated with controlling and preventing the spread of COVID-19, clinicians performing kidney transplantation should be aware of the risk of perioperative infection. By publishing this case report, we hope to provide a reference for kidney transplant teams seeking to effectively manage post-transplant patient recovery.

CASE PRESENTATION

Chief complaints

Elevated creatinine detected for 3 + years, regular hemodialysis admitted for 2 + years.

History of present illness

Three years before, the patient had a cough with no obvious cause. The cough was intermittent, with no sputum, and was accompanied by a loss of appetite, vomiting, and shortness of breath, although no nausea or chest tightness. Examination at the local hospital showed a creatinine level of 800 μmol/L and blood pressure of 180/90 mmHg. The patient was diagnosed with renal failure and was discharged from the hospital after symptomatic treatment. The patient wished to have a kidney transplant and was waiting for a suitable kidney donor after matching. After finding a suitable kidney donor, the patient was admitted to our department with a diagnosis of chronic renal failure, and surgery was scheduled. Since the onset of the disease, the patients' spirit, appetite, and sleep were fine, the stool was normal, the urine volume had decreased to 800 mL/d, and there was no significant change in body weight.

History of past illness

He had a prior history of hypertension with blood pressure levels of up to 180/90 mmHg managed through the long-term use of controlled-relates nifedipine tablets. He had no history of diabetes mellitus, hepatitis, or tuberculosis.

Personal and family history

The patient was a non-smoker and did not drink alcohol. He was a public servant, lived in an area with no endemic diseases, and had not been vaccinated against SARS-CoV-2. He had been born, raised, and lived in his native region and had no history of foreign travel. Additionally, he was not aware of any hereditary diseases in his family.

Physical examination

The patient had been free of nausea, vomiting, and diarrhea since the onset of the disease, and did not exhibit any masses or positive signs, including abdominal pressure, rebound pain, or abdominal muscle tone upon examination.

Laboratory examinations

On admission, his nucleic acid test results indicated that he was negative for COVID-19 pneumonia. On day two following admission, the patients' creatinine was 320 μmol/L, his estimated glomerular filtration rate was 25 mL/min, and his hemoglobin level was 108 g/L.

Imaging examinations

Repeated chest computed tomography (CT) scans revealed patchy shadows in both lungs consistent with the possibility of viral pneumonia (Figure 1A).

FINAL DIAGNOSIS

A pharyngeal swab was collected for SARS-CoV-2 reverse transcription polymerase chain reaction (RT-PCR) testing, which was positive for the presence of the virus. In conjunction with the patients' clinical presentation, etiologic evidence, and imaging findings, a diagnosis of COVID-19 pneumonia was made.

TREATMENT

A 39-year-old male was admitted to the Affiliated Hospital of Guizhou Medical University (Guiyang, China) on December 19, 2022, due to a three-year history of elevated creatinine levels and 2 years of regular hemodialysis. He had expressed interest in receiving a transplanted kidney and was awaiting a suitable donor following a matching test. On admission, his nucleic acid test results indicated that he was negative for COVID-19 pneumonia.

On the third day, he underwent allogeneic kidney transplantation under general anesthesia, with rabbit anti-human thymocyte immunoglobulin for immune induction and mescaline sodium + prednisone acetate + tacrolimus for immune maintenance. He was administered an empirical antimicrobial treatment consisting of piperacillin sodium/tazobactam sodium (4.5 g/d). Sputum and urine culture results were negative, and serum calcitoninogen was negative and interleukin 164 pg/mL. On day 14 of admission, the patient began exhibiting a persistent future. Given the recent rise in COVID-19 infections in the country, the patient was regarded as possibly being infected with COVID-19 and he was thus placed in an isolated single-occupancy room. A pharyngeal swab was collected for SARS-CoV-2 RT-PCR testing, which was positive for the presence of this virus. Repeated chest CT scans revealed patchy shadows in both lungs consistent with the possibility of viral pneumonia (Figure 1A). On the day of diagnosis, his arterial pO2 had fallen to 74 mmHg and continuous oxygenation was initiated *via* nasal cannula and a face mask. Oral paxlovid (nirmatrelvir, 150 mg and ritonavir, 100 mg, Pfizer) Q12 h was administered, while the anti-rejection drugs mescaline sodium and tacrolimus were discontinued. The patients' interleukin-6 (IL-6) levels were rechecked and had risen to 314 pg/mL. After a discussion with our infectious specialist and obtaining written informed consent from the patient, tocilizumab was intravenously administered at a dose of 8 mg/kg diluted in 100 mL of 0.9% saline. After 4 d the patient exhibited no improvements in clinical symptoms and chest CT revealed significant worsening relative to the previous scan (Figure 1B). Following further discussion with our team of physicians, we speculated that reductions in leukocyte counts may be related to the activity of tocilizumab. In an effort to improve the overall immune status of this patient, we administered 5 g/d of intravenous immunoglobulin. Administration was continued for one week. One week following COVID-19 pneumonia, the patients' pO2 levels gradually rose and were maintained at 90%-95% following the discontinuation of paxlovid and tocilizumab treatment. When IL-16 levels were measured 5 d after r drug administration, they had fallen to 42.42 pg/mL.

On day 7 after onset, a chest CT scan showed some degree of absorption relative to previous scans (Figure 1C). On day 28 following admission, the patient was discharged. At the time of discharge, he was free of fever or sputum production, exhibited a pO2 of 96%, a respiratory rate of 16 breaths/min, and a controlled blood pressure of 136/82 mmHg. Repeat chest CT (Figure 1D) and pharyngeal swab testing for COVID-19 were negative on 10 d after the confirmed diagnosis. Tacrolimus and prednisone acetate were continued, and the patient was advised to undergo repeat outpatient testing after 1 wk.

OUTCOME AND FOLLOW-UP

After a period of hospitalization in our hospital, the patients' condition gradually recovered.

DISCUSSION

The ongoing COVID-19 pandemic caused by the SARS-CoV-2 virus has caused over 500 million confirmed infections and 8 million deaths throughout 223 countries and territories[10,11]. The highest number of confirmed cases to date has been reported in the United States. Specific treatment options are lacking, with only symptomatic and routine care for infected individuals. Emerging mutant strains of SARS-CoV-2 represent a particularly substantial threat to post-transplant patients, as these individuals often need to attend outpatient check-up appointments and are more often hospitalized

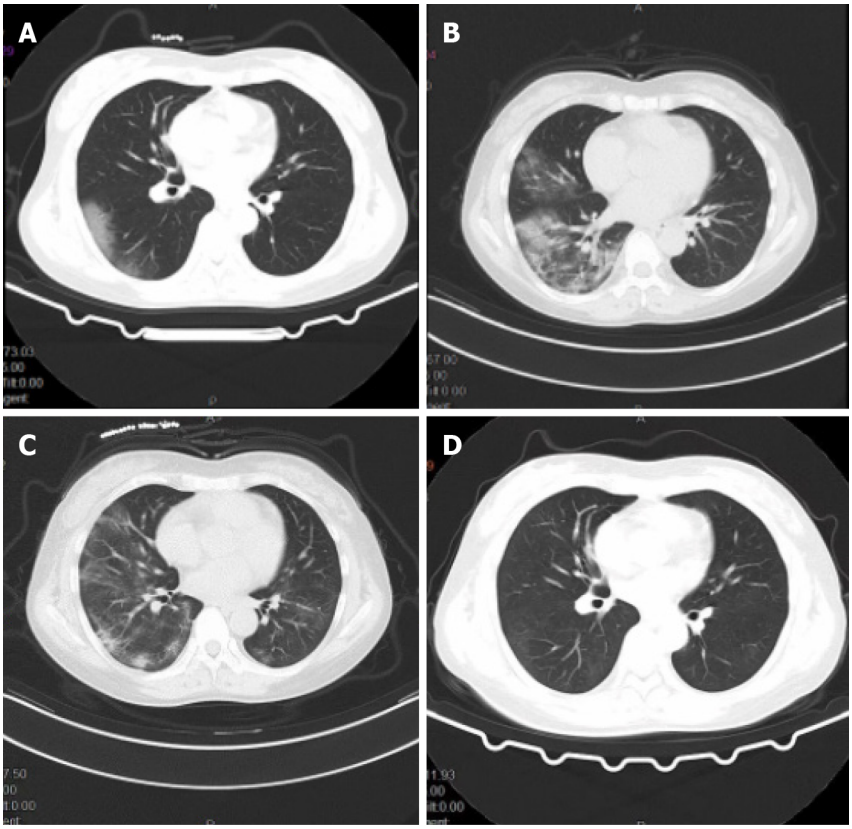

DOI: 10.12998/wjcc.v11.i25.6012

Figure 1 Computed tomography of the chest showing changes in the patients' condition. A: Multiple foci of exudate in both lungs, consider viral pneumonia; B: Multiple foci of exudate in both lungs are more than before, viral pneumonia is considered, and review after treatment is recommended; C: Foci of exudate in both lungs are more resorbed than before, viral pneumonia is considered, and continued treatment is recommended; D: Resorption of foci of infection in both lungs.

dues to their immunosuppressed status[12,13]. These unique population characteristics can place these individuals at a high risk of severe illness or death.

The incubation period for COVID-19 infections reportedly varies from 1-24 d[14]. The initial presenting symptoms in infected patients are relatively nonspecific and can include fever and an upper respiratory tract infection[15]. These signs and symptoms also vary among patients, and the early detection and management of COVID-19 infections is thus vital to improving therapeutic outcomes and reducing the odds that patients develop severe disease[16,17].

After undergoing organ transplantation, patients face a persistent risk of severe illness and death upon COVID-19 infection owing to their impaired immune function[18]. Most kidney transplant patients have also not been vaccinated against COVID-19, and those that have generally exhibit relatively weak vaccine-induced humoral immunity such that they face very high rates of morbidity and mortality[19]. When they do contract COVID-19, these patients are more likely to progress to severe disease such that they are a particularly important group to provide with therapeutic interventions when possible. However, the precise efficacy of different interventional regimens in COVID-19 patients that are also transplant recipients is likely to vary as the virus continues to mutate.

In the present case, when our patient was diagnosed with COVID-19 pneumonia we initially elected to discontinue immunosuppressive treatment with tacrolimus and mycophenolate while maintaining low-dose steroid treatment in light of the high risk of simultaneous bacterial infection[20]. Paxlovid is a recently developed COVID-19 treatment developed by Pfizer that consists of a combination of nirmatrelvir and ritonavir, a peptidomimetic analog of Mpro (3C-like protease)that serves as the primary protease used by SARS-CoV-2[21]. Ritonavir can inhibit the metabolic processing of nirmatrelvir by cytochrome P4503A (CYP3A), thus increasing the circulating levels of the drug (Figure 2). Paxlovid received emergency use authorization from the United States Food and Drug Administration as a treatment for mild-to-moderate COVID-19 in light of its favorable efficacy. Several studies have confirmed that paxlovid administration within the first 5 d after SARS-CoV-2 infection can expedite viral clearance[22]. However, some researchers have questioned the methodology employed in these studies and have suggested that the results are exaggerated. Even so, given the lack of more effective treatment options, paxlovid represents a promising candidate treatment for patients recovering from kidney transplantation who are infected with COVID-19. Accordingly, we elected to use paxlovid to treat our patient following confirmed SARS-CoV-2 infection, with a total paxlovid treatment course lasting 5 d.

Some reports have indicated that infection with SARS-CoV-2 can result in severe lung damage as a consequence of cytokine release syndrome mediated by an overzealous host immune response to the virus. Those patients with severe disease tend to exhibit higher levels of IL-6 as compared to patients with less severe disease. Tocilizumab is initially used to treat adult patients with moderately severe active rheumatoid arthritis that have failed to satisfactorily respond to

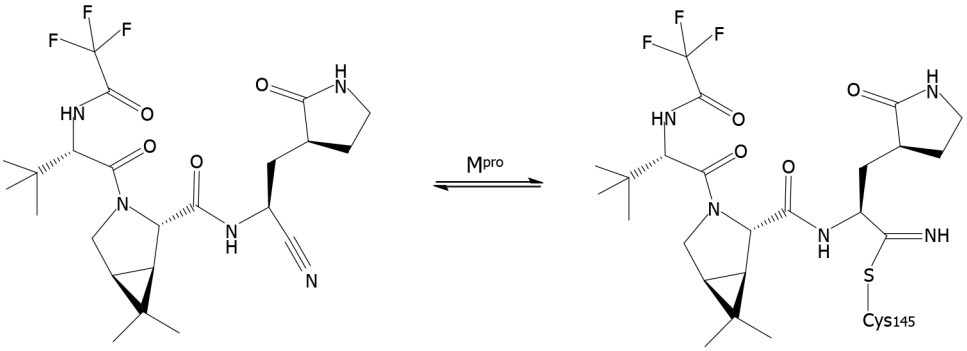

DOI: 10.12998/wjcc.v11.i25.6012 **Copyright** ©The Author(s) 2023.

Figure 2 Mechanism and major binding sites of niamatrelvir for suppressing the severe acute respiratory syndrome coronavirus 2 main prorease.

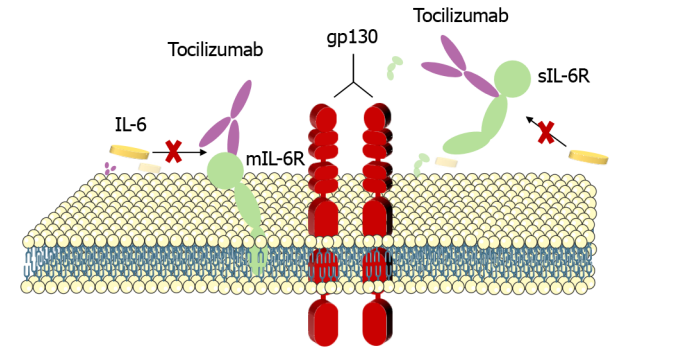

DOI: 10.12998/wjcc.v11.i25.6012 **Copyright** ©The Author(s) 2023.

Figure 3 Tocilizumab binding to the interleukin-6 (IL-6) receptor (gp80) inhibits IL-6 binding and signal transduction. IL-6: Interleukin-6.

disease-modifying anti-rheumatic drug treatment[23]. In a prospective, multicenter, open-label, randomized, controlled trial, investigators found that tocilizumab appeared to be more effective in patients with COVID-19 who had high IL-6 concentrations[24]. Some COVID-19 patients will experience severe disease characterized by dyspnea, respiratory failure, and acute respiratory distress syndrome driven by IL-6 and other components of cytokine release syndrome in critical cases. Blocking of IL-6 production is an attractive means of targeting excessive inflammation during SARS-CoV-2 infection, as IL-6 is known to play a critical role in the COVID-19-induced cytokine storm. Tolizumab is a competitive inhibitor of membrane-bound and soluble IL-6 receptors that blocks the downstream signaling of IL-6 (Figure 3). The use of the IL-6 receptor antagonist tocilizumab as a treatment for severely ill COVID-19 patients thus has the potential to mitigate these severe outcomes[25]. In this case, we treated our patient with tocilizumab given his high circulating IL-6 concentrations in an effort to protect against further lung lesions and associated pulmonary distress. At present, there is no consensus regarding the optimal timing of tocilizumab administration when treating COVID-19, and given that our patient experienced positive clinical outcomes with a single dose of tocilizumab, we did not administer any further doses. It is important to note that IL-6 Levels may remain temporarily elevated following the initiation of tocilizumab treatment as the antibody blocks the IL-6 receptor, whereas the ligand itself remains in circulation and degrades over time. In the present case, the patient was also administered immunoglobulin to enhance his immune system.

The treatment of patients with COVID-19 has forced physicians to choose between trying unproven therapeutic agents and hoping that they work or providing standard supportive care for patients with severe respiratory disease until the identification of an optimal therapeutic agent by randomized controlled clinical trials. The platform trial PEMAP-CAP (randomized, embedded, multi-factorial, adaptive platform trial for community-acquired pneumonia-for critically ill patients) aims to turn the frantic attempts to save lives on the front line into an ongoing international trial with the goal of rapidly identifying the best treatments for terminally ill patients. Because pandemics are unpredictable and can occur suddenly, it is important to have the appropriate infrastructure in place to generate evidence on optimal treatments during a pandemic so that clinicians and policymakers can use this information to improve patient prognosis.

In summary, we have herein detailed a case of COVID-19 pneumonia that developed during the perioperative period in a patient that underwent kidney transplantation to treat end-stage kidney disease. The patient was successfully treated with a series of drugs including paxlovid, tocilizumab, and human immunoglobulin together with the temporary discontinuation of the immunosuppressive therapy given following transplantation. While informative, this case is subject to several limitations. As this is a single case, it is not sufficient to formulate treatment guidelines for these multiple, and the self-healing process in COVID-19 patients following kidney transplantation remains to be fully elucidated. Even so, we believe that this case will provide a valuable reference to clinicians in transplant units, aiding in the recognition and

potential treatment of COVID-19 pneumonia among individuals in the perioperative period following transplantation.

CONCLUSION

Given the sustained high rates of COVID-19 infections throughout the globe, we believe that descriptions of the effective management of exceptional cases are important as a focus of concern for transplant surgeons until sufficiently large volumes of data are available from clinical studies to provide more robust guidance.

ACKNOWLEDGEMENTS

Thank you to all the medical staff of the Organ Transplantation Department of the Affiliated Hospital of Guizhou Medical University.

FOOTNOTES

Author contributions: Chen Q and Niu YL wrote and collated the manuscript; Niu YL reviewed the manuscript; All authors contributing to the article and approving the submitted version.

Supported by Guiyang Science and Technology Program, No. 2019-9-1-39.

Informed consent statement: Informed written consent was obtained from the patient and her parents for the publication of this report and any accompanying images.

Conflict-of-interest statement: All the authors report no relevant conflicts of interest for this article.

CARE Checklist (2016) statement: The authors have read the CARE Checklist (2016), and the manuscript was prepared and revised according to the CARE Checklist (2016).

Country/Territory of origin: China

ORCID number: Qian Chen 0000-0002-8918-0313.

S-Editor: Qu XL
L-Editor: A
P-Editor: Yuan YY

REFERENCES

1 **Guan WJ**, Zhong NS. Clinical Characteristics of Covid-19 in China. Reply. *N Engl J Med* 2020; **382**: 1861-1862 [PMID: 32220206 DOI: 10.1056/NEJMc2005203]
2 **Zu ZY**, Jiang MD, Xu PP, Chen W, Ni QQ, Lu GM, Zhang LJ. Coronavirus Disease 2019 (COVID-19): A Perspective from China. *Radiology* 2020; **296**: E15-E25 [PMID: 32083985 DOI: 10.1148/radiol.2020200490]
3 **Mo P**, Xing Y, Xiao Y, Deng L, Zhao Q, Wang H, Xiong Y, Cheng Z, Gao S, Liang K, Luo M, Chen T, Song S, Ma Z, Chen X, Zheng R, Cao Q, Wang F, Zhang Y. Clinical Characteristics of Refractory Coronavirus Disease 2019 in Wuhan, China. *Clin Infect Dis* 2021; **73**: e4208-e4213 [PMID: 32173725 DOI: 10.1093/cid/ciaa270]
4 **Arimoto KI**, Miyauchi S, Troutman TD, Zhang Y, Liu M, Stoner SA, Davis AG, Fan JB, Huang YJ, Yan M, Glass CK, Zhang DE. Expansion of interferon inducible gene pool *via* USP18 inhibition promotes cancer cell pyroptosis. *Nat Commun* 2023; **14**: 251 [PMID: 36646704 DOI: 10.1038/s41467-022-35348-5]
5 **Sarier M**, Demir M, Emek M, Usta SS, Soylu A, Konuk EY, Turgut H. Comparison of spermiograms of infertile men before and during the COVID-19 pandemic. *Rev Assoc Med Bras (1992)* 2022; **68**: 191-195 [PMID: 35239880 DOI: 10.1590/1806-9282.20210935]
6 **Onder G**, Rezza G, Brusaferro S. Case-Fatality Rate and Characteristics of Patients Dying in Relation to COVID-19 in Italy. *JAMA* 2020; **323**: 1775-1776 [PMID: 32203977 DOI: 10.1001/jama.2020.4683]
7 **Hippisley-Cox J**, Coupland CA, Mehta N, Keogh RH, Diaz-Ordaz K, Khunti K, Lyons RA, Kee F, Sheikh A, Rahman S, Valabhji J, Harrison EM, Sellen P, Haq N, Semple MG, Johnson PWM, Hayward A, Nguyen-Van-Tam JS. Risk prediction of covid-19 related death and hospital admission in adults after covid-19 vaccination: national prospective cohort study. *BMJ* 2021; **374**: n2244 [PMID: 34535466 DOI: 10.1136/bmj.n2244]

8 **Desai A**, Gainor JF, Hegde A, Schram AM, Curigliano G, Pal S, Liu SV, Halmos B, Groisberg R, Grande E, Dragovich T, Matrana M, Agarwal N, Chawla S, Kato S, Morgan G, Kasi PM, Solomon B, Loong HH, Park H, Choueiri TK, Subbiah IM, Pemmaraju N, Subbiah V; COVID19 and Cancer Clinical Trials Working Group. COVID-19 vaccine guidance for patients with cancer participating in oncology clinical trials. *Nat Rev Clin Oncol* 2021; **18**: 313-319 [PMID: 33723371 DOI: 10.1038/s41571-021-00487-z]

9 **Mahalingasivam V**, Su G, Iwagami M, Davids MR, Wetmore JB, Nitsch D. COVID-19 and kidney disease: insights from epidemiology to inform clinical practice. *Nat Rev Nephrol* 2022; **18**: 485-498 [PMID: 35418695 DOI: 10.1038/s41581-022-00570-3]

10 **Safiabadi Tali SH**, LeBlanc JJ, Sadiq Z, Oyewunmi OD, Camargo C, Nikpour B, Armanfard N, Sagan SM, Jahanshahi-Anbuhi S. Tools and Techniques for Severe Acute Respiratory Syndrome Coronavirus 2 (SARS-CoV-2)/COVID-19 Detection. *Clin Microbiol Rev* 2021; **34** [PMID: 33980687 DOI: 10.1128/CMR.00228-20]

11 **Yüce M**, Filiztekin E, Özkaya KG. COVID-19 diagnosis -A review of current methods. *Biosens Bioelectron* 2021; **172**: 112752 [PMID: 33126180 DOI: 10.1016/j.bios.2020.112752]

12 **Fernandes Q**, Inchakalody VP, Merhi M, Mestiri S, Taib N, Moustafa Abo El-Ella D, Bedhiafi T, Raza A, Al-Zaidan L, Mohsen MO, Yousuf Al-Nesf MA, Hssain AA, Yassine HM, Bachmann MF, Uddin S, Dermime S. Emerging COVID-19 variants and their impact on SARS-CoV-2 diagnosis, therapeutics and vaccines. *Ann Med* 2022; **54**: 524-540 [PMID: 35132910 DOI: 10.1080/07853890.2022.2031274]

13 **Azzi Y**, Parides M, Alani O, Loarte-Campos P, Bartash R, Forest S, Colovai A, Ajaimy M, Liriano-Ward L, Pynadath C, Graham J, Le M, Greenstein S, Rocca J, Kinkhabwala M, Akalin E. COVID-19 infection in kidney transplant recipients at the epicenter of pandemics. *Kidney Int* 2020; **98**: 1559-1567 [PMID: 33069762 DOI: 10.1016/j.kint.2020.10.004]

14 **Cravedi P**, Mothi SS, Azzi Y, Haverly M, Farouk SS, Pérez-Sáez MJ, Redondo-Pachón MD, Murphy B, Florman S, Cyrino LG, Grafals M, Venkataraman S, Cheng XS, Wang AX, Zaza G, Ranghino A, Furian L, Manrique J, Maggiore U, Gandolfini I, Agrawal N, Patel H, Akalin E, Riella LV. COVID-19 and kidney transplantation: Results from the TANGO International Transplant Consortium. *Am J Transplant* 2020; **20**: 3140-3148 [PMID: 32649791 DOI: 10.1111/ajt.16185]

15 **Nair V**, Jandovitz N, Hirsch JS, Nair G, Abate M, Bhaskaran M, Grodstein E, Berlinrut I, Hirschwerk D, Cohen SL, Davidson KW, Dominello AJ, Osorio GA, Richardson S, Teperman LW, Molmenti EP. Covid-19 in kidney transplant recipients. *American journal of transplantation: official journal of the American Society of Transplantation and the American Society of Transplant Surgeons* 2020; **20**: 1819-1825 [DOI: 10.1111/ajt.15967]

16 **Radcliffe C**, Palacios CF, Azar MM, Cohen E, Malinis M. Real-world experience with available, outpatient COVID-19 therapies in solid organ transplant recipients during the omicron surge. *Am J Transplant* 2022; **22**: 2458-2463 [PMID: 35583664 DOI: 10.1111/ajt.17098]

17 **Goffin E**, Candellier A, Vart P, Noordzij M, Arnol M, Covic A, Lentini P, Malik S, Reichert LJ, Sever MS, Watschinger B, Jager KJ, Gansevoort RT; ERACODA Collaborators. COVID-19-related mortality in kidney transplant and haemodialysis patients: a comparative, prospective registry-based study. *Nephrol Dial Transplant* 2021; **36**: 2094-2105 [PMID: 34132811 DOI: 10.1093/ndt/gfab200]

18 **Abu Jawdeh BG**. COVID-19 in Kidney Transplantation: Outcomes, Immunosuppression Management, and Operational Challenges. *Adv Chronic Kidney Dis* 2020; **27**: 383-389 [PMID: 33308503 DOI: 10.1053/j.ackd.2020.07.004]

19 **Karatas M**, Tatar E, Simsek C, Yıldırım AM, Ari A, Zengel B, Uslu A. COVID-19 pneumonia in kidney transplant recipients: A promising treatment algorithm in the absence of a disease-specific drug. *J Med Virol* 2021; **93**: 5789-5797 [PMID: 34050953 DOI: 10.1002/jmv.27110]

20 **El Karoui K**, De Vriese AS. COVID-19 in dialysis: clinical impact, immune response, prevention, and treatment. *Kidney Int* 2022; **101**: 883-894 [PMID: 35176326 DOI: 10.1016/j.kint.2022.01.022]

21 **Najjar-Debbiny R**, Gronich N, Weber G, Khoury J, Amar M, Stein N, Goldstein LH, Saliba W. Effectiveness of Paxlovid in Reducing Severe Coronavirus Disease 2019 and Mortality in High-Risk Patients. *Clin Infect Dis* 2023; **76**: e342-e349 [PMID: 35653428 DOI: 10.1093/cid/ciac443]

22 **RECOVERY Collaborative Group**. Lopinavir-ritonavir in patients admitted to hospital with COVID-19 (RECOVERY): a randomised, controlled, open-label, platform trial. *Lancet* 2020; **396**: 1345-1352 [PMID: 33031764 DOI: 10.1016/S0140-6736(20)32013-4]

23 **Rosas IO**, Diaz G, Gottlieb RL, Lobo SM, Robinson P, Hunter BD, Cavalcante AW, Overcash JS, Hanania NA, Skarbnik A, Garcia-Diaz J, Gordeev I, Carratalà J, Gordon O, Graham E, Lewin-Koh N, Tsai L, Tuckwell K, Cao H, Brainard D, Olsson JK. Tocilizumab and remdesivir in hospitalized patients with severe COVID-19 pneumonia: a randomized clinical trial. *Intensive Care Med* 2021; **47**: 1258-1270 [PMID: 34609549 DOI: 10.1007/s00134-021-06507-x]

24 **Declercq J**, Van Damme KFA, De Leeuw E, Maes B, Bosteels C, Tavernier SJ, De Buyser S, Colman R, Hites M, Verschelden G, Fivez T, Moerman F, Demedts IK, Dauby N, De Schryver N, Govaerts E, Vandecasteele SJ, Van Laethem J, Anguille S, van der Hilst J, Misset B, Slabbynck H, Wittebole X, Liénart F, Legrand C, Buyse M, Stevens D, Bauters F, Seys LJM, Aegerter H, Smole U, Bosteels V, Hoste L, Naesens L, Haerynck F, Vandekerckhove L, Depuydt P, van Braeckel E, Rottey S, Peene I, Van Der Straeten C, Hulstaert F, Lambrecht BN. Effect of anti-interleukin drugs in patients with COVID-19 and signs of cytokine release syndrome (COV-AID): a factorial, randomised, controlled trial. *Lancet Respir Med* 2021; **9**: 1427-1438 [PMID: 34756178 DOI: 10.1016/S2213-2600(21)00377-5]

25 **Somers EC**, Eschenauer GA, Troost JP, Golob JL, Gandhi TN, Wang L, Zhou N, Petty LA, Baang JH, Dillman NO, Frame D, Gregg KS, Kaul DR, Nagel J, Patel TS, Zhou S, Lauring AS, Hanauer DA, Martin E, Sharma P, Fung CM, Pogue JM. Tocilizumab for treatment of mechanically ventilated patients with COVID-19. *medRxiv* 2020 [PMID: 32577684 DOI: 10.1101/2020.05.29.20117358]

World Journal of Clinical Cases

Submit a Manuscript: https://www.f6publishing.com

World J Clin Cases 2023 September 6; 11(25): 6019-6024

DOI: 10.12998/wjcc.v11.i25.6019

ISSN 2307-8960 (online)

CASE REPORT

Diagnosis and treatment of Whipple disease after kidney transplantation: A case report

Qian Chen, Yu-Lin Niu, Tao Zhang

Specialty type: Biology

Provenance and peer review: Unsolicited article; Externally peer reviewed.

Peer-review model: Single blind

Peer-review report's scientific quality classification

Grade A (Excellent): 0
Grade B (Very good): 0
Grade C (Good): C, C
Grade D (Fair): 0
Grade E (Poor): 0

P-Reviewer: Susak YM, Ukraine; Teng X, China

Received: July 6, 2023
Peer-review started: July 6, 2023
First decision: July 18, 2023
Revised: July 20, 2023
Accepted: August 1, 2023
Article in press: August 1, 2023
Published online: September 6, 2023

Qian Chen, Yu-Lin Niu, Tao Zhang, Department of Organ Transplantation, Affiliated Hospital of Guizhou Medical University, Guiyang 550000, Guizhou Province, China

Corresponding author: Tao Zhang, PhD, Chief Physician, Department of Organ Transplantation, Affiliated Hospital of Guizhou Medical University, No. 28 Guimedical Street, Yunyan District, Guiyang 550000, Guizhou Province, China. enric_olivera@sina.com

Abstract

BACKGROUND

Kidney transplantation is the standard treatment for end-stage renal disease. Particularly, rare and specific pathogenic infections which are asymptomatic are often difficult to diagnose, causing delayed and ineffective treatment and thus seriously affecting prognosis. *Tropheryma whipplei* (*T. whipplei*) is a Gram-positive actinomycete widely found in soil, sewage, and other external environments and is present in the population as an asymptomatic pathogen. There is relatively little documented research on *T. whipplei* in renal transplant patients, and there are no uniform criteria for treating this group of post-transplant patients. This article describes the treatment of a 42-year-old individual with post-transplant *T. whipplei* infection following kidney transplantation.

CASE SUMMARY

To analyze clinical features of Whipple's disease and summarize its diagnosis and treatment effects after renal transplantation. Clinical data of a Whipple's disease patient treated in the affiliated hospital of Guizhou Medical University were collected and assessed retrospectively. The treatment outcomes and clinical experience were then summarized *via* literature review. The patient was admitted to the hospital due to recurrent diarrhea for 1 mo, shortness of breath, and 1 wk of fever, after 3 years of renal transplantation. The symptoms of the digestive and respiratory systems were not significantly improved after adjusting immunosuppressive regimen and anti-diarrheal, empirical antibiotic treatments. Bronchoscopic alveolar fluid was collected for meta-genomic next-generation sequencing (mNGS). The deoxyribonucleic acid sequence of *Tropheryma whipplei* was detected, and Whipple's disease was diagnosed. Meropenem, ceftriaxone, and other symptomatic treatments were given, and water-electrolyte balance was maintained. Symptoms resolved quickly, and the patient was discharged after 20 d of hospitalization. The compound sulfamethoxazole tablet was continued for 3 mo after discharge. No diarrhea, fever, and other symptoms occurred during the 6-month follow-up.

CONCLUSION
Whipple's disease is rare, with no specific symptoms, which makes diagnosis difficult. Polymerase chain reaction or mNGS should be immediately performed when the disease is suspected to confirm the diagnosis.

Key Words: Kidney transplantation; Immunosuppression; Whipple disease; Whipple's nutrient barrier; Macrogenomics second-generation sequencing technology; Case report

Core Tip: Whipple disease is rare and has no specific symptoms, which makes diagnosis difficult. When the disease is suspected, polymerase chain reaction or meta-genomic next-generation sequencing should be performed immediately to confirm the diagnosis.

Citation: Chen Q, Niu YL, Zhang T. Diagnosis and treatment of Whipple disease after kidney transplantation: A case report. *World J Clin Cases* 2023; 11(25): 6019-6024
URL: https://www.wjgnet.com/2307-8960/full/v11/i25/6019.htm
DOI: https://dx.doi.org/10.12998/wjcc.v11.i25.6019

INTRODUCTION

Kidney transplantation is standard treatment for end-stage renal disease[1,2]. Human and kidney survival rates have improved significantly after kidney transplantation with the development of immunosuppressive drugs, advancements in surgical techniques, and improved perioperative management protocols[3,4]. However, infectious diseases are significantly more frequent in post-transplant recipients than in general population due to prolonged immunosuppressive medication, and infection has become one of the main causes of death after kidney transplantation[5]. Particularly, rare and specific pathogenic infections which are asymptomatic are often difficult to diagnose, causing delayed and ineffective treatment and thus seriously affecting prognosis[6]. *Tropheryma whipplei (T. whipplei)*, a Gram-positive actinomycete, is widely found in soil, sewage, and other external environments and is present in the population as an asymptomatic pathogen[7,8]. Historically, the symptoms of Whipple's disease included intermittent and recurrent arthralgia or arthritis with chronic diarrhea, abdominal pain, weight loss, and central nervous and cardiovascular systems effects[9,10]. The occurrence of Whipple's disease after renal transplantation has not been reported yet. A patient with Whipple's disease was admitted with respiratory and digestive systems infections after renal transplantation and the treatment outcomes were good. This case aimed to report clinical data and treatment outcomes. Furthermore, the relevant domestic and international literature was also included to provide a reference for the timely diagnosis and treatment of this rare disease.

CASE PRESENTATION

Chief complaints

Diarrhea for 1 mo, shortness of breath with fever for 1 wk.

History of present illness

A 46 years old male patient was enrolled at the affiliated hospital of Guizhou Medical University for the uremic stage of chronic renal failure (primary nephropathy unknown) and underwent a living donor kidney transplant in July 2019. The patient received left kidney of his father. The donor-recipient blood type is A. The human leukocyte antigen mismatch was 2. The recipient had a negative preoperative penal reactive antibody and a complement-dependent cytotoxicity test of 3%. The donor underwent laparoscopic kidney resection, and the recipient underwent conventional kidney transplantation at the right iliac fossa. The rabbit anti-human thymocyte immunoglobulin (r-ATG) was administered intra- and post-operatively at 50 and 25 mg from D1 to D4, respectively. There were no postoperative complications, and the patient was discharged 14 days after the surgery. With regular follow-up after discharge, a triple immunosuppressive regimen of tacrolimus + morte-tacrolimus + glucocorticoids was used to prolong anti-rejection and tacrolimus trough maintained between 5 and 10 ng/mL was prescribed. The patient with 1 mo of diarrhea visited the hospital; he had 5-6 stools per day, diluted and watery, without mucus, pus, and blood. Outpatient treatment with symptomatic anti-diarrhea and intestinal flora regulation did not significantly relieve diarrhea symptoms. Subsequently, the immunosuppressive regimen was adjusted, and diarrhea frequency decreased to 2 to 3 times daily. After one week, the patient developed shortness of breath with fever after activity with no apparent cause, with a maximum temperature of 38.5 °C. He was diagnosed with "diarrhea and fever to be investigated" and was admitted to the hospital without cough, sputum, nausea, vomiting, and frequent and urgent urination. On the day of admission, he relieved loose stools twice and urinated 1200

mL. He had lost about 2.5 kg of weight in the past month.

History of past illness

Denied unclean diet, cold and close contact with febrile patients before the disease onset, hypertension, diabetes, coronary heart disease, tuberculosis, hepatitis B, *etc*. There was no history of trauma, blood transfusion, drug or food allergy, living in infected areas, contact with infected water or sources, or exposure to radiation, toxins, or drugs. Furthermore, there was no residence history in areas with medium to high risk of neoconiosis or close contact.

Personal and family history

Born and raised in Guizhou Province, no history of extended travel outside the country, no smoking or drinking. Parents, children and spouse are all healthy.

Physical examination

The initial checkup indicated a temperature of 37.8 °C, pulse 106/min, respiration 28/min, blood pressure 123/85 mmHg, and finger pulse oxygen 91%. After a physical examination, he was clear and had shortness of breath, with a medium body shape, general nutrition, and cooperation. The pupils were equally large and rounded bilaterally, and the light reflex was sensitive. There was no yellowing of the skin and sclera, and no petechiae were observed on the skin mucosa. No enlargement of superficial lymph nodes was detected throughout the body. Breath sounds were coarse in both lungs, and a few wet rales could be heard in the middle and lower lungs. He had a uniform heart rhythm with no murmur in the valves. Abdominal and neurological investigations were negative; no abnormal external genitalia development or external urethral discharge was identified. Furthermore, there was no abnormal joint movement of the limbs.

Laboratory examinations

The blood profile revealed the following: Leukocytes = 8.94 × 10^9/L, lymphocyte = 4.3%, absolute lymphocyte value = 0.38 × 10^9/L, neutrophil = 90.5%, absolute neutrophil value = 8.09 × 10^9/L, calcitoninogen = 0.45 μg/L, creatinine = 131.0 μmol/L, blood sodium = 132.1 mmol/L, blood chloride = 79.9, blood glucose = 8.43 mmol/L, albumin = 32.5 g/L, and ultrasensitive C-reactive protein = 24.94 mg/L. The routine stool test and Vibrio cholera, Salmonella, and Shigella culture were negative. Tacrolimus blood concentration was 4.76 ng/mL.

Imaging examinations

Chest computed tomography (CT) showed multiple exudates in both lungs, and infection was considered.

FINAL DIAGNOSIS

Whipple disease.

TREATMENT

After the admission, the cardiac profile was monitored, nasal catheter oxygenation was administered, the empirical anti-infection regime of moxifloxacin was initiated, mortification with mortification, symptomatic anti-diarrhea medication was started, the water-electrolyte acid-base balance was carefully maintained for active infection improvement and pathogenesis-related tests were performed.

Blood and urine BK and human cytomegalovirus virus deoxyribonucleic acid were negative, fungal (1,3)-β-D glucan ≤ 37.5 pg/mL, Aspergillus galactomannan = 0.205 S/CO, and antibodies to 12 common respiratory pathogens were also negative. After 3 d of empirical anti-infective treatment, the patient's shortness of breath and fever did not improve; the fever peak rose to 38.9 °C and was mainly experienced from 2 pm to 10 pm daily. Therefore, the anti-infective regimen was adjusted to moxifloxacin + cefoperazone-sulbactam sodium with micafungin (antifungal). Furthermore, blood bacterial and fungal cultures and fiberoptic bronchoscopy were performed, which were negative. Fibronectomy indicated abnormal trachea and bronchi. On brush examination of the posterior segment of the right lung's upper lobe, ciliated columnar cells, a few erythrocytes, and phagocytes were seen microscopically, and no acid-resistant bacilli were found on antacid staining. Bronchoalveolar lavage fluid (BALF) was obtained for metagenomics next-generation sequencing (mNGS), which Whipple's nutrient barrier sequence was detected after 2 days. Since this was a rare pathogen and our department has no previous experience with this disease, literatures weas reviewed, and multidisciplinary consultation (MDT) with the Department of Infection, Clinical Pharmacy, Respiratory Medicine, and Gastroenterology was requested to change the anti-infective regimen to meropenem alone. After 48 h of this new regime, the patient's temperature dropped to 36.8 °C and fluctuated within the normal range after that. After 9 d, the regimen was changed to ceftriaxone; post- 5 days of ceftriaxone, it was changed to oral cotrimoxazole.

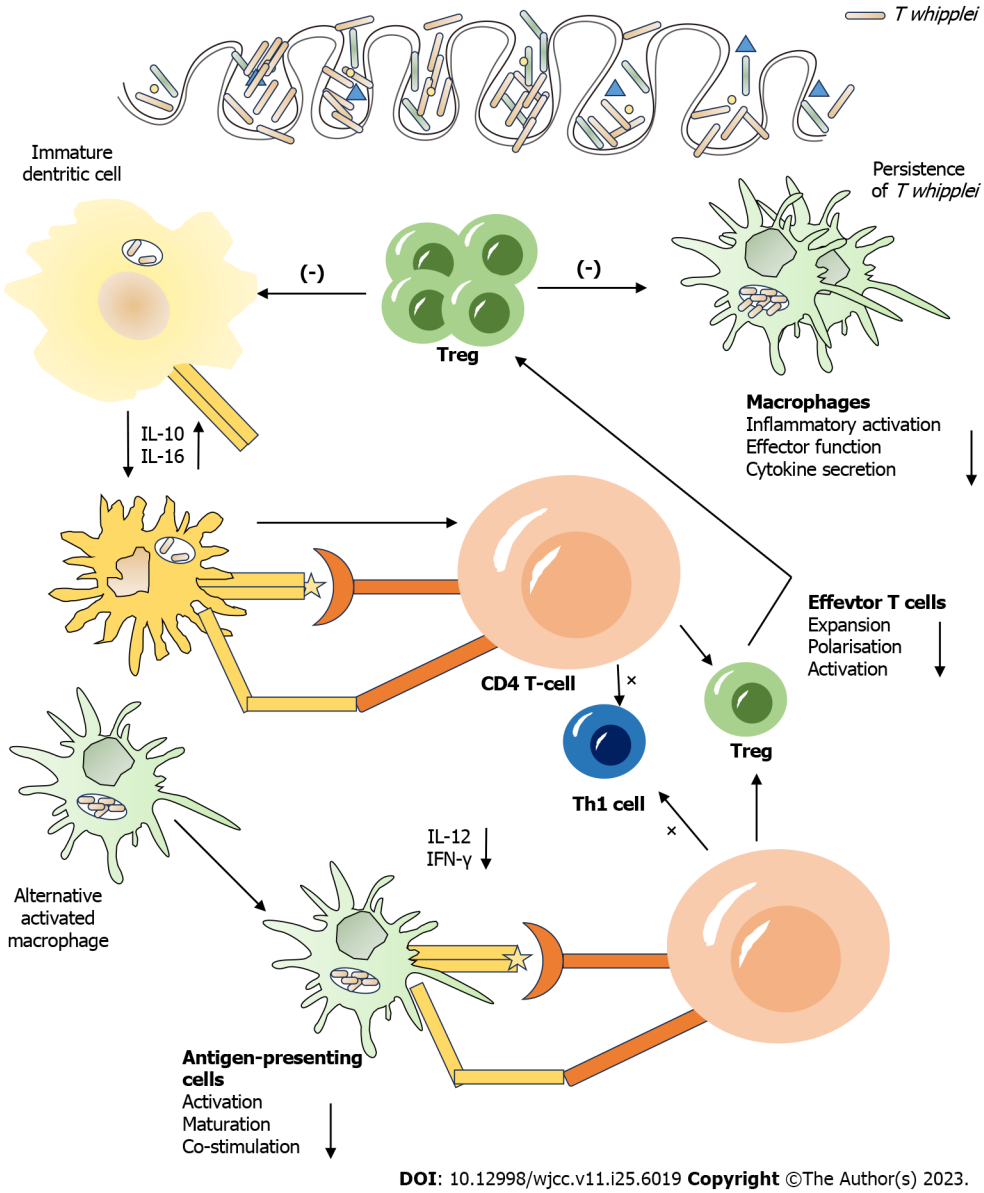

Figure 1 Pathogenesis of Whipple's disease. IL: Interleukin; IFN: Interferons; *T. whipplei*: *Tropheryma whipplei*.

OUTCOME AND FOLLOW-UP

The patient was discharged after 20 d of hospitalization and continued on oral cotrimoxazole for 3 mo after discharge. At 6 mo post-discharge follow-up, the patient's transplanted renal function was stable, no significant abnormalities were observed in the relevant biochemical indices, and no extended symptoms such as diarrhea or fever occurred.

DISCUSSION

Whipple's disease is a rare systemic infection caused by *T. whipplei*, most frequently observed in patients with diabetes, chronic kidney disease, liver disease, and immunodeficiency[11,12]. Its Pathogenesis of Whipple's disease is shown in Figure 1. It is also detected in the general population as an asymptomatic pathogen. A study reported its incidence to be 3 in a million, and no relevant epidemiological report from China exists[13]. It is primarily manifested with intermittent and recurrent arthralgia or arthritis with chronic diarrhea, abdominal pain, and weight loss. It can affect multiple systems such as cardiovascular, central nervous, respiratory, and skin systems. If left untreated, many serious complications can occur, with poor prognosis[14]. Because of the rarity, non-specific clinical manifestations, and absence of classical diagnostic techniques (smear microscopy, microbial culture, antigenic antibody testing, *etc.*) to identify *T. whipplei* nurturing bodies, the disease is difficult to diagnose and is mainly confirmed using tissue biopsy and pathogenetic genetic testing[15]. Upon suspicion, despite gastrointestinal symptoms, small intestinal mucosal specimens should be obtained *via* microscopy for periodic acid Schiff staining, polymerase chain reaction (PCR), and mNGS testing[16]. If the results of small intestinal tissue examination are not diagnostic, the above tests should be performed by sampling the

corresponding lesion sites (synovial membrane, lymph nodes, alveolar lavage fluid, cerebrospinal fluid, blood, *etc*.) according to the patient's clinical manifestations. With the rapid development of molecular biology techniques, the application of mNGS for pathogenic detection has been increasing, especially for clinically rare, atypical, or caustic microorganisms with important diagnostic value[17,18]. mNGS also allow the detection of multiple pathogens simultaneously in a single specimen, dismissing repeated sampling, and multiple testing[19].

In review, the patient received long-term maintenance therapy with immunosuppressive drugs after renal transplantation and had recurrent diarrhea with weight loss as the first symptom. Diarrhea is frequent in most post-transplant patients and is mostly considered non-infectious and caused by morte-macrolides. The diarrhea was slightly relieved after routine adjustment of immunosuppressants and symptomatic anti-diarrhea medications. Subsequently, the patient developed respiratory symptoms, including chest tightness, shortness of breath with fever, and inflammatory exudate in both lungs, evident by chest CT. Although monism was applied to explain the digestive and respiratory symptoms, we could not find a disease or pathogen linked with the incidence of all the clinical symptoms simultaneously, and conventional pathogenic tests were not positive. Therefore, only a preliminary diagnosis of non-infectious diarrhea combined with community-acquired pneumonia was made, and the two systems were treated separately, which was ineffective. The patient's diagnosis was confirmed when BALF was examined by fiberoptic bronchoscopy for mNGS, and a sequence of *T. whipplei* nutrient blockers was detected. This case highlighted that in the future, if a patient with diarrhea and combined motor, cardiovascular, respiratory, or other systemic symptoms is admitted after renal transplantation and the conventional treatment is ineffective, the possibility of Whipple's disease should be considered, and specimen from the appropriate site should be collected for PCR or mNGS testing.

Currently, there are no guidelines or expert consensus on treating Whipple's disease. The primary treatment includes anti-infective therapy against the pathogen and supportive symptomatic therapy against the corresponding systemic symptoms. Effective anti-infective drugs reported in the literature include meropenem, ceftriaxone, cotrimoxazole, doxycycline, and hydroxychloroquine[20,21]. In this case, meropenem was selected as an anti-infection after MDT consultation because of severe respiratory symptoms, which quickly improved the patient's fever and was subsequently stepped down to ceftriaxone. Furthermore, A research reported that a recurrence rate of this disease was 30% to 40%[22]; therefore, an oral combination of sulfamethoxazole or doxycycline + hydroxychloroquine for 3 mo to 1 year was proposed. The patient continued using sulfamethoxazole for 3 mo after discharge. The followed up of > 6 mo reported no further symptoms of diarrhea and fever, as well as had stable transplant renal function[23].

CONCLUSION

In summary, prolonged immunosuppressive medication in organ transplant patients can cause opportunistic infections, especially some relatively rare pathogens in the normal population, and often causes difficulties in clinical management. Whipple's disease after renal transplantation is rarely reported. Therefore, if a patient enrolls with diarrhea and symptoms of motor, respiratory, cardiovascular, or other systems after renal transplantation and indicates poor outcomes after conventional management, Whipple's disease should be considered. PCR or mNGS testing can be performed on the appropriate specimens for early detection of pathogens for targeted anti-infective treatment.

FOOTNOTES

Author contributions: Chen Q and Zhang T wrote and collated the manuscript; Niu YL and Chen Q collected and collated patient data, and Chen Q, Niu YL, and Zhang T reviewed and received funding for the manuscript. All authors contribute to the article and approve submitted versions.

Supported by Guiyang Science and Technology Program, No. 2019-9-1-39.

Informed consent statement: All authors have read the manuscript and agreed to its publication.

Conflict-of-interest statement: All authors declare that there is no conflict of interest in this study.

CARE Checklist (2016) statement: The authors have read the CARE Checklist (2016), and the manuscript was prepared and revised according to the CARE Checklist (2016).

Country/Territory of origin: China

ORCID number: Qian Chen 0000-0002-8918-0313; Tao Zhang 0009-0008-5334-3791.

S-Editor: Liu JH
L-Editor: A

P-Editor: Yuan YY

REFERENCES

1 **Chitty DW**, Hartley-Brown MA, Abate M, Thakur R, Wanchoo R, Jhaveri KD, Nair V. Kidney transplantation in patients with multiple myeloma: narrative analysis and review of the last two decades. *Nephrol Dial Transplant* 2022; **37**: 1616-1626 [PMID: 33295615 DOI: 10.1093/ndt/gfaa361]

2 **Tingle SJ**, Figueiredo RS, Moir JA, Goodfellow M, Talbot D, Wilson CH. Machine perfusion preservation versus static cold storage for deceased donor kidney transplantation. *Cochrane Database Syst Rev* 2019; **3**: CD011671 [PMID: 30875082 DOI: 10.1002/14651858.CD011671.pub2]

3 **Mason P**, Robb ML. Improving Access to Renal Transplantation for Highly Sensitized Patients. *Transplantation* 2022; **106**: 2299-2300 [PMID: 35973049 DOI: 10.1097/TP.0000000000004239]

4 **Slagter JS**, Outmani L, Tran KTCK, Ijzermans JNM, Minnee RC. Robot-assisted kidney transplantation as a minimally invasive approach for kidney transplant recipients: A systematic review and meta-analyses. *Int J Surg* 2022; **99**: 106264 [PMID: 35183735 DOI: 10.1016/j.ijsu.2022.106264]

5 **Sigera LSM**, Denning DW. Invasive Aspergillosis after Renal Transplantation. *J Fungi (Basel)* 2023; **9** [PMID: 36836369 DOI: 10.3390/jof9020255]

6 **Danger R**, Le Berre L, Cadoux M, Kerleau C, Papuchon E, Mai HL, Nguyen TV, Guérif P, Morelon E, Thaunat O, Legendre C, Anglicheau D, Lefaucheur C, Couzi L, Del Bello A, Kamar N, Le Quintrec M, Goutaudier V, Renaudin K, Giral M, Brouard S; DIVAT Consortium. Subclinical rejection-free diagnostic after kidney transplantation using blood gene expression. *Kidney Int* 2023; **103**: 1167-1179 [PMID: 36990211 DOI: 10.1016/j.kint.2023.03.019]

7 **Boumaza A**, Ben Azzouz E, Arrindell J, Lepidi H, Mezouar S, Desnues B. Whipple's disease and Tropheryma whipplei infections: from bench to bedside. *Lancet Infect Dis* 2022; **22**: e280-e291 [PMID: 35427488 DOI: 10.1016/S1473-3099(22)00128-1]

8 **Wiech T**, Reinhard L, Wulf S, Giuffrida AE, Longhitano E, Caruso R, Gröne HJ, Stahl RAK, Zipfel PF, Kikhney J, Moter A, Hoxha E, Santoro D. Bacterial infection possibly causing autoimmunity: Tropheryma whipplei and membranous nephropathy. *Lancet* 2022; **400**: 1882-1883 [PMID: 36328044 DOI: 10.1016/S0140-6736(22)02039-6]

9 **Yoon S**, Choi YJ, Lim YK, Kweon OJ, Kim HR, Kim TH, Lee MK. Prevalence and detection of Tropheryma whipplei in the stools of Korean patients with diarrhea using real-time PCRs. *Ann Clin Microbiol Antimicrob* 2022; **21**: 55 [PMID: 36474214 DOI: 10.1186/s12941-022-00543-1]

10 **Meyer S**, Puéchal X, Quesne G, Marques I, Jamet A, Ferroni A. Contribution of PCR to Differential Diagnosis between Patients with Whipple Disease and Tropheryma whipplei Carriers. *J Clin Microbiol* 2023; **61**: e0145722 [PMID: 36656022 DOI: 10.1128/jcm.01457-22]

11 **Ioannou P**, Kourtidis M, Mytilinis DO, Psyllaki A, Baliou S, Kofteridis D. Whipple's disease-associated infective endocarditis: a systematic review. *Infect Dis (Lond)* 2023; **55**: 447-457 [PMID: 37198913 DOI: 10.1080/23744235.2023.2214610]

12 **Manini A**, Querzola G, Lovati C, Pantoni L. Rapidly progressive dementia and intractable diarrhea: a teaching case report and a systematic review of cognitive impairment in Whipple's disease. *Neurol Sci* 2022; **43**: 907-926 [PMID: 34981284 DOI: 10.1007/s10072-021-05844-5]

13 **Hajduczenia MM**, Klefisch FR, Hopf AGM, Grubitzsch H, Stegemann MS, Pfäfflin F, Puhlmann B, Ocken M, Kretzler L, von Schöning D, Falk V, Moter A, Kikhney J. New Perspectives for Prosthetic Valve Endocarditis: Impact of Molecular Imaging by FISHseq Diagnostics. *Clin Infect Dis* 2023; **76**: 1050-1058 [PMID: 36318608 DOI: 10.1093/cid/ciac860]

14 **Makka S**, Papadogiannaki I, Voulgari-Kokota A, Georgakopoulou T, Koutantou M, Angelakis E. Tropheryma whipplei Intestinal Colonization in Migrant Children, Greece. *Emerg Infect Dis* 2022; **28**: 1926-1928 [PMID: 35997529 DOI: 10.3201/eid2809.220068]

15 **Wang L**, Su P, Song L, Sai L. Subcutaneous Nodules Caused by Tropheryma whipplei Infection. *Emerg Infect Dis* 2022; **28**: 761-763 [PMID: 35202530 DOI: 10.3201/eid2803.211989]

16 **Lin M**, Wang K, Qiu L, Liang Y, Tu C, Chen M, Wang Z, Wu J, Huang Y, Tan C, Chen Q, Zheng X, Liu J. Tropheryma whipplei detection by metagenomic next-generation sequencing in bronchoalveolar lavage fluid: A cross-sectional study. *Front Cell Infect Microbiol* 2022; **12**: 961297 [PMID: 36061864 DOI: 10.3389/fcimb.2022.961297]

17 **Diao Z**, Han D, Zhang R, Li J. Metagenomics next-generation sequencing tests take the stage in the diagnosis of lower respiratory tract infections. *J Adv Res* 2022; **38**: 201-212 [PMID: 35572406 DOI: 10.1016/j.jare.2021.09.012]

18 **Liu H**, Zhang Y, Yang J, Liu Y, Chen J. Application of mNGS in the Etiological Analysis of Lower Respiratory Tract Infections and the Prediction of Drug Resistance. *Microbiol Spectr* 2022; **10**: e0250221 [PMID: 35171007 DOI: 10.1128/spectrum.02502-21]

19 **Yang A**, Chen C, Hu Y, Zheng G, Chen P, Xie Z, Fan H, Sun Y, Wu P, Jiang W, Wang C, Zhang J, Zhang D, Wang J, Hu X, Xia H, Yin G, Guo Y. Application of Metagenomic Next-Generation Sequencing (mNGS) Using Bronchoalveolar Lavage Fluid (BALF) in Diagnosing Pneumonia of Children. *Microbiol Spectr* 2022; **10**: e0148822 [PMID: 36169415 DOI: 10.1128/spectrum.01488-22]

20 **Feurle GE**, Junga NS, Marth T. Efficacy of ceftriaxone or meropenem as initial therapies in Whipple's disease. *Gastroenterology* 2010; **138**: 478-86; quiz 11 [PMID: 19879276 DOI: 10.1053/j.gastro.2009.10.041]

21 **Lagier JC**, Fenollar F, Lepidi H, Giorgi R, Million M, Raoult D. Treatment of classic Whipple's disease: from in vitro results to clinical outcome. *J Antimicrob Chemother* 2014; **69**: 219-227 [PMID: 23946319 DOI: 10.1093/jac/dkt310]

22 **Marth T**, Moos V, Müller C, Biagi F, Schneider T. Tropheryma whipplei infection and Whipple's disease. *Lancet Infect Dis* 2016; **16**: e13-e22 [PMID: 26856775 DOI: 10.1016/S1473-3099(15)00537-X]

23 **Feurle GE**, Moos V, Bläker H, Loddenkemper C, Moter A, Stroux A, Marth T, Schneider T. Intravenous ceftriaxone, followed by 12 or three months of oral treatment with trimethoprim-sulfamethoxazole in Whipple's disease. *J Infect* 2013; **66**: 263-270 [PMID: 23291038 DOI: 10.1016/j.jinf.2012.12.004]

World Journal of Clinical Cases

Submit a Manuscript: https://www.f6publishing.com

World J Clin Cases 2023 September 6; 11(25): 6025-6030

DOI: 10.12998/wjcc.v11.i25.6025

ISSN 2307-8960 (online)

CASE REPORT

Monkeypox presenting as a chancre-like rash: A case report

Wei-Fang Zhu, Shu-Juan Song, Lin-Wei Wei, Jian-Jun Qiao

Specialty type: Infectious diseases

Provenance and peer review: Unsolicited article; Externally peer reviewed.

Peer-review model: Single blind

Peer-review report's scientific quality classification

Grade A (Excellent): 0
Grade B (Very good): 0
Grade C (Good): C, C
Grade D (Fair): 0
Grade E (Poor): 0

P-Reviewer: Al-Nazawi AM, Saudi Arabia; Ihekweazu C, Niger

Received: July 14, 2023
Peer-review started: July 14, 2023
First decision: August 2, 2023
Revised: August 4, 2023
Accepted: August 9, 2023
Article in press: August 9, 2023
Published online: September 6, 2023

Wei-Fang Zhu, Lin-Wei Wei, Jian-Jun Qiao, Division of Dermatology, First Affiliated Hospital, Zhejiang University School of Medicine, Hangzhou 310003, Zhejiang Province, China

Shu-Juan Song, Hangzhou Center of Disease Control and Prevention, Hangzhou Center of Disease Control and Prevention, Hangzhou 310000, Zhejiang Province, China

Corresponding author: Jian-Jun Qiao, MD, PhD, Doctor, Division of Dermatology, First Affiliated Hospital, Zhejiang University School of Medicine, No. 79 Qingchun Road, Hangzhou 310003, Zhejiang Province, China. qiaojianjun@zju.edu.cn

Abstract

BACKGROUND

Since May 2022, outbreaks of monkeypox have occurred in many countries around the world, and several cases have been reported in China.

CASE SUMMARY

A 38-year-old man presented with a small, painless, shallow ulcer on the coronary groove for 8 d. One day after the rash appeared, the patient developed inguinal lymphadenopathy with fever. The patient had a history of male-male sexual activity and denied a recent history of travel abroad. Monkeypox virus was detected by quantitative polymerase chain reaction from the rash site and throat swab. Based on the epidemiological history, clinical manifestations and nucleic acid test results, the patient was diagnosed with monkeypox.

CONCLUSION

Monkeypox is an emerging infectious disease in China. Monkeypox presenting as a chancre-like rash is easily misdiagnosed. Diagnosis can be made based on exposure history, clinical manifestations and nucleic acid test results.

Key Words: Monkeypox; Chancre-Like rash; China; Case report

Core Tip: We reported an indigenous case of monkeypox transmitted by male-male sexual activity, suggesting the beginning of community transmission of monkeypox in the mainland of China. Monkeypox presenting as genital ulcers is easily misdiagnosed as chancre or other skin diseases. Clinicians should improve the awareness of monkeypox to avoid possible misdiagnosis and prevent the spread of monkeypox in the community.

Citation: Zhu WF, Song SJ, Wei LW, Qiao JJ. Monkeypox presenting as a chancre-like rash: A case report. *World J Clin Cases* 2023; 11(25): 6025-6030
URL: https://www.wjgnet.com/2307-8960/full/v11/i25/6025.htm
DOI: https://dx.doi.org/10.12998/wjcc.v11.i25.6025

INTRODUCTION

Monkeypox is a zoonotic disease caused by the monkeypox virus (MPXV) that infects both humans and animals. It used to be predominantly prevalent in West and Central Africa. However, since May 2022, there have been multiple global outbreaks of monkeypox with different transmission routes and clinical presentations compared to the classical form[1]. In September 2022, China reported its first imported case, followed by sporadic cases within the country[2]. This article reports a recently diagnosed case of indigenous monkeypox and reviews the relevant literature.

CASE PRESENTATION

Chief complaints

A 38-year-old male pet shop worker presented to our dermatologic clinic with coronary ulcers for 8 d.

History of present illness

Eight days ago, the patient developed a small, painless shallow ulcer near the coronary sulcus of the glans without obvious inducement. The ulcer was not relieved by self-topical mupirocin treatment and became deeper. Seven days ago, the patient developed inguinal lymphadenopathy and fever, with a maximum body temperature of 38.6 °C. He self-administered ibuprofen for symptomatic relief. One day ago, new rashes appeared on the neck and limbs, prompting him to seek medical help at our department.

History of past illness

The patient was healthy in the past.

Personal and family history

The patient had a history of unprotected male-male sexual activity approximately 11 d before the rash onset and denied a recent history of travel abroad.

Physical examination

Physical examination revealed redness and swelling of the pharynx and enlargement of bilateral inguinal lymph nodes. Multiple grayish-white plaques with a central ulceration were observed in the coronal groove of the glans penis, without obvious secretions on the surface (Figure 1A). There were scattered tender papules, papulopustules and crusts on the neck, palms, and inner thighs (Figures 1B and C).

Laboratory examinations

The treponema pallidum particle agglutination assay, toluidine red unheated serum test, and human immunodeficiency virus antigen antibody combination test (HIV-P24) were negative. The white blood cell count was 6.98×10^9/L, with an atypical lymphocyte proportion of 4%, and the C-reactive protein level was 16.04 mg/L. There were no obvious abnormalities in liver or kidney function. Monkeypox virus quantitative polymerase chain reaction testing was performed on swabs taken from the rash site and throat secretion. The computed tomography (CT) values for the rash on the glans penis and the throat swab were 23 and 37, respectively. The virus was identified as the West African strain by sequencing by the Hangzhou Center of Disease Control and Prevention.

FINAL DIAGNOSIS

Based on the epidemiological history, clinical manifestations, and nucleic acid test results, the patient was diagnosed with monkeypox.

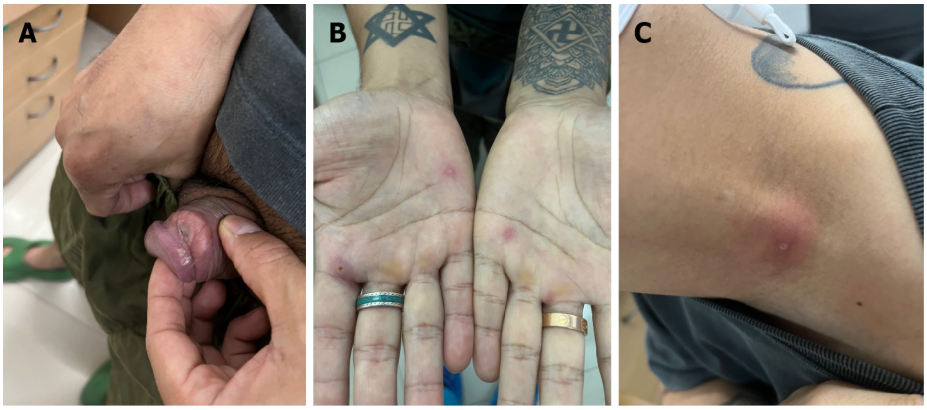

DOI: 10.12998/wjcc.v11.i25.6025

Figure 1 Skin and mucosal lesions on physical examination. A: Multiple grayish-white plaques with central ulcerations on the coronal groove, without obvious secretions on the surface; B and C: Scattered papulopustules with tenderness on the neck and palms.

TREATMENT

The patient was admitted to the ward and placed in droplet and contact isolation. Antiviral treatment with acyclovir and symptomatic treatment with celecoxib were administered. Topical application of recombinant human interferon alpha-2b spray was used for antiviral therapy. Four days later, the patient's body temperature returned to normal, and no new rashes appeared. He was discharged but still needed to continue medication at home and self-isolate.

OUTCOME AND FOLLOW-UP

By telephone follow-up, all the rashes crusted and fell off 14 d after discharge, leaving superficial depressed scars on the neck and hypopigmentations on the other sites. At present, the patient has been released from self-isolation.

DISCUSSION

Monkeypox virus is a double-stranded DNA virus belonging to the genus Orthopoxvirus of the Poxviridae family. Its primary hosts are African rodents. The first case of human monkeypox infection was reported in the Democratic Republic of the Congo in 1970[3]. Subsequently, sporadic outbreaks occurred in some countries in West and Central Africa, with a few travel-associated cases reported in Europe, North America, and Asia[1]. From May 2022, monkeypox started to spread extensively and had outbreaks in multiple nontraditional endemic countries and regions. As a result, in July 2022, the World Health Organization declared the outbreak of monkeypox a Public Health Emergency of International Concern.

Monkeypox can be transmitted through two main routes: animal-to-human and human-to-human transmission. Transmission between humans occurs through the inhalation of large respiratory droplets, close or direct contact with skin lesions, vertical transmission, or indirect contact through fomites[1]. Currently, there is no clear evidence of sexual transmission through semen or vaginal secretions[4]. In the current global outbreak of human MPXV infection, most diagnosed cases are among men who have sex with men, and direct contact with infectious lesions is the main route of transmission[4-6]. Subclinical or asymptomatic monkeypox infections are rare[1]. However, in the 2022 outbreak, approximately half of the transmissions occurred during the presymptomatic stage, indicating a need for further research to determine the possibility of transmission by asymptomatic individuals[1,7]. In this case, the patient engaged in unprotected sexual behavior with a male before the rash appeared, which aligns with male-to-male transmission.

In the 2022 outbreak, the average incubation period after exposure was 7-10 d[4,8-10]. Systemic symptoms are common and typically present as fever, fatigue, or myalgia[1]. These symptoms can occur before or shortly after the onset of rash, although reports of skin lesions without systemic illness have also been observed[5,8]. The rash of monkeypox usually lasts for 2-3 wk. It initially appears as small spots and then evolves into papules, vesicles, and pustules, which crust, dry, and eventually slough off after 7 d to 14 d[1]. Skin lesions can appear on any part of the body, and different stages of lesions may coexist[6]. In previous outbreaks, the rash typically first appeared on the face and gradually spread to the trunk and limbs. However, in the 2022 outbreak, the lesions were mainly located in the anogenital and perioral regions[4,6]. Genital rash in male patients may manifest as one or multiple lesions[5]. Approximately a quarter of patients are concurrently diagnosed with sexually transmitted diseases[4,5]. In this case, the patient's rash initially occurred in the coronal sulcus, presenting as a chancroid-like genital ulcer, which can often be misdiagnosed as chancroid.

In September 2022, the first imported case of the mainland of China was reported in Chongqing municipality[2]. According to the statistics on the WHO website, as of June 27, 2023, there have been 6 confirmed cases in the mainland of

China (https://worldhealthorg.shinyapps.io/mpx_global/). Two recently reported cases of local transmission in the mainland of China were both males who had sex with men[11,12]. In one case, the initial manifestation was gray-white plaques in the coronal sulcus, followed by fever, sore throat, and generalized rash[11]. In the other case, the patient developed erythema, papules, pustules, and ulcers on the penis and pubis three days after the onset of fever[12]. The epidemiological characteristics and clinical presentations of our case were similar to those of the above two cases, with an incubation period of approximately 11 d. The initial presentation is painless ulceration in the coronal sulcus, followed by fever and enlarged lymph nodes one day later. It can be misdiagnosed as syphilis chancre, lymphogranuloma venereum, chancroid, genital herpes, or balanitis. Chancre has an average incubation period of 2 wk to 4 wk and is often solitary with a clean, smooth base and cartilaginous hardness without systemic symptoms. Monkeypox, however, often has multiple rashes, presenting as papulopustules, umbilical-like papules, *etc.*, with surrounding redness and swelling, and often has systemic symptoms before or after the onset of rash[5]. Lymphogranuloma venereum is characterized by small superficial vesicles or ulcers, followed by inguinal lymphadenopathy, ulceration, and suppuration, while lymphadenopathy of monkeypox often resolves within a short period. Chancroid presents as painful, purulent ulcers in the genital area, often accompanied by suppurative lymphadenitis in the inguinal region, whereas monkeypox skin lesions are not associated with severe pain. Genital herpes manifests as multiple vesicles that progress to erosions, which are smaller and shallower than monkeypox lesions. After the onset of generalized rash, monkeypox needs to be differentiated from varicella. Compared to monkeypox, varicella lesions were polymorphic and centripetal distributed, with denser lesions on the trunk than on the face and limbs, and developed rapidly without lymph node enlargement. In contrast, monkeypox skin lesions usually start on the genital area or face and spread in a centrifugal manner, involving the chest, arms and legs, followed by the palms and soles[13]. In this case, there were vesicular eruptions on both palms. Additionally, monkeypox needs to be distinguished from other poxvirus infections, secondary syphilis, pyoderma, and aphthous ulcers[1].

Timely diagnosis is crucial for controlling the spread of monkeypox. The diagnosis of monkeypox is based on a comprehensive assessment of clinical manifestations, epidemiological history, and laboratory testing results. Skin lesion specimens are preferred for testing due to high viral load and positive nucleic acid detection rates[14]. In this case, the nucleic acid test result from the skin lesion had a lower CT value than the throat swab, supporting transmission through close contact. A relatively high proportion of patients with monkeypox were HIV positive or had sexually transmitted diseases[4,5], so testing for HIV and other sexually transmitted infections should be conducted for monkeypox patients. Once diagnosed, the patients should be promptly isolated until all skin lesions crust over and fall off. Monkeypox is self-limiting and generally has a good prognosis. Most patients do not need special treatment, and symptomatic care, such as antipyretic and analgesic therapy, is sufficient. However, monkeypox in individuals with advanced and uncontrolled HIV infection may have a higher risk of developing serious and prolonged illness, which should be given high attention [15]. Effective antimicrobial therapy should be administered for secondary bacterial skin infections. Currently, there are no specific antiviral drugs for treating monkeypox. Antiviral treatment with tecovirimat is preferred for severe cases and immunocompromised individuals[16]. In this case, the patient did not have any other sexually transmitted diseases, and his condition improved after symptomatic antipyretic treatment without complications.

CONCLUSION

In China, monkeypox is a newly emerging infectious disease. Currently, the number of monkeypox cases in the mainland of China is gradually increasing. Clinical physicians need to enhance their understanding of this disease. For individuals with a high-risk exposure history, especially a history of male-to-male sexual contact, and the presence of papules, vesicles, pustules or ulcers around the genital and anal areas, with or without fever and lymphadenopathy, the possibility of monkeypox should be considered. Immediate MPXV nucleic acid testing should be performed to confirm the diagnosis, and the patient should be isolated and treated in time. In addition, it is necessary to improve the reporting and monitoring system, strengthen health education for high-risk populations, and administer vaccines to high-risk individuals when necessary to curb community transmission of monkeypox.

FOOTNOTES

Author contributions: Zhu WF, Song SJ, and Wei LW contributed to manuscript writing and editing and data collection; Qiao JJ contributed to conceptualization and supervision; and all authors have read and approved the final manuscript.

Informed consent statement: Informed written consent was obtained from the patient for publication of this report and any accompanying images.

Conflict-of-interest statement: The authors declare that they have no conflict of interest to disclose.

CARE Checklist (2016) statement: The authors have read the CARE Checklist (2016), and the manuscript was prepared and revised according to the CARE Checklist (2016).

Country/Territory of origin: China

ORCID number: Wei-Fang Zhu 0000-0003-2587-0160; Shu-Juan Song 0009-0009-0850-2666; Lin-Wei Wei 0000-0003-2199-7586; Jian-Jun Qiao 0000-0003-3386-297X.

S-Editor: Chen YL
L-Editor: A
P-Editor: Chen YL

REFERENCES

1 **Mitjà O**, Ogoina D, Titanji BK, Galvan C, Muyembe JJ, Marks M, Orkin CM. Monkeypox. *Lancet* 2023; **401**: 60-74 [PMID: 36403582 DOI: 10.1016/S0140-6736(22)02075-X]

2 **Zhao H**, Wang W, Zhao L, Ye S, Song J, Lu R, Zong H, Wu C, Huang W, Huang B, Deng Y, A R, Xie W, Qi L, Xu W, Ling H, Tan W. The First Imported Case of Monkeypox in the Mainland of China - Chongqing Municipality, China, September 16, 2022. *China CDC Wkly* 2022; **4**: 853-854 [PMID: 36284686 DOI: 10.46234/ccdcw2022.175]

3 **Ladnyj ID**, Ziegler P, Kima E. A human infection caused by monkeypox virus in Basankusu Territory, Democratic Republic of the Congo. *Bull World Health Organ* 1972; **46**: 593-597 [PMID: 4340218]

4 **Thornhill JP**, Barkati S, Walmsley S, Rockstroh J, Antinori A, Harrison LB, Palich R, Nori A, Reeves I, Habibi MS, Apea V, Boesecke C, Vandekerckhove L, Yakubovsky M, Sendagorta E, Blanco JL, Florence E, Moschese D, Maltez FM, Goorhuis A, Pourcher V, Migaud P, Noe S, Pintado C, Maggi F, Hansen AE, Hoffmann C, Lezama JI, Mussini C, Cattelan A, Makofane K, Tan D, Nozza S, Nemeth J, Klein MB, Orkin CM; SHARE-net Clinical Group. Monkeypox Virus Infection in Humans across 16 Countries - April-June 2022. *N Engl J Med* 2022; **387**: 679-691 [PMID: 35866746 DOI: 10.1056/NEJMoa2207323]

5 **Girometti N**, Byrne R, Bracchi M, Heskin J, McOwan A, Tittle V, Gedela K, Scott C, Patel S, Gohil J, Nugent D, Suchak T, Dickinson M, Feeney M, Mora-Peris B, Stegmann K, Plaha K, Davies G, Moore LSP, Mughal N, Asboe D, Boffito M, Jones R, Whitlock G. Demographic and clinical characteristics of confirmed human monkeypox virus cases in individuals attending a sexual health centre in London, UK: an observational analysis. *Lancet Infect Dis* 2022; **22**: 1321-1328 [PMID: 35785793 DOI: 10.1016/S1473-3099(22)00411-X]

6 **Angelo KM**, Smith T, Camprubí-Ferrer D, Balerdi-Sarasola L, Díaz Menéndez M, Servera-Negre G, Barkati S, Duvignaud A, Huber KLB, Chakravarti A, Bottieau E, Greenaway C, Grobusch MP, Mendes Pedro D, Asgeirsson H, Popescu CP, Martin C, Licitra C, de Frey A, Schwartz E, Beadsworth M, Lloveras S, Larsen CS, Guagliardo SAJ, Whitehill F, Huits R, Hamer DH, Kozarsky P, Libman M; GeoSentinel Network Collaborators. Epidemiological and clinical characteristics of patients with monkeypox in the GeoSentinel Network: a cross-sectional study. *Lancet Infect Dis* 2023; **23**: 196-206 [PMID: 36216018 DOI: 10.1016/S1473-3099(22)00651-X]

7 **Ward T**, Christie R, Paton RS, Cumming F, Overton CE. Transmission dynamics of monkeypox in the United Kingdom: contact tracing study. *BMJ* 2022; **379**: e073153 [PMID: 36323407 DOI: 10.1136/bmj-2022-073153]

8 **Tarín-Vicente EJ**, Alemany A, Agud-Dios M, Ubals M, Suñer C, Antón A, Arando M, Arroyo-Andrés J, Calderón-Lozano L, Casañ C, Cabrera JM, Coll P, Descalzo V, Folgueira MD, García-Pérez JN, Gil-Cruz E, González-Rodríguez B, Gutiérrez-Collar C, Hernández-Rodríguez Á, López-Roa P, de Los Ángeles Meléndez M, Montero-Menárguez J, Muñoz-Gallego I, Palencia-Pérez SI, Paredes R, Pérez-Rivilla A, Piñana M, Prat N, Ramirez A, Rivero Á, Rubio-Muñiz CA, Vall M, Acosta-Velásquez KS, Wang A, Galván-Casas C, Marks M, Ortiz-Romero PL, Mitjà O. Clinical presentation and virological assessment of confirmed human monkeypox virus cases in Spain: a prospective observational cohort study. *Lancet* 2022; **400**: 661-669 [PMID: 35952705 DOI: 10.1016/S0140-6736(22)01436-2]

9 **McFarland SE**, Marcus U, Hemmers L, Miura F, Iñigo Martínez J, Martínez FM, Montalbán EG, Chazelle E, Mailles A, Silue Y, Hammami N, Lecompte A, Ledent N, Vanden Berghe W, Liesenborghs L, Van den Bossche D, Cleary PR, Wallinga J, Robinson EP, Johansen TB, Bormane A, Melillo T, Seidl C, Coyer L, Boberg R, Jurke A, Werber D, Bartel A. Estimated incubation period distributions of mpox using cases from two international European festivals and outbreaks in a club in Berlin, May to June 2022. *Euro Surveill* 2023; **28** [PMID: 37410383 DOI: 10.2807/1560-7917.ES.2023.28.27.2200806]

10 **Miura F**, van Ewijk CE, Backer JA, Xiridou M, Franz E, Op de Coul E, Brandwagt D, van Cleef B, van Rijckevorsel G, Swaan C, van den Hof S, Wallinga J. Estimated incubation period for monkeypox cases confirmed in the Netherlands, May 2022. *Euro Surveill* 2022; **27** [PMID: 35713026 DOI: 10.2807/1560-7917.ES.2022.27.24.2200448]

11 **Wang TZ**, Chu TS, Huai PC, Wang M, Feng FF, Liu YX, Wang C, Tian HQ, Zhang FR. A case of monkeypox with plaques on the balanus as the first manifestation and literature review. *Chin J Lepr Skin Dis* 2023; **39**: 551-554 [DOI: 10.12144/zgmfskin202308551]

12 **Yang LG**, An NB, Wen Yj. A case of monkeypox and literature review. *J Diagn Ther Dermato-Venereol* 2023; **30**: 187-189 [DOI: 10.3969/j.issn.1674-8468.2023.03.001]

13 **Sukhdeo S**, Mishra S, Walmsley S. Human monkeypox: a comparison of the characteristics of the new epidemic to the endemic disease. *BMC Infect Dis* 2022; **22**: 928 [PMID: 36503476 DOI: 10.1186/s12879-022-07900-7]

14 **Lim CK**, McKenzie C, Deerain J, Chow EPF, Towns J, Chen MY, Fairley CK, Tran T, Williamson DA. Correlation between monkeypox viral load and infectious virus in clinical specimens. *J Clin Virol* 2023; **161**: 105421 [PMID: 36893717 DOI: 10.1016/j.jcv.2023.105421]

15 **Miller MJ**, Cash-Goldwasser S, Marx GE, Schrodt CA, Kimball A, Padgett K, Noe RS, McCormick DW, Wong JM, Labuda SM, Borah BF, Zulu I, Asif A, Kaur G, McNicholl JM, Kourtis A, Tadros A, Reagan-Steiner S, Ritter JM, Yu Y, Yu P, Clinton R, Parker C, Click ES, Salzer JS, McCollum AM, Petersen B, Minhaj FS, Brown E, Fischer MP, Atmar RL, DiNardo AR, Xu Y, Brown C, Goodman JC, Holloman A, Gallardo J, Siatecka H, Huffman G, Powell J, Alapat P, Sarkar P, Hanania NA, Bruck O, Brass SD, Mehta A, Dretler AW, Feldpausch A, Pavlick J, Spencer H, Ghinai I, Black SR, Hernandez-Guarin LN, Won SY, Shankaran S, Simms AT, Alarcón J, O'Shea JG, Brooks JT, McQuiston J, Honein MA, O'Connor SM, Chatham-Stephens K, O'Laughlin K, Rao AK, Raizes E, Gold JAW, Morris SB; CDC Severe Monkeypox Investigations Team. Severe Monkeypox in Hospitalized Patients - United States, August 10-October 10, 2022. *MMWR Morb*

Mortal Wkly Rep 2022; **71**: 1412-1417 [PMID: 36327164 DOI: 10.15585/mmwr.mm7144e1]

16 **Sherwat A**, Brooks JT, Birnkrant D, Kim P. Tecovirimat and the Treatment of Monkeypox - Past, Present, and Future Considerations. *N Engl J Med* 2022; **387**: 579-581 [PMID: 35921403 DOI: 10.1056/NEJMp2210125]

Published by **Baishideng Publishing Group Inc**
7041 Koll Center Parkway, Suite 160, Pleasanton, CA 94566, USA
Telephone: +1-925-3991568
E-mail: bpgoffice@wjgnet.com
Help Desk: https://www.f6publishing.com/helpdesk
https://www.wjgnet.com